NASA

Earth Resources
A Continuing Bibliography with Indexes

NASA SP-7041(35)
October 1982

National Aeronautics and Space Administration

Earth Resources Earth Resources Earth Resources Earth Resources Earth Resources Earth Resources Earth Resources

ACCESSION NUMBER RANGES

Accession numbers cited in this Supplement fall within the following ranges.

STAR (N-10000 Series)	N82-22141 - N82-28242
IAA (A-10000 Series)	A82-28539 - A82-38102

This bibliography was prepared by the NASA Scientific and Technical Information Facility operated for the National Aeronautics and Space Administration by PRC Government Information Systems.

NASA SP-7041(35)

EARTH RESOURCES

A CONTINUING BIBLIOGRAPHY WITH INDEXES

Issue 35

A selection of annotated references to unclassified reports and journal articles that were introduced into the NASA scientific and technical information system and announced between July 1 and September 30, 1982 in

- *Scientific and Technical Aerospace Reports (STAR)*
- *International Aerospace Abstracts (IAA).*

NASA Scientific and Technical Information Branch 1982
National Aeronautics and Space Administration
Washington, DC

This supplement is available as NTISUB/038/093 from the National Technical Information Service (NTIS), Springfield, Virginia 22161 at the price of $10 50 domestic; $21.50 foreign for standing orders. Please note. Standing orders are subscriptions which do not terminate at the end of a year, as do regular subscriptions, but continue indefinitely unless specifically terminated by the subscriber.

INTRODUCTION

The technical literature described in this continuing bibliography may be helpful to researchers in numerous disciplines such as agriculture and forestry, geography and cartography, geology and mining, oceanography and fishing, environmental control, and many others. Until recently it was impossible for anyone to examine more than a minute fraction of the Earth's surface continuously. Now vast areas can be observed synoptically, and changes noted in both the Earth's lands and waters, by sensing instrumention on orbiting spacecraft or on aircraft.

This literature survey lists 587 reports, articles, and other documents announced between July 1 and September 30, 1982 in *Scientific and Technical Aerospace Reports (STAR)*, and *International Aerospace Abstracts (IAA)*.

The coverage includes documents related to the identification and evaluation by means of sensors in spacecraft and aircraft of vegetation, minerals, and other natural resources, and the techniques and potentialities of surveying and keeping up-to-date inventories of such riches. It encompasses studies of such natural phenomena as earthquakes, volcanoes, ocean currents, and magnetic fields; and such cultural phenomena as cities, transportation networks, and irrigation systems. Descriptions of the components and use of remote sensing and geophysical instrumentation, their subsystems, observational procedures, signature and analyses and interpretive techniques for gathering data are also included. All reports generated under NASA's Earth Resources Survey Program for the time period covered in this bibliography will also be included. The bibliography does not contain citations to documents dealing mainly with satellites or satellite equipment used in navigation or communication systems, nor with instrumentation not used aboard aerospace vehicles.

The selected items are grouped in nine categories. These are listed in the Table of Contents with notes regarding the scope of each category. These categories were especially chosen for this publication, and differ from those found in *STAR* and *IAA*.

Each entry consists of a standard bibliographic citation accompanied by an abstract. The citations and abstracts are reproduced exactly as they appeared originally in *STAR*, or *IAA*, including the original accession numbers from the respective announcement journals. This procedure, which saves time and money, accounts for the variation in citation appearance.

Under each of the nine categories, the entries are presented in one of two groups that appear in the following order:

IAA entries identified by accession number series A82-10,000 in ascending accession number order;

STAR entries identified by accession number series N82-10,000 in ascending accession number order.

After the abstract section, there are six indexes:

subject, personal author, corporate source, contract number, report/accession number, and accession number.

AVAILABILITY OF CITED PUBLICATIONS

IAA ENTRIES (A82-10000 Series)

All publications abstracted in this Section are available from the Technical Information Service, American Institute of Aeronautics and Astronautics, Inc (AIAA), as follows Paper copies of accessions are available at $8.00 per document Microfiche[1] of documents announced in *IAA* are available at the rate of $4 00 per microfiche on demand, and at the rate of $1 35 per microfiche for standing orders for all *IAA* microfiche

Minimum air-mail postage to foreign countries is $2 50 and all foreign orders are shipped on payment of pro-forma invoices

All inquiries and requests should be addressed to AIAA Technical Information Service Please refer to the accession number when requesting publications

STAR ENTRIES (N82-10000 Series)

One or more sources from which a document announced in *STAR* is available to the public is ordinarily given on the last line of the citation. The most commonly indicated sources and their acronyms or abbreviations are listed below. If the publication is available from a source other than those listed, the publisher and his address will be displayed on the availability line or in combination with the corporate source line

Avail: NTIS. Sold by the National Technical Information Service Prices for hard copy (HC) and microfiche (MF) are indicated by a price code preceded by the letters HC or MF in the *STAR* citation Current values for the price codes are given in the tables on page vii.

Documents on microfiche are designated by a pound sign (#) following the accession number The pound sign is used without regard to the source or quality of the microfiche.

Initially distributed microfiche under the NTIS SRIM (Selected Research in Microfiche) is available at greatly reduced unit prices For this service and for information concerning subscription to NASA printed reports, consult the NTIS Subscription Section, Springfield, Va 22161

NOTE ON ORDERING DOCUMENTS: When ordering NASA publications (those followed by the * symbol), use the N accession number NASA patent applications (only the specifications are offered) should be ordered by the US-Patent-Appl-SN number Non-NASA publications (no asterisk) should be ordered by the AD, PB, or other *report* number shown on the last line of the citation, not by the N accession number. It is also advisable to cite the title and other bibliographic identification

Avail SOD (or GPO) Sold by the Superintendent of Documents, U.S. Government Printing Office, in hard copy The current price and order number are given following the availability line. (NTIS will fill microfiche requests, at the standard $4.00 price, for those documents identified by a # symbol)

Avail NASA Public Document Rooms Documents so indicated may be examined at or purchased from the National Aeronautics and Space Administration, Public Document Room (Room 126), 600 Independence Ave., S.W , Washington, D.C 20546, or public document rooms located at each of the NASA research centers, the NASA Space Technology Laboratories, and the NASA Pasadena Office at the Jet Propulsion Laboratory

(1) A microfiche is a transparent sheet of film 105 by 148 mm in size containing as many as 60 to 98 pages of information reduced to micro images (not to exceed 26 1 reduction)

Avail. DOE Depository Libraries. Organizations in U.S. cities and abroad that maintain collections of Department of Energy reports, usually in microfiche form, are listed in *Energy Research Abstracts.* Services available from the DOE and its depositories are described in a booklet, *DOE Technical Information Center - Its Functions and Services* (TID-4660), which may be obtained without charge from the DOE Technical Information Center.

Avail: Univ. Microfilms Documents so indicated are dissertations selected from *Dissertation Abstracts* and are sold by University Microfilms as xerographic copy (HC) and microfilm All requests should cite the author and the Order Number as they appear in the citation.

Avail: USGS. Originals of many reports from the U S. Geological Survey, which may contain color illustrations, or otherwise may not have the quality of illustrations preserved in the microfiche or facsimile reproduction, may be examined by the public at the libraries of the USGS field offices whose addresses are listed in this introduction. The libraries may be queried concerning the availability of specific documents and the possible utilization of local copying services, such as color reproduction.

Avail: HMSO. Publications of Her Majesty's Stationery Office are sold in the U.S. by Pendragon House, Inc (PHI), Redwood City, California. The U S. price (including a service and mailing charge) is given, or a conversion table may be obtained from PHI.

Avail: BLL (formerly NLL): British Library Lending Division, Boston Spa, Wetherby, Yorkshire, England. Photocopies available from this organization at the price shown (If none is given, inquiry should be addressed to the BLL.)

Avail: Fachinformationszentrum, Karlsruhe. Sold by the Fachinformationszentrum Energie, Physik, Mathematik GMBH, Eggenstein Leopoldshafen, Federal Republic of Germany, at the price shown in deutschmarks (DM).

Avail: Issuing Activity, or Corporate Author, or no indication of availability Inquiries as to the availability of these documents should be addressed to the organization shown in the citation as the corporate author of the document

Avail U.S. Patent and Trademark Office. Sold by Commissioner of Patents and Trademarks, U.S. Patent and Trademark Office, at the standard price of 50 cents each, postage free.

Other availabilities: If the publication is available from a source other than the above, the publisher and his address will be displayed entirely on the availability line or in combination with the corporate author line.

ADDRESSES OF ORGANIZATIONS

American Institute of Aeronautics and Astronautics
Technical Information Service
555 West 57th Street, 12th Floor
New York, New York 10019

British Library Lending Division,
Boston Spa, Wetherby, Yorkshire,
England

Commissioner of Patents and Trademarks
U S. Patent and Trademark Office
Washington, D C 20231

Department of Energy
Technical Information Center
P O. Box 62
Oak Ridge, Tennessee 37830

ESA-Information Retrieval Service
ESRIN
Via Galileo Galilei
00044 Frascati (Rome) Italy

Fachinformationszentrum Energie, Physik, Mathematik GMBH
7514 Eggenstein Leopoldshafen
Federal Republic of Germany

Her Majesty's Stationery Office
P.O. Box 569, S.E. 1
London, England

NASA Scientific and Technical Information Facility
P.O. Box 8757
B W I Airport, Maryland 21240

National Aeronautics and Space Administration
Scientific and Technical Information Branch (NST-41)
Washington, D C 20546

National Technical Information Service
5285 Port Royal Road
Springfield, Virginia 22161

Pendragon House, Inc.
899 Broadway Avenue
Redwood City, California 94063

Superintendent of Documents
U S Government Printing Office
Washington, D C. 20402

University Microfilms
A Xerox Company
300 North Zeeb Road
Ann Arbor, Michigan 48106

University Microfilms, Ltd
Tylers Green
London, England

U S. Geological Survey
1033 General Services Administration Building
Washington, D.C 20242

U.S. Geological Survey
601 E Cedar Avenue
Flagstaff, Arizona 86002

U.S. Geological Survey
345 Middlefield Road
Menlo Park, California 94025

U S. Geological Survey
Bldg 25, Denver Federal Center
Denver, Colorado 80225

NTIS PRICE SCHEDULES

Schedule A

STANDARD PAPER COPY PRICE SCHEDULE

(Effective January 1, 1982)

Price Code	Page Range	North American Price	Foreign Price
A01	Microfiche	$ 4 00	$ 8 00
A02	001-025	6 00	12 00
A03	026-050	7 50	15 00
A04	051-075	9 00	18 00
A05	076-100	10 50	21 00
A06	101-125	12 00	24 00
A07	126-150	13 50	27 00
A08	151-175	15 00	30 00
A09	176-200	16 50	33 00
A10	201-225	18 00	36 00
A11	226-250	19 50	39 00
A12	251-275	21 00	42 00
A13	276-300	22 50	45 00
A14	301-325	24 00	48 00
A15	326-350	25 50	51 00
A16	351-375	27 00	54 00
A17	376-400	28 50	57 00
A18	401-425	30 00	60 00
A19	426-450	31 50	63 00
A20	451-475	33 00	66 00
A21	476-500	34 50	69 00
A22	501-525	36 00	72 00
A23	526-550	37 50	75 00
A24	551-575	39 00	78 00
A25	576-600	40 50	81 00
	601-up	-- 1/	-- 2/

A99 - Write for quote

1/ Add $1 50 for each additional 25 page increment or portion thereof for 601 pages up

2/ Add $3 00 for each additional 25 page increment or portion thereof for 601 pages and more

Schedule E

EXCEPTION PRICE SCHEDULE

Paper Copy & Microfiche

Price Code	North American Price	Foreign Price
E01	$ 6 50	$ 13 50
E02	7 50	15 50
E03	9 50	19 50
E04	11 50	23 50
E05	13 50	27 50
E06	15 50	31 50
E07	17 50	35 50
E08	19 50	39 50
E09	21 50	43 50
E10	23 50	47 50
E11	25 50	51 50
E12	28 50	57 50
E13	31 50	63 50
E14	34 50	69 50
E15	37 50	75 50
E16	40 50	81 50
E17	43 50	88 50
E18	46 50	93 50
E19	51 50	102 50
E20	61 50	123 50

E-99 - Write for quote

N01	30 00[1]	45 00

TABLE OF CONTENTS

Page

Category 01 Agriculture and Forestry 1
Includes crop forecasts, crop signature analysis, soil identification, disease detection, harvest estimates, range resources, timber inventory, forest fire detection, and wildlife migration patterns.

Category 02 Environmental Changes and Cultural Resources 21
Includes land use analysis, urban and metropolitan studies, environmental impact, air and water pollution, geographic information systems, and geographic analysis.

Category 03 Geodesy and Cartography 31
Includes mapping and topography.

Category 04 Geology and Mineral Resources 40
Includes mineral deposits, petroleum deposits, spectral properties of rocks, geological exploration, and lithology.

Category 05 Oceanography and Marine Resources 49
Includes sea-surface temperature, ocean bottom surveying imagery, drift rates, sea ice and icebergs, sea state, fish location

Category 06 Hydrology and Water Management 59
Includes snow cover and water runoff in rivers and glaciers, saline intrusion, drainage analysis, geomorphology of river basins, land uses, and estuarine studies.

Category 07 Data Processing and Distribution Systems 63
Includes film processing, computer technology, satellite and aircraft hardware, and imagery.

Category 08 Instrumentation and Sensors 76
Includes data acquisition and camera systems and remote sensors.

Category 09 General 82
Includes economic analysis.

Subject Index A-1
Personal Author Index B-1
Corporate Source Index C-1
Contract Number Index D-1
Report / Accession Number Index E-1
Accession Number Index F-1

TYPICAL CITATION AND ABSTRACT FROM *STAR*

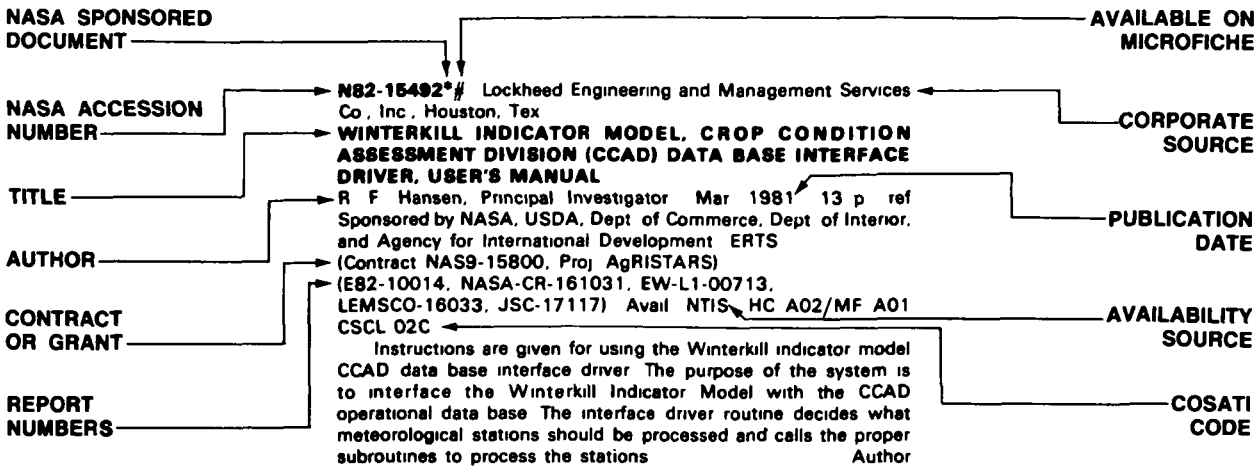

TYPICAL CITATION AND ABSTRACT FROM *IAA*

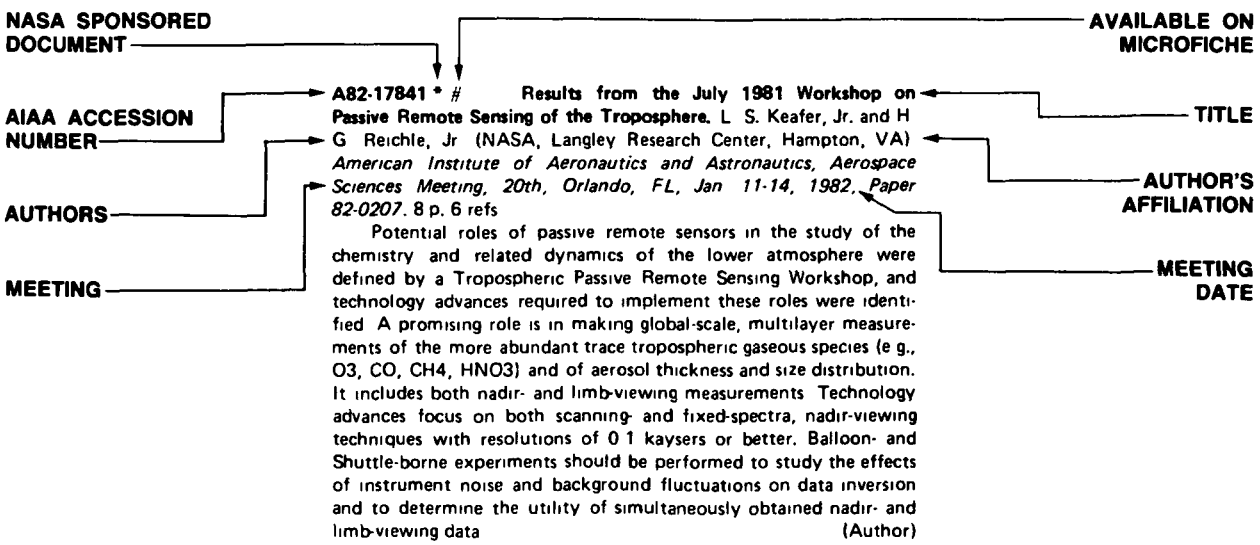

EARTH RESOURCES

A Continuing Bibliography (Issue 35)

OCTOBER 1982

01

AGRICULTURE AND FORESTRY

Includes crop forecasts, crop signature analysis, soil identification, disease detection, harvest estimates, range resources, timber inventry, forest fire detection, and wildlife migration patterns.

A82-22539
A REPORT ON THE 'COSMIC RAY PROPAGATION PROBLEM'
P. S. FREIER (Minnesota, University, Minneapolis, MN) In: International Cosmic Ray Conference, 17th, Paris, France, July 13-25, 1981, Conference Papers. Volume 2. Gif-sur-Yvette, Essonne, France, Commissariat a l'Energie Atomique, 1981, p. 182-185 refs

Data on abundances of elements are now of such quality, that the major source of discrepancies in cosmic ray propagation results is believed to be due to a difference in the propagation programs being used by different groups Nine groups were therefore asked to use a standardized source, E equals 2 3 GeV/n with no energy loss, and propagate it through a 5 g/sq cm exponential path length of hydrogen, using their values of the Silverberg and Tsao cross sections at 2 3 GeV/n (1973, 1977, 1979). Results indicate significant discrepancies arising from propagation, demonstrating the differences that can result when different physical conditions are assumed. J.F.

A82-22541* Chicago Univ., Ill.
THE QUESTION OF SHORT PATHLENGTHS IN INTERSTELLAR PROPAGATION
M GARCIA-MUNOZ, T. G. GUZIK, J. A SIMPSON, and J. P. WEFEL (Chicago, University, Chicago, IL) In. International Cosmic Ray Conference, 17th, Paris, France, July 13-25, 1981, Conference Papers. Volume 2. Gif-sur-Yvette, Essonne, France, Commissariat a l'Energie Atomique, 1981, p 192-195. refs
(Contract NAS5-25731; NGL-14-001-006)

Interstellar propagation calculations for cosmic rays, He-4 - Ni-64, are compared with currently available abundance ratios for B/C and sub-Fe/Fe The calculations show that an exponential pathlength distribution (leaky box model) cannot reproduce both secondary to primary ratios in the interval 0 5-1 GeV/n unless some values of the propagation parameters are modified. The calculated ratios are shown to be particularly sensitive to the adopted cross sections, the presence of the sub-Fe elements in the source regions, the shape of the source energy spectrum, and ionization energy loss. (Author)

A82-22542* National Aeronautics and Space Administration Goddard Space Flight Center, Greenbelt, Md.
THE COSMIC RAY POSITRON SPECTRUM
R. J. PROTHEROE (NASA, Goddard Space Flight Center, Laboratory for High Energy Astrophysics, Greenbelt, MD) In International Cosmic Ray Conference, 17th, Paris, France, July 13-25, 1981, Conference Papers. Volume 2. Gif-sur-Yvette, Essonne, France, Commissariat a l'Energie Atomique, 1981, p. 198-201 refs

A calculation is made of the flux of secondary positrons expected above 100 MeV for various disk-halo diffusion models, which are consistent with the observed grammage and Be-10 abundance. It is found that models which give a high surviving fraction of Be-10 (about 0.3) give a secondary positron spectrum which is consistent with the observations, while a model predicting a low Be-10 abundance (about 0.1 surviving) gives a poorer fit at high energies hinting at the presence of a primary positron component. Implications of these results are discussed. (Author)

A82-22543
THE ELECTRON AND POSITRON SPECTRA IN PRIMARY COSMIC RAYS
L C TAN and L. K. NG (University of Hong Kong, Hong Kong) In: International Cosmic Ray Conference, 17th, Paris, France, July 13-25, 1981, Conference Papers. Volume 2 Gif-sur-Yvette, Essonne, France, Commissariat a l'Energie Atomique, 1981, p 202-205. refs

It is contended that variations in the results of various authors' positron calculations derive mainly from differences between the local interstellar electron spectrum and those derived from radio data. It is found that, among the spectra derived from radio data, that of Rockstroh and Webber (1978) is the most consistent with the description using the usual 'leaky box' model. In addition, it is shown that the electron injection spectrum with a single power *law cannot satisfactorily explain the primary electron spectrum.* Analysis also shows that the leaky box model is able to account for the mean behavior of interstellar positrons and electrons in a cosmic ray containment volume whose galactic scale height and width around the earth are, respectively, 0 5-1 kpc and 2-3 kpc C.R

A82-22544
COMPARISON OF THE MEASURED ANTIPROTON FLUX WITH THAT PREDICTED BY THE 'LEAKY BOX' MODEL
L C TAN and L. K. NG (University of Hong Kong, Hong Kong) In: International Cosmic Ray Conference, 17th, Paris, France, July 13-25, 1981, Conference Papers. Volume 2 Gif-sur-Yvette, Essonne, France, Commissariat a l'Energie Atomique, 1981, p. 210-213 refs

A82-22552
STEADY-STATE COSMIC RAY ELECTRON SPECTRUM UNDER DIFFUSION, CONVECTION, ADIABATIC DECELERATION AND SYNCHROTRON LOSSES
I LERCHE (Chicago, University, Chicago, IL) and R SCHLICKE6SER (Max-Planck-Institut fur Radioastronomie, Bonn, West Germany) In International Cosmic Ray Conference, 17th, Paris, France, July 13-25, 1981, Conference Papers. Volume 2. Gif-sur-Yvette, Essonne, France, Commissariat a l'Energie Atomique, 1981, p. 244-247 Deutsche Forschungsgemeinschaft refs
(Contract DFG-SCHL-201/1)

A82-22557
MASS PER CHARGE RATIO IN HOT PLASMAS AND COSMIC RAY SOURCE COMPOSITION
C J CESARSKY, R ROTHENFLUG, and M CASSE (Commissariat a l'Energie Atomique, Centre d'Etudes Nucleaires de Saclay, Gif-sur-Yvette, Essonne, France) In: International Cosmic Ray Conference, 17th, Paris, France, July 13-25, 1981, Conference Papers Volume 2. Gif-sur-Yvette, Essonne, France, Commissariat a l'Energie Atomique, 1981, p. 269-272. refs

Some models of shock acceleration of cosmic rays assume that particles are injected out of the thermal plasma behind the shock and are selected according to their effective charge (Eichler, 1979; Ellison et al., 1981). The pattern of compositions that could emerge from such a selection starting from plasmas in ionization equilibrium at various temperatures greater than or equal to 100,000 K and containing no grains is considered. It is found that, in the case of steady state ionization equilibrium and of time-dependent cooling of a hot plasma, which are possible descriptions of the hot ISM and of the halo gas, it is not possible to reproduce the observed cosmic ray composition with this simple scheme
(Author)

A82-22559
PHYSICAL STATE OF THE BIRTH PLACE OF COSMIC RAYS AND ITS IMPLICATION TO THE ACCELERATION PROCESSES
K SAKURAI (Kanagawa University, Yokohama, Japan) In: International Cosmic Ray Conference, 17th, Paris, France, July 13-25, 1981, Conference Papers Volume 2. Gif-sur-Yvette, Essonne, France, Commissariat a l'Energie Atomique, 1981, p. 277-280 refs

To explain the observed chemical composition of galactic cosmic rays at their sources, it is suggested that this composition is the result of an acceleration mechanism, possibly related to the charge states of particles ambient in the source regions. Since it is likely that most of the particles are partially ionized in these regions, the ambient temperature there will be less than 100,000 K before the start of acceleration. C.R

A82-22560
ON VOLATILITY, FIRST IONIZATION POTENTIAL, AND S- AND R-PROCESSES
J. P MEYER (Commissariat a l'Energie Atomique, Centre d'Etudes Nucleaires de Saclay, Gif-sur-Yvette, Essonne, France) In International Cosmic Ray Conference, 17th, Paris, France, July 13-25, 1981, Conference Papers Volume 2 Gif-sur-Yvette, Essonne, France, Commissariat a l'Energie Atomique, 1981, p 281-284 refs

The possibility of a correlation between the first ionization potential and volatility (in that elements of low potential tend to be refractory and those of high potential volatile) is considered. It is noted that the apparent correlation between galactic cosmic ray source (GCRS) elemental abundances and the first ionization potential may in fact be based on volatility. Attention is given here to compositional clues which may determine whether volatility or the first ionization potential is the relevant parameter. The correlation between the first ionization potential and volatility is examined, and those elements which do not fit into the correlation are isolated Attention is also given to possible ambiguities in interpreting the charge spectrum beyond Ni that derive from coincidences between regions of change in the first ionization (and volatility) and the s- and r-process peaks. C.R.

A82-22561
INTERSTELLAR GRAINS AS SEEDS FOR GALACTIC COSMIC RAYS
J.-P. BIBRING (CNRS, Centre de Spectrometrie Nucleaire et de Spectrometrie de Masse, Orsay, Essonne, France) and C. J CESARSKY (Commissariat a l'Energie Atomique, Centre d'Etudes Nucleaires de Saclay, Gif-sur-Yvette, Essonne, France) In: International Cosmic Ray Conference, 17th, Paris, France, July 13-25, 1981, Conference Papers. Volume 2 Gif-sur-Yvette, Essonne, France, Commissariat a l'Energie Atomique, 1981, p. 289-291. refs

A82-22563
ORIGIN OF GALACTIC COSMIC RAYS FROM NE ISOTOPIC COMPOSITION
J. AUDOUZE (CNRS, Institut d'Astrophysique, Paris; CNRS, Centre de Spectrometrie Nucleaire et de Spectrometrie de Masse, Orsay, Essonne, France), M. CASSE, J. A PAUL (Commissariat a l'Energie Atomique, Centre d'Etudes Nucleaires de Saclay, Gif-sur-Yvette, Essonne, France), J P. CHIEZE (CNRS, Institut d'Astrophysique, Paris; Centre d'Etudes Nucleaires de Bruyere-le-Chatel, Montrouge, Hauts-de-Seine, France), and G MALINIE (CNRS, Institut d'Astrophysique, Paris, France) In: International Cosmic Ray Conference, 17th, Paris, France, July 13-25, 1981, Conference Papers Volume 2 Gif-sur-Yvette, Essonne, France, Commissariat a l'Energie Atomique, 1981, p. 296-298. refs

The possibility that a cosmic ray composition reflecting that of the interstellar medium may account for the observed enhancement of the cosmic ray Ne-22/Ne-20 abundance ratio with respect to the solar value is examined Processes leading to the observed solar system abundances of Ne-22 are discussed, and it is suggested that explosive hydrogen burning might be a significant source, since secondary production of this isotope as a by-product of the CNO cycle in intermediate and massive stars is incapable of accounting for the present abundance Calculations are presented which show that neither Ne-22 enrichment of the interstellar medium by low-mass stars after the birth of the sun nor a cosmic ray origin in the inner galaxy account for the observed cosmic ray enrichment. It is thus concluded that Ne-22 cannot have been significantly enriched in the interstellar medium during the last 4.6 billion years, and thus cosmic rays are accelerated in the vicinity of Ne-22 sources. A.L.W.

A82-22564
EVIDENCE FOR THE STOCHASTIC ACCELERATION OF COSMIC RAYS IN SUPERNOVA REMNANTS
T. W. HARQUIST (University College, London, England) and G. E. MORFILL (Max-Planck-Institut fuer Kernphysik, Heidelberg, West Germany) In: International Cosmic Ray Conference, 17th, Paris, France, July 13-25, 1981, Conference Papers. Volume 2. Gif-sur-Yvette, Essonne, France, Commissariat a l'Energie Atomique, 1981, p 300-302 refs

Ionization rates in several locations in an expanding shell, probably formed by the passage of a shock driven by the expansion of an old supernova remnant in the Per OB2 association, have been derived from molecular observations The production of 1-2 MeV cosmic rays by the second order Fermi mechanism in the ionized regions of the remnant would explain these and a number of other molecular observations (Author)

A82-22565
THE GALACTIC ORIGIN OF COSMIC RAYS. I
S. A. COLGATE (Los Alamos National Laboratory, Los Alamos, New Mexico Institute of Mining and Technology, Socorro, NM) In: International Cosmic Ray Conference, 17th, Paris, France, July 13-25, 1981, Conference Papers. Volume 2. Gif-sur-Yvette, Essonne, France, Commissariat a l'Energie Atomique, 1981, p. 303-306. refs
(CONF-810711-1; LA-UR-81-965)

The theoretical basis for the supernova envelope shock origin of cosmic rays is reviewed. The theoretical explanation of the SN Type I light curve requires the ejection of a relativistic mass fraction. The criterion of the adiabatic deceleration by Alfven wave trapping neither applies in theory, when beta is greater than 1, or practice, as in the Starfish high-altitude nuclear explosion experiment. Arguments of delayed acceleration due to K-capture are not applicable to SN ejecta because a period of prompt recombination exists before subsequent stripping in propagation. (Author)

A82-22571
ORIGIN OF COSMIC RAYS IN GALACTIC CENTRE SOURCES
S S. SAID, A W. WOLFENDALE (Durham, University, Durham, England), M GILER (Lodz, Uniwersytet, Lodz, Poland), and J. WDOWCZYK (Instytut Badan Jadrowych, Lodz, Poland) In: International Cosmic Ray Conference, 17th, Paris, France, July 13-25, 1981, Conference Papers Volume 2 Gif-sur-Yvette, Essonne, France, Commissariat a l'Energie Atomique, 1981, p 344-347. refs

A model is proposed which attributes the origin of cosmic rays to rare explosive events in galactic nuclei. In accordance with the model, the individual explosions are separated by times of the order of 100 million years, and the duration of each explosion is much shorter than the period of separation Particles produced with a power-law spectrum would propagate by diffusion throughout the Galaxy, and in its simplest form, there would be simple three-dimensional diffusion with a diffusion coefficient independent of position. The proposed model could provide an explanation for the very low electron-to-proton ratio (about 3 percent at 1 GeV) of cosmic radiation at the earth. V.L.

A82-22572
ACCELERATION PROCESSES NEAR MASSIVE BLACK HOLES
M KAFATOS (George Mason University, Fairfax, VA), R SILBERBERG, and M. M. SHAPIRO (U S. Navy, Naval Research Laboratory, Washington, DC) In International Cosmic Ray Conference, 17th, Paris, France, July 13-25, 1981, Conference Papers. Volume 2 Gif-sur-Yvette, Essonne, France, Commissariat a l'Energie Atomique, 1981, p. 348-351. refs

Ultra-massive accreting black holes in the nuclei of active galaxies have been proposed as the central sources of energy emission, especially of the nonthermal kind Accretion disks around massive black holes in the centers of active galactic nuclei are shown to be likely sites of particle acceleration Electrons can be accelerated to relativistic energies by electromagnetic processes as well as purely gravitational processes (e g., Penrose pair production). Protons are also accelerated to very high energies by processes such as (1) Fermi acceleration, (2) betatron acceleration, (3) shock wave acceleration, and (4) in beams via the electromagnetic dynamo process The stochastic Fermi process acting over a period of only about a day in the ergosphere suffices for efficient acceleration of protons, even to high energies.
(Author)

A82-22584* National Aeronautics and Space Administration. Goddard Space Flight Center, Greenbelt, Md.
INTERPLANETARY PARTICLE OBSERVATIONS ASSOCIATED WITH SOLAR FLARE GAMMA-RAY LINE EMISSION
T. T. VON ROSENVINGE, R. RAMATY, and V. REAMES (NASA, Goddard Space Flight Center, Laboratory for High Energy Astrophysics, Greenbelt, MD) In: International Cosmic Ray Conference, 17th, Paris, France, July 13-25, 1981, Conference Papers Volume 3. Gif-sur-Yvette, Essonne, France, Commissariat a l'Energie Atomique, 1981, p. 28-31 refs

Observations of particle emissions during three solar flares which were observed to emit 2.22 MeV gamma rays as recorded by the Solar Maximum Mission are discussed. The 2 22 MeV line is produced by neutron capture by hydrogen, and additional attention is given to a 4.4 MeV emission line of June 7, 1980, with estimates made of the particle density 1 AU from the sun assuming a good magnetic connection between the earth and the sun. The measurements were made from the ISEE-3 and HELIOS-1 spacecraft. The connectedness of the earth and the sun in a magnetic field leads to conclusions that few particles actually escaped into interplanetary space M.S.K.

A82-22587
COMPUTER SIMULATION OF THE TIME DEPENDENCE OF THE PHOTON ENERGY SPECTRA PRODUCED IN PROTON AND ELECTRON BREMSTRAHLUNG
S. R. KELNER, IU. D KOTOV, A. S ROSHAL, and V. N. RUSSKIKH (Moskovskii Inzherno-Fizicheskii Institut, Moscow, USSR) In: International Cosmic Ray Conference, 17th, Paris, France, July 13-25, 1981, Conference Papers. Volume 3. Gif-sur-Yvette, Essonne, France, Commissariat a l'Energie Atomique, 1981, p. 41-44 refs

An analytic model of the time dependence of the photon generation spectra resulting from proton and electron bremsstrahlung in matter is presented. The lifetimes of the protons and electrons with the same Lorentz factor are shown to differ by a factor of at least three, which implies that the time dependence of photon energy spectra resulting from pulse beam injection of accelerated particles into a generation region depends on the types of particles accelerated. Basic equations are formulated for the evolution of the proton distribution function in matter, with consideration given to path lengths which remain or pass from the matter The proton energy spectrum is then defined and the generation function for the production of gamma rays in a target block is derived, taking into account the density of the target Similar calculations for electrons showed that with time the energy spectra becames harder for electrons. M.S.K.

A82-22589
POSSIBLE EVIDENCE FOR ATTENUATION OF AN MHD SHOCK BY A MAGNETIC NEUTRAL SHEET IN THE SOLAR CORONA
D. J. MULLAN (Franklin Institute, Bartol Research Foundation, Newark, DE) In· International Cosmic Ray Conference, 17th, Paris, France, July 13-25, 1981, Conference Papers. Volume 3. Gif-sur-Yvette, Essonne, France, Commissariat a l'Energie Atomique, 1981, p. 51-54. refs
(Contract NSF ATM-78-20936-01)

The possibility that H-alpha filaments in the solar chromosphere are markers beneath regions where coronal shocks experience severe attenuation, and are thus the areas where particles can be ejected from the corona, is examined from data from flares of Aug 4, 1972 and Nov. 9, 1979 Both flares produced gamma rays with 2.2 MeV energy, and data exists for the energetic protons received at earth stations. The efficiency of transport was high for the August event and two magnitudes lower for the November event. H-alpha filtergrams of the two flares show that in the second flare the shock propagation crossed two or three filaments lying in its path. The low efficiency of particle transport is taken to indicate a degraded shock in the region above the filaments, indicating that the particles needed a different route to escape.
M.S K

A82-22591* Chicago Univ., Ill
THE RELATION OF TYPE II RADIO BURSTS TO SOLAR ENERGETIC PARTICLES OBSERVED AT EARTH
P EVENSON, P. MEYER (Chicago, University, Chicago, IL), and S. YANAGITA In: International Cosmic Ray Conference, 17th, Paris, France, July 13-25, 1981, Conference Papers Volume 3. Gif-sur-Yvette, Essonne, France, Commissariat a l'Energie Atomique, 1981, p. 59-62. refs
(Contract NAS5-20674)

Observations of particle events associated with type II radio bursts as recorded on the ISEE-3 spacecraft are reported. Data on burst events following flares of Sept 23,1978 and Aug. 18, 1979 yield time histories of the particle fluxes, which exceeded 25 MeV energy. The profiles of the Category-1 type II bursts display a continuous release of particles, which was concluded by no decrease in the fluxes until after the passage of the shock. The continuous nature of the recorded events suggests that the secondary acceleration process associated with the type II bursts is maintained as the flare shock propagates through interplanetary space, and may be the source of the energetic particles which propagate with the shock M.S.K.

A82-22592* National Aeronautics and Space Administration. Goddard Space Flight Center, Greenbelt, Md.
A SURVEY OF SOLAR PROTONS AND ALPHA DIFFERENTIAL SPECTRA BETWEEN 1 AND GREATER THAN 400 MEV/NUCLEON
R E. MCGUIRE, T. T VON ROSENVINGE, and F. B MACDONALD (NASA, Goddard Space Flight Center, Greenbelt; Maryland, University, College Park, MD) In: International Cosmic Ray Conference, 17th, Paris, France, July 13-25, 1981, Conference Papers. Volume 3 Gif-sur-Yvette, Essonne, France, Commissariat a l'Energie Atomique, 1981, p 65-68 refs

Attempts to systematically measure and fit a large sample of flare spectra from IMP 7 and 8 satellite data to determine the spectral forms that characterize the data and the range of spectral slopes are reported Proton spectra are constructed covering the range 0 9 to over 400 MeV, and alpha fluxes from 1 4-80 MeV/nucleon The event spectra are composed of fluxes measured at different times at each energy, and fitting procedures were employed such as a power law in kinetic energy, an exponential in rigidity, an exponential in energy, and a Bessel function of momentum/nucleon. Best fits were obtained with the exponential in rigidity and the Bessel function, with the Bessel function having a better numerical accuracy for all 21 proton spectra considered M.S.K

A82-22593
ENERGETIC SOLAR PARTICLE SPECTRA ACCORDING TO VENERA-11, 12 AND PROGNOZ-5, 6
V G KURT, IU I. LOGACHEV, V. G STOLPOVSKII, and E. I. DAIBOG (Moskovskii Gosudarstvennyi Universitet, Moscow, USSR) In: International Cosmic Ray Conference, 17th, Paris, France, July 13-25, 1981, Conference Papers. Volume 3. Gif-sur-Yvette, Essonne, France, Commissariat a l'Energie Atomique, 1981, p 69-72. refs

Proton and electron spectra of solar flares measured from 0.1-500 MeV and 0.03-3.0 MeV, respectively, on board the Venera 11, 12, and the Prognoz 5, 6, satellites are reported, along with analyses of the integral peak flux and density dependence in relation to the kinetic energy. All the spectra were fitted by either one or a set of two power functions, with the proton spectra having more complicated characteristics than the electron spectra. The number of high energy protons undergoing stochastic particle propagation was found to depend on the shock wave speed. Energy losses were calculated on the basis of deviation from a power law, of a deceleration down to the observation point, and from a numerical estimate of the rate of proton energy change in the adiabatic solar wind expansion An event of Nov 22, 1977 is notable for the absence of protons with energy less than 1 MeV. M.S.K.

A82-22594
EVOLUTION OF THE SOLAR PROTON SPECTRUM IN INTERPLANETARY SPACE
N. N. KONTOR (Moskovskii Gosudarstvennyi Universitet, Moscow, USSR) In: International Cosmic Ray Conference, 17th, Paris, France, July 13-25, 1981, Conference Papers. Volume 3. Gif-sur-Yvette, Essonne, France, Commissariat a l'Energie Atomique, 1981, p. 73-76. refs

Exponential forms suitable for describing two-three orders wide energy ranges of proton spectra emitted during solar flares are examined. The rigidity exponent form shows a good fit over a broad range except during the onset of a proton shower. A parabolic spectral shape is presented which becomes a power law at narrower energy ranges. Application of the parabolic formula to available flare data reveals that energetic protons arrive first at the detectors, followed by lower energy particles. M S.K.

A82-22600
A DESCRIPTION OF RELATIVISTIC SOLAR PARTICLE PROPAGATION
H DEBRUNNER, H. NEUENSCHWANDER, A. F WAGNER (Bern, Universitaet, Berne, Switzerland), and J A. LOCKWOOD (New Hampshire, University, Durham, NH) In International Cosmic Ray Conference, 17th, Paris, France, July 13-25, 1981, Conference Papers Volume 3. Gif-sur-Yvette, Essonne, France, Commissariat a l'Energie Atomique, 1981, p. 102-105. Research supported by the Swiss National Science Foundation and NSF.

The intensity-time profiles and anisotropies of the solar cosmic-ray ground level events (GLEs) on November 22, 1977 and May 7, 1978 were addressed by means of a Monte Carlo simulation of relativistic solar flare protons propagation in the interplanetary magnetic field. Pitch angle scattering mean free paths of 0.5 AU and more than 3 AU are deduced. The injection of the solar flare protons has an extended time structure, correlated with the X-ray burst profiles in the 1-8 A and 0.5-4.0 A bands, respectively, for the November 1977 and May 1978 GLEs. O.C.

A82-22601
NON-FLARE INJECTION OF PROTONS INTO INTERPLANETARY SPACE
V. DOMINGO, B. SANAHUJA, and K.-P. WENZEL (ESA, Space Science Dept , Noordwijk, Netherlands) In International Cosmic Ray Conference, 17th, Paris, France, July 13-25, 1981, Conference Papers. Volume 3. Gif-sur-Yvette, Essonne, France, Commissariat a l'Energie Atomique, 1981, p. 109-112. refs

The superimposition of a second proton population associated with a solar wind regime, and bounded by a pair of shocks, is found to be superimposed upon the first in an investigation of 35-1600 KeV solar protons observed during an April, 1979 nonflare event by ISEE-3 The source of the particles and the solar wind regime appear to be closely associated with intense solar filament activity near the central meridian The temporal evolution of velocity spectra and anisotropy distributions during this period are discussed O.C.

A82-22602
LOW-ENERGY PARTICLES IN INTERPLANETARY MAGNETIC FIELD NEAR THE SECTORIAL BOUNDARY ON SEPTEMBER 26, 1977
M. A ZELDOVICH and B. M KUZHEVSKII (Moskovskii Gosudarstvennyi Universitet, Moscow, USSR) In. International Cosmic Ray Conference, 17th, Paris, France, July 13-25, 1981, Conference Papers Volume 3. Gif-sur-Yvette, Essonne, France, Commissariat a l'Energie Atomique, 1981, p. 113-116 refs

Prognoz-6 data are used to examine effects of the sign reversal in the interplanetary magnetic field of September 26, 1977 on the 70-keV to 40 MeV proton fluxes, and the 10-30 keV and 40-500 keV electron fluxes. The sectorial boundary of interplanetary magnetic field traversed the earth at 2300 UT, and in that period the interplanetary space was filled with the solar cosmic ray particles generated in the flare of September 24, 1977, whose intensity decreased in time. Results indicate that the event of September 26, 1977 was the first observation where effects of the sectorial boundary were traced up to proton energies of 40-50 MeV. D.L G

A82-22610
COULOMBIAN ENERGY LOSSES AND THE NUCLEAR COMPOSITION OF THE SOLAR COSMIC RAYS
S. S TRIVEDI and S. BISWAS (Tata Institute of Fundamental Research, Bombay, India) In: International Cosmic Ray Conference, 17th, Paris, France, July 13-25, 1981, Conference Papers. Volume 3. Gif-sur-Yvette, Essonne, France, Commissariat a l'Energie Atomique, 1981, p. 157-160. refs

Coulombian energy losses suffered by fast ions in a two component plasma are discussed quantitatively Their dependence on the temperature and density of the ambient plasma is also investigated. It is shown that these losses coupled with the transient nature of the flare can give rise to selectivity effects. The ionic charge states are also discussed. (Author)

A82-22611* National Aeronautics and Space Administration. Goddard Space Flight Center, Greenbelt, Md
HEAVY-ELEMENT ABUNDANCES IN HE/3/-RICH EVENTS
D. V. REAMES and T. T. VON ROSENVINGE (NASA, Goddard Space Flight Center, Laboratory for High Energy Astrophysics, Greenbelt, MD) In International Cosmic Ray Conference, 17th, Paris, France, July 13-25, 1981, Conference Papers. Volume 3. Gif-sur-Yvette, Essonne, France, Commissariat a l'Energie Atomique, 1981, p. 162-165. refs

Abundances of the elements He through Fe observed on the ISEE-3 during He(3) rich events are reported. Ratios of He(3)-He(4) of not less than about 1, and Fe/O of greater than 1 are found, and rather large event-to-event variations in C, O, Ne, Mg, Si, and S are seen superposed upon the general trend of heavy element enhancement It is concluded that the discontinuous variation of the neighboring elements in the He(3) rich events could result from differences in the electron temperature of the material prior to injection that give rise to differences in the dominant charge states and cyclotron frequencies of different elements. D.L.G.

A82-22612* Max-Planck-Institut fuer Physik und Astrophysik, Garching (West Germany)
A COMPARISON OF HELIUM AND HEAVY ION SPECTRA IN HE/3/ RICH SOLAR FLARES WITH A MODEL CALCULATION
E MOBIUS, D HOVESTADT, B. KLECKER, M SCHOLER (Max-Planck-Institut fur Physik und Astrophysik, Garching, West Germany), and G GLOECKLER (Maryland, University, College Park, MD) In: International Cosmic Ray Conference, 17th, Paris, France, July 13-25, 1981, Conference Papers. Volume 3. Gif-sur-Yvette, Essonne, France, Commissariat a l'Energie Atomique, 1981, p 166-169. Bundesministerium fur Forschung und Technologie refs
(Contract BMFT-RV14-B8/74; NAS5-20062)

He isotopes, O and Fe in He(3) rich solar flares are studied during the 1977 to 1979 period with the MPI/UoMd particle experiment on ISEE-1 and ISEE-3. The study revealed that the He(3) spectrum is generally harder than that of He(4), and the O spectrum is harder than that of Fe The spectra are compared with a stationary model based on stochastic Fermi acceleration in Alfven turbulence including a rigidity dependent particle loss. Model calculations fit the He(3) and He(4) spectra between 0.4 and 4.0 MeV/nucleon, with discrepancies at lower and higher energies, and the O and Fe spectra cannot be fitted simultaneously.
D L G.

A82-22617
THE ENERGY SPECTRA OF COSMIC RAY VARIATIONS INFERRED FROM THE STRATOSPHERIC MEASUREMENTS IN 1972-1979
A K. SVIRZHEVSKAIA, IU. I. STOZHKOV (Akademiia Nauk SSSR, Fizicheskii Institut, Moscow, USSR), and T. N. CHARAKHCHIAN (Moskovskii Gosudarstvennyi Universitet, Moscow, USSR) In International Cosmic Ray Conference, 17th, Paris, France, July 13-25, 1981, Conference Papers. Volume 3. Gif-sur-Yvette, Essonne, France, Commissariat a l'Energie Atomique, 1981, p. 187-190.

A82-22618
PRIMARY SPECTRAL VARIATIONS OF COSMIC RAYS ABOVE 1 GV
P. H. STOKER (Potchefstroom University for Christian Higher Education, Potchefstroom, Republic of South Africa) In: International Cosmic Ray Conference, 17th, Paris, France, July 13-25, 1981, Conference Papers. Volume 3. Gif-sur-Yvette, Essonne, France, Commissariat a l'Energie Atomique, 1981, p 193-196. refs

Observations on proton spectra of solar flare GLEs and data from a latitude survey are used to determine specific yield functions for the neutron moderated detector (4NMD) and the 3NM64 neutron monitor at Sanae, Antarctica. Monthly average count rates of the 4NMD and 3NM64 do not follow each other better than 1 percent on long term modulation. No definite physical explanation is singled out to account for the observed excessive variability, which is presumably related to a phase lag effect or hysteresis effect between changes in intensities of particles of different rigidities and the level of solar modulation. D.L G

A82-29435
REMOTE SENSING OF THE WEEDINESS OF CROP FIELDS [DISTANTSIONNOE OPREDELENIE ZASORENNOSTI SEL'SKOKHOZIAISTVENNYKH POLEI]
K. IA KONDRATEV, A. I. BELIAVSKII, O M. POKROVSKII, and P. P FEDCHENKO (Glavnaia Geofizicheskaia Observatoriia, Leningrad, USSR) Akademiia Nauk SSSR, Doklady, vol. 263, Mar.-Apr 1982, p 251-253 In Russian.

A82-29526
COLOR AERIAL PHOTOGRAPHY IN THE PLANT SCIENCES AND RELATED FIELDS; PROCEEDINGS OF THE EIGHTH BIENNIAL WORKSHOP, LURAY, VA, APRIL 21-23, 1981
Workshop sponsored by the Society of American Foresters, American Society of Photogrammetry, U S Geological Survey, et al. Falls Church, VA, American Society of Photogrammetry, 1981. 174 p $20

Aerial photography methods, equipment, targets, and the effectiveness of remote sensing of vegetation are discussed Analysis with color or IR equipment is examined, and color aerial photography of riparian vegetation in northeastern California, wildlife on an island, and the use of color IR photography for vegetative monitoring are described. Specific photography of loblolly pine plantations, Alaskan resources, forest land changes, rangeland cover proportions, Oregon vegetation, and fir trees infested by beetles are considered. Spectral scanning of SO2-affected winter wheat and soybeans is presented, along with IR color photography of damaged citrus crops, the application of a scanning microdensitometer in plant science studies, and the development of an IR exposure meter M.S.K.

A82-29527
DEVELOPMENT AND APPLICATION OF PANORAMIC AERIAL PHOTOGRAPHY IN FOREST PEST MANAGEMENT
W. M. CIESLA (U.S. Forest Service, Davis, CA) In: Color aerial photography in the plant sciences and related fields, Proceedings of the Eighth Biennial Workshop, Luray, VA, April 21-23, 1981 Falls Church, VA, American Society of Photogrammetry, 1981, p 19-28. refs

Characteristics of panoramic aerial photography and its use in forest pest management are reviewed Applications to date include estimating losses caused by the mountain pine beetle and planning salvage operations of insect killed timber in California. Advantages of the optical bar panoramic aerial camera system include the ability to acquire high-resolution photography over large areas of land rapidly. Disadvantages include a relatively high acquisition cost, a limited acquisition capability, unconventional film size, and a changing photo scale. (Author)

A82-29528
RIPARIAN VEGETATION MAPPING IN NORTHEASTERN CALIFORNIA USING HIGH ALTITUDE COLOR INFRARED AERIAL PHOTOGRAPHY
K G. BONNER (U.S. Forest Service, San Francisco, CA) In: Color aerial photography in the plant sciences and related fields; Proceedings of the Eighth Biennial Workshop, Luray, VA, April 21-23, 1981 Falls Church, VA, American Society of Photogrammetry, 1981, p 29-37 Research supported by the California State Resources Agency. refs

A82-29529
INVENTORY OF WILDLIFE HABITAT FROM COLOR INFRARED AERIAL PHOTOGRAPHY FOR COBB ISLAND, VIRGINIA
J. T. HEINEN and R. A. MEAD (Virginia Polytechnic Institute and State University, Blacksburg, VA) In: Color aerial photography in the plant sciences and related fields; Proceedings of the Eighth Biennial Workshop, Luray, VA, April 21-23, 1981. Falls Church, VA, American Society of Photogrammetry, 1981, p. 39-44, 160. refs

A82-29530
CONSIDERATIONS IN USING COLOR INFRARED PHOTOGRAPHS FOR VEGETATIVE INTERPRETATION
P M SEEVERS (U S. Geological Survey, EROS Data Center, Sioux Falls, SD) In: Color aerial photography in the plant sciences and related fields; Proceedings of the Eighth Biennial Workshop, Luray, VA, April 21-23, 1981 Falls Church, VA, American Society of Photogrammetry, 1981, p. 45-49. refs

The literature suggests that the infrared wavelengths are the most significant when color infrared film records the reflectance of vegetation. Some evidence, however, suggests that the relative sensitivity of the infrared sensitive emulsion layer of the film and the apparent intensity of near infrared reflectance from plants combine to saturate that layer when the film is used to photograph agricultural crops at low altitude. In addition, some physiological considerations of plant characteristics also suggest that the red- and green-sensitive emulsion layers would be affected before the infrared-sensitive layer. Observations indicate that tissue damage in most crops is relatively severe before it becomes detectable on color infrared film. It is also then visible to the human eye. This effect suggests that previsual detection of crop damage is not likely on color infrared film. Furthermore, the perceptability of color contrasts by the human eye tends to be a deterrent to visual detection of plant symptoms, both in the field and in the interpretations of color-infrared photographs. (Author)

A82-29531
COLOR AERIAL PHOTOGRAPHY DETECTS NUTRIENT STATUS OF LOBLOLLY PINE PLANTATIONS
A. LYONS and E. BUCKNER (Tennessee, University, Knoxville, TN) In: Color aerial photography in the plant sciences and related fields; Proceedings of the Eighth Biennial Workshop, Luray, VA, April 21-23, 1981. Falls Church, VA, American Society of Photogrammetry, 1981, p. 53-58. Research supported by the Champion International Corp. refs

A82-29532
MULTI-RESOURCE INVENTORY IN INTERIOR ALASKA
K. M. HEGG (U.S. Forest Service, Washington, DC), F. R LARSON, D. R. MEAD, and K. C WINTERBERGER (Pacific Northwest Forest and Range Experiment Station, Anchorage, AK) In: Color aerial photography in the plant sciences and related fields; Proceedings of the Eighth Biennial Workshop, Luray, VA, April 21-23, 1981. Falls Church, VA, American Society of Photogrammetry, 1981, p. 59-65. refs

Data reduction, conversion, and application of NASA small scale color IR photography for Alaskan renewable resource evaluation are described. The photographs are taken at a 1:120,000 scale, and special overlay ink and film allow suitable definitions of forest and woodland, although brush heights and tundra are undiscernable The study is concentrated along the Susitna River basin, where rapid development is occurring along the road between Anchorage and Fairbanks. Interpretation involves classification of forest, woodland, nonforest, and nonvegetated groups, with forest and woodland further defined into closed or open crown areas, depending on exceeding 50% cover It is recommended that relating ground sample selection based on photopoint interpretation to a digitized map be accomplished by completing the map digitization prior to field plot selection, and statistically tieing photointerpretation sampling schemes to detailed inplace digitized map sampling schemes M.S.K.

A82-29533
APPLICATION OF 35MM COLOR AERIAL PHOTOGRAPHY TO FOREST LAND CHANGE DETECTION
N. L. MILLER and M. P. MEYER (Minnesota, University, St. Paul, MN) In Color aerial photography in the plant sciences and related fields; Proceedings of the Eighth Biennial Workshop, Luray, VA, April 21-23, 1981 Falls Church. VA, American Society of Photogrammetry, 1981, p. 67-72. Research sponsored by the U.S. Forest Service.

Attention is called to the high cost ($280 per plot) of examining the sample plots that form the data base in forestry surveys. The use of 35-mm color aerial photography for detecting change in these plots is investigated With the method envisaged here, only those sample plots found to be significantly changed (logging, fire, blowdown, insect damage, disease) would be examined, the rest would be updated by computer growth projection models. Trial runs with 35-mm color aerial photography in Minnesota and Michigan yielded good results at a cost estimated at $20 per plot. C.R.

A82-29534
ESTIMATING RANGELAND COVER PROPORTIONS WITH LARGE-SCALE COLOR-INFRARED AERIAL PHOTOGRAPHS
C. J VAN ZEE (U.S. Geological Survey, EROS Data Center, Sioux Falls, SD) and K. G. BONNER (U S. Forest Service, San Francisco, CA) In: Color aerial photography in the plant sciences and related fields; Proceedings of the Eighth Biennial Workshop, Luray, VA, April 21-23, 1981. Falls Church, VA, American Society of Photogrammetry, 1981, p 73-82. refs

A82-29535
MAPPING RIPARIAN VEGETATION IN SOUTHEASTERN OREGON USING DIGITIZED LARGE SCALE COLOR INFRA-RED AERIAL PHOTOGRAPHY
D. S LINDEN (Technicolor Graphic Services, Denver, CO) and D. M. CONCANNON (U.S. Bureau of Land Management, Denver, CO) In: Color aerial photography in the plant sciences and related fields; Proceedings of the Eighth Biennial Workshop, Luray, VA, April 21-23, 1981. Falls Church, VA, American Society of Photogrammetry, 1981, p. 83-89. refs

A82-29536
REMOTE SENSING OF DOUGLAS-FIR TREES NEWLY INFESTED BY BARK BEETLES
P. M. HALL, P A. MURTHA, and J. A. MCLEAN (British Columbia, University, Vancouver, Canada) In: Color aerial photography in the plant sciences and related fields; Proceedings of the Eighth Biennial Workshop, Luray, VA, April 21-23, 1981. Falls Church, VA, American Society of Photogrammetry, 1981, p. 91-98, 157 refs

Two study plots containing Douglas-fir (Pseudotsuga menziesii /Mirb/ Franco) newly infested by Douglas-fir beetle (Dendroctonus pseudotsugae Hopk) were photographed with large-scale (1:1000), color infrared film on July 29, 1979 - approximately three months after possible insect attack. Significant differences were found between the ratios of the optical density values of the images of healthy and attacked trees It is concluded that trees which have been successfully attacked by beetles can be detected on color infrared air photos approximately three months after initial attack when the trees still support visually green, healthy-appearing foliage. (Author)

A82-29537#
SPECTRAL SCANNING OF EXPERIMENTAL PLOTS OF SO2-AFFECTED WINTER WHEAT AND SOYBEANS FOR MISSION PLANNING
C D. SAPP (Tennessee Valley Authority, Chattanooga, TN) In: Color aerial photography in the plant sciences and related fields, Proceedings of the Eighth Biennial Workshop, Luray, VA, April 21-23, 1981. Falls Church, VA, American Society of Photogrammetry, 1981, p 101-114. refs

A series of TVA experiments is described wherein plots of soybeans and winter wheat plants were grown to the critical

seed-filling stage of development, exposed to controlled doses of SO2, observed systematically for foliar effects, then scanned row by row with a spectroradiometer The spectral curves were statistically analyzed to determine the changes in spectral reflectance that occur after plants are stressed by SO2 emissions. For soybeans, the affected subplots had higher visible reflectance, lower IR reflectance, and a lower IR/red ratio. Variance analysis showed significant differences in IR and IR/red reflectance between chlorotic soybeans and unaffected ones, and in red reflectance, IR reflectance and IR/red ratio between necrotic and unaffected ones. Since the wheat subplots showed no chlorosis, analysis of reflectance data concentrates on necrosis, which showed a significant difference in red, IR, and IR/red reflectance between classes of differentially injured wheat. C D

A82-29538* National Aeronautics and Space Administration John F. Kennedy Space Center, Cocoa Beach, Fla.
DETECTION AND DAMAGE ASSESSMENT OF CITRUS TREE LOSSES WITH AERIAL COLOR INFRARED PHOTOGRAPHY /ACIR/
C H. BLAZQUEZ, F. W. HORN, JR (NASA, Kennedy Space Center, Applications Projects Branch, Cocoa Beach, FL), and G. J. EDWARDS (Florida, University, Lake Alfred, FL) In: Color aerial photography in the plant sciences and related fields, Proceedings of the Eighth Biennial Workshop, Luray, VA, April 21-23, 1981. Falls Church, VA, American Society of Photogrammetry, 1981, p. 115-126. refs

Detection and disease damage assessment of citrus tree losses in a Florida citrus grove were made by establishing a registration (grove site location) coordinate system, developing a damage assessment system, and testing sequential aerial color infrared (ACIR) photography at the scale of 1 in. = 333 ft (2 5 cm = 100 m) during the winter, spring, and summer seasons of 1978 and spring of 1979. Spring photography was the easiest to photo interpret, showed the greatest differences between healthy and diseased trees, and had the least shadow and background interference for photo interpretation. Trees showing slight disease damage were detected in ACIR before they were found in ground surveys. (Author)

A82-29539* Minnesota Univ , St. Paul
APPLICATION OF SCANNING MICRODENSITOMETER DATA IN SELECTED PLANT SCIENCE CASE STUDIES
T. M. LILLESAND and D E. MEISNER (Minnesota, University, St. Paul, MN) In· Color aerial photography in the plant sciences and related fields; Proceedings of the Eighth Biennial Workshop, Luray, VA, April 21-23, 1981 Falls Church, VA, American Society of Photogrammetry, 1981, p. 127-136, 164, 165. Research supported by the Minnesota State Department of Agriculture and University of Minnesota refs
(Contract NGL-24-005-263)

This paper treats a representative sample of projects aimed at vegetation mapping and assessment via analysis of both digital photographic and Landsat data projects and illustrates the potential for using scanning microdensitometric data extracted from color infrared photographs in the following applications: freshwater wetlands mapping, tree type mapping, and yield vs reflectance modeling in corn fertilization experiments. These case studies are presented to illustrate the general applicability of scanning microdensitometer data in the contexts of image classification and enhancement as well as quantitative modeling of ground parameters. (Author)

A82-29747
DESERT LOCUST HABITAT MONITORING WITH SATELLITE REMOTE SENSING A NEW TECHNOLOGY FOR AN OLD PROBLEM
J. U. HIELKEMA (United Nations, Food and Agriculture Organization, Rome, Italy) ITC Journal, no 4, 1981, p. 387-417 refs

Precipitation and vegetation remote sensing techniques developed during Phase I of the UN Food and Agricultural Organization program to monitor rainfall and vegetation conditions known to presage desert locust plagues are described. Landsats 2 and 3 multispectral scanners were used, along with Tiros-N and Meteosat and Goes satellite data, to quantify the location, extent, duration, and intensity of rainfall events in the recession area, that region where locusts live as ordinary grasshoppers until conditions which lead to population explosions and subsequent swarming are present. Outbreak areas were sought, along with ecological conditions which induced the outbreaks Landsat data handling procedures are reviewed, and it is noted that mosaic image construction has resulted in the construction of 10 maps for the north Africa locust recession area of Morocco, Algeria, Tunisia, and Libya. M.S K.

A82-32701#
PANORAMIC AERIAL PHOTOGRAPHY IN FOREST PEST MANAGEMENT
W. M. CIESLA (U.S Forest Service, Fort Collins, CO), R A ALLISON (U.S. Forest Service, Washington, DC), and F. P WEBER (U.S Forest Service, Houston, TX) Photogrammetric Engineering and Remote Sensing, vol 48, May 1982, p. 719-723 refs

The combination of high image resolution and large-area coverage inherent in panoramic photography is shown to make possible 100% coverage of forest pest outbreak areas, as well as the extraction of both stratification and detailed crown counts from a single set of photos. Attention is given to the deployment of the KA-80A optical bar panoramic camera aboard the U-2 high-speed, high-altitude aircraft operated by NASA. Continuous coverage of forested areas allows photos acquired for vegetation damage assessment to be used by such other disciplines as land-use planning, watershed evaluation, road location, or timber-sale planning, suggesting the sharing of photo-acquisition costs. Unfortunately, no aircraft other than the U-2, with its 65,000-foot cruise altitude, is able to use this camera system efficiently. O.C.

A82-32703#
ESTIMATING BARK BEETLE-KILLED LODGEPOLE PINE WITH HIGH ALTITUDE PANORAMIC PHOTOGRAPHY
W. H KLEIN (U S. Forest Service, Davis, CA) Photogrammetric Engineering and Remote Sensing, vol. 48, May 1982, p. 733-737. refs

A82-32704#
ESTIMATING MOUNTAIN PINE BEETLE-KILLED PONDEROSA PINE OVER THE FRONT RANGE OF COLORADO WITH HIGH ALTITUDE PANORAMIC PHOTOGRAPHY
R. D. DILLMAN (Lockheed Engineering and Management Services Co., Inc., Houston, TX) and W. B. WHITE (U.S Forest Service, Fort Collins, CO) Photogrammetric Engineering and Remote Sensing, vol. 48, May 1982, p. 741-747. U S. Department of Agriculture refs
(Contract USDA-53-3187-8-25)

A82-32705#
OPTICAL BAR PANORAMIC PHOTOGRAPHY FOR PLANNING TIMBER SALVAGE IN DROUGHT-STRESSED FORESTS
J. CAYLOR, J PIERCE, and W. SALAZAR (U.S. Forest Service, San Francisco, CA) Photogrammetric Engineering and Remote Sensing, vol. 48, May 1982, p 749-753. refs

Panoramic aerial photographs were obtained over 40 million acres of forest land in northern California during the period July, 1978, through September, 1979 These were used as an aid in planning timber salvage sales to locate concentrations of bark beetle-caused tree mortality following a severe drought. Several innovative procedures devised to effectively use these unconventional format photographs under field conditions are described. The photos were used in 223 salvage sales, resulting in a harvest of 532.2 million board feet of bark beetle killed timber during the period July, 1978, through May 1979. (Author)

A82-32707
EVALUATION OF SPRUCE-FIR FORESTS USING SMALL-FORMAT PHOTOGRAPHS
J. MCCARTHY (Vermont, University, Burlington, VT), C. E OLSON, JR , and J. A WITTER (Michigan, University, Ann Arbor, MI) Photogrammetric Engineering and Remote Sensing, vol. 48, May 1982, p. 771-778 Research supported by the McIntire-Stennis Funds and University of Michigan, U.S. Department of Agriculture refs
(Contract USDA-23-178)

The effectiveness of large-scale, 1 4800 small-format color aerial photographs in the evaluation of tree conditions and identification of the balsam fir and white spruce hosts of the spruce budworm is assessed. Contingency tables allowed comparisons of tree condition and species identification from aerial and ground data It is shown that photointerpretation of small-format photographs provided mean aerial estimates of tree conditions within one-half of a ranking class of the mean from ground truth data, with balsam fir and white spruce separable at a frequency of 80% and host specie mortality aerial estimates within 10% of the ground test data. O.C.

A82-32708* Cornell Univ., Ithaca, N. Y.
LANDSAT DETECTION OF HARDWOOD FOREST CLEARCUTS
W R. HAFKER and W. R. PHILIPSON (Cornell University, Ithaca, NY) Photogrammetric Engineering and Remote Sensing, vol. 48, May 1982, p. 779, 780. refs
(Contract NGL-33-010-171)

In a study of hardwood forests in Pennsylvania, the detection of clearcuts by means of visual analysis of Landsat summer imagery was accomplished best using band 5 images; however, a higher percentage of clearcuts could be detected using bands 5 or 7 winter images acquired during periods of snow cover. (Author)

A82-32897* National Aeronautics and Space Administration. Goddard Space Flight Center, Greenbelt, Md.
REMOTE SENSING OF LEAF WATER CONTENT IN THE NEAR INFRARED
C. J. TUCKER (NASA, Goddard Space Flight Center, Earth Resources Branch, Greenbelt, MD) Remote Sensing of Environment, vol. 10, Aug. 1980, p. 23-32. refs
(Previously announced in STAR as N80-20768)

A82-32905* National Aeronautics and Space Administration. Goddard Space Flight Center, Greenbelt, Md.
EFFECTS OF VEGETATION CANOPY STRUCTURE ON REMOTELY SENSED CANOPY TEMPERATURES
D. S. KIMES (NASA, Goddard Space Flight Center, Earth Resources Branch, Greenbelt, MD) Remote Sensing of Environment, vol. 10, Nov. 1980, p. 165-174 refs
(Previously announced in STAR as N79-33530)

A82-32907
THE RESPONSE CHARACTERISTICS OF VEGETATION IN LANDSAT MSS DIGITAL DATA
K. R. MCCLOY (South Australian Institute of Technology, Ingle Farm, Australia) Remote Sensing of Environment, vol. 10, Nov. 1980, p. 185-190. refs

Empirical evidence is used to propose a model of the response due to a vegetative canopy. The model is a simplification, and hence approximation, of the complex relationship between physical conditions in the canopy and the resultant spectral reflectance However, the model can be quantified to yield at least two, and possibly more, independent response parameters from the Landsat response data. These independent response parameters can be used to derive estimates of more than one independent physical characteristic of the canopy. Further, the model specifies its limitations, for a given data input, and indicates how further auxiliary data may be used to extract more information from the model. (Author)

A82-32909* National Aeronautics and Space Administration. Lyndon B. Johnson Space Center, Houston, Tex.
FIELD SIZE, LENGTH, AND WIDTH DISTRIBUTIONS BASED ON LACIE GROUND TRUTH DATA
D. E. PITTS and G. BADHWAR (NASA, Johnson Space Center, Houston, TX) Remote Sensing of Environment, vol. 10, Nov. 1980, p. 201-213 refs

The development of agricultural remote sensing systems requires knowledge of agricultural field size distributions so that the sensors, sampling frames, image interpretation schemes, registration systems, and classification systems can be properly designed. Malila et al. (1976) studied the field size distribution for wheat and all other crops in two Kansas LACIE (Large Area Crop Inventory Experiment) intensive test sites using ground observations of the crops and measurements of their field areas based on current year rectified aerial photomaps. The field area and size distributions reported in the present investigation are derived from a representative subset of a stratified random sample of LACIE sample segments In contrast to previous work, the obtained results indicate that most field-size distributions are not log-normally distributed. The most common field size observed in this study was 10 acres for most crops studied. G.R

A82-32913* National Aeronautics and Space Administration. Goddard Space Flight Center, Greenbelt, Md.
LANDSAT DIGITAL ANALYSIS OF THE INITIAL RECOVERY OF BURNED TUNDRA AT KOKOLIK RIVER, ALASKA
D. K. HALL, J. P. ORMSBY (NASA, Goddard Space Flight Center, Hydrological Sciences Branch, Greenbelt, MD), L JOHNSON (U.S Army, Cold Regions Research and Engineering Laboratory, Fairbanks, AK), and J BROWN (U S. Army, Cold Regions Research and Engineering Laboratory, Hanover, NH) Remote Sensing of Environment, vol. 10, Dec. 1980, p 263-272 Research supported by the U.S. Geological Survey refs
(Previously announced in STAR as N80-19588)

A82-32914* National Aeronautics and Space Administration. Goddard Space Flight Center, Greenbelt, Md.
VIEW ANGLE EFFECTS IN THE RADIOMETRIC MEASUREMENT OF PLANT CANOPY TEMPERATURES
D S. KIMES (NASA, Goddard Space Flight Center, Earth Resources Branch, Greenbelt, MD), S B. IDSO, P. J. PINTER, JR , R. J REGINATO, and R. D. JACKSON (U.S Water Conservation Laboratory, Phoenix, AZ) Remote Sensing of Environment, vol. 10, Dec 1980, p 273-284. refs

The thermal infrared sensor response from a wheat canopy was extremely non-Lambertian because of spatial variations in energy flow processes; the effective radiant temperature of the sensor varied as much as 13 C with changing view angle. This variation of sensor response was accurately quantified (root-mean-square of deviations between theoretical and measured responses reduced to 1.1 C) as a function of vegetation canopy geometry, vertical temperature distribution of canopy components, and sensor view angle The results have important implications for optimizing sensor view angles for remote sensing missions. (Author)

A82-34179* New York State Univ., Syracuse.
EVALUATION OF NOAA-AVHRR DATA FOR CROP ASSESSMENT
M. J. DUGGIN, D. PIWINSKI (New York, State University, Syracuse, NY), V. WHITEHEAD, and G. RYLAND (Lockheed Engineering and Management Services Co., Inc., Houston, TX) Applied Optics, vol. 21, June 1, 1982, p. 1873-1875. refs
(Contract NAS9-16514)

A study has been carried out in order to determine the angular limits which should be imposed upon NOAA06 and -7 satellite advanced very high-resolution radiometer (AVHRR) data used in vegetation assessment. The study involved simulations of anticipated sensor output over a wheat crop and empirical investigation of sensor data over vegetated areas. The conclusion drawn from both approaches is that less than 10% variation in

the simulated vegetative index may be anticipated across the swath of imagery used if only the central 512 pixels are utilized. V.L.

A82-34706
INTERPRETATION OF VEGETATIVE COVER IN WETLANDS USING FOUR-CHANNEL SAR IMAGERY
E WEDLER (Ontario Centre for Remote Sensing, Toronto, Canada) and R. KESSLER (Freiburg, Universitaet, Freiburg im Breisgau, West Germany) In. American Society of Photogrammetry, Annual Meeting, 47th, Washington, DC, February 22-27, 1981, ASP Technical Papers. Falls Church, VA, American Society of Photogrammetry, 1981, p 111-124. refs

As a part of a Canada-West Germany scientific exchange program, SAR imagery obtained over areas in Southern Ontario was investigated. A unique and varied image response was noted at certain wetland sites. A description is provided of the results of an extension of the early observations to other wetland sites, taking into account preliminary correlations between the SAR image response and the wetland cover type It was found that the effects produced by wetland conditions in Southern Ontario on SAR X- and L-band backscatter make it possible to interpret vegetative cover and moisture conditions from SAR imagery. X-band SAR is sensitive to smaller-scale vegetative content in the wetlands, while L-band SAR is sensitive to larger-scale vegetative content in the wetlands. G R.

A82-34710
PROBLEMS ASSOCIATED WITH REMOTELY DETECTING AND MONITORING SALINE SITES WITHIN IRRIGATED ALBERTA
D. B HARKER (Alberta Agriculture, Irrigation Div, Lethbridge, Canada) In American Society of Photogrammetry, Annual Meeting, 47th, Washington, DC, February 22-27, 1981, ASP Technical Papers. Falls Church, VA, American Society of Photogrammetry, 1981, p 154-163. refs

Of the 400,000 ha of land irrigated in Alberta, from 10% to 30% has been estimated to be adversely affected by high water tables and soil salinity. To facilitate optimum rehabilitation planning, those lands which are affected or are likely to become affected under new irrigation must be identified and monitored. Over the last 25 years several attempts have been made to identify and monitor affected acreages using panchromatic air photos. Recently, 1:10,000 color and other photographic sensors and scales have been utilized and preliminary work with Landsat digital data has begun In an evaluation of these activities, attention is given to mapping details, mapping efficiency, the affected area, visual pattern recognition problems, and ground truth requirements Plans for future work are also discussed G R.

A82-34716
A COMPUTERIZED SPATIAL ANALYSIS SYSTEM FOR ASSESSING WILDLIFE HABITAT FROM VEGETATION MAPS
R. A. MEAD, T L SHARIK, S P. PRISLEY, and J. T. HEINEN (Virginia Polytechnic Institute and State University, Blacksburg, VA) In· American Society of Photogrammetry, Annual Meeting, 47th, Washington, DC, February 22-27, 1981, ASP Technical Papers Falls Church, VA, American Society of Photogrammetry, 1981, p. 212-220. refs

A82-34729* Florida Univ., Lake Alfred.
EFFECTS OF ALTITUDE, FOCAL LENGTH, AND FILTER COMBINATIONS ON COLOR INFRARED PHOTOGRAPHY OF CITRUS GROVES
C. H. BLAZQUEZ (Florida, University, Lake Alfred, FL), F. W. HORN, JR. (NASA, Kennedy Space Center, Cocoa Beach, FL), and E. RHODES (Florida, Dept. of Transportation, Tallahassee, FL) In American Society of Photogrammetry, Annual Meeting, 47th, Washington, DC, February 22-27, 1981, ASP Technical Papers. Falls Church, VA, American Society of Photogrammetry, 1981, p 351-366. refs

A82-34730* National Aeronautics and Space Administration Goddard Space Flight Center, Greenbelt, Md.
DEFINING THE TEMPORAL WINDOW FOR MONITORING FOREST CANOPY DEFOLIATION USING LANDSAT
R. F NELSON (NASA, Goddard Space Flight Center, Earth Resources Branch, Greenbelt, MD) In: American Society of Photogrammetry, Annual Meeting, 47th, Washington, DC, February 22-27, 1981, ASP Technical Papers Falls Church, VA, American Society of Photogrammetry, 1981, p 367-382. refs

An analysis of Landsat imagery of forested areas near Williamsport, Pennsylvania shows that the effects of defoliation by insects can be assessed over a two month period beginning in early June. Within this window heavily defoliated forest can be successfully delineated from moderately defoliated and healthy forest Consequently, the effects of insect damage can be assessed at times other than peak defoliation, doubling the probability that useful satellite data can be acquired in the Williamsport area. (Author)

A82-34731
USE OF LANDSAT MULTISPECTRAL SCANNER DATA IN VEGETATION MAPPING OF A FORESTED AREA
S. KHORRAM and E. F. KATIBAH (California, University, Berkeley, CA) In. American Society of Photogrammetry, Annual Meeting, 47th, Washington, DC, February 22-27, 1981, ASP Technical Papers. Falls Church, VA, American Society of Photogrammetry, 1981, p. 383-392. refs

Landsat digital data combined with U-2 color infrared photography of the scale 1 120,000 are used for vegetation mapping of a forested area in northern California. The approach involves geometric correction of Landsat digital data, selection of ten training sites, unsupervised classification of training sites, and supervised classification of the entire study area. Best results for unsupervised classification are achieved when each training site is analyzed independently USGS topographic maps of the scale 1:250,000 are useful in the location of control points, delineation of watershed boundary, and geometric correction of Landsat digital data. It is concluded that Landsat repetitive data are a useful means of mapping the area under investigation. D.L G.

A82-34732
REMOTE SENSING - A POTENTIAL AID IN THE PREPARATION OF AN URBAN TREE INVENTORY
P. A GOLDBERG In American Society of Photogrammetry, Annual Meeting, 47th, Washington, DC, February 22-27, 1981, ASP Technical Papers Falls Church, VA, American Society of Photogrammetry, 1981, p 393-401. refs

Remote sensing is a reliable tool for the compilation of urban tree inventories An assessment of the quantity and quality of the Omaha-Bellevue, Nebraska tree population was made the summer of 1979. After digitizing the data several analytical techniques were explored, among them factor analysis Preliminary results indicated that the use of aerial surveys and computer analysis prove more cost effective and accurate than traditional forest field surveys. (Author)

A82-34733
MONITORING DEFORESTATION IN THE EASTERN PART OF THE STATE OF GUERRERO, MEXICO
D. RODRIGUEZ-BEJARANO (Guerrero, Universidad Autonoma, Chilpancingo, Mexico) In. American Society of Photogrammetry, Annual Meeting, 47th, Washington, DC, February 22-27, 1981, ASP Technical Papers Falls Church, VA, American Society of Photogrammetry, 1981, p. 402-411. refs

A research project carried out by the University of Guerrero to investigate deforestation and other land use and land cover changes is described Landsat imagery, aerial photographs, and cartographic maps are used in determining changes in forest vegetation between 1972 and 1979 The area covered by forest fell from 112,250 hectares to 76,250 hectares. During the period investigated, the population density rose from 35 persons/sq km to 46 persons/sq km. The forest cover comprises tropical and semitemperate forests. C R.

A82-35139
STATUS AND PROSPECTS OF THE AUTOMATED PROCESSING OF REMOTE-SENSING DATA /USING FOREST SURVEYS AS AN EXAMPLE/ [SOSTOIANIE I PERSPEKTIVY AVTOMATIZATSII OBRABOTKI AEROKOSMICHESKOI INFORMATSII /NA PRIMERE MATERIALOV S'EMKI LESA/]
V. I SUKHIKH and R. I ELMAN In: Study of the hydrological cycle by aerospace methods. Moscow, Izdatel'stvo Radio i Sviaz', 1982, p 80-85. In Russian

Attention is given to the following techniques of the automated processing of remote-sensing data: the delineation of forest boundaries and homogeneous areas; the delineation of extended land areas and their schematic representation, and the determination of the reserves, completeness, diameter, and other characteristics of plantations The automatic delineation of such land categories as forest-covered areas, fire-consumed areas, cleared spaces, and swamps is considered. It is shown that the most informative features for the determination of forest-evaluation indices are the combination of the image texture patterns of the delineated area with the landscape characteristics and generalized features of the external appearance of these images. B.J.

A82-37194
C-BAND RADAR FOR DETERMINING SURFACE SOIL MOISTURE
R. BERNARD, P. MARTIN, D. VIDAL-MADJAR (CNRS and CNET, Centre de Recherche en Physique de l'Environnement Terrestre et Planetaire, Issy-les-Moulineaux, Hauts-de-Seine, France), J. L THONY, and M VAUCLIN (Institut de Mecanique, Grenoble, France) Remote Sensing of Environment, vol 12, July 1982, p 189-200. Centre National d'Etudes Spatiales refs
(Contract CNES-214; CNES-272)

A C band radar calibration method is presented The experiment has been conducted in an agricultural area near Paris on three different types of surface: wheat stubble, sugar beet, and corn. It has been found that the sensitivity of the radar backscattering coefficient to surface soil moisture agrees well with the results obtained by Ulaby et al. (1979) when soil moisture values are expressed as percentage of the field capacity. (Author)

A82-37503
REMOTE SENSING OF SALT MARSH VEGETATION IN THE FIRST FOUR PROPOSED THEMATIC MAPPER BANDS
J. T. C BUDD (Portsmouth Polytechnic, Portsmouth, England) and E. J. MILTON (Southampton, University, Southampton, England) International Journal of Remote Sensing, vol. 3, Apr -June 1982, p 147-161. Research supported by Portsmouth Polytechnic and University of Reading. refs

The potential of the first four proposed TM bands for estimating above-ground biomass and discriminating species groups was evaluated in an area of intertidal salt marsh in Chichester Harbor, Southern England. Ground spectral data were collected using a portable multiband radiometer during August 1979. The correlation and variance-covariance matrices of the data are shown, as are the results of principal-components analysis of the ground spectral data and of canonical variate analysis. Individual sites for four types of algae are graphed for principal components and canonical variates. For biomass estimation, the relationship between bidirectional reflectance and dry biomass is shown for the algae C.D.

A82-37589
THE INFLUENCE OF SOIL CHARACTERISTICS ON REGIONAL CONVECTION DIFFERENCES ABOVE NORTHERN GERMANY [DIE AUSWIRKUNG VON BODENEIGENSCHAFTEN AUF DIE REGIONALEN KONVEKTIONSUNTERSCHIEDE UEBER NORDDEUTSCHLAND]
D. MUELLER and C KOTTMEIER (Hannover, Technische Universitaet, Hanover, West Germany) Meteorologische Rundschau, vol. 35, June 1982, p 84-91 In German. refs

The present investigation is concerned with the various factors which can affect the intensity of convection Soil moisture and orography are found to have significant influence on the convection. Regional differences concerning soil and soil moisture are used as a basis to develop a map which can provide information regarding the local differences of the intensity of convection. The map shows good agreement with observations made by glider pilots above the North German Plain. However, in the mountainous area south of the northern lowlands, orography appears to have a greater effect than soil moisture G.R.

N82-22623*# Purdue Univ , Lafayette, Ind. Lab. for Applications of Remote Sensing.
SPECTRAL PROPERTIES OF AGRICULTURAL CROPS AND SOILS MEASURED FROM SPACE, AERIAL, FIELD, AND LABORATORY SENSORS
M E. BAUER, Principal Investigator, V. C. VANDERBILT, B F. ROBINSON, and C S. T DAUGHTRY Nov. 1981 21 p refs Repr. from Proc of the Intern Arch. of Photogrammetry, v. 23(B7) p 56-73 Presented at the 14th Congr. of the Intern. Soc. for photogrammetry, Hamburg, 13-15 Jul 1980 Sponsored by NASA, USDA, Dept of Commerce, Dept. of the Interior, and Agency for International Development ERTS
(Contract NAS9-15466; PROJ. AGRISTARS)
(E82-10189; NASA-CR-168617, SR-P1-04200; NAS 1 26:168617; LARS-07138) Avail· NTIS HC A02/MF A01 CSCL 20F

Investigations of the multispectral reflectance characteristics of crops and soils as measured from laboratory, field, aerial, and satellite sensor systems are reviewed. The relationships of important biological and physical characteristics to the spectral properties of crops and soils are addressed. J.D

N82-22626*# Environmental Research Inst. of Michigan, Ann Arbor
ANALYSIS OF SCANNER DATA FOR CROP INVENTORIES *Progress Report, 15 Nov. 1980 - 14 Feb. 1981*
R. HORVATH, Principal Investigator, R C. CICONE, R. J. KAUTH, W. A. MALILA, W. PONT, B THELEN, and A. SELLMAN Apr. 1981 141 p ERTS
(Contract NAS9-15476)
(E82-10192, NASA-CR-161047, NAS 1 26.161047, ERIM-152400-4-P) Avail· NTIS HC A07/MF A01 CSCL 02C

Accomplishments for a machine-oriented small grains labeler T&E, and for Argentina ground data collection are reported. Features of the small grains labeler include temporal-spectral profiles, which characterize continuous patterns of crop spectral development, and crop calendar shift estimation, which adjusts for planting date differences of fields within a crop type. Corn and soybean classification technology development for area estimation for foreign commodity production forecasting is reported. Presentations supporting quarterly project management reviews and a quarterly technical interchange meeting are also included. T M.

N82-23116*# *Evangel Coll., Springfield, Mo*
USE OF LANDSAT DATA TO DEFINE SOIL BOUNDARIES IN CARROLL COUNTY, MISSOURI
S E DAVIDSON *In* Houston Univ. The 1981 NASA ASEE Summer Fac. Fellowship Program, Vol 1 12 p 20 Aug. 1981 refs
Avail. NTIS HC A14/MF A01 CSCL 08M

Bands 4, 5 and 7 false color composite photographs were prepared using data from LANDSAT scenes acquired during April 1977 and April 1981 on computer compatible tapes, and these color composites were compared with band 7 black and white photographs prepared for the entire county. Delineations of soil boundaries at the soil association level were achieved using LANDSAT spectral reflectance data and slope maps for a portion of Carroll County, Missouri. Forty two spectral reflectance classes from April 1977 LANDSAT data were overlaid on digitized slope maps of nine USGS 7.5 minute series topographic quadrangle slope maps to achieve boundary delineations of the soil associations. Author

N82-23133*# Mississippi State Univ , State College
A COMPARISON OF STRATIFIED VERSUS REGRESSION ESTIMATORS Final Report
H. C TAKACS *In* Houston Univ. The 1981 NASA ASEE Summer Fac. Fellowship Program, Vol 2 17 p 20 Aug 1981 refs
Avail: NTIS HC A17/MF A01 CSCL 05B

LANDSAT data acquired over an agricultural area along with ground enumeration of the same area are used to obtain crop acreage estimates which are better (as measured in terms of bias and variance) than can be obtained from either data source alone. Two basic approaches considered within the AgRISTARS program are a stratified crop acreage estimator and a regression estimator A statement of the problem was mathematically formulated and some theorems were proved which relate to the variance of the two estimators For a particular set of data, the regression and stratified estimators are compared in terms of certain easily computed parameters. S L.

N82-23564*# National Aeronautics and Space Administration Lyndon B. Johnson Space Center, Houston, Tex
A METEOROLOGICALLY DRIVEN MAIZE STRESS INDICATOR MODEL
T. W TAYLOR and F W RAVET, Principal Investigators Apr. 1981 20 p refs Sponsored by NASA, USDA, Dept. of Commerce, Dept. of the Interior, and Agency for International Development ERTS
(Contract PROJ. AGRISTARS)
(E82-10112, NASA-TM-84201, JSC-173991, NAS 1.15:84201; EW-UI-04119) Avail: NTIS HC A02/MF A01 CSCL 02C

A maize soil moisture and temperature stress model is described which was developed to serve as a meteorological data filter to alert commodity analysts to potential stress conditions in the major maize-producing areas of the world The model also identifies optimum climatic conditions and planting/harvest problems associated with poor tractability. Author

N82-23565*# Lockheed Engineering and Management Services Co , Inc., Houston, Tex.
AGRISTARS: FOREIGN COMMODITY PRODUCTION FORECASTING. THE 1980 US/CANADA WHEAT AND BARLEY EXPLORATORY EXPERIMENT
R. W. PAYNE, Principal Investigator Jul. 1981 30 p refs Sponsored by NASA, USDA, Dept. of Commerce, Dept. of the Interior, and Agency for International Development ERTS
(Contract NAS9-15800, PROJ AGRISTARS)
(E82-10126; NASA-CR-167404; JSC-17406; NAS 1.26:16740, LEMSCO-16921; FC-L1-04127) Avail. NTIS HC A03/MF A01 CSCL 02C

The crop identification procedures used performed were for spring small grains and are conducive to automation. The performance of the machine processing techniques shows a significant improvement over previously evaluated technology, however, the crop calendars require additional development and refinements prior to integration into automated area estimation technology. The integrated technology is capable of producing accurate and consistent spring small grains proportion estimates Barley proportion estimation technology was not satisfactorily evaluated because LANDSAT sample segment data was not available for high density barley of primary importance in foreign regions and the low density segments examined were not judged to give indicative or unequvocal results. Generally, the spring small grains technology is ready for evaluation in a pilot experiment focusing on sensitivity analysis to a variety of agricultural and meteorological conditions representative of the global environment. Author

N82-23566*# Purdue Univ , Lafayette, Ind Lab for Applications of Remote Sensing
DIURNAL CHANGES IN REFLECTANCE FACTOR DUE TO SUN-ROW DIRECTION INTERACTIONS
M E BAUER, Principal Investigator, V C VANDERBILT, J. C. KOLLENKARK, L. L BIEHL, B F. ROBINSON, and K J. RANSON Sep. 1981 13 p refs Repr from Intern Colloq. on Spectral Signatures of Objects in Remote Sensing (France), 1980 Colloq. held in Avignon, France, 8-11 Sep. 1980 Sponsored by NASA, USDA, Dept of Commerce, Dcpt. of the Interior, and Agency for International Development ERTS
(Contract NAS9-15466; PROJ AGRISTARS)
(E82-10128; NASA-CR-167403, NAS 1 26·167403; LARS-090881, SR-P1-04140) Avail: NTIS HC A02/MF A01 CSCL 02C

Over a two year period, data were collected regarding the canopies of soybeans grown in rows in planter boxes placed on a turntable in an effort to investigate changes in the spectral reflectance factor related to row direction, Sun direction, soil background, and crop development stage Results demonstrate that the direction of rows in a soybean canopy can affect the reflectance factor of the canopy by as much as 230%. The results for the red spectral region tend to support the validity of canopy reflectance models, results for the infrared region do not. A R H.

N82-23578*# Washington Univ., St. Louis, Mo Dept. of Earth and Planetary Sciences.
STRUCTURE OF THE ST. FRANCOIS MOUNTAINS AND SURROUNDING LEAD BELT, S. E. MISSOURI: INFERENCES FROM THERMAL IR AND OTHER DATA SETS Quarterly Report, 1 Aug. - 31 Oct. 1981
R. E ARVIDSON, Principal Investigator 15 Dec. 1981 5 p Original contains imagery. Original imagery may be purchased from NASA, Goddard Space Flight Center, (code 601), Greenbelt, Md 20771. Domestic users send order to 'Attn : National Space Science Data Center', nondomestic users send order to 'Attn : World Data Center A for Rockets and Satellites HCMM
(Contract NAS5-26533)
(E82-10205, NASA-CR-168632, NAS 1.26·168632) Avail: NTIS HC A02/MF A01 CSCL 08G

Day-IR, day-visible, and night-IR image data sets were analyzed. All three images were contrast enhanced, using a linear stretch. The night-IR image was destriped using a box-car filtering approach. Apparent thermal inertia images were generated from the data. The enhanced data and the apparent thermal inertia image were also registered and overlayed onto shaded relief images depicting topography and onto a colored version of the Missouri geologic map. The combination of the apparent thermal inertial image and the shaded relief map proved to have the greatest discriminability in terms of portraying linear features. The reason seems to be that the vegetation canopy on the Ozark Plateau is different topography, tend to emphasize subtle topographic effects.
E.A.K

N82-23579*# Lockheed Engineering and Management Services Co., Inc., Houston, Tex.
AGRISTARS: FOREIGN COMMODITY PRODUCTION FORECASTING. THE 1980 US CORN AND SOYBEANS EXPLORATORY EXPERIMENT Final Report
J T. MALIN and J G. CARNES, Principal Investigators Oct. 1981 183 p refs Sponsored by NASA, USDA, Dept of Commerce, Dept. of the Interior and Agency for International Development ERTS
(Contract NAS9-15800, PROJ. AGRISTARS)
(E82-10206; NASA-CR-167485, JSC-17138; NAS 1.26:167485, LEMSCO-16573; FC-L1-04096) Avail: NTIS HC A09/MF A01 CSCL 02C

The U.S corn and soybeans exploratory experiment is described which consisted of evaluations of two technology components of a production forecasting system: classification procedures (crop labeling and proportion estimation at the level of a sampling unit) and sampling and aggregation procedures. The results from the labeling evaluations indicate that the corn and soybeans labeling procedure works very well in the U.S. corn belt with full season

(after tasseling) LANDSAT data. The procedure should be readily adaptable to corn and soybeans labeling required for subsequent exploratory experiments or pilot tests. The machine classification procedures evaluated in this experiment were not effective in improving the proportion estimates The corn proportions produced by the machine procedures had a large bias when the bias correction was not performed. This bias was caused by the manner in which the machine procedures handled spectrally impure pixels. The simulation test indicated that the weighted aggregation procedure performed quite well. Although further work can be done to improve both the simulation tests and the aggregation procedure, the results of this test show that the procedure should serve as a useful baseline procedure in future exploratory experiments and pilot tests. M.G.

N82-23580*# Department of Agriculture, Houston, Tex
EVALUATION OF THE DORAISWAMY-THOMPSON WINTER WHEAT CROP CALENDAR MODEL INCORPORATING A MODIFIED SPRING RESTART SEQUENCE
T. W. TAYLOR, F. W RAVET, and D. SMIKA, Principal Investigators Nov. 1981 11 p refs Sponsored by NASA, USDA, Dept. of Commerce, Dept of the Interior, and Agency for International Development ERTS
(Contract PROJ. AGRISTARS)
(E82-10207, NASA-CR-167486; JSC-17801; NAS 1 26:167486, EW-U1-04212) Avail· NTIS HC A02/MF A01 CSCL 02C

The Robertson phenology was used to provide growth stage information to a wheat stress indicator mode. A stress indicator model demands two acurate predictions from a crop calendar. date of spring growth initiation; and crop calendar stage at growth initiation. Several approaches for restarting the Robertson phenology model at spring growth initiation were studied. Although best results were obtained with a solar thermal unit method, an alternate approach which indicates soil temperature as the controlling parameter for spring growth initiation was selected and tested. The modified model (Doraiswamy-Thompson) is compared to LACIE-Robertson model predictions E.A.K.

N82-23581*# Lockheed Engineering and Management Services Co., Inc., Houston, Tex.
AGRISTARS: SUPPORTING RESEARCH. SPRING SMALL GRAINS PLANTING DATE DISTRIBUTION MODEL
T. HODGES and J. A. ARTLEY, Principal Investigators Mar. 1981 33 p refs Sponsored by NASA, USDA, Dept. of Commerce, Dept. of the Interior, and Agency for International Development ERTS
(Contract NAS9-15800; PROJ. AGRISTARS)
(E82-10208; NASA-CR-167487, JSC-16858, NAS 1 26.167487; LEMSCO-16018; SR-L1-04032) Avail: NTIS HC A03/MF A01 CSCL 02C

A model was developed using 996 planting dates at 51 LANDSAT segments for spring wheat and spring barley in Minnesota, Montana, North Dakota, and South Dakota in 1979 Daily maximum and minimum temperatures and precipitation were obtained from the cooperative weather stations nearest to each segment. The model uses a growing degree day summation modified for daily temperature range to estimate the beginning of planting and uses a soil surface wetness variable to estimate how a fixed number of planting days are distributed after planting begins For 1979, the model predicts first, median, and last planting dates with root mean square errors of 7.91, 6 61, and 7.09 days, respectively. The model also provides three or four dates to represent periods of planting activity within the planting season. Although the full model was not tested on an independent data set, it may be suitable in areas other than the U.S. Great Plains where spring small grains are planted as soon as soil and air temperatures become warm enough in the spring for plant growth. T.M

N82-23582*# Lockheed Engineering and Management Services Co., Inc , Houston, Tex
DESCRIPTION OF HISTORICAL CROP CALENDAR DATA BASES DEVELOPED TO SUPPORT FOREIGN COMMODITY PRODUCTION FORECASTING PROJECT EXPERIMENTS
W L. WEST, III, Principal Investigator Oct 1981 19 p refs Sponsored by NASA, USDA, Dept. of Commerce, Dept of the Interior, and Agency for International Development ERTS
(Contract NAS9-15800; PROJ. AGRISTARS)
(E82-10209; NASA-CR-167488; JSC-17417; NAS 1 26:167488; LEMSCO-16929; FC-L1-04142) Avail. NTIS HC A02/MF A01 CSCL 02C

The content, format, and storage of data bases developed for the Foreign Commodity Production Forecasting project and used to produce normal crop calendars are described. In addition, the data bases may be used for agricultural meteorology, modeling of stage sequences and planting dates, and as indicators of possible drought and famine. M G

N82-23585*# Purdue Univ , Lafayette, Ind. Lab. for Applications of Remote Sensing.
SPECTRAL PROPERTIES OF AGRICULTURAL CROPS AND SOILS MEASURED FROM SPACE, AERIAL, FIELD, AND LABORATORY SENSORS
M E BAUER, Principal Investigator, V C. VANDERBILT, B. F. ROBINSON, and C. S. T DAUGHTRY Nov. 1982 21 p refs Repr. from Proc. of the Intern. Arch of Photogrammetry (West Germany), v 23(B7), 1980 p 56-73 Presented at the 14th Congr. of the Intern Soc. for Photogrammetry, Hamburg, 13-15 Jul 1980 Sponsored by NASA, USDA, Dept of Commerce, Dept. of the Interior, and Agency for International Development ERTS
(Contract NAS9-15466, PROJ. AGRISTARS)
(E82-10212; NASA-CR-167507, SR-P1-04200, NAS 1.26:167507; LARS-071380) Avail: NTIS HC A02/MF A01 CSCL 02C

The state of knowledge of the multispectral reflectance characteristics of crops and soils as measured from laboratory, field, aerial, and satellite sensor systems is reviewed emphasizing current investigations. The relationships of important biological and physical characteristics to their spectral properties of crops and soils are addressed. Future research needs are defined. M.G.

N82-23588*# Purdue Univ , Lafayette, Ind Lab. for Applications of Remote Sensing
DETERMINATION OF THE OPTIMAL LEVEL FOR COMBINING AREA AND YIELD ESTIMATES
M E. BAUER, Principal Investigator, M. M. HIXSON, and C. D. JOBUSCH 12 Oct. 1981 71 p refs Sponsored by NASA, USDA, Dept. of Commerce, Dept. of the Interior, and Agency for International Development ERTS
(Contract NAS9-15466; PROJ. AGRISTARS)
(E82-10215; NASA-CR-167511, FC-P1-04197, NAS 1 26:167511; LARS-101281) Avail: NTIS HC A04/MF A01 CSCL 02C

Several levels of obtaining both area and yield estimates are considered: county, refined strata, refined/split strata, crop reporting district, and state Using the CCEA model form and smoothed weather data, regression coefficients at each level were derived to compute yield and its variance The variance of the yield estimates was largest at the state and smallest at the county level for the two crops studied corn and soybeans. The refined strata had somewhat larger variances than those associated with the refined/split strata and CRD. For production estimates, the difference in standard deviations among levels was not large for corn, but for soybeans the standard deviation at the state level was more than 50% greater than for the other levels. The refined strata had the smallest standard deviations T.M.

N82-23589*# National Aeronautics and Space Administration. Lyndon B. Johnson Space Center, Houston, Tex.
AGRISTARS. PRELIMINARY TECHNICAL RESULTS REVIEW OF FY81 EXPERIMENTS, VOLUME 2: FISCAL YEAR 1981/1982 'CORN AND SOYBEANS PILOT' EXPERIMENT
29 Sep. 1981 170 p Sponsored by NASA, USDA, Dept. of Commerce, Dept of the Interior, and Agency for International Development ERTS
(Contract PROJ. AGRISTARS)
(E82-10216; NASA-TM-84206; JSC-17433-VOL-2, NAS 1.15:84206; FC-J1-04175-VOL-2) Avail: NTIS HC A08/MF A01 CSCL 02C

The performance of the technology exhibited significant proportion estimation errors, specifically, high mean error in both corn and soybeans area estimation. The data systems, technical approaches, and data assessment of the pilot experiment were reviewed. Results of proportion estimations procedure performance evaluations, and sensitivity evaluations are presented. The role of the pilot experiment in foreign technology development is discussed. T.M.

N82-23590*# Lockheed Engineering and Management Services Co., Inc., Houston, Tex
APPLICATION OF THERMAL MODEL FOR PAN EVAPORATION TO THE HYDROLOGY OF A DEFINED MEDIUM, THE SPONGE
M H. TRENCHARD and J. A ARTLEY, Principal Investigators Nov. 1981 23 p refs Sponsored by NASA, USDA, Dept. of Commerce, Dept of the Interior, and Agency for International Development ERTS
(Contract NAS9-15800; PROJ AGRISTARS)
(E82-10217; NASA-CR-167479; JSC-17440, NAS 1.26:167479; LEMSCO-16935, FC-L1-04192) Avail: NTIS HC A02/MF A01 CSCL 02C

A technique is presented which estimates pan evaporation from the commonly observed values of daily maximum and minimum air temperatures. These two variables are transformed to saturation vapor pressure equivalents which are used in a simple linear regression model. The model provides reasonably accurate estimates of pan evaporation rates over a large geographic area The derived evaporation algorithm is combined with precipitation to obtain a simple moisture variable. A hypothetical medium with a capacity of 8 inches of water is initialized at 4 inches. The medium behaves like a sponge: it absorbs all incident precipitation, with runoff or drainage occurring only after it is saturated. Water is lost from this simple system through evaporation just as from a Class A pan, but at a rate proportional to its degree of saturation The contents of the sponge is a moisture index calculated from only the maximum and minium temperatures and precipitation.
T M.

N82-23591*# National Aeronautics and Space Administration. Lyndon B. Johnson Space Center, Houston, Tex.
A METEOROLOGICALLY DRIVEN GRAIN SORGHUM STRESS INDICATOR MODEL
T. W. TAYLOR (Agricultural Research Service, Houston, Tex) and F. W. RAVET, Principal Investigators Nov 1981 18 p refs Sponsored by NASA, USDA, Dept. of Commerce, Dept of the Interior, and Agency for International Development ERTS
(Contract PROJ. AGRISTARS)
(E82-10218; NASA-TM-84740; JSC-17797; NAS 1 15 84740; EW-U1-04208) Avail NTIS HC A02/MF A01 CSCL 02C

A grain sorghum soil moisture and temperature stress model is described. It was developed to serve as a meteorological data filter to alert commodity analysts to potential stress conditions and crop phenology in selected grain sorghum production areas. The model also identifies optimum conditions on a daily basis and planting/harvest problems associated with poor tractability.
T M.

N82-23592*# National Aeronautics and Space Administration Lyndon B Johnson Space Center, Houston, Tex
AGRISTARS. PROJECT MANAGEMENT REPORT: PROGRAM REVIEW PRESENTATION TO LEVEL 1, INTERAGENCY COORDINATION COMMITTEE
3 Nov. 1981 105 p Sponsored by NASA, USDA, Dept. of Commerce, Dept. of the Interior, and Agency for International Development ERTS
(Contract PROJ AGRISTARS)
(E82-10219, NASA-TM-84203, JSC-17792; NAS 1.15 84203; SR-J1-04195) Avail: NTIS HC A06/MF A01 CSCL 02C

The AgRISTARS supporting research projects in the areas of data systems, scene radiation, and pattern recognition are reviewed The objectives, activities, and accomplishments of FY-80 and the objectives and status of FY-81 programs are described
M.G

N82-23593*# National Aeronautics and Space Administration Ames Research Center, Moffett Field, Calif
AIRBORNE OBSERVED SOLAR ELEVATION AND ROW DIRECTION EFFECTS ON THE NEAR-IR/RED RATIO OF COTTON
J P. MILLARD, R. D JACKSON (Science and Education Administration, Phoenix, Ariz.), R. C GOETTELMAN (EAL Corp, Richmond, Calif.), and M J. LEROY, Principal Investigators (DCA Corp., Palo Alto, Calif) Aug. 1981 14 p refs Sponsored by NASA, USDA, Dept of Commerce, Dept of the Interior, and Agency for International Development ERTS
(Contract PROJ AGRISTARS)
(E82-10220; NASA-TM-84204; JSC-17420; NAS 1 15:84204, EW-U1-04144) Avail NTIS HC A02/MF A01 CSCL 02C

An airborne multispectral scanner was used to obtain data over two adjacent cotton fields having rows perpendicular to one another, at three times of day (different solar elevations), and on two dates (different plant size) The near IR/red ratios were displayed in image form, so that within-field variations and differences between fields could be easily assessed The ratio varied with changing Sun elevation for north-south oriented rows, but no variation was detected for east-west oriented rows
A.R H

N82-23594*# Lockheed Engineering and Management Services Co., Inc., Houston, Tex
NORMAL CROP CALENDARS. VOLUME 3: THE CORN AND SOYBEAN STATES OF ILLINOIS, INDIANA, AND IOWA
W. L WEST, III, Principal Investigator Oct. 1981 79 p refs Sponsored by NASA, USDA, Dept. of Commerce, Dept. of the Interior, and Agency for International Development
(Contract NAS9-15800; PROJ. AGRISTARS)
(E82-10221; NASA-CR-167446; JSC-17432; NAS 1.26 167446, LEMSCO-16944; FC-L1-04172) Avail. NTIS HC A05/MF A01 CSCL 02C

The state and crop reporting distric crop calendars for Iowa, Illinois, and Indiana are presented. Crop calendars for corn, soybeans, sorghum, oats, wheat, barley, clover, flax, sugar beets, and tobacco are included J.D

N82-23595*# Lockheed Engineering and Management Services Co , Inc , Houston, Tex
SELECTION OF THE AUSTRALIAN INDICATOR REGION
C. R. REED, Principal Investigator Sep 1981 73 p refs Sponsored by NASA, USDA, Dept. of Commerce, Dept. of the Interior, and Agency for International Development ERTS
(Contract NAS9-15800, PROJ AGRISTARS)
(E82-10222; NASA-CR-167406; JSC-17421; NAS 1.26 167406; LEMSCO-15682; FC-L1-04145) Avail: NTIS HC A04/MF A01 CSCL 02C

Each Australian state was examined for the availability of LANDSAT data, area, yield, and production characteristics, statistics, crop calendars, and other ancillary data. Agrophysical conditions that could influence labeling and classification accuracies were identified in connection with the highest producing states as determined from available Australian crop statistics.

Based primarily on these production statistics, Western Australia and New South Wales were selected as the wheat indicator region for Australia. The general characteristics of wheat in the indicator region, with potential problems anticipated for proportion estimation are considered. The varieties of wheat, the diseases and pests common to New South Wales, and the wheat growing regions of both states are examined. A.R.H

N82-23597*# Lockheed Engineering and Management Services Co., Inc , Houston, Tex.

AGRISTARS: RENEWABLE RESOURCES INVENTORY. LAND INFORMATION SUPPORT SYSTEM IMPLEMENTATION PLAN AND SCHEDULE

S. S. YAO, Principal Investigator Sep 1981 29 p Sponsored by NASA, USDA, Dept. of Commerce, Dept. of the Interior, and Agency for International Development ERTS

(Contract NAS9-15800; PROJ. AGRISTARS)

(E82-10224, NASA-CR-167441; JSC-17434, NAS 1.26:167441, LEMSCO-17276; RR-L1-00641) Avail: NTIS HC A03/MF A01 CSCL 05B

The planning and scheduling of the use of remote sensing and computer technology to support the land management planning effort at the national forests level are outlined. The task planning and system capability development were reviewed A user evaluation is presented along with technological transfer methodology. A land management planning pilot test of the San Juan National Forest is discussed. T.M.

N82-23598*# Science and Education Administration, Weslaco, Tex.

AGRISTARS: EARLY WARNING AND CROP CONDITION ASSESSMENT. PLANT COVER, SOIL TEMPERATURE, FREEZE, WATER STRESS, AND EVAPOTRANSPIRATION CONDITIONS Final Report, 1 Dec. 1977 - Sep. 1 1980

C L. WIEGAND, Principal Investigator, P. R. NIXON, H. W GAUSMAN, L. N. NAMKEN, R W LEAMER, and A J. RICHARDSON Aug 1981 185 p refs Sponsored by NASA, USDA, Dept. of Commerce, Dept. of the Interior, and Agency for International Development ERTS

(Contract NASA ORDER S-40198B, PROJ. AGRISTARS)

(E82-10225; NASA-CR-167440; JSC-17143; NAS 1.26:167440, EW-U1-04103) Avail: NTIS HC A09/MF A01 CSCL 02C

Emissive (10 5 to 12 5 microns) and reflective (0.55 to 1.1 microns) data for ten day scenes and infrared data for six night scenes of southern Texas were analyzed for plant cover, soil temperature, freeze, water stress, and evapotranspiration. Heat capacity mapping mission radiometric temperatures were: within 2 C of dewpoint temperatures, significantly correlated with variables important in evapotranspiration, and related to freeze severity and planting depth soil temperatures. Author

N82-23600*# Purdue Univ., Lafayette, Ind Lab for Applications of Remote Sensing

APPLICATION OF COMPUTER AXIAL TOMOGRAPHY (CAT) TO MEASURING CROP CANOPY GEOMETRY

M. E. BAUER, V. C. VANDERBILT, Principal Investigators, and R W KILGORE Jun. 1981 9 p refs Repr. from 1981 Intern. Geosci. and Remote Sensing Sym. (IGARSS'81), IEEE Catalog no 81CH1656-8, 1981 p 1162-1167 Sym. held in Washington, D.C., 8-10 Jun. 1981 ERTS

(Contract NAS9-15466; PROJ. AGRISTARS)

(E82-10227; NASA-CR-167397, NAS 1.26:167397, LARS-TR-060881; SR-P1-04141) Avail. NTIS HC A02/MF A01 CSCL 02C

The feasibility of using the principles of computer axial topography (CAT) to quantify the structure of crop canopies was investigated because six variables are needed to describe the position-orientation with time of a small piece of canopy foliage Several cross sections were cut through the foliage of healthy, green corn and soybean canopies in the dent and full pod development stages, respectively. A photograph of each cross section representing the intersection of a plane with the foliage was enlarged and the air-foliage boundaries delineated by the plane were digitized. A computer program was written and used to reconstruct the cross section of the canopy. The approach used in applying optical computer axial tomography to measuring crop canopy geometry shows promise of being able to provide needed geometric information for input data to canopy reflectance models. The difficulty of using the CAT scanner to measure large canopies of crops like corn is discussed and a solution is proposed involving the measurement of plants one at a time A R.H.

N82-23601*# Agricultural Research Services, Beltsville, Md.

AGRICULTURAL RESEARCH SERVICE RESEARCH HIGHLIGHTS IN REMOTE SENSING FOR CALENDAR YEAR 1980 Annual Report

J. C. RITCHIE, Principal Investigator Jul. 1981 27 p Sponsored by NASA, USDA, Dept. of Commerce, Dept of the Interior, and Agency for International Development ERTS

(Contract PROJ. AGRISTARS)

(E82-10228, NASA-CR-167408; EW-R1-04147; NAS 1 26:167408) Avail NTIS HC A03/MF A01 CSCL 02C

The AR research mission in remote sensing is to develop the basic understanding of the soil plant animal atmosphere continuum in agricultural ecosystems and to determine when remotely sensed data can be used to provide information about these agricultural ecosystems. A brief statement of the significant results of each project is given A list of 1980 publication and location contacts is also given. T M.

N82-23602*# Purdue Univ., Lafayette, Ind. Lab. for Applications of Remote Sensing

LINEAR POLARIZATION OF LIGHT BY TWO WHEAT CANOPIES MEASURED AT MANY VIEW ANGLES

M. E BAUER, Principal Investigator, V C VANDERBILT, L. L. BIEHL, B. F. ROBINSON, and A. S. VANDERBILT Sep. 1981 11 p refs Repr. from Intern Colloq on Spectral Signatures of Objects in Remote Sensing, 1980 Collog. held in Avignon, France, 8-11 Sep 1980 Sponsored by NASA, USDA, Dept of Commerce, Dept. of the Interior, and Agency for International Development ERTS

(Contract NAS9-15466; PROJ AGRISTARS)

(E82-10229; NASA-CR-167419, NAS 1.26:167419, LARS-TR-090981; SR-P1-04139) Avail NTIS HC A02/MF A01 CSCL 20F

The linear polarization and reflection of visible light by wheat as a function of sun-view diections, crop development stage, and wavelength were examined. Two-hundred spectra were taken continuously in wave-lengths from 0.45 to 0 72 Micron in 33 view directions using an Exotech model 20C spectroradiometer six meters above two wheat canopies in the boot and fully headed maturity stages. The analysis results show that the amount of linearly polarized light from the wheat canopies is greatest in the blue spectral region and decreases gradually with increasing wavelength. The results also show that the linearly polarized light from the canopies is generally greatest in the azimuth direction of the Sun and tends toward zero as the view direction tends toward the direction of the hot spot or anti-solar point. It is demonstrated that the single, angle of incidence of sunlight on the leaf, explains almost all of the variation of the amount of polarized light with Sun-view direction M.G

N82-23603*# Lockheed Engineering and Management Services Co., Inc , Houston, Tex.

EVALUATION OF THE PROCEDURE FOR SEPARATING BARLEY FROM OTHER SPRING SMALL GRAINS

E R. MAGNESS, Principal Investigator Aug. 1980 77 p refs Sponsored by NASA, USDA, Dept. of Commerce, Dept. of the Interior, and Agency for International Development ERTS

(Contract NAS9-15800; PROJ. AGRISTARS)

(E82-10230; NASA-CR-160888; JSC-16752, NAS 1.26.160888, LEMSCO-14598; FC-LO-00472) Avail: NTIS HC A05/MF A01 CSCL 02C

The success of the Transition Year procedure to separate and label barley and the other small grains was assessed. It was decided that developers of the procedure would carry out the

exercise in order to prevent compounding procedural problems with implementation problems The evaluation proceeded by labeling the spring small grains first. The accuracy of this labeling was, on the average, somewhat better than that in the Transition Year operations. Other departures from the original procedure included a regionalization of the labeling process, the use of trend analysis, and the removal of time constraints from the actual processing. Segment selection, ground truth derivation, and data available for each segment in the analysis are discussed. Labeling accuracy is examined for North Dakota, South Dakota, Minnesota, and Montana as well as for the entire four-state area. Errors are characterized. A.R H

N82-23604*# National Aeronautics and Space Administration Lyndon B. Johnson Space Center, Houston, Tex.
AGRISTARS. PROJECT MANAGEMENT REPORT: PROGRAM REVIEW PRESENTATION TO LEVEL 1, INTERAGENCY COORDINATION COMMITTEE Semiannual Report
Nov. 1981 232 p Sponsored by NASA, USDA, Dept of Commerce, Dept of the Interior, and Agency for International Development
(Contract PROJ. AGRISTARS)
(E82-10231; NASA-TM-84205; JSC-17438; NAS 1.15:84205; FC-J1-04181) Avail: NTIS HC A10/MF A01 CSCL 02C

Accomplishments relating to the development of crop calendars and production estimates for spring small grains, corn, and soybeans and the associated data acquisition and processing systems are reviewed The areas of interest included the Great Plains Corridor and Argentina. M G.

N82-23606*# Purdue Univ., Lafayette, Ind. Lab for Applications of Remote Sensing.
A MODEL OF PLANT CANOPY POLARIZATION
V. C. VANDERBILT Jun. 1980 12 p refs Repr from Machine Process. of Remotely Sensed Data, Jun 1980 p 98-108 Sponsored by NASA, USDA, Dept of Commerce, Dept. of the Interior, and Agency for International Development ERTS
(Contract NAS9-15466, PROJ AGRISTARS)
(E82-10233; NASA-CR-167415; SR-P1-04170; NAS 1.26:167415; LARS-060580) Avail: NTIS HC A02/MF A01 CSCL 20F

A model for the amount of linearly polarized light reflected by the shiny leaves of grain crops is based on the morphological and phenological characteristics of the plant canopy and upon the Fresnel equations which describe the light reflection process at the smooth boundary separating two dielectrics. The theory used demonstrates that, potentially, measurements of the linearly polarized light from a crop canopy may be used as an additional feature to discriminate between crops such as wheat and barley, two crops which are so spectrally similar that they are misclassified with unacceptable frequency Examination of the model suggests that, potentially, satellite polarization measurements may be used to monitor crop development stage, leaf water content, leaf area index, hail damage, and certain plant diseases. The information content of these measurements is needed to evaluate the proposed polarization sensor for the satellite-borne multispectral resource sampler. A.R H

N82-23607*# Lockheed Engineering and Management Services Co , Inc., Houston, Tex.
USE AND APPLICABILITY OF THE VEGETATION COMPONENT OF THE NATIONAL SITE CLASSIFICATION SYSTEM
C. A. CLARK, Principal Investigator Apr 1981 43 p refs Sponsored by NASA, USDA, Dept. of Commerce, Dept. of the Interior, and Agency for International Development Original contains color imagery. Original photography may be purchased from the EROS Data Center, Sioux Falls, S.D 57198 ERTS
(Contract NAS9-15800; PROJ AGRISTARS)
(E82-10234, NASA-CR-167416; JSC-17122, NAS 1.26:167416; LEMSCO-15173, RR-LO-00466) Avail: NTIS HC A03/MF A01 CSCL 02C

Existing vegetation on a site in Sumter National Forest, South Carolina was classified using high altitude aerial optical bar color infrared photography in an effort to determine if the National Site Classification (NSC) system could be used in the heterogeneously forested southeastern United States where it had not previously been used Results show that the revised UNESCO international classification and mapping of vegetation system, as incorporated into the NSCS, is general enough at the higher levels and specific enough at the lower levels to adequately accommodate densely forested, heterogeneous areas as well as the larger, more homogeneous regions of the Pacific Northwest. The major problem is of existing vegetation versus natural vegetation. A.R.H.

N82-23608*# Lockheed Engineering and Management Services Co , Inc., Houston, Tex
DESCRIPTION OF THE FORTRAN IMPLEMENTATION OF THE SPRING SMALL GRAINS PLANTING DATE DISTRIBUTION MODEL
J A ARTLEY, Principal Investigator Aug 1981 55 p refs Sponsored by NASA, USDA, Dept of Commerce, Dept of the Interior, and Agency for International Development ERTS
(Contract NAS9-15800; PROJ. AGRISTARS)
(E82-10235; NASA-CR-167411; JSC-17414, NAS 1 26:167411; LEMSCO-16854, SR-L1-00309) Avail· NTIS HC A04/MF A01 CSCL 02C

The Hodges-Artley spring small grains planting date distribution model was coded in FORTRAN. The PLDRVR program, which implements the model, is described and a copy of the code is provided. The purpose, calling procedure, local variables, and input/output devices for each subroutine are explained to supplement the user's guide A.R H

N82-23609*# National Aeronautics and Space Administration. Lyndon B. Johnson Space Center, Houston, Tex
AGRISTARS: AGRICULTURE AND RESOURCES INVENTORY SURVEYS THROUGH AEROSPACE REMOTE SENSING Annual Report
Jun 1981 68 p Sponsored by NASA, USDA, Dept of Commerce, Dept. of the Interior, and Agency for International Development ERTS
(Contract PROJ. AGRISTARS)
(E82-10236; NASA-TM-84202; JSC-17398, NAS 1.15:84202; AP-J0-04111) Avail: NTIS HC A04/MF A01 CSCL 02C

The major objectives and FY 1980 accomplishments are described of a long term program designed to determine the usefulness, cost, and extent to which aerospace remote sensing data can be integrated into existing or future USDA systems to improve the objectivity, reliability, timeliness, and adequacy of information. A general overview, the primary and participating agencies, and the technical highlights of each of the following projects are presented: early warning/crop condition assessment; foreign commodity production forecasting; yield model development; supporting research, soil moisture; domestic crops and land cover; renewable resources incentory; and conservation and pollution. A.R.H

N82-23610*# Purdue Univ., Lafayette, Ind. Lab. for Applications of Remote Sensing.
CANOPY REFLECTANCE AS INFLUENCED BY SOLAR ILLUMINATION ANGLE
M. E. BAUER, Principal Investigator, J. C. KOLLENKARK, V. C. VANDERBILT, and C S. T. DAUGHTRY Mar 1981 24 p refs Sponsored by NASA, USDA, Dept of Commerce, Dept. of the Interior, and Agency for International Development ERTS
(Contract NAS9-15466; PROJ. AGRISTARS)
(E82-10237; NASA-CR-167402; SR-P1-04039; NAS 1.26:167402; LRS-021681) Avail: NTIS HC A02/MF A01 CSCL 20F

The interaction of the solar illumination angle and row azimuth angle of the measured reflectance factor (RF) of soybean canopies was investigated Diurnal changes of nearly 140% were observed in the red wavelength region when canopies covered 64% of the soil. The amount of shadow observed was a function of the plant geometry and row width. As soil cover approached 100%, the diurnal changes diminished. A function tht describes the solar illumination angle with respect to the row azimuth explained most of the diurnal variation in the measured RF. Variation in near

infrared response was much less and did not appear to be as strongly related to Sun-row angle interactions. The near infrared/red ratio was highly sensitive to Sun angle-row direction interactions, whereas the greenness function, utilizing all four spectral bands, was not. J.D.

N82-23611*# National Aeronautics and Space Administration Goddard Space Flight Center, Greenbelt, Md

A MULTI-FREQUENCY RADIOMETRIC MEASUREMENT OF SOIL MOISTURE CONTENT OVER BARE AND VEGETATED FIELDS

J. R. WANG, T. J. SCHMUGGE, J. E MCMURTREY, III (Dept of Agriculture, Beltsville, Md.), W I GOULD, W. S. GLAZAR, and J. E. FUCHS, Principal Investigators Oct. 1981 16 p refs Submitted for publication Sponsored by NASA, USDA, Dept. of Commerce, Dept of the Interior, and Agency for International Development ERTS

(Contract PROJ AGRISTARS)

(E82-10238, NASA-TM-83842; SM-GI-04178; NAS 1.15.83842) Avail. NTIS HC A02/MF A01 CSCL 08M

A USDA Beltsville Agricultural Research Center site was used for an experiment in which soil moisture remote sensing over bare, grass, and alfalfa fields was conducted over a three-month period using 0.6 GHz, 1.4 GHz, and 10.6 GHz Dicke-type microwave radiometers mounted on mobile towers. Ground truth soil moisture content and ambient air and sil temperatures were obtained concurrently with the radiometric measurements Biomass of the vegetation cover was sampled about once a week Soil density for each of the three fields was measured several times during the course of the experiment. Results of the radiometric masurements confirm the frequency dependence of moisture sensing sensitivity reduction reported earlier Observations over the bare, wet field show that the measured brightness temperature is lowest at 5.0 GHz and highest of 0.6 GHz frequency, a result contrary to expectation based on the estimated dielectric permittivity of soil water mixtures and current radiative transfer model in that frequency range. Author

N82-24519*# Environmental Research Inst. of Michigan, Ann Arbor.

ANALYSIS OF SCANNER DATA FOR CROP INVENTORIES Progress Report, 15 Feb. - 30 Jun. 1981

R HORVATH, Principal Investigator, R. C. CICONE, R. J. KAUTH, and W A MALILA Aug 1981 273 p refs Sponsored by NASA, USDA, Dept. of Commerce, Dept. of Interior and Agency for Intern. Develop ERTS

(Contract NAS9-15476, PROJ AGRISTARS)

(E82-10241; NASA-CR-167391; NAS 1 26·167391; ERIM-152400-6-P) Avail NTIS HC A12/MF A01 CSCL 02C

Progress and technical issues are reported in the development of corn/soybeans area estimation procedures for use on data from South America, with particular emphasis on Argentina Aspects related to the supporting research section of the AgRISTARS Project discussed include: (1) multisegment corn/soybean estimation, (2) through the season separability of corn and soybeans within the U.S corn belt, (3) TTS estimation; (4) insights derived from the baseline corn and soybean procedure; (5) small fields research, and (6) simulating the spectral appearance of wheat as a function of its growth and development To assist the foreign commodity production forecasting, the performance of the baseline corn/soybean procedure was analyzed and the procedure modified Fundamental limitations were found in the existing guidelines for discriminating these two crops. The temporal and spectral characteristics of corn and soybeans must be determined because other crops grow with them in Argentina. The state of software technology is assessed and the use of profile techniques for estimation is considered. A.R H.

N82-24523*# National Aeronautics and Space Administration. Ames Research Center, Moffett Field, Calif.

MULTILEVEL MEASUREMENTS OF SURFACE TEMPERATURE OVER UNDULATING TERRAIN PLANTED TO BARLEY Final Report, 1 Nov. 1977 - 31 Oct. 1980

R. J REGINATO, Principal Investigator (USDA, Phoenix, Ariz.), J. P. MILLARD, J. L HATFIELD (California Univ., David), and R D. JACKSON (USDA, Phoenix, Ariz.) Mar 1981 74 p refs Original contains color imagery. Original may be obtained from the EROS Data Center. Sioux Falls, S D. 57198 ERTS

(Contract NASA ORDER S-40255-B)

(E82-10245; NASA-CR-168826; NAS 1.26·168826) Avail· NTIS HC A04/MF A01 CSCL 04B

A ground and aircraft program was conducted to extend ground based methods for measuring soil moisture and crop water stress to aircraft and satellite altitudes A 260ha agricultural field in California was used over the 1977-78 growing season For cloud free days ground based temperature measurements over bare soil were related to soil moisture content. Water stress resulted from too much water, not from lack of it, as was expected A theoretical examination of the canopy air temperature difference as affected by vapor pressure deficit and net radiation was developed This analysis shows why surface temperatures delineate crop water stress under conditions of low humidity, but not under high humidity conditions. Multilevel temperatures acquired from the ground, low and high altitude aircraft, and the Heat Capacity Mapping Mission (HCMM) spacecraft were compared for two day and one night overpasses The U-2 and low altitude temperatures were within 0.5 C The HCMM data were analyzed using both the pre- and post-launch calibrations, with the former being considerably closer in agreement with the aircraft data than the latter M.G.

N82-24563*# National Aeronautics and Space Administration. National Space Technology Labs., Bay Saint Louis, Miss.

AN ANALYSIS OF LANDSAT MSS SCENE-TO-SCENE REGISTRATION ACCURACY

B. R SEYFARTH and P. W COOK, Principal Investigators (USDA) Dec 1981 14 p Sponsored by NASA, USDA, Dept. of Commerce, Dept of Interior, and Agency for International Development ERTS

(Contract PROJ AGRISTARS)

(E82-10285; NASA-TM-84694; DC-Y1-04156, NSTL/ERL-198; NAS 1.15.84694) Avail: NTIS HC A02/MF A01 CSCL 02C

Measurements were made for 12 registrations done by ERL for 8 registrations done by SRS. The results indicate that the ERL method is significantly more accurate in five of the eight comparison. The difference between the two methods are not significant in the other three cases There are two possible reasons for the differences. First, the ERL model is a piecewise linear model and the EDITOR model is a cubic polynomial model Second, the ERL program resamples using bilinear interpolation while the EDITOR software uses a nearest neighbor resampling. This study did not indicate how much of the difference is attributable to each factor. The average of all merged scene error values for ERL was 31.6 meters and the average for the eight common areas was 32.6 meters The average of the eight merged scene error values for SRS was 40 1 meters. T.M

N82-24564*# National Aeronautics and Space Administration. National Space Technology Labs., Bay Saint Louis, Miss.

AN ALGORITHM FOR AUTOMATING THE REGISTRATION OF USDA SEGMENT GROUND DATA TO LANDSAT MSS DATA

M H. GRAHAM, Principal Investigator Dec 1981 31 p refs Sponsored by NASA, USDA, Dept. of Commerce, Dept. of Interior and Agency for International Development ERTS

(Contract PROJ. AGRISTARS)

(E82-10286; NASA-TM-84695; DC-YI-04211, NSTL/ERL-201; NAS 1 15:84695) Avail: NTIS HC A03/MF A01 CSCL 02C

The algorithm is referred to as the Automatic Segment Matching Algorithm (ASMA). The ASMA uses control points or the annotation record of a P-format LANDSAT compter compatible tape as the initial registration to relate latitude and longitude to LANDSAT rows and columns. It searches a given area of LANDSAT data

with a 2x2 sliding window and computes gradient values for bands 5 and 7 to match the segment boundaries. The gradient values are held in memory during the shifting (or matching) process The reconstructed segment array, containing ones (1's) for boundaries and zeros elsewhere are computer compared to the LANDSAT array and the best match computed Initial testing of the ASMA indicates that it has good potential for replacing the manual technique. T.M.

N82-24565*# National Aeronautics and Space Administration. National Space Technology Labs., Bay Saint Louis, Miss.
ANALYSIS OF THEMATIC MAPPER SIMULATOR DATA ACQUIRED DURING WINTER SEASON OVER PEARL RIVER, MISSISSIPPI, TEST SITE
J E. ANDERSON and M. T. KALCIC, Principal Investigators Mar. 1982 45 p refs Sponsored by NASA, USDA, Dept. of Commerce Dept. of Interior and Agency for International Development Original contains color imagery. Original photography may be purchased from EROS Data Center, Sioux Falls, S D 57198 ERTS
(Contract PROJ. AGRISTARS)
(E82-10287; NASA-TM-84696; RR-Y1-04217, NSTL/ERL-202, NAS 1 15:84696) Avail: NTIS HC A03/MF A01 CSCL 05B

Digital processed aircraft-acquired thematic mapping simulator (TMS) data collected during the winter season over a forested site in southern Mississippi are presented to investigate the utility of TMS data for use in forest inventories and monitoring Analyses indicated that TMS data are capable of delineating the mixed forest land cover type to an accuracy of 92.5 % correct. The accuracies associated with river bottom forest and pine forest were 95.5 and 91.5 % correct. The accuracies associated with river bottom forest and pine forest were 95.5 and 91 5 % correct, respectively. The figures reflect the performance for products produced using the best subset of channels for each forest cover type. It was found that the choice of channels (subsets) has a significant effect on the accuracy of classification produced, and that the same channels are not the most desirable for all three forest types studied. Both supervised and unsupervised spectral signature development techniques are evaluated, the unsupervised methods proved unacceptable for the three forest types considered. E.A K

N82-24574*# Pennsylvania State Univ., University Park. Office for Remote Sensing of Earth Resources.
DELINEATION OF SOIL TEMPERATURE REGIMES FROM HCMM DATA Quarterly Report
R. L. DAY and G W. PETERSEN, Principal Investigators 31 Mar. 1982 3 p refs HCMM
(E82-10298; NASA-CR-168867; NAS 1 26 168867) Avail. NTIS HC A02/MF A01 CSCL 08M

The subsetting of HCMM data into ORSER format was completed for four dates using a modified SUBSET program. Large areas (approximately 2500 scan lines, 1680 elements) were selected to increase the occurrrence of suitable control points for registration Average daily temperatures (ADT) were calculated for each date. The MERGE program combined registered daytime temperature (DAY-IR) with nighttime temperature (NIGHT-IR) to form a separate two-channel data set The SUBTRAN program averaged the DAY-IR and NIGHT-IR creating a third ADT channel. Registration equations for the four ADT data sets were generated. A one dimensional soil heat flow equation was modified to allow for mean annual soil temperature predictions using merged ADT data sets A.R.H.

N82-24575*# Florida Univ , Gainesville.
USE OF THERMAL INERTIA DETERMINED BY HCMM TO PREDICT NOCTURNAL COLD PRONE AREAS IN FLORIDA Quarterly Report, 16 Sep. - 15 Dec. 1981
L. H ALLEN, JR., Principal Investigator, E CHEN, J. D. MARTSOLF, and P. H. JONES 15 Dec 1981 15 p refs HCMM
(Contract NAS5-26453)
(E82-10299; NASA-CR-168868; NAS 1 26:168868) Avail NTIS HC A02/MF A01 CSCL 04B

Surface temperatures derived from HCMM data were compared with to those obtained by GOES satellite and the apparent thermal inertia (ATI) calculated. For two dates, the HCMM temperatures appear to be about 5 C lower than the GOES temperatures. The ATI for excessively-drained to well-drained mineral soils was greater than for drained organic soils possibly because of long periods of low rainfall during late 1980 and early 1981 Organic soils cropped to sugar cane showed lower ATI after a severe killing freeze. With dead leaves, there was less transpiration and more solar radiation probably reached the dark soil surface. This would explain the larger diurnal temperature amplitude observed. A.R.H.

N82-24576*# Instituto Geografico Nacional, Madrid (Spain).
THERMAL MAPPING, GEOTHERMAL SOURCE LOCATION, NATURAL EFFLUENTS AND PLANT STRESS IN THE MEDITERRANEAN COAST OF SPAIN Final Report, Sep. 1978 - Aug. 1980
R. N. DELASCUEVAS, Principal Investigator and A M. DEARAGON 31 Mar. 1981 218 p Sponsored by NASA Original contains color imagery. Original imagery may be purchased from NASA Goddard Space Flight Center, (code 601), Greenbelt, Md. 20070 Domestic users send orders to 'Attn: National Space Science Data Center', non-domestic users send orders to 'Attn· World Data Center A for Rockets and Satellites' HCMM (E82-10300; NASA-CR-168869; NAS 1.26 168869) Avail: NTIS HC A10/MF A01 CSCL 08G

Data obtained by HCMM satellite over a complex area in eastern Spain were evaluated and found to be most useful in studying macrostructures in geology and in analyzing marine currents, layers, and areas (although other satellites provide more data) The upper scale to work with HCMM data appears to be 1:2.000.000 Techniques used in preprocessing, processing, and analyzing imagery are discussed as well as methods for pattern recognition. Surface temperatures obtained for soils, farmlands, forests, geological structures, and coastal waters are discussed Suggestions are included for improvements needed to achieve better results in geographic areas similar to the study area.
E A K.

N82-24585*# Pennsylvania State Univ., University Park Dept of Meteorology.
A METHOD FOR INFERRING AVAILABLE SURFACE MOISTURE USING REMOTE SURFACE TEMPERATURE MEASUREMENTS: AN ASSESSMENT
T. N. CARLSON, Principal Investigator Feb 1982 33 p refs Sponsored by NASA ERTS
(E82-10311; NASA-CR-168886; NAS 1.26 168886) Avail: NTIS HC A03/MF A01 CSCL 08M

A method for inferring surface moisture availability, which combines a numerical boundary layer model with remote estimates of surface-temperature, is evaluated with regard to its ability to provide significant results. Some analyses of surface moisture availability based on GOES and on HCMM surface temperature measurements are presented for an urban area (St. Louis) and for a drought situation over Kansas Patterns of moisture availability clearly indicate a relationship between land use, particularly vegetation cover, and derived moisture availability over urban areas and also suggest a relationship between antecedent rainfall and derived moisture availability over vegetated regions. Author

N82-24602*# South Dakota State Univ., Brookings Remote Sensing Inst.

EVALUATION OF HCMM DATA FOR ASSESSING SOIL MOISTURE AND WATER TABLE DEPTH Final Report, Jun. 1977 - Mar. 1981

D. G. MOORE, J. L HEILMAN, J A. TUNHEIM, F C. WESTIN, W E HEILMAN, G. A. BEUTLER, and S D NESS, Principal Investigators Aug. 1981 205 p refs Original contains imagery Original imagery may be purchased from NASA Goddard Space Flight Center, (code 601), Greenbelt, Md. 20770 Domestic users send orders to 'Attn National Space Science Data Center', nondomestic users send orders to 'Attn World Data Center A for Rockets and Satellites' HCMM

(Contract NAS5-24206)

(E82-10329; NASA-CR-168944; NAS 1.26:168944; SDSU-RS1-81-04) Avail NTIS HC A10/MF A01 CSCL 08M

Soil moisture in the 0-cm to 4-cm layer could be estimated with 1-mm soil temperatures throughout the growing season of a rainfed barley crop in eastern South Dakota Empirical equations were developed to reduce the effect of canopy cover when radiometrically estimating the soil temperature. Corrective equations were applied to an aircraft simulation of HCMM data for a diversity of crop types and land cover conditions to estimate the soil moisture. The average difference between observed and measured soil moisture was 1.6% of field capacity. Shallow alluvial aquifers were located with HCMM predawn data. After correcting the data for vegetation differences, equations were developed for predicting water table depths within the aquifer. A finite difference code simulating soil moisture and soil temperature shows that soils with different moisture profiles differed in soil temperatures in a well defined functional manner A significant surface thermal anomaly was found to be associated with shallow water tables. A R H

N82-25605*# Texas A&M Univ., College Station. Remote Sensing Center.

ORBITING PASSIVE MICROWAVE SENSOR SIMULATION APPLIED TO SOIL MOISTURE ESTIMATION Final Report

R. W. NEWTON, Principal Investigator, B V CLARK, W. M PITCHFORD, and J F PARIS (Houston Univ., Clear Lake City) Dec. 1979 219 p Original contains imagery Original photography may be purchased from the EROS Data Center, Sioux Falls, S.D 57198 ERTS

(Contract NSG-5266)

(E82-10343; NASA-CR-168960, NAS 1.26:168960, RSC-3753) Avail NTIS HC A10/MF A01 CSCL 08M

A sensor/scene simulation program was developed and used to determine the effects of scene heterogeneity, resolution, frequency, look angle, and surface and temperature relations on the performance of a spaceborne passive microwave system designed to estimate soil water information. The ground scene is based on classified LANDSAT images which provide realistic ground classes, as well as geometries. It was determined that the average sensitivity of antenna temperature to soil moisture improves as the antenna footprint size increased. Also, the precision (or variability) of the sensitivity changes as a function of resolution M.G

N82-25606*# Purdue Univ., Lafayette, Ind Lab for Applications of Remote Sensing

FOREST RESOURCE INFORMATION SYSTEM. PHASE 3: SYSTEM TRANSFER REPORT Final Report, 1 Apr. 1979 - 31 Dec. 1980

R P. MROCZYNSKI, Principal Investigator 30 Jul 1981 142 p refs Original contains imagery Original photography may be purchased from the EROS Data Center, Sioux Falls, S.D. 57198 ERTS

(Contract NAS9-15325)

(E82-10344; NASA-CR-167544, NAS 1.26:167544; LARS-073081) Avail: NTIS HC A07/MF A01 CSCL 02F

Transfer of the forest reserve information system (FRIS) from the Laboratory for Applications of Remote Sensing to St Regis Paper Company is described. Modifications required for the transfer of the LARYS image processing software are discussed. The reformatting, geometric correction, image registration, and documentation performed for preprocessing transfer are described Data turnaround was improved and geometrically corrected and ground-registered CCT LANDSAT 3 data provided to the user The technology transfer activities are summarized An application test performed in order to assess a Florida land acquisition is described. A benefit/cost analysis of FRIS is presented. J D.

N82-25607*# Utah Univ., Salt Lake City. Center for Remote Sensing and Cartography

INVENTORY OF WETLANDS AND AGRICULTURAL LAND COVER IN THE UPPER SEVIER RIVER BASIN, UTAH

R A JAYNES, L. D CLARK, JR , and K. F. LANDGRAF, Principal Investigator 31 Oct. 1981 40 p refs ERTS

(Contract NAGW-95)

(E82-10345, NASA-CR-168961) Avail. NTIS HC A03/MF A01 CSCL 08B

The use of color infrared aerial photography in the mapping of agricultural land use and wetlands in the Sevier River Basin of south central utah is described. The efficiency and cost effectiveness of utilizing LANDSAT multispectral scanner digital data to augment photographic interpretations are discussed Transparent overlays for 27 quadrangles showing delineations of wetlands and agricultural land cover were produced. A table summarizing the acreage represented by each class on each quadrangle overlay is provided J D.

N82-25608*# National Aeronautics and Space Administration, Washington, D C

PLAN OF RESEARCH FOR INTEGRATED SOIL MOISTURE STUDIES. RECOMMENDATIONS OF THE SOIL MOISTURE WORKING GROUP

Oct. 1980 111 p refs

(NASA-TM-84731; NAS 1.15 84731) Avail NTIS HC A06/MF A01 CSCL 08M

Soil moisture information is a potentially powerful tool for applications in agriculture, water resources, and climate At present, it is difficult for users of this information to clearly define their needs in terms of accuracy, resolution and frequency because of the current sparsity of data. A plan is described for defining and conducting an integrated and coordinated research effort to develop and refine remote sensing techniques which will determine spatial and temporal variations of soil moisture and to utilize soil moisture information in support of agricultural, water resources, and climate applications The soil moisture requirements of these three different application areas were reviewed in relation to each other so that one plan covering the three areas could be formulated. Four subgroups were established to write and compile the plan, namely models, ground-based studies, aircraft experiments, and spacecraft missions A.R.H.

N82-26742*# Purdue Univ., Lafayette, Ind Lab for Applications of Remote Sensing

SPECTRAL ESTIMATES OF SOLAR RADIATION INTERCEPTED BY CORN CANOPIES

M E. BAUER, Principal Investigator, C. S. T. DAUGHTRY, and K. P. GALLO Mar. 1982 17 p refs Sponsored by NASA, USDA, Dept of Commerce, Dept. of the Interior, and Agency for International Development ERTS

(Contract NAS9-15466, PROJ AGRISTARS)

(E82-10003; NASA-CR-167643, SR-P2-04236, NAS 1 26 169032; LARS-030182) Avail. NTIS HC A02/MF A01 CSCL 20F

Reflectance factor data were accquired with a Landsat band radiometer throughout two growing seasons for corn (Zea mays L.) canopies differing in planting dates, populations, and soil types. Agronomic data collected included leaf area index (LAI), biomass, development stage, and final grain yields The spectral variable, greenness, was associated with 78 percent of the variation in LAI over all treatments Single observations of LAI or greenness have limited value in predicting corn yields. The proportions of solar radiation intercepted (SRI) by these canopies were estimated using either measured LAI or greenness Both SRI estimates, when accumulated over the growing season, accounted for approximately

65 percent of the variation in yields. Models which simulated the daily effects of weather and intercepted solar radiation on growth had the highest correlations to grain yields This concept of estimating intercepted solar radiation using spectral data represents a viable approach for merging spectral and meteorological data for crop yield models. Author

N82-26745*# Morgan State Coll, Baltimore, Md. Dept. of Biology.
RELATING THEMATIC MAPPER BANDS TM3, TM4, AND TM5 TO AGRONOMIC VARIABLES FOR CORN, COTTON, SUGARBEET, SOYBEAN, SORGHUM, SUNFLOWER AND TOBACCO Final Technical Report, 1 Apr. 1981 - 31 Mar. 1982
C. J FAN, Principal Investigator 31 Mar. 1982 25 p refs ERTS
(Contract NAG5-12)
(E82-10347; NASA-CR-168856; NAS 1.26:168856) Avail NTIS HC A02/MF A01 CSCL 02C

Red, photographic infrared, near infrared spectral data of corn, cotton, soybeans, sugar beets, sorghum, sunflowers and tobacco were collected throughout the entire growing season by using a three band handheld radiometer Different radiance patterns were found among these crops based on their morphology, green biomass duration and leaf size. Results show near infrared radiance is a good indicator of water content in plant tissue under small scale experimental conditions. E.A.K.

N82-26747*# California Univ., Santa Barbara Geography Remote Sensing Unit
MULTISPECTRAL DETERMINATION OF SOIL MOISTURE-2 Annual Technical Report
J. E. ESTES, D S SIMONETT, Principal Investigators, E J HAJIC, B. M. HILTON, and R D. LEES Apr. 1982 252 p refs Prepared in cooperation with Texas A and M Univ., College Station ERTS
(Contract NCC5-5)
(E82-10349, NASA-CR-168967, NAS 1.26:168967) Avail: NTIS HC A12/MF A01 CSCL 08M

Soil moisture data obtained using scatterometers, modular multispectral scanners and passive microwave radiometers were revised and grouped into four field cover types for statistical anaysis. Guymon data are grouped as alfalfa, bare, milo with rows perpendicular to the field view, and milo viewed parallel to the field of view Dalhart data are grouped as bare combo, stubble, disked stubble, and corn field Summary graphs combine selected analyses to compare the effects of field cover. The analysis for each of the cover types is presented in tables and graphs. Other tables show elementary statistics, correlation matrices, and single variable regressions. Selected eigenvectors and factor analyses are included and the highest correlating sensor typs for each location are summarized. E.A.K.

N82-26749*# Kansas Univ. Center for Research, Inc., Lawrence. Remote Sensing Lab
EVALUATION OF THE SOIL MOISTURE PREDICTION ACCURACY OF A SPACE RADAR USING SIMULATION TECHNIQUES Final Report
F. T. ULABY, Principal Investigator, M. C. DOBSON, J. A. STILES, R. K MOORE, and J. C. HOLTZMAN May 1981 208 p refs Original contains imagery. Original photography may be purchased from the EROS Data Center, Sioux Falls, S.D. 57198 ERTS
(Contract NAS5-25807)
(E82-10351; NASA-CR-166801; NAS 1.26:166801; RSL-TR-429-1)
Avail: NTIS HC A10/MF A01 CSCL 08M

Image simulation techniques were employed to generate synthetic aperture radar images of a 17.7 km x 19.3 km test site located east of Lawrence, Kansas The simulations were performed for a space SAR at an orbital altitude of 600 km, with the following sensor parameters. frequency = 4.75 GHz, polarization = HH, and angle of incidence range = 7 deg to 22 deg from nadir. Three sets of images were produced corresponding to three different spatial resolutions; 20 m x 20 m with 12 looks, 100 m x 100 m with 23 looks, and 1 km x 1 km with 1000 looks Each set consisted of images for four different soil moisture distributions across the test site. Results indicate that, for the agricultural portion of the test site, the soil moisture in about 90% of the pixels can be predicted with an accuracy of = + or - 20% of field capacity Among the three spatial resolutions, the 1 km x 1 km resolution gave the best results for most cases, however, for very dry soil conditions, the 100 m x 100 m resolution was slightly superior. A R.H.

N82-26751*# Environmental Research Inst. of Michigan, Ann Arbor Infrared and Optics Div
ASSOCIATION OF SPECTRAL DEVELOPMENT PATTERNS WITH DEVELOPMENT STAGES OF CORN Technical Report, 1 Nov. 1981 - 31 Jan. 1982
E. P. CRIST, Principal Investigator Feb 1982 37 p refs Sponsored by NASA, USDA, Dept of Commerce, Dept. of the Interior, and Agency for International Development ERTS
(Contract NAS9-16538, PROJ. AGRISTARS)
(E82-10353; NASA-CR-167604; NAS 1.26:167604, IT-E2-04235, ERIM-160300-7-T) Avail: NTIS HC A03/MF A01 CSCL 02C

Association is made between the development stages of corn as defined by Hanway and the temporal-spectral development pattern of corn in a transformed data space derived from Landsat-MSS band reflectance values, using field-collected reflectance and associated data. Results indicate that the spectral vegetation index used (a reflectance equivalent of Tasseled Cap Greenness) reaches a maximum well before the stage at which corn is expected to achieve its peak leaf area index. Possible physiological and canopy geometry related causes for this and other results are presented. Author

N82-26752*# Utah Univ, Salt Lake City Center for Remote Sensing and Cartography
MAPPING OF WILDLIFE HABITAT IN FARMINGTON BAY, UTAH
R. A JAYNES and R. D. WILLIE, Principal Investigators 1982 15 p refs ERTS
(Contract NAGW-95)
(E82-10354; NASA-CR-168975; NAS 1.26:168975, CRSC-82-1)
Avail NTIS HC A02/MF A01 CSCL 08B

Mapping was accomplished through the interpretation of high-altitude color infrared photography. The feasibility of utilizing LANDSAT digital data to augment the analysis was explored; complex patterns of wildlife habitat and confusion of spectral classes resulted in the decision to make limited use of LANDSAT data in the analysis. The final product is a map which delineates wildlife habitat at a scale of 1:24,000. The map is registered to and printed on a screened U S G S. quadrangle base map. Screened delineations of shoreline contours, mapped from a previous study, are also shown on the map Intensive field checking of the map was accomplished for the Farmington Bay Waterfowl Management Area in August 1981; other areas on the map received only spot field checking. Author

N82-26753*# Utah Univ., Salt Lake City. Center for Remote Sensing and Cartography.
DETECTION OF VARIATIONS IN ASPEN FOREST HABITAT FROM LANDSAT DIGITAL DATA: BEAR RIVER RANGE, UTAH
J A MEROLA and R. A JAYNES, Principal Investigators 17 Mar. 1982 34 p refs Sponsored in part by US Forest Service ERTS
(Contract NAGW-95; NSF SPI-80-03978)
(E82-10355; NASA-CR-168976; NAS 1.26.168976; CRSC-82-2)
Avail: NTIS HC A03/MF A01 CSCL 02F

The aspen forests of the Bear River Range were analyzed and mapped using data recorded on July 2, 1979 by the LANDSAT III satellite; study efforts yielded sixty-seven light signatures for the study area, of which three groups were identified as aspen and mapped at a scale of 1 24,000. Analysis and verification of the three groups were accomplished by random location of twenty-six field study plots within the LANDSAT-defined aspen areas All study plots are included within the Cache portion of the

Wasatch-Cache National Forest. The following selected site characteristics were recorded for each study plot: a list of understory species present, average percent cover density for understory species; aspen canopy cover estimates and stem measurements; and general site topographic characteristics The study plot data were then analyzed with respect to corresponding Landsat spectral signatures. Field studies show that all twenty-six study plots are associated with one of the three aspen groups. Further study efforts concentration on characterizing the differences between the site characteristics of plots falling into each of the three aspen groups Author

N82-26754*# Utah Univ, Salt Lake City Center for Remote Sensing and Cartography
IRRIGATED ACREAGE IN THE BEAR RIVER BASIN AS OF THE 1975 GROWING SEASON
M. K. RIDD, R A. JAYNES, K F LANDGRAF, and L. D CLARK, JR., Principal Investigators 8 Apr 1982 28 p refs Original contains color imagery Original photography may be purchased *from the EROS Data Center, Sioux Falls, S D. 57198* ERTS
(Contract NAGW-95)
(E82-10356, NASA-CR-168977; NAS 1.26:168977; CRSC-82-3)
Avail NTIS HC A03/MF A01 CSCL 02C

The irrigated cropland in the Bear River Basin as of the 1975 growing season was inventoried from satellite imagery LANDSAT color infrared images (scale 1 125,000) were examined for early, mid, and late summer dates, and acreage was estimated by use of township/section overlays. The total basin acreage was estimated to be 573,435 acres, with individual state totals as follows: Idaho 234,370 acres, Utah 265,505 acres, and Wyoming 73,560 acres As anticipated, wetland areas intermingled among cropland appears to have produced an over-estimation of irrigated acreage. According to a 2% random sample of test sites evaluated by personnel from the Soil Conservation Service such basin-wide over-estimation is 7.5%; individual counties deviate significantly from the basin-wide figure, depending on the relative amount of wetland areas intermingled with cropland. Author

N82-26755*# South Dakota State Univ., Brookings Remote Sensing Inst.
IRRIGATION MANAGEMENT WITH REMOTE SENSING Final Technical Report, Apr. 1980 - Sep. 1981
C. HARLAN, J. HEILMAN, D. MOORE, and V. MYERS, Principal Investigators Feb. 1982 48 p refs
(Contract NAG5-37)
(E82-10357; NASA-CR-168978; NAS 1.26:168978;
SDSU-RSI-82-02) Avail: NTIS HC A03/MF A01 CSCL 08H

Two visible/near IR hand held radiometers and a hand held thermoradiometer were used along with soil moisture and lysimetric measurements in a study of soil moisture distribution in afalfa fields on the Navajo Indian Irrigation Project near Farmington, New Mexico. Radiances from irrigated plots were measured and converted to reflectances. Surface soil water contents (o cm to 4 cm) were determined gravimetrically on samples collected at the same time as the spectral measurements. The relationship between the spectral measurements and the crop coefficient were evaluated to demonstrate potential for using spectral measurement to estimate crop coefficient E A.K.

N82-26759*# Texas A&M Univ., College Station. Remote Sensing Center.
MEASUREMENT OF SOIL MOISTURE TRENDS WITH AIRBORNE SCATTEROMETERS Final Report
C. L. JONES, M. J. MCFARLAND, W. D. ROSETHAL, and S. W THEIS, Principal Investigators Feb. 1982 194 p refs ERTS
(Contract NSG-5134)
(E82-10361, NASA-CR-169010; NAS 1.26.169010;
RSC-3458-131) Avail. NTIS HC A09/MF A01 CSCL 08M

In an effort to investigate aircraft multisensor responses to soil moisture and vegetation in agricultural fields, an intensive ground sampling program was conducted in Guymon, Oklahoma and Dalhart, Texas in conjunction with aircraft data collected for visible/infrared and passive and active microwave systems Field selections, sampling techniques, data processing, and the aircraft schedule are discussed for both sites. Field notes are included along with final (normalized and corrected) data sets A.R.H

N82-26760*# Texas A&M Univ, College Station. Remote Sensing Center
MULTIFREQUENCY REMOTE SENSING OF SOIL MOISTURE Final Report
S. W THEIS, M. J MCFARLAND, W D. ROSENTHAL, and C. L JONES, Principal Investigator Feb. 1982 145 p refs ERTS
(Contract NSG-5134)
(E82-10362; NASA-CR-169011, NAS 1 26.169011,
RSC-3458-129) Avail. NTIS HC A07/MF A01 CSCL 08M

Multifrequency sensor data collected at Guymon, Oklahoma and Dalhart, Texas using NASA's C-130 aircraft were used to determine which of the all-weather microwave sensors demonstrated the highest correlation to surface soil moisture over optimal bare soil conditions, and to develop and test techniques which use visible/infrared sensors to compensate for the vegetation *effect in this sensor's response to soil moisture The L-band passive* microwave radiometer was found to be the most suitable single sensor system to estimate soil moisture over bare fields. In comparison to other active and passive microwave sensors the L-band radiometer (1) was influenced least by ranges in surface roughness, (2) demonstrated the most sensitivity to soil moisture differences in terms of the range of return from the full range of soil moisture; and (3) was less sensitive to errors in measurement in relation to the range of sensor response. L-band emissivity related more strongly to soil moisture when moisture was expressed as percent of field capacity. The perpendicular vegetation index as determined from the visible/infrared sensors was useful as a measure of the vegetation effect on the L-band radiometer response to soil moisture. A R.H.

N82-26761*# Texas A&M Univ., College Station. Remote Sensing Center.
DEVELOPMENT OF VISIBLE/INFRARED/MICROWAVE AGRICULTURE CLASSIFICATION AND BIOMASS ESTIMATION ALGORITHMS Final Report
W. D. ROSENTHAL, M J MCFARLAND, S. W. THEIS, and C. L JONES, Principal Investigtors Feb. 1982 221 p refs ERTS
(Contract NSG-5134)
(E82-10363, NASA-CR-169012) Avail: NTIS HC A10/MF A01 CSCL 02C

Agricultural crop classification models using two or more spectral regions (visible through microwave) are considered in an effort to estimate biomass at Guymon, Oklahona Dalhart, Texas Both grounds truth and aerial data were used Results indicate that inclusin of C, L, and P band active microwave data, from look angles greater than 35 deg from nadir, with visible and infrared data improve crop discrimination and biomass estimates compared to results using only visible and infrared data. The microwave frequencies were sensitive to different biomass levels. The K and C band were sensitive to differences at low biomass levels, while P band was sensitive to differences at high biomass levels. Two indices, one using only active microwave data and the other using data from the middle and near infrared bands, were well correlated to total biomass It is implied that inclusion of active microwave sensors with visible and infrared sensors on future satellites could aid in crop discrimination and biomass estimation. E.A.K.

N82-26762# California Univ, Santa Barbara.
THE USE OF SOIL TEXTURE AND FIELD CAPACITY TO NORMALIZE MICROWAVE SOIL MOISTURE MEASUREMENTS: SOME PROBLEMS M.S. Thesis
R. D. LEES May 1982 72 p refs Sponsored by Texas A & M Univ.
Avail: NTIS HC A04/MF A01

Soil moisture normalizing techniques attempt to explain variations in soil-water content between soils in terms of soil texture based on the percent sand, silt and clay in the soil. A critical analysis of these techniques was made to examine their *effectiveness in comparing soils of varying texture and soil moisture*

content in relation to their microwave (radar) backscatter While the particle size distribution is recognized as a significant factor in the soil-water relationship, its influence is regulated by a number of other factors Results indicate that 'normalization' by use of field capacity - derived from the percentages of sand, silt and clay - actually reduced the sensitivity of backscattering coefficient to soil-water content. The water holding capacity of soils is variably influenced by properties such as soil structure, clay mineral type, organic matter content, aeration, soil layering, and hysteresis and related water addition and extraction processes. B.W.

02

ENVIRONMENTAL CHANGES AND CULTURAL RESOURCES

Includes land use analysis, urban and metroplitan studies, environmental impact, air and water pollution, geographic information systems, and geographic analysis

A82-22545
DEPENDENCE OF EARTH SPECTRUM OF POSITRONS AND ANTIPROTONS ON PROPAGATION MODELS
S A STEPHENS (Tata Institute of Fundamental Research, Bombay, India) In: International Cosmic Ray Conference, 17th, Paris, France, July 13-25, 1981, Conference Papers Volume 2. Gif-sur-Yvette, Essonne, France, Commissariat a l'Energie Atomique, 1981, p 214-217 refs

A calculation of the equilibrium spectra of positrons and antiprotons for different models are presented. A total of five propagation models is considered, comprising a simple leak box, a modified leaky box, a nested leaky box, a simple closed galaxy, and a modified closed galaxy The antiproton spectrum is noted to be dependent only on the propagation model and not on the solar modulation, which supports the use of an antiproton spectrometer in monitoring the degree of solar modulation Kinetic energy fluxes are determined for the two components as predicted for each model, and observed antiproton fluxes are shown to rule out the modified and nested leaky box models. The modified closed galaxy model is found to accurately predict solar modulation from low energy data, and positron data at high energies is taken to quantify the mean gas density in a region of total confinement to be 0 05 atoms/cu cm. M.S.K.

A82-22562
ON THE STELLAR ORIGIN OF THE NE-22 EXCESS IN COSMIC RAYS
M. CASSE and J. A. PAUL (Commissariat a l'Energie Atomique, Centre d'Etudes Nucleaires de Saclay, Gif-sur-Yvette, Essonne, France) In International Cosmic Ray Conference, 17th, Paris, France, July 13-25, 1981, Conference Papers. Volume 2. Gif-sur-Yvette, Essonne, France, Commissariat a l'Energie Atomique, 1981, p. 293-295. refs

A82-22566
COSMIC RAY ACCELERATION BY STELLAR WINDS. I - TOTAL DENSITY, PRESSURE AND ENERGY FLUX
G. M. WEBB, W. I AXFORD (Max-Planck-Institut fuer Aeronomie, Katlenburg, West Germany), and M A. FORMAN (New York, State University, Stony Brook, NY) In. International Cosmic Ray Conference, 17th, Paris, France, July 13-25, 1981, Conference Papers. Volume 2. Gif-sur-Yvette, Essonne, France, Commissariat a l'Energie Atomique, 1981, p. 309-312. refs

A82-22567
ON THE STELLAR ORIGIN OF LOW ENERGY COSMIC RAYS
S BISWAS, N DURGAPRASAD, and S S TRIVEDI (Tata Institute of Fundamental Research, Bombay, India) In. International Cosmic Ray Conference, 17th, Paris, France, July 13-25, 1981, Conference Papers. Volume 2. Gif-sur-Yvette, Essonne, France, Commissariat a l'Energie Atomique, 1981, p 314-317 refs

The hypothesis is proposed that energetic ions of He, C, N, O, etc., in the low energy (1 to 50 MeV/amu) anomalous component of cosmic rays, originate from O-type stars which manifest very strong stellar winds with very high mass loss rates of about 3 x 10 to the -6th solar mass/yr These have terminal velocities of 1200-4000 km/s which are typically several times their escape velocities. These velocities correspond to ion energies of 10 to 200 keV/amu. These ions of energy of about 100 keV/amu are in partly ionized states and are accelerated in the interstellar shock fronts to about 10 MeV/amu, thus accounting for the observed anomalous component of low-energy cosmic rays (Author)

A82-22569
REMARKS ON COSMIC RAY ORIGIN
V. L. GINZBURG (Akademiia Nauk SSSR, Fizicheskii Institut, Moscow, USSR) and V. S PTUSKIN (Akademiia Nauk SSSR, Institut Zemnogo Magnetizma Ionosfery i Rasprostraneniia Radiovoln, Troitsk, USSR) In: International Cosmic Ray Conference, 17th, Paris, France, July 13-25, 1981, Conference Papers Volume 2. Gif-sur-Yvette, Essonne, France, Commissariat a l'Energie Atomique, 1981, p 336-339. refs

Various problems related to current work on the origins of cosmic rays are considered. The acceleration of cosmic ray particles at the spherical front of an interstellar shock wave is analyzed, and a value of 10 to the 12th eV is obtained for the upper limit to accelerated particle energies. Transport in the Galaxy by means of large-scale turbulent motions is shown to produce a cosmic ray diffusion coefficient that is too low, while acceleration due to scattering by isotropic magnetohydrodynamic turbulence is also small A possible method for the estimation of the contribution of local sources to cosmic ray concentrations observed near the earth is also presented, and possible explanations are suggested for the recent gamma ray observations of lowered cosmic ray electron concentrations at a distance less than 2 kpc from the galactic center. A.L W.

A82-22570
PULSAR MODELS AND COSMIC-RAY ACCELERATION
F. C. MICHEL and A. J DESSLER (Rice University, Houston, TX) In: International Cosmic Ray Conference, 17th, Paris, France, July 13-25, 1981, Conference Papers. Volume 2. Gif-sur-Yvette, Essonne, France, Commissariat a l'Energie Atomique, 1981, p. 340-343. refs

It is argued that radio pulsars and X-ray pulsars differ mainly in the fact that the the latter are surrounded by an inward moving accretion disk while the former are surrounded by an outward moving fossil collapse disk presumably left over from the formation event. Cosmic rays of more-or-less 'solar' composition can be accelerated to energies of 10 to the 20th eV shortly after the formation event. (Author)

A82-22583
SOLAR GAMMA-RAY EXPERIMENT ON ASTRO-A SATELLITE
K. OKUDAIRA, Y HIRASIMA, M. YOSHIMORI (Rikkyo University, Tokyo, Japan), and I. KONDO (Tokyo, University, Tanashi, Japan) In: International Cosmic Ray Conference, 17th, Paris, France, July 13-25, 1981, Conference Papers Volume 3 Gif-sur-Yvette, Essonne, France, Commissariat a l'Energie Atomique, 1981, p. 11-14 refs

The instrumentation and performance parameters of the Japanese Astro-A satellite for measuring solar gamma ray lines and continua associated with solar flares are described. A gamma ray spectrometer which is a phoswich scintillator covers the gamma ray range from 0.24-6.48 MeV with a resolution of 10 percent at 662 keV. Techniques to discern gamma ray from particle events are discussed, along with the 128 channel pulse height analyzer

with three regions for the pulse height spectrum. Low bit rates are recorded during quiet modes, and high speed rates are enacted during a solar flare The spacecraft was launched in Feb 1981 and is in-flight calibrated by reference to the atmospheric positron annihilation line at 0.51 MeV M.S K

A82-22588
HIGH-ENERGY SOLAR PROTONS
N. N VOLODICHEV and I. A SAVENKO (Moskovskii Gosudarstvennyi Universitet, Moscow, USSR) In: International Cosmic Ray Conference, 17th, Paris, France, July 13-25, 1981, Conference Papers. Volume 3. Gif-sur-Yvette, Essonne, France, Commissariat a l'Energie Atomique, 1981, p 45-48. refs

Evidence is presented for a second particle acceleration phase following the explosive phase of a solar flare. Cerenkov and scintillation counters were employed on the Prognoz satellite to detect the arrival of protons with energies greater than 100 MeV or 500 MeV, respectively. Delays of several minutes to several tens of minutes were observed for the arrival of protons from radiobursts in the cm range and X ray bursts during solar flare activity A similar delay was recorded on the Proton-3 satellite during a burst event of Nov. 22, 1977, using the same measurement techniques. The existence of a second acceleration phase, when protons are accelerated to high energies and electrons up to relativistic energies, is noted to not contradict a model of the explosive phase of the flare as a process of disappearance and break of the current layer in the region of a highly dense plasma M.S.K.

A82-22605* Maryland Univ , College Park.
TIME AND ENERGY DEPENDENCE OF HEAVY ION ABUNDANCES IN SOLAR FLARE ENERGETIC PARTICLE EVENTS
G. M MASON, H. WEISS, G GLOECKLER (Maryland, University, College Park, MD), and D. HOVESTADT (Max-Planck-Institut fuer Physik und Astrophysik, Garching, West Germany) In: International Cosmic Ray Conference, 17th, Paris, France, July 13-25, 1981, Conference Papers Volume 3. Gif-sur-Yvette, Essonne, France, Commissariat a l'Energie Atomique, 1981, p 124-127 refs
(Contract NAS5-11063; NAS5-25735; NGR-21-002-316)

Data from a survey of solar flare events undertaken by the UMD/MPI ULET telescope on the IMP-8 satellite during the period 1973-1977 yields examples of time and energy dependence of the abundances and spectra of the He, C, O and Fe heavy ions. Time variations are found in the O/He, O/C and Fe/O ratios which appear to be inconsistent with models based entirely on rigidity-dependent propagation in the interplanetary medium It is speculated that such other factors as the abundance differences at the flare site on the sun, or features of the acceleration and release mechanisms, may play an important role in the variations discussed O.C

A82-22606* California Inst of Tech., Pasadena.
HIGH RESOLUTION MEASUREMENTS OF SOLAR FLARE ISOTOPES
R. A. MEWALDT, J. D. SPALDING, E. C. STONE, and R. E. VOGT (California Institute of Technology, Pasadena, CA) In: International Cosmic Ray Conference, 17th, Paris, France, July 13-25, 1981, Conference Papers Volume 3. Gif-sur-Yvette, Essonne, France, Commissariat a l'Energie Atomique, 1981, p. 131-134. refs
(Contract NAS5-20721; NGR-05-002-160)

The individual isotopes of C, N and O are measured in the large solar particle event of August 1978 Limits are placed on mass dependent selection effects occurring in the solar flare by fitting a simple mass fractionation law to measurements of the C, N, O and Mg isotopes, to relate the SEP composition more directly to the composition of the sun. The individual isotopes are found to be consistent with solar system abundances, and the absence of any observable fractionation for C, O and Mg leads to the conclusion that solar neon is most likely neon-A with Ne-22/Ne-20 equals 0 12. D.L.G.

A82-22616
11-YEAR MODULATION AND SPECTRUM OF COSMIC RAYS IN THE INTERSTELLAR SPACE
A. G ZUSMANOVICH (Akademiia Nauk Kazakhskoi SSR, Sektor Ionosfery, Alma-Ata, Kazakh SSR) In: International Cosmic Ray Conference, 17th, Paris, France, July 13-25, 1981, Conference Papers Volume 3. Gif-sur-Yvette, Essonne, France, Commissariat a l'Energie Atomique, 1981, p. 183-186 refs

The 11-year modulation in cosmic ray intensity is examined with a view towards the study of cosmic ray spectra in interstellar space. The steady-state, homogeneous solution of the cosmic ray modulation equation is used to determine a value of 0 4 plus or minus 0.1 for the modulation coefficient and a value between 15 and 20 GV for the rigidity of the unmodulated spectrum. Cosmic ray spectra outside the modulation region are then calculated from the modulation coefficient and differential energy spectra measured near earth at solar activity minimum, taking into account cosmic ray energy changes during passage through interplanetary space. Results are shown to be in agreement with measurements of galactic gamma ray intensities A.L.W.

A82-29327
DETECTION OF ENVIRONMENTAL DISTURBANCE USING COLOR AERIAL PHOTOGRAPHY AND THERMAL INFRARED IMAGERY
S. ARONOFF and G A. ROSS (Calgary, University, Calgary, Alberta, Canada) Photogrammetric Engineering and Remote Sensing, vol 48, Apr 1982, p. 587-591. Research supported by the Alberta Oil Sands Environmental Research Program. refs

Characteristics of a program for satellite remote sensing for long-period environmental monitoring are examined, noting that establishing early mapping surveys of areas of concern aids in detection of stressful environmental conditions The process is described with an example from IR and color photography of a 30,000 sq km area in the Athabasca Oil Sands, with the photography carried out from aircraft and satellite The IR data was gathered between 8-14 microns and the photographs were taken at a 1:11,000 scale. Water-related disturbances detected included turbidity which indicated the possible presence of oil, and higher thermal emission near a tailings pond which also suggested an oil source. The presence of surface aquatic vegetation is an indicator of nutrient imbalance in a pond near a sewage pond. Finally, dead trees were observed near improperly installed culverts along new roads. M S K

A82-29332* South Carolina Univ., Columbia.
DETECTING RESIDENTIAL LAND-USE DEVELOPMENT AT THE URBAN FRINGE
J. R. JENSEN (South Carolina, University, Columbia, SC) and D. L. TOLL (NASA, Goddard Space Flight Center, Greenbelt, MD) Photogrammetric Engineering and Remote Sensing, vol. 48, Apr. 1982, p 629-643. refs

Problems associated with the use of Landsat multispectral scanner (MSS) imagery for the detection of urban growth and land use patterns are discussed. The presence of vegetation, either original or added between scanning periods, has been found to dramatically effect the range of signatures in a given area. Different land use developmental stages have been successfully identified by means of 1:50,000 scale panchromatic aerial photography, a resolution only considered possible by spaceborne instrumentation with the advent of the Landsat D satellite. Textural information generated through the grey-tone spatial-dependency matrix for the Landsat band 5 data is compared for different years and a change detection algorithm is described. It is found that the addition of vegetation during development after the removal of natural vegetation resulted in error of omission in the single band data, which must therefore only be used in concert with other data sources. M.S.K.

A82-30293
AIRCRAFT MONITORING OF SURFACE CARBON DIOXIDE EXCHANGE
R L. DESJARDINS, E. J BRACH (Agriculture Canada, Ottawa, Canada), P. ALVO, and P. H SCHUEPP (McGill University, Sainte Anne de Bellevue, Quebec, Canada) Science, vol. 216, May 14, 1982, p. 733-735 Research supported by Agriculture Canada and National Research Council. refs

Aircraft-mounted sensors were used to measure the exchange of carbon dioxide above a cornfield, a forest, and a lake under midday conditions Mean absorption values of 3400, 1200, and 100 milligrams of carbon dioxide per square meter per hour, respectively, are consistent with reported ground-based observations of carbon dioxide flux. Such information, gathered by aircraft, could be used to provide a quantitative evaluation of source and sink distributions of carbon dioxide in the biosphere, to establish a correlation between satellite data and near-surface measurements, and to monitor crop performance (Author)

A82-30307
PROBLEMS OF THE INTERPRETATION OF AERIAL AND SATELLITE IMAGES OF INDUSTRIAL SMOKE [PROBLEMY INTERPRETACJI LOTNICZYCH I SATELITARNYCH ZDJEC DYMOW PRZEMYSLOWYCH]
T. Z. DWORAK (Instytut Meteorologii i Gospodarki Wodnej, Krakow, Poland) Przeglad Geofizyczny, vol 25, no. 1, 1980, p 33-38. In Polish refs

Methods for the interpretation of aerial and satellite photographs of industrial smoke emissions are considered, with particular attention given to the difficulties of the qualitative interpretation of such images. Conditions that should be taken into account in an approximate solution of the radiative-transfer equations are examined. Recommendations on the practical solution of a specific satellite remote-sensing problem are presented B J

A82-31295#
DETECTION OF VOLCANIC SMOKE AND ASH-FALL AREA AT VOLCANO ASO, FROM LANDSAT MSS DATA
Y TANAKA (Meteorological Research Institute, Isukuba, Ibaraki, Japan), K. TSUCHIYA, and Y YAMAURA (National Space Development Agency of Japan, Tokyo, Japan) Papers in Meteorology and Geophysics, vol 32, Dec 1981, p. 275-290. refs

Landsat imagery is employed to determine the extent of volcanic smoke and ashfall associated with the eruptions of the volcano ASO in 1979 and 1980, and a comparison is made with nearby meteorological data. Pictures from four bands 0.5-0.6, 0.6-0.7, 0.7-0 8, and 0.8-1.1 micron, are analyzed for information on volcanic smoke, polluted sea water, vegetation, clouds, and visibility over urban areas The imagery comprises natural, false, and Ektachrome colors, taken from multispectral band scanners on Landsats 2 and 3 A qualitative analysis of volcanic smoke is developed, and a comparison of topographic data with the Landsat images showed that the Landsat pictures are useful and sufficiently accurate for detecting terrain changes due to the volcanic activity, including the forms of caldera. Assessment of the volcanic state, smoke, and ashfall were also possible using the Landsat imagery. M.S K.

A82-31990* Lincoln Lab., Mass Inst of Tech , Lexington.
DETECTION OF REGIONAL AIR POLLUTION EPISODES UTILIZING SATELLITE DIGITAL DATA IN THE VISUAL RANGE
H.-H. K. BURKE (MIT, Lincoln Laboratory, Lexington, MA) IEEE Transactions on Geoscience and Remote Sensing, vol GE-20, Apr. 1982, p. 154-158. refs
(Contract NAS1-15301)

Digital analyses of satellite visible data for selected high-sulfate cases over the northeastern U.S., on July 21 and 22, 1978, are compared with ground-based measurements. Quantitative information on total aerosol loading derived from the satellite digitized data using an atmospheric radiative transfer model is found to agree with the ground measurements, and it is shown that the extent and transport of the haze pattern may be monitored from the satellite data over the period of maximum intensity for the episode Attention is drawn to the potential benefits of satellite monitoring of pollution episodes demonstrated by the model O.C

A82-32342* Liverpool Univ (England)
SYSTEM ALBEDO AS SENSED BY SATELLITES - ITS DEFINITION AND VARIABILITY
N A HUGHES (Liverpool, University, Liverpool, England) and A HENDERSON-SELLERS (NASA, Goddard Institute for Space Studies, New York, NY; Liverpool, University, Liverpool, England) International Journal of Remote Sensing, vol. 3, Jan.-Mar. 1982, p. 1-11 Natural Environment Research Council refs
(Contract NERC-GR3/3941)

System albedo, an important climatological and environmental parameter, is considered. Some of the problems and assumptions involved in evaluating albedo from satellite data are discussed. Clear-sky and cloud albedos over the United Kingdom and parts of northwest Europe are treated Consideration is given to the spectral, temporal, and spatial variations and the effect of averaging The implications of these results for those using and archiving albedo values and for future monitoring of system albedo are discussed Normalization is of especial importance since this correction alters many albedo values The pronounced difference in spectral albedo of the two visible channels reemphasizes the problem of attempting to calculate integrated albedo values from meteorological satellite data The assumption of isotropic reflection is seen to be invalid, hindering the computation of accurate albedo values C R

A82-32348* Alabama Univ , Huntsville
REMOTE SENSING OF TORNADIC STORMS FROM GEOSYNCHRONOUS SATELLITE INFRARED DIGITAL DATA
R. J HUNG (Alabama, University, Huntsville, AL) and R. E. SMITH (NASA, Marshall Space Flight Center, Huntsville, AL) International Journal of Remote Sensing, vol. 3, Jan -Mar 1982, p. 69-81 refs
(Contract NAS8-33726)

Two cases of GOES digital infrared data were analyzed during the three-hour period immediately prior to the tornado touchdown times. Clouds associated with tornadoes were compared to those without tornadoes using a combination of satellite infrared and rawinsonde data On the basis of this limited data sample, it appears as if the altitude to which the overshooting cloud top penetrated above the tropopause is the factor which determines whether or not a tornado is formed. In these cases, the overshooting cloud top collapsed about 15 to 30 min before the tornado touchdown. (Author)

A82-32441* Jet Propulsion Lab , California Inst. of Tech., Pasadena.
RESOURCE INVENTORY TECHNIQUES USED IN THE CALIFORNIA DESERT CONSERVATION AREA
R G. MCLEOD (California Institute of Technology, Jet Propulsion Laboratory Image Processing Laboratory, Pasadena, CA) and H. B. JOHNSON (U.S. Department of Agriculture, Grassland Soil and Water Research Laboratory, Temple, TX) In: Imaging spectroscopy; Proceedings of the Seminar, Los Angeles, CA, February 10, 11, 1981. Bellingham, WA, SPIE - The International Society for Optical Engineering, 1981, p 2-16. refs
(Contract NAS7-100)

A variety of conventional and remotely sensed data for the 25 million acre California Desert Conservation Area (CDCA) have been integrated and analyzed to estimate range carrying capacity Multispectral classification was performed on a digital mosaic of ten Landsat frames. Multispectral classes were correlated with low level aerial photography, quantified and aggregated by grazing allotment, land ownership, and slope. (Author)

A82-32711
SAMPLE DESIGN FOR ESTIMATING CHANGE IN LAND USE AND LAND COVER
G. H. ROSENFIELD (U.S. Geological Survey, Reston, VA) Photogrammetric Engineering and Remote Sensing, vol. 48, May 1982, p. 793-801. refs

The tasks of the field of applied statistics known as sample design are enumerated as: (1) sampling within a specified population, (2) consideration of sampling distribution; (3) determination of sample size; (4) determination of sample selection procedure; and (5) estimation of population means, totals, variances and confidence limits from the sample information This methodology, which is used in the estimation of land use and land cover change, is sufficiently general to extend to the determination of change in any type of time-variant thematic mapping An opportunity is presented for the determination of land use and land cover change in the state of Pennsylvania over a 20-year period O.C

A82-32899
IMPACTS OF REMOTE SENSING ON U.S. GEOGRAPHY
J. E ESTES, D. S. SIMONETT (California, University, Santa Barbara, CA), and J R JENSEN (Georgia, University, Athens, GA) Remote Sensing of Environment, vol. 10, Aug. 1980, p. 43-80. refs

Attention is called to the fact that few senior academic geographers are doing research in remote sensing and that few economic geographers have even considered the possibilities opened up by this technique. This dearth of research is even more pronounced among regional geographers with interests in less-developed countries Programs of study in remote sensing are considered vital because remote sensing can provide the geographer with significant improvements in the quantity, quality, and timeliness of data. C.R

A82-32901
EFFECT OF ATMOSPHERIC CONDITIONS ON REMOTE SENSING OF VEGETATION PARAMETERS
J V. DAVE (IBM Scientific Center, Palo Alto, CA) Remote Sensing of Environment, vol 10, Sept. 1980, p. 87-99. refs

The effects of atmospheric and observational conditions on the remote sensing of vegetation parameters are studied in simulations of the ratios of radiances in the 0 76-0 90 micron and 0.52-0.60 micron bands (Landsat Thematic Mapper bands 4 and 2, respectively) as a function of leaf water content in blue grama grass. The simulations were performed based on spectral flux reflectance and canopy data for 35 plots with different leaf water levels and three different models of the cloud-free midlatitude summer atmosphere with no, moderate and high aerosol contents at solar zenith angles from 0 to 80 deg, heights from the top to the bottom of the atmosphere, nadir angles from 0 to 75 deg and azimuth angles from 0 to 180 deg. Selected results demonstrate that the slope and intercept of the straight line expressing the dependence of radiance ratio on leaf water content can be significantly affected by atmospheric conditions and viewing geometry. A.L.W.

A82-33652
SOUFRIERE VOLCANO, ST. VINCENT - OBSERVATIONS OF ITS 1979 ERUPTION FROM THE GROUND, AIRCRAFT, AND SATELLITES
R. S. FISKE (Smithsonian Institution, Washington, DC) and H. SIGURDSSON (Rhode Island, University, Kingston, RI) Science, vol. 216, June 4, 1982, p. 1105, 1106. refs

The 1979 eruption of Soufriere Volcano, St Vincent, is described. The initial vulcanian explosive phase from April 13 to 26 was a series of discrete vertical explosions, blasting a new vent through the 1971-1972 lava island in the middle of the 1-km-wide crater lake. The second phase was characterized by the quiet extrusion of viscous basaltic andesite lava, resulting in the growth of a dome over the vent. The importance of the geologic, seismic and ground-deformation data gathered prior to the eruption is discussed. D.L.G

A82-33654
GEOSTATIONARY SATELLITE OBSERVATIONS OF THE APRIL 1979 SOUFRIERE ERUPTIONS
A. F KRUEGER (NOAA, National Weather Service, Washington, DC) Science, vol. 216, June 4, 1982, p 1108, 1109. refs

Infrared images from the geostationary satellite SMS-1 were used to study the growth of the eight major eruptions of Soufriere, St. Vincent, during April, 1979 These eruptions differed considerably in growth and intensity, the most intense being that of April 17, which formed an ash cloud of 96,000 square kilometers in 4 hours The weakest eruption formed a cloud of only 16,000 square kilometers. (Author)

A82-33655
METEOROLOGICAL ANALYSIS OF THE ERUPTION OF SOUFRIERE IN APRIL 1979
S. BARR (Los Alamos National Laboratory, Los Alamos, NM) and J. L HEFFTER (NOAA, Air Resources Laboratory, Silver Spring, MD) Science, vol 216, June 4, 1982, p. 1109-1111. refs

Meteorological upper-air data, in conjunction with satellite imagery, lidar light detection and ranging returns, and aircraft sampling, aid in the determination of plume altitude and transport. The estimated trajectories indicate that the ash was transported eastward across the Atlantic to Africa in 3 to 5 days and that there was modest meridional transport as far as 15 deg poleward during the first week of travel. (Author)

A82-33656
SKIRT CLOUDS ASSOCIATED WITH THE SOUFRIERE ERUPTION OF 17 APRIL 1979
S. BARR (Los Alamos National Laboratory, Los Alamos, NM) Science, vol 216, June 4, 1982, p. 1111, 1112.

A fortuitous and dramatic photograph of the Soufriere eruption column of April 17, 1979 displays a series of highly structured skirt clouds. The gentle distortion of thin, quasi-horizontal layers of moist air has been documented in meteorological situations. It is proposed that at St. Vincent subhorizontal layers of moist air were intensely deformed by the rapidly rising eruption column and were carried to higher altitudes, where they condensed to form the skirt clouds (Author)

A82-33657* National Aeronautics and Space Administration. Langley Research Center, Hampton, Va.
AIRBORNE LIDAR MEASUREMENTS OF THE SOUFRIERE ERUPTION OF 17 APRIL 1979
W. H. FULLER, JR , S SOKOL (NASA, Langley Research Center, Hampton, VA), and W. H HUNT (Wyle Laboratories, Hampton, VA) Science, vol 216, June 4, 1982, p. 1113-1115 refs

At the time of the Soufriere, St. Vincent, volcanic eruption of April 17, 1979, a NASA P-3 aircraft with an uplooking lidar (light detection and ranging) system onboard was airborne 130 kilometers east of the island. Lidar measurements of the fresh volcanic ash were made approximately 2 hours after the eruption, 120 kilometers to the northeast and east. On the evening of April 18, the airborne lidar, on a southerly flight track, detected significant amounts of stratospheric material in layers at 16, 17, 18, and 19 5 kilometers. These data, and measurements to the north on April 19, indicate that the volcanic plume penetrated the stratosphere to an altitude of about 20 kilometers and moved south during the first 48 hours after the eruption. (Author)

A82-33659* National Aeronautics and Space Administration. Langley Research Center, Hampton, Va
FINE PARTICLES IN THE SOUFRIERE ERUPTION PLUME
D C. WOODS (NASA, Langley Research Center, Hampton, VA) and R L CHUAN (Brunswick Corp., Costa Mesa, CA) Science, vol. 216, June 4, 1982, p. 1118, 1119. refs

The size distributions of fine particles measured at tropospheric altitudes in the periphery of the eruption plume formed during the April 17, 1979 eruption of Soufriere Volcano and in the low-level effluents on May 15, 1979 were found to be bimodal, having peak concentrations at geometric mean diameters of 1.1 and 0 23 micrometers. Scanning electron microscopy and energy-dispersive

X-ray analysis of the samples revealed an abundance of aluminum and silicon and traces of sodium, magnesium, chlorine, potassium, calcium, and iron in the large-particle mode The submicrometer-sized particles were covered with liquid containing sulfur, assumed to be in the form of liquid sulfuric acid. (Author)

A82-33865
EPA'S NEW BUBBLE AND BANKING POLICIES
M. R. DELAND (U.S. Environmental Protection Agency, Environmental Monitoring Systems Laboratory, Las Vegas, NV) Environmental Science and Technology, vol. 16, June 1982, p. 338A-346A refs

The uses of multispectral scanning (MSS), laser technology, and aerial photography in remote sensing programs to monitor potential and existing environmental problems are examined. Airborne MSS applications involve the detection of visible and IR emissions from the earth's surface for electronic cleaning of the imagery and reproduction of the sensed scene. Spectroscopic coding of the images allows identification of pollutants, the health of vegetative cover, and the state of observable water quality Airborne laser sensing of chlorophyll-a in water bodies has allowed association of dissolved organic nutrients, due mainly to sewage discharges, with increases in the population of the algae Lidar measurements permit digitized air quality measurements from aircraft. The development of a differential absorption lidar (DIAL) system, using two lasers close in frequency output, is paving the way for specific species labeling M S K.

A82-34218* National Aeronautics and Space Administration Goddard Space Flight Center, Greenbelt, Md
THE USE OF LANDSAT-3 THERMAL DATA TO HELP DIFFERENTIATE LAND COVERS
J. P. ORMSBY (NASA, Goddard Space Flight Center, Earth Survey Applications Div., Greenbelt, MD) Remote Sensing of Environment, vol. 12, May 1982, p. 97-105. refs

Landsat-3 Multispectral Scanner Subsystem (MSS) digital data of the Baltimore, Maryland area gathered on May 24, 1978, are examined to show the usefulness of thermal data in providing better discrimination between agricultural and residential areas, certain types of urban/industrial areas and water, cloud shadows and water, and bare-extractive areas and bright urban cover types High altitude aircraft imagery taken on May 3, 1978, provides ground truth and training site verification. Two classifications are made for each training site· the initial one using bands 4, 5, and 7 and a second in which the thermal data are included with the visible and near infrared data. This permits a direct comparison of areas spectrally similar with and without the inclusion of the thermal data. Commission errors determined from selected subsets of the data show reductions of 95% for the urban/industrial versus water themes, 84% for the residential versus agriculture themes, 64.0% for the bare-extractive versus bright urban themes, and 24% for the cloud shadow versus water themes when the thermal data are included in the signature C R.

A82-34711
SITE SELECTION AND ENGINEERING ISSUES FOR A MAJOR INDUSTRIAL COMPLEX - APPLICATION OF IMAGE AND MAP INTERPRETATION
D. S WAY (Harvard University, Cambridge, MA) In· American Society of Photogrammetry, Annual Meeting, 47th, Washington, DC, February 22-27, 1981, ASP Technical Papers. Falls Church, VA, American Society of Photogrammetry, 1981, p 164-169

A major port and industrial complex is being developed in Indonesia near Singapore. Little existing data is available facilitating application of remote sensing techniques for site evaluation and planning. Over eight hundred square kilometers of area was analyzed. Landsat images, aerial photographs, and topographic maps where interpreted for geology, geomorphology, soils, hydrology, and visual resources Evaluations were made for both environmental and development/engineering issues culminating in a phased master plan The data contributed by remote sensing represented a significant savings in site reconnaissance, design and construction. (Author)

A82-34739
A NEW APPROACH TO MULTIRESOURCE INVENTORIES USING REMOTE SENSING AND GEOGRAPHIC INFORMATION SYSTEMS TECHNOLOGIES
J. VAN ROESSEL, P. G. LANGLEY, C. SHEFFIELD, and M. C PLACE (Earth Satellite Corp , Berkeley, CA) In American Society of Photogrammetry, Annual Meeting, 47th, Washington, DC, February 22-27, 1981, ASP Technical Papers. Falls Church, VA, American Society of Photogrammetry, 1981, p. 499-510. refs

The design for a new multiresource inventory system is presented Two geographic information systems are employed in concert to support a sampling system which can provide estimates for multiple resource parameters One GIS (the upper level) is cell- and tape- oriented and incorporates various types of Landsat processing The other (the lower level) is a disk-based polygon system that holds high resolution sample maps The two systems are connected through a linear regression model. The results of a pilot test of a prototype system in South Carolina are presented. (Author)

A82-34743* Jet Propulsion Lab., California Inst. of Tech., Pasadena.
IMPROVED LAND USE CLASSIFICATION FROM LANDSAT AND SEASAT SATELLITE IMAGERY REGISTERED TO A COMMON MAP BASE
J. CLARK (California Institute of Technology, Jet Propulsion Laboratory, Pasadena, CA) In American Society of Photogrammetry, Annual Meeting, 47th, Washington, DC, February 22-27, 1981, ASP Technical Papers. Falls Church, VA, American Society of Photogrammetry, 1981, p 591-599. refs
(Contract NAS7-100)

In the case of Landsat Multispectral Scanner System (MSS) data, ambiguities in spectral signature can arise in urban areas. A study was initiated in the belief that Seasat digital SAR could help provide the spectral separability needed for a more accurate urban land use classification. A description is presented of the results of land use classifications performed on Landsat and preprocessed Seasat imagery that were registered to a common map base. The process of registering imagery and training site boundary coordinates to a common map has been reported by Clark (1980). It is found that preprocessed Seasat imagery provides signatures for urban land uses which are spectrally separable from Landsat signatures This development appears to significantly improve land use classifications in an urban setting for class 12 (Commercial and Services), class 13 (Industrial), and class 14 (Transportation, Communications, and Utilities) G.R

A82-34744* National Aeronautics and Space Administration Goddard Inst. for Space Studies, New York
LONGWAVE INFRARED OBSERVATION OF URBAN LANDSCAPES
S N. GOWARD (NASA, Goddard Institute for Space Studies; Columbia University, New York, NY) In American Society of Photogrammetry, Annual Meeting, 47th, Washington, DC, February 22-27, 1981, ASP Technical Papers. Falls Church, VA, American Society of Photogrammetry, 1981, p 600-609. Research supported by the Indiana Academy of Science and Indiana State University. refs

An investigation is conducted regarding the feasibility to develop improved methods for the identification and analysis of urban landscapes on the basis of a utilization of longwave infrared observations. Attention is given to landscape thermal behavior, urban thermal properties, modeled thermal behavior of pavements and buildings, and observed urban landscape thermal emissions. The differential thermal behavior of buildings, pavements, and natural areas within urban landscapes is found to suggest that integrated multispectral solar radiant reflectance and terrestrial radiant emissions data will significantly increase potentials for analyzing urban landscapes. In particular, daytime satellite observations of the considered type should permit better identification of urban areas and an analysis of the density of buildings and pavements within urban areas. This capability should

enhance the utility of satellite remote sensor data in urban applications. G.R.

A82-35534
OBSERVED MAGNETIC SUBSTORM SIGNATURES AT SYNCHRONOUS ALTITUDE
T. NAGAI Journal of Geophysical Research, vol. 87, June 1, 1982, p. 4405-4417. refs

Magnetic field data from the geostationary satellites GOES 2 and GOES 3 are examined to study the development of substorm activity in the near-earth nightside magnetosphere (around a radial distance of 6.6 earth radii). Substorm events are those in which a well-defined single onset is seen at low latitudes on the ground. The field configuration change from more taillike to more dipolelike starts initially in a longitudinally localized region in association with the ground onset, and it develops westward and eastward, even when the simultaneous onset of the low-latitude positive bay is recorded in a wide longitudinal region on the ground. It is also found that the variation caused by the field-aligned current starts at the ground onset and reaches a peak at the time of the field change. The present results are consistent with the view that a substorm is associated with a disruption and subsequent conversion of the cross-tail current to the field-aligned current connected with the polar ionosphere. It is indicated that the cross-tail current near synchronous orbit and its disruption are important in producing the field configuration change at synchronous orbit (Author)

A82-35542* Maryland Univ , College Park
GENERATION OF THE AURORAL KILOMETRIC RADIATION
C. S. WU, H. K. WONG (Maryland, University, College Park, MD), D. J GORNEY (Aerospace Corp , Space Sciences Laboratory, El Segundo, CA), and L C. LEE (Alaska, University, Fairbanks, AK) Journal of Geophysical Research, vol. 87, June 1, 1982, p. 4476-4487. refs
(Contract F04701-80-C-0081; NSF ATM-81-16045; NGL-21-002-005)

Data collected from the S3-3 spacecraft in the auroral kilometric radiation (AKR) source region are employed to form a stability theory from which numerical results are obtained and discussed. The distribution function was found to be isotropic outside the auroral atmospheric loss-cone region, which was partially filled with upcoming electrons A parallel electric field was observed to be modifying the loss-cone distribution A model distribution function is formulated, along with a magnetic field model expressed in terms of the electron cyclotron frequency Models for the parallel electric field are also introduced, the first with the field distributed over a broad altitude range, while the second assumes a potential drop only above 4000 km. The presence of the field is found to enhance the growth rate of the AKR. At higher altitudes, the cutoff frequency of the X mode is affected by the rising energetic electrons. Finally, the folding distances of spatial amplification are calculated. M.S K.

A82-35895
OBSERVATION OF THE DIURNAL VARIATION OF ATMOSPHERIC OZONE
J. L. LEAN (Adelaide, University, Adelaide, Australia) Journal of Geophysical Research, vol 87, June 20, 1982, p. 4973-4980. Research supported by the World Meteorological Organization. refs

Ozone densities in the stratosphere and mesosphere have been derived from broad-band photometer measurements of Hartley band absorption of middle ultraviolet radiation. Seven rockets were launched during October-November 1979 from Wallops Island. Six rockets, each carrying one detector comprising two UV photometers, were launched at different times of the day. A seventh rocket, with three similar detectors each having three UV photometers, was launched at the time of a full moon and provided estimates of the nighttime ozone densities. Results from these rocket flights form a basis for investigating ozone diurnal variations. The number of flights provide greater statistical reliability for the ozone profiles than is generally afforded from in situ measurements with a single rocket. During the night, an enhancement in ozone densities occurred at altitudes above about 50 km At 70 km, for example, the nighttime ozone was determined to be a factor of 6.4 greater than at sunset. In addition, these experiments suggest that near 40 km the magnitude of the ozone density at noon may be greater by 10-15% than the nighttime concentration (Author)

A82-36053*# National Meteorological Center, Washington, D. C
TOTAL OZONE VARIATIONS 1970-74 USING BACKSCATTERED ULTRAVIOLET /BUV/ AND GROUND-BASED OBSERVATIONS
A J MILLER, R. M. NAGATANI, T G. ROGERS (NOAA, National Meteorological Center, Washington, DC), A. J. FLEIG, and D F HEATH (NASA, Goddard Space Flight Center, Greenbelt, MD) *Journal of Applied Meteorology*, vol 21, May 1982, p. 621-630. NASA-supported research. refs

The most long-lived satellite set of ozone observations, to date, is that derived from the Backscatter Ultraviolet (BUV) ozone sensor on Nimbus 4 and extends from April 1970 through 1976. Unfortunately, this experiment suffered spacecraft power limitations which limited the spatial and temporal coverage and also appears to have suffered from long-term drifts which may be associated with changes in the instrument characteristics or the incident solar flux Techniques have been developed to account for these problems, and this paper presents results of the BUV total ozone variations and compares them with those from ground-based observations, specifically the computations of Angell and Korshover (1978). After adjustments for the spatial gaps and comparison with concurrent Dobson ground-based observations, no significant trend was found in the BUV data over the years 1970-74 This finding is in contrast to a general decrease of about 2% during the same period appearing in the data of Angell and Korshover. The difference in these results is discussed in terms of the geographic sampling and the methods of hemispheric integration (Author)

A82-36247#
AIRCRAFT MEASUREMENTS OF NO/X/ IN THE LOWER TROPOSPHERE ABOVE THE COAST OF JAPAN
Y KONDO, M. TAKAGI, Y. MORITA, and A. IWATA Nagoya University, Research Institute of Atmospherics, Proceedings, vol. 29, Mar 1982, p 85-91. Research supported by the Nissan Science Foundation. refs

Concentrations of NO(x) in altitude regions of 0.5-3.0 km above the coastal area of Japan were measured. The measured mixing ratios range from 1 to 30 ppb depending on the altitude, location and time of the observations. From the measured mixing ratio, it can be said that relatively large amounts of NO(x) emitted at ground level are often transported at least as far as 3 km vertically and 200 km horizontally (Author)

A82-36268
CHARACTERISTICS OF FIELD-ALIGNED E-REGION IRREGULARITIES OVER IIOKA /36 N/, JAPAN. I
T TANAKA and S. V. VENKATESWARAN (California, University, Los Angeles, CA) Journal of Atmospheric and Terrestrial Physics, vol. 44, May 1982, p. 381-393, 395-397, 399-406 refs
(Contract NSF ATM-77-24843)

Measurements with a 25-MHz radar over Iioka, Japan, reveal that field-aligned E-region irregularities occur mainly at night in association with sporadic E (Es) layers at an altitude range of about 100-110 km and that they drift predominantly westward with speeds of the order of 60 m/s. It is shown that these observed characteristics of the irregularities are in reasonable agreement with quantitative predictions of the gradient drift instability theory. The predictions are based on appropriate models for neutral air densities and temperatures, ionic composition and ionospheric electric field, and available observations of electron density profiles of the E and Es layers. Observations of multifrequency (4-64 MHz) echoes with an oblique incidence ionosonde and of Doppler spectra with a fixed frequency (25 MHz) radar are then presented and discussed. It is shown that the ionosonde observations are capable of being explained in terms of the linear theory of cross-field or

gradient-drift instability, which is presumed to generate the field-aligned irregularities C.R

A82-36292* National Aeronautics and Space Administration. Langley Research Center, Hampton, Va.
TROPOSPHERIC CO MEASUREMENT EXPERIMENT FROM THE SECOND SPACE SHUTTLE FLIGHT
H. G REICHLE, JR. (NASA, Langley Research Center, Hampton, VA) American Meteorological Society, American Geophysical Union, and NASA, Symposium on the Composition of the Nonurban Troposphere, 2nd, Williamsburg, VA, May 25-28, 1982, Paper. 4 p refs

The MAPS experiment was designed to remotely measure the mixing ratio of carbon monoxide in the middle and upper troposphere using a gas filter radiometer as the sensing instrument The asymmetrical worldwide distribution of CO is discussed as background, and the experimental scientific and technical objectives are briefly stated. The gas filter radiometer is described in detail, and the second Shuttle mission is summarized Auxiliary and correlative data were obtained in order to evaluate the performance of the measurement system, to assess the effect of stratospheric ozone on the radiometer signals, and to determine the effect of the underlying surface. The experiment acquired about 32 hours of data between 38 deg N and 38 deg S, signal-to-noise ratios were as predicted and the instrument achieved satisfactory stability in spite of large temperature variations. Data reduction is in progress. C.D.

A82-36293* National Aeronautics and Space Administration Langley Research Center, Hampton, Va
AMMONIA AND THE NOX BUDGET OF THE TROPOSPHERE
J. S LEVINE, T. R. AUGUSTSSON, and J. M. HOELL (NASA, Langley Research Center, Hampton, VA) American Meteorological Society, American Geophysical Union, and NASA, Symposium on the Composition of the Nonurban Troposphere, 2nd, Williamsburg, VA, May 25-28, 1982, Paper. 3 p. refs

Liu et al (1980) suggested that NOx transported from the stratosphere, as opposed to the anthropogenic source of NOx, may be the dominant source that controls the distribution of NOx in the global troposphere. These ideas require a reinvestigation, and, in particular, an assessment of the role of the oxidation of ammonia as a source of NOx. Attention is given to the results of an ammonia measurement program, in which the vertical distribution of ammonia in the troposphere and lower stratosphere could be studied with the aid of the Infrared Heterodyne Radiometer (IHR), a solar-viewing remote sensor. A one-dimensional photochemical model of the troposphere reported by Levine et al. (1980) was employed to study the chemical and physical processes that control the loss of ammonia in the troposphere. The results of the considered investigation suggest that the oxidation of ammonia may indeed be a significant source of NOx in the troposphere G.R.

A82-36362*# National Aeronautics and Space Administration. Goddard Space Flight Center, Greenbelt, Md.
ATMOSPHERIC OZONE DETERMINATION BY SOLAR OCCULTATION USING THE UV SPECTROMETER ON THE SOLAR MAXIMUM MISSION
A. C. AIKIN, B. WOODGATE (NASA, Goddard Space Flight Center, Greenbelt, MD), and H. J. P SMITH (Visidyne, Inc., Burlington, MA) Applied Optics, vol. 21, July 1, 1982, p. 2421-2424. refs

The UV spectrometer polarimeter instrument on the Solar Maximum Mission spacecraft has been used to measure ozone in the 53-75 km altitude interval by the technique of solar occultation A 1 x 180 arcsec entrance aperture spectrometer with 0.04-A spectral resolution was employed. Resulting high-quality data are reduced by expressing measured UV attenuation as a Volterra integral equation. Solution of the equation is accomplished by expressing the integral in terms of a series representing the sum of ozone densities contained in concentric shells through tangent points separated by specified altitude increments Sample ozone vs altitude profiles are presented for the equatorial region. These data show reproducibility to better than 10%. The density at 60 km is 7.3 + or - 0 15 x 10 to the 9th/cu cm for 2.5 deg latitude and longitudes between 81 and 105 deg west in September 1980 Density vs altitude profile exhibits changes in slope between 50 and 75 km (Author)

A82-36405#
SENSITIVITY OF DOBSON TOTAL OZONE ESTIMATIONS TO WAVELENGTH BAND CALIBRATION UNCERTAINTIES
R E. BASHER (New Zealand Meteorological Service, Wellington, New Zealand) In: Quadrennial International Ozone Symposium, Boulder, CO, August 4-9, 1980, Proceedings. Volume 1. Boulder, CO, International Association of Meteorology and Atmospheric Physics, 1981, p 33-36 refs

It is pointed out that calibration uncertainties in the center wavelength, bandwidth, and shape of the Dobson instrument's bands propagate uncertainty into extraterrestrial constants, ozone absorption coefficients, standard lamp calibrations, and total ozone estimations. Detailed calculations of these uncertainties have been conducted for a wide range of conditions of calibration and operation It is emphasized that all of the considered calculations refer to the defined 'well calibrated', 'well operated' instrument. It is found that the percent standard errors in total ozone are very dependent on airmass and ozone amount. The errors are greatest at low airmass and low ozone, especially for the D and CD band combinations. The AD combination generally has the least error of the double wavelength pairs, and for the directly intercompared instruments has a standard error of 1 1% or less G.R

A82-36406#
THE EFFECT OF THE SPECTRAL ATTENUATION OF UV RADIATION BY AEROSOL ON THE TOTAL OZONE MEASUREMENTS
A. DZIEWULSKA-LOSIOWA (Polska Akademia Nauk, Instytut Geofizyki, Warsaw, Poland) In: Quadrennial International Ozone Symposium, Boulder, CO, August 4-9, 1980, Proceedings Volume 1. Boulder, CO, International Association of Meteorology and Atmospheric Physics, 1981, p. 38-45. U S Environmental Protection Agency refs
(Contract EPA-5-536-4)

The effect of aerosol in the atmosphere on ozone measurements is considered. Shah (1976) had concluded that changes in aerosol concentration and particle size distribution affect the measurement results only slightly. DeLuisi (1975), on the other hand, had found that substantial differences exist between values for ozone content obtained by taking into account scattering, and values calculated without regard to scattering effects. Instrumental errors are analyzed and the statistical relationship between measurements at different wavelengths are investigated. It is found that differences between the results of measurements related to different wavelength pairs are greater than instrumental errors. It is shown that these results are connected with the spectral extinction of the atmospheric aerosol G.R

A82-36414#
APPLICATION OF INFRARED TECHNIQUES TO THE STUDY OF ATMOSPHERIC OZONE [APPLICATION DES TECHNIQUES INFRAROUGES A L'ETUDE DE L'OZONE ATMOSPHERIQUE]
C SECROUN, A. BARBE, P MARCHE, and P JOUVE (Reims, Universite, Reims, France) In: Quadrennial International Ozone Symposium, Boulder, CO, August 4-9, 1980, Proceedings. Volume 1. Boulder, CO, International Association of Meteorology and Atmospheric Physics, 1981, p. 108-113 In French. refs

The present investigation is concerned with the utilization of the infrared wavelength region for the study of the ozone in the atmosphere, taking into account three atmospheric windows including the wavelength ranges near 10, 5, and 3 micrometers. More than 3200 spectral lines could be assigned to different bands of the ozone spectrum Laboratory studies formed one part of the investigation Spectral frequencies, absorption line intensities, and linewidths were determined for ozone. Some of the obtained results were employed in connection with data provided by the radiometric probe LIMS on board the Nimbus-7 satellite The second part of the investigation involved a study of the atmosphere. The same

spectrometer as in the laboratory study was utilized, and the sun was employed as radiation source The obtained results were compared with data provided by a Dobson spectrophotometer Attention is also given to vertical concentration profiles. It is concluded that infrared absorption spectroscopy represents a suitable technique for studies of atmospheric ozone. G R

A82-36415*# Jet Propulsion Lab , California Inst. of Tech., Pasadena.
MICROWAVE MEASUREMENT OF STRATOSPHERIC AND MESOSPHERIC OZONE
J W. WATERS (California Institute of Technology, Jet Propulsion Laboratory, Pasadena, CA) In· Quadrennial International Ozone Symposium, Boulder, CO, August 4-9, 1980, Proceedings. Volume 1. Boulder, CO, International Association of Meteorology and Atmospheric Physics, 1981, p. 114-121. refs

It is pointed out that ozone has a rich rotational spectrum with many lines at millimeter wavelengths Measurement of these lines can provide a means of remotely sensing stratospheric and mesospheric ozone. Technology has recently advanced to the state where it is reasonable to consider monitoring upper atmospheric O3 on a global scale by microwave radiometers in earth orbit An investigation indicates that approximately 1% accuracy and approximately 2 km vertical resolution O3 mixing ratio measurements are reasonable goals for limb-viewing microwave radiometers in earth orbit. Mesospheric ozone can also be measured by the considered techniques using stronger (but more temperature-sensitive) O3 lines. A balloon-borne microwave limb sounder has recently been constructed to test the practical limitations on the measurement concepts. Also under study is a microwave limb sounder for operation in earth orbit. G R

A82-36422#
TOTAL OZONE RETRIEVAL FROM SATELLITE METEOR 28 FOURIER SPECTROMETER MEASUREMENTS
U FEISTER and D SPAENKUCH (Meteorologisches Hauptobservatorium, Potsdam, East Germany) In: Quadrennial International Ozone Symposium, Boulder, CO, August 4-9, 1980, Proceedings. Volume 1 Boulder, CO, International Association of Meteorology and Atmospheric Physics, 1981, p 168-175. refs

The efficiency and accuracy of four different algorithms for deriving total ozone from IR radiance measurements made with Fourier spectrometers are assessed. For a total of more than 1,100 spectrometer-interferometer spectra measured between July and September 1977, 40 corresponding Dobson ozone values are found with a maximum spatial distance between the subsatellite point and the Dobson station of 300 km and an average distance of 175 km; 35 values here are from midlatitudes of the Northern Hemisphere. The Dobson ozone values are used in determining a different number of coefficients for each method applying the least square method With these coefficients, ozone values are calculated. The original number of spectral channels is then reduced to two intervals. It is found that a radiometer with one or two channels in the 9 6/micron band in the window and in the 15/micron band is sufficient for the total ozone determination A highly significant positive correlation is found between spectrometer-interferometer ozone and calculated relative topographies of the lower stratosphere. This correlation holds even if the latitudinal dependence and autocorrelation of ozone values and relative topographies are eliminated. C.R.

A82-36428#
OPTICAL STOP AND FOCUSSING EFFECTS IN THE DOBSON INSTRUMENT
R. E. BASHER (New Zealand Meteorological Service, Wellington, New Zealand) In Quadrennial International Ozone Symposium, Boulder, CO, August 4-9, 1980, Proceedings. Volume 1 Boulder, CO, International Association of Meteorology and Atmospheric Physics, 1981, p. 216-218

The present investigation shows that the 'directional effect' observed in connection with the photoelectric spectrometer designed by Dobson (1931) is caused by defects in optical stopping and focusing The considered effect consists of two parts, related to different field-of-view boundaries for the two wavelength bands being measured, and varying relative sensitivity across the field of view for the two bands The stop problem is readily tested for and corrected, and it may affect only a limited number of instruments. The focussing problem, however, affects all but the earliest instruments, and its solution will require a careful consideration of the involved aspects G.R.

A82-36431#
DOBSON SPECTROPHOTOMETER CALIBRATIONS, POSSIBLE ERRORS IN OZONE ABSORPTION COEFFICIENTS, AND ERRORS DUE TO INTERFERING POLLUTANT GASES
W. D. KOMHYR, R D GRASS (NOAA, Air Resources Laboratories, Boulder, CO), R. D EVANS, and R K. LEONARD (Cooperative Institute for Research in Environmental Sciences, Boulder, CO) In Quadrennial International Ozone Symposium, Boulder, CO, August 4-9, 1980, Proceedings Volume 1. Boulder, CO, International Association of Meteorology and Atmospheric Physics, 1981, p 230-235. Research supported by the World Meteorological Organization; U S. Department of Transportation refs
(Contract DOT-FA78WAI-850)

In connection with the employment of Dobson spectrophotometers as standard instruments for measurements of total ozone, it is imperative that the accuracy of the total ozone measurements be properly assessed Research within the Geophysical Monitoring for Climatic Change program into the accuracy of ozone observations is currently focussed on possible variations of the Dobson instrument extraterrestrial constants Attention is given to spectrophotometer calibrations, the systematic ozone measurement error, and interfering trace gas pollutants. It is pointed out that ozone produced photochemically in polluted air near ground level can also be considered an interferer since it renders unreliable background measurements of total ozone. G.R.

A82-36444#
OBSERVATIONS AND ANALYSES OF THE TOTAL AMOUNT OF ATMOSPHERIC OZONE IN THE BEIJING REGION AND IN THE REGION OF JOLMOLUNGMA MOUNTAIN IN TIBET
D WEI (Chinese Academy of Sciences, Atmospheric Physics Institute, Beijing, People's Republic of China) and C WEN (Sichuan, Institute of Geography, Sichuan, People's Republic of China) In· Quadrennial International Ozone Symposium, Boulder, CO, August 4-9, 1980, Proceedings Volume 1 Boulder, CO, International Association of Meteorology and Atmospheric Physics, 1981, p. 340-346.

A82-36472#
OSO-8 LOWER MESOSPHERIC OZONE NUMBER DENSITY PROFILES
F. MILLIER (CNRS, Laboratoire de Physique Stellaire et Planetaire, Verrieres-le-Buisson, Essonne, France), B. A. EMERY, and R. G. ROBLE (National Center for Atmospheric Research, Boulder, CO) In: Quadrennial International Ozone Symposium, Boulder, CO, August 4-9, 1980, Proceedings Volume 1. Boulder, CO, International Association of Meteorology and Atmospheric Physics, 1981, p 572-579 refs

Solar occultation data gathered by the French ultraviolet spectrophotometer telescope on the NASA Orbiting Solar Observatory, scanning between about 50 deg N and 50 deg S between June 1975 and June 1976, are presented. The occultation profiles, observed near 2800 A, contain information on the ozone concentration at altitudes between about 52 and 75 km. Results obtained between June 5 and August 4, 1975 are discussed, longitudinal and latitudinal variations are demonstrated, and comparisons with published ozone density profiles are shown. C.D.

A82-36477#
COMPARISON OF OZONE IN POLLUTED AND CLEAN AIR MASSES OVER LAKE MICHIGAN
A. J ALKEZWEENY, W. E. DAVIS, and R. C. EASTER (Battelle Pacific Northwest Laboratories, Richland, WA) In: Quadrennial International Ozone Symposium, Boulder, CO, August 4-9, 1980, Proceedings. Volume 1. Boulder, CO, International Association of Meteorology and Atmospheric Physics, 1981, p 616-623 refs

A82-36534*# National Aeronautics and Space Administration Goddard Space Flight Center, Greenbelt, Md
THE SEASONAL VARIATIONS OF OZONE AND TEMPERATURE IN THE MIDDLE AND THE UPPER STRATOSPHERE
S. CHANDRA (NASA, Goddard Space Flight Center, Laboratory for Planetary Atmospheres, Greenbelt, MD) In. Quadrennial International Ozone Symposium, Boulder, CO, August 4-9, 1980, Proceedings. Volume 2 Boulder, CO, International Association of Meteorology and Atmospheric Physics, 1981, p. 1083-1090 refs

The seasonal variations in ozone and temperature inferred from the Nimbus-4 BUV (Backscatter Ultraviolet Spectrometer) and the SCR (Selective Chopper Radiometer) experiments are compared with predictions based on a simplified radiative photochemical model. It is shown that the observations, in agreement with the model calculations, show a systematic phase shift from a summer maximum at 10 mb to a winter maximum at 1 mb with equinoctial maxima at intermediate heights In contrast, the temperature between these pressure levels shows no appreciable phase shift and the summer maximum prevails at all heights. The observed phase differences in ozone and temperature are shown to be a manifestation of the radiative feedback on the photochemistry of the upper stratosphere (Author)

A82-36741
ON THE APPLICATION OF A MODEL OF BOUNDARY-LAYER FLOW OVER LOW HILLS TO REAL TERRAIN
J L WALMSLEY, J. R SALMON, and P. A. TAYLOR (Department of the Environment, Atmospheric Environment Service, Downsview, Ontario, Canada) Boundary-Layer Meteorology, vol 23, May 1982, p. 17-46 Research supported by the National Research Council of Canada. refs

Attempts to apply a computer model (Walmsley et al., 1980) to neutrally-stratified, boundary-layer flow over an isolated hill of moderate slope (Kettles Hill, Alberta) lead to velocity perturbation fields which probably overemphasize the impact of small-scale topographic features. Some numerical smoothing of the digitized terrain input field is found to be helpful in reducing this effect, although such a procedure is somewhat arbitrary. An extension of the original theory results in an improved representation of the effect of small-scale terrain components. These modifications are described and some results of an application of the extended model to Kettles Hill are presented (Author)

A82-37405* Aerospace Corp., El Segundo, Calif.
SOFT X-RAYS FROM THE SUNLIT EARTH'S ATMOSPHERE
D L. MCKENZIE, H. R. RUGGE (Aerospace Corp., Space Sciences Laboratory, El Segundo, CA), and P. A. CHARLES (California, University, Berkeley, CA) Journal of Atmospheric and Terrestrial Physics, vol 44, June 1982, p 499-508. Research supported by the Aerospace Corp refs
(Contract NAS8-33235; NASW-3338; CIT-44-727600; NAS5-23315 , F04701-79-C-0080)

Observations of soft X-ray emission from the sunlit earth atmosphere are presented and compared with the predictions of an earth albedo X-ray theory. The exact theory accounts for the flux of Thomson scattered solar X rays and fluorescently excited K X rays that arise following the absorption of incident X rays as a function of observing geometry Observations were made at widely separated geometries with the two low-energy detectors of the A-2 experiment on the HEAO-1 satellite Fitting of the model to the observed spectra results in values for the solar coronal temperature and emission measure that are in good agreement with expected values for the nonflaring sun, indicating that X-ray observations of the sunlit atmosphere may be a useful monitor of solar activity for satellites unable to view the sun directly The total measured fluorescent line flux is also in agreement with calculations, although the N/O line ratio is not. X-ray fluorescence measurements from the sunlit atmosphere will thus be useful in monitoring atmospheric composition only to the extent that the total line counting rates depend upon the composition. A.L.W.

A82-37502
SPATIAL RESOLUTION REQUIREMENTS FOR URBAN STUDIES
R. WELCH (Georgia, University, Athens, GA) International Journal of Remote Sensing, vol 3, Apr.-June 1982, p. 139-146. refs

Remote sensor data with spatial resolutions corresponding to 0 5-10 m IFOV are required to define adequately the high frequency detail which characterizes the urban scene. Effective analyses of the small parcels, compact structures and narrow street patterns typical of Asian environments will necessitate data of much higher resolution than are required for Western countries. Consequently it is unlikely that satellite image data expected for the 1980s will replace aerial photographs as a primary source of information about urban areas. (Author)

N82-23043# Comptroller General of the United States, Washington, D C
STREAMLINING AND ENSURING MINERAL DEVELOPMENT MUST BEGIN AT LOCAL LAND MANAGEMENT LEVELS Report to the Chairman, Committee on Energy and Commerce, House of Representatives
4 Dec 1981 24 p refs
(EMD-82-10, B-205344) Avail SOD

A study of the use of Federal lands, particularly military lands, concluded that success in streamling and accelerating mineral development on Federal lands depends on the Bureau of Land Management state offices ultimately responsible for the implementation of Department of Interior minerals policies. It was found the eastern States Office of the Bureau of Land Management did not effectively deal with potential Federal mineral trespass in the East, and was unable to issue mineral leases and permits on a timely basis. Moreover, it was unable to effectively deal with new areas of mineral interest because of Department actions. Recommendations to improve the mineral trespass program help relieve lease and permit backlogs, maintain dedicated staff, and improve headquarters communications with State offices were made R J F

N82-23793# California Univ., Berkeley Lawrence Berkeley Lab Engineering and Technical Service Div
ENVIRONMENTAL MONITORING REPORT OF THE LAWRENCE BERKELEY LABORATORY, 1980 Annual Report
G. E SCHLEIMER, ed. Apr. 1981 33 p refs
(Contract W-7405-ENG-48)
(LBL-12604) Avail. NTIS HC A03/MF A01

The environmental monitoring program of the Lawrence Berkeley Laboratory is described Data for 1980 are presented and general trends are discussed Airborne and waterborne radionuclides are discussed. The radiation dose on the surrounding population is discussed R J.F.

N82-23891# National Oceanic and Atmospheric Administration, Washington, D. C. National Earth Satellite Service.
COMPARISON OF SATELLITE DERIVED RADIATION BUDGET MEASUREMENTS OVER MONEX DURING 1979 TO 1980
P. K. RAO IN WMO Intern. Conf on Early Results of FGGE and Large-Scale Aspects of its Monsoon Expt. 7 p Apr. 1981 Avail: NTIS MF A01; HC WMO

Earth atmosphere radiation budgets derived from polar orbiting satellite radiometers are compared for May to August 1979 and 1980 The data are the differences in outgoing fluxes and albedos between 1980 and 1979. The low values in outgoing longwave radiation are associated with high and thick clouds which are relatively cold. High albedo values over this region are associated with clouds and snow over the mountains; moderately high values are observed over Saudi Arabia. Author (ESA)

N82-23963# Intermountain Forest and Range Experiment Station, Ogden, Utah. Aviation and Fire Management Staff.
REMOTE AUTOMATIC WEATHER STATION FOR RESOURCE AND FIRE MANAGEMENT AGENCIES
J. R. WARREN and D L. VANCE Aug. 1981 15 p refs
(PB82-107335; FSGTR/INT-116) Avail NTIS HC A02/MF A01 CSCL 04B

A weather station that operates automatically in remote areas, without power or communication lines was developed and is commercially available. Remote automatic weather stations (RAWS) transmit precipitation, windspeed, air temperature,temperature, humidity, and barometric pressure data via satellite Data may be acquired by direct dialing or through a fire forecasting program. GRA

N82-24566*# Mississippi State Univ , Mississippi State. Remote Sensing Center.
APPLICATION OF REMOTE SENSING TO STATE AND REGIONAL PROBLEMS Semiannual Progress Report, 1 May - 31 Oct. 1981
W. F MILLER, J R. CLARK, J L. SOLOMON, B. DUFFY, K. MINCHEW, and L. H. WRIGHT, Principal Investigator 1 Nov 1981 89 p refs ERTS
(Contract NGL-25-001-054)
(E82-10288; NASA-CR-168857, NAS 1.26:168857; SAPR-16)
Avail: NTIS HC A05/MF A01 CSCL 06B

The objectives, accomplishments, and future plans of several LANDSAT applications projects in Mississippi are discussed. The applications include land use planning in Lowandes County, strip mine inventory and reclamation, white tailed deer habitat evaluation, data analysis support systems, discrimination of forest habitats in potential lignite areas, changes in gravel operations, and determination of freshwater wetlands for inventory and monitoring. In addition, a conceptual design for a LANDSAT based information system is discussed. M G.

N82-24567*# Utah Univ., Salt Lake City. Center for Remote Sensing and Cartography
IDENTIFYING ENVIRONMENTAL FEATURES FOR LAND MANAGEMENT DECISIONS Annual Report
27 Oct. 1981 55 p refs Original contains color imagery Original photography may be purchased from the EROS Data Center, Sioux Falls, S. D. 57198 ERTS
(Contract NAGW-95)
(E82-10289; NASA-CR-168858) Avail: NTIS HC A04/MF A01 CSCL 05B

Advances in digital processing of LANDSAT imagery and in the interpretation of aerial photography are reported as well as the development of a geographic information system and the acquisition of cartographic equipment. Services to technical specialists and dignitaries are also described. The status of the following studies is discussed: Farmington Bay waterfowl; Sevier River wetland and agriculture, Davis County foothill development; Bear River Range aspen habitat; Wasatch-Cache riparian habitats; irrigated acreage in the Bear River Basin; the Parker Mountain rangeland inventory; and the development of techniques for inventorying aspen and aspen conifer stands. The cooperative project with NASA-Ames to verify LANDSAT digital maps of the forest and range resources on the LaSal Mountains is also considered. A.R.H.

N82-24598*# Instituto de Pesquisas Espaciais, Sao Jose dos Campos (Brazil).
COMPARISON OF STORM-TIME CHANGES OF GEOMAGNETIC FIELD AT GROUND AND AT MAGSAT ALTITUDES, PART 2
N. DEJESUSPARADA, Principal Investigator, R P KANE, and N. B TRIVEDI Apr. 1982 42 p Sponsored by NASA ERTS
(E82-10325; NASA-CR-168904, NAS 1 26 168904, INPE-2367-RA/161-PT-2) Avail NTIS HC A03/MF A01 CSCL 08N

Geomagnetic field variations were studied by considering the parameter delta H which indicated H(observed) minus H(model), where H = (X squared + Y squared) (1/2) where X, Y, and Z are the components actually observed. Quiet time base values for 5 deg longitude belts were estimated After subtracting these from the observed values, the residual delta H (dawn) and delta H (dusk) were studied for the two major storms. It was noticed that the dusk values attained larger (negative) values for a longer time, than the dawn value Some changes in delta Y and delta Z were also noticed, indicating possibilities of either meridional currents and/or noncoincidence of the central plane of the ring current with the equatorial plane of the Earth Other details are described. M.G.

N82-25661*# National Aeronautics and Space Administration. Langley Research Center, Hampton, Va.
IN SITU OZONE DATA FOR COMPARISON WITH LASER ABSORPTION REMOTE SENSOR: 1980 PEPE/NEROS PROGRAM
D S. MCDOUGAL, R. B. LEE, III, and R. J. BENDURA May 1982 42 p refs
(NASA-TM-84471; NAS 1 15:84471) Avail: NTIS HC A03/MF A01 CSCL 13B

Several sets of in situ ozone (O3) measurements were made by a NASA aircraft in support of the laser absorption spectrometer (LAS) remote sensor These measurements were designed to provide comparative O3 data for the LAS sensor. The LAS, which was flown on a second aircraft, remotely measured the vertical burden of O3 from the aircraft to the surface. In situ results of the air quality (O3 and B sub scat) and meteorological (temperature and dewpoint) parameters for three correlative missions are presented The aircraft flight plans, in situ concentration profiles and vertical burdens, and measurement errors are summarized B W.

N82-26757*# Instituto de Pesquisas Espaciais, Sao Jose dos Campos (Brazil).
COMPARISON OF STORM-TIME CHANGES OF GEOMAGNETIC FIELD AT GROUND AND MAGSAT ALTITUDES
N DEJESUSPARADA, Principal Investigator, R. P. KANE, and N. B TRIVEDI Jan. 1982 17 p refs Sponsored by NASA and Fundo Nacional de Desenvolvimento Cientifico e Tecnologio ERTS
(E82-10359; NASA-CR-168980; NAS 1.26:168980; INPE-2297-RPE/401) Avail: NTIS HC A02/MF A01 CSCL 04B

The MAGSAT data for the period Nov. 2-20, 1979 were studied. From the observed H, the HMD predicted by model was subtracted. The residue delta H = H-HMD shows storm-time variations similar to geomagnetic Dst, at least qualitatively Delta H sub 0, i.e., equatorial values of delta H were studied separately for dusk and dawn and show some differences T.M.

N82-27737# California Univ , Livermore Lawrence Livermore Lab
FEASIBILITY OF LASER-SEPARATION OF 36 S AND ITS USE AS AN ATMOSPHERIC TRACER
I. P. HERMAN 18 Aug. 1981 14 p refs
(Contract W-7405-ENG-48)
(DE82-000965, UCID-19167) Avail NTIS HC A02/MF A01

The use of laser produced sulfur isotopes to analyze the acid rain situation is considered. The proposed use of isotopically labelled SO2, in particular of (56)SO2, as a tracer can help elucidate the chemical and transport facets in a unified experiment. Separation of a sufficient quantity of the rare (36)S isotope to perform several of these tracer studies appears to be practical and economical T.M.

N82-27802# Tennessee Valley Authority, Chattanooga. Office of Natural Resources.
REMOTE SENSING OF SULFUR DIOXIDE EFFECTS ON VEGETATION. VOLUME 1: SUMMARY Final Report
C. D. SAPP Jul. 1981 31 p 2 Vol.
(Contract EPA-IAG-D8-E721)
(DE82-900580; TVA/ONR/ARP-81/5-VOL-1; EPA-660/7-81-113)
Avail: NTIS HC A03/MF A01

Three techniques for detecting and mapping sulfur dioxide (SO2) effects on the foliage of sensitive crops and trees near large, coal-fired power plants were tested and evaluated: spectroradiometry, photometric analysis of aerial photographs, and computer analysis of airborne multispectral scanner data. DOE

N82-27803# Tennessee Valley Authority, Chattanooga Office of Natural Resources
REMOTE SENSING OF SULFUR DIOXIDE EFFECTS ON VEGETATION. VOLUME 2: DATA Final Report
C. D. SAPP Jul. 1981 280 p refs 2 Vol
(Contract EPA-IAG-D8-E721)
(DE82-900581, TVA/ONR/ARP-81/6-VOL-2, EPA-600/7-81-114)
Avail: NTIS HC A13/MF A01

Airborne multispectral scanner data covering affected soybean fields were analyzed using three computer-assisted procedures: unsupervised, supervised, and pseudosupervised. The last method provided the best results. LANDSAT imagery was also investigated, but the foliar effects of SO2 were too subtle to detect from orbit. DOE

03

GEODESY AND CARTOGRAPHY

Includes mapping and topography

A82-22294* Pittsburg Univ., Pa
A COLOR-RATIO MAP OF MERCURY
B. HAPKE, C CHRISTMAN, B. RAVA (Pittsburgh, University, Pittsburgh, PA), and J. MOSHER (California Institute of Technology, Jet Propulsion Laboratory, Pasadena, CA) In: Lunar and Planetary Science Conference, 11th, Houston, TX, March 17-21, 1980, Proceedings. Volume 1. New York, Pergamon Press, 1980, p. 817-821. refs

Orange and UV frames are used to construct a color-ratio map of the portion of Mercury imaged by Mariner 10, with at least two independent color-ratio images being used for each region in order to prevent spurious, blemish-induced color Color differences appear to be smaller than those of the moon, and many apparently fresh craters and their ray systems tend to be bluer than their surroundings Regions of interesting color contrast are noted, and it is concluded that there is little evident correlation of color with either geology or topography. O C.

A82-22595
PREFLARE INCREASES IN SOLAR COSMIC RAYS RELEVANT TO THE MODE OF ENERGY ACCUMULATION IN THE ACTIVE REGIONS ASSOCIATED WITH LARGE FLARES
G. M. BLOKH, O. P. GRIGORIAN, and B. M KUZEVSKII (Moskovskii Gosudarstvennyi Universitet, Moscow, USSR) In: International Cosmic Ray Conference, 17th, Paris, France, July 13-25, 1981, Conference Papers. Volume 3. Gif-sur-Yvette, Essonne, France, Commissariat a l'Energie Atomique, 1981, p. 77-80. refs

Evidence of preflare increases in the electron and proton solar cosmic ray components is analyzed to develop a model of the processes involved. Data from the Prognoz-6 and Helios-1 and -2 satellites are cited as proof of a temporal form of particle arrival similar to a flare-produced event. The electron data indicates a set of individual events of acceleration up to 5 MeV and proton data shows the same process up to tens of MeV, implying a quasicontinuous generation of particles The low-energy particle increase has been observed to occur several days in advance of a flare, with the particle acceleration happening in subregions of an imminent flare event It is suggested that Coulomb interactions in the two-component plasma are responsible for the accelerations, *which do not culminate in a flare until the ionization energy loss* on the electrons and protons becomes insignificant compared to the acceleration rate M.S.K.

A82-22596
COMPARISON OF SOLAR PROTON ACTIVITY IN 1967 AND 1969 WITH THAT IN 1978 AND 1979 AS MEASURED ONBOARD VENERA 4, 6, 11, 12 SPACE PROBES
S. I ERMAKOV, N. N KONTOR, G. P. LIUBIMOV, N. V. PERESLEGINA, and T G. KHOTILOVSKAIA (Moskovskii Gosudarstvennyi Universitet, Moscow, USSR) In: International Cosmic Ray Conference, 17th, Paris, France, July 13-25, 1981, Conference Papers. Volume 3. Gif-sur-Yvette, Essonne, France, Commissariat a l'Energie Atomique, 1981, p. 81-84.

A comparison of the proton activity in 1967 and 1969 with that in 1978-1979 shows that proton activity in 1967 was much below the level of 1978-1979 owing to the high solar activity during the rise phase of the 21st cycle It is also found that the activity in 1969 was much above the level of 1978-1979, although the smoothed sunspot number was approximately 110 This is seen as indicating that proton activity is weakly correlated with the smoothed sunspot number and is determined largely by the phase of the solar cycle. The greatest proton activity was observed in phases of maximum solar activity and solar activity decay C.R.

A82-22598
SPACECRAFT DETERMINATION OF ENERGETIC PARTICLE PROPAGATION PARAMETERS - THE 1 JANUARY 1978 SOLAR EVENT
K. KECSKEMETY, T. I. GOMBOSI, A. J. SOMOGYI, A SZENTGALI (Magyar Tudomanyos Akademia, Kozponti Fizikai Kutato Intezet, Budapest, Hungary), G. WIBBERENZ, G GREEN, H. KUNOW, V. STEFFENS (Kiel, Neue Universitaet, Kiel, West Germany), V. G. KURT, and IU. I. LOGACHEV (Moskovskii Gosudarstvennyi Universitet, Moscow, USSR) In: International Cosmic Ray Conference, 17th, Paris, France, July 13-25, 1981, Conference Papers Volume 3. Gif-sur-Yvette, Essonne, France, Commissariat a l'Energie Atomique, 1981, p. 89-92. refs

Intensity-time profiles in similar energy intervals measured by the longitudinally separated Helios 1/2 and Prognoz 6 spacecraft are used in studying coronal injection and interplanetary propagation. The scattering mean free path for the interplanetary propagation turns out to be in essence the same for the three locations If the coronal propagation is described by a Reid-Axford type diffusion model, the diffusion coefficient is approximately constant below 200 MeV (about 0.1 AU), above this rigidity it exhibits a power law increase. C.R.

A82-22614
THE MODEL OF THE COSMIC RAY ENRICHMENT BY HELIUM-3
L. G. KOCHAROV (Leningradskii Politekhnicheskii Institut, Leningrad, USSR) In: International Cosmic Ray Conference, 17th, Paris, France, July 13-25, 1981, Conference Papers. Volume 3. Gif-sur-Yvette, Essonne, France, Commissariat a l'Energie Atomique, 1981, p. 175-178. refs

A model of He(3) enrichment is used to demonstrate that a stratified electron shock front propagating through the upper chromosphere may produce the He(3) enrichment in solar cosmic rays. The model also shows that bursts of hard X-rays, microwaves and UV radiation are produced An analysis of available data shows that He(3) rich events are accompanied by hard X-rays, whose fluxes are in good agreement with theoretical estimations by Kocharov et al. (1980) D L.G.

A82-29615*# National Aeronautics and Space Administration Goddard Space Flight Center, Greenbelt, Md
GRAVITY MODEL IMPROVEMENT FOR SEASAT
F J LERCH, J. G MARSH (NASA, Goddard Space Flight Center, Geodynamics Branch, Greenbelt, MD), S. M KLOSKO, and R G. WILLIAMSON (EG&G Washington Analytical Services Center, Inc , Riverdale, MD) Journal of Geophysical Research, vol 87, Apr. 30, 1982, p. 3281-3296 refs
(Previously announced in STAR as N80-20749)

A82-30306
WORK RELATED TO THE BLUE ROAD GEOTRAVERSE AT THE FINNISH GEODETIC INSTITUTE
J MAKINEN (Geodeettinen Laitos, Helsinki, Finland) Earth Evolution Sciences, vol 1, Mar. 1981, p 71-76. refs
Finnish Geodetic Institute research work and research capabilities relevant to Blue Road Geotraverse studies are described Institute activities cover precise levelling, high-precision gravimetry on land uplift gravity lines, earth tide observations, gravity mapping, geoid calculations, satellite geodesy, VLBI techniques, and geometric geodesy. O.C.

A82-30314
MAGNETIC ANOMALIES AS A REFERENCE FOR GROUND-SPEED AND MAP-MATCHING NAVIGATION
C. TYREN Journal of Navigation, vol. 35, May 1982, p. 242-254
The use of the earth's magnetic field for ground referenced motion and position measurements is discussed A magnetic terrain-navigation concept is set forth, and its sensor configuration, data processing and data storage unit, and navigation data interface unit are discussed. The navigational accuracy of the system is assessed, one particular advantage of terrain navigation systems is that ground-speed accuracy is independent of vehicle speed until speeds are reached at which the sensors and/or computer operations are too slow to track the vehicle path. The system is therefore excellent at low speeds and can advantageously be used for hovering operations. The results of field tests indicate that the feasibility of both ground-speed and map-matching methods is indeed promising. C D.

A82-30778
MAGNETIC CHARTS OF CANADA DERIVED FROM MAGSAT DATA
L. R. NEWITT, E. DAWSON, R. L. COLES, and A NANDI (Department of Energy, Mines, and Resources, Div of Geomagnetism, Ottawa, Canada) Geophysical Research Letters, vol 9, Apr 1982, p 246-249 refs
The feasibility of regional magnetic chart production by means of Magsat scalar and vector data is assessed through comparisons of Magsat north, east, vertical and total field charts with Canadian aeromagnetic data. After reducing all satellite and aeromagnetic data to sea-level, gridding at 1-deg intervals of longitude and latitude, and contouring the charts, it was determined that good agreement exists between the two data sets, with an overall rms difference of 150 nT. In all components, the greatest discrepancies between data sets occur in the northern U S and along the east coast of Canada O.C.

A82-30784* National Aeronautics and Space Administration Goddard Space Flight Center, Greenbelt, Md
INITIAL SCALAR MAGNETIC ANOMALY MAP FROM MAGSAT
R. A LANGEL (NASA, Goddard Space Flight Center, Greenbelt, MD), J D PHILLIPS (U.S. Geological Survey, Reston, VA), and R. J. HORNER (Computer Sciences Corp , Silver Spring, MD) Geophysical Research Letters, vol. 9, Apr. 1982, p. 269-272. refs
Magsat data acquired during the November 1979-June 1980 mission was used to derive a scalar magnetic anomaly map covering +50 to -50 deg geographic latitude, and the separation of anomaly fields from core and external fields was accomplished by techniques developed for POGO satellite data Except in the Atlantic and Pacific at latitudes south of -15 deg, comparison of the Magsat map with its POGO data-derived counterpart shows basic anomaly patterns to be reproducible, and higher resolution due to Magsat's lower measurement altitude Color-coded scalar anomaly maps are presented for both satellites O C

A82-30785* National Aeronautics and Space Administration. Goddard Space Flight Center, Greenbelt, Md
INITIAL VECTOR MAGNETIC ANOMALY MAP FROM MAGSAT
R. A. LANGEL, C. C SCHNETZLER (NASA, Goddard Space Flight Center, Greenbelt, MD), J. D. PHILLIPS (U S. Geological Survey, Reston, VA), and R. J HORNER (Computer Sciences Corp., Silver Spring, MD) Geophysical Research Letters, vol 9, Apr. 1982, p. 273-276. refs
Global magnetic component anomaly field maps have been derived from the Magsat vector magnetometer data obtained from November 1979 through May 1980 The amplitude of variations of the components over the maps are between 10 and 15 nT, well above the noise in the data. Averaged data, in 2-by-2 deg blocks, exhibit standard errors of the mean of about 1 nT over most of the X and Z maps, and about 2 nT over most of the Y maps. Errors rise to about twice these amounts near the auroral belts. Most of the anomalies in the component data are consistent with a crustal magnetization model which incorporates dipoles aligned only in the direction of the main field. However, there appear to be some regions which require dipoles aligned in some other direction i.e., remanent magnetization (Author)

A82-30787* Wisconsin Univ., Madison
MAGSAT MAGNETIC ANOMALIES OVER ANTARCTICA AND THE SURROUNDING OCEANS
M. H. RITZWOLLER and C. R BENTLEY (Wisconsin, University, Madison, WI) Geophysical Research Letters, vol. 9, Apr. 1982, p. 285-288 refs
(Contract NAS5-25977)

A82-30788* Analytic Sciences Corp., Reading, Mass.
SPATIAL RESOLUTION AND REPEATABILITY OF MAGSAT CRUSTAL ANOMALY DATA OVER THE INDIAN OCEAN
R. V. SAILOR, A R. LAZAREWICZ, and R F. BRAMMER (Analytic Sciences Corp , Reading, MA) Geophysical Research Letters, vol. 9, Apr 1982, p 289-292. refs
(Contract NAS5-26424)
Preliminary results from analysis of individual Magsat tracks in the eastern Indian Ocean demonstrate the resolution capability and repeatability of these data. Spectrum analysis indicates that 250 km is the absolute lower limit for resolving crustal magnetic anomalies in Magsat along-track data Spectral coherence analysis of closely-spaced tracks shows that magnetic anomaly features with wavelengths greater than 700 km are highly repeatable from track to track (Author)

A82-30789* Purdue Univ , Lafayette, Ind
VERIFICATION OF THE CRUSTAL COMPONENT IN SATELLITE MAGNETIC DATA
R. R. B. VON FRESE, W. J. HINZE, J. L SEXTON, and L. W. BRAILE (Purdue University, West Lafayette, IN) Geophysical Research Letters, vol 9, Apr. 1982, p 293-295.
(Contract NAS5-25030)

A82-30790* North Carolina State Coll , Raleigh.
A PRELIMINARY COMPARISON OF THE MAGSAT DATA AND AEROMAGNETIC DATA IN THE CONTINENTAL U.S.
I. J. WON and K H. SON (North Carolina State University, Raleigh, NC) Geophysical Research Letters, vol 9, Apr 1982, p. 296-298.
(Contract NAS5-26157)
A preliminary regional scale magnetic anomaly map derived from the Magsat data over the continental U S. shows reasonably good correlations when compared with the corresponding aeromagnetic map This conclusion is based upon the analysis of the fine attitude scalar Magsat data of about a two-month duration starting November 2, 1979 and the analysis of the Project Magnet U.S. aeromagnetic data in the same region. (Author)

A82-30795* Purdue Univ., Lafayette, Ind.
A SATELLITE MAGNETIC MODEL OF NORTHEASTERN SOUTH AMERICAN AULACOGENS
M. B. LONGACRE, W. J. HINZE, and R. R. B. VON FRESE (Purdue University, West Lafayette, IN) Geophysical Research Letters, vol. 9, Apr. 1982, p 318-321 refs
(Contract NAS5-25030)

Magnetic modeling of the Amazon River and Takatu Aulacogens in northeastern South America illustrate the utility of satellite magnetic data in characterizing the properties and structure of the lithosphere. Specifically, reduction of preliminary Magsat scalar magnetic anomaly data to an equivalent condition of vertical polarization shows a general correlation between magnetic anomaly minima and the Amazon River and Takatu Aulacogens. Surface gravity data demonstrate a correlative positive anomaly Spherical earth modeling of the magnetic data indicates a less magnetic crust associated with the aulacogens which is compatible with previous studies over the Mississippi River Aulacogen and Rio Grande Rift in North America. (Author)

A82-30796
PRELIMINARY INTERPRETATION OF MAGNETIC ANOMALIES OVER JAPAN AND ITS SURROUNDING AREA
M. YANAGISAWA, T. YUKUTAKE, N. FUKUSHIMA (Tokyo, University, Tokyo, Japan), and M. KONO (Tokyo Institute of Technology, Tokyo, Japan) Geophysical Research Letters, vol. 9, Apr. 1982, p 322-324 refs

A82-30849
ALBEDO AND ANGULAR CHARACTERISTICS OF THE REFLECTANCE OF THE UNDERLYING SURFACE AND CLOUDS [AL'BEDO I UGLOVYE KHARAKTERISTIKI OTRAZHENIIA PODSTILAIUSHCHEI POVERKHNOSTI I OBLAKOV]
K. IA. KONDRATEV, V. I. BINENKO, L. N. DIACHENKO, V. I. KORZOV, and V V MUKHENBERG Leningrad, Gidrometeoizdat, 1981 232 p In Russian refs

Information on the reflectance in the short-wave region of the spectrum of clouds and of the system comprising the earth's surface and atmosphere is discussed. Data are presented on the total albedo of the underlying surface and on the geographical distribution of albedo. Attention is given to the principles determining the spectral distribution of the albedo. Also considered are the laws governing the angular distribution of the reflectance of various types of natural formations C R.

A82-31994* Kansas Univ Center for Research, Inc., Lawrence.
THE RECOGNITION OF EXTENDED TARGETS - SAR IMAGES FOR LEVEL AND HILLY TERRAIN
J A. STILES, V. S. FROST, J. C HOLTZMAN, and K S SHANMUGAM (University of Kansas Center for Research, Inc., Lawrence, KS) IEEE Transactions on Geoscience and Remote Sensing, vol. GE-20, Apr 1982, p. 205-211. Research supported by the California Institute of Technology refs
(Contract NAS7-100)

Radar image simulation techniques are used to determine the character of SAR images of area-extensive targets, for the cases of flat underlying terrain and of moderate relief, with a view to the severity of elevation change effects on the detection and recognition of boundaries and shapes. The experiment, which demonstrated these effects on shapes and boundaries, was performed in order to establish Seasat-A SAR performance. Attention is given to the geometry/propagation effects in range perspective imaging that must be known for information extraction. O.C.

A82-32077* Ohio State Univ., Columbus.
REFERENCE COORDINATE SYSTEMS FOR EARTH DYNAMICS - A PREVIEW
I. I. MUELLER (Ohio State University, Columbus, OH) In Reference coordinate systems for earth dynamics; Proceedings of the Fifty-sixth Colloquium, Warsaw, Poland, September 8-12, 1980 Dordrecht, D Reidel Publishing Co, 1981, p 1-22. Deutsche Forschungsgemeinschaft refs
(Contract DFG-4810/79; NSG-5265)
(Previously announced in STAR as N81-12525)

A82-32078* Joint Inst. for Lab. Astrophysics, Boulder, Colo
ESTABLISHMENT OF TERRESTRIAL REFERENCE FRAMES BY NEW OBSERVATIONAL TECHNIQUES
P L. BENDER (Joint Institute for Laboratory Astrophysics, National Bureau of Standards, Quantum Physics Div, Boulder, CO) In Reference coordinate systems for earth dynamics, Proceedings of the Fifty-sixth Colloquium, Warsaw, Poland, September 8-12, 1980. Dordrecht, D. Reidel Publishing Co., 1981, p 23-36 NBS-supported research refs
(Contract NASA ORDER S-65000-B)

It is anticipated that terrestrial reference systems for geodynamics studies which include adopted plate motion models will be introduced for the analysis of both LAGEOS satellite and very long baseline interferometry ranging data. One of the possible approaches involves adjustment of ground station coordinates in conjunction with solutions for Universal Time 1 (UT1) and polar motions as functions of time. Another method uses principal value decomposition to reduce the number of degrees of freedom being solved for by three In a third alternative, the values of UT1 and polar motion derived from the available data by means of the initial set of coordinates are kept fixed, and an appropriate block of data is reanalyzed using the previously determined values of UT1 and polar motion so that a new set of station coordinates can be derived O C.

A82-32084
THE DEFINITION OF THE TERRESTRIAL COORDINATE FRAME BY LONG BASELINE INTERFEROMETRY
W. H. CANNON (York University, Toronto, Canada) and M. G ROCHESTER (Newfoundland, Memorial University, St. John's, Canada) In. Reference coordinate systems for earth dynamics, Proceedings of the Fifty-sixth Colloquium, Warsaw, Poland, September 8-12, 1980. Dordrecht, D. Reidel Publishing Co., 1981, p. 111-118. refs

This paper examines the question of the definition of the celestial and terrestrial coordinate frames by the technique of long baseline interferometry. It demonstrates how the celestial coordinate frame may be usefully defined in terms of basis I-forms associated with the advancing phase fronts of the radiation fields from compact radio sources using only interferometer observables. The paper then proceeds to show how the terrestrial coordinate frame could be usefully defined, incorporating fully the effects of plate tectonics and secular motion of the observatories, by an application of the theory of continuum mechanics to interferometer observations. (Author)

A82-32090
ON REFERENCE COORDINATE SYSTEMS USED IN POLAR MOTION DETERMINATIONS
B. KOLACZEK (Polska Akademia Nauk, Centrum Badan Kosmicznych, Warsaw, Poland) and G. TELEKI (Astronomiska Opservatorija, Belgrade, Yugoslavia) In: Reference coordinate systems for earth dynamics, Proceedings of the Fifty-sixth Colloquium, Warsaw, Poland, September 8-12, 1980 Dordrecht, D. Reidel Publishing Co, 1981, p. 165-173. Research supported by the Smithsonian Institution. refs

A short review of the reference pole presently used in polar motion determinations by classical astrometric methods is followed by a discussion of the systematic differences between systems of polar coordinates and the influence of the mean latitude of stations on pole position The importance of homogenous processing of astrometric data is stressed. (Author)

A82-32096
SOME CONSIDERATIONS IN THE USE OF VERY-LONG-BASELINE-INTERFEROMETRY TO ESTABLISH REFERENCE COORDINATE SYSTEMS FOR GEODYNAMICS
D. S ROBERTSON (NOAA, National Geodetic Survey and National Ocean Survey, Rockville, MD) In. Reference coordinate systems for earth dynamics; Proceedings of the Fifty-sixth Colloquium, Warsaw, Poland, September 8-12, 1980. Dordrecht, D. Reidel Publishing Co., 1981, p. 205-216. refs

A82-32099
ORIGIN AND SCALE OF COORDINATE SYSTEMS IN SATELLITE GEODESY
J. B. ZIELINSKI (Polska Akademia Nauk, Centrum Badan Kosmicznych, Warsaw, Poland) In: Reference coordinate systems for earth dynamics, Proceedings of the Fifty-sixth Colloquium, Warsaw, Poland, September 8-12, 1980. Dordrecht, D. Reidel Publishing Co , 1981, p 239-250. refs

The center of mass of the earth is commonly taken as origin for the coordinate systems used in satellite geodesy In this paper the notion of the 'geocenter' is discussed from the point of view of mechanics and geophysics. It is shown that processes in and above the crust have practically no impact on the position of the geocenter It is possible however that motions of the inner core may cause variations of the geocenter of the order of 1 m. Nevertheless the geocenter is the best point for the origin of a coordinate system Mather's method of monitoring geocenter motion is discussed, and some other possibilities are mentioned. Concerning the scale problem, the role of the constant GM and time measurements in satellite net determinations are briefly discussed. (Author)

A82-32646* California Univ , Los Angeles.
GEOID HEIGHT-AGE RELATION FROM SEASAT ALTIMETER PROFILES ACROSS THE MENDOCINO FRACTURE ZONE
D. T. SANDWELL and G. SCHUBERT (California, University, Los Angeles, CA) Journal of Geophysical Research, vol 87, May 10, 1982, p. 3949-3958. refs
(Contract NAG5-152)

Twenty-eight Seasat altimeter profiles crossing the Mendocino Fracture Zone are used together with seafloor ages determined from magnetic lineations to estimate the change in oceanic geoid height with age, between ages of 15 and 135 m.y. An unbiased estimate of the overall geoid offset along each profile is determined from a least-squares fit of the along-track derivative of the geoid to the geoid slope predicted from a simple two-layer gravitational edge effect model. Uncertainties based upon the statistical properties of each profile are also determined A geoid slope-age relation is constructed by normalizing the geoid offsets and uncertainties by the age offsets. The results are in agreement with geoid slope-age relations determined from symmetrically spreading ridges (Sandwell and Schubert, 1980). However, the fracture zone estimates have smaller uncertainties and show less scatter. A comparison of these results with the geoid slope-age prediction of the boundary layer cooling model shows that the thermal structure begins to deviate from this model at an early age (20-40 m.y.). A plate cooling model with a thickness of 125 km is most compatible with the geoid slope-age estimates, although significant deviations occur, these may indicate that the lithospheric thermal structure is not entirely age dependent. (Author)

A82-33293
ESTABLISHING GEODETIC-GEODYNAMIC PARAMETERS USING LUNAR LASER RANGE MEASUREMENTS [DIE BESTIMMUNG GEODAETISCH-GEODYNAMISCHER PARAMETER MIT HILFE VON LASERDISTANZMESSUNGEN ZUM MOND]
L. BALLANI (Deutsche Akademie der Wissenschaften, Zentralinstitut fuer Physik der Erde, Potsdam, East Germany) Gerlands Beitraege zur Geophysik, vol. 91, no. 2, 1982, p. 121-140. In German. refs

The state of the art of lunar laser range measurements is reviewed. The transit time of the signals is simulated to determine if the effects of the final signal speed should be taken into account, and modeling of the signal time delay is treated in the frame of earth-moon dynamics. Results concerning coordinates and distances of laser stations in the United States, USSR and Austria, and essential UTO and UT1 analyses are presented Conditions for establishing the geodetic-geodynamic parameters are determined, and preliminary estimations are made. (Author)

A82-33295
THE SIMULTANEOUS EMPLOYMENT OF GEODETIC MEASUREMENTS FOR BLOCK ADJUSTMENTS USING THE METHOD OF INDEPENDENT MODELS [EIN BEITRAG ZUR SIMULTANEN VERWENDUNG GEODAETISCHER MESSUNGEN BEI BLOCKAUSGLEICHUNGEN NACH DER METHODE DER UNABHAENGIGEN MODELLE]
R.-D DUEPPE (Darmstadt, Technische Hochschule, Darmstadt, West Germany) Bildmessung und Luftbildwesen, vol 50, May 1, 1982, p. 81-90. In German. refs

A method is proposed which involves the simultaneous adjustment of some types of geodetic measurements using independent models. Fields of application for the simultaneous adjustment are reviewed, and the photogrammetric consideration of geodetic measurements using the block adjustments with independent models is discussed. The method is presented with regard to a computer program development, and is demonstrated by several examples. D.L.G

A82-34719
COMPARING LINEAMENTS INTERPRETED FROM LANDSAT IMAGERY AND TOPOGRAPHIC MAPS WITH REPORTED FAULTS IN SOUTHWEST MONTANA
R. C. HOWE and D M. THOMPSON (Indiana State University, Terre Haute, IN) In: American Society of Photogrammetry, Annual Meeting, 47th, Washington, DC, February 22-27, 1981, ASP Technical Papers. Falls Church, VA, American Society of Photogrammetry, 1981, p 237-246 refs

Poor resolution has usually prevented detection of features smaller than 60 by 80 meters on Landsat imagery. However, features previously not known to be related have been shown to be continuous or semicontinuous over large distances as a result of the synoptic view provided by satellites. In particular, numerous authors have noted the usefulness of Landsat imagery for lineament interpretations. The present investigation has the objective to compare the results of the lineament interpretation from Landsat imagery and topographic maps with reported faults in a portion of southwest Montana. The 1:1,000,000 color composite Landsat image was found to be clearly superior to 1:250,000 topographic maps for detecting lineaments Almost twice as many lineaments were visible on the image as could be interpreted from the maps. However, the number of reported faults matching lineaments interpreted from each of these two data bases was similar. G.R.

A82-34918* National Aeronautics and Space Administration. Goddard Space Flight Center, Greenbelt, Md.
SATELLITE AND SURFACE GEOPHYSICAL EXPRESSION OF ANOMALOUS CRUSTAL STRUCTURE IN KENTUCKY AND TENNESSEE
M. A. MAYHEW (BTS, Inc , Seabrook, MD), H. H THOMAS, and P. J. WASILEWSKI (NASA, Goddard Space Flight Center, Greenbelt, MD) Earth and Planetary Science Letters, vol 58, no 3, May 1982, p. 395-405. refs
(Previously announced in STAR as N82-17715)

A82-37175
THE PROCESSING OF SATELLITE NAVIGATION DATA FOR MARINE GEODESY [OBRABOTKA SPUTNIKOVOI NAVIGATSIONNOI INFORMATSII DLIA MORSKOI GEODEZII]
IU. G FIRSOV and B. D. IAROVOI Geodeziia i Kartografiia, May 1982, p. 37-42 In Russian. refs

Various aspects of the use of satellite navigation systems to solve problems of marine geodesy, i.e., to determine ship coordinates, are examined. Particular consideration is given to the use of the integral Doppler method; the parametric equation and

the solution of the problem in a spatial coordinate system; the determination of coordinates in a spatial polar system; allowance for different times of Doppler measurements in determining the coordinates of a mobile station; and tack equalization with allowance for feedback of satellite determinations. B.J.

A82-37962*# National Aeronautics and Space Administration Goddard Space Flight Center, Greenbelt, Md.
INFORMATION THEORY LATERAL DENSITY DISTRIBUTION FOR EARTH INFERRED FROM GLOBAL GRAVITY FIELD
D. P. RUBINCAM (NASA, Goddard Space Flight Center, Geodynamics Branch, Greenbelt, MD) Journal of Geophysical Research, vol 87, July 10, 1982, p. 5541-5552. NASA-supported research. refs
(Previously announced in STAR as N82-19731)

N82-22621*# Sao Paulo Univ. (Brazil).
STRUCTURE, COMPOSITION AND THERMAL STATE OF THE CRUST IN BRAZIL Progress Report, Feb. - May 1981
I. I. G. PACCA, Principal Investigator and W. SHUKOWSKY May 1981 41 p refs Sponsored by NASA ERTS
(E82-10187, NASA-CR-168615; NAS 1.26.168615) Avail NTIS HC A03/MF A01 CSCL 08G

Efforts in support of a geomagnetic survey of the Brazilian area are described Software to convert MAGSAT data tapes to the Burroughs/B-6700 binary format was developed and tested. A preliminary analysis of the first total intensity anomaly map was performed and methodologies for more intensive analysis were defined. The sources for correlative geological, aeromagnetic, and gravimetric data are described M.G.

N82-22628*# Purdue Univ, Lafayette, Ind Dept of Geosciences.
STUDY OF GRAVITY AND MAGNETIC ANOMALIES USING MAGSAT DATA Quarterly Progress Report, Apr. - Jun. 1981
L. W. BRAILE, W. J HINZE, and R. R B VONFRESE, Principal Investigators 1 Jul 1981 9 p ERTS
(E82-10194, NASA-CR-168621; NAS 1.26:168621) Avail NTIS HC A02/MF A01 CSCL 08B

The results of modeling satellite-elevation magnetic and gravity data using the constraints imposed by near surface data and seismic evidence shows that the magnetic minimum can be accounted for by either an intracrustal lithologic variation or by an upwarp of the Curie point isotherm. The long wavelength anomalies of the NOO's-vector magnetic survey of the conterminous U S. were contoured and processed by various frequency filters to enhance particular characteristics. A preliminary inversion of the data was completed and the anomaly field calculated at 450 km from the equivalent magnet sources to compare with the POGO satellite data. Considerable progress was made in studing the satellite magnetic data of South America and adjacent marine areas. Preliminary versions of the 1 deg free-air gravity anomaly map (20 m gal contour interval) and the high cut (lambda approximately 8 deg) filtered anomaly maps are included A.R.H.

N82-22832# National Academy of Sciences - National Research Council, Washington, D C Committee on Geodesy.
GEODETIC MONITORING OF TECTONIC INFORMATION. TOWARD A STRATEGY
1981 118 p refs
Avail: NTIS HC A06/MF A01 CSCL 08G

The time scale and time lapse over which crustal movements are traditionally monitored by geodesy and seismology was studied. Efforts are made to bridge this gap through increasing the frequency of geodetic measurements in the regions of particular interests, establishment of a global network of long and ultralong period seismometers, and development of geophysical and geodetic intrumentation that should be capable of measuring rates of crustal deformation over arbitrary time scales. The following measurements were undertaken: (1) on a global scale; (2) deformation near active plate boundaries; (3) deformation within plate interiors and other neotectonic motion; and (4) instrumentation for measuring tectonic deformation. E.A K.

N82-22846*# National Academy of Sciences - National Research Council, Washington, D. C. Panel on Crustal Movement Measurements.
GEODETIC MONITORING OF TECTONIC DEFORMATION: TOWARD A STRATEGY Final Report
Nov. 1981 121 p refs Sponsored in part by Defense Mapping Agency, Washington, NASA, Washington; NOAA, Washington; and Geological Survey, Reston, Va.
(NASA-CR-168784, NAS 1 26 168784; PB82-137118) Avail: NTIS HC A06/MF A01 CSCL 08E

Issues of interest and importance to society and science are presented. The problems considered are of national concern; their solutions may contribute to a better understanding of tectonic deformation and earthquake hazards The need for additional field data, the role of geodetic measurements, the importance of both ground and space techniques, and the need for advanced instrumentation development are discussed. GRA

N82-23563*# Consiglio Nazionale delle Ricerche, Naples (Italy). Osservatorio Vesuviano
CRUSTAL STRUCTURES UNDER THE ACTIVE VOLCANIC AREAS OF CENTRAL AND EASTERN MEDITERRANEAN (M-44) Progress Report
P GASPARINI, Principal Investigator, M. S. M. MANTOVANI, F. MONACO, D. PIERATTINI, and M. FEDI 10 Jan. 1981 4 p Sponsored by NASA ERTS
(E82-10096; NASA-CR-168845; NAS 1.26.168845) Avail NTIS HC A02/MF A01 CSCL 08G

Programs are being adapted to the UNIVAC 1000 computer and others are being developed for immediate utilization in processing MAGSAT data. The magnetization intensity, susceptability, Koeningsberger ratio, NMR stbility against alternated fields and temperature, and the Curie temperature were determined for some rock formations with mineralogical compositions stable to the intermediate for lower continental crust and to upper manele conditions. Attempts to residuate crustal anomalies from one selected profile passing through western mediterranean using procedures commonly used at NASA yielded dubious results because of uncertainties in the adoption of coefficients in the expression accounting for the effect of equatorial ring currents and the empirical approach used for other corrections. Instead, filtering techniques are to be applied to each profile once invesigator B tapes relative to the whole planet are received.
A.R.H.

N82-23571*# Colorado Univ., Boulder. Dept. of Astrogeophysics.
INVESTIGATION OF GEOMAGNETIC FIELD FORECASTING AND FLUID DYNAMICS OF THE CORE Quarterly Status Technical Progress Report, 1 Apr. - 30 Jun. 1981
E. R. BENTON, Principal Investigator 1 Jul. 1981 10 p ERTS (Contract NAS5-25957)
(E82-10198, NASA-CR-168625, NAS 1.26:168625, QSTPR-6)
Avail: NTIS HC A02/MF A01 CSCL 08G

Progress in the use of MAGSAT data to confirm that the radius of the Earth's core-mantle boundary can be accurately determined magnetically is reported. The MAGSAT data was used in conjunction with a high quality manfield model for epoch 1965. The unsigned flux linking the core and mantle of the Earth is considered to be a legitimate invariant for a span of time. The value from MAGSAT of this constant is 16.056 GWb (gigawebers). J D.

N82-23573*# Washington Univ , St Louis, Mo Dept of Earth and Planetary Science.
STRUCTURE OF THE ST. FRANCOIS MOUNTAINS AND SURROUNDING LEAD BELT, S. E. MISSOURI: INFERENCES FROM THERMAL IR AND OTHER DATA SETS Quarterly Report, 13 May - 31 Jul. 1981
R. E. ARVIDSON, Principal Investigator 1 Nov 1981 5 p HCMM
(Contract NAS5-26533)
(E82-10200, NASA-CR-168627; NAS 1.26:168627) Avail: NTIS HC A02/MF A01 CSCL 08G

Heat Capacity Mapping Mission (HCMM) in the form of an apparent thermal inertia image were merged with shaded relief maps and Bouguer gravity maps. The HCMM data show that the dominant structural grain in Missouri strikes in a northwesterly direction The strike is the same as a major basement fault or flexure identified on the basis of gravity images. M.G.

N82-23577*# Analytic Sciences Corp , Reading, Mass.
BATHYMETRIC AND TECTONICS OF INDIAN OCEAN USING MAGSAT DATA Quarterly Progress Report, 1 Jul. - 30 Sep. 1981
R. V. SAILOR and A. R. LAZAREWICZ, Principal Investigators 15 Oct. 1981 22 p refs ERTS
(Contract NAS5-26424)
(E82-10204; NASA-CR-168631; NAS 1.26:168631) Avail: NTIS HC A02/MF A01 CSCL 05B

The quality of the MAGSAT data was assessed, especially the characterization of spikes The spectral passbands of significance to geophysical analysis were analyzed, including computations of spectral coherence between nearby repeating satellite tracks A spectrum modeling effort was begun which is designed to show the effect of spacecraft attitude on the observability of magnetic anomalies The data obtained is to be used to compute crustal anomaly maps by modeling the equivalent dipoles in the project area. A.R.H.

N82-23587*# Geological Survey, Denver, Colo
TOPOGRAPHIC SLOPE CORRECTION FOR ANALYSIS OF THERMAL INFRARED IMAGES
K. WATSON, Principal Investigator 1982 14 p refs HCMM
(Contract NASA ORDER S-40256-B)
(E82-10214; NASA-CR-168774; NAS 1.26:168774) Avail: NTIS HC A02/MF A01 CSCL 08B

A simple topographic slope correction using a linearized thermal model and assuming slopes less than about 20 degrees is presented The correction can be used to analyzed individual thermal images or composite products such as temperature difference or thermal inertia Simple curves are provided for latitudes of 30 and 50 degrees. The form is easily adapted for analysis of HCMM images using the DMA digital terrain data
Author

N82-24520*# Purdue Univ , Lafayette, Ind Dept of Geosciences.
SPHERICAL-EARTH GRAVITY AND MAGNETIC ANOMALY MODELING BY GAUSS-LEGENDRE QUADRATURE INTEGRATION Quarterly Progress Report, Jul. - Sep. 1981
R. R. B. VONFRESE, W. J. HINZE, L W. BRAILE, and A. J. LUCA, Principal Investigators (Chevron Geophysical Co., Calgary, Alberta) 1 Oct. 1981 11 p refs Repr. from J. Geophys. vol 49, 1981 p 234-242 ERTS
(Contract NAS5-25030)
(E82-10242; NASA-CR-168823, NAS 1.26:168823) Avail: NTIS HC A03/MF A01 CSCL 05B

The anomalous potential of gravity and magnetic fields and their spatial derivatives on a spherical Earth for an arbitrary body represented by an equivalent point source distribution of gravity poles or magnetic dipoles were calculated The distribution of equivalent point sources was determined directly from the coordinate limits of the source volume Variable integration limits for an arbitrarily shaped body are derived from interpolation of points which approximate the body's surface envelope. The versatility of the method is enhanced by the ability to treat physical property variations within the source volume and to consider variable magnetic fields over the source and observation surface A number of examples verify and illustrate the capabilities of the technique, including preliminary modeling of potential field signatures for Mississippi embayment crustal structure at satellite elevations. T.M.

N82-24522*# Tokyo Univ (Japan). Geophysics Research Lab.
INVESTIGATION FROM JAPANESE MAGSAT TEAM. PART A. CRUSTAL STRUCTURE NEAR JAPAN AND IN ANTARCTIC STATION. PART B. ELECTRIC CURRENTS AND HYDROMAGNETIC WAVES IN THE IONOSPHERE AND THE MAGNETOSPHERE Progress Report, 15 Jul. - 15 Nov. 1981
N FUKUSHIMA, Principal Investigator 15 Dec 1981 13 p refs Sponsored by NASA ERTS
(E82-10244; NASA-CR-168825; NAS 1.26:168825; PR-4) Avail. NTIS HC A02/MF A01 CSCL 05B

Preliminary results of MAGSAT data analysis are described. Regional anomaly maps (deviations from the MGST model field) for X,Y,Z, and F in the area of 115 to 155 deg E and 20 to 60 deg N were obtained. A similar map for the geomagnetic total force anomaly in the vicinity of Japan showed that the observed anomaly can be explained by the difference in crustal magnetization between the Japan Sea and the Japan Island, which reflects a difference of 25 km in the thickness of the magnetized layer. The MAGSAT record of a sudden comencement of a magnetic storm above the South Atlantic Ocean showed a reverse impulse particularly in the D-component. Results relating to toroidal currents in the ionosphere, transverse and parallel perturbations over the polar regions, the relationship between field aligned currents and precipitating electrons, and the calculation of the subsatellite electric field are also discussed M.G.

N82-24573*# Business and Technological Systems, Inc., Seabrook, Md.
AN EQUIVALENT LAYER MAGNETIZATION MODEL FOR THE UNITED STATES DERIVED FROM MAGSAT DATA
M. A MAYHEW and S. C GALLIHER, Principal Investigators 1982 8 p refs ERTS
(Contract NAS5-26328)
(E82-10297; NASA-CR-168866; NAS 1.26:168866) Avail NTIS HC A02/MF A01 CSCL 05B

Long wavelength anomalies in the total magnetic field measured field measured by MAGSAT over the United States and adjacent areas are inverted to an equivalent layer crustal magnetization distribution. The model is based on an equal area dipole grid at the Earth's surface Model resolution having physical significance, is about 220 km for MAGSAT data in the elevation range 300-500 km The magnetization contours correlate well with large-scale tectonic provinces. Author

N82-24577*# Analytic Sciences Corp , Reading, Mass.
ANALYZING THE BROKEN RIDGE AREA OF THE INDIAN OCEAN USING MAGNETIC AND GRAVITY ANOMALY MAPS AND GEOID UNDULATION AND BATHYMETRY DATA Quarterly Progress Report, 1 Jan. - 31 Mar. 1982
A. R. LAZAREWICZ and R. V. SAILOR, Principal Investigators 15 Apr. 1982 19 p refs ERTS
(Contract NAS5-26424)
(E82-10303; NASA-CR-168878; NAS 1.26:168878) Avail. NTIS HC A02/MF A01 CSCL 08G

A higher resolution anomaly map of the Broken Ridge area (2 degree dipole spacing) was produced and reduced to the pole using quiet time data for this area. The map was compared with equally scaled maps of gravity anomaly, geoid undulation, and bathymetry. The ESMAP results were compared with a NASA MAGSAT map derived by averaging data in two-degree bins. A survey simulation was developed to model the accuracy of MAGSAT anomaly maps as a function of satellite altitude, instrument noise level, external noise model, and crustal anomaly field model. A preliminary analysis of the geophysical structure of

Broken Ridge is presented and unresolved questions are listed. A.R.H

N82-24578*# Analytic Sciences Corp., Reading, Mass.
INVESTIGATING TECTONIC AND BATHYMETRIC FEATURES OF THE INDIAN OCEAN USING MAGSAT MAGNETIC ANOMALY DATA Quarterly Progress Report, 1 Sep. - 31 Dec. 1981
A. R. LAZAREWICZ and R. V. SAILOR, Principal Investigators 22 Jan. 1982 17 p refs ERTS
(Contract NAS5-26424)
(E82-10304, NASA-CR-168879; NAS 1 26 168879; PR-1325-4)
Avail. NTIS HC A02/MF A01 CSCL 08G

MAGSAT Investigator-B tapes were preprocessed by (1) removing all data points with obvious erroneous values and location errors; (2) removing smaller spikes (typically 15 nT or more), and deleting data tracks with fewer than 20 points; and (3) removing a linear trend from each track. The remaining data were recorded on tape for use by the equivalent source mapping (ESMAP) program which uses a least squares algorithm to fit the magnetization parameter of the grid of equivalent source dipoles in the crust to satellite data acquired at different times and locations. ESMAP was implemented on the TASC computing system and modified to read preprocessed MAGSAT tapes and interface with TASC plotting software. Some verification of the software was accomplished. Gridded 1-degree mean values of gravity anomaly and sea surface undulation computed from SEASAT radar altimeter were obtained and brought on line. A.R.H.

N82-24582*# Wisconsin Univ., Madison
INVESTIGATION OF ANTARCTIC CRUST AND UPPER MANTLE USING MAGSAT AND OTHER GEOPHYSICAL DATA Quarterly Status Technical Progress Report
C. R. BENTLEY, Principal Investigator 14 Jan. 1982 1 p ERTS
(Contract NAS5-25977)
(E82-10308; NASA-CR-168883; NAS 1 26 168883; QSTPR-8)
Avail: NTIS HC A02/MF A01 CSCL 08G

Development of a spectral analysis technique to determine the depth to the Curie Isotherm from MAGSAT data over Antarctica is reported. The analysis of the power spectra of a number of MAGSAT passes over Antarctica indicates on the average two power maxima for each flight pass, one with spatial wavelength of approximately 2000 km and the other with a wavelength of approximately 700 km. It was not determined whether these spectral peaks are geological or mathematical in origin. T.M

N82-24583*# Wisconsin Univ, Madison
INVESTIGATION OF ANTARCTIC CRUST AND UPPER MANTLE USING MAGSAT AND OTHER GEOPHYSICAL DATA Quarterly Status Technical Progress Report
C. R. BENTLEY, Principal Investigator 16 Apr. 1982 1 p ERTS
(Contract NAS5-25977)
(E82-10309; NASA-CR-168884; NAS 1.26:168884; QSTPR-9)
Avail: NTIS HC A02/MF A01 CSCL 08G

Plans to create an improved version of the MAGSAT magnetic anomaly map by more carefully scrutinizing the accepted data for field-aligned current effects are discussed. Data are continued to a 300 km surface for the compilation of a final map. Based on this set of data, vector anomaly maps over Antarctica are planned. A high-pass anomaly map with a cut-off wavelength of approximately 1500 km is also envisioned It is suspected that longer-wavelength features have their origin outside the crust. T.M.

N82-24584*# Colorado Univ, Boulder Dept. of Astro-Geophysics.
INVESTIGATION OF GEOMAGNETIC FIELD FORECASTING AND FLUID DYNAMICS OF THE CORE Quarterly Progress Report, 1 Jan. - 31 Mar. 1982
E. R. BENTON, Principal Investigator 1 Apr. 1982 7 p refs ERTS
(Contract NAS5-25957)
(E82-10310, NASA-CR-168885; NAS 1.26:168885, QPR-9) Avail NTIS HC A02/MF A01 CSCL 08G

It was established that the total absolute magnetic flux crossing the core- mantle boundary has been a constant of the core motion for the last 50 years This provides a scalar constraint that could be added to the geometric modelling procedure. The GSFC 8 8/80 model is being evaluated. The absolute magnetic flux linking the CMB to that model was plotted as a function of time during the span covered by the data, and increasing truncation level. The inclusion of the standard error of each Gauss coefficient derived from the statistics of fit in the GSFC 9/80 model is useful. The magnitude and sense (upwelling or downe welling) of vertical fluid motion adjacent to the core-mantle boundary was calculated using the model. Standard errors were found to be sufficiently small at all but one or two of the 40 or more critical points of B sub r They do not nearly overlap the value gamma u/gamma r = 0. It is concluded that the core is upwelling and downwelling at an observationally detectable level A.R.H.

N82-24586*# Purdue Univ, Lafayette, Ind Dept of Geosciences
MAGNETIC AND GRAVITY ANOMALIES IN THE AMERICAS Quarterly Progress Report, Oct. - Dec. 1981
L W. BRAILE, W. J. HINZE, and R. R. B. VONFRESE, Principal Investigators 30 Dec 1981 7 p Sponsored by NASA ERTS
(E82-10312; NASA-CR-168888; NAS 1 26·168888) Avail· NTIS HC A02/MF A01 CSCL 05B

The cleaning and magnetic tape storage of spherical Earth processing programs are reported. These programs include. NVERTSM which inverts total or vector magnetic anomaly data on a distribution of point dipoles in spherical coordinates; SMFLD which utilizes output from NVERTSM to compute total or vector magnetic anomaly fields for a distribution of point dipoles in spherical coordinates; NVERTG; and GFLD. Abstracts are presented for papers dealing with the mapping and modeling of magnetic and gravity anomalies, and with the verification of crustal components in satellite data. T.M.

N82-24587*# Phoenix Corp., McLean, Va.
IMPROVED DEFINITION OF CRUSTAL MAGNETIC ANOMALIES FOR MAGSAT DATA Final Report
R. D. BROWN, J. F. FRAWLEY, W. M. DAVIS, R. D RAY, E DIDWALL, and R D. REGAN, Principal Investigators 15 Mar. 1982 23 p refs ERTS
(Contract NAS5-25882)
(E82-10314; NASA-CR-168889, NAS 1 26 168889) Avail: NTIS HC A02/MF A01 CSCL 08G

The routine correction of MAGSAT vector magnetometer data for external field effects such as the ring current and the daily variation by filtering long wavelength harmonics from the data is described. Separation of fields due to low altitude sources from those caused by high altitude sources is affected by means of dual harmonic expansions in the solution of Dirichlet's problem. This regression/harmonic filter procedure is applied on an orbit by orbit basis, and initial tests on MAGSAT data from orbit 1176 show reduction in external field residuals by 24.33 nT RMS in the horizontal component, and 10.95 nT RMS in the radial component J.D.

N82-24589*# Technicolor Graphic Services, Inc., Sioux Falls, S. Dak.
AN INVESTIGATION OF MAGSAT AND COMPLEMENTARY DATA EMPHASIZING PRECAMBRIAN SHIELDS AND ADJACENT AREAS OF WEST AFRICA AND SOUTH AMERICA Quarterly Report, period ending 30 Sep. 1981
D A HASTINGS, Principal Investigator 30 Sep. 1981 34 p Sponsored by NASA ERTS
(Contract DI-14-08-0001-16439)
(E82-10316; NASA-CR-168897; NAS 1.26:168897) Avail: NTIS HC A03/MF A01 CSCL 08B

Accomplishments with regard to the mapping and analysis of MAGSAT data for the investigation of correlations between the magnetic field characteristics of South American and African shields are reported Significant results in the interpretation of the global total-field anomalies and the anomaly patterns of Africa and South America are discussed. The central position of the Brazilian shield tends to form a negative total-field anomaly, consistent with findings for shields in equatorial Africa. Sedimentary sequences in the Amazon basin and in the Rio de Janeiro-Sao Paolo areas exhibit positive anomalies, also consistent with equatorial Africa. Results for the Caribbean Sea and Guyana regions are also described. M.G.

N82-24590*# Technicolor Graphic Services, Inc , Sioux Falls, S Dak
AN INVESTIGATION OF MAGSAT AND COMPLEMENTARY DATA EMPHASIZING PRECAMBRIAN SHIELDS AND ADJACENT AREAS OF WEST AFRICA AND SOUTH AMERICA Quarterly Report, 1 Oct. - 31 Dec. 1981
D. A HASTINGS, Principal Investigator 31 Dec. 1981 13 p Sponsored by NASA ERTS
(Contract DE-14-08-0001-16439)
(E82-10317, NASA-CR-168895, NAS 1.26.168895) Avail NTIS HC A02/MF A01 CSCL 08G

Several possible causes for the east-west striping of the MAGSAT anomaly maps are listed and discussed including· (1) the inadequacy of the field model used for core-crustal separation of geomagnetic anomalies; (2) external field noise remaining in the available maps, (3) east-west trends of crustal uplift and depression; (4) east-west trends to convection patterns in the mantle; (5) bands of crustal materials of similar metamorphic grade, (6) variations in the depth of the Curie isotherm; and (7) the data processing techniques used to overcome the absence of tie lines and orbital path of MAGSAT M.G.

N82-24591*# Technicolor Graphic Services, Inc., Sioux Falls, S. Dak.
AN INVESTIGATION OF MAGSAT AND COMPLEMENTARY DATA EMPHASIZING PRECAMBRIAN SHIELDS AND ADJACENT AREAS OF WEST AFRICA AND SOUTH AMERICA Quarterly Report, 1 Jan. - 31 Mar. 1982
D. A. HASTINGS, Principal Investigator 31 Mar. 1982 14 p Sponsored by NASA ERTS
(Contract DI-14-08-0001-21249)
(E82-10318, NASA-CR-168896; NAS 1.26 168896) Avail. NTIS HC A02/MF A01 CSCL 08B

The problems associated with the use of an interactive magnetic modeling program are reported and a publication summarizing the MAGSAT anomaly results for Africa and the possible tectonic associations of these anomalies is provided. An overview of the MAGSAT scalar anomaly map for Africa suggested a correlation of MAGSAT anomalies with major crustal blocks of uplift or depression and different degrees of regional metamorphism The strongest MAGSAT anomalies in Africa are closely correlated spatially with major tectonic features. Results indicate that the Bangui anomaly may be caused by a central old Precambrian shield, flanked to the north and south by two relatively young sedimentary basins. M.G.

N82-24592*# Texas Univ. at El Paso. Dept of Geological Sciences.
THE CRUSTAL STRUCTURE AND TECTONICS OF SOUTH AMERICA Quarterly Report, 1 Jul. - 30 Sep. 1981
G R. KELLER and E G. LIDIAK, Principal Investigators 30 Sep. 1981 4 p refs ERTS
(Contract NAS5-26326)
(E82-10319; NASA-CR-168898, NAS 1.26·168898) Avail: NTIS HC A02/MF A01 CSCL 08G

A preliminary crustal structure map and a bibliography of crustal and upper mantle studies for South America are given Work on the surface wave analysis and tectonic characterizations continues M.G

N82-24593*# Texas Univ. at El Paso Dept. of Geological Sciences
GEOTECTONICS OF SOUTH AMERICA Quarterly Report, 1 Oct. 1981 - 31 Mar. 1982
G. R. KELLER and E. G LIDIAK, Principal Investigators 31 Mar. 1982 36 p refs ERTS
(Contract NAS5-26326)
(E82-10320, NASA-CR-168899, NAS 1 26.168899) Avail: NTIS HC A03/MF A01 CSCL 08G

Preliminary satellite scalar magnetic anomaly data (MAGSAT) reduced to vertical polarization and long wavelength-pass filtered free air gravity anomaly data of South and Central America are compared to major tectonic features. In addition, a geotectonic overview of South America is presented. M G

N82-24599*# Paris VI Univ. (France)
MAGSAT ANOMALY MAP AND CONTINENTAL DRIFT Progress Report
J. L LEMOUEL, Principal Investigator, A. GALDEANO, and J. DUCRUIX 1 Dec 1981 5 p refs Sponsored by NASA ERTS
(E82-10326; NASA-CR-168905; NAS 1.26:168905) Avail: NTIS HC A02/MF A01 CSCL 08G

Anomaly maps of high quality are needed to display unambiguously the so called long wave length anomalies. The anomalies were analyzed in terms of continental drift and the nature of their sources is discussed. The map presented confirms the thinness of the oceanic magnetized layer. Continental magnetic anomalies are characterized by elongated structures generally of east-west trend. Paleomagnetic reconstruction shows that the anomalies found in India, Australia, and Antarctic exhibit a fair consistency with the African anomalies. It is also shown that anomalies are locked under the continents and have a fixed geometry. T.M.

N82-24603*# Miami Univ., Fla School of Marine and Atmospheric Science
INVESTIGATIONS OF MEDIUM WAVELENGTH MAGNETIC ANOMALIES IN THE EASTERN PACIFIC USING MAGSAT DATA Interim Report, Oct. - Dec. 1981
C. G. A HARRISON, Principal Investigator Feb. 1982 3 p ERTS
(E82-10330; NASA-CR-168909; NAS 1.26:168909) Avail: NTIS HC A02/MF A01 CSCL 08G

Efforts concerning spherical harmonic modeling of the Earth's magnetic field and the use of such models in removing core produced magnetic fields from magnetic fields of crustal origin are discussed Results indicate that the terms of a spherical harmonic expansion do not uniquely determine a given wavelength of signal as the terms in a Fourier series do. Addition of terms of higher degree and order to a spherical harmonic expansion tend to fine tune the amplitude of the terms of lower degree and order. As a result, removal of such a model from a regional data set will not remove long wavelengths completely M.G

N82-25601*# Purdue Univ., Lafayette, Ind Dept. of Geosciences
AEROMAGNETIC AND SATELLITE MAGNETIC ANOMALLY MAPPING Quarterly Progress Report, Jan. - Mar. 1982
L W. BRAILE, W. J HINZE, and R. R. B VONFRESE, Principal Investigators 31 Mar. 1982 8 p Sponsored by NASA ERTS (E82-10339, NASA-CR-168958; NAS 1.26:168958) Avail. NTIS HC A02/MF A01 CSCL 05B

Efforts to process 2 deg-averaged MAGSAT data for a radially polarized map of Africa and western Europe and investigator B data tapes were initiated M G.

N82-25604*# Colorado Univ., Boulder. Dept. of Astrogeophysics.
INVESTIGATION OF GEOMAGNETIC FIELD FORECASTING AND FLUID DYNAMICS OF THE CORE Quarterly Status Technical Progress Report, 1 Oct. - 31 Dec. 1981
E R. BENTON, Principal Investigator 1 Jan. 1982 3 p ERTS (Contract NAS5-25957)
(E82-10342; NASA-CR-168959; NAS 1 26·168959; QSTPR-8) Avail: NTIS HC A02/MF A01 CSCL 08G

Accomplishments to date were summarized in three parts submitted for publication. Goddard models and MAGSAT data were used heavily in the investigation which address· (1) the sensitivity of selected geomagnetic properties to truncation level of spherical harmonic expansions; (2) the pole strength of the Earth from MAGSAT, and magnetic determination of the core radius, and (3) frozen flux upper limits to the MAGSAT geomagnetic coefficients and relative multipole indices for Earth. A.R H

N82-25748# Woods Hole Oceanographic Institution, Mass Dept. of Geology and Geophysics.
COMPUTER-PROCESSED GEOPHYSICAL ATLAS OF DIGITAL DATA FOR THE EAST COAST MARGIN OF THE UNITED STATES FROM SURFACE AND SPACECRAFT DATA
C. BOWIN, J. MILLIGAN, and K. DUNKLE Dec 1981 36 p refs Sponsored in part by Joint Oceanograph Inst., Inc.
(Contract N00014-82-C-0019)
(AD-A111388; WHOI-81-104) Avail: NTIS HC A03/MF A01 CSCL 08J

This atlas comprises maps for the East Coast margin of the United States of free-air gravity anomaly, geoid anomaly, regional geoid anomaly, residual geoid anomaly, magnetic crustal anomaly, and bathymetry Data from surface measurements, GEOS-III and MAGSAT Satellites, GEM-9 spherical harmonic coefficients, and SYNBAPS bathymetry profiling systems were utilized Estimated error maps for the geoid data are not included because for the marine areas, these data are uniformly of very low error The data are presented in three sets of maps of northern, central, and southern portions of the margin Author (GRA)

N82-26268# Defense Mapping Agency Hydrographic and Topographic Center, Washington, D.C.
A COMPARISON OF POLE POSITIONS DERIVED FROM GPS SATELLITE AND NAVY NAVIGATION SATELLITE OBSERVATIONS
W. H. WOODEN, II 6 Jan. 1982 18 p refs Presented at the 3rd Intern. Geodetic Symp. on Satellite Doppler Positioning
(AD-A110765) Avail: NTIS HC A02/MF A01 CSCL 17G

The observation of the motion of the Earth's spin axis with respect to the crust has been done continuously since the latter part of 1899 by the International Service. With the advent of new technologies, new determinations of polar motion have been possible Doppler tracking of the Navy Navigation Satellites has provided estimates of the polar motion on a permanent basis since 1969. Currently, these estimates are done at the Defense Mapping Agency and are distributed to several agencies including the Bureau International de l'Heure (BIH), which has the responsibility of centralizing polar motion data. The NAVSTAR Global Positioning System (GPS) is a new navigation satellite system which will eventually replace the existing Navy Navigation Satellite System. As a byproduct of the orbit estimation process for the GPS satellites, values for the position of the pole are determined. In this paper the two different methods for computing the pole's position from satellite observations are described The most recent results from each method are compared to each other and to the standard BIH values Author (GRA)

N82-26748*# Washington Univ., St Louis, Mo. Center for the Space Sciences.
STRUCTURE OF THE SAINT FRANCOIS MOUNTAINS AND SURROUNDING LEAD BELT, S.E. MISSOURI: INFERENCE FROM THERMAL IR AND OTHER DATA SETS Quarterly Report, 1 Nov. 1981 - 30 Apr. 1982
R E ARVIDSON, Principal Investigator 11 May 1982 65 p refs Original contains color imagery. Original imagery may be purchased from NASA Goddard Space Flight Center, (code 601), Greenbelt, Md 20770 Domestic users send orders to Attn. National Space Science Data Center , non-domestic users send orders to Attn: World Data Center A for Rockets and Satellites. . HCMM
(Contract NAS5-26533)
(E82-10350, NASA-CR-168969; NAS 1.26:168969) Avail· NTIS HC A04/MF A01 CSCL 08G

Progress in the preparation of manuscripts on the discovery of a Precambrian rift running NW-SE through Missouri as seen in free air and Bouguer gravity anomalies and in HCMM data, and on digital image processing of potential field and topographic data on the rift is reported. Copies of the papers are attached Contrast-enhanced HCMM images that have been transformed to Mercator projections are presented. Shaded relief map overlays of thermal and apparent thermal inertia images used as part of a masers thesis examining correlations between HCMM data products, linears, and geologic units are presented Progress in examination of the difference in information content of daytime infrared, night time infrared, albedo, and thermal inertia images and their application to he identification of linears not directly controlled by topography is repored. Thermal infrared and albedo data were coded as hue, saturation and brightness values to generate a color display, which is included. J D.

N82-26915# California Univ., Livermore. Lawrence Livermore Lab
SEISMIC AND GEODETIC STUDIES OF THE IMPERIAL VALLEY, CALIFORNIA Final Technical Report
D. D. JACKSON (UCLA) 1 May 1981 50 p refs
(Contract W-7405-ENG-48)
(DE82-001686, UCRL-15382) Avail· NTIS HC A03/MF A01

Patterns of gravitational and thermal anomalies, strike slip faulting, volcanism in the Imperial Valley were investigated These patterns suggest that the continental crust may still be spreading. In recent years, the United States Geological Survey and Caltech have added new seismic stations into a dense network in the Imperial Valley to study in detail the relationship between geothermal areas and earthquakes, and to understand the tectonic processes taking place there The following areas were examined: (1) crustal structure data on P wave arrival times of local earthquakes; (2) leveling data for evidence of tectonic subsidence or uplift, and (3) correlations between seismicity, seismic velocity, geodetic motion, geothermal activity, and local geology. DOE

N82-27882# National Oceanic and Atmospheric Administration, Boulder, Colo. Wave Propagation Lab.
FIELD MEASUREMENTS IN SUPPORT OF DISPERSION MODELING IN COMPLEX TERRAIN (1980) Annual Report
W. EBERHARD Jul. 1981 26 p refs
(PB82-148644; NOAA-81102005) Avail NTIS HC A03/MF A01 CSCL 13B

The EPA is engaged in a concerted effort to develop models for prediction of air quality in complex terrain. Remote sensors and an instrumented aircraft from the Wave Propagation Laboratory and other elements of NOAA's Environmental Research Laboratory are participating with EPA in a series of field experiments that are necessary for development and validation of such models. A calibrated particulate mapping lidar with multiwavelength capability is the principal remote sensor NOAA's accomplishments during

the first year (February 1980 - January 1981) under the EPA-NOAA Interagency Agreement for Energy and Environment are participation by lidar and other sensors in EPA's Small Hill Impaction Study No. 1 studying plume impingement or elevated terrain; preliminary experiment by instrumented aircraft on power plant plumes near Farmington, New Mexico, lidar participation in DOE's 1980 ASCOT experiment investigating nocturnal drainage flows in mountainous terrain; and improvements to the lidar for plume mapping applications GRA

N82-27900# Ohio State Univ, Columbus. Dept. of Geodetic Science and Surveying.
THE EARTH'S GRAVITY FIELD TO DEGREE AND ORDER 180 USING SEASAT ALTIMETER DATA, TERRESTRIAL GRAVITY DATA AND OTHER DATA
R. H. RAPP Hanscom AFB, Mass AFGL Dec. 1981 58 p refs
(Contract F19628-79-C-0027, AF PROJ. 2309)
(AD-A113098, DGS-322; SCIENTIFIC-12; AFGL-TR-82-0019)
Avail: NTIS HCA04/MF A01 CSCL 08N

The spherical harmonic expansion of the Earth's gravitational field has been obtained to degree 180 by combining several sources of data The first data set was an a priori set of potential coefficients to degree 36 based on number of recent solutions including a substantial of resonance terms. A second data set was a 1 x 1 deg anomaly field derived from the SEASAT data set, while the third data set was an updated 1 x 1 deg terrestrial field The last two fields were combined into one set containing 56761 1 x 1 deg values. The remaining values were computed from the a priori potential coefficients. A rigorous combination solution was not carried out. Instead all anomalies were weighted in such a way that the normal equations were diagonal The results of the adjustment were 64800 1 x 1 deg anomalies that were expanded into spherical harmonics using the optimum quadrature procedure developed by Colombo Accuracy estimates for each coefficient were obtained considering noise propagation and sampling error caused by the finite block size in which the anomalies are given The percentage error of the solution reaches 100% near degree 120. The coefficients and their accuracy to degree 50 are listed in an appendix. GRA

04

GEOLOGY AND MINERAL RESOURCES

Includes mineral deposits, petroleum deposits, spectral properties of rocks, geological exploration, and lithology.

A82-22574
EXTRAGALACTIC COSMIC RAYS, THEIR SOURCES AND SPECTRUM
R. SILBERBERG and M. M SHAPIRO (U.S. Navy, Naval Research Laboratory, Washington, DC) In: International Cosmic Ray Conference, 17th, Paris, France, July 13-25, 1981, Conference Papers. Volume 2. Gif-sur-Yvette, Essonne, France, Commissariat a l'Energie Atomique, 1981, p. 356-359 refs

Studies of air showers, particularly by Watson et al (1980), have shown that cosmic rays at energies above 10 to the 19th eV are likely to be extragalactic in origin. The energy density above 10 to the 19th eV is 3 x 10 to the -8th eV/cu cm, and the exponent of the integral energy spectrum is -1.4 plus or minus 0.1. For estimating the energy density of relativistic protons (E greater than GeV) in metagalactic space an energy input rate W sub p into protons similar to that for relativistic electrons (W sub e) in active galactic nuclei is assumed. For cosmic rays in the supercluster, W sub p is found to be 10 to the -4th (plus or minus 1) eV/cu cm. This estimate for W sub p is supported by the following internal consistency argument: this spectrum at 10 to the 9th eV, when extended with an exponent -1.4, smoothly joins the extragalactic spectrum at 10 to the 19th eV, having a similar spectral slope (The exponent -1 4 also is that of galactic cosmic rays when corrected for rigidity-dependent leakage from the Galaxy.) (Author)

A82-22604
THE APPROXIMATE 1 GEV SOLAR COSMIC RAYS IN THE FORBUSH-EFFECT OF FEBRUARY 15, 1978
G P. LIUBIMOV, V I TULUPOV, and E A. CHUCHKOV (Moskovskii Gosudarstvennyi Universitet, Moscow, USSR) In: International Cosmic Ray Conference, 17th, Paris, France, July 13-25, 1981, Conference Papers. Volume 3. Gif-sur-Yvette, Essonne, France, Commissariat a l'Energie Atomique, 1981, p. 121-123 refs

Differences in the behavior of the galactic cosmic-ray intensity are studied using the data from the Alert and Deep River neutron monitors from February 14 to 17, 1978. The behavior of the intensity at Alert and Deep River is normalized to the initial stage of February 14, before the Forbush effect, and the additional differential flux reaches 15 percent. The observed anomalous differences are explained by an additional particle flux of about 1 GeV of solar origin in the Forbush effect. D L.G.

A82-22607* Maryland Univ., College Park
OBSERVATIONS OF THE IONIZATION STATES OF ENERGETIC PARTICLES ACCELERATED IN SOLAR FLARES
G. GLOECKLER, H. WEISS, F. M IPAVICH (Maryland, University, College Park, MD), D. HOVESTADT, B. KLECKER, M. SCHOLER (Max-Planck-Institut fuer extraterrestrische Physik, Garching, West Germany), L. A FISK (New Hampshire, University, Durham, NH), C. Y FAN (Arizona, University, Tucson, AZ), and J. J. OGALLAGHER (Chicago, University, Chicago, IL) In. International Cosmic Ray Conference, 17th, Paris, France, July 13-25, 1981, Conference Papers Volume 3 Gif-sur-Yvette, Essonne, France, Commissariat a l'Energie Atomique, 1981, p 136-139. Bundesministerium fuer Forschung und Technologie refs
(Contract NAS5-20062, BMFT-RV14-B8/74,
BMFT-01-OI-017-ZA/WF/WRK-1754; NGR-21-002-224,
NGR-21-002-316)

The ionization states and spectra of 0.3 to 2.4 MeV/nuc He, C, O and Fe are measured in a survey of ten solar flare particle events. He(plus) is found to be present in all events, which indicates the common presence of energetic He(plus) in the source material from which solar particles are accelerated. The distribution functions of He(plus), He(plus plus) and heavier elements are represented by simple exponentials of the particle speed times its rigidity to a power n, where n is between 0 and 1, and equal e-folding values. Results are consistent with a model where ions are accelerated in the corona by multi-dimensional shocks out of a population taken from both hot and cold coronal regions. D.L.G.

A82-22609
A TENTATIVE ORDERING OF ALL AVAILABLE SOLAR ENERGETIC PARTICLES ABUNDANCE OBSERVATIONS. I - THE MASS UNBIASED BASELINE. II - DISCUSSION AND COMPARISON WITH CORONAL ABUNDANCES
J. P. MEYER (Commissariat a l'Energie Atomique, Centre d'Etudes Nucleaires de Saclay, Gif-sur-Yvette, Essonne, France) In: International Cosmic Ray Conference, 17th, Paris, France, July 13-25, 1981, Conference Papers. Volume 3. Gif-sur-Yvette, Essonne, France, Commissariat a l'Energie Atomique, 1981, p. 145-152. refs

A82-22613* Maryland Univ., College Park.
ON THE ANTICORRELATION BETWEEN THE HE/3//HE/4/ RATIO AND PROTON INTENSITY IN HE/3/ RICH FLARES
M. E. PESSES (Maryland, University, College Park, MD) In: International Cosmic Ray Conference, 17th, Paris, France, July 13-25, 1981, Conference Papers. Volume 3. Gif-sur-Yvette, Essonne, France, Commissariat a l'Energie Atomique, 1981, p 171-174. refs
(Contract NAS5-20062)

A model is presented to explain the observed anticorrelation between the size of the He(3)/He(4) abundance ratio at not less

than about 10 MeV/nuc and the peak intensity of about 10 MeV protons in the He(3) rich events. The anticorrelation is shown to be a natural consequence of producing abundance enhancement by a two step acceleration process, where He(3) is preaccelerated with respect to He(4) prior to the main ion acceleration phase, which has an effective injection cutoff varying from flare to flare. D L.G.

A82-30304
REGIONAL GEOLOGICAL, TECTONIC AND GEOPHYSICAL FEATURES OF NORDLAND, NORWAY
R. H. GABRIELSEN, I. B. RAMBERG (Oslo, Universitetet, Oslo, Norway), M. B E. MORK (Universitets Minelarogisk Geologiske Museum, Oslo, Norway), and B TVEITEN (BP Petroleum Development of Norway, A/S, Stavanger, Norway) Earth Evolution Sciences, vol. 1, Mar. 1981, p. 14-26. Research supported by the Norges Almenvitenskapelige Forskningsrad, Committee for Geophysics and Geology and Norges Teknisk-Naturvitenskapelige Forskningsrad refs
(Contract NTNF PROJECT 18108075)

Foliation and lineament patterns from Landsat imagery, gravity and magnetic data mapping of Nordland, Norway shows a high degree of correlation with known tectonostratigraphic units and suggests other, previously unidentified tectonic units. Attention is given to regionally important lineament systems, one striking approximately ENE-WSW, and a younger one N-S. It is indicated by the large-scale residual gravity lows along the Norway-Sweden border, which are associated with basement domes, and by magnetic data and lineament patterns, that the eastern basement windows represent large-scale culminations By contrast, the western domes represent smaller, perhaps granitic cores of recumbent fold nappes. A positive correlation is found between the seismotectonic coastal zones of Nordland and the area's Bouguer gravity anomally maximum gradient O.C.

A82-30305
SATELLITE IMAGE INTERPRETATION OF THE EASTERN CALEDONIAN PART OF THE BLUE ROAD GEOTRAVERSE AND ITS GEOLOGICAL IMPLICATIONS /NORDLAND, VASTERBOTTEN, SCANDINAVIA/
R. GREILING (Mainz, Universitaet, Mainz, West Germany) Earth Evolution Sciences, vol. 1, Mar. 1981, p. 27-30. refs

An 80% coincidence of known geological features with the lineaments interpreted in the satellite image presented by Ehrenborg (1977) is found through the quantitative study of Landsat interpretations for the case of a Precambrian area in southeastern Sweden Because of its probable connection with the quaternary glacial erosion, the distribution of joints and faults may be interpreted as (1) E-W-striking lineaments locally correlated with faults affecting Caledonian low-angle thrusts and folliations, (2) NW-SE lineaments locally correlated with leucocratic dikes, and (3) NNW-SSW lineaments generally parallel to the present coast which, by contrast to the region farther west, is of minor importance. O.C.

A82-30786* National Aeronautics and Space Administration Goddard Space Flight Center, Greenbelt, Md.
MAGSAT SCALAR ANOMALY DISTRIBUTION - THE GLOBAL PERSPECTIVE
H. FREY (NASA, Goddard Space Flight Center, Geophysics Branch, Greenbelt, MD) Geophysical Research Letters, vol. 9, Apr. 1982, p. 277-280. refs

It is established that geographic coincidences exist between high-altitude Magsat scalar anomalies and major geologic and tectonic structures, with oceanic abyssal plains overlain by negative anomalies agreeing well in spatial extent and position and submarine platforms lying beneath positive scalar anomalies. In addition, geographic coincidence is found in the continents between many high-latitude positive anomalies and shields and cratons in North America, Eurasia and Australia. While these correlations are qualitative, they serve to identify regions for detailed study. *The global distribution of anomalies provides a basis for* comparative study which will be enhanced when reduced-to-pole versions of the Magsat data become available O C.

A82-32442* Jet Propulsion Lab., California Inst. of Tech , Pasadena
SPECTROSCOPIC REMOTE SENSING FOR GEOLOGICAL APPLICATIONS
A F. H. GOETZ (California Institute of Technology, Jet Propulsion Laboratory, Pasadena, CA) In Imaging spectroscopy; Proceedings of the Seminar, Los Angeles, CA, February 10, 11, 1981. Bellingham, WA, SPIE - The International Society for Optical Engineering, 1981, p. 17-21. refs
(Contract NAS7-100)

Remote sensing is being used with increasing frequency in the development of geologic maps and in the exploration process *Spectral data from airborne and spaceborne multispectral scanners* provide information on rock type and vegetation stress, important in geologic applications. Emphasis is now being placed on direct identification of materials rather than discrimination among geologic units. To do this, higher spectral resolution systems with wider spectral coverage than currently available are required. Imaging spectroscopy in the 0 4 - 14 microns region appears to be the answer (Author)

A82-32898
POSSIBLE FAULT DETECTION IN COTTONBALL BASIN, CALIFORNIA AN APPLICATION OF RADAR REMOTE SENSING
G. L BERLIN, G. G SCHABER, and K. C. HORSTMAN (U.S. Geological Survey, Flagstaff, AZ) Remote Sensing of Environment, vol 10, Aug. 1980, p. 33-42 refs

An analysis of a 3-cm wavelength radar image of Cottonball Basin in Death Valley National Monument has revealed the existence of two suspect fault traces in evaporite deposits that are less than 2000-yr old The traces are well defined on the image because the radar system was able to differentiate surface roughness variations at the centimeter scale. The features are not recognizable on data sets recorded ,in the visible and near-infrared spectral bands. Results indicate the potential of radar images as a tool to help locate recent breaks along a fault when the disturbed zone is represented by a somewhat rougher surface than is found in immediately adjacent areas. (Author)

A82-33402
AEROGEOPHYSICAL METHODS OF FINDING URANIUM DEPOSITS [AEROGEOFIZICHESKIE METODY PROGNOZIROVANIIA MESTOROZHDENII URANA]
A I KRASNOV, E. B. VYSOKOOSTROVSKAIA, V. A. SMIRNOV, IU. B NOVIKOV, E. I ZUBOV, G B. MUKAREVA, L. V. DIORDIENKO, and V. G. ZAITSEV Moscow, Atomizdat, 1980. 132 p. In Russian. refs

Geophysical prospecting for uranium with the aid of a large-scale, comprehensive gamma-spectrometric, aeromagnetic, and aeroelectric survey is considered. The development in the USSR and in other countries of aerogeophysical prospecting for uranium is surveyed. Features of geophysical fields that are characteristic of regions containing endogenous and exogenous deposits of uranium are analyzed. Direct and indirect radiogeochemical, magnetogeophysical, and electrogeophysical indicators of uranium-bearing structures are described. The methods described here rely on a comprehensive interpretation of *aerogeophysical, geological, and other types of data.* C.R

A82-34721* National Aeronautics and Space Administration. Goddard Space Flight Center, Greenbelt, Md.
LANDSAT IN THE SEARCH FOR APPALACHIAN HYDROCARBONS
H. W. BLODGET (NASA, Goddard Space Flight Center, Eastern Regional Remote Sensing Applications Center, Greenbelt, MD) In: American Society of Photogrammetry, Annual Meeting, 47th, Washington, DC, February 22-27, 1981, ASP Technical Papers Falls Church, VA, American Society of Photogrammetry, 1981, p. 259-262. refs

A study has been conducted to determine the applicability of enhanced Landsat imagery for oil and gas exploration in Appalachia Attention was given to the feasibility to employ lineaments identified on Landsat imagery as a tool in petroleum exploration. Lineaments, as defined in this connection, are linear or sublinear traces seen on Landsat imagery. They frequently reflect subsurface geological structures. The investigation was conducted in two stages The first was designed to identify the specific Landsat imagery enhancement best suited for displaying lineaments. The second stage consisted of plotting lineaments and conducting an analysis of the lineament trends with regard to both local geological structure and regional tectonics A close relationship was observed between lineaments identified on Landsat imagery and known oil and gas reservoirs. This result suggests that lineaments can be related to the structural control of oil and gas reservoirs throughout Appalachia G R

A82-36298* Lunar and Planetary Inst., Houston, Tex.
INFLUENCE OF CO2 ON MELTING OF MODEL GRANULITE FACIES ASSEMBLAGES - A MODEL FOR THE GENESIS OF CHARNOCKITES
R. F. WENDLANDT (Lunar and Planetary Institute, Houston, TX) American Mineralogist, vol. 66, 1981, 1164-1174. refs
(Contract NASW-3389)

A model is described for the melting of a simple granulite assemblage, in the presence of CO2-rich fluid phases, which can occur between 750 and 1000 C at crustal pressures and is therefore within the range estimated for such regional metamorphism as that of the Adirondacks For melting which occurs at about 750 C in the presence of both H2O and CO2, pressures corresponding to the deep crust are required to generate a melt enriched in pyroxene and feldspar components, while melting the precense of pure CO2 at about 1000 C generates analogous melt compositions at lower pressures. These experimental reactions are in keeping with observations constraining charnockite occurrences (1) pressure and temperature constraints; (2) mineralogical constraints, and (3) constraints on the compositions of volatiles associated with peak conditions of charnockite formation O C.

A82-37198
SIGNIFICANCE OF TECTONICS IN LINEAR FEATURE DETECTION AND INTERPRETATION ON SATELLITE IMAGES
F. CSILLAG (Eotvos Lorand Tudomanyegyetem, Budapest, Hungary) Remote Sensing of Environment, vol. 12, July 1982, p. 235-245. refs

There are two main concepts of linear feature evaluation based on satellite images. One puts emphasis on finding equivalence between the image and the field data, in the other, the basic aim is to correlate them after their more or less separate interpretation A comparative study of the two methods has been carried out on a test field in Southwest Hungary using several kinds of geological and geophysical data as reference Combining the statistical and deterministic approach a block-faulting mechanism can be recognized and described with ENE-WSW main axis. Correlation of satellite and reference data proved the tectonic difference of the northern and southern parts of the test field This led to the conclusion that one can derive textural information on tectonics from a Landsat image concerning especially short lines. This implies that not only the present surface expression of faults and tectonics is detectable but the determination of the latest tectonically active surface is also possible. (Author)

N82-22624*# Bureau de Recherches Geologiques et Minieres, Minieres, Paris (France).
SPATIAL THERMAL RADIOMETRY CONTRIBUTION TO THE MASSIF ARMORICAIN AND THE MASSIF CENTRAL FRANCE LITHO-STRUCTURAL STUDY Final Report
J Y. SCANVIC, Principal Investigator Nov 1980 85 p refs Sponsored by NASA Original contains imagery. Original imagery may be purchased from NASA Goddard Space Flight Center, (code 601), Greenbelt, Md 20771. Domestic users send orders to 'Attn: National Space Science Data Center', nondomestic users send orders to 'Attn· World Data Center A for Rockets and Satellites'. HCMM
(E82-10190; NASA-CR-168618, NAS 1.26:168618; REPT-80-SGN-848-GEO-REPT-3) Avail. NTIS HC A05/MF A01 CSCL 08G

Thermal zones delimited on HCMM images, by visual interpretation only, were correlated with geological units and carbonated rocks, granitic, and volcanic rocks were individualized rock signature is evolutive parameter and some distinctions were made by addition of day, night and seasonal thermal image interpretation This analysis also demonstrated that forest cover does not mask the underlying rocks thermal signature. Thermal linears are associated with known tectonics but the observed thermal variations from day to night and from one to another represent a promising concept to be studied in function of neotectonics and hydrogeology The thermal anomalies discovered represent a potential interest which is to be evaluated. Significant results were obtained in the Mont Dore area and additional geological targets were defined in the Paris Basin and the Montmarault granite. Author

N82-22636# Natural Environment Research Council, London (England)
OVERSEAS GEOLOGY AND MINERAL RESOURCES NUMBER 56: A GEOLOGICAL INTERPRETATION OF LANDSAT IMAGERY AND AIR PHOTOGRAPHY OF BOTSWANA
D. I. J MALLICK, F HABGOOD, and A. C SKINNER 1981 41 p refs Original contains color maps Original contains color illustrations
(OGMR-56, ISBN-0-11-884138-6) Avail: NTIS HC A03/MF A01; HMSO 5

A 1 1 million geological map compiled from LANDSAT and air photography of Botswana and border areas is presented. The distribution of 22 geological units of Karoo and Precambrian age is shown together with the post-Karoo deposits, differentiated into 7 units, based on geomorphological criteria. The data help distinguish volcanics of the Kanye Group from those of the Ventersdorp Group, and the Transvaal Supergroup from those of the Waterberg Group at localities far from their better exposed outcrop areas in the southeast of the country. Eolian, lacustrine and alluvial components of Kalahari desert superficial deposits are differentiated. The fracture and lineament pattern is only partly evident from the photographs. Author (ESA)

N82-23569*# Texas Univ. at El Paso
CHARACTERIZATION OF THE STRUCTURE AND TECTONIC OF SOUTH AMERICA Quarterly Report, 1 Mar. - 30 Jun. 1981
G. R KELLER and E. G. LIDIAK, Principal Investigators 30 Jun. 1981 4 p ERTS
(Contract NAS5-26326)
(E82-10196, NASA-CR-168623; NAS 1.26·168623) Avail: NTIS HC A02/MF A01 CSCL 08G

Geologic studies of the South American plate were undertaken. The Guayana shield is reasonably well studied, and although data are sparce, the central Brazilian shield appears similar. Both the Amazon and Parnaiba basins seem to be related to an aulocogen structure. The collection of crustal structure information and the generation of measurement of surface wave dispersion in the shield areascontinues Long period seismograms are digitized and analyzed Existing crusted and upper mantle studies were indexed. Both MAGSAT scaler and vector magnetic anomaly data were used with regional gravity anomaly data to investigate the regional tectonic features of the South American plate. E.A.K.

N82-23621# Western Geophysical Co of America, Houston, Tex. Aero Service Div.
AIRBORNE GAMMA-RAY SPECTROMETER AND MAGNETOMETER SURVEY. ROSEAU QUADRANGLE, MINNESOTA, VOLUME 1 Final Report
May 1981 98 p refs Prepared for Bendix Field Engineering Corp., Grand Junction, Colo. 2 Vol.
(Contract DE-AC13-76GJ-01664)
(DE82-001031; GJBX-329-81-VOL-1) Avail. NTIS HC A05/MF A01

An airborne high sensitivity gamma ray spectrometer and magnetometer survey was conducted over the Roseau map area in Minnesota. Radiometric multiple parameter, magnetic, and ancillary parameter stacked profiles are discussed. Hostograms, anomaly, and computer printer maps are also discussed. Stratigraphy is described Geochemical, printer contour, and anomaly map analyses are provided N W

N82-23623# Western Geophysical Co of America, Houston, Tex. Aero Service Div.
AIRBORNE GAMMA-RAY SPECTROMETER AND MAGNETOMETER SURVEY. BARROW QUADRANGLE, ALASKA, VOLUME 1 Final Report
Mar. 1981 100 p refs 2 Vol.
(Contract DE-AC13-76GJ-01664)
(DE82-000334, GJBX-295-81-VOL-1) Avail: NTIS HC A05/MF A01

From July to August 1980, an airborne high sensitivity gamma ray spectrometer and magnetometer survey over eleven 30 by 10 and one 40 by 10 quadrangles of the Alaskan North Slope were conducted. The results obtained over the Barrow area are presented in four different forms: on magnetic tape; on microfiche, in graphic form as profiles and histograms; and in map form as anomaly maps, flight path maps, and computer printer maps Complete data listings of both the reduced single record and the reduced averaged record data are given. DOE

N82-23624# Western Geophysical Co. of America, Houston, Tex. Aero Service Div
AIRBORNE GAMMA-RAY SPECTROMETER AND MAGNETOMETER SURVEY. WAINWRIGHT QUADRANGLE, ALASKA, VOLUME 2 Final Report
Mar. 1981 125 p 2 Vol.
(Contract DE-AC13-76GJ-01664)
(DE82-000341; GJBX-296-81-VOL-2) Avail: NTIS HC A06/MF A01

The flight path map, multiparameter profiles, histograms, and anomaly maps for uranium, thorium, potassium, uranium/potassium, uranium/thorium, and thorium/potassium are given for the survey conducted in the Wainwright area, Alaska. DOE

N82-23625# Western Geophysical Co. of America, Houston, Tex. Aero Service Div.
AIRBORNE GAMMA-RAY SPECTROMETER AND MAGNETOMETER SURVEY, KENORA QUADRANGLE, MINNESOTA, VOLUME 1 Final Report
Mar. 1981 87 p refs
(Contract DE-AC13-76GJ-01664)
(DE82-001029; GJBX-328-81-VOL-1) Avail: NTIS HC A05/MF A01

During the months of June through October, 1980, Aero Service Division Western Geophysical Company of America conducted an airborne high sensitivity gamma-ray spectrometer and magnetometer survey over eleven (11) 20 x 10 NTMS quadrangles located in the states of Minnesota and Wisconsin and seven (7) 20 x 10 NTMS quadrangles in North and South Dakota. The results obtained over the Kenora map area of Minnesota are discussed. The final data are presented in four different forms: on magnetic tape; on microfiche; in graphic form as profiles and histograms: and in map form as anomaly maps, flight path maps, and computer printer maps. DOE

N82-23626# Western Geophysical Co. of America, Houston, Tex. Aero Service Div.
AIRBORNE GAMMA-RAY SPECTROMETER AND MAGNETOMETER SURVEY. MEADE RIVER QUADRANGLE, ALASKA, VOLUME 2 Final Report
Feb 1981 173 p
(Contract DE-AC13-76GJ-01664)
(DE82-000340, GJBX-297-81-VOL-2) Avail NTIS HC A08/MF A01

The flight path map, multiparameter profiles, histograms, and anomaly maps for uranium, thorium, potassium are given for the Beechey point area, Alaska DOE

N82-23627# Western Geophysical Co. of America, Houston, Tex. Aero Service Div
AIRBORNE GAMMA-RAY SPECTROMETER AND MAGNETOMETER SURVEY. TESHEKPUK QUADRANGLE, ALASKA, VOLUME 2 Final Report
Mar 1981 88 p
(Contract DE-AC13-76GJ-01664)
(DE82-000310, GJBX-298-81-VOL-2) Avail NTIS HC A05/MF A01

The flight path map, multiparameter profiles, histograms, and anomally maps for uranium, thorium, potassium uranium/potassium, uranium/thorium, and thorium/potassium are given. DOE

N82-23628# Western Geophysical Co. of America, Houston, Tex Aero Service Div.
AIRBORNE GAMMA-RAY SPECTROMETER AND MAGNETOMETER SURVEY. HARRISON BAY QUADRANGLE, ALASKA, VOLUME 2 Final Report
Feb. 1981 120 p
(Contract DE-AC13-76GJ-016664)
(DE82-000315, GJBX-299-81-VOL-2) Avail NTIS HC A06/MF A01

The flight path map, multiparameter profiles, histograms, and anomaly maps for uranium, thorium, potassium, uranium/potassium, uranium/thorium, and thorium/potassium are given DOE

N82-23629# Western Geophysical Co. of America, Houston, Tex. Aero Service Div.
AIRBORNE GAMMA-RAY SPECTROMETER AND MAGNETOMETER SURVEY: BEECHEY PT., QUADRANGLE, ALASKA, VOLUME 2 Final Report
Feb. 1981 76 p
(Contract DE-AC13-76GJ-01664)
(DE82-000309; GJBX-300-81-VOL-2) Avail NTIS HC A05/MF A01

Aerial survey data are presented including the flight path map, multiparameter profiles, histograms, and anomaly maps for uranium, thorium, potassium, uranium/potassium, uranium/thorium, and thorium/potassium. DOE

N82-23630# Western Geophysical Co. of America, Houston, Tex. Aero Service Div
AIRBORNE GAMMA-RAY SPECTROMETER AND MAGNETOMETER SURVEY. POINT LAY QUADRANGLE, ALASKA, VOLUME 2 Final Report
Feb. 1981 101 p
(Contract DE-AC13-76GJ-01664)
(DE82-000308, GJBX-301-81-VOL-2) Avail: NTIS HC A06/MF A01

Data from magnetic and spectral surveys of the Point Lay area, Alaska are given including the flight path map, multiparameter profiles, histograms, and anomaly maps for uranium, thorium, and potassium DOE

N82-23631# Western Geophysical Co. of America, Houston, Tex. Aero Service Div
AIRBORNE GAMMA-RAY SPECTROMETER AND MAGNETOMETER SURVEY. UTUKIK RIVER QUADRANGLE, ALASKA, VOLUME 2 Final Report
Mar. 1981 208 p
(Contract DE-AC13-76GJ-01664)
(DE82-000316; GJBX-302-81-VOL-2) Avail: NTIS HC A10/MF A01

The flight path map, multiparameter profiles, histograms, and anomaly maps for uranium, thorium, potassium, uranium/potassium, uranium/thorium, and thorium/potassium are presented. DOE

N82-23632# Western Geophysical Co. of America, Houston, Tex Aero Service Div.
AIRBORNE GAMMA-RAY SPECTROMETER AND MAGNETOMETER SURVEY. SAGAVANIRKTOK QUADRANGLE, ALASKA, VOLUME 2 Final Report
Mar 1981 114 p
(Contract DE-AC13-76GJ-01664)
(DE82-000311; GJBX-306-81-VOL-2) Avail: NTIS HC A06/MF A01

Magnetic and gamma ray spectral data are given including the flight path map, multiparameter profiles, histograms, and anomaly maps for uranium, thorium, potassium, uranium/potassium, uranium/thorium, and thorium/potassium DOE

N82-23633# Western Geophysical Co. of America, Houston, Tex. Aero Service Div.
AIRBORNE GAMMA-RAY SPECTROMETER AND MAGNETOMETER SURVEY: DULUTH QUADRANGLE, MINNESOTA, VOLUME 2 Final Report
Apr. 1981 56 p
(Contract DE-AC13-76GJ-01664)
(DE82-001027; GJBX-330-81-VOL-2) Avail. NTIS HC A04/MF A01

The flight path map, multiparameter profiles, histograms, and anomaly maps for uranium, thorium, potassium, uranium/potassium, uranium/thorium, and thorium/potassium are included. DOE

N82-23634# Western Geophysical Co. of America, Houston, Tex. Aero Service Div.
AIRBORNE GAMMA-RAY SPECTROMETER AND MAGNETOMETER SURVEY. ROSEAU QUADRANGLE, MINNESOTA, VOLUME 2 Final Report
Apr. 1981 50 p 2 Vol
(Contract DE-AC13-76GJ-01664)
(DE82-001025; GJBX-329-81-VOL-2) Avail NTIS HC A03/MF A01

Multiparameter profiles, histograms, and flight path and anomaly maps are provided for uranium, thorium and potassium deposits. N W.

N82-23635# Western Geophysical Co. of America, Houston, Tex Aero Service Div.
AIRBORNE GAMMA-RAY SPECTROMETER AND MAGNETOMETER SURVEY. DEVIL'S LAKE QUADRANGLE, NORTH DAKOTA, VOLUME 1 Final Report
May 1981 98 p refs 2 Vol.
(Contract DE-AC13-76GJ-01664)
(DE82-004161; GJBX-354-81-VOL-1) Avail: NTIS HC A05/MF A01

During the months of June through October, 1980, an airborne high sensitivity gamma ray spectrometer and magnetometer survey was conducted over eleven 20 X 10 NTMS quadrangles located in the states of Minnesota and Wisconsin and seven 20 x 10 NTMS quadrangles in North and South Dakota. The results obtained over the Devil's Lake map area of North Dakota are discussed. The final data are presented in four different forms: on magnetic tape; on microfiche, in graphic form as profiles and histograms; and in map form as anomaly maps, flight path maps, and computer printer maps DOE

N82-23636# Western Geophysical Co. of America, Houston, Tex. Aero Service Div
AIRBORNE GAMMA-RAY SPECTROMETER AND MAGNETOMETER SURVEY. DEVIL'S LAKE QUADRANGLE, NORTH DAKOTA, VOLUME 2 Final Report
Apr. 1981 98 p 2 Vol.
(Contract DE-AC13-76GJ-01664)
(DE82-004168; GJBX-354-81-VOL-2) Avail: NTIS HC A05/MF A01

Volume 2 on airborne gamma ray spectrometer and magnetometer surveys contains the flight path map, radiometric multiple parameter stacked profiles, magnetic and ancillary parameter stacked profiles, histograms, and anomaly maps for uranium, potassium, thorium, uranium/potassium, uranium/thorium, and thorium/potassium. DOE

N82-23637# Western Geophysical Co of America, Houston, Tex. Aero Service Div.
AIRBORNE GAMMA-RAY SPECTROMETER AND MAGNETOMETER SURVEY. BEMIDJI QUADRANGLE, MINNESOTA, VOLUME 1 Final Report
May 1981 102 p refs 2 Vol.
(Contract DE-AC13-76GJ-01664)
(DE82-001032; GJBX-331-81-VOL-1) Avail: NTIS HC A06/MF A01

The results obtained over the Bemidji map area of Minnesota by airborne high sensitivity gamma ray spectrometer and magnetometer surveys are discussed The final data are presented in four different forms: on magnetic tape; on microfiche, in graphic form as profiles and histograms, and in map form as anomaly maps, flight path maps, and computer printer maps. Complete data listings of both the reduced single record and the reduced averaged record data are also reported. DOE

N82-23638# Western Geophysical Co. of America, Houston, Tex. Aero Service Div.
AIRBORNE GAMMA-RAY SPECTROMETER AND MAGNETOMETER SURVEY. BEMIDJI QUADRANGLE, MINNESOTA, VOLUME 2 Final Report
Mar. 1981 50 p 2 Vol
(Contract DE-AC13-76GJ-01664)
(DE82-001026; GJBX-331-81-VOL-2) Avail: NTIS HC A03/MF A01

Aerial surveys of the Bemidji quadrangle, Minnesota are reported In volume 2 the flight path map, multiparameter profiles, histograms and anomaly maps fo uranium, thorium, potassium, uranium/potassium, uranium/thorium and thorium/potassium are presented DOE

N82-23639# Western Geophysical Co. of America, Houston, Tex Aero Service Div
AIRBORNE GAMMA-RAY SPECTROMETER AND MAGNETOMETER SURVEY. HIBBING QUADRANGLE, MINNESOTA, VOLUME 1 Final Report
Apr 1981 111 p refs 2 Vol.
(Contract DE-AC13-76GJ-01664)
(DE82-004159, GJBX-355-81-VOL-1) Avail NTIS HC A06/MF A01

An airborne high sensitivity gamma-ray spectrometer and magnetometer survey over eleven 20 x 10 NTMS quadrangles located in the states of Minnesota and Wisconsin and seven 20 x 10 NTMS quadrangles in North and South Dakota was conducted The results obtained over the Hibbing, Minnesota map area are presented in four different forms: on magnetic tape; on microfiche; in graphic form as profiles and histograms, and in map form as anomaly maps, flight path maps, and computer printer maps. DOE

N82-23640# Western Geophysical Co. of America, Houston, Tex. Aero Service Div.
AIRBORNE GAMMA-RAY SPECTROMETER AND MAGNETOMETER SURVEY. HIBBING QUADRANGLE, MINNESOTA, VOLUME 2 Final Report
Apr. 1981 138 p 2 Vol.
(Contract DE-AC13-76GJ-01664)
(DE82-004165; GJBX-355-81-VOL-2) Avail: NTIS HC A07/MF A01

The flight path map, radiometric multiple-parameter stacked profiles, magnetic and ancillary parameter stacked profiles, and histograms are presented Anomaly maps for uranium, thorium, potassium, uranium/potassium, uranium/thorium, and thorium/potassium are included DOE

N82-23641# Western Geophysical Co of America, Houston, Tex. Aero Service Dept
AIRBORNE GAMMA-RAY SPECTROMETER AND MAGNETOMETER SURVEY. ABERDEEN QUADRANGLE, SOUTH DAKOTA, VOLUME 1 Final Report
Apr 1981 99 p refs 2 Vol
(Contract DE-AC13-76GJ-01664)
(DE82-004152; GJBX-357-81-VOL-1) Avail: NTIS HC A05/MF A01

An airborne high sensitivity gamma-ray spectrometer and magnetometer survey over eleven 20 x 10 NTMS quadrangles located in the states of Minnesota and Wisconsin and seven 20 x 10 NTMS quadrangles in North and South Dakota were conducted. The results obtained over the Aberdeen, South Dakota map area are discussed. The final data are presented in four different forms: on magnetic tape, on microfiche; in graphic form as profiles and histograms; and in map form as anomaly maps, flight path maps, and computer printer maps. DOE

N82-23642# Western Geophysical Co of America, Houston, Tex. Aero Service Div
AIRBORNE GAMMA-RAY SPECTROMETER AND MAGNETOMETER SURVEY. ABERDEEN QUADRANGLE, SOUTH DAKOTA, VOLUME 2 Final Report
Apr. 1981 106 p 2 Vol.
(Contract DE-AC13-76GJ-01664)
(DE82-004164; GJBX-357-81-VOL-2) Avail: NTIS HC A06/MF A01

The flight path map, radiometric and multiple-parameter stacked profiles, magnetic and ancillary parameter stacked profiles, and histograms are presented. Anomaly maps for uranium, thorium, potassium, uranium/potassium, uranium/thorium, and thorium/potassium are included. DOE

N82-23643# Western Geophysical Co of America, Houston, Tex Aero Service Div.
AIRBORNE GAMMA-RAY SPECTROMETER AND MAGNETOMETER SURVEY. INTERNATIONAL FALLS QUADRANGLE, MINNESOTA, VOLUME 1 Final Report
Apr. 1981 107 p refs 2 Vol
(Contract DE-AC13-76GJ-01664)
(DE82-004151; GJBX-356-81-VOL-1) Avail NTIS HC A06/MF A01

Results obtained using an airborne high sensitivity gamma-ray spectrometer and magnetometer to survey the International Falls map area of Minnesota are presented on magnetic tape; on microfiche; in graphic form as profiles and histograms; and in map form as anomaly maps, flight path maps, and computer printer maps. DOE

N82-23644# Western Geophysical Co. of America, Houston, Tex. Aero Service Div
AIRBORNE GAMMA-RAY SPECTROMETER AND MAGNETOMETER SURVEY. INTERNATIONAL FALLS QUADRANGLE, MINNESOTA, VOLUME 2 Final Report
Apr. 1981 104 p 2 Vol.
(Contract DE-AC13-76GJ-01664)
(DE82-004166; GJBX-356-81-VOL-2) Avail: NTIS HC A06/MF A01

The flight path map is presented as well as radiometric multiple-parameter stacked profiles, magnetic and ancillary parameter stacked profiles, histograms, and anomaly maps for uranium, potassium, thorium, uranium/potassium, thorium/potassium, and uranium/thorium. DOE

N82-24518*# Geological Survey, Denver, Colo
APPLICATION OF HCMM DATA TO REGIONAL GEOLOGIC ANALYSIS FOR MINERAL AND ENERGY RESOURCE EVALUATION Progress Report, Sep. - Nov. 1981
K. WATSON, Principal Investigator and S. H. MILLER Nov. 1981 4 p Sponsored by NASA HCMM
(E82-10153; NASA-CR-168538, NAS 1 26.168538) Avail: NTIS HC A02/MF A01 CSCL 08G

A more accurate algorithm was developed to compute thermal inertia from temperature difference and albedo information. The error of this algorithm is about 1/3 of the measurement error in HCMM as opposed to the current algorithm which can have an error 5 times larger A northeast trending lineament was discovered in southewestern Arizona on enhanced thermal inertia images. Author

N82-24521*# Geological Survey, Denver, Colo. Petrophysics and Remote Sensing Branch.
APPLICATION OF HCMM DATA TO REGIONAL GEOLOGIC ANALYSIS FOR MINERAL AND ENERGY RESOURCE EVALUATION Progress Report, Mar. - May 1981
K. WATSON, Principal Investigator and S H MILLER May 1981 4 p Sponsored by NASA HCMM
(E82-10243; NASA-CR-168824, NAS 1.26:168824) Avail: NTIS HC A02/MF A01 CSCL 08G

The effects of topographic elevation and slope on thermal images were examined using representative field obstructions of the solar and sky radiation and a simple linearized thermal model. The forms are easily adapted for analysis of HCMM images using the DMA digital terrain data From a representative set of field observations, it was found that flux variations with elevation can cause changes in the mean diurnal temperature gradient from -4 deg to -14 deg per km evaluated at 2000 m Changes in the temperature difference gradient of 1 to 2 C per km are also produced which is equivalent to an effective thermal inertia gradient of 100 W s to the 1/2 power/sq m K/1 per km Exposed bedrock on topographic ridges will appear to have a lower thermal inertia due to the additional effect E A.K.

N82-24579*# Massachusetts Univ, Amherst. Dept. of Geology
THE MINERALOGY OF GLOBAL MAGNETIC ANOMALIES Progress Report, Sep. 1981 - Jan. 1982
S E. HAGGERTY, Principal Investigator 15 Feb 1982 31 p refs ERTS
(Contract NAS5-26414)
(E82-10305; NASA-CR-168880; NAS 1.26:168880) Avail: NTIS HC A03/MF A01 CSCL 08G

Problems with the Curie balance, which severely hindered the acquisition of data, were rectified. Chemical analytical activities are proceeding satisfactorily. The magnetization characteristics of metamorphic suites were analyzed and susceptibility data for a wide range of metamorphic and igneous rocks These rock magnetic signatures are discussed as well as the relationships between geology, gravity and MAGSAT anomalies of West Africa A.R.H.

N82-24594*# Iowa Univ., Iowa City. Dept of Geology
USE OF MAGSAT ANOMALY DATA FOR CRUSTAL STRUCTURE AND MINERAL RESOURCES IN THE US MIDCONTINENT Quarterly Report, period ending 31 Mar. 1982
R S. CARMICHAEL, Principal Investigatoret al 24 Mar 1982 2 p ERTS
(Contract NAS5-26425)
(E82-10321, NASA-CR-168900; NAS 1.26:168900; QR-5) Avail: NTIS HC A02/MF A01 CSCL 08G

Personnel matters related to the processing and interpretation of MAGSAT data are reported Efforts are being initiated to determine the crustal geology, structure, and potential economic consequences to be deduced from the satellite magnetic anomalies in conjuction with correlative data A.R H.

N82-24596*# Iowa Univ , Iowa City Dept. of Geology.
USE OF MAGSAT ANOMALY DATA FOR CRUSTAL STRUCTURE AND MINERAL RESOURCES IN THE US MIDCONTINENT Quarterly Report, period ending 31 Dec. 1981
R. S. CARMICHAEL, Principal Investigator 31 Dec. 1981 31 p refs ERTS
(Contract NAS5-26425)
(E82-10323; NASA-CR-168902; NAS 1.26 168902; QR-4) Avail. NTIS HC A03/MF A01 CSCL 08G

The analysis and preliminary interpretation of investigator-B MAGSAT data are addressed. The data processing included: (1) removal of spurious data points; (2) statistical smoothing along individual data tracks, to reduce the effect of geomagnetic transient disturbances; (3) comparison of data profiles spatially coincident in track location but acquired at different times, (4) reduction of data by weighted averaging to a grid with 1 deg xl deg latitude/longitude spacing, and with elevations interpolated and weighted to a common datum of 400 km; (5) wavelength filtering; and (6) reduction of the anomaly map to the magnetic pole Agreement was found between a magnitude data anomaly map and a reduce-to-the-pole map supporting the general assumption that, on a large scale (long wavelength), it is induced crustal magnetization which is responsible for major anamalies Anomalous features are identified and explanations are suggested with regard to crustal structure, petrologic characteristics, and Curie temperature isotherms. M.G.

N82-25603*# National Aeronautics and Space Administration. Goddard Space Flight Center, Greenbelt, Md.
THE INFLUENCE OF AUTOCORRELATION IN SIGNATURE EXTRACTION: AN EXAMPLE FROM A GEOBOTANICAL INVESTIGATION OF COTTER BASIN, MONTANA
M. L. LABOVITZ and E. J MASUOKA, Principal Investigators Dec 1981 28 p refs Submitted for publication ERTS
(E82-10341; NASA-TM-83871; NAS 1.15.83871) Avail NTIS HC A03/MF A01 CSCL 05B

The presence of positive serial correlation (autocorrelation) in remotely sensed data results in an underestimate of the variance-covariance matrix when calculated using contiguous pixels. This underestimate produces an inflation in F statistics. For a set of Thematic Mapper Simulator data (TMS), used to test the ability to discriminate a known geobotanical anomaly from its background, the inflation in F statistics related to serial correlation is between 7 and 70 times. This means that significance tests of means of the spectral bands initially appear to suggest that the anomalous site is very different in spectral reflectance and emittance from its background sites. However, this difference often disappears and is always dramatically reduced when compared to frequency distributions of test statistics produced by the comparison of simulated training sets possessing equal means, but which are composed of autocorrelated observations Author

N82-25620# High Life Helicopters, Inc., Puyallup, Wash.
AIRBORNE GAMMA-RAY SPECTROMETER AND MAGNETOMETER SURVEY, TORONTO QUADRANGLE NEW YORK, VOLUME 2A Final Report
1981 90 p refs Prepared in cooperation with QEB, Inc. 3 Vol.
(Contract DE-AC13-79GJ-01692)
(DE81-027158, GJBX-211-81-VOL-2A) Avail: NTIS HC A05/MF A01

No uranium anomalies meet the minimum statistical requirements as defined and no anomaly map is presented Potassium (%K), equivalent Uranium (ppm eU), equivalent Thorium (ppm eTh), eU/eTh, eU/K, eTh/K, and magnetic pseudo-contour maps are presented. Stacked Profiles showing geologic strip maps along each flight-line, together with sensor data, and ancillary data are also presented. All maps and profiles were prepared on a scale of 1.250,000, but were reduced to 1·500,000 for presentation DOE

N82-25621# High Life Helicopters, Inc., Puyallup, Wash.
AIRBORNE GAMMA-RAY SPECTROMETER AND MAGNETOMETER SURVEY, KINGSTON QUADRANGLE NEW YORK, VOLUME 2C Final Report
1981 64 p refs Prepared in cooperation with QEB, Inc. 3 Vol.
(Contract DE-AC13-79CJ-01692)
(DE81-027161; GJBX-211-81-VOL-2C) Avail. NTIS HC A04/MF A01

No uranium anomalies meet the minimum statistical requirements as defined. No Uranium Anomaly Map is given Potassium (%K), equivalent Uranium (ppm eU), equivalent Thorium (ppm eTh), eU/eTh, eU/K, eTh/K, and magnetic pseudo-contour maps are presented Stacked Profiles showing geologic strip maps along each flight-line, together with sensor data, and ancillary data are also presented. All maps and profiles were prepared on a scale of 1 250,000, but were reduced to 1·500,000 for presentation DOE

N82-25622# High Life Helicopters, Inc., Puyallup, Wash.
AIRBORNE GAMMA-RAY SPECTROMETER AND MAGNETOMETER SURVEY, ROCHESTER QUADRANGLE NEW YORK, VOLUME 2D Final Report
1981 143 p refs Prepared in cooperation with QEB, Inc. 3 Vol.
(Contract DE-AC13-79GJ-01692)
(DE81-027156, GJBX-211-81-VOL-2D) Avail: NTIS HC A07/MF A01

One uranium anomaly met the minimum statistical requirements as defined This anomaly is listed and is shown on the Uranium Anomaly Interpretation Map. Potassium (%K), equivalent Uranium (ppm eU), equivalent Thorium (ppm eTh), eU/eTh, eU/K, eTh/K, and magnetic pseudo-contour maps are also presented. Stacked Profiles showing geologic strip maps along each flight-line, together with sensor data, and ancillary data are presented. All maps and profiles were prepared on a scale of 1:250,000, but were reduced to 1 500,000 for presentation Anomaly number 1 is over an area underlain by shale and dolomite of the upper Silurian Camillus and Syracuse formations (Scy). DOE

N82-25623# Western Geophysical Co of America, Houston, Tex. Aero Service Div
AIRBORNE GAMMA-RAY SPECTROMETER AND MAGNETOMETER SURVEY. BARROW QUADRANAGLE, ALASKA, VOLUME 2 Final Report
Mar. 1981 63 p refs 2 Vol.
(Contract DE-AC13-76GJ-01664)
(DE82-000342, GJBX-295-81-VOL-2) Avail: NTIS HC A04/MF A01

Volume II contains the flight path map, multiparamenter profiles, histograms, and anomaly maps for potassium, uranium, thorium, uranium/potassium, uranium/thorium, and thorium/potassium GRA

N82-25625# Western Geophysical Co. of America, Houston, Tex. Aero Service Div

AIRBORNE GAMMA-RAY SPECTROMETER AND MAGNETOMETER SURVEY. LOOKOUT RIDGE QUADRANGLE, ALASKA, VOLUME 2 Final Report

Feb. 1981 190 p refs 2 Vol

(Contract DE-AC13-76GJ-01664)

(DE82-000313, GJBX-303-81-VOL-2) Avail: NTIS HC A09/MF A01

The flight path map, multiparameter profiles, histograms, and anomaly maps are included. Uranium, thorium, potassium, uranium/potassium, uranium/thorium, and thorium/potassium are investigated. DOE

N82-26750*# Brown Univ., Providence, R. I Dept. of Geological Sciences.

AN INVESTIGATION INTO THE UTILIZATION OF HCMM *THERMAL DATA FOR THE DISCRIMINATION OF VOLCANIC* AND EOLIAN GEOLOGICAL UNITS Quarterly Progress Report, 1 Sep. 1981 - 28 Feb. 1982

J W HEAD, III, Principal Investigator 28 Feb. 1982 1 p HCMM

(Contract NAS5-26728)

(E82-10352; NASA-CR-168996, NAS 1.26:168996) Avail. NTIS HC A02/MF A01 CSCL 08G

The nature of the HCMM data set and the general geologic application of thermal inertia imaging using HCMM data were studied. The CCT's of five sites of interest were obtained and displayed. The upgrading of the image display system was investigated. Fragment/block size distributions in various terrain types wre characterized with emphasis on volcanic terrain. The SEASAT L-band radar images of volcanic landforms at Newberry Volcano, Oregon, were analyzed and compared to imagery from LANDSAT band 7. E.A.K.

N82-27804# Western Geophysical Co. of America, Houston, Tex. Aero Service Div

AIRBORNE GAMMA-RAY SPECTROMETER AND MAGNETOMETER SURVEY: NORTH/SOUTH TIELINE, VOLUME 1 Final Report

May 1981 38 p refs 2 Vol.

(Contract DE-AC13-76GJ-01664)

(DE82-005542; GJBX-386-81-VOL-1) Avail NTIS HC A03/MF A01

An airborne high sensitivity gamma ray spectrometer and magnetometer survey was conducted along the 990 longitude meridian from the Canadian border southward to the Mexican border A total of 1555 line miles of geophysical data were acquired. The program acquires and compiles geologic and other information to assess the magnitude and distribution of uranium resources and to determine areas favorable for the occurrence of uranium in the United States. DOE

N82-27805# Western Geophysical Co. of America, Houston, Tex. Aero Service Div.

AIRBORNE GAMMA-RAY SPECTROMETER AND MAGNETOMETER SURVEY: NORTH/SOUTH TIELINE, VOLUME 2 Final Report

May 1981 108 p refs 2 Vol

(Contract DE-AC13-76GJ-01664)

(DE82-005570; GJBX-386-81-VOL-2) Avail: NTIS HC A06/MF A01

Data from an airborne high sensitivity gamma-ray spectrometer and magnetometer survey along the 990 longitude meridian from the Canadian border southward to the Mexican border are presented. The purpose of this study is to acquire and compile geologic and other information with which to assess the magnitude and distribution of uranium resources and to determine areas favorable for the occurrence of uranium in the US. DOE

N82-27806# Western Geophysical Co. of America, Houston, Tex. Aero Service Div.

AIRBORNE GAMMA-RAY SPECTROMETER AND MAGNETOMETER SURVEY: SIOUX FALLS QUADRANGLE, SOUTH DAKOTA, VOLUME 1 Final Report

May 1981 99 p refs Sponsored in part by Bendix Field Engineering Corp 2 Vol

(Contract DE-AC13-76GJ-01664)

(DE82-005533, GJBX-389-81-VOL-1) Avail NTIS HC A05/MF A01

Computer printer maps of the magnetic total intensity and the six radiometric parameters were prepared in addition to the radiometric anomaly maps for this area The magnetic total intensity map displays a rather subdued response pattern of broad low amplitude anomalies over much of the area with an average magnetic intensity of approximately 58,900 gammas. The radiometric response over much of the area is relatively low Equivalent concentrations of uranium, thorium and potassium only rarely exceed 3 2 ppM, 7 5 ppM and 1.4% respectively A number of these zones of increased concentrations show corresponding anomalous responses on the uranium/potassium and/or uranium/thorium pseudo-contour maps Based on this set of computer printer maps alone however, it is, at times, difficult to discern the contribution of coinciding local decreases in the potassium and thorium parameters to these ratio anomalies Based on the criteria stated in the general section on interpretation, a total of seven uranium and seven thorium anomalies were outlined on the interpretation map. DOE

N82-27807# Western Geophysical Co. of America, Houston, Tex Aero Service Div

AIRBORNE GAMMA-RAY SPECTROMETER AND MAGNETOMETER SURVEY: SIOUX FALLS QUADRANGLE, SOUTH DAKOTA, VOLUME 2 Final Report

May 1981 132 p Sponsored in part by Bendix Field Engineering Corp 2 Vol.

(Contract DE-AC13-76GJ-01664)

(DE82-005574; GJBX-389-81-VOL-2) Avail: NTIS HC A07/MF A01

The flight path, radiometric multiparameter stacked profiles, magnetic and ancillary parameter stacked profiles, histograms, and anomaly maps for the Sioux Falls Quadrangle in South Dakota are presented. These data are used to assess the magnitude and distribution of uranium resources and to determine areas favorable for the occurrence of uranium. DOE

N82-27808# Texas Univ., El Paso. Dept of Geological Sciences.

EVALUATION AND COMBINED GEOPHYSICAL INTERPRETATIONS OF NURE AND RELATED GEOSCIENCE DATA IN THE VAN HORN, PECOS, MARFA, FORT STOCKTON, PRESIDIDO, AND EMORY PEAK QUADRANGLES, TEXAS, VOLUME 1 Final Report

G R. KELLER, W. J. HINZE, C L. V. AIKEN, P. C GOODELL, R. F. ROY, and N E. PINGITORE Sep. 1981 451 p refs 2 Vol

(Contract DE-AC13-76GJ-01664)

(DE82-005554; GJBX-365-81) Avail· NTIS HC A20/MF A01

The six Trans-Pecos Texas quadrangles (Van Horn, Pecos, Marfa, Port Stockton, Presidio, and Emory Park) were surveyed. The aeromagnetic gravity and geochemical data, their processing, and their analysis are discussed The geologic history and setting of the Trans-Pecos are discussed along with the uranium potential of the region. Uranium anomalies and occurrences are present in the study area, and information is presented on 33 drill holes into these targets. A folio of maps reduced to a scale of 1:500,000. Geologic maps for each of the six quadrangles are included and the geophysical maps have been prepared to be overlays for the geologic maps. Residual aeromagnetic anomaly, complete Bougner gravity anomaly, flight line index, gravity station index, and anomaly interpretative maps were prepared for each quadrangle. A large suite of digitally processed maps of gravity and aeromagnetic are included. DOE

N82-27809# Texas Univ , El Paso. Dept of Geological Sciences.
EVALUATION AND COMBINED GEOPHYSICAL INTERPRETATIONS OF NURE AND RELATED GEOSCIENCE DATA IN THE VAN HORN, PECOS, MARFA, FORT STOCKTON, PRESIDIO, AND EMORY PEAK QUADRANGELS, TEXAS Final Report
G. R KELLER, W J. HINZE, C. L. V. AIKEN, R. C GOODELL, R. F. ROY, and N. E PINGITORE Sep. 1981 88 p 2 Vol.
(Contract DE-AC13-76GJ-01664)
(DE82-005560; GJBX-365-81-VOL-2) Avail NTIS HC A05/MF A01

An atlas containing the geophysical data publicly available in the Van Horn, Pecos, Marfa, Fort Stockton, Presidio, and Emory Peak quadrangles and a major file of basic data which are the *object of much industrial interest is presented. Narrative discussion* of the maps and contour maps of the aeromagnetic and gravity data, as well as maps of flight path recovery and gravity station locations are included. Geologic maps, key radiometric data, and ground truth sample location and data are also displayed A scale of 1:500,000 is employed so that the maps can be overlain for qualitative comparisons. The maps refer to the qualitative analysis, particularly the interpretative anomaly index maps DOE

N82-27810# *Carson Helicopters, Inc., Perkasie, Pa*
NURE AERIAL GAMMA-RAY AND MAGNETIC RECONNAISSANCE SURVEY OF PORTIONS OF NEW MEXICO, ARIZONA AND TEXAS. VOLUME 2: NEW MEXICO-CARLSBAD QUADRANGLE Final Report
Sep 1981 184 p refs Prepared for Bendix Field Engineering Corp.
(Contract DE-AC13-76GJ-01664)
(DE82-005527; GJBX-412-81-VOL-2C) Avail: NTIS HC A09/MF A01

A rotary wing high sensitivity radiometric and magnetic survey was flown covering the Carlsbad Quadrangle of the State of New Mexico. The survey was flown with a Sikorsky SS8T helicopter equipped with a high sensitivity gamma ray spectrometer and the dynamic test range at Lake Mead, Arizona Instrumentation and data reduction methods are presented in Volume I of this report. The reduced data is presented in the form of stacked profiles, standard deviation anomaly plots, histogram plots and microfiche listings. The results of the geologic interpretation of the radiometric data together with the profiles, anomaly maps and histograms are presented in this Volume II final report. DOE

N82-27811# *Bendix Field Engineering Corp , Grand Junction,* Colo.
AIRBORNE GAMMA-RAY SPECTROMETER AND MAGNETOMETER SURVEY: SUSANVILLE QUADRANGLE, CALIFORNIA, VOLUME 1 Final Report
May 1981 115 p refs
(Contract DE-AC13-76GJ-01664)
(DE82-005538, GJBX-410-81-VOL-1) Avail: NTIS HC A06/MF A01

An airborne high sensitivity gamma ray spectrometer and magnetometer survey was conducted over ten areas over northern California and southwestern Oregon These include the 20 x 10 NTMS quadrangles of Roseburg, Medford, Weed, Alturas, Redding, Susanville, Ukiah, and Chico along with the 10 x 30 areas of the Coos bay quadrangle and the Crescent City/Eureka areas combined Traverse lines were flown in an east-west direction at a line spacing of six (6) miles. The lines were flown north-south approximately eighteen (18) miles apart. A total of 16,880,5 line miles of geophysical data were acquired, compiled, and interpreted during the survey, of which 1642.8 line miles are in this quadrangle Geologic and other information with which to assess the magnitude *and distributing of uranium resources and to determine areas* favorable for the occurrence of uranium in the United States were computed. Author

N82-27812# Bendix Field Engineering Corp., Grand Junction, Colo
AIRBORNE GAMMA-RAY SPECTROMETER AND MAGNETOMETER SURVEY: ROSEBURG QUADRANGLE, OREGON, VOLUME 2 Final Report
Mar 1981 134 p refs
(Contract DE-AC13-76GJ-01664)
(DE82-005568; GJBX-388-81-VOL-2) Avail. NTIS HC A07/MF A01

Data from an airborne high sensitivity gamma ray spectrometer and magnetometer survey of the Roseburg quadrangle, Oregon are presented The magnitude and distribution of uranium resources and favorable areas for occurrence of uranium in the US are discussed DOE

N82-27813# *Western Geophysical Co. of America, Houston,* Tex. Aero Service Div.
AIRBORNE GAMMA-RAY SPECTROMETER AND MAGNETOMETER SURVEY: UKIAH QUADRANGLE, CALIFORNIA, VOLUME 1 Final Report
May 1981 110 p refs Sponsored in part by Bendix Field Engineering Corp 2 Vol.
(Contract DE-AC13-79GJ-01664)
(DE82-005541; GJBX-390-81-VOL-1) Avail NTIS HC A06/MF A01

Transverse lines were flown in an east to west direction at a line spacing of six miles. Tie lines were flown north to south approximately eighteen miles apart A total of 16,880.5 line miles of geophysical data were acquired, compiled and interpreted during the survey, of which 1517 line miles are in this quadrangle Geologic and other information was compiled with which to assess the magnitude and distribution of uranium in the United States DOE

N82-27814# Western Geophysical Co. of America, Houston, Tex. Aero Service Div
AIRBORNE GAMMA-RAY SPECTROMETER AND MAGNETOMETER SURVEY: HURON QUADRANGLE, SOUTH DAKOTA Final Report
Apr. 1981 98 p refs Prepared for Bendix Field Engineering Corp.
(Contract DE-AC13-76GJ-01664)
(DE82-005540, GJBX-405-81-VOL-1) Avail: NTIS HC A05/MF A01

Geologic and other information with which to assess the magnitude and distribution of uranium resources and to determine areas favorable for the occurrence of uranium in the United States were acquired An airborne high sensitivity gamma ray spectrometer and magnetometer survey was conducted over eleven 20 x 10 NTMS quadrangles located in the states of Minnesota and Wisconsin and seven 20 x 10 NTMS quadrangles in North and South Dakota The quadrangles located within the North and South Dakota survey area include Devil's Lake, New Rockford, Jamestown, Aberdeen, Huron, Mitchell, and Sioux Falls The results obtained over the Huron map area are discussed Traverse lines were flown in an east-west direction at a line spacing of six miles. The lines were flown north-south approximately 24 miles apart. DOE

N82-27815# Western Geophysical Co. of America, Houston, Tex. Aero Service Div
AIRBORNE GAMMA-RAY SPECTROMETER AND MAGNETOMETER SURVEY: CHICO QUADRANGLE, CALIFORNIA Final Report
May 1981 127 p refs Prepared for Bendix Field Engineering Corp.
(Contract DE-AC13-76GJ-01664)
(DE82-005543, GJBX-407-81-VOL-1) Avail: NTIS HC A07/MF A01

The magnitude and distribution of uranium resources with which to assess the magnitude and distribution of uranium resources *and to determine areas favorable for the occurrence of uranium* in the United States was investigated An airborne high sensitivity gamma ray spectrometer and magnetometer survey was conducted

over 10 areas over northern California and southwestern Oregon. These include the 20 x 10 NTMS quadrangles of Roseburg, Medford, Weed, Alturas, Redding, Susanville, Ukiah, and Chico along with the 10 x 20 areas of the Coos Bay quadrangle and the Crescent City/Eureka areas combined. The results obtained over the Chico, California, map area are discussed DOE

05

OCEANOGRAPHY AND MARINE RESOURCES

Includes sea-surface temperature, ocean bottom surveying imagery, drift rates, sea ice and icebergs, sea state, fish location

A82-22306* California Inst. of Tech., Pasadena.
LABORATORY STUDIES OF ACTINIDE METAL-SILICATE FRACTIONATION
J. H. JONES and D S. BURNETT (California Institute of Technology, Pasadena, CA) In: Lunar and Planetary Science Conference, 11th, Houston, TX, March 17-21, 1980, Proceedings Volume 2. New York, Pergamon Press, 1980, p 995-1001. refs
(Contract NSG-7202)

Actinide and Sm partition coefficients between silicate melt and several metallic phases have been measured. Under reducing conditions Si, Th, U and Pu can be reduced to metals from silicate melts and alloyed with a platinum-gold alloy. U and Pu enter a molten Pt-Si alloy with roughly equal affinity but U strongly partitions into the solid Pt. Th behaves qualitatively the same as Pu but is much less readily reduced than U, and Sm appears to remain unreduced Experiments with Fe metal have shown that the partition coefficients of the actinides between Fe and silicate liquid are extremely low, suggesting a very low actinide concentration in planetary cores Experiments show that platinum metals can efficiently fractionate actinides and fractionate actinides from lanthanides and this process may be relevant to the condensation behavior of these elements from the solar nebula. Pt-metal grains in Allende Ca-Al-rich inclusions appear to be U-poor, although the sub-class of Zr-bearing Pt metals may have high U contents.
(Author)

A82-22619
FEATURES OF COSMIC RAY VARIATIONS DUE TO VARIATIONS IN THE TOTAL MAGNETIC FIELD OF THE SUN
A. N. CHARAKHCHIAN (Akademiia Nauk SSSR, Fizicheskii Institut, Moscow, USSR) and T. N. CHARAKHCHIAN (Moskovskii Gosudarstvennyi Universitet, Moscow, USSR) In: International Cosmic Ray Conference, 17th, Paris, France, July 13-25, 1981, Conference Papers Volume 3 Gif-sur-Yvette, Essonne, France, Commissariat a l'Energie Atomique, 1981, p. 202-205. refs

The characteristics of the large-scale variations in cosmic ray intensity associated with variations in the total solar magnetic field are discussed. Particular attention is given to cosmic ray effects connected with solar magnetic field inversion and the presence in the stratosphere of short-range particles during periods of increasing total solar magnetic field, and to zonal cosmic ray modulation in the primary energy range 5-20 GeV which is due largely to magnetic field variations at the periphery of the heliosphere. A L.W

A82-28907* National Aeronautics and Space Administration. Goddard Space Flight Center, Greenbelt, Md.
REMOTE SENSING OF PRECIPITABLE WATER OVER THE OCEANS FROM NIMBUS 7 MICROWAVE MEASUREMENTS
C. PRABHAKARA, A. T. C. CHANG (NASA, Goddard Space Flight Center, Laboratory for Atmospheric Sciences, Greenbelt, MD), and H. D. CHANG (NASA, Goddard Space Flight Center, Laboratory for Atmospheric Sciences, Greenbelt; Computer Sciences Corp., Silver Spring, MD) Journal of Applied Meteorology, vol. 21, Jan 1982, p. 59-68. refs
(Previously announced in STAR as N81-24504)

A82-29601* Jet Propulsion Lab., California Inst. of Tech., Pasadena.
SEASAT MEASUREMENT SYSTEM EVALUATION - ACHIEVEMENTS AND LIMITATIONS
D B. LAME and G H BORN (California Institute of Technology, Jet Propulsion Laboratory, Pasadena, CA) Journal of Geophysical Research, vol 87, Apr. 30, 1982, p. 3175-3178. refs
(Contract NAS7-100)

The Seasat project, which demonstrated the feasibility of microwave oceanographic remote sensing, was sponsored by the National Aeronautics and Space Administration and managed by the Jet Propulsion Laboratory. The evaluation of the measurement system (elements of the satellite, the sensors, the data handling, and data processing subsystems) was a key activity of the Seasat project. This paper summarizes the primary achievements and highlights the generic limitations of the evaluation process. Other papers in this issue present details of the geophysical evaluation process carried out under the auspices of the Seasat project
(Author)

A82-29602* Texas Univ., Austin.
THE SEASAT ALTIMETER DATA AND ITS ACCURACY ASSESSMENT
B. D. TAPLEY (Texas, University, Austin, TX), G. H BORN, and M. E. PARKE (California Institute of Technology, Jet Propulsion Laboratory, Pasadena, CA) Journal of Geophysical Research, vol. 87, Apr. 30, 1982, p. 3179-3188. NASA-supported research. refs

A description is given of the Seasat satellite radar altimeter, which was designed to measure (1) the altitude of the satellite above the ocean surface, (2) surface wave height, and (3) the ocean-surface backscatter coefficient from which wind speed may be inferred. The atmospheric and geophysical effects influencing radar altimeter measurement accuracies and the attendant correction models adopted for the altimeter geophysical data record are summarized, along with Seasat Altimeter/Precision Orbit Determination Experiment Team activities directed towards the validation and improvement of these models and investigations assessing the accuracy of both the altimeter measurements and the computed satellite altitude ephemeris. O.C.

A82-29603* National Aeronautics and Space Administration. Goddard Space Flight Center, Greenbelt, Md.
SEASAT ALTIMETER HEIGHT CALIBRATION
R KOLENKIEWICZ (NASA, Goddard Space Flight Center, Geodynamics Branch, Greenbelt, MD) and C F. MARTIN (EG&G Washington Analytical Services Center, Inc., Riverdale, MD) Journal of Geophysical Research, vol. 87, Apr 30, 1982, p. 3189-3197. refs
(Previously announced in STAR as N81-19526)

A82-29604#
TIDAL AND GEODETIC OBSERVATIONS FOR THE SEASAT ALTIMETER CALIBRATION EXPERIMENT
J M. DIAMANTE, B C. DOUGLAS, D L. PORTER, and R. P. MASTERSON, JR. (NOAA, National Ocean Survey, Rockville, MD) Journal of Geophysical Research, vol. 87, Apr. 30, 1982, p 3199-3206. refs

As part of the Seasat calibration activities of September and October 1978, a tide gage was installed by the National Ocean Survey at an open coastal location on Bermuda to provide instantaneous sea surface height determinations during Seasat overflights of the island Because the tide gage was geodetically tied to the laser tracking station on Bermuda, the satellite's position relative to the sea surface could be determined independently for comparison with altimeter measurements. A root sum square error of 4 0 cm in the laser's vertical position determination, relative to the sea surface, has been estimated apart from possible errors arising from the present lack of precise information on the elevation of the Bermuda geoid. O.C.

A82-29607* Jet Propulsion Lab., California Inst. of Tech., Pasadena
AN EMPIRICAL DETERMINATION OF THE EFFECTS OF SEA STATE BIAS ON SEASAT ALTIMETRY
G. H. BORN, M A. RICHARDS (California Institute of Technology, Jet Propulsion Laboratory, Pasadena, CA), and G. W ROSBOROUGH (Texas, University, Austin, TX) Journal of Geophysical Research, vol. 87, Apr 30, 1982, p 3221-3226. NASA-supported research. refs

A linear empirical model has been developed for the correction of sea state bias effects, in Seasat altimetry data altitude measurements, that are due to (1) electromagnetic bias caused by the fact that ocean wave troughs reflect the altimeter signal more strongly than the crests, shifting the apparent mean sea level toward the wave troughs, and (2) an independent instrument-related bias resulting from the inability of height corrections applied in the ground processor to compensate for simplifying assumptions made for the processor aboard Seasat After applying appropriate corrections to the altimetry data, an empirical model for the sea state bias is obtained by differencing significant wave height and height measurements from coincident ground tracks Height differences are minimized by solving for the coefficient of a linear relationship between height differences and wave height differences that minimize the height differences. In more than 50% of the 36 cases examined, 7% of the value of significant wave height should be subtracted for sea state bias correction. O C.

A82-29608*# National Aeronautics and Space Administration. Wallops Flight Center, Wallops Island, Va
SEA-STATE-RELATED ALTITUDE ERRORS IN THE SEASAT RADAR ALTIMETER
G S HAYNE and D. W. HANCOCK, III (NASA, Wallops Flight Center, Wallops Island, VA) Journal of Geophysical Research, vol. 87, Apr. 30, 1982, p. 3227-3231 refs

A significant waveheight-dependent bias is identified in Seasat-measured surface heights which cannot be neglected when using Seasat data at accuracies within 10 cm. Ten-second averages of the data from 63 waveform sampling rates in the Seasat radar altimeter were least squares fitted with a six-parameter model, the time-origin parameter of which provides a measure of the position of the actual mean radar waveform relative to the sampling rate and therefore provides altitude measurement corrections. Attention is given to actual altimeter point target response function, waveform sampler noise baseline, waveform sampler gain calibration, attitude angle and sea surface skewness, as effects not accounted for in Seasat altimeter measurements and standard data processing O C

A82-29609*# National Aeronautics and Space Administration Goddard Space Flight Center, Greenbelt, Md
SEASAT ALTIMETER TIMING BIAS ESTIMATION
J G MARSH (NASA, Goddard Space Flight Center, Geodynamics Branch, Greenbelt, MD) and R G WILLIAMSON (EG & G Washington Analytical Services Center, Inc, Riverdale, MD) Journal of Geophysical Research, vol. 87, Apr 30, 1982, p 3232-3238. refs

A technique developed for the solution of time lag bias based on the analysis of sea surface height discrepancies at ground track intersections, prompted by the presence of a time calibration bias in Seasat altimeter data that produced measurement errors in excess of 1 m, is shown to yield a separation of the dominant, once-per-revolution ephemeris error amounting to about 1.5 m rms from the timing error signature The technique does not depend on precise geoid data, and in application to a global Seasat altimeter data set covering July 28-August 9, 1978, has yielded a time lag value of -81.0 + or - 2 msec This corroborates the -79.4 msec revised value derived from a reexamination of internal instrument time delays. O C.

A82-29610* Texas Univ, Austin.
EVALUATION OF THE SEASAT ALTIMETER TIME TAG BIAS
B E. SCHUTZ, B D. TAPLEY, and C. SHUM (Texas, University, Austin, TX) Journal of Geophysical Research, vol. 87, Apr. 30, 1982, p. 3239-3245 refs
(Contract NOAA-MO-A01-78-00-4325, JPL-954703)

Two methods were used in analyses of Seasat altimeter data, aimed at the corroboration of an inherent altimeter microprocessor delay compensation value of -79.4 msec, which benefited from a global data distribution in the oceanic areas: (1) the crossover method, using altimeter data differenced at points where the Seasat ground track intersected with itself, and (2) the direct use of the altimeter data Because the former method is independent of errors in the geoid model, it is considered the more reliable. For all crossover method results, the adopted value of -79.4 msec is within the bounds of the standard deviation associated with the estimates, of which -78.1 + or - 2.0 msec is considered the best representative O C

A82-29611*# National Aeronautics and Space Administration Goddard Space Flight Center, Greenbelt, Md.
COMPARISON DATA FOR SEASAT ALTIMETRY IN THE WESTERN NORTH ATLANTIC
R E. CHENEY (NASA, Goddard Space Flight Center, Geodynamics Branch, Greenbelt, MD) Journal of Geophysical Research, vol 87, Apr. 30, 1982, p. 3247-3253 refs
(Previously announced in STAR as N81-19529)

A82-29612
WAVEHEIGHT AND WIND SPEED MEASUREMENTS FROM THE SEASAT RADAR ALTIMETER
L S. FEDOR (NOAA, Wave Propagation Laboratory, Boulder, CO) and G. S BROWN (Applied Science Associates, Inc, Apex, NC) Journal of Geophysical Research, vol 87, Apr 30, 1982, p. 3254-3260 refs
(Contract NOAA-NA-79SAC00723)

A similarity to the results of earlier comparisons with the GEOS-3 radar altimeter data is noted, in the mean difference of -0.25 m/sec and standard deviation of 1 58 m/sec found upon comparison of Seasat radar altimeter-derived winds with buoy-recorded winds in the 1-10 m/sec range It has therefore been demonstrated by means of two different radars and data sets that radar altimetry can provide accurate estimates of ocean surface wind speeds. Although the altimeter cannot provide the large-swath coverage provided by the Seasat scatterometer, its ability to produce accurate, simultaneous estimates of wind speed and waveheight may be important to future oceanographic research O.C

A82-29613* California Univ., La Jolla.
SEASAT ALTIMETER DETERMINATION OF OCEAN CURRENT VARIABILITY
R. L BERNSTEIN, R. H WHRITNER (California, University, La Jolla, CA), and G H. BORN (California Institute of Technology, Jet Propulsion Laboratory, Pasadena, CA) Journal of Geophysical Research, vol. 87, Apr. 30, 1982, p. 3261-3268. refs
(Contract NAS7-100)

An experiment conducted in the Kuroshio Current, east of Japan, has confirmed the ability of radar altimeters of precision on the order of 10 cm, such as that of the Seasat satellite, to measure the small oceanic height variations associated with geostrophic ocean currents Changes in surface dynamic height were inferred from data gathered by air-expendable bathythermographs, which had been dropped to coincide with the Seasat subtrack, for the periods between the flights of September 25 and October 5 and 13, 1978. The changes registered generally agreed to within + or - 10 cm of the height changes observed in the altimeter data. O.C.

A82-29614*# National Aeronautics and Space Administration Goddard Space Flight Center, Greenbelt, Md
THE SEASAT ALTIMETER MEAN SEA SURFACE MODEL
J. G. MARSH (NASA, Goddard Space Flight Center, Geodynamics Branch, Greenbelt, MD) and T. V. MARTIN (EG & G Washington Analytical Services Center, Inc., Riverdale, MD) Journal of Geophysical Research, vol 87, Apr. 30, 1982, p. 3269-3280. refs

Gridding techniques are used to combine an 18-day set of Seasat altimeter data and two precisely-computed Seasat ephemerides, in order to arrive at global contour maps of the mean sea surface topography The altimeter data have an rms agreement of 111 cm with the SS3 mean sea surface computed by means of the PGS-S3 ephemerides, and of 70 cm with the SS4 mean surface derived from the PGS-S4 ephemerides. While comparisons with the GEM 10B 1 x 1 deg gravimetric geoid have yielded rms differences of 2.8 m, those with a global mean sea surface derived from GEOS 3 altimeter data show rms differences of 1.3 m and 1.1 m for the cases of the SS3 and SS4 surfaces, respectively. An SS4 mean sea surface topograph is featured among the study findings presented Further improvements in the representation of mean sea surface topography are expected with the development of more accurate gravity models for orbit computation. O.C

A82-29616*# General Electric Co , Philadelphia, Pa
THE SEASAT-A SATELLITE SCATTEROMETER - THE GEOPHYSICAL EVALUATION OF REMOTELY SENSED WIND VECTORS OVER THE OCEAN
W. L. JONES (General Electric Co , Space Div , Philadelphia, PA), L. C. SCHROEDER, E M. BRACALENTE (NASA, Langley Research Center, Hampton, VA), D H BOGGS (California Institute of Technology, Jet Propulsion Laboratory, Pasadena, CA), R A. BROWN (Washington, University, Seattle, WA), G. J. DOME (University of Kansas Center for Research, Inc , Lawrence, KS), W J. PIERSON (New York, City University, New York, NY), and F. J. WENTZ (Remote Sensing Systems, Inc., Sausalito, CA) Journal of Geophysical Research, vol. 87, Apr. 30, 1982, p. 3297-3317. refs

A description is given of the algorithm used to convert Seasat-A satellite microwave scatterometer measurements of ocean normalized radar cross section to the neutral stability vector wind at 19 5 m height, as well as to compare these winds with high-quality surface observations The wind vector algorithm used an empirical normalized radar cross section model function to describe the ocean normalized radar cross section's dependence on the 19.5-m neutral stability wind vector. In addition, two model functions were evaluated by means of an independent set of in situ surface wind observations from the Joint Air Sea Interaction experiment (JASIN). Better results were produced by these comparisons than the stipulated Seasat wind speed and direction accuracy specifications of + or - 2 m/sec and + or - 20 deg, respectively, over the 0-16 m/sec range of winds observed during JASIN O.C.

A82-29617*# National Aeronautics and Space Administration Langley Research Center, Hampton, Va.
THE RELATIONSHIP BETWEEN WIND VECTOR AND NORMALIZED RADAR CROSS SECTION USED TO DERIVE SEASAT-A SATELLITE SCATTEROMETER WINDS
L. C. SCHROEDER, W. L. JONES (NASA, Langley Research Center, Hampton, VA), D H. BOGGS, I. M. HALBERSTAM (California Institute of Technology, Jet Propulsion Laboratory, Pasadena, CA), G DOME (University of Kansas Center for Research, Inc , Lawrence, KS), W J PIERSON (New York, City University, New York, NY), and F. J. WENTZ (Remote Sensing Systems, Inc., Sausalito, CA) Journal of Geophysical Research, vol 87, Apr. 30, 1982, p 3318-3336. refs

The Seasat-A Satellite Scatterometer (SASS) ocean normalized radar cross section (NRCS) dependence on the 19.5-m neutral stability wind vector may be specified as a function of radar incidence angle, the angle between wind direction and radar azimuth, and the neutral stability wind speed expressed in m/sec at a height of 19 5 m An account is given of the development of models both expressing this relationship and providing the basis of inversion of NRCS to SASS winds, from initially aircraft scatterometer measurement-based forms to three Seasat field-validation experiments which furnish model NRCS versus surface windspeed data for comparison with SASS data O C

A82-29618* Kansas Univ. Center for Research, Inc., Lawrence.
EVALUATION OF ATMOSPHERIC ATTENUATION FROM SMMR BRIGHTNESS TEMPERATURE FOR THE SEASAT SATELLITE SCATTEROMETER
R. K MOORE, I J BIRRER (University of Kansas Center for Research, Inc., Lawrence, KS), E. M. BRACALENTE (NASA, Langley Research Center, Hampton, VA), G J. DOME (Bell Telephone Laboratories, Inc , Holmdel, NJ), and F J. WENTZ (Remote Sensing Systems, Inc., Sausalito, CA) Journal of Geophysical Research, vol 87, Apr. 30, 1982, p 3337-3354. refs

The effect of attenuation in precipitation regions of the sea, which must be considered in order to measure the radar backscatter from the ocean with sufficient accuracy to allow determination of the wind vector, can be ascertained from a knowledge of the brightness temperature observed by a microwave radiometer such as the Seasat multifrequency scanning radiometer. Two algorithms relating radiometric measurements and attenuation, and thereby correcting measured scattering coefficient values, were compared with wind vectors reported by surface observers and those determined by the Seasat scatterometer measurements with and without correction for atmospheric attenuation. Although the attenuation correction yields some improvements, it is constrained by both radiometer footprint differences and different scan patterns. O C

A82-29619* Washington Univ., Seattle.
SURFACE WIND ANALYSES FOR SEASAT
R. A. BROWN (Washington, University, Seattle, WA), V J CARDONE (Oceanweather, Inc., White Plains, NY), T. GUYMER (Institute of Oceanographic Sciences, Wormley, Surrey, England), J. HAWKINS (NOAA, National Hurricane and Experimental Meteorology Laboratory, Bay Saint Louis, MS), J E. OVERLAND (NOAA, Pacific Marine Environment Laboratory, Seattle, WA), W. J. PIERSON (City College, New York, NY), S. PETEHERYCH (Department of the Environment, Atmospheric Environment Service, Downsview, Ontario, Canada), J. C WILKERSON (NOAA, Camp Springs, MD), P M. WOICESHYN (California Institute of Technology, Jet Propulsion Laboratory, Pasadena, CA), and M WURTELE (California, University, Los Angeles, CA) Journal of Geophysical Research, vol. 87, Apr. 30, 1982, p. 3355-3364. refs

During the 99 days of Seasat operation, two large-scale experiments were conducted which established the satellite sensors' wind measuring capabilities: (1) the Gulf of Alaska Experiment (GOASEX), and (2) the Joint Air Sea Interaction Experiment (JASIN), which unlike GOASEX was independent of the Seasat program and undertook comprehensive air and sea investigations which furnished excellent comparison data for Seasat. Qualitative comparison windfields were also provided by several storms. The point measurements in GOASEX and JASIN were averaged in conjunction with Seasat scatterometer regions and, on the basis of comparisons between several anemometers on buoys and meteorological ships and the calculation of various averaging times, a 20-min average yields a scatterometer scale windfield accuracy of up to + or 1 m/sec and + or - 10 deg in well-behaved windfields. O.C.

A82-29621* Remote Sensing Systems, Sausalito, Calif
INTERCOMPARISON OF WIND SPEEDS INFERRED BY THE SASS, ALTIMETER, AND SMMR
F. J WENTZ (Remote Sensing Systems, Inc., Sausalito, CA), V. J. CARDONE (Oceanweather, Inc., White Plains, NY), and L S. FEDOR (NOAA, Wave Propagation Laboratory, Boulder, CO) Journal of Geophysical Research, vol 87, Apr. 30, 1982, p. 3378-3384 refs
(Contract NAS1-16032; NAS7-100)

The operational theory, control algorithms, and comparisons with surface-determined wind speeds for the scatterometer (SASS), altimeter (ALT), and passive microwave radiometer (SMMR) on board the Seasat satellite are presented. Radiative scattering combining specular reflections and Bragg resonance scattering are noted to occur at tilting waves and sea foam, two conditions highly correlated with wind speed. SASS scans swaths of 70, 200, and 700 km from nadir, the SMMR covers a 150 km strip. Normalized radar sections are derived from the SASS and ALT telemetry, and brightness temperature from the SMMR ALT winds were found to be biased about 3 m/sec low, while intercomparison between the SMMR and SASS data showed a mean difference of 0.3 m/sec with a standard deviation from measured winds of 1.7 m/sec or less. The effects of land thermal emissions, rain, and sun glint are discussed, and good viewing conditions are concluded to result in 2 m/sec accuracy M.S K.

A82-29622* Jet Propulsion Lab., California Inst. of Tech., Pasadena
DESCRIPTION OF SEASAT RADIOMETER STATUS AND RESULTS
R. G LIPES (California Institute of Technology, Jet Propulsion Laboratory, Pasadena, CA) Journal of Geophysical Research, vol 87, Apr. 30, 1982, p 3385-3395. refs
(Contract NAS7-100)

Improved geophysical algorithms are shown to be able to determine sea surface temperature (SST) to an accuracy of 1 C (1 sigma) under favorable surface and atmospheric conditions over an SST range of 10-30 C. Under similar conditions, the radiometer wind retrievals track the scatterometer winds within a scatter of 2 m/s (1 sigma) over a wind speed range of 0-25 m/s These conditions require that contamination from land, rain, sun glint, and radio frequency interference be avoided What is more, water vapor determinations in the midlatitudes and in the tropical Pacific are found to agree with estimates of precipitable water from radiosondes to within 10%. C.R.

A82-29623* Stanford Univ., Calif.
THE OBSERVATION OF OCEAN SURFACE PHENOMENA USING IMAGERY FROM THE SEASAT SYNTHETIC APERTURE RADAR - AN ASSESSMENT
J. F VESECKY (Stanford University, Stanford, CA) and R. H STEWART (California Institute of Technology, Jet Propulsion Laboratory, Pasadena, California, University, La Jolla, CA) Journal of Geophysical Research, vol. 87, Apr 30, 1982, p. 3397-3430. refs
(Contract N00014-75-C-0356; NOAA-MO-A01-78-00-4318)

The principles governing synthetic aperture radar (SAR) and its use on the Seasat spacecraft are reviewed. The way in which wind stress, surface currents, long gravity waves, and surface films modulate the scattering properties of resonant (approximately 30-cm-wavelength) waves is discussed, with particular emphasis placed on the mechanisms that could produce images of long gravity waves. Doppler effects by ocean motion are also described. Measurements of long (wavelength more than about 100 m) gravity waves made using Seasat SAR imagery are compared with surface measurements during several experiments. Combining these results, it is found that dominant wavelength and direction are measured by Seasat SAR within + or - 12% and + or - 15 deg, respectively. It is noted, however, that ocean waves are not always visible in SAR images, and detection criteria are discussed in terms of wave height, length, and direction. C.R.

A82-29624* National Oceanic and Atmospheric Administration, Seattle, Wash
SEASAT WIND AND WAVE OBSERVATIONS OF NORTHEAST PACIFIC HURRICANE IVA, AUGUST 13, 1978
F. I. GONZALEZ (NOAA, Pacific Marine Environmental Laboratory, Seattle, WA), T. W. THOMPSON (Science Applications, Inc., Planetary Science Institute, Pasadena, CA), W. E BROWN, JR. (California Institute of Technology, Jet Propulsion Laboratory, Pasadena, CA), and D. E WEISSMAN (Hofstra University, Hempstead, NY) Journal of Geophysical Research, vol 87, Apr. 30, 1982, p. 3431-3438 NOAA-supported research refs
(Contract NAS7-100)

The paper examines Seasat wind and wave observations collected in the eye of hurricane Iva on August 13, 1978 in the northeast Pacific. A maximum wind speed of 25-30 m/s is observed, along with a banana-shape high-wind-speed distribution. Two-dimensional Fourier transforms of selected SAR scenes show a dominant wavefield characterized by wavelengths of 166-211 m, with a fanlike distribution of propagation directions. A simple geometric model is proposed to explain the dominant wave field in terms of prior storm intensity and location, which is combined with the Ross parametric hurricane wave model and Seasat wind and wave data to estimate a value of 43 km for the effective radial distance from the storm center to the region of maximum winds. D.L.G.

A82-30666#
A STUDY OF THE EARTH'S RADIATION BUDGET USING A GENERAL CIRCULATION MODEL
J. M. SLINGO (Meteorological Office, Bracknell, Berks., England) Royal Meteorological Society, Quarterly Journal, vol. 108, Apr. 1982, p 379-405. refs

A model clarifying the roles played by clouds and the surface in determining the seasonal variations in the radiation budget is described The model employs an interactive radiation scheme with seasonally varying climatological sea surface temperatures, incoming solar radiation, and zonal mean climatological cloud amounts. Since its simulation of the various components of the earth's radiation compares favorably with results from satellites, its results are used in explaining certain aspects of the observed budgets. The model results are also used to estimate the earth's annual mean total energy budget and, in particular, the poleward flux of heat by the oceans. The oceanic heat flux implied by the model compares favorably with estimates based on observations, the main differences being at the equator and near the North Pole. C.R.

A82-30810
A SEARCH FOR SEAMOUNTS IN THE SOUTHERN COOK AND AUSTRAL REGION
K. LAMBECK and R. COLEMAN (Australian National University, Canberra, Australia) Geophysical Research Letters, vol. 9, Apr. 1982, p. 389-392. refs

A82-31294#
EMISSIVITY AND REFLECTANCE OF THE MODEL SEA SURFACE FOR THE USE OF AVHRR DATA OF NOAA SATELLITES
T. TAKASHIMA and Y. TAKAYAMA (Meteorological Research Institute, Tsukuba, Ibaraki, Japan) Papers in Meteorology and Geophysics, vol. 32, Dec. 1981, p. 267-274.

The emissivity and reflectance of the sea surface, modeled from AVHRR advanced radiometer sensing from the NOAA-6 satellites, are derived as a function of the incident and emergent directions of radiation The sea surface is modeled numerically with slope components varying according to a gaussian distribution, including isotropy if independent of the wind direction, and anisotropy if dependent on the wind direction. The geometry of the slope with changing incident and reflecting angles is formulated in terms of spherical trigonometry. Treatment of the surface as a specular reflector is found to be acceptable except for visible light, where the reflection depends on the surface characteristics and a bivariate gaussian analysis is necessary. Additional influences

due to oil slicks are considered, particularly for reflectance reduction. M.S.K

A82-31995* National Aeronautics and Space Administration. Goddard Space Flight Center, Greenbelt, Md.
RETRIEVAL OF OCEAN SURFACE AND ATMOSPHERIC PARAMETERS FROM MULTICHANNEL MICROWAVE RADIOMETRIC MEASUREMENTS
A. T. C. CHANG (NASA, Goddard Space Flight Center, Earth Survey Application Div., Greenbelt, MD) and A. S. MILMAN (Systems and Applied Sciences Corp., Riverdale, MD) IEEE Transactions on Geoscience and Remote Sensing, vol GE-20, Apr. 1982, p. 217-224. refs

Methods for the retrieval of ocean surface temperature, surface wind speed, rain rate, cloud height, and the amounts of water vapor and nonprecipitated liquid water over the ocean from Scanning Multichannel Microwave Radiometer (SMMR) data are presented. The sensitivity of retrieval algorithms for wind speed and sea surface temperature, in the absence of rain, to the undetected presence of rain, is discussed along with the accuracy of a more general method for the retrieval of rain rate in conjunction with other meteorological parameters. It is concluded that the inability to retrieve the average rain rate accurately at small rain angles is due to the inability of SMMR to distinguish between small raindrops and nonprecipitating droplets. O C.

A82-32559#
LASER-INDUCED BIOLUMINESCENCE
G. D. HICKMAN (Applied Science Technology, Inc , Arlington, VA) and R. V. LYNCH, III (U.S. Navy, Naval Research Laboratory, Washington, DC) In Los Alamos Conference on Optics '81, 2nd, Los Alamos, NM, April 7-10, 1981, Proceedings. Bellingham, WA, SPIE - The International Society for Optical Engineering, 1981, p. 263-268. refs
(Contract N00014-80-C-0673)

A project has been initiated to determine the feasibility of developing a complete airborne remote sensing system for rapidly mapping high concentration patches of bioluminescent organisms in the world's oceans. Conceptually, this system would be composed of a laser illuminator to induce bioluminescence and a low light level image intensifier for detection of light. Initial laboratory measurements consisted of using a 2-J flash lamp pulsed optical dye laser to excite bioluminescence in the marine dinoflagellate Pyrocustis lunula at ambient temperature using Rhodamine 6G as the lasing dye (585 nm) and a laser pulse width of 1 microsec. After a latency period of 15-20 msec, the bioluminescence maximum occurred in the blue (480 nm is the wavelength maximum for most dinoflagellate bioluminescence) with the peaking occurring approximately 65 msec after the laser pulse Planned experiments will investigate the effect of different excitation wavelengths and energies at various temperatures and salinities of the cultures. (Author)

A82-32651
A SHIP AND SATELLITE VIEW OF HYDROGRAPHIC FEATURES IN THE WESTERN GULF OF MEXICO
D. A. BROOKS (Texas A & M University, College Station, TX) and R. V LEGECKIS (Texas A & M University, College Station, TX; NOAA National Earth Satellite Service, Washington, DC) Journal of Geophysical Research, vol. 87, May 20, 1982, p. 4195-4206. refs
(Contract NSF OCE-79-24606; NSF OCE-78-22481)

In April 1980, nearly synoptic hydrographic observations were obtained in the western Gulf of Mexico by satellite and ship. A meandering surface thermal front which turned northeastward from the Mexican coast near 23 deg N was prominent in the satellite infrared observations The front separated a southern anticyclone and a northern cyclone, both of which had horizontal scales of several 100 km and were prominent in the subsurface hydrographic observations The eastward geostrophic volume transport in the confluent leg of the two features was roughly equal to that of the Florida Current. A shallow layer of fresh, cool water from the Texas shelf region extended about 300 km seaward into the cyclone along the northern side of the front. Remnant Subtropical Underwater in the core of the April anticyclone indicates its origin in the eastern Gulf Loop Current (Author)

A82-32881
ON THE SYNTHETIC APERTURE RADAR IMAGING OF OCEAN SURFACE WAVES
A. V. IVANOV (Akademiia Nauk SSSR, Institut Radiotekhniki i Elektroniki, Moscow, USSR) IEEE Journal of Oceanic Engineering, vol. OE-7, Apr. 1982, p. 96-103. refs

A process of synthetic aperture radar imaging of ocean surface waves is considered on the basis of the two-scale model of microwave scattering by a disturbed sea surface. Analytical expressions are obtained to relate characteristics of a large-scale wave image, averaged over an ensemble of realizations of the small-scale ripple, with the wave, radar, and viewing scheme as parameters. It is shown that the wave image would be defocused as an image of a target moving in the along-track direction with a speed equal to a half of the wave phase speed projection on the line of flight. The defocusing magnitude was measured experimentally for the ocean swells images, obtained with an airborne S-band radar, and the results are found to be in satisfactory agreement with the model prediction (Author)

A82-32882* Jet Propulsion Lab , California Inst. of Tech , Pasadena.
OCEAN WAVE HEIGHT MEASUREMENT WITH SEASAT SAR USING SPECKLE DIVERSITY
A. JAIN, G. MEDLIN, and C. WU (California Institute of Technology, Jet Propulsion Laboratory, Pasadena, CA) IEEE Journal of Oceanic Engineering, vol OE-7, Apr 1982, p. 103-107. refs
(Contract NAS7-100)

Measurement of ocean wave heights with the synthetic aperture radar can be accomplished with high spatial resolution by determining the variation of speckle intensity with the frequency and angle of illumination A comparison of data obtained by the SEASAT SAR with surface truth measurements obtained during the GOASEX and the JASIN experiments demonstrates this concept. (Author)

A82-32902
INFRARED SENSING OF SEA SURFACE TEMPERATURE FROM SPACE
M SIDRAN (Bernard Baruch College, New York, NY) Remote Sensing of Environment, vol. 10, Sept 1980, p. 101-114. refs

The retrieval of sea surface temperature information from the infrared signals received by remote sensing satellites is examined. Factors influencing the received signal are evaluated, including surface emissivity, spectral radiance, atmospheric transmittance, and sources of error in lengthy computer retrievals based on the integration of the radiative transfer equation related to imperfections in atmospheric transmittance models, uncertainties in the vertical profiles of atmospheric pressure, temperature and humidity profiles, temperature discontinuities at the air-sea interface, differences between surface and bulk water temperatures and the neglect of surface emissivity and reflectance are pointed out. The simple retrieval scheme of Prabhakara et al. (1974), which makes use of three spectral bands to achieve an rms error of + or - 1.1 K, is then reviewed, and a simplified version of this scheme based on only two bands is presented which reduces the rms error to + or - 1.0 K A.L W.

A82-32903
NEARSHORE CURRENT PATTERN OFF SOUTH TEXAS - AN INTERPRETATION FROM AERIAL PHOTOGRAPHS
R. E. HUNTER and G. W. HILL (U S. Geological Survey, Menlo Park, CA) Remote Sensing of Environment, vol. 10, Sept. 1980, p. 115-134 refs

Turbidity patterns seen on aerial photographs of nearshore waters are analyzed to derive the current patterns in a 4-km wide zone along the south Texas coast. Series of color aerial photographs were taken vertically from an altitude of 3700 m on December 23, 1968, following the passage of a cold front

accompanied by strong northwesterly to northeasterly winds. Examination of photographs taken from 6 to 80 min apart indicate the presence of southward currents nearly parallel to the shore, with velocities increasing from about 17 cm/sec off shore to about 40 cm/sec at the line of breaking waves Rip-current plumes were observed to drift with the longshore current and be deformed by the horizontal shear. The turbidity by which these currents were traced originated in Aransas pass, a tidal inlet connecting several estuarine bays to the Gulf of Mexico, and a preceding ebb-tidal plume from the same inlet A linear pattern of turbid and less turbid bands also suggests the development of Langmuir circulation with cell axes parallel to the shelf current. A L W

A82-32917
MEASURING SEA SURFACE TEMPERATURE FROM SATELLITES - A GROUND TRUTH APPROACH
D. C. MCCONAGHY (NOAA, Southwest Fisheries Center, La Jolla, CA) Remote Sensing of Environment, vol 10, Dec. 1980, p 307-310.

Determining the correction for atmospheric attenuation is a major problem in processing thermal infrared digital data from very high resolution radiometers aboard NOAA Polar Orbiting Satellites. An empirical equation for estimating this correction is developed. The coefficients of the equation are determined by using regression techniques and comparing satellite observations to sea surface temperature measurements. Although there is not sufficient data to fully evaluate this procedure, initial satellite measurements are within 0 5 C of independent sea surface temperature measurements (Author)

A82-33322*# National Aeronautics and Space Administration Langley Research Center, Hampton, Va
DEPRESSION OF BRIGHTNESS TEMPERATURE OF SEA SURFACES COVERED WITH MONOMOLECULAR OIL FILMS RELATIVE TO CLEAN WATER SURFACES AT 1.43 GHZ
H.-J C. BLUME (NASA, Langley Research Center, Hampton, VA) Institute of Electrical and Electronics Engineers, International Geoscience and Remote Sensing Symposium, Munich, West Germany, June 1-4, 1982, Paper 6 p. refs

A82-33438*# National Aeronautics and Space Administration Langley Research Center, Hampton, Va
CHARACTERISTICS OF 13.9 GHZ RADAR SCATTERING FROM OIL FILMS ON THE SEA SURFACE
J. W JOHNSON and W. F. CROSWELL (NASA, Langley Research Center, Hampton, VA) Radio Science, vol 17, May-June 1982, p. 611-617. refs

Aircraft microwave scatterometer measurements are presented, which were made in 1979 as part of a project to study the response of a number of active and passive microwave and optical remote sensors to an oil-covered sea surface conducted by NASA Langley Research Center. A 13.9-GHz Doppler scatterometer with a fan beam antenna and coherent detection was used to measure radar backscatter as a function of incidence angle The radar scattering signature of the clear surface and signatures of the surface covered with various crude oil films are compared Reductions in Ku band microwave backscatter up to 14 dB are observed for both treated and untreated LaRosa and Murban crude oil films deposited on the sea surface. Maximum Ku band sensitivity to the effects of the oil in terms of differential scatter is observed in the 25-35 deg incidence angle region. D.L G.

A82-33717
SATELLITE OBSERVATIONS OF SEA SURFACE TEMPERATURE AROUND THE BRITISH ISLES
R. W. SAUNDERS, N R. WARD, C. F. ENGLAND, and G E. HUNT (University College, London, England) American Meteorological Society, Bulletin, vol 63, Mar 1982, p. 267-272. Research supported by the European Space Agency, Natural Environmental Research Council, and Science and Engineering Research Council. refs

TIROS-N Advanced Very High Resolution Radiometer (AVHRR) imagery has been used to study the temperature structure of the sea surface around the British Isles The satellite imagery from both TIROS-N, METEOSAT and conventional synoptic data are combined to obtain a calibration for both 11-micron infrared channels, which gave sea surface temperatures accurate to + or - 1 K. The changes in the sea surface temperature around the British Isles for July 12, 1979 are shown well by the satellite data. In particular, a study is made of an anomalously warm patch in the North Sea that appeared at local noon over an area where the surface winds were weak, inhibiting surface mixing. (Author)

A82-34219
COASTAL ENVIRONMENT CHANGE ANALYSIS BY LANDSAT MSS DATA
J -K. HONG (Tokyo University of Agriculture and Technology, Tokyo, Japan) and J. IISAKA (IBM Japan, Ltd., Tokyo, Japan) Remote Sensing of Environment, vol. 12, May 1982, p. 107-116 refs

A case study of coastal environmental change is conducted using computer-assisted analysis of Landsat scenes for three different years The Kanto area in Japan is divided into three study areas on the basis of social and geographical factors Land use changes along the bay from November 26, 1972, to November 11, 1980, are studied and the results are interpreted by referring to the ground truth data. The results show a continuous decrease in the area of shallow water along the bay and changes in land use in the coastal areas. The changes are recognized as being closely related to the bay area changes; they are found to correspond well to differences in social developments in the study areas. Landsat data are thus shown to provide sufficient information on the environmental changes taking place. C.R

A82-36005
ESTIMATION OF THE TEMPERATURE OF THE UPPER BOUNDARY OF CLOUD COVER OVER THE WORLD OCEAN [OTSENKA TEMPERATURY VERKHNEI GRANITSY OBLACHNOSTI NAD MIROVYM OKEANOM]
O. AVASTE, O. KIARNER, and S. KEEVALLIK (Akademiia Nauk Estonskoi SSR, Institut Astrofiziki i Fiziki Atmosfery, Tartu, Estonian SSR) Meteorologiia i Gidrologiia, June 1982, p. 54-59. In Russian refs

The temperature of the upper boundary of cloud cover over the world ocean is estimated on the basis of cloud-amount estimates made by Avaste et al. (1981), climatological means of ocean surface temperature, and mean monthly values of outgoing radiation fluxes. Mean monthly upper-cloud-boundary temperatures over the world ocean are estimated for the 30 deg N to 30 deg S latitude belt Data from the Nimbus-3 and NOAA meteorological satellites were used in the estimation. B.J

A82-36341
INTERANNUAL VARIATIONS OF OUTGOING IR ASSOCIATED WITH TROPICAL CIRCULATION CHANGES DURING 1974-1978
B. LIEBMANN and D. L. HARTMANN (Washington, University, Seattle, WA) Journal of the Atmospheric Sciences, vol. 39, May 1982, p. 1153-1162. refs
(Contract NSF 78-07369; NSF 81-06099)

Interannual variability of outgoing IR in the tropical Pacific Ocean is studied using measurements derived from the NOAA scanning radiometer In addition to the usual mean maps, seasonal anomaly maps are constructed from June, July, August 1974-December 1977, and January, February 1978. Time series representing the equatorial eastern Pacific sea-surface temperature (SST) anomalies and monthly anomalies at various locations are also plotted During this period a warming event occurs, in which SSTs in the eastern Pacific rapidly become anomalously warm. Dramatic changes in outgoing IR occur simultaneously with this SST increase. The region of convergence over Indonesia shifts eastward and connects to a well-developed intertropical convergence zone (ITCZ). The South Pacific convergence zone (SPCZ) is also connected to the Indonesian convergence zone, but develops more slowly and does not reach its maximum strength until more than a year after the SST increases occur By this time the ITCZ has returned to its

prewarming state. Eastward movement of the SPCZ is also apparent (Author)

A82-37195
DETERMINATION OF WINTER TEMPERATURE PATTERNS, FRONTS, AND SURFACE CURRENTS IN THE YELLOW SEA AND EAST CHINA SEA FROM SATELLITE IMAGERY
Q. A. ZHENG and V. KLEMAS (Delaware, University, Newark, DE) Remote Sensing of Environment, vol 12, July 1982, p. 201-218. refs

A82-37196
ESTIMATION OF THE PRECIPITABLE WATER FROM THE IR CHANNEL OF THE GEOSTATIONARY SATELLITE
T AOKI (Meteorological Satellite Center, Kiyose, Tokyo, Japan) and T INOUE (Meteorological Research Institute, Yatabe, Ibaraki, Japan) Remote Sensing of Environment, vol. 12, July 1982, p 219-228. refs

It has been shown that over the tropical oceans the total precipitable water can be estimated from the infrared radiometer data (10 5-12.5 microns) of the Geostationary Meteorological Satellite. The satellite derived values are in good agreement with the radiosonde data, with a 0.53 g/sq cm rms difference The weekly mean distribution of the precipitable water over the tropical ocean of western Pacific has been obtained in both summer and winter seasons The pattern of this distribution is in reasonable agreement with other authors and climatological data. (Author)

A82-37390*# National Aeronautics and Space Administration Wallops Flight Center, Wallops Island, Va
PULSE-TO-PULSE CORRELATION IN SATELLITE RADAR ALTIMETERS
E. J. WALSH (NASA, Wallops Flight Center, Wallops Island, VA) Radio Science, vol. 17, July-Aug. 1982, p. 786-800 refs

Pulse-to-pulse correlation in satellite radar altimeters is examined to determine if range jitter in future altimeters could be reduced by increasing the pulse repetition frequency (PRF) Data from the Skylab radar altimeter is analyzed and compared with rules of thumb and the results of a Monte Carlo simulation Altimeter range tracker configurations are reviewed and a simple curve is developed for the PRF below which decorrelation is assured. An adaptive PRF for future altimeters is recommended to conserve mission power while optimizing data collection during high-sea states. (Author)

A82-37505
A QUANTITATIVE MULTISPECTRAL ANALYSIS SYSTEM FOR AERIAL PHOTOGRAPHS APPLIED TO COASTAL PLANNING
C. VALERIO (Aix-en-Provence, Centre d'Etudes Techniques de l'Equipement, Les Milles, Bouches-du-Rhone, France) and A LLEBARIA (CNRS, Laboratoire d'Astronomie Spatiale, Marseille, France) International Journal of Remote Sensing, vol 3, Apr.-June 1982, p. 181-197. refs

A system that may be used to study the dispersion of effluents in the sea either by means of their color or by using a fluorescent tracer, rhodamine B, is described, and its use is illustrated with the study of the dispersion over one day of a release of rhodamine in seawater. The underlying principle is the adjustment of the data acquisition device to the optical properties of the phenomenon being studied, so that the signal-to-noise ratio is optimized A very accurate digitizing microdensitometer is used, and the data processing system is adapted to allow for correction of radiometric, spatial, and temporal variations. A simple mathematical representation of the interaction of sunlight with the environments encountered before reaching the negative is employed. An experimental procedure that eliminates the need for sampling from boats is used to follow the evolution of the plume, giving maps showing quantity of rhodamine to an accuracy of about five percent. C.D

N82-23614*# National Aeronautics and Space Administration. Langley Research Center, Hampton, Va.
ANALYSIS OF OCEAN COLOR SCANNER DATA FROM THE SUPERFLUX III EXPERIMENT
C. W. OHLHORST Mar 1982 30 p refs
(NASA-TM-83290, NAS 1.15:83290) Avail: NTIS HC A03/MF A01 CSCL 08J

The scanner collected data on October 15, 20, and 22, 1980. Single-channel gray-scale data products generated 5 minutes after the scanner were collected and showed details of the Chesapeake plume structure, suggesting that this quick-look capability could have potential use for experiments in real time. The Chesapeake Bay plume extended offshore about 5 nautical miles on October 15, and 7 nautical miles on October 20. Using the October 15 1980, data, a correlation coefficient of r = 0 889 was obtained between chlorophyll 'A' and the ratio of band 7 (664-684 nanometers) to band 9 (746-766 nanometers). This ratio was then used to calculate the average surface chlorophyll 'A' concentration of the water flowing out of the Chesapeak Bay. A ratio from the Ocean Color Scanner bands was created to simulate the ratio that the Multichannel Ocean Color Sensor uses to calculate chlorophyll A concentrations Using the October 15, 1980, data set, this ratio has a correlation coefficient of r = -0 739 with the log of the chlorophyll 'A' and the ratio of band 2 minus band 4 to band 2 plus band 4 of the Ocean Color Scanner No correlation is found between the Ocean Color Scanner data and total suspended solid measurements made on October 15, 1980.
T M.

N82-23852# Wisconsin Univ., Madison.
THE IMPACT OF METEOROLOGICAL SATELLITES ON THE FIRST GARP GLOBAL EXPERIMENT (FGGE)
V. E SUOMI *In* WMO Intern. Conf. on Early Results of FGGE and Large-Scale Aspects of its Monsoon Expt. 7 p Apr. 1981
Avail: NTIS MF A01, HC WMO

The impact of meteorological satellite observations is presented Drifting buoys provide sea level atmospheric pressure and sea surface temperature for Tiros N temperature sounder retrievals. Geostationary satellites help to construct more accurate long range forecasting models. The Indian monsoon is observed.
Author (ESA)

N82-23856# Commonwealth Scientific and Industrial Research Organization, Mordialoc (Australia). Div. of Atmospheric Physics.
MEAN SEA-LEVEL PRESSURE IN THE SOUTHERN HEMISPHERE DURING THE FGGE PERIOD
W. L. PHYSICK and G B. TUCKER *In* WMO Intern. Conf. on Early Results of FGGE and Large-Scale Aspects of its Monsoon Expt. 5 p Apr. 1981 refs
Avail NTIS MF A01; HC WMO

Drifting buoy recordings of mean sea level pressure (MSLP) are assessed as a means for investigating climate. Data from FGGE buoys were compared to long term MSLP's computed from daily numerical analyses and MSLP's from nine weather stations. Pressures observed in high latitude oceans during FGGE are lower than average for every month. The maximum difference is 12 mb. The MSLP is significantly different from normal. Mean zonal winds at 500 mb are significantly stronger by up to 50%. Buoys are useful data sources, but because the data is anomalous, they should not be used as reference points Author (ESA)

N82-23879# Centre National de la Recherche Scientifique, Paris (France). Lab. de Meteorologie Dynamique.
REPRESENTATIVENESS OF CLOUD MOTION WINDS DEDUCED FROM GOES INDIAN OCEAN SATELLITE IMAGERY FOR THE DESCRIPTION OF THE INDIAN SUMMER MONSOON
M. DESBOIS *In* WMO Intern. Conf. on Early Results of FGGE and Large-Scale Aspects of its Monsoon Expt 5 p Apr. 1981 refs
Avail. NTIS MF A01; HC WMO

A technique which extracts wind fields from cloud motions is described and data thus produced are compared with cloud winds extracted by standard methods, dropsondes and balloon winds of

the BALSAMINE experiment. A set of successive pictures is presented in loops. Each picture can be moved relative to the others. Pictures are aligned using landmarks and cloud motions are measured by moving the pictures so that the observed cloud appears motionless during the loop. The relative displacement of the pictures and the location of the cloud elements are recorded and the results are processed on a computer that plots them on a map It takes 4 hr to obtain a field Results compare well with other methods and indicate that low cloud tracers follow the wind like constant level balloons. Over the Indian Ocean low cloud winds are representative of the 900-850 mb layer. Cloud winds are advocated as a tool for investigating monsoons
Author (ESA)

N82-23898# National Meteorological Center, Washington, D C.
SHORT TERM INFLUENCE RADIUS OF MONSOONAL OVERTURNINGS
J. PAEGLE (Utah Univ.) *In* WMO Intern. Conf. on Early Results of FGGE and Large-Scale Aspects of its Monsoon Expt. 9 p Apr. 1981 refs
Avail: NTIS MF A01; HC WMO

The FGGE 3 b analyses and NOAA satellite data are used to delineate periods of intense convective activity over the central and western Pacific Ocean For periods of stronger convection, the transient kinetic energy is relatively stronger over the deep tropics and into the subtropics than for times of less active tropical overturnings. Regions which are predominantly convective correspond to areas where the balance equation is nonelliptic. For these areas only steady states which are strongly divergent and with small or vanishing absolute vorticity are possible. Correlations of upper level outflows with wind components suggest substantial influence of the tropics upon the subtropics in time scales of 3 days. The need to include tropical processes in numerical weather prediction for tropical and subtropical numerical weather prediction is shown. Author (ESA)

N82-23900# Indian Inst of Tropical Meteorology, Poona
IMPACT OF ADDITIONAL SUMMER MONEX WIND DATA ON THE PREDICTION OF MONSOON DEPRESSIONS DURING JUNE - AUGUST 1979 WITH TWO VERSIONS OF PRIMITIVE EQUATION (PE) BAROTROPIC MODEL
D. R. SIKKA, S. SINHA, S. S. SINGH, P. L KULKANNI, and A A. KULKARNI *In* WMO Intern. Conf. on Early Results of FGGE and Large-Scale Aspects of its Monsoon Expt 4 p Apr. 1981 refs Sponsored in part by Colorado State Univ.
Avail: NTIS MF A01, HC WMO

The reliability of barotropic prediction and the influence of MONEX data was investigated Streamlines and isotachs data for 700 mb are analyzed using (1) regular weather station observations and (2) additional data from Monex platforms Two versions of the P.E. barotropic model, which differ only in the dynamic initialization procedure, are used and it is found that they perform equally well. They perform best on those structures in which the easterly flow is of comparable strength to monsoon westerlies at 700 mb The impact of additional data is not positive consistently because the easterlies around the depression are weaker than westerlies and the additional data are better defined the westerly maxima. Westward motion of monsoon depression is linked with the convergence ahead of the system and the preferential convection in the forward sector. It is concluded that the P.E barotropic model is not the best one to study the impact of additional data. Author (ESA)

N82-23908# Miami Univ , Fla.
MONEX OCEANOGRAPHIC OBSERVATIONS ALONG THE EAST AFRICAN COAST
O. B. BROWN and F SCHOTT *In* WMO Intern. Conf on Early Results of FGGE and Large-Scale Aspects of its Monsoon Expt. 16 p Apr. 1981 refs
Avail: NTIS MF A01; HC WMO

Ship, buoy, and satellite current, temperature and air pressure data were used in order to study the Somali current Wind field development, near surface circulation and upwelling were noted Temperature, salinity, and potential density were recorded. The salinity profiles show several layers which deviate by more than 0 1 ppt from the mean. The density profile is smooth So-called anomalous flow and expected flow often occur in the same year. Results suggest a mesoscale ocean-atmosphere interaction driven by the large horizontal difference in ocean surface temperature along the East African coast. Author (ESA)

N82-23909# Naval Physical and Oceanographic Lab., Cochin (India).
ON THE SPACE-TIME VARIABILITY OF OCEAN SURFACE MIXED LAYER CHARACTERISTICS OF CENTRAL AND EASTERN ARABIAN SEA DURING MONSOON-77
R R RAO, P. G. K. MURTY, M G JOSEPH, and K. V. S RAMAN *In* WMO Intern. Conf. on Early Results of FGGE and Large-Scale Aspects of its Monsoon Expt. 8 p Apr 1981 refs
Avail NTIS MF A01; HC WMO

Surface mixed layer deepening and cooling of the Arabian Sea, which occurs in a nonhomogeneous manner during the monsoon season, is described Ship polygons collected data on mixed layer (MLD) characteristics Average MLD and vertical temperature gradient below MLD were recorded spatially and temporally. Deepening and cooling rates are higher over the central Arabian Sea than over the eastern Arabian Sea. In the central Arabian sea, deepening is greatest at the northern end. In the eastern Arabian Sea the layer deepening is higher at the southern location. The observed deepening shows good agreement with the computed layer depth, considering convective turnover caused by surface cooling. However, wind induced mixing contributes to the observed layer depth more in Phase-1U than Phase-2U. Vertical flow at the base of the mixed layer is upward, causing entrainment of colder waters from the upper thermocline and leading to mixed layer deepening and cooling Author (ESA)

N82-23910# Wisconsin Univ , Madison
ESTIMATES OF SEA SURFACE STRESS FOR SUMMER MONEX FROM CLOUD MOTIONS
B B HINTON and D. P WYLIE *In* WMO Intern. Conf. on Early Results of FGGE and Large-Scale Aspects of its Monsoon Expt. 5 p Apr. 1981 refs
(Contract NSF ATM-79-13097)
Avail NTIS MF A01; HC WMO

Numerical modeling of surface wind stress is described. Satellite winds, cloud motions and monthly ship data are analyzed Cloud motion speed is plotted as a function of the speed measured by a collocated ship. A regression line extrapolates speed from cloud to ship level Regression relations are exploited for direction changes, e g. veering. Cloud and ship data are merged in order to produce daily stress maps. Results agree with observed published data. The method is accurate over a wide area, at a 2 deg or more resolution, for several days. Cross correlations indicate that gridded cloud motion measurements error characteristics are compatable with ship wind measurements Author (ESA)

N82-23912# Australian Numerical Meteorology Research Center, Melbourne.
THE ONSET OF THE AUSTRALIAN NORTHWEST MONSOON DURING WINTER MONEX: BROADSCALE FLOW REVEALED BY AN OBJECTIVE ANALYSIS SCHEME
B. J MCAVANEY, N. E. DAVIDSON, and J. L. MCBRIDE *In* WMO Intern. Conf on Early Results of FGGE and Large-Scale Aspects of its Monsoon Expt 5 p Apr. 1981
Avail NTIS MF A01; HC WMO

The structure and time changes of the seasonal movement of the equatorial trough were studied using an univariate, three-dimensional optimum interpolation objective analysis scheme Wind field and surface pressure are analyzed. Analyses are cycled so that the analysis from 12 hr previous is used as the first guess field. Ships, aircraft, land stations, ocean platforms, satellite and archive data are analyzed The monsoon onset is a large scale event (10 deg latitude by 30 deg longitude). It is not preceeded by a similar change in the Northern Hemisphere. Forcing comes

from changes in the Southern Hemisphere subtropical circulation. These changes are well simulated by numerical prediction models on the 3 to 4 day time scale. Author (ESA)

N82-23929# Brookhaven National Lab , Upton, N. Y. Atmospheric Sciences Div.

MARINE BOUNDARY LAYER WIND STRUCTURE OVER THE BAY OF BENGAL DURING MONEX-79

S. SETHURAMAN *In* WMO Intern. Conf. on Early Results of FGGE and Large-Scale Aspects of its Monsoon Expt 7 p Apr 1981 refs Sponsored by NSF

Avail: NTIS MF A01; HC WMO

The role of the atmospheric boundary layer in monsoon formation was investigated through a micrometeorological tower which observed turbulent fluxes of heat and momentum over the ocean, a weather station that continuously recorded mean parameters, and pilot balloon observations to a height of 1 km Wind profiles and surface/layer fluxes of momentum and heat indicate a change in the direction of the heat flux (in a vertical plane). Surface heat flux is upward with small values for cases with large downward heat fluxes in the upper layers. This occurs when the monsoon trough is far northward causing a break in the monsoon When the trough moves to its normal position, there is a strong convective boundary layer over the Bay of Bengal Author (ESA)

N82-23939# Main Geophysical Observatory, Leningrad (USSR).

ESTIMATES OF THE STATISTICAL STRUCTURE OF THE ATMOSPHERIC PRESSURE FIELD IN SUMMER MONEX-79 AREA

I. A. DUYBKIN, E. A. SOSNINA, and N. A. SHKABURA *In* WMO Intern. Conf on Early Results of FGGE and Large-Scale Aspects of its Monsoon Expt. 4 p Apr 1981 refs

Avail: NTIS MF A01, HC WMO

Atmospheric pressure measurements (P) obtained from ships and three stationary polygons are presented Diurnal course values, the temporal correlation structural functions, and their 95% confidence intervals were calculated using data with the diurnal course included and excluded These show that in the northwest Indian Ocean the mean background of pressure oscillates within the limits 1011, 9 + or - 0, 7gPa and the scatter of singular measurements is within 1011, 9 + or - 2, 8gPa in the premonsoon period. During transition to monsoon circulation it is within 1008, 7 + or - 1, 2gPa and 1008, 7 + or - 3, 7gPa. During the monsoon onset it is 1007, 4 + or - 1, 2gPa and 1007, 4 + or - 3, 2gPa. The mean pressure field variability sigma p shows no significant differences for the polygons. It is within 1,4 sigma p 1, 7gPa. Author (ESA)

N82-23945# All-Union Scientific Research Inst. of Hydrometeorological Information, Moscow (USSR). World Data Centre.

ANALYSIS OF OCEAN AND ATMOSPHERE THERMODYNAMICAL CHARACTERISTICS DURING THE ONSET OF SOUTHWEST MONSOON OVER THE ARABIAN SEA

P. V. NUZHDIN *In* WMO Intern Conf on Early Results of FGGE and Large-Scale Aspects of its Monsoon Expt. 2 p Apr. 1981

Avail: NTIS MF A01; HC WMO

Ship surface and oceanographic data are used to analyze the onset of the Arabian Sea monsoon. Areas of marked heat storage, such as the central Arabian Sea are treated as centers of air sea coupling. A positive enthalpy anomaly is formed in this area from April to June, together with the Somali current, determines monsoon intensity. Enthalpy (H) and potential energy (Ep) were computed for the ocean layers 0 to 100 and 0 to 500 m as well as latent heat and sensible heat fluxes in the surface atmospheric layer over the ocean. The difference between the series of these characteristics for the premonsoon period and the period of the steady enthalpy decrease and heat and moisture flux increase is significant. Monsoon onset can be predicted from the moment when H and Ep stop oscillating drastically and H starts decreasing steadily Author (ESA)

N82-24597*# Defence Science and Technology Organisation, Edgecliff (Australia).

HIGH RESOLUTION SATELLITE OBSERVATIONS OF MESOSCALE OCEANOGRAPHY IN THE TASMAN SEA, 1978 - 1979 Final Report, period ending 31 Mar. 1981

C S. NILSSON, J C. ANDREWS (Australian Inst of Marine Science, Townsville), M. HORNIBROOK (CSIRO, North Ryde), A. R LATHAM, G C. SPEECHLEY, and P SCULLY-POWER, Principal Investigators Feb 1982 88 p refs Sponsored by NASA Original contains imagery Original imagery may be purchased from NASA Goddard Space Flight Center, (code 601), Greenbelt, Md. 20770. Domestic users send orders to 'Attn. National Space Data Center'; non-domestic users send orders to 'Attn: World Data Center A for Rockets and Satellites'. HCMM

(E82-10324; NASA-CR-168903; NAS 1.26:168903; RANRL-1/82, AR-002-695) Avail: NTIS HC A05/MF A01 CSCL 08J

Of the Nearly 1000 standard infrared photographic images received, 273 images were on computer compatible tape. It proved necessary to digitally enhance the scene contrast to cover only a select few degrees K over the photographic grey scale appropriate to the scene-specific range of sea surface temperature (SST). Some 178 images were so enhanced. Comparison with sea truth show that SST, as seen by satellite, provides a good guide to the ocean currents and eddies off East Australia, both in summer and winter. This is in contrast, particularly in summer, to SST mapped by surface survey, which usually lacks the necessary spatial resolution. Author

N82-25609*# Jet Propulsion Lab., California Inst. of Tech., Pasadena.

SEA-ICE MISSION REQUIREMENTS FOR THE US FIREX AND CANADA RADARSAT PROGRAMS

F. D. CARSEY, R. O RAMSEIER (Atmospheric Environment Service), and W. F. WEEKS (Army Cold Regions Research and Engineering Lab., Hanover, New Hampshire) Jan. 1982 83 p refs Presented at Bilateral Ice Study Team Workshop, Cornwall, Ontario, 11-13 Feb 1981

(Contract NAS7-100)

(NASA-CR-168984; NAS 1.26 168984) Avail: NTIS HC A05/MF A01 CSCL 08F

A bilateral synthetic aperture radar (SAR) satellite program is defined. The studies include addressing the requirements supporting a SAR mission posed by a number of disciplines including science and operations in sea ice covered waters Sea ice research problems such as ice information and total mission requirements, the mission components, the radar engineering parameters, and an approach to the transition of spacecraft SAR from a research to an operational tool were investigated. S.L.

N82-26525*# Remote Sensing Systems, Sausalito, Calif.

THE EFFECT OF SEA-SURFACE SUN GLITTER ON MICROWAVE RADIOMETER MEASUREMENTS

F. J. WENTZ 4 Nov. 1981 58 p refs

(Contract JPL-954958)

(NASA-CR-169083, JPL-9950-652; NAS 1 26.169083, RSS-TR-110481) Avail: NTIS HC A04/MF A01 CSCL 20N

A relatively simple model for the microwave brightness temperature of sea surface Sun glitter is presented. The model is an accurate closeform approximation for the fourfold Sun glitter integral The model computations indicate that Sun glitter contamination of on orbit radiometer measurements is appreciable over a large swath area. For winds near 20 m/s, Sun glitter affects the retrieval of environmental parameters for Sun angles as large as 20 to 25 deg The model predicted biases in retrieved wind speed and sea surface temperature due to neglecting Sun glitter are consistent with those experimentally observed in SEASAT SMMR retrievals. A least squares retrieval algorithm that uses a combined sea and Sun model function shows the potential of retrieving accurate environmental parameters in the presence of

Sun glitter so long as the Sun angles and wind speed are above 5 deg and 2 m/s, respectively Author

N82-26758*# Instituto de Pesquisas Espaciais, Sao Jose dos Campos (Brazil)

A STUDY OF ATMOSPHERIC DIFFUSION FROM THE LANDSAT IMAGERY

N. DEJESUSPARADA, Principal Investigator, Y. VISWANADHAM, and J. A. TORSANI Dec. 1981 58 p refs Submitted for publication Sponsored by NASA Original contains color imagery. Original photography may be purchased from the EROS Data Center, Sioux Falls, S.D. 57198 ERTS

(E82-10360; NASA-CR-168981; NAS 1.26:168981; INPE-2284-PRE/060) Avail: NTIS HC A04/MF A01 CSCL 04A

LANDSAT multispectral scanner data of the smoke plumes which originated in eastern Cabo Frio, Brazil and crossed over into the Atlantic Ocean, are analyzed to illustrate how high resolution LANDSAT imagery can aid meteorologists in evaluating specific air pollution events. The eleven LANDSAT images selected are for different months and years. The results show that diffusion is governed primarily by water and air temperature differences. With colder water, low level air is very stable and the vertical diffusion is minimal; but water warmer than the air induces vigorous diffusion The applicability of three empirical methods for determining the horizontal eddy diffusivity coefficient in the Gaussian plume formula was evaluated with the estimated standard deviation of the crosswind distribution of material in the plume from the LANDSAT imagery The vertical diffusion coefficient in stable conditions is estimated using Weinstock's formulation These results form a data base for use in the development and validation of meso scale atmospheric diffusion models. Author

N82-26764# Army Cold Regions Research and Engineering Lab, Hanover, N H.

ICE DISTRIBUTION AND WINTER SURFACE CIRCULATION PATTERNS, KACHEMAK BAY, ALASKA

L. W. GATTO Dec 1981 52 p refs

(AD-A110806; CRREL-81-22) Avail: NTIS HC A04/MF A01 CSCL 08C

Development of the hydropower potential of Bradley Lake, Alaska, would nearly double winter freshwater discharge from the Bradley River into upper Kachemak Bay, and the Corps of Engineers is concerned about possible subsequent increased ice formation and related ice-induced problems. The objectives of this investigation were to describe winter surface circulation in the bay and document ice distribution patterns for predicting where additional ice might be transported if it forms Fifty-one LANDSAT MSS band 5 and 7 and RBV images with 70% cloud cover or less, taken between 1 November and 30 April each year, were analyzed for the eight winters from 1972 to 1980 with standard photointerpretation techniques Results of this analysis showed that glacial sediment discharged into Kachemak Bay acts as a natural tracer in the water Inner Kachemak Bay circulation in the winter is predominantly counterclockwise, with northeasterly nearshore currents along the south shore and southwesterly nearshore currents along the north shore. Most of the ice in the inner bay forms at its northeast end and is discharged by the Fox, Sheep and Bradley Rivers. Some ice becomes shorefast on the tidal flats at the head of the bay, while some moves southwestward along the north shore pushed by winds and currents. When this ice reaches Coal Bay, it accumulates between Homer Spit and the north shore. This buildup extended out to Coal Point at the tip of Homer Spit in February 1976 and 1979; ice was not observed in the nearshore zone along the south shore of the inner bay. GRA

N82-26766# Scripps Institution of Oceanography, La Jolla, Calif.

SATELLITE OBSERVATIONS IN FRONTS 80

M. L. VANWOERT Nov 1981 44 p refs

(Contract N00014-80-C-0440)

(AD-A111080; SIO-REF-81-38) Avail: NTIS HC A03/MF A01 CSCL 08J

Early observations in the Central North Pacific indicate a general decrease in temperature and salinity as one moves northward from the equator. The change is not a smooth function of latitude, but rather, superimposed on a steady poleward decrease of temperature and salinity are regions of abrupt change called fronts (Seckel, 1968; Roden 1972). The general strength and location of the mid-ocean fronts are well-known. Near 45 deg. N latitude is the Pacific Subarctic Front. It separates the Pacific Subarctic water mass from the North Pacific Central water mass and is characterized by a change of 4 C per 30km and 0 6% per 30km across the front. In the vicinity of 32 deg. N is the Pacific Subtropical Front. It separates the North Pacific Central water mass from the Pacific Equatorial water mass and is characterized by a change of 2 deg. C per 30km and 0 25% per 30km across the front (Roden, 1975). A schematic map of the Central North Pacific Fronts is shown. Although the general location and strength of the mid-ocean fronts are well documented, little is known about variability associated with frontal strength and position. In December 1979 a large observational program (FRONTS 80) was undertaken to obtain basic scale information on a mid-ocean front. The North Pacific Subtropical Front, near 31 deg. N, 153 deg. W was chosen as the experiment site because of its logistical proximity to the U S. mainland and Hawaii, and because extensive historical data exists for this region. GRA

N82-26944# Office of Technology Assessment, Washington, D C

TECHNOLOGY AND OCEANOGRAPHY: AN ASSESSMENT OF FEDERAL TECHNOLOGIES FOR OCEANOGRAPHIC RESEARCH AND MONITORING. VOLUME 2: WORKING PAPERS ON FISHERY RESEARCH TECHNOLOGY

Jun. 1981 245 p refs

Avail: NTIS HC A11/MF A01

The existing Federal research programs on ocean fisheries and other living oceanic resources are reviewed. The research technology and the programs provide the needed management information are evaluated and preparation for future demands on that technology and on the programs using it is discussed. The fishery research which is needed by international fishery agreements and by all regional fishery management councils is discussed. The stocks, measuring the abundance of each, and forecasting the effects on them of fishing and of environmental changes are described. E.A K

N82-26945# Naval Postgraduate School, Monterey, Calif. Dept. of Systems Technology.

RAPID OCEANOGRAPHIC DATA GATHERING: SOME PROBLEMS IN USING REMOTE SENSING TO DETERMINE THE HORIZONTAL AND VERTICAL THERMAL DISTRIBUTIONS IN THE NORTHEAST PACIFIC OCEAN M.S. Thesis

G. W. LUNDELL Sep 1981 189 p refs

(AD-A111005; NPS68-81-006) Avail: NTIS HC A09/MF A01 CSCL 08J

NOAA-6 satellite AVHRR data and AXBT data were collected in the Northeast Pacific Ocean in late 1980 as part of the Naval Postgraduate School-sponsored Acoustic Storm Transfer and Response Experiment which was in turn part of the U.S -Canadian Storm Transfer and Response Experiment (STREX) Some of the problems in transferring AXBT geographical positions to satellite images were solved by designing a computer program with accuracies of less than 2 pixels Thermal comparisons were made between AXBT, NOAA-6, and GOSSTCOMP data with the result that NOAA-6 data was on the average of 2.9 C colder than AXBT data and 3 2 C colder than GOSSTCOMP data. Linear regression methods reduced to 0.3 C the difference between NOAA-6 and AXBT data. Use of this method over a period of 15 days produced

a mean error of 0 5 C. Although NOAA-6 cannot sense directly the subsurface thermal structure, it is excellent for observing surface manifestations of horizontal thermal features. Further investigation into using satellite data as the basis of an empirical relationship between the surface temperature and the subsurface vertical thermal structure is warranted. Author (GRA)

N82-26948# Scripps Institution of Oceanography, La Jolla, Calif. Center for Coastal Studies.
FLUID-SEDIMENT INTERACTIONS ON BEACHES AND SHELVES Progress Report, 1980 - 1981
D L. INMAN, C D WINANT, R. T. GUZA, and R E FLICK 11 Sep. 1981 91 p refs
(Contract N00014-75-C-0300)
(AD-A110838, SIO-REF-81-27) Avail· NTIS HC A05/MF A01 CSCL 08C

This research seeks to predict shelf and beach forms and their changes from knowledge of local bathymetry and the driving forces due to winds, waves and currents and their complicated interactions with nearshore sediments. The work falls into three distinct but interdependent areas of research· wave and current dynamics; fluid-sediment interactions; coastal zone remote sensing. The principal area of interest in wave and current dynamics continues to be wind generated, surface gravity waves and the currents and other fluid motions which derive their energy from surface waves. The fluid sediment interaction studies lead to an understanding of the shelf and beach sediment response including the fundamental rheology of granular fluids, the longshore and on-offshore transport of sand and the formation of features like cusps and bars The coastal zone remote sensing tasks are largely exploratory in nature, with the general objective of determining the extent to which signatures from remote sensors can be used to define the broader spatial characteristics of driving forces, and the larger scale ocean surface patterns that are characteristic of nearshore dynamics Author (GRA)

N82-26949# Florida State Univ., Tallahassee. Dept. of Meteorology
METEOROLOGICAL AND AIRCRAFT DATA FOR CUE 2 1973
D. W STUART and J D HAWKINS Jul 1981 57 p refs
(Contract NSF OCE-77-27735)
(PB82-149246, CUEA-74; FSU-MET-STU-81/5; NSF/IDOE-81-88) Avail· NTIS HC A02/MF A01 CSCL 08J

Documentation of the various meteorological observations made in support of the CUE II experiment in coastal upwelling of Oregon during the summer 1975 is presented. Details of the instruments, observational techniques, and data recording systems, digitizing and reduction techniques are discussed. Selected parameters from land stations are presented as time plots All sea surface temperature maps prepared via the aircraft are included GRA

N82-27816# Technical Univ of Denmark, Lyngby. Electromagnetics Inst.
MOVEMENT OF ICE MARKERS MEASURED BY SATELLITE RANGING
P. GUDMANDSEN, C. CARLE, and J. MAALOEE · Paris ESA Jun. 1981 82 p refs
(Contract ESA-4634/81)
(R-240, ESA-CR(P)-1547) Avail: NTIS HC A05/MF A01

A method for determining the surface velocity of large ice sheets in Greenland and Antarctica involves measuring the change of distance between fixed markers and those on ice sheets, using ERS-1 for altimetry and radar ranging. An acceptable signal to noise ratio can be obtained with the ERS-1 high gain antenna and a marker, consisting of a square trihedral corner reflector, with side length = 1.5 m, radar cross section 55 dB. The high gain antenna limits the area investigated to an 18 km swath, assuming a 5 deg incidence angle. A Swerling type radar cross section of the corner reflector results in a 62% detection probability for 6-pulse integration. Displacement of markers can only be measured at crossing ground tracks when the satellite is operated in a rigid orbit mode, i.e., a 20 X 20 km area Accuracy of 78 cm is possible Author (ESA)

N82-27949# National Weather Service, Fort Worth, Tex. National Hurricane Center.
SOME EMPIRICAL RULES FOR FORECASTING FOG AND STATUS OVER NORTHERN FLORIDA, SOUTHERN GEORGIA AND ADJACENT COASTAL WATERS
E. L. RICKS Aug. 1981 15 p refs
(PB82-154006; NOAA-TM-NWS-SR-104, NOAA-81111608) Avail. NTIS HC A02/MF A01 CSCL 04B

Strong low-level winds, especially strong vertical wind shear, generate and maintain enough mixing below the subsidence inversion over southern Georgia and northern Florida to counteract, or inhibit, low stratus and fog formation Weaker northeast and east winds flavor low stratus and fog formation over southern Georgia and northern Florida when the trajectory is from the Atlantic coast GRA

06

HYDROLOGY AND WATER MANAGEMENT

Includes snow cover and water runoff in rivers and glaciers, saline intrusion, drainage analysis, geomorphology of river basins, land uses, and estuarine studies.

A82-13528#
EFFECTIVE ELECTROMAGNETIC SHIELDING IN MULTILAYER PRINTED CIRCUIT BOARDS
K. G. WILES and J. L MOE (General Dynamics Corp., Fort Worth, TX) In· Digital Avionics Systems Conference, 4th, St. Louis, MO, November 17-19, 1981, Collection of Technical Papers. New York, American Institute of Aeronautics and Astronautics, 1981, p 593-596.
(AIAA 81-2333)

Multilayer printed circuit boards have proven to be recurrent abettors of electromagnetic coupling problems created by the incessantly faster response times in integrated circuit technologies Coupling within multilayer boards has not only inhibited meeting certain EMI requirements but has also precipitated 'self-inflicted' malfunctions commonly experienced during development of avionic systems. A recent avionic system, interfacing two asynchronous processors through a fourteen-layer motherboard, permitted coupling through ground plane connector apertures of sufficient amplitude and duration as to cause unintentional intercommunication and system malfunctions. The coupling mechanism and ground plane modifications which reduced this coupling by 40 dB and eliminated the incompatibility are discussed in this paper (Author)

A82-22615
THE MODULATION CHARACTERISTICS OF THE 19TH AND 20TH SOLAR ACTIVITY CYCLES
N N KONTOR, G. P. LIUBIMOV, N. V. PERESLEGINA, and T. I. STEPINA (Moskovskii Gosudarstvennyi Universitet, Moscow, USSR) In: International Cosmic Ray Conference, 17th, Paris, France, July 13-25, 1981, Conference Papers Volume 3. Gif-sur-Yvette, Essonne, France, Commissariat a l'Energie Atomique, 1981, p 179-182 refs

The intensity modulation of galactic cosmic rays at 1 AU from the sun is described in terms of the nonstationary model. The dependencies of the modulation coefficients are found, which characterize the galactic cosmic ray fluxes to and from the sun on the solar activity level, and consideration is given to the dependencies of the modulation parameters on time and cosmic ray energy. Significant variations are observed in the modulation factors, even for the smoothed data, and the transparency coefficient is proportional to the particle energy, while the transfer coefficient is inverse D.L G.

A82-29333
A SIMULATION STUDY OF SOIL MOISTURE ESTIMATION BY A SPACE SAR
F. T ULABY, C. DOBSON, J. STILES, R. K. MOORE, and J. HOLTZMAN (University of Kansas Center for Research, Inc , Lawrence, KS) Photogrammetric Engineering and Remote Sensing, vol 48, Apr 1982, p. 645-660. refs

An evaluation of the accuracy of soil moisture estimates available from satellite radar remote sensing is made, along with an assessment of the effects of spatial resolution on the estimation accuracy Synthetic aperture radar (SAR) images of a 17.7 x 19 3 km test site were generated by image simulation techniques for a space SAR orbiting at 600 km and operating at 4 75 GHz, an HH polarization, and an angle of incidence range between 7-22 deg from nadir Data bases were constructed of U-2 color IR photographs, 20 m x 20 m pixel soil elements from the USDA totalling 800,000 pixels classified for target class, soil texture, and surface elevation Three sets of images were generated for four varying soil moisture distributions across the site Soil moisture in 90% of the 20 m x 20 m pixels were found to be predictable in terms of moisture capacity to within 20%. A 100 m x 100 m resolution was best for very dry soil conditions M.S K

A82-32896* Texas Univ. at Austin.
INTERPRETATION OF SURFACE-WATER CIRCULATION, ARANSAS PASS, TEXAS, USING LANDSAT IMAGERY
R. J. FINLEY and R. W BAUMGARDNER, JR (Texas, University, Austin, TX) Remote Sensing of Environment, vol. 10, Aug. 1980, p.3-22. refs
(Contract NAS5-20986)

The development of plumes of turbid surface water in the vicinity of Aransas Pass, Texas has been analyzed using Landsat imagery The shape and extent of plumes present in the Gulf of Mexico is dependent on the wind regime and astronomical tide prior to and at the time of satellite overpass. The best developed plumes are evident when brisk northerly winds resuspend bay-bottom muds and flow through Aransas Pass is increased by wind stress. Seaward diversion of nearshore waters by the inlet jetties was also observed. A knowledge of surface-water circulation through Aransas Pass under various wind conditions is potentially valuable for monitoring suspended and surface pollutants (Author)

A82-32910* National Aeronautics and Space Administration. Goddard Space Flight Center, Greenbelt, Md
A COMPARATIVE STUDY OF MICROWAVE RADIOMETER OBSERVATIONS OVER SNOWFIELDS WITH RADIATIVE TRANSFER MODEL CALCULATIONS
A. T. C. CHANG and J. C. SHIUE (NASA, Goddard Space Flight Center, Laboratory for Atmospheric Sciences, Greenbelt, MD) Remote Sensing of Environment, vol 10, Nov. 1980, p. 215-229 refs

(Previously announced in STAR as N79-30611)

A82-33329
THE GROWTH OF SNOW IN WINTER STORMS - AN AIRBORNE OBSERVATIONAL STUDY
K K. LO and R. E. PASSARELLI, JR (MIT, Cambridge, MA) Journal of the Atmospheric Sciences, vol. 39, Apr. 1982, p. 697-706. refs
(Contract F19628-80-C-0021)

In studies of precipitation growth, comparisons between theory and observation are difficult because of the problem in obtaining a complete four-dimensional (space and time) description of the kinematic, thermodynamic and microphysical properties of the atmosphere. A new flight plan has been devised which permits one to observe the height evolution of snow-size spectra in a reference frame where the effects of horizontal gradients and temporal changes are minimized. The flight plan, termed the advecting spiral descent (ASD), requires an aircraft to start aloft in a mesoscale precipitation area and then spiral downward in a constant bank angle, descending at approximately the mean fallspeed of snow. Qualitative comparisons between ASD observations and particle growth theory suggest that snow evolves through at least three stages characterized by deposition, aggregation and breakup. The breakup process serves to limit the number of large snow particles and interacts with aggregation to produce a limiting value of the slope of the snow-size spectrum (Author)

A82-34734
AUTOMATED CLASSIFICATION OF RUNOFF COEFFICIENTS FROM LANDSAT MULTISPECTRAL DATA
F ASKARI (Ohio State University, Columbus, OH) and N. L. FAUST (Georgia Institute of Technology, Atlanta, GA) In: American Society of Photogrammetry, Annual Meeting, 47th, Washington, DC, February 22-27, 1981, ASP Technical Papers. Falls Church, VA, American Society of Photogrammetry, 1981, p. 426-439. Research supported by the Ohio State University Research Foundation refs

Multispectral data from Landsat are used with aircraft color infrared photography to derive the runoff coefficients for watersheds in Mill Creek, Ohio Regression models are developed from the treatment of the runoff coefficient of each sample site as the dependent variable, and the mean radiance measurements in the four Landsat channels as the independent variables. A comparison of classification results illustrates the spatial and temporal variations of runoff potential for the surface. Single cover test fields and test watersheds are used to verify the model results, and the mean runoff coefficients derived for the test watersheds from the multispectral data analysis technique compare favorably with those obtained from ground truth D L G.

A82-34735
DIGITAL AND VISUAL EVALUATION OF GOES AND TIROS/NOAA IMAGE DATA FOR COVER TYPE EFFECTS ON SNOWFIELD OBSERVATIONS
T. M. LILLESAND, D E MEISNER, A L DOWNS, and R. L DEUELL (Minnesota, University, St. Paul, MN) In: American Society of Photogrammetry, Annual Meeting, 47th, Washington, DC, February 22-27, 1981, ASP Technical Papers. Falls Church, VA, American Society of Photogrammetry, 1981, p. 450-465. Research supported by the University of Minnesota refs
(Contract NOAA-NA-80AAD0019)

A82-34736* National Aeronautics and Space Administration. Goddard Space Flight Center, Greenbelt, Md.
USE OF AERIAL PHOTOGRAPHY IN DETERMINING LAND USE AND STREAMFLOW RELATIONSHIPS ON SMALL DEVELOPING WATERSHEDS
M. OWE (NASA, Goddard Space Flight Center, Hydrological Sciences Branch, Greenbelt, MD) In American Society of Photogrammetry, Annual Meeting, 47th, Washington, DC, February 22-27, 1981, ASP Technical Papers. Falls Church, VA, American Society of Photogrammetry, 1981, p 466-475. refs

Using aerial photographs dating back to 1937, the historical trends of five land use classes (crop, forest, open field, urban and suburban) are determined. The relationships between these and various flow regime parameters are investigated Annual runoff is found to be 7 5 inches greater now than in the year 1932 It is also found that growing season runoff increased by 3.5 inches during the same period This increase is approximately equivalent to 160 area inches of excess runoff during the 45-year period of observation. The increase in runoff is found to be positively correlated with the percent basin area in the urban, suburban and open field land use classes. A negative correlation is established with forest and crop land Although poor correlations are found with high flow, low flow, flow interval and flow date data, it is thought that a more precise quantification of land use or a smaller basin area may possibly have yielded more positive results for streamflow timing data. C.R.

A82-34745
AERIAL PHOTOGRAPHY VS. LANDSAT FOR DIGITAL LAND-COVER MAPPING IN AN URBAN WATERSHED
B. K. QUIRK and F. L. SCARPACE (Wisconsin, University, Madison, WI) In American Society of Photogrammetry, Annual Meeting, 47th, Washington, DC, February 22-27, 1981, ASP Technical Papers. Falls Church, VA, American Society of Photogrammetry, 1981, p 610-617. refs

A comparison was made between digital analyses of color infrared film and Landsat to provide land-cover information in an urban watershed. The results were compared to a manual photo interpretation of a black and white infrared photograph. Both the color infrared and Landsat produced similar land-cover acreages and both were similar to the black and white interpretation. However, the color infrared was found to be a better representation. (Author)

A82-35126
STUDY OF THE HYDROLOGICAL CYCLE BY AEROSPACE METHODS [IZUCHENIE GIDROLOGICHESKOGO TSIKLA AEROKOSMICHESKIMI METODAMI]
K. IA. KONDRATEV, (ED.) and IU V KURILOVA Moscow, Izdatel'stvo Radio i Sviaz', 1982. 100 p. In Russian

Topics discussed include principles and methods of the study of the hydrological cycle on the basis of remote-sensing methods, water-balance differentiation of natural complexes on the basis of satellite photographs, the use of remote sensing to study the hydrology of elementary watersheds, and methods for the analysis of the melting of firn complexes on the basis of satellite photographs. The mapping of snow lines in the central part of the European USSR, the forecasting of pluvial floods in Mongolia on the basis of remote-sensing data, the measurement of water-surface temperature by means of airborne infrared radiometers, the use of multispectral photography to study littoral zones, and the use of remote sensing to study the space-time variability of water quality are also considered. B J.

A82-35127
PRINCIPLES AND METHODS OF THE STUDY OF THE HYDROLOGICAL CYCLE ON THE BASIS OF AEROSPACE DATA [PRINTSIPY I METODY IZLUCHENIIA GIDROLOGICHESKOGO TSIKLA PO AEROKOSMICHESKOI INFORMATSII]
IU. V. KURILOVA, A. M. GRIN, and P A KOLOSOV In: Study of the hydrological cycle by aerospace methods. Moscow, Izdatel'stvo Radio i Sviaz', 1982, p. 5-18. In Russian. refs

The paper examines the possibilities and advantages of using satellite data to study various aspects of the hydrological cycle. Methods for evaluating the separate components of the cycle are generalized. In addition, indirect methods for determining slowly and rapidly varying parameters of the cycle on the basis of global TV and IR data acquired by satellites are proposed. Attention is also given to the principles of dynamic regionalization according to types of processes and landscape features on the basis of multispectral data B J

A82-35129
WATER-BALANCE DIFFERENTIATION OF NATURAL COMPLEXES ON THE BASIS OF SATELLITE PHOTOGRAPHS [VODNOBALANSOVAIA DIFFERENTSIATSIIA PRIRODNYKH KOMPLEKSOV NA OSNOVE ISPOL'ZOVANIIA KOSMICHESKIKH SNIMKOV]
A. V. LEBEDEV In: Study of the hydrological cycle by aerospace methods. Moscow, Izdatel'stvo Radio i Sviaz', 1982, p 25-29. In Russian. refs

The paper examines methods for assessing the role of natural complexes, particularly forest complexes, in hydrology These methods are then used to evaluate techniques of the differentiation and mapping of hydrological parameters on the basis of the structural elements of natural-territorial complexes. As an example, attention is given to the thermal and water-balance characteristics of the natural complexes of the middle and southern taiga of the Ob-Yenisei interfluve as determined from satellite photographs B J.

A82-35130
THE POSSIBILITY OF USING REMOTE-SENSING METHODS TO STUDY THE HYDROLOGY OF ELEMENTARY WATERSHEDS [VOZMOZHNOSTI PRIMENENIIA DISTANTSIONNYKH METODOV V OBLASTI GIDROLOGII ELEMENTARNYKH VODOSBOROV]
K. KASPRZHAK and F. SHABELA In Study of the hydrological cycle by aerospace methods Moscow, Izdatel'stvo Radio i Sviaz', 1982, p. 30-35. In Russian. refs

Theoretical and experimental determinations of the microwave radiation characteristics of wet soils are compared. A survey is then presented of methods for measuring the hydrological regimes of soils in the visible, infrared, and microwave ranges. Particular emphasis is placed on the use of active-radar techniques at wavelengths of 0.3-30 cm and even 100 cm, which make it possible to analyze the hydrological regimes of soils at great depths. B.J

A82-35131
THE SEASONAL SNOW-LINE WITHIN THE FERGANA BASIN AND THE POSSIBILITY OF USING IT FOR HYDROLOGICAL FORECASTING [SEZONNAIA SNEGOVAIA GRANITSA V PREDELAKH FERGANSKOI KOTLOVINY I VOZMOZHNOSTI EE ISPOL'ZOVANIIA V GIDROPROGNOZAKH]
O. P. SHCHEGLOVA and V IU. CHERNOV In Study of the hydrological cycle by aerospace methods. Moscow, Izdatel'stvo Radio i Sviaz', 1982, p 36-41 In Russian. refs

TV data acquired by meteorological satellites during 1969-1978 are used to study snow cover within the mountain region of the Fergana basin. The dynamics of the seasonal snow-line during spring thaw is investigated, and the positions of the seasonal snow-line for individual days in 1969 are given The data are used to evaluate the possibility of making hydrological forecasts on the basis of relationships between the monthly average water discharge and the height of the snow line at the end of the preceding month B.J.

A82-35132
THE USE OF SATELLITE PHOTOGRAPHS TO STUDY SNOW-COVER DYNAMICS AND TO DETERMINE THE AVERAGE WATER DISCHARGE OF THE AMUDARYA DURING A VEGETATION PERIOD [ISPOL'ZOVANIE SPUTNIKOVYKH SNIMKOV DLIA IZUCHENIIA DINAMIKI SNEZHNOGO POKROVA I OTSENKI SREDNEGO RASKHODA VODY AMUDAR'I ZA VEGETATSIONNYI PERIOD]
M V. DZHORZHIO, M V SITNIKOVA, and B. K. TSAREV In Study of the hydrological cycle by aerospace methods. Moscow, Izdatel'stvo Radio i Sviaz', 1982, p. 42-45 In Russian refs

A82-35133
METHOD FOR THE ANALYSIS OF THE MELTING OF A FIRN COMPLEX ON THE BASIS OF AEROSPACE PHOTOGRAPHS [METODIKA RASCHETA TAIANIIA KOMPLEKSA SNEZHNIKOV PO AEROKOSMICHESKIM SNIMKAM]
N. I. OSOKIN In Study of the hydrological cycle by aerospace methods Moscow, Izdatel'stvo Radio i Sviaz', 1982, p. 46-49. In Russian. refs

The characteristics of firn melting are investigated on the basis of field studies performed in the polar Urals, Crimea, and Kamchatka, as well as on the basis of satellite data It is shown that the intensity of melting is determined by the dimensions and shape of the firn basin. A dimensionless parameter for the shape of a firn basin is proposed which makes it possible to calculate the melting rate of individual firn basins as well as their complexes Methods of automated processing of satellite photographs are examined, which may be used to determine this parameter in hydrometeorological calculation and forecasting. B J.

A82-35134
EXPERIENCE WITH THE COMPILATION OF MAPS OF SNOW-COVER MELTING IN THE CENTRAL PART OF THE EUROPEAN USSR ON THE BASIS OF SATELLITE DATA [OPYT SOSTAVLENIIA KART SKHODA SNEZHNOGO POKROVA TSENTRAL'NOI CHASTI ETS PO DANNYM SPUTNIKOVOI INFORMATSII]
M S. DELEUR, E. I. PANKRATOVA, and L. P. BABKINA In. Study of the hydrological cycle by aerospace methods Moscow, Izdatel'stvo Radio i Sviaz', 1982, p 50-54. In Russian.

The paper examines techniques for the compilation of snow-cover melting maps from satellite photographs as well as methods for the interpretation of snow-cover features for various territories. Attention is given to the possibility of determining the following features from satellite photographs: the position of snow lines and the velocity of their motion, and the extent of snow in river drainage systems The accuracy with which snow lines can be depicted on maps is examined B J

A82-35136
EVALUATION OF THE ACCURACY OF WATER-SURFACE TEMPERATURE MEASUREMENT BY MEANS OF AIRBORNE INFRARED RADIOMETERS [OTSENKA TOCHNOSTI IZMERENIIA TEMPERATURY POVERKHNOSTI VODY SAMOLETNYM RADIATSIONNYM TERMOMETROM]
A. M. NIKITIN and S. N. TEMNIKOV In: Study of the hydrological cycle by aerospace methods. Moscow, Izdatel'stvo Radio i Sviaz', 1982, p. 62-64. In Russian.

Two sets of experiments are described whose objective was to evaluate the accuracy of the MIR-3 small-scale infrared radiometer, installed on the Il-14 aircraft, for measuring the surface temperature of natural water bodies The first set involved measurements of the surface temperature of Lake Issyk-Kul, carried out in July 1977. The second set involved five series of measurements of the surface temperature of the Aral Sea and five series of measurements of the surface temperature of Lake Issyk-Kul. The effect of atmospheric attenuation on the performance of the radiometers was evaluated. B.J.

A82-35138
THE USE OF REMOTE-SENSING DATA TO IDENTIFY THE SPACE-TIME VARIABILITY OF THE QUALITY OF NATURAL WATERS [ISPOL'ZOVANIE AEROKOSMICHESKOI INFORMATSII DLIA OBNARUZHENIIA PROSTRANSTVENNO-VREMENNOI IZMENCHIVOSTI KACHESTVA PRIRODNYKH VOD]
V. A. KRIULKOV, IU V. ZAVOLOKIN, V. I NOSACHEV, L. A. SHLIAKHOVA, and S. T. LAPCHENKOV In· Study of the hydrological cycle by aerospace methods. Moscow, Izdatel'stvo Radio i Sviaz', 1982, p 75-79 In Russian

Remote-sensing techniques for obtaining the quantitative characteristics of the space-time variability of water quality and reservoir pollution are assessed with particular attention given to the possibility of developing an operational system for the monitoring of water quality Optimal spectral ranges of measurements, photointerpretation keys, and zones of relatively constant concentration values are determined on the basis of ground-based and airborne measurements. Algorithms for the processing of remote-sensing images obtained by different techniques are examined, and a hybrid system based on the synthesis of TV and digital data is proposed B J.

A82-35140
COMPARISON OF BRIGHTNESS INDICATRIXES OF SNOW COVER MEASURED FROM AN AIRCRAFT AND CALCULATED THEORETICALLY FOR DIFFERENT HEIGHTS OF THE ATMOSPHERE [SRAVNENIE INDIKATRIS IARKOSTI SNEZHNOGO POKROVA, IZMERENNYKH S SAMOLETA I RASSCHITANNYKH TEORETICHESKI DLIA OTDEL'NYKH VYSOT ATMOSFERY]
V. V. KOZODEROV In Study of the hydrological cycle by aerospace methods. Moscow, Izdatel'stvo Radio i Sviaz', 1982, p. 86-88. In Russian. refs

A82-37174
THE USE OF SPACE PHOTOGRAPHS IN THE MAPPING OF GLACIERS AND WATER BODIES [ISPOL'ZOVANIE KOSMICHESKIKH SNIMKOV PRI KARTOGRAFIROVANII LEDNIKOV V VODNYKH OB'EKTOV]
M. A ALIMUKHAMEDOV, IU N. LESNIK, and A. M. TIMOSHENKO Geodeziia i Kartografiia, May 1982, p 24-30 In Russian refs

The use of black and white, multispectral, and color space photographs for the investigation of glaciers and water resources in the Middle Asiatic region has made possible the operational monitoring of their state and dynamics. Morphometric indices for the Fedchenko glacier, the Aidaro-Arnasaiskii water complex, and Lake Sarykamysh obtained from the interpretation of space photographs were found to be sufficiently accurate for various practical needs of the economy. B.J.

A82-37501
REMOTE SENSING IN SCOTLAND USING DATA RECEIVED FROM SATELLITES - A STUDY OF THE TAY ESTUARY REGION USING LANDSAT MULTISPECTRAL SCANNING IMAGERY
A P CRACKNELL, N. MACFARLANE, K MCMILLAN, J. A. CHARLTON, J. MCMANUS (Dundee, University, Dundee, Scotland), and K. A ULBRICHT (Deutsche Forschungsund Versuchsanstalt fuer Luft- und Raumfahrt, Oberpfaffenhofen, West Germany) International Journal of Remote Sensing, vol 3, Apr.-June 1982, p. 113-137 Research supported by the Carnegie Trust and Science and Engineering Research Council. refs

Multispectral scanning data from Landsat are used to study the sandbanks and tidal flats in the Tay Estuary, and the specialized digital image-processing system used in the study is briefly described. Several examples of Landsat-2 images of the Tay Estuary and its environs are presented as false-color composites and monochrome pictures, and a qualitative interpretation and several quantitative ones are presented. The low-water mark for sandbanks in the upper and lower estuary is determined and the results are compared with existing charts and maps, showing that changes in the positions of sandbanks of the size found in the estuary can be monitored satisfactorily using satellite imagery. The position of an estuarine front is mapped and also observed in situ in the position indicated by this image. An attempt at quantitative bathymetry, using a high tide Landsat image, indicated that depths up to three or four meters can be determined from the satellite data, but the accuracy is rather poor. C.D.

N82-22625*# Environmental Research and Technology, Inc., Concord, Mass.
THE APPLICATION OF HEAT CAPACITY MAPPING MISSION (HCMM) THERMAL DATA TO SNOW HYDROLOGY Final Report, Sep. 1977 - Mar. 1981
J. C. BARNES, Principal Investigator, C J BOWLEY, M. D SMALLWOOD, and J. H WILLAND Mar. 1981 112 p refs Original contains imagery. Original imagery may be purchased from NASA Goddard Space Flight Center, (code 601), Greenbelt, Md. 20771. Domestic users send orders to 'Attn: National Space Science Data Center', non-domestic users send orders to 'Attn. World Data Center A for Rockets and Satellites'. HCMM (Contract NAS5-24316)
(E82-10191; NASA-CR-168619; NAS 1.26.168619; ERT-P-2061-F) Avail. NTIS HC A06/MF A01 CSCL 08L

The application of HCMM thermal infrared data to snow hydrology and the prediction of snowmelt runoff was evaluated. Data for the Salt Verde watershed in central Arizona and the southern Sierra Nevada in California were analyzed and compared to LANDSAT and NOAA satellite data, U-2 thermal data, and other correlative data. It was determined that HCMM thermal imagery provides data as accurate for snow mapping as does visible imagery, and that in comparison with the reslution of other satellite imagery, it may be the most useful. Data from the HCMM thermal channel, with careful calibration, provides useful snow surface temperature data for hydrological purposes An approach to an automated method of analysis is presented. J.D.

N82-22644# National Oceanic and Atmospheric Administration, Rockville, Md. Ocean Technology and Engineering Services Office.

BIAS CORRECTION PROCEDURES FOR AIRBORNE LASER HYDROGRAPHY

G. C. GUENTHER and R. W. L. THOMAS Aug. 1981 110 p refs Prepared in cooperation with EG and G Washington Analytical Services Center, Inc., Rockville, Md. sponsored in part by Naval Ocean Research and Development Activity, NSTL Station, Miss. (PB82-130089; NOAA-TR-OTES-03; NOAA-8110502) Avail. NTIS HC A06/MF A01 CSCL 08J

Depending on the entry nadir angle of the beam and the optical properties of the water, one of two opposing effects, multiple scattering and geometric 'undercutting', will dominate and result in either a deep or shallow depth measurement bias, respectively. The magnitude of this bias can greatly exceed international hydrographic accuracy standards, and hence bias correctors must be calculated and applied to the raw depths in postflight data processing to attain the required accuracy for the overall system. The magnitudes of the bias correctors depend not only on the water and flight parameters, but also on the basic design of the receiver electronics. Several typical systems and procedures required to calculate a set of bias correctors for any given system are described and a cookbook approach for the necessary postflight data processing algorithms are included. GRA

N82-22854# National Oceanic and Atmospheric Administration, Rockville, Md. Earth Satellite Lab

A STATISTICAL APPROACH TO RAINFALL ESTIMATION USING SATELLITE AND CONVENTIONAL DATA

L. F WHITNEY, JR. Apr 1982 55 p refs (NOAA-TR-NESS-89) Avail NTIS HC A04/MF A01

A statistical approach is employed in an attempt to estimate convective rainfall using both satellite and conventional data. A variety of variables derived from both satellite and conventional meteorological sources are presented. From among these variables, a screening regression method selects those which best explain area-averaged rainfall. Among the cases studied, the relationship of each variable to rainfall is weak to poor, particularly as cases are combined. Although multivariate selections improve the relationships, inconsistency of selection develops from one case to another and from one time to another, even in the same meteorological situation Regression equations are found to estimate the amount inadequately, even when using dependent data At best, rainfall is not likely to be measured quantitively by such an approach and, at worst, concern is raised about the validity of using the variables investigated to estimate rainfall. B.W

N82-24569*# Instituto de Pesquisas Espaciais, Sao Jose dos Campos (Brazil).

DYNAMIC STUDY OF THE UPPER SAO FRANCISCO RIVER AND TRES MARIAS RESERVOIR USING MSS/LANDSAT IMAGES M.S. Thesis

N. DEJESUSPARADA, Principal Investigator and T M SAUSEN Oct. 1981 272 p refs In PORTUGUESE, ENGLISH summary ERTS (E82-10291; NASA-CR-168860; NAS 1 26:168860, INPE-2249-TDL/066) Avail: NTIS HC A12/MF A01 CSCL 05B

The relationship between the dispersion and concentration of sediment in the superficial layers of the Tres Marias reservoir and the dynamics of the drainage basins of its tributaries was verified using LANDSAT MSS imagery. The drainage network, dissection patterns, and land use of each watershed were considered in an analysis of multispectral images, corresponding to bands 4,5, and 7, of dry and rainy seasons in 1973, 1975, 1977, and 1978. The superficial layer water layers of the reservoir were also divided according to the grey level pattern of each image. Two field trips were made to collect Secchi depths and in situ water reflectance. It is concluded that it is possible to determine the main factors that act in the dynamics of the drainage basins of a reservoir by simultaneous control of the physical variables and the antropic action of each basin. A.R.H.

N82-24601*# Brigham Young Univ., Provo, Utah. Dept. of Civil Engineering.

HCMM HYDROLOGICAL ANALYSIS IN UTAH Quarterly Progress Report

28 Feb. 1982 43 p Sponsored by NASA HCMM (E82-10328, NASA-CR-168907, NAS 1.26:168907; QPR-3) Avail: NTIS HC A03/MF A01 CSCL 05B

Temperature calibration and groundwater depth location studies were finalized. Distinctions among algae species and among suspended materials (turbidity) using HCMM data were investigated. Field evaluations of algae's effect on evaporation pan readings were completed and related to the lake and HCMM data. Additional correlations among infrared and reflectivity data were made using the color graphics capabilities developed during this project E A.K

07

DATA PROCESSING AND DISTRIBUTION SYSTEMS

Includes film processing, computer technology, satellite and aircraft hardware, and imagery

A82-22538* New Hampshire Univ , Durham

FRAGMENTATION OF FE NUCLEI ON CARBON, HYDROGEN AND CH2 TARGETS. I - INDIVIDUAL CHARGE CHANGING AND TOTAL CROSS SECTIONS. II - ISOTOPIC CROSS SECTIONS

D. A BRAUTIGAM, J. H CHAPELL, J. C. KISH, G. A. SIMPSON, and W R. WEBBER (New Hampshire, University, Durham, NH) In: International Cosmic Ray Conference, 17th, Paris, France, July 13-25, 1981, Conference Papers Volume 2. Gif-sur-Yvette, Essonne, France, Commissariat a l'Energie Atomique, 1981, p 173-180. refs (Contract NGR-30-002-052)

The fragmentation of Fe nuclei in carbon and CH2 targets at energies of 650, 800, and 950 MeV/nuc has been studied. Direct measurements of the interaction between Fe nuclei and the carbon and CH2 targets were carried out. The Fe to H charge changing cross sections derived for selected nuclei showed a clear energy dependence, consistent with the results of Westfall et al. (1979) Values for the total inelastic cross section Fe to H charge changing were obtained by two methods: the first method involved subtracting the total CH2 and C cross sections (values of 703 plus or minus 9 mb and 65 plus or minus 10 mb at 950 MeV/nuc and 650 MeV/nuc, respectively were obtained). The same cross sections were obtained by adding the individual charge changing cross sections A cross section for Fe to fragment into lower mass Fe isotopes of 65 plus or minus 5 mb was also observed, giving total inelastic mass changing cross sections of 768 plus or minus 11 mb and 716 plus or minus 12 mb, respectively. In addition, the individual isotopic cross sections for Z equals 16-25 are reported. J F.

A82-22540

ON THE CHARACTERISTICS OF THE VERY LOW ENERGY GALACTIC COSMIC RAYS IN THE INTERSTELLAR SPACE

M. B. KRAINEV (Akademiia Nauk SSSR, Fizicheskii Institut, Moscow, USSR) In: International Cosmic Ray Conference, 17th, Paris, France, July 13-25, 1981, Conference Papers. Volume 2. Gif-sur-Yvette, Essonne, France, Commissariat a l'Energie Atomique, 1981, p. 186-189 refs

The interstellar spectra of several cosmic ray nuclei and ions (H, He, C, O) are calculated in the energy range T less than 1 MeV/n, where the charge-exchange processes become significant. The ionization energy loss and the processes of electron loss and capture are taken into account. The cosmic ray intensity calculation is discussed in detail, and spectra results are presented and interpreted J.F.

A82-22555* New Hampshire Univ., Durham
THE CHARGE AND ISOTOPIC COMPOSITION OF Z EQUALS 7-16 COSMIC RAY NUCLEI AT THEIR SOURCE
W. R WEBBER (New Hampshire, University, Durham, NH) In. International Cosmic Ray Conference, 17th, Paris, France, July 13-25, 1981, Conference Papers. Volume 2. Gif-sur-Yvette, Essonne, France, Commissariat a l'Energie Atomique, 1981, p 261-264 refs
(Contract NGR-30-002-052)

Using the combined data from our 1976 and 1977 balloon flights, the charge and isotopic composition of Z equals 7-16 cosmic ray nuclei have been determined A low abundance of both N and Ne in the cosmic ray source relative to solar cosmic rays is observed. However, the cosmic ray source ratio, Ne-22/Ne is 2.75 plus or minus 0.42 times the solar ratio. A possible enhancement of the Mg-26/Mg ratio, which is 1.29 plus or minus 0.14 times the solar ratio is also observed. (Author)

A82-22558
COSMIC RAY COMPOSITION FROM ACCELERATION OF THERMAL MATTER
J. PEREZ-PERAZA (Universidad Nacional Autonoma de Mexico, Villa Obregon, Mexico) In: International Cosmic Ray Conference, 17th, Paris, France, July 13-25, 1981, Conference Papers Volume 2. Gif-sur-Yvette, Essonne, France, Commissariat a l'Energie Atomique, 1981, p 273-276.

The source composition of cosmic rays is thought to be controlled by Coulombian interactions during the acceleration of thermal matter A given element is representative of the source or depletion depending on whether the predominant ionic state at the temperature of the source is lower than a threshold imposed by Coulombian losses Coupling this restriction to the theory of ionization equilibrium, the source abundances are calculated. The results corroborate sources of relatively low temperature. C.R.

A82-22568
ACCELERATION OF COSMIC RAYS IN ACCRETION SHOCKS
R COWSIK (Tata Institute of Fundamental Research, Bombay, India) and M A LEE (New Hampshire, University, Durham, NH) In: International Cosmic Ray Conference, 17th, Paris, France, July 13-25, 1981, Conference Papers Volume 2. Gif-sur-Yvette, Essonne, France, Commissariat a l'Energie Atomique, 1981, p. 318-321. refs

Spherically symmetric accretion around condensed astronomical objects like white dwarfs, neutron stars and black holes very often go through a quasi-stationary shock close to the object. The transport of radiation, energetic particles and neutrinos in such flows is studied, and it is found that these are accelerated to high energies very efficiently The generated spectra are seen to have power-law behavior when the diffusion coefficient is independent of particle momentum. The possibility that the bulk of the galactic cosmic rays are accelerated by approximately 10,000 neutron stars which are surrounded by dense interstellar clouds is briefly discussed. (Author)

A82-22573
THE GALACTIC ORIGIN OF COSMIC RAYS. II
S. A. COLGATE (Los Alamos National Laboratory, Los Alamos; New Mexico Institute of Mining and Technology, Socorro, NM) In: International Cosmic Ray Conference, 17th, Paris, France, July 13-25, 1981, Conference Papers. Volume 2. Gif-sur-Yvette, Essonne, France, Commissariat a l'Energie Atomique, 1981, p. 352-355. refs
(CONF-810711-2; LA-UR-81-966)

The cosmic ray pressure limit to cosmic ray acceleration in the interstellar medium (ISM) is considered It is found that the beta equals 1 Alfven speed streaming limit imposes a new and strong constraint on supernova-ISM shock models of cosmic-ray acceleration. A more detailed analysis is, therefore, required. Ultra-high energy cosmic rays are also discussed, giving attention to sources of cosmic rays inside and outside the Galaxy. In connection with complexities and constraints, one source for all energies within all galaxies is finally considered, taking into account a flattening of the source in slope and the characteristics of spectrum and flux produced by the shock ejection of the envelope of a type I supernova. G.R.

A82-22575
ASTROPHYSICAL SCENARIOS FOR CRITICALLY EVALUATING A ZERO-POINT FIELD ACCELERATION MECHANISM
A. RUEDA (Universidad de los Andes, Bogota, Colombia) In. International Cosmic Ray Conference, 17th, Paris, France, July 13-25, 1981, Conference Papers Volume 2 Gif-sur-Yvette, Essonne, France, Commissariat a l'Energie Atomique, 1981, p. 361-364. refs

If the electromagnetic zero-point field of ordinary quantum theory is considered as a real field that may act on particles in the usual way that random fields act in classical electrodynamics, it is possible to show that electromagnetically interacting particles perform a random walk in velocity space to ever-increasing translational kinetic energies. As the zero-point field has a Lorentz invariant energy density spectrum, it can be shown that, in a very high vacuum an unconfined gas of infinitely many of those particle displays an energy spectrum of the form E to the (-eta) (eta is a parameter) when in equilibrium with the zero-point field Scenarios are presented in order to critically discuss and evaluate the possible astrophysical relevance of the model as applied to the acceleration of particles in intergalactic space (Author)

A82-22576
CALCULATION OF PRODUCTION RATES OF COSMOGENIC NUCLIDES BY MONTE CARLO METHOD
S TOKAR and P. POVINEC (Komenskeho Univerzita, Bratislava, Czechoslovakia) In. International Cosmic Ray Conference, 17th, Paris, France, July 13-25, 1981, Conference Papers. Volume 2 Gif-sur-Yvette, Essonne, France, Commissariat a l'Energie Atomique, 1981, p 374-377 refs

A method is presented for the calculation of production rates of cosmogenic nuclides based on Monte Carlo simulations of hadronic cascade processes in matter Calculations are carried out for the case of a semi-infinite iron slab with a thickness of 2 5 m, and the hadronic cascade is assumed to consist only of nucleons and pions The nuclide production is found to exhibit only a weak energy dependence, especially at higher energies D L G.

A82-22577
MEASUREMENT OF COSMOGENIC NUCLIDES USING A MULTI-CRYSTAL GAMMA-RAY COINCIDENCE SPECTROMETER
J. C BARTON (North London, Polytechnic, London, England) In: International Cosmic Ray Conference, 17th, Paris, France, July 13-25, 1981, Conference Papers. Volume 2. Gif-sur-Yvette, Essonne, France, Commissariat a l'Energie Atomique, 1981, p 378-381.

The activities of Na-22 and Al-26 in a recently fallen meteorite, Mayo Belwa, have been measured using an improved gamma-ray spectrometer. This uses six sodium iodide detectors, arranged symmetrically, so that extended samples can be measured. By recording total rates, 2-fold and 3-fold coincidences simultaneously, it is possible to correct for source absorption and other instrumental effects The absolute intensity of Al-26 was found to be comparable to that found in other meteorites, but that of Na-22 is anomalously high (Author)

A82-22578
NUCLEOSYNTHESIS OF LIGHT AND BY-PASSED ISOTOPES IN THE SOLAR SYSTEM MATTER
A. K. LAVRUKHINA and R. I. KUZNETSOVA (Akademiia Nauk SSSR, Institut Geokhimii i Analiticheskoi Khimii, Moscow, USSR) In: International Cosmic Ray Conference, 17th, Paris, France, July 13-25, 1981, Conference Papers. Volume 2. Gif-sur-Yvette, Essonne, France, Commissariat a l'Energie Atomique, 1981, p 382-385. refs

A model of nucleosynthesis of light and by-passed isotopes is proposed, which is based on the idea that a supernova event led simultaneously to nuclei explosion burning, to collective

acceleration of particles up to relativistic energies by shock waves, and to spallation reactions It is shown that solar system matter was formed in two main events of intensive nucleosynthesis. The first event led to the formation of about 99 percent of K-40, V-50, and the by-passed isotopes with A not less than 113. The second event led to the formation of observed abundances of isotopes and about 1 percent of other products of spallation reactions. Proton fluxes, the alpha/p value, the gamma value, irradiation duration, and the sequence of nucleosynthesis processes are obtained. D.L.G.

A82-22579
MAGNETIC MONOPOLE PAIR AND ITS OBSERVATION IN COSMIC RAYS
L LUO (Nei Monggol University, Hohhot, People's Republic of China) and T. LU (Nanjing University, Nanjing, People's Republic of China) In International Cosmic Ray Conference, 17th, Paris, France, July 13-25, 1981, Conference Papers. Volume 2. Gif-sur-Yvette, Essonne, France, Commissariat a l'Energie Atomique, 1981, p 388-391

The bound system of a magnetic monopole and an antimonopole is analyzed It is pointed out that the angular momentum of the ground state may be 48 or 194. Some unexplained events in cosmic rays may be identified as the monopole pairs with high spin. (Author)

A82-22580
INTERNATIONAL COSMIC RAY CONFERENCE, 17TH, PARIS, FRANCE, JULY 13-25, 1981, CONFERENCE PAPERS. VOLUME 3 [CONFERENCE INTERNATIONALE SUR LE RAYONNEMENT COSMIQUE, 17TH, PARIS, FRANCE, JULY 13-25, 1981, CONFERENCE PAPERS. VOLUME 3]
Conference sponsored by CEA, IUPAP, CESR, et al Gif-sur-Yvette, Essonne, France, Commissariat a l'Energie Atomique, 1981. 543 p. In French and English.

The sun and heliosphere are examined from satellite data of solar cosmic ray events recorded by satellite and theories of the interplanetary propagation of particles and particle acceleration within the heliosphere Attention is given to X ray, radio, energetic electron, gamma ray, and nuclear reactions of energetic protons observations of solar activity. Ground-, balloon-, and satellite-based detection of particle events are discussed, along with data relevant to the propagation of particles, especially for He-3 enriched events. Modulation of galactic cosmic rays by the solar cycle is explored, and theories of the interplanetary propagation of particles and of the heliospheric medium are presented Theoretical models of the acceleration of particles within the heliosphere are investigated, including the effect of planetary magnetospheres on the solar-accelerated particles. M S K.

A82-22581
MODEL FOR SOLAR HARD X-RAY BURSTS
M. YOSHIMORI (Rikkyo University, Tokyo, Japan) In: International Cosmic Ray Conference, 17th, Paris, France, July 13-25, 1981, Conference Papers Volume 3. Gif-sur-Yvette, Essonne, France, Commissariat a l'Energie Atomique, 1981, p. 4-7.

Balloon-borne observations of the hard X ray burst event of Sept 19, 1979 are presented as a basis for a description of the temporal behavior of a number of electrons. One NaI(Tl) monitor and four NaI(Tl) counters provided measurements in the energy ranges 30-50, 50-80, 80-120, and 120-200 keV with a counting rate of 1 sec. The energy spectra of the hard X rays were correlated with solar flares and sunspots, and were fitted to power law forms evaluated at the sampling time. A trap-plus-precipitation model describes accelerated electrons as being magnetically trapped and precipitated onto a denser region, leading to hard X ray emission, yielding an electron/X ray ratio calculated to be 1,700,000, in accord with other observations. A thermal model approximated the energy spectrum of hard X-rays by the thermal radiation spectrum from hot plasma, with variations in temperature and emission. M S.K.

A82-22582
THE DETERMINATION OF DIFFERENTIAL X-RAY SPECTRUM OF THE SOLAR FLARE USING IONOSPHERIC DATA
I D KOZIN (Akademiia Nauk Kazakhskoi SSR, Sektor Ionosfery, Alma-Ata, Kazakh SSR) In: International Cosmic Ray Conference, 17th, Paris, France, July 13-25, 1981, Conference Papers. Volume 3. Gif-sur-Yvette, Essonne, France, Commissariat a l'Energie Atomique, 1981, p. 8-10.

The ionization velocity of X rays from a solar flare entering the lower ionosphere is determined by first assuming that the X ray spectrum outside the atmosphere is described by a third degree polynomial. The absorption of monochromatic radiation is modeled as a function of atmospheric density, of the absorption cross-section, and of the path length. The ionosphere is divided into three levels, from which coefficients are calculated from data on ionization from the X ray flux Substitution of the coefficients into the third degree polynomial equation yields the differential X ray spectrum. M S.K

A82-22585* Chicago Univ., Ill.
UNUSUAL PROPERTIES OF PARTICLE EVENTS ASSOCIATED WITH SOLAR FLARE GAMMA RAY EVENTS
P EVENSON, P. MEYER, and S. YANAGITA (Chicago, University, Chicago, IL) In: International Cosmic Ray Conference, 17th, Paris, France, July 13-25, 1981, Conference Papers. Volume 3. Gif-sur-Yvette, Essonne, France, Commissariat a l'Energie Atomique, 1981, p. 32-35. refs
(Contract NAS5-20674)

An attempt to establish a link between gamma rays observed at the earth with solar flare areas highly enriched with electrons is presented Two hour averages of the counting rates of 5-100 MeV electrons and 25-145 MeV protons performed on the ISEE-3 spacecraft were correlated with solar flares with a maximum intensity of 6-11 MeV electrons and 25-44 MeV protons recorded by other observers. The coverage was part of the Solar Maximum Mission, which attained a 50 percent coverage. Gamma ray associated events showed high ratios of electrons to protons, about 0 2, and electrons with energies greater than 80 MeV were observed, which are values high enough to produce the highest gamma rays observed, 40 MeV. The available data for electron, proton, and rare isotope fluxes and the time histories of the fluxes are noted to provide a data base for further information on solar flares and particle acceleration mechanisms M.S K.

A82-22586* Maryland Univ., College Park.
OBSERVATIONS OF INTERPLANETARY ENERGETIC CHARGED PARTICLES FROM GAMMA-RAY LINE SOLAR FLARES
M. E PESSES, G GLOECKLER (Maryland, University, College Park, MD), B KLECKER, and D. HOVESTADT (Max-Planck-Institut fur extraterrestrische Physik, Garching, West Germany) In: International Cosmic Ray Conference, 17th, Paris, France, July 13-25, 1981, Conference Papers. Volume 3. Gif-sur-Yvette, Essonne, France, Commissariat a l'Energie Atomique, 1981, p 36-39. Bundesministerium fur Forschung und Technologie refs
(Contract BMFT-RV14-B8/74,
BMFT-01-01-017-ZA/WF/WRK-1754; NAS5-20062)

Results from ISEE-3 experiments on interplanetary energetic charged particles on June 7, June 21, and July 1, 1980 dealing with gamma ray producing solar flares are reported The data were gathered by the Ultra Low Energy Wide Angle Telescope, which comprises a thin window, flow through proportional counter/solid-state detector composition telescope. Evidence of a specified time delay from an observed flare and the recording of 0.44-1.3 MeV electrons on ISEE-3 combined with quiescent periods of at least two hours before the observations and recording provides a link between the events The data indicates interplanetary energetic particle enhancement, and a second, similar set of occurrences was also observed Protons were accelerated up to 10-20 MeV. No enrichment of either He-3 or Fe was found.
M S.K.

A82-22590
AZIMUTHAL PROPAGATION OF FLARE PARTICLES IN THE HELIOSPHERE
J PEREZ-PERAZA and J. MARTINELL (Universidad Nacional Autonoma de Mexico, Villa Obregon, Mexico) In: International Cosmic Ray Conference, 17th, Paris, France, July 13-25, 1981, Conference Papers Volume 3 Gif-sur-Yvette, Essonne, France, Commissariat a l'Energie Atomique, 1981, p. 55-58. refs

Empirically determined properties of solar coronal particle transport are used to quantitatively describe coronal propagation. A velocity dependence of the transport is formulated based on the diffusive nature of the transport and the observation that a drift motion acts on the particles. Both characteristics are assumed to be applicable outside of the fast propagation region, where convective processes dominate. An evolution of particle density is defined, and time profiles of the distribution are calculated for the two regions just before propagation into outer space. A prediction of prompt particles is made, and is caused by contact between the expanding magnetic bottle and field lines of opposite polarity, which leads to a tearing mode instability and a transfer of energy excess to thermal particles. A calculation of the growth time of the instability shows that particles will be observed before the flare particles appear. M S.K

A82-22597
THE SOLAR PROTON FLUXES IN APRIL, 1979
S. I ERMAKOV, N. N KONTOR, T. I MOROZOVA, T I STEPINA, and G. O. KHACHATURIAN (Moskovskii Gosudarstvennyi Universitet, Moscow, USSR) In International Cosmic Ray Conference, 17th, Paris, France, July 13-25, 1981, Conference Papers Volume 3. Gif-sur-Yvette, Essonne, France, Commissariat a l'Energie Atomique, 1981, p. 85-87.

Increases in the solar low-energy proton intensity near the earth detected in April 1979 by the Venera-11 space probe are discussed During that period the probe was located at approximately 55 deg west of the sun-earth line. A comparison between the proton intensity profiles measured on Venera-11 and on earth shows that the proton propagation conditions during the period of high solar activity were essentially inhomogeneous in the azimuthal direction. C.R.

A82-28905
SURFACE TEMPERATURE DETERMINATION FROM AN AMALGAMATION OF GOES AND TIROS-N RADIANCE MEASUREMENTS
J. A. ZANDLO, W. P. MENZEL (Wisconsin, University, Madison, WI), W. L SMITH, and C M HAYDEN (Wisconsin, University; NOAA, National Earth Satellite Service, Madison, WI) Journal of Applied Meteorology, vol. 21, Jan 1982, p 44-50.

A technique for exploiting the TIROS-N capability of measuring the earth skin surface temperature and the GOES ability to monitor surface changes with fine temporal and horizontal resolution is described. Atmospheric absorption due to water vapor is assumed to vary slowly in space and time relative to the same scales of the GOES observations, thus allowing a horizontally varying correction field derived from 6-hr TIROS-N data to be used to obtain quasi-continuous surface temperature features from the GOES data. Additionally, a field of temperature differences between the corrected TIROS-N window channel brightness temperatures and uncorrected GOES brightness temperatures are specified. The GOES temperatures are then correctable to within six hours Two examples are provided of regional temperature assessments with comparison with surface-measured data and accuracy with the satellite data is within 1 K. M S.K.

A82-29326* National Aeronautics and Space Administration. Earth Resources Labs , Bay St. Louis, Miss.
DEVELOPMENT OF THREE-DIMENSIONAL SPATIAL DISPLAYS USING A GEOGRAPHICALLY BASED INFORMATION SYSTEM
B. G JUNKIN (NASA, National Space Technology Laboratories, Earth Resources Laboratory, Bay Saint Louis, MS) Photogrammetric Engineering and Remote Sensing, vol 48, Apr 1982, p. 577-586. refs

Procedures necessary for the development of a generalized three-dimensional perspective software capability in support of graphic, topographic, and color mapping of Landsat data are reviewed The NASA Earth Resources Laboratory developed the procedures in order to facilitate the processing and analysis of disparate, geographically oriented base maps from aircraft and satellite sensors Perspective displays are obtained through a translation of the space-viewed object to a vantage point coordinate system, followed by a rotation through two angles for alignment along the vantage line of sight, and finally a perspective transformation to yield two-dimensional displays with no hidden lines Matrix equations for the transformations are reviewed, including scaling, and block diagrams are provided of the data and perspective software systems The classification data plane may be mapped onto a topographic elevation data plane M.S.K.

A82-29328
THE USE OF RESIDUAL IMAGES IN LANDSAT IMAGE ANALYSIS
D. L. B JUPP and K. K MAYO (Commonwealth Scientific and Industrial Research Organization, Div. of Land Use Research, Canberra, Australia) Photogrammetric Engineering and Remote Sensing, vol 48, Apr. 1982, p. 595-604. refs

Methods of classification of Landsat data for interactive image display and analysis are reviewed, and the use of the residual image to improve the postclassification analysis is examined The mean image is formed from an accumulation of the mean radiance values from four channels, while the residual image is generated in the form of pixels in terms of the difference between the class mean and the actual measured radiance The residual image facilitates detection of departures from hierarchical classes and patterns. A reference model is developed to standardize residual images, and gains in texture analysis during visual analysis are noted with inclusion of the residual images Examples are provided of land cover mapping an area in southeast Australia, and spectral class mapping on the northeast coast, where differences between inland and coastal vegetation are made visible using residual imagery M S K.

A82-29409
DESCRIPTION OF GRAY LEVEL PICTURE USING A COLLECTION OF DENSITY CONTOUR LINES
T AGUI, M NAKAJIMA, and K MATSUBARA (Tokyo Institute of Technology, Yokohama, Japan) Institute of Electronics and Communication Engineers of Japan, Transactions, Section E (English), vol E 65, Jan 1982, p. 36-43 refs

An extraction method of density contour lines of gray level pictures is described Two kinds of quads composed of four image pixels and non-image pixels are defined for making the density contour lines simple closed paths From the resultant density contour lines of simple closed paths, a tree graph is made for executing the recognition of a house included in a monochromatic aerial photo of an urban area. (Author)

A82-29762#
RELATING LANDSAT DIGITAL COUNT VALUES TO GROUND REFLECTANCE FOR OPTICALLY THIN ATMOSPHERIC CONDITIONS
A. J. RICHARDSON (U S. Department of Agriculture, Agricultural Research Service, Weslaco, TX) Applied Optics, vol 21, Apr. 15, 1982, p. 1457-1464. refs

The relation of Landsat digital count (DCc) values to ground-measured bidirectional reflectance (R), in data from seven previous investigations that are summarized and examined as a unified data set, is shown to be useful in the estimation of R by

means of a simplified linear formulation for conditions approximating optically thin atmospheres. All digital count values and formulas were corrected to appear as though obtained at a sun zenith angle of 39 deg, with a Landsat-2 calibration for the January 22-July 15, 1975 period The relations for R4-7 are: -5.9 + 0.476DCc4, -1 94 + 0.373DCc5, -1.40 + 0.412DCc6, and -0.49 + 1 220DCc7, respectively O.C

A82-32033
EXTRACTION OF LINE SHAPED OBJECTS FROM AERIAL IMAGES USING A SPECIAL OPERATOR TO ANALYZE THE PROFILES OF FUNCTIONS
W.-D. GROCH (Karlsruhe, Universitaet, Karlsruhe, West Germany) Computer Graphics and Image Processing, vol. 18, Apr. 1982, p 347-358. Research supported by the Bundesministerium fuer Forschung und Technologie and U S Army refs

Line-shaped objects are extracted sequentially by object-guided and object-specific methods with the facility for interactive support. The line following starts at locations which reliably are part of line-shaped objects. Two different object-guided methods may be initialized at these starting points The methods follow the object by applying special operators to extract line segments. The operator is described that analyzes the function profiles, the detection of starting points, the two methods for line following and the combination of all methods in a system for the extraction of line-shaped objects from discrete gray level pictures. Results of a test are shown. C.D.

A82-32343* National Aeronautics and Space Administration. Goddard Space Flight Center, Greenbelt, Md.
PRELIMINARY EVIDENCE FOR THE INFLUENCE OF PHYSIOGRAPHY AND SCALE UPON THE AUTOCORRELATION FUNCTION OF REMOTELY SENSED DATA
M. L. LABOVITZ, D L TOLL (NASA, Goddard Space Flight Center, Greenbelt, MD), and R. E KENNARD (Computer Sciences Corp , Silver Spring, MD) International Journal of Remote Sensing, vol. 3, Jan.-Mar 1982, p. 13-30. refs

(Previously announced in STAR as N81-19530)

A82-32344
DEPENDENT FEATURE TREES FOR DENSITY APPROXIMATION. I - OPTIMAL CONSTRUCTION AND CLASSIFICATION RESULTS
C. B. CHITTINENI (Conoco, Inc., Ponca City, OK) International Journal of Remote Sensing, vol. 3, Jan.-Mar. 1982, p 31-44. refs

This paper deals with the approximation of probability density functions with dependent feature trees. The optimal dependent feature trees are proposed to be constructed using criteria of mutual information and distance measures. Expressions are derived for the criteria when the distributions of the features are Gaussian Expressions are developed for the covariances between the features connected by a path in a dependent feature tree. The case when the nodes in a dependent feature tree represent a set of features is also considered. Furthermore, experimental results from the classification of remotely sensed multispectral scanner imagery data are presented. (Author)

A82-32345* National Aeronautics and Space Administration. Goddard Space Flight Center, Greenbelt, Md.
EVALUATION OF TEMPORAL REGISTRATION OF LANDSAT SCENES
R. NELSON and G. GREBOWSKY (NASA, Goddard Space Flight Center, Greenbelt, MD) International Journal of Remote Sensing, vol. 3, Jan.-Mar. 1982, p. 45-50. refs

The registration of Landsat images is important for multitemporal classification and for detecting change. Landsat data are now rectified to a ground coordinate system during preprocessing, hence scenes obtained over the same area are registered The machine responsible for preprocessing the Landsat multispectral scanner data is the master data processor (MDP). This paper describes the rectification approach taken by the MDP, reviews the accuracy standards of the resultant product, and provides an assessment of the accuracy of the scene to scene registration of two Landsat images. (Author)

A82-32346
THE USE OF CONTEXTUAL INFORMATION TO DETECT CUMULUS CLOUDS AND CLOUD SHADOWS IN LANDSAT DATA
C M. GURNEY (Reading, University, Reading, England) International Journal of Remote Sensing, vol 3, Jan -Mar. 1982, p 51-62 Research supported by the Atomic Energy Research Establishment. refs

The use of contextual information to identify areas of cloud and cloud shadow in digital Landsat data is described The distance from cloud to shadow is calculated from sun elevation and azimuth, cloud base height and image geometry Pixels with a gray level above a given threshold are considered to be potential cloud. A 3 x 3 pixel window centered at the calculated shadow position is searched. Pixels in this window with gray levels below a second threshold are classed as cloud shadow. If no shadow pixels are found the potential cloud is rejected. Modifications to allow for overlapping cloud and shadow are included The detection procedure was found to work well for bands 5, 6, or 7 of Landsat data. (Author)

A82-32347
THE ESTIMATION OF WAVE HEIGHT FROM DIGITALLY PROCESSED SAR IMAGERY
M. H. B. THOMAS (Atomic Energy Research Establishment, Materials Physics Div , Harwell, Oxon, England) International Journal of Remote Sensing, vol. 3, Jan -Mar 1982, p 63-68 Research supported by the Department of Industry. refs

A simple method has been developed for estimating wave height from synthetic aperture radar (SAR) imagery obtained by the Seasat satellite The method is based on measuring the contrast of the image and the wavelength of the dominant wave. A calculation has been made for two orbits made by the satellite over the North Atlantic in 1978, using digitally processed data supplied by DFVLR in West Germany. Comparison with sea truth measurements shows agreement to within about 20 per cent. (Author)

A82-32507
DIGITALLY ENHANCED VISUAL DISPLAYS FACILITATE THE ANALYSIS OF LANDSAT IMAGERY
R N COLWELL (Earth Satellite Corp., Berkeley, CA) In Display technology II; Proceedings of the Meeting, Los Angeles, CA, February 10, 11, 1981. Bellingham, WA, SPIE - The International Society for Optical Engineering, 1981, p. 118-126.

There have been efforts during most of the past decade to increase the interpretability of Landsat multispectral scanner (MSS) imagery through the performance of various kinds of image enhancement. Attention is given to research recently conducted for the U S. Forest Service (USFS) with the objective to develop improved 'multiresource inventory methods' entailing the direct visual analysis of Landsat MSS imagery. The establishment of the resource categories to be identified is discussed along with approaches for producing the digitally enhanced visual displays, the preparation of the image analysis keys, the selection of personnel to evaluate the imagery, and the administration of the image interpretability tests Preliminary results clearly showed that the studied procedure of enhanced visual display (color composite image in opaque print form) was significantly more interpretable than the conventional Landsat color composite imagery. G.R.

A82-32581* Lowell Observatory, Flagstaff, Ariz
SUBTLETIES IN THE FLAT-FIELDING OF CHARGE-COUPLED DEVICE /CCD/ IMAGES
W. A. BAUM, B. THOMSEN, and T. J. KREIDL (Lowell Observatory, Flagstaff, AZ) In: Solid state imagers for astronomy, Proceedings of the Meeting, Cambridge, MA, June 10, 11, 1981 Bellingham, WA, SPIE - The International Society for Optical Engineering, 1981, p. 24-27.
(Contract NAS5-25451; NAS5-25488)

Astronomical photometry with CCDs will often involve relatively low signal levels (less than 1000 charge carriers per pixel), at which nonlinear effects sometimes become significant These effects will probably play a role in the processing of Space Telescope data. The problem apparently arises because signal charges are not read out equally completely from all columns and all pixels It is shown that, although a first-order correction can be made by subtracting a low-level flat field from all frames before conventional processing, higher accuracy can be achieved by modeling the response with a nonlinear function B.J.

A82-32709
COMPUTATION WITH PHYSICAL VALUES FROM LANDSAT DIGITAL DATA
C. J. ROBINOVE (U.S Geological Survey, Reston, VA) Photogrammetric Engineering and Remote Sensing, vol 48, May 1982, p. 781-784.

Although the analysis of Landsat digital images by using the digital numbers for each pixel recorded on a computer-compatible magnetic tape may be adequate when only a single, internally-consistent image is used, incorrect results will be given by the procedure if more than one image is used for analysis, as in mosaics or temporal overlays. The digital numbers for each pixel should in such cases be converted to their dimensionless equivalents, such as (1) radiance, as measured at the satellite, in mW/sq cm per steradian (sr), or (2) reflectance, both of which vary depending on the calibration of satellite MSS, sun angle, atmospheric state, terrain slope and aspect, and surface cover. Equations are given for radiance and reflectance calculations for the cases of five radiometric conditions, neglecting atmospheric correction O.C.

A82-32900
GEOGRAPHIC LOCATION OF INDIVIDUAL PIXELS
D. C. MCCONAGHY (NOAA, National Marine Fisheries Service, La Jolla, CA) Remote Sensing of Environment, vol 10, Aug. 1980, p 81-84. refs

A major problem in processing thermal infrared digital data from very high resolution radiometers aboard NOAA Polar Orbiting Satellites is the geographic placement of digital data fields. Geographic placement is especially difficult over oceanic areas because of the lack of landmarks. Using a series of geometric constructions, an analytical approach can be developed for geographic location of individual data pixels The errors associated with this method are generally less than 0.1 deg latitude and longitude. (Author)

A82-32904* California Univ., Santa Barbara.
THE USE OF PRIOR PROBABILITIES IN MAXIMUM LIKELIHOOD CLASSIFICATION OF REMOTELY SENSED DATA
A. H. STRAHLER (California, University, Santa Barbara, CA) Remote Sensing of Environment, vol. 10, Sept 1980, p 135-163 refs
(Contract NAS9-15509; NAS7-100, NSG-2377)

Possibilities for the improvement of classification accuracies by the use of prior information about the expected distribution of classes in the maximum likelihood classification of remote sensing data are examined The modification of the maximum likelihood decision rule to take into account one or several sets of probabilities for the occurrence of classes which probabilities are based on independent knowledge of the area surveyed is demonstrated. It is then shown that the use of prior probabilities is sufficiently versatile so as to allow the prior weighting of output classes based on their anticipated sizes as well as the merging of continuously varying measurements with discrete collateral information data sets and the construction of time-sequential classification systems in which an earlier classification modifies the outcome of a latter one A.L.W

A82-32906
MONITORING LAND-COVER CHANGE BY PRINCIPAL COMPONENT ANALYSIS OF MULTITEMPORAL LANDSAT DATA
G. F. BYRNE, P F. CRAPPER, and K. K. MAYO (Commonwealth Scientific and Industrial Research Organization, Div. of Land Use Research, Canberra, Australia) Remote Sensing of Environment, vol. 10, Nov 1980, p. 175-184. refs

Two four-channel Landsat scenes of the same area, which were recorded on different dates, were superimposed and treated as a single eight-dimensional (channel) data array Principal component analysis (PCA) of this array resulted in the gross differences associated with overall radiation and atmospheric changes appearing in the major component images and statistically minor changes associated with local changes in land cover appearing in the minor component images. (Author)

A82-32911
TERRAIN ANALYSIS FROM LANDSAT USING A COLOR TV ENHANCEMENT SYSTEM
T. H. L. WILLIAMS (Kansas, University, Lawrence, KS) and J. M. GOODMAN (Oklahoma, University, Norman, OK) Remote Sensing of Environment, vol. 10, Nov 1980, p. 231-237.

Visual interpretation of Landsat false-color composite imagery was employed to map terrain types on the Navajo Indian Reservation in northeastern Arizona and northwestern New Mexico. Three main difficulties were encountered in the visual analysis: (1) determination of the exact boundary positions; (2) repeatability of the boundary decisions over an area; and (3) discrimination among subtle tone differences associated with certain terrain type groupings. A simple image enhancement technique, based on a color television system was developed to make the visual analysis more accurate A color TV camera was used to view the image and a color monitor used for the display Image enhancement was achieved by use of the chroma, hue, contrast, and brightness controls on the monitor. The use of a zoom lens on the camera allowed rapid scale change and facilitated study of small areas of the image By working directly from a color image, the technique obviated the need for separation positives with their attendant registration problems. (Author)

A82-32916
APPEARANCE OF IRREGULAR TREE CANOPIES IN NIGHTTIME HIGH-RESOLUTION THERMAL INFRARED IMAGERY
L. K. BALICK and S. K. WILSON (Los Alamos National Laboratory, Los Alamos, NM) Remote Sensing of Environment, vol. 10, Dec. 1980, p. 299-305 refs

A82-34225
SEPARATION OF DIFFUSE FROM SHARP-EDGED FEATURES IN DIGITAL IMAGERY
G. F. BYRNE, P. F. CRAPPER, B. G. WILLIAMS, and M. J. GOODSPEED (Commonwealth Scientific and Industrial Research Organization, Div. of Land Use Research, Canberra, Australia) Remote Sensing of Environment, vol. 12, May 1982, p. 181-186. refs

A new classification procedure that removes sharp-edge features from digital imagery and that more clearly reveals any patterns more diffuse in nature that may be present is proposed. The procedure relies on the hypothesis that the sharp edges separate areas of uniform but differing optical density. These differences are frequently sufficiently large to obscure other patterns that are more diffuse ('fuzzy') in nature The technique is illustrated by application to a Landsat scene where a suspected mosaic arising from soil variability is overlain by agricultural fields. C.R.

A82-34469
EVALUATION OF THE EFFECTIVENESS OF SYSTEMATIC IMAGE DISTORTION COMPENSATION [OTSENKA EFFEKTIVNOSTI KOMPENSATSII SISTEMATICHESKIKH ISKAZHENII IZOBRAZHENIIA]
N G. BARABANOVA, K. N GERTSENOVA, and S S. NEKHIN Geodeziia i Kartografiia, Apr. 1982, p. 32-36. In Russian

The improvements in image accuracy afforded by two methods for the compensation of systematic distortions in aerial photographs are studied The techniques of field calibration, which involves the correction of image coordinates by interpolation from the coordinates of selected calibration points, and polynomial correction using additional reference points, in which the distortion field is approximated by second- and third-degree polynomials, were applied to aerial photographs subject to four different types of distortions Examination of the errors in the determination of the coordinates of control points and the maximum errors of their mutual positioning indicates field calibration to be more effective for sign-changing point displacements, while polynomial approximation is more effective for regular displacements.
A L W.

A82-34702
A PRACTICAL STUDY OF GROSS-ERROR DETECTION IN BUNDLE ADJUSTMENT
S. F. EL-HAKIM (National Research Council, Ottawa, Canada) In: American Society of Photogrammetry, Annual Meeting, 47th, Washington, DC, February 22-27, 1981, ASP Technical Papers. Falls Church, VA, American Society of Photogrammetry, 1981, p. 1-17. refs

A special bundle adjustment program has been developed with built-in automatic gross-error detector by the data snooping approach. The program computes, in an efficient way, the exact values of the redundancy numbers for each image point. Using actual data, many of the factors affecting the reliability of bundle adjustment and the ability of the technique to detect gross errors are studied. The effects of different block parameters, point type and location, and the use of additional constraints are presented.
(Author)

A82-34717
AN INFORMATION-THEORIC SPATIAL TRANSFORM
J. S. POWERS (Mississippi State University, Mississippi State, MS) In. American Society of Photogrammetry, Annual Meeting, 47th, Washington, DC, February 22-27, 1981, ASP Technical Papers Falls Church, VA, American Society of Photogrammetry, 1981, p. 221-225. refs

Significant improvements in the sensitivity of existing computer algorithms for digital remote-sensor image classification may be effected without involving any software modification of these systems. An information-theoric spatial transform may be applied to the raw multispectral data set, and synthetic channels thus created may be utilized in the classification process. The transform is analogous in operation to the transform which occurs in the retina of higher organisms, a processing stage which has been omitted in most existing classification schemes. The transform algorithm is described and preliminary results of the application of the algorithm to the study of forest ecosystems from Landsat MSS image data are discussed (Author)

A82-34720* Jet Propulsion Lab., California Inst. of Tech , Pasadena.
BATHYMETRIC IMAGING
P. R PALUZZI (California Institute of Technology, Jet Propulsion Laboratory, Pasadena, CA) and M. C MALIN (Arizona State University, Tempe, AZ) In American Society of Photogrammetry, Annual Meeting, 47th, Washington, DC, February 22-27, 1981, ASP Technical Papers. Falls Church, VA, American Society of Photogrammetry, 1981, p. 247-258. refs
(Contract NAS7-100)

Digital topography has, for some years, been formatted and processed into shaded relief images for specific studies involving land use and thermal properties Application to bathymetry is a new and seemingly fruitful extension of these techniques. Digital terrain models of the earth - combining subaerial topography with an extensive collection of bathymetric soundings - have been processed to yield shaded relief images. These images provide new and exciting insights into submarine geomorphology and portray many aspects of plate tectonic physiography in a manner not previously possible (Author)

A82-34722
A QUANTITATIVE METHOD TO TEST FOR SIMILARITY BETWEEN PHOTO INTERPRETERS
R. G CONGALTON and R. A. MEAD (Virginia Polytechnic Institute and State University, Blacksburg, VA) In. American Society of Photogrammetry, Annual Meeting, 47th, Washington, DC, February 22-27, 1981, ASP Technical Papers Falls Church, VA, American Society of Photogrammetry, 1981, p. 263-266.

Photo interpretation is the art and science of identifying objects and deducing their significance on aerial photos The judgment involved is generally qualitative in nature, and, therefore, difficult to evaluate or compare with interpretations made by others. The present investigation is concerned with an approach which makes it possible to quantify photo interpretation results, taking into account a statistical method for comparing these results. The proposed procedure can be employed in tests regarding the degree of similarity between interpreters or the consistency of the same interpreter over time. The procedure is based on the employment of an error matrix and the conduction of a discrete multivariate analysis to test the degree of similarity between the error matrices. G R

A82-34723
TERRAIN CLASSIFICATION BY FOURIER ANALYSIS - ACCURACY AND ECONOMY
P. FREDERIKSEN and O. JACOBI (Danmarks Tekniske Hojskole, Lyngby, Denmark) In: American Society of Photogrammetry, Annual Meeting, 47th, Washington, DC, February 22-27, 1981, ASP Technical Papers Falls Church, VA, American Society of Photogrammetry, 1981, p. 267-284. refs

The Fourier transformation is applied to terrain profiles for classification purposes. Areas with different geology are considered, and the power spectra are estimated. The spectrum is used to predict the accuracy of a digital terrain model and to calculate some economic consequences of the relation between type of terrain, accuracy of measurements, point density, and surveying expenses. (Author)

A82-34726
RAMS-1, A RESOURCE ANALYSIS AND MAPPING SYSTEM
R. J MADILL (Systemhouse, Ltd., Ottawa, Canada) In: American Society of Photogrammetry, Annual Meeting, 47th, Washington, DC, February 22-27, 1981, ASP Technical Papers. Falls Church, VA, American Society of Photogrammetry, 1981, p. 306-310.

RAMS-1 is a Resource Analysis and Mapping System developed by Systemhouse. RAMS-1 will produce colour shaded thematic overlays as well as planimetric base maps This paper describes the hardware configuration and software facilities of the SHL RAMS-1 system (Author)

A82-34940
PRESENT STATUS OF ON-LINE ANALYTICAL TRIANGULATION
V. KRATKY (National Research Council, Ottawa, Canada) Photogrammetria, vol. 38, May 1982, p 1-12 refs

Basic principles of solutions suitable for analytical aerial triangulation are outlined and analyzed in the context of existing on-line photogrammetric systems Two basic categories of procedures are considered: those which primarily aim for a quality controlled data acquisition followed by an off-line adjustment, and those which make the adjustment a part of the on-line procedure proper. The discussion covers geometrical as well as numerical considerations and emphasizes practical and methodological aspects which may bring about a higher efficiency of work and a reduction of preparatory operations. (Author)

A82-35141
ALLOWANCE FOR THE EFFECT OF THE ATMOSPHERE IN THE PROCESSING OF SATELLITE REMOTE-SENSING IMAGES [UCHET VLIIANIIA ATMOSFERY PRI OBRABOTKE KOSMICHESKOI VIDEOINFORMATSII]
V. V KOZODEROV and N D LIUBOVNYI In Study of the hydrological cycle by aerospace methods. Moscow, Izdatel'stvo Radio i Sviaz', 1982, p. 90-94. In Russian. refs

A method for the radiative correction of multispectral imagery is proposed which relies on the physicomathematical modeling of the formation of the outgoing-radiation field on the basis of experimental data concerning the distribution of atmospheric aerosol and average statistical data on the distribution of the gaseous constituents of the atmosphere As an example, attention is given to the radiative correction of Meteor-satellite data, realized by a special-purpose image-processing system. B J.

A82-35650* National Aeronautics and Space Administration. Goddard Space Flight Center, Greenbelt, Md
INFLUENCE OF SKY RADIANCE DISTRIBUTION ON THE RATIO TECHNIQUE FOR ESTIMATING BIDIRECTIONAL REFLECTANCE
J. A. KIRCHNER (NASA, Goddard Space Flight Center, Earth Resources Branch, Greenbelt, MD), S YOUKHANA, and J A. SMITH (Colorado State University, Fort Collins, CO) Photogrammetric Engineering and Remote Sensing, vol 48, June 1982, p 955-959. refs
(Contract DACW39-77-C-0073, DARG29-79-C-0199)

The technique of ratioing scene radiance to the radiance obtained from standard Lambertian reference panels in order to estimate bidirectional reflectance factors may depend on the angular distribution of the diffuse irradiance field as well as the direct solar irradiance. A simulation study was performed to estimate the magnitude of this effect for differing clear sky irradiance distributions for a variety of vegetated surfaces. For the seven surfaces and wavelengths analyzed, the error induced in the estimation of bidirectional reflectance factors using the standard ratio technique was less than 5 percent for zenith view and sun angles less than 55 degrees (Author)

A82-35824* Business and Technological Systems, Inc., Seabrook, Md.
APPLICATION OF SATELLITE MAGNETIC ANOMALY DATA TO CURIE ISOTHERM MAPPING
M. A. MAYHEW (Business and Technological Systems, Inc., Seabrook, MD) Journal of Geophysical Research, vol. 87, June 10, 1982, p. 4846-4854 refs
(Contract NAS5-25720)

A82-36043#
THE METEOROLOGICAL PRODUCT - 'CLOUD-TOP HEIGHT'
R. A. BOWEN (ESA, European Space Operations Centre, Darmstadt, West Germany) ESA Bulletin, no. 30, May 1982, p. 16-20.

The rationale for choices made in the method of presenting Meteosat IR and visual imagery to commercial users for visual analyses are examined. IR, at 11 microns, and water vapor (WV), at 6 microns, channels are noted to produce pictures in 2500 x 2500 pixel grids, while the 0.4-11 micron visible channel yields 5000 x 2500 pixel images. It was found necessary to digitally compress every picture by four in both directions for direct transmission to users. A resolution of 20 km was then available at the subsatellite point. Eight grey levels showed clouds above 12,000 m height in 1500 m steps to the 300 m level A correction for the semitransparency of clouds is numerically determined, particularly for overlying cirrus formations. User-activated corrections to images from remote terminals is described. A time lag of a little over two hours existed between Meteosat-1 acquisition and dissemination M.S.K.

A82-36935
SATELLITE RADIATION MEASUREMENTS FOR THE RETRIEVAL OF THE VERTICAL TEMPERATURE PROFILES [PRZETWARZANIE SATELITARNYCH POMIAROW PROMIENIOWANIA NA PIONOWE PROFILE TEMPERATUR]
Z. BUNSCH-MAKAREWICZ, B. BRAUN, and R. GOSS-ZUREK Acta Geophysica Polonica, vol 29, no. 3, 1981, p 235-246. In Polish refs

The physical basis underlying satellite IR determination of vertical temperature profiles in the atmosphere is detailed The earth is treated as a black-body emitting radiation at temperatures dependent only on the concentration, temperature, and absorption coefficient of the absorbents present in the atmosphere Consideration is given to regression analysis, the inverse matrix method, and direct retrieval techniques, noting that regression is preferred as the first choice in all cases and is the only method when transmission properties are not known The level of agreement between derived profiles and measured values is shown to depend on the number of spectral frequency measurements. Good correlations are found, with the in situ data being slightly higher than the satellite figures. Examples are cited from TIROS N and NOAA spacecraft data M S.K.

A82-37048
DESIGN GUIDELINES FOR SATELLITE IMAGE DATA DISTRIBUTION SYSTEMS
D. L. HALL, K H. MILLER, W. T. BISIGNANI, and J. W. VERA (Mitre Corp., McLean, VA) In EASCON '81, Electronics and Aerospace Systems Conventions, Washington, DC, November 16-19, 1981, Record New York, Institute of Electrical and Electronics Engineers, Inc., 1981, p 328-337.

A modular, systems level design for satellite systems which produce images is presented. This is a three-stage, ten-step iterative design technique which applies to the data flow from the sensing instruments through the processing system to the image product users Procedures for converting operational requirements into functional architectures are described. The resulting architectures are translated into a subsystem level design by using an array of building blocks An important feature of this structured approach is the parametric characterization of the interfaces between building blocks. B J.

A82-37200
LANDSAT D TO YIELD MORE PRECISE DATA
C. COVAULT Aviation Week and Space Technology, vol. 117, July 5, 1982, p. 40, 41, 46-48, 51.

The Landsat D spacecraft to be launched in mid 1982 will offer new multispectral and thermal imaging capabilities. The satellite is designed to improve the monitoring of renewable resources and to provide rock discrimination data for mineral and pertroleum geologists The expanded features of the new satellite include a seven-band thematic mapper with spectral ranges from 0.45-0.52 microns to 2.08-2.35 microns and a multispectral scanner capable of higher resolution and spectral fidelity than used in previous Landsats. The development of the Landsat D has been complicated by project changes both in the Space Shuttle and the Tracking and Data Relay Satellite Program, which resulted in an increase in weight (now 4400 lb.), an additional hydrazine tank and narrow band tape recorders Other details on the spacecraft include total array output power of 2200 W, operational altitude of 705 km and launching on a Delta 3920 N.B.

A82-37810*# National Aeronautics and Space Administration Goddard Space Flight Center, Greenbelt, Md.
ADVANCED TECHNOLOGY FOR EARTH OBSERVATION - DATA PROCESSING
P. HEFFNER and E CONNELL (NASA, Goddard Space Flight Center, Mission and Data Operations Directorate, Greenbelt, MD) American Astronautical Society and Deutsche Gesellschaft fuer Luft- und Raumfahrt, Goddard Memorial Symposium on Spacelab, Space Platforms and the Future, 20th, Greenbelt, MD, Mar. 17-19, 1982, AAS 18 p.
(AAS PAPER 82-130)

The Experimental Land Observing System (ELOS) is to demonstrate major advances in space-based land observation. Program success will depend upon successful demonstration of both space-segment performance and ground-system capabilities. Increases in data-rate, volume, and processing requirements present substantial challenges to the ground data processing system. ELOS is based on the utilization of the multispectral linear array (MLA) sensor, a solid-state, electronically scanned instrument. Current MLA instrument designs offer a number of capabilities beyond those provided in the Landsat imaging devices. These capabilities include greater resolution, inherent registration, onboard calibration, off-nadir pointing capability, and fore/aft pointing capability The proposed MLA flight mission scenario will be one of continued growth and will include flights on the Space Transportation System. Attention is also given to ground-to-ground data transport, data capture, and the use of high speed computers G.R

N82-22622*# Herzberg Inst. of Astrophysics, Ottawa (Ontario)
STUDIES OF HIGH LATITUDE CURRENT SYSTEMS USING MAGSAT VECTOR DATA Progress Report, 16 Nov. 1980 - 31 Aug. 1981
J. R. BURROWS, Principal Investigator, T. J. HUGHES, D D. WALLIS, and M. D. WILSON 31 Aug. 1981 19 p Sponsored by NASA ERTS
(E82-10188; NASA-CR-168616; NAS 1.26:168616, PR-3) Avail: NTIS HC A02/MF A01 CSCL 04A

The magnetic disturbance fields caused by global external current systems are considered with particular emphasis on improving the understanding of the physical processes which control high latitude current systems. Following processing the MAGSAT data were routinely plotted in the Universal Time (UT) format as well as in a polar plot format. The H'D'U' coordinate system, was adopted as the standard for representing the MAGSAT residual magnetic field vectors A data file was generated and the TPOLAR computer code was developed to determine from the orbital elements, the time, latitude, and MLT of the extremum latitude of each transpolar segment of orbit. The precision of the vector data set from MAGSAT prompted an extended exploratory phase for data analysis procedures, modeling techniques and phenomenology A.R.H.

N82-22627*# North Carolina State Univ., Raleigh Dept. of Marine, Earth, and Atmospheric Sciences.
MAGSAT AND AEROMAGNETIC DATA IN THE NORTH AMERICAN CONTINENT Progress Report
8 Jun. 1981 2 p ERTS
(Contract NAS5-26157)
(E82-10193; NASA-CR-168620; NAS 1.26:168620) Avail: NTIS HC A02/MF A01 CSCL 05B

Problems were encountered in deriving a proper reference field to be subtracted from the aeromagnetic data obtained from Project MAGNET. Field models tried thus far do not seem to eliminate properly the main field. The MAGSAT data in the North American continent for the period November 1 to December 22, 1979 are being compiled and compared with MAGNET data Efforts are being made to eliminate the orbital bias errors. A computer program was developed and successfully tested which computes a topographic profile of the Curie depth isotherm which fits best to the observed vector or scalar field magnetic data. A.R.H

N82-22629*# Texas Univ at Dallas, Richardson. Center for Space Sciences
INVESTIGATION OF THE EFFECTS OF EXTERNAL CURRENT SYSTEMS ON THE MAGSAT DATA UTILIZING GRID CELL MODELING TECHNIQUES Quarterly Status Technical Progress Report, 1 Apr. - 30 Jun. 1981
D. M. KLUMPAR, Principal Investigator 8 Jul. 1981 12 p ERTS
(Contract NAS5-26309)
(E82-10195; NASA-CR-168622; NAS 1.26:168622, UTD-E0533-01; QSTRP-5) Avail: NTIS HC A02/MF A01 CSCL 05B

Refinements to the modeling procedure developed to compute the magnetic fields at satellite orbit due to current distributions in the ionosphere and magnetosphere are described. The modeling technique utilizes a linear current element representation of the large scale space current system. A model polar current system is presented and magnetic field perturbations resulting from this system are computed along two hypothetical satellite orbits M G

N82-23567*# Business and Technological Systems, Inc., Seabrook, Md.
EQUIVALENT SOURCE MODELING OF THE MAIN FIELD USING MAGSAT DATA Quarterly Report, 1 Jan. - 31 Mar. 1981
31 Mar. 1981 4 p ERTS
(Contract NAS5-26047)
(E82-10151, NASA-CR-168536; NAS 1.26 168536; QR-5) Avail. NTIS HC A02/MF A01 CSCL 05B

Modeling and software development of the main field using MAGSAT data is discussed The cause of the apparent bulge in the power spectrum of Dipole model no. 4 was investigated by simulation with POGO crustal anomaly field model. Results for cases with and without noise, and the spectra of selected reslts are given It is indicated that the beginning of the bump in the spectrum of Dipole no 4 is due to crustal influence, while the departure of the spectrum from that of MGST (12/80-2) around expansion order 17 is due to the resolution limits of the Dipole density. E.A.K.

N82-23570*# Analytic Sciences Corp., Reading, Mass
ANALYSES OF MAGSAT TRACKS CROSSING THE STUDY REGION IN THE INDIAN OCEAN Quarterly Progress Report, 2 Dec. 1980 - 31 Mar. 1981
R. V SAILOR and A. R LAZAREWICZ, Principal Investigators 7 May 1981 15 p ERTS
(Contract NAS5-26424)
(E82-10197; NASA-CR-168624; NAS 1.26 168624; PR-1325-1) Avail: NTIS HC A02/MF A01 CSCL 05B

Progress in software development and in preliminary analysis of MAGSAT tracks crossing the Indian Ocean is reported Tracks crossing the Java Trench, Broken Ridge, the Southeast Indian Ridge, and the Ninetyeast Ridge show that magnetic anomalies correlate with some of these features. Preliminary study of anomaly profiles indicates that tracks of anomaly data (the observations minus a core field model) have a power spectrum decreasing as the inverse square of the spatial frequency. An apparent noise floor of about one to two gammas rms is reached at wavelengths of about 360 km, corresponding to approximately 10 samples of the decimated Investigator tape data at a sampling rate of approximately 4.9 sec/sample. J D.

N82-23572*# Business and Technological Systems, Inc., Seabrook, Md.
MAGSAT SCIENCE INVESTIGATIONS Quarterly Report
1982 3 p ERTS
(Contract NAS5-26328)
(E82-10199; NASA-CR-168626) Avail NTIS HC A02/MF A01 CSCL 05B

Progress in the development and modification of software to accommodate total field anomaly data and for spectral analysis of aeromagnetic profile data and computation of depth to magnetic bottom is reported. J.D.

N82-23574*# Applied Physics Lab., Johns Hopkins Univ., Laurel, Md
INVESTIGATION OF MAGSAT AND TRIAD MAGNETOMETER DATA TO PROVIDE CORRECTIVE INFORMATION ON HIGH-LATITUDE EXTERNAL FIELDS Progress Report, 1 Jul. - 30 Sep. 1981
T A. POTEMRA, Principal Investigator 4 Nov 1981 10 p Sponsored by NASA Original contains color imagery. Original photography may be purchased from the EROS Data Center, Sioux Falls, S D. 57198 ERTS
(E82-10201; NASA-CR-168628; NAS 1.26:168628) Avail: NTIS HC A02/MF A01 CSCL 04A

The compilation of a catalog of the MAGSAT-observed high altitude disturbances is discussed and an example of contents and format is given. The graphs allow the investigation of Birkeland current signatures which are superimposed upon the main geomagnetic field. An example of a display of the MAGSAT orbital tracks in a polar geomagnetic coordinate system with the locations, flow directions, and intensities of field aligned currents shown in color is also given. The display was generated using an interactive color graphics terminal. M.G

N82-23575*# Indian Inst. of Geomagnetism, Bombay
MAGSAT FOR GEOMAGNETIC STUDIES OVER INDIAN REGION Progress Report, 1 Jan. - 31 Oct. 1981
R G. RASTOGI, B. N. BHARGAVA, B. P. SINGH, D. R. K RAO, G. K. RANGARAJAN, R. RAJARAM, M ROY, B. R. ARORA, and A SETH, Principal Investigators 31 Oct. 1981 42 p refs Sponsored by NASA ERTS
(E82-10202; NASA-CR-168629; NAS 1.26.168629, PR-1) Avail: NTIS HC A03/MF A01 CSCL 08G

Progress in the preparation of software for converting data tapes produced on an IBM system to data readable on a DEC-10 system, in the creation of awareness of the utility of MAGSAT data among users in India, and in making computer programs supplied by NASA operational on the DEC-10 system is reported Papers presented to Indian users, at the IAGA fourth scientific assembly, at a symposium on interdisciplinary approaches to geomagnetism, and a paper published in Science Today are included. J.D

N82-23576*# Institute of Geological Sciences, Edinburgh (Scotland).
SPHERICAL HARMONIC REPRESENTATION OF THE MAIN GEOMAGNETIC FIELD FOR WORLD CHARTING AND INVESTIGATIONS OF SOME FUNDAMENTAL PROBLEMS OF PHYSICS AND GEOPHYSICS Progress Report
D R. BARRACLOUGH, R. HIDE (Meteorological Office), B. R. LEATON, F J. LOWES (Newcastle-Upon-Tyne Univ.), S. R. C MALIN, and R. L. WILSON, Principal Investigators (Liverpool Univ.) 1 Jun. 1981 4 p Sponsored by NASA ERTS
(E82-10203; NASA-CR-168630; NAS 1.26:168630) Avail: NTIS HC A02/MF A01 CSCL 08G

The data processing of MAGSAT investigator B test tapes and data tapes, and tapes of selected data on 15 magnetically quiet days is reported. The 1980 World Chart spherical model was compared with the MAGSAT (3/80) and MAGSAT vector data were used in the models. An article on modelling the geomagnetic field using satellite data is included. T M.

N82-23583*# Geological Survey, Denver, Colo
REGISTRATION OF HEAT CAPACITY MAPPING MISSION DAY AND NIGHT IMAGES
K. WATSON, S. HUMMER-MILLER, and D. L SAWATZKY, Principal Investigators 1982 17 p refs Submitted for publication Sponsored by NASA Original contains imagery. Original imagery may be purchased from NASA, Goddard Space Flight Center, (code 601), Greenbelt, Md. 20771. Domestic users send orders to 'Attn: National Space Science Data Center'; non-domestic users send orders to 'Attn World Data Center A for Rockets and Satellites'. HCMM
(E82-10210; NASA-CR-168773) Avail: NTIS HC A02/MF A01 CSCL 05B

Neither iterative registration, using drainage intersection maps for control, nor cross correlation techniques were satisfactory in registering day and night HCMM imagery A procedure was developed which registers the image pairs by selecting control points and mapping the night thermal image to the daytime thermal and reflectance images using an affine transformation on a 1300 by 1100 pixel image. The resulting image registration is accurate to better than two pixels (RMS) and does not exhibit the significant misregistration that was noted in the temperature-difference and thermal-inertia products supplied by NASA. The affine transformation was determined using simple matrix arithmetic, a step that can be performed rapidly on a minicomputer. A.R H.

N82-23584*# Geological Survey, Denver, Colo.
GROUND SUPPORT DATA FROM JULY 10 TO JULY 29, 1978, FOR HCMM THERMAL SATELLITE DATA OF THE POWDER RIVER BASIN, WYOMING
S. HUMMER-MILLER, K WATSON, and R. KIPFINGER, Principal Investigators 1980 48 p refs Sponsored by NASA HCMM
(E82-10211, NASA-CR-168772, NAS 1 26.168772;
USGS-OFR-80-469) Avail: NTIS HC A03/MF A01 CSCL 08I

Radiometric and meteorological data acquired at three ground stations located approximately 150 km apart in the Powder River Basin, Wyoming, are summarized. The data were collected between July 10 and July 29, 1978, to support the HCMM thermal satellite data acquired during this time period. The parameters measured are direct solar radiance, total solar radiance, sky radiance, air temperature, relative humidity, wind speed, and wind direction A tabulation of the measurement accuracies is presented J.D.

N82-23586*# Purdue Univ., Lafayette, Ind Lab. for Applications of Remote Sensing.
MULTISTAGE CLASSIFICATION OF MULTISPECTRAL EARTH OBSERVATIONAL DATA: THE DESIGN APPROACH
M E. BAUER, Principal Investigators, M. J. MUASHER, and D. A LANDGREBE Dec. 1981 181 p refs Sponsored by NASA, USDA, Dept. of Commerce, Dept. of the Interior, and Agency for International Development ERTS
(Contract NAS9-15466; PROJ. AGRISTARS)
(E82-10213; NASA-CR-167508; NAS 1.26:167508, LARS-101481; SR-P1-04194) Avail: NTIS HC A09/MF A01 CSCL 02C

An algorithm is proposed which predicts the optimal features at every node in a binary tree procedure. The algorithm estimates the probability of error by approximating the area under the likelihood ratio function for two classes and taking into account the number of training samples used in estimating each of these two classes. Some results on feature selection techniques, particularly in the presence of a very limited set of training samples, are presented. Results comparing probabilities of error predicted by the proposed algorithm as a function of dimensionality as compared to experimental observations are shown for aircraft and LANDSAT data. Results are obtained for both real and simulated data. Finally, two binary tree examples which use the algorithm are presented to illustrate the usefulness of the procedure.
Author

N82-23596*# Lockheed Engineering and Management Services Co., Inc, Houston, Tex
EVALUATION OF VICAR SOFTWARE CAPABILITY FOR LAND INFORMATION SUPPORT SYSTEM NEEDS
S. S. YAO, Principal Investigator Sep 1981 19 p Sponsored by NASA, USDA, Dept of Commerce, Dept of the Interior, and Agency for International Development ERTS
(Contract NAS9-15800; PROJ. AGRISTARS)
(E82-10223; NASA-CR-167442; JSC-17431; NAS 1.26:167442; LEMSCO-17269, RR-L1-17269) Avail: NTIS HC A02/MF A01 CSCL 09B

A preliminary evaluation of the processing capability of the VICAR software for land information support system needs is presented. The geometric and radiometric properties of four sets of LANDSAT data taken over the Elk River, Idaho quadrangle were compared. Storage of data sets, the means of location, pixel resolution, and radiometric and geometric characteristics are described. Recommended modifications of VICAR programs are presented. J.D.

N82-23599*# Texas Univ. at Dallas. Center for Space Sciences.
INVESTIGATION OF THE EFFECTS OF EXTERNAL CURRENT SYSTEMS ON THE MAGSAT DATA UTILIZING GRID CELL MODELING TECHNIQUES Quarterly Status Technical Progress Report, 1 Oct. - 31 Dec. 1981
D. M. KLUMPAR, Principal Investigator 9 Jan. 1982 10 p ERTS
(Contract NAS5-26309)
(E82-10226; NASA-CR-168800; NAS 1.26:168800, QSTPR-5)
Avail: NTIS HC A02/MF A01 CSCL 05B

Efforts in support of the development of a model of the magnetic fields due to ionospheric and magnetospheric electrical currents are discussed. Specifically, progress made in reading MAGSAT tapes and plotting the deviation of the measured magnetic field components with respect to a spherical harmonic model of the main geomagnetic field is reported Initial tests of the modeling procedure developed to compute the ionosphere/magnetosphere-induced fields at satellite orbit are also described. The modeling technique utilizes a liner current element representation of the large scale current system M G

N82-23605*# Texas Univ. at Dallas. Center for Space Sciences.
INVESTIGATION OF THE EFFECTS OF EXTERNAL CURRENT SYSTEMS ON THE MAGSAT DATA UTILIZING GRID CELL MODELING TECHNIQUES Quarterly Status Technical Progress Report, 1 Jul. - 30 Sep. 1981
D. M. KLUMPAR, Principal Investigator 12 Oct. 1981 9 p Original contains color imagery. Original photography may be purchased from the EROS Data Center, Sioux Falls, S.D. 57198. ERTS
(Contract NAS5-26309)
(E82-10232; NASA-CR-168801, NAS 1.26:168801; QSTPR-4)
Avail: NTIS HC A02/MF A01 CSCL 08G

Progress is reported in reading MAGSAT tapes in modeling procedure developed to compute the magnetic fields at satellite orbit due to current distributions in the ionosphere. The modeling technique utilizes a linear current element representation of the large-scale space-current system Author

N82-23612*# Tokyo Univ (Japan).
INVESTIGATION FROM JAPANESE MAGSAT TEAM Progress Report, 15 Mar. 1980 - 15 Jul. 1981
N. FUKUSHIMA, Principal Investigator 20 Jul. 1981 10 p Sponsored by NASA ERTS
(E82-10239, NASA-CR-168755; NAS 1.26:168755, PR-3) Avail: NTIS HC A02/MF A01 CSCL 05B

The acquisition of tapes which contain vector and scalar data decimated at an interval of 0.5 sec, together with time and position data, is reported. Progress in the study of magnetic anomalies in the vicinity of Japan and in electric currents in the ionosphere and magnetosphere is also reported. MAGSAT data was used in obtaining a map of total force anomaly for the area of latitude 10-70 deg N and longitude 110-170 deg E. One of the outstanding features in the map of the magnetic anomaly is a negative magnetic anomaly in the Okhotsk Sea, which is of geophysical interest because of its possible connection with high heat flow values in that area. T M

N82-23613*# Miami Univ., Fla School of Marine and Atmospheric Science
INVESTIGATIONS OF MEDIUM WAVELENGTH MAGNETIC ANOMALIES IN THE EASTERN PACIFIC USING MAGSAT Interim Report, Jul. - Sep. 1981
C. G A. HARRISON, Principal Investigator Nov. 1981 2 p Sponsored by NASA ERTS
(E82-10240; NASA-CR-168756; NAS 1.26.168756) Avail: NTIS HC A02/MF A01 CSCL 08G

Progress in study of the details of spherical harmonic representations of the Earth's magnetic field is reported The first of the Investigator B quiet time tapes were received and determined to be error free. J.D.

N82-24517# Technische Hogeschool, Delft (Netherlands). Lab. of Engineering Mechanics.
NONLINEAR THEORY FOR ELASTIC BEAMS AND RODS AND ITS FINITE ELEMENT REPRESENTATION
J. F. BESSELING Oct. 1981 25 p refs
(WTHD-143) Avail: NTIS HC A02/MF A01

Expressions for large curvatures of elastic beams and rods are given in terms of displacement components and angular coordinates. The application of these expressions to bifurcation and stability problems, based on the principle of virtual work is discussed This approach is compared with another finite element representation, and an error in this representation is corrected. The condition of zero extension of the axis in the case of the Euler column is shown to require division into a large number of finite elements in order to ensure an accurate result for the stability coefficient. The conditions of zero extension of the axis and zero curvature about one principal axis of the cross section in the case of the lateral buckling of the end loaded cantilever have similar consequences. Author (ESA)

N82-24570*# Survey of India, Dehra Dun. Geodetic and Research Branch.
REPORT OF MAGSAT PROJECT BY SURVEY OF INDIA Status Report
J. L. SAWHNEY 18 Aug. 1981 4 p refs Sponsored by NASA ERTS
(E82-10293; NASA-CR-168916; NAS 1.26:168916) Avail: NTIS HC A02/MF A01 CSCL 08G

Magsat data fo quiet days for the period 4.11.79, 17.11.79 to 24.11.79, which pertains to 44 passes, was screened to exclude the the period of exclude the period of maximum diurnal variation The results of this screening process is a data set that has the effect, (or at least the major part of the effect), of the external field removed from it. Such a data set is the basis for further analysis which is in hand. The data set is now being reduced to horizontal plane. The mathematical techniques uses a finite harmonic series representation of the three dimensional data, combined with least squares approach for the solution of coefficients. A computer programme was developed to reduce satellite data to a common elevation A.R.H.

N82-24572*# Indian Inst. of Geomagnetism, Bombay.
MAGSAT FOR GEOMAGNETIC STUDIES OVER INDIAN REGION Progress Report, 1 Nov. 1981 - 31 Mar. 1982
R. G. RASTOGI, B P SINGH, D. R. K RAO, G K. RANGARAJAN, R. RAJARAM, M ROY, and B. R. ARORA, Principal Investigators 1 Apr 1982 5 p ERTS
(E82-10296; NASA-CR-168865; NAS 1.26.168865; M-38; PR-2)
Avail: NTIS HC A02/MF A01 CSCL 08G

The major activities of the period are summarized. Data tapes generated on an IBM system were read on DEC-10 system new tapes compatible with DEC-10 system were prepared for data

sections of interest. Core and external current contributions were removed from selected passes over the Indian region and the residuals analyzed. Possible equatorial electrojet contributions to the MAGSAT data were studied. J.D.

N82-24580*# Texas Univ. at Dallas, Richardson. Center for Space Sciences
INVESTIGATION OF THE EFFECTS OF EXTERNAL CURRENT SYSTEMS ON THE MAGSAT DATA UTILIZING GRID CELL MODELING TECHNIQUES Quarterly Status Technical Progress Report, 1 Jan. - 31 Mar. 1982
D M. KLUMPAR, Principal Investigator 27 Apr. 1982 11 p ERTS
(Contract NAS5-26309)
(E82-10306, NASA-CR-168881; NAS 1.26:168881; STPR-6)
Avail: NTIS HC A02/MF A01 CSCL 05B

Progress made in reducing MAGSAT data and displaying magnetic field perturbations caused primarily by external currents is reported. A periodic and repeatable perturbation pattern is described that arises from external current effects but appears as unique signatures associated with upper middle latitudes on the Earth's surface Initial testing of the modeling procedure that was developed to compute the magnetic fields at satellite orbit due to current distributions in the ionosphere and magnetosphere is also discussed. The modeling technique utilizes a linear current element representation of the large scale space current system. M.G

N82-24581*# North Carolina State Univ., Raleigh Dept. of Marine, Earth and Atmospheric Sciences.
MAGSAT SCALAR AND VECTOR ANOMALY DATA ANALYSIS Progress Report, period ending 31 Jan. 1982
1 Feb. 1982 1 p ERTS
(Contract NAS5-26157)
(E82-10307; NASA-CR-168882; NAS 1 26:168882) Avail: NTIS HC A02/MF A01 CSCL 08B

Efforts on the analysis of MAGSAT scalar anomaly data, the application of the scalar analysis results to three component vector data, and the comparison of MAGSAT data with corresponding MAGNET aeromagnetic and free air gravity anomaly data are briefly described M.G.

N82-24588*# Zentralstelle fuer Geo-Photogrammetrie und Fernerkundung, Munich (West Germany).
MULTIDISCIPLINARY INVESTIGATIONS ON HCMM DATA OVER MIDDLE EUROPE AND MAROCCO Final Report, 1979 - 1981
R. HAYDN, Principal Investigator, G DALKE, J. HENKEL, and H. KAUFMANN 10 Mar. 1982 86 p Sponsored by NASA, Deutsche Forschungsgemeinschaft and Bundesministerium fuer Forschung und Technologie Original contains color imagery. Original imagery may be purchased from NASA Goddard Space Flight Center, (code 601), Greenbelt, Md. 20070. Domestic users send orders to 'Attn: National Space Science Data Center', nondomestic users send orders to 'Attn World Data Center A for Rockets and Satellites'. HCMM
(E82-10315; NASA-CR-168910, NAS 1.26:168910) Avail: NTIS HC A05/MF A01 CSCL 05B

The development approaches in presenting HCMM data in combination with LANDSAT for improved interpretability is presented. The techniques are based on the IHS (intensity hue and saturation) concept which permits the calculation of LANDSAT/HCMM merges exhibiting the high spatial resolution of LANDSAT along with the HCMM thermal recordings coded into perceivable and interpretable colors. A further approach is based on the calculation of synthetic LANDSAT stereo images showing HCMM thermal recording as a quasitopography. The feasibility of these approaches are discussed on the tests The feasibility of these approaches are discussed on the basis of HCMM and LANDSAT images representing the test sites. On the basis of a scene covering an area of the Anti Atlas, the relationship between geological phenomena and their interpretability via LANDSAT/HCMM merged products. E.A.K.

N82-24595*# Tokyo Univ. (Japan). Geophysics Research Lab.
REPORT OF INVESTIGATION FROM JAPANESE MAGSAT TEAM Progress Report, 1 Dec. 1981 - 30 Mar. 1982
N. FUKUSHIMA, H. MAEDA, T. YUKUTAKE, M. TANAKA, S OSHIMA, K. OGAWA, M. KAWAMURA, Y. MIYAZAKI, S UYEDA, K KOBAYASHI, Principal Investigatorset al. 5 Apr. 1982 13 p refs Submitted for publication ERTS
(E82-10322, NASA-CR-168901, NAS 1.26:168901, PR-5) Avail: NTIS HC A02/MF A01 CSCL 08G

Progress in the data processing and data acquisition of computer compatible MAGSAT tapes is reported. Investigations focused on the crustal structure near Japan and its Antarctic station, and electric currents and hydrodynamic waves in the ionosphere and the magnetosphere The magnetization of the crust in the northwestern Pacific region is discussed. T.M

N82-24600*# Paris VI Univ (France).
MODELS AND MAPS OF THE MAIN FIELD Progress Report
J L LEMOUEL, Principal Investigator, C. GIRE, and J. DUCRUIX 1 Apr 1982 13 p refs Sponsored by NASA ERTS
(E82-10327; NASA-CR-168906; NAS 1 26:168906) Avail: NTIS HC A02/MF A01 CSCL 08B

The difference between the models comes from the difference in the procedures of data selection and depends on the aim the model is intended for: regional studies necessitates locally higher density of data and for downward continuation the reduction of external variations must be as careful as possible. Refinements of preliminary models MAGP1 and MAGP2 are presented. Models MAGP1 and MAGP2 are found to have drawbacks coming from insufficient reduction of the external variations and from the inhomogeneity in the distribution of the measurement points. New analysis was performed to overcome these shortcomings The quality of the new models is characterized by the average rms of the differences measurement model. T.M.

N82-25611# University of Southern California, Los Angeles. Image Processing Inst.
IMAGE UNDERSTANDING RESEARCH Final Technical Report, 1 Apr. - 30 Sep. 1981
R. NEVATIA and A. A. SAWCHUK 30 Sep. 1981 138 p refs
(Contract F33615-80-C-1080; DARPA ORDER 3119)
(AD-A110746; USCIPI-1050) Avail: NTIS HC A07/MF A01 CSCL 05H

This technical report summarizes the image understanding and VLSI system research activities performed by the University of Southern California and the Hughes Research Laboratories during 1 April 1981 through 30 September 1981 under contract number F-33615-80-C-1080 with the Defense Advanced Research Projects Agency, Information Processing Techniques Office. The purpose of this research program is to develop techniques and systems for understanding images, particularly for mapping applications. The research activity includes low level image analysis and feature extraction, statistical and structural texture analysis, symbolic image representations, and image to map correspondence using relational structures Additional activity is concerned with VLSI architectures for implementation of image analysis and image understanding operations. GRA

N82-25612# Defense Mapping Agency Aerospace Center, St. Louis, Mo. Aerospace Cartography Dept
MATRIX DATA ANALYSIS: COLOR/B AND W CODING IS NOT ALWAYS ENOUGH Interim Report, 1976 - 1981
M. B. FAINTICH, G. B. SIGLER, and J. D. SIMPSON 1981 31 p refs Presented at the Inter-Congr. Symp., Inter. Soc. of Phot and Remote Sensing Comm 3, Otaniemi, Finland, 7-11 Jun. 1982
(AD-A111401) Avail NTIS HC A03/MF A01 CSCL 08B

The Defense Mapping Agency produces digital data bases that describe the physical appearance of the surface of the Earth These data bases include, but are not limited to, terrain elevation, culture including landscape characteristics and vertical features. This data is collected from digitized source maps, from optically or digitally correlated stereo-pairs of photographic imagery, and

from digital multi-spectral sensor data. A dramatic impact has been made in the ability to analyze these digital data bases by applying state-of-the-art digital image technology processing and display concepts. These include a variety of color and/or black and white displays of not only intensity/color coded matrix data, but also image processed data using specialized convolution filters, texture discrimination, and special color representation techniques. In addition, computer generated imagery from these data bases serves as a final analysis tool. GRA

N82-25613# Measurement Concept Corp , Rome, N. Y.
SOURCE ASSESSMENT SYSTEM Final Technical Report
R. H. SENN, M L. TAYLOR, R BURNS, and M SMITH Griffiss AFB, N.Y. RADC Nov 1981 153 p refs
(Contract F30602-80-C-0040, AF PROJ. 4303)
(AD-A111223; RADC-TR-81-303) Avail: NTIS HC A08/MF A01 CSCL 09B

This report contains an analysis of the Source Assessment Procedures at both Defense Mapping Agency (DMA) production facilities (Aerospace Center DMAAC in St. Louis MO and Hydrographic Topographic Center DMAHTC in Washington DC). Following the analysis, the report documents a design trade off of various approaches to a Source Assessment System. Finally, a Design Plan for the selected approach analog-digital video system, is presented. Author (GRA)

N82-25614# Army Engineer Topographic Labs., Fort Belvoir, Va.
COORDINATION OF STEREO IMAGE REGISTRATION AND PIXEL CLASSIFICATION Computer Sciences Lab.
M. A. CROMBIE 20 Mar. 1982 10 p refs Presented at the ACSM-ASP Ann. Conv., Denver, 1982
(AD-A111307; ETL-R034) Avail: NTIS HC A02/MF A01 CSCL 14E

An inadequate concept of how corresponding points relate to one another on dissimilar images has a greater effect than exposure geometry or data collection on registration problems in stereo photogrammetry Conventional correlation, or one of its relatives, is the measure of similarity used in all automated stereo correlation systems. Correlation, a measure of the linear dependence between two sets of data, is an inadequate measure when there is less than, or more than, a moderate amount of image structure at and around points selected for image matching. The existence of structure should be recognized and utilized in an appropriate manner for image matching Similarly, the absence of structure should be recognized, and the surrounding imagery should be used to complete matches where it is possible. The concurrent determination of what a pixel is, as well as where it is, can alleviate much of the registration problem. A variety of features including point-density data, texture, and edges, as well as existing cartographic knowledge, can be combined and organized through rules in order to more completely describe a point. The overall throughput of the compilation process will be improved in both time and accuracy if those functions which tend to support one another are concurrently, rather than sequentially, performed. If the compilation process takes place in image space, then the image matching operation as well as the other feature extraction operations, can be ordered by the data processing manager to best suit the function of the process Author (GRA)

N82-26027# Instituto de Pesquisas Espaciais, Sao Jose dos Campos (Brazil).
SMS/GOES DATA COLLECTION PLATFORM SYSTEM [PLATFORMA DE COLETA DE DADOS SISTEMA SMS/GOES]
V. RODRIGUES *In its* Minutes of the 1st Seminar on Use of the Natl System for Collection of Satellite Data p 21-30 Jul. 1981 In PORTUGUESE
Avail NTIS HC A12/MF A01

The SMS/GOES synchronous meteorological satellite system, consisting of the satellite, ground stations, and data collection platforms, is described. The objectives of the system and the services it performs are listed. Applications of the data collection platforms are surveyed and the platforms described The parameters of the data collected are listed. Transl by J.D

N82-26037# European Space Agency, Toulouse (France). METEOSAT Data Management Dept
THE METEOSAT DATA COLLECTION SYSTEM AND ITS APPLICATION
A ROBSON and H. HOVET *In* Instituto de Pesquisas Espaciais 1st Seminar on Use of the Natl. System for Collection of Satellite Data p 191-206 Jul. 1981
Avail: NTIS HC A12/MF A01

The METEOSAT data collection system and its applications are described Use of the system for collection of meteorological data at remote land sites in Greenland, for meteorological and sea state monitoring at offshore sites in the North and Baltic Seas, for hydrological monitoring in Great Britain, and for meteorological data collection from aircraft is discussed. J.D.

N82-26756*# Survey of India, Dehra Dun.
ANALYSIS OF MAGSAT DATA OF THE INDIAN REGION Progress Report, 10 Jan. 1981 - 1 Feb. 1982
K L. KHOSLA, Principal Investigators, M G ARUR, S R. M. GUPTA, S. P. S BAINS, S. J. LAL, J. G NEGI (NGRI), P. K. AGARWAL (NGRI), B. N. P. AGARWAL (Indian School of Mines), and B. SAHAI (Space Application Centre, Ahmedabad, India) 31 Mar. 1982 3 p refs Sponsored by NASA ERTS
(E82-10358; NASA-CR-168979; NAS 1.26 168979; REPT-2; REPT-3) Avail NTIS HC A02/MF A01 CSCL 05B

Progress in the development of software for reading MAGSAT data tapes and for the reduction of anomaly data, and in the preparation of data for magnetic anomaly maps is reported J D.

N82-26763*# Environmental Systems Research Inst., Redlands, Calif
EXPLORATION INTO TECHNICAL PROCEDURES FOR VERTICAL INTEGRATION Final Contractor Report
R. J. MICHEL and K D MAW Sep. 1979 29 p refs
(Contract NASA ORDER A-65111-B)
(NASA-CR-166352; NAS 1.26:166352) Avail. NTIS HC A03/MF A01 CSCL 08G

Issues in the design and use of a digital geographic information system incorporating landuse, zoning, hazard, LANDSAT, and other data are discussed. An eleven layer database was generated. Issues in spatial resolution, registration, grid versus polygonal structures, and comparison of photointerpreted landuse to LANDSAT land cover are examined. Author

N82-26765# Earth Satellite Corp., Washington, D C.
EXPERIMENTAL ASSESSMENT OF IMPROVED SPATIAL RESOLUTION LANDSAT DATA Final Report
C. SHEFFIELD, M PLACE, D GAROFALO, J. DYKSTRA, and L. HALL Ft Belvoir, Va. ETL 30 Sep. 1981 82 p refs
(Contract DAAK70-80-C-0016)
(AD-A110538, E/S-1234; ETL-0268) Avail: NTIS HC A05/MF A01 CSCL 14E

This report describes the possible uses of higher resolution (25 meter) space-derived images for delineating and measuring surface features of interest in the Corps of Engineers' Civil Works Program Following a discussion of imaging sensors and computer processing methods, test evaluations are described in which LANDSAT multispectral scanner data and SEASAT SAR data were interpreted for surface features. The comparative advantages of the two data sources are discussed, and the complementary nature of LANDSAT MSS and SEASAT SAR images is displayed in the image analyses. Image examples are included for both background discussion and test site evaluation. Author (GRA)

N82-26907# Massachusetts Univ., Amherst. Astronomy Research Facility.
STRATOSPHERIC EMISSION DATA ANALYSIS Final Report, 1 Jan. 1979 - 31 Jan. 1982
H. SAKAI Feb. 1982 32 p refs
(Contract F19628-79-C-0062; AF PROJ. 2310)
(AD-A112337; UMASS-ARF-82-321; AFGL-TR-82-0055) Avail: NTIS HC A03/MF A01 CSCL 04A

The work described in this report constitutes a data-processing and data analysis part of the AFGL SCRIBE (Stratospheric Cryogenic Interferometer Balloon Experiment) program. This work may be summarized into three major categories: (1) extraction of the interferogram data from the PCM telemetry data tape, (2) processing of the interferogram data for spectral retrieval; and (3) analysis of the obtained atmospheric emission data. GRA

08

INSTRUMENTATION AND SENSORS

Includes data acquisition and camera systems and remote sensors.

A82-22608
IS THE NEON COMPOSITION OF OUR SUN, PLANETARY OR SOLAR
M. N. RAO, C. M. NAUTIYAL, and T. R. VENKATESAN (Physical Research Laboratory, Ahmedabad, India) In. International Cosmic Ray Conference, 17th, Paris, France, July 13-25, 1981, Conference Papers. Volume 3. Gif-sur-Yvette, Essonne, France, Commissariat a l'Energie Atomique, 1981, p. 141-144. refs

The surficial solar wind from the feldspar grain-size separates of lunar soils is removed by selective chemical etching to determine whether the long term average solar flare Ne composition is planetary or solar. Mineral residues mostly containing solar flare implanted noble gas components are analyzed by step wise gas release mass spectrometric methods. Results do not show any major differences in the Ne ratios of solar flares and solar wind, and the long term average composition of low energy solar flares implanted Ne is similar to solar wind neon instead of planetary, although variations of Ne isotopic ratios in solar flares over short time scales is not ruled out D.L G.

A82-29541
AN INFRARED EXPOSURE METER
R. W. DANA (U.S. Forest Service, Fort Collins, CO) In: Color aerial photography in the plant sciences and related fields; Proceedings of the Eighth Biennial Workshop, Luray, VA, April 21-23, 1981. Falls Church, VA, American Society of Photogrammetry, 1981, p. 145-156. refs

It is noted that, since the commonly used color infrared aerial film has less latitude to variations in scene brightness than most normal color films, camera exposure adjustment is crucial in the infrared aerial photography of natural resources A description is given of a spotmeter sensitive in the wavelength band of infrared films developed to aid the aerial photographer in adjusting camera settings for optimum exposure of a variety of scenes. Also discussed are airborne tests undertaken to evaluate the meter for agricultural, forest, and range cover. The problems encountered in using photographic photometry to evaluate luminance readings from a hand-held instrument fall into three groups: instrument pointing problems, film sensitometry, and camera calibration. The optimum exposure for quantitative density analysis is thought to be about three-fourths of a stop lower than for visual interpretation. The results of regression analysis suggest that the infrared meter marks an improvement over conventional spotmeters in predicting the infrared response of the film. C.R.

A82-29922
THERMOGRAPHY - A REMOTE SENSING METHOD WITH MANY PERSPECTIVES [THERMOGRAFIE - EINE PERSPEKTIVREICHE FERNERKUNDUNGSMETHODE]
A. GESCHKE (Gesellschaft fuer Internationalen Flugverkehr mbH, Berlin, East Germany) Technisch-oekonomische Information der zivilen Luftfahrt, vol. 17, no. 4, 1981, p 169-171. In German.

Thermography, as considered in this report, is concerned with the utilization of the electromagnetic radiation of the far-infrared region for the formation of images. Possibilities for such a utilization improved greatly with the development of cooled semiconductor sensing devices during the last twenty years. Thermographs were designed as far-infrared image-forming devices which provide a thermal photograph by scanning a far-infrared image of an object or a scene. A description is provided of investigations in which such devices, carried on board of a helicopter or a fixed-wing aircraft, were used to obtain thermal images of an area on the ground. Thermography is found to be a valuable approach for the study of energetic aspects, geologic structures, groundwater budget questions, the vitality of forests and agricultural areas, and water pollution. G R

A82-31019
LARGE AMPLITUDE UNDULATIONS ON THE EQUATORWARD BOUNDARY OF THE DIFFUSE AURORA
A. T. Y. LUI, C.-I. MENG, and S. ISMAIL (Johns Hopkins University, Laurel, MD) Journal of Geophysical Research, vol. 87, Apr 1, 1982, p. 2385-2400. refs
(Contract AF-AFOSR-79-0010, NSF ATM-79-23240; NSF ATM-79-25987)

A description is presented of the first observation of large scale undulations in the equatorward boundary of the diffuse aurora by pictures of global auroral displays in the afternoon-evening sector. These observations are made by a broad band scanning radiometer on the Defense Meteorological Satellite Program (DMSP) satellites. Attention is given to four periods during which the equatorward boundary of the diffuse aurora is undulated Three of these are taken in the southern polar region and one in the northern polar region. The duration of the undulations is considered along with geomagnetic and interplanetary conditions. All undulations are found to occur during the period of a geomagnetic storm near the peak development of the storm-time ring current. All are accompanied by substorm patterns of discrete auroras. G.R

A82-31020
EXTREMELY HIGH LATITUDE AURORAS
M. S. GUSSENHOVEN (Boston College, Chestnut Hill, MA) Journal of Geophysical Research, vol. 87, Apr. 1, 1982, p. 2401-2412 refs
(Contract F19628-81-K-0032; AF-AFOSR-79-0012)

It is pointed out that imaging devices on the polar orbiting ISIS and Defense Meteorological Satellite Program (DMSP) satellites have greatly increased the extent of polar cap and auroral zone coverage and have prompted several studies of polar cap arcs. A description is presented of a statistical study of the occurrence conditions for arcs recorded in DMSP images at extremely high latitudes, taking into account corrected geomagnetic latitudes equal to or greater than 80 deg. The 80 deg boundary is chosen to minimize the problems associated with defining a polar cap boundary Attention is given to the data base and categorization of extremely high latitude auroras, the relationship to magnetic activity, and the relationship to solar wind conditions. It is found that one category of extremely high latitude auroras is distinctly different from the rest. This category includes the oval auroras which expand poleward in the midnight sector G.R.

A82-31991
A SYSTEM DESIGN FOR A MULTISPECTRAL SENSOR USING TWO-DIMENSIONAL SOLID-STATE IMAGING ARRAYS
R. M. HODGSON (Canterbury, University, Christchurch, New Zealand), F. M CADY (Montana State University, Bozeman, MT), and D PAIRMAN (Department of Scientific and Industrial Research, Physics and Engineering Laboratories, Lower Hutt, New Zealand) IEEE Transactions on Geoscience and Remote Sensing, vol. GE-20, Apr 1982, p. 177-179 Research supported by the University of Canterbury and University Grants Committee. refs

A system developed for remote sensing from light aircraft in the 400-1100 nm wavelength range possesses an architecture which permits the simultaneous capture of up to four images from solid-state, two-dimensional image sensors In operation, the array sensor captures a series of relatively rapid, approximately 10 msec exposures at intervals as long as 10 sec. This mode of operation has the advantage of nearly the same degree of distortion due to aircraft roll in all image elements. The software generation of sensor drive signals is incorporated in the system. O C.

A82-32440
IMAGING SPECTROSCOPY; PROCEEDINGS OF THE SEMINAR, LOS ANGELES, CA, FEBRUARY 10, 11, 1981
D. D. NORRIS, (ED.) (California Institute of Technology, Jet Propulsion Laboratory, Pasadena, CA) Seminar sponsored by SPIE - The International Society for Optical Engineering. Bellingham, WA, SPIE - The International Society for Optical Engineering (SPIE Proceedings. Volume 268), 1981 204 p
MEMBERS, $34.; NONMEMBERS, $40

The seminar concentrated on the science applications of spectral imaging, multispectral imaging sensors, and spectral filtering. Papers are presented on spectroscopic remote sensing for geological applications, spectral mapping of Jupiter, system design of an interferometer imaging sounder and a common module imaging spectral radiometer. Other topics discussed include the performance and application of an intensified linear self-scanned array instrument, tunable optical filtering using an interferometer for selective modulation, design studies for a spectrally agile staring sensor system, and acousto-optic tunable filters for high-resolution spectral analysis. V L.

A82-32443* Columbia Univ , New York
HIGH SPECTRAL RESOLUTION AIRBORNE SPECTROMETRY
W. COLLINS, S. CHANG, J T. KUO (Columbia University, New York, NY), M. DOUMA, S. MARSHALL (Massachusetts Manufacturing Corp., Cambridge, MA), and P. MURPHY (Sanders Associates, Inc., Nashua, NH) In: Imaging spectroscopy; Proceedings of the Seminar, Los Angeles, CA, February 10, 11, 1981 Bellingham, WA, SPIE - The International Society for Optical Engineering, 1981, p 22-28
(Contract JPL-955832; NSF ENG-78-24432)

An airborne spectroradiometer system developed at Columbia University has been providing new spectral data for use in remote sensing for natural resources. The system has been improved by addition of a solid state silicon detector array, and has been extended into the infrared by addition of a 64 element lead sulfide detector array. The infrared data in the 2000 to 2500 nm region especially holds large potential for mineral and oil exploration. (Author)

A82-32447* Santa Barbara Research Center, Goleta, Calif.
THEMATIC MAPPER - AN OVERVIEW OF SPECTRAL BAND REGISTRATION
W. H. FREUDENSTEIN (Santa Barbara Research Center, Goleta, CA) In: Imaging spectroscopy; Proceedings of the Seminar, Los Angeles, CA, February 10,11, 1981 Bellingham, WA, SPIE - The International Society for Optical Engineering, 1981, p. 50-63.
(Contract NAS5-24200)

The Thematic Mapper (TM) is a high-resolution radiometer designed for earth resources classification and mapping. The TM employs multispectral scanning in a near polar orbit to sweep a 185-km swath. Data are obtained through a combination of spacecraft motion and the sweeping action of the scan mirror. These data are transmitted either directly to ground stations around the world or through a relay to the central data processing facility at White Sands, NM Seven spectral passbands are employed, and applications include coastal water mapping, soil vegetation differentiation, biomass surveys, water body delineation, vegetation moisture measurement, plant heat stress management, and hydrothermal mapping Attention is given to the scan mirror assembly, scan nonlinearities, the characterization and compensation of scan profiles, experimental performance, and a procedure for midscan correction. G R.

A82-32448* Jet Propulsion Lab., California Inst of Tech , Pasadena
MULTISPECTRAL MAPPER - IMAGING SPECTROSCOPY AS APPLIED TO THE MAPPING OF EARTH RESOURCES
J. B. WELLMAN (California Institute of Technology, Jet Propulsion Laboratory, Observational Systems Div., Pasadena, CA) In Imaging spectroscopy; Proceedings of the Seminar, Los Angeles, CA, February 10,11, 1981 Bellingham, WA, SPIE - The International Society for Optical Engineering, 1981, p 64-73. refs
(Contract NAS7-100)

An instrument concept that uses solid-state array imaging has been developed for a future land observing system. The design concept is responsive to a variety of use needs and provides improved capabilities over the planned Landsat Thematic Mapper A comparison of the differing approaches to the instrument design was made, resulting in the selection of a concept which uses a spectrograph coupled to a line-array imager to provide simultaneous spatial and spectral resolution. The design provides an inherent solution to the problem of achieving precise registration among the spectral bands Data processing on the focal plane is used to select the spectral bands and their band widths Onboard capabilities include radiometric correction, selection of instantaneous field-of-view and swath width, and data compression (Author)

A82-32658* Massachusetts Inst. of Tech., Cambridge
INVERSION OF DATA FROM DIFFRACTION-LIMITED MULTIWAVELENGTH REMOTE SENSORS. II - NONLINEAR DEPENDENCE OF OBSERVABLES ON THE GEOPHYSICAL PARAMETERS
P. W. ROSENKRANZ (MIT, Cambridge, MA) Radio Science, vol. 17, Jan -Feb. 1982, p. 245-267. refs
(Contract NAS5-22929, NAG5-10)

Linear shift-invariant spatial filtering is applied to inversion of radiometric measurements of the earth in both polarizations at the following frequencies: 6.6, 10.7, 18, 21, and 37 GHz. For purposes of radiative transfer calculations at these frequencies, the state of the ocean-atmosphere system is described by a seven-parameter model. The parameters are near-surface wind speed, sea surface temperature, integrated water vapor mass, scale height of water vapor in an exponential distribution, integrated liquid water mass, height of the liquid water, and characteristic drop radius in a Best (1950) drop size distribution. Also described is a spatial filtering algorithm by means of which geophysical parameters are retrieved from measurements made over the ocean by the scanning multichannel microwave radiometer on the Nimbus 7 satellite. The parameters here are near-surface wind speed, sea surface temperature, rain rate, integrated atmospheric water vapor content, and integrated liquid water content (including rain). C R.

A82-32702#
PHOTOGRAMMETRIC METHODS FOR MAPPING RESOURCE DATA FROM HIGH ALTITUDE PANORAMIC PHOTOGRAPHY
R. L. LISTON (U S. Forest Service, Washington, DC) Photogrammetric Engineering and Remote Sensing, vol. 48, May 1982, p. 725-732. refs

Characteristics of the Itek KA-80A optical bar panoramic camera are discussed. Two computer based mapping systems designed to correct for variations in photo scale are described Panoramic Grid (PANGRID) is a computer program that creates a panoramic

image overlay of an equal area grid assumed to lie on flat ground. The Photographic Mapping System (PMS) provides for the generation of both map registered grid overlays and mapping of digitized point, line, and polygon data Both programs make use of single frame resection techniques and digital terrain data.
(Author)

A82-32766
SIMPLIFIED TECHNIQUES TO STUDY COMPONENTS OF SOLAR RADIATION UNDER HAZE AND CLOUDS
M. L. WESELY (Argonne National Laboratory, Argonne, IL) Journal of Applied Meteorology, vol. 21, Mar. 1982, p 373-383 Research sponsored by the U.S. Department of Energy. refs

A82-32824#
AN OPTICAL OBJECTIVE LENS FOR EARTH OBSERVATIONS BY SATELLITES [UN OBJECTIF OPTIQUE POUR L'OBSERVATION DE LA TERRE A PARTIR DE SATELLITES]
E. MATHIEU (Wild Heerbrugg AG, Heerbrugg, Switzerland), E. SEIN (Centre National d'Etudes Spatiales, Centre Spatial de Toulouse, Toulouse, France), and J.-P. DURPAIRE (ESA, Toulouse, France) ESA Journal, vol. 6, no. 1, 1982, p. 71-81. In French. European Space Agency
(Contract ESA-4422/80)

The features and performance of objective lenses intended for transmission of optical images of the earth to deposition on the detectors of CCDs onboard the ESA land application satellite system/optical imaging instrument are described. Trials to determine satisfactory durability for space-based uses are reviewed The lenses were required to have an angular field of 16 deg, a 105 mm aperture, cover the spectral bands 0.6, 0.69, 0.8, and 0.9 micron, the panchromatic band from 0.52-0 9 micron, have a focal distance to within 3 mm of 567 mm, cause less than 1 percent distortion in the image size, and less than 1.5 micron error in the spectral domain Other requirements were for a 0 75 transmittance, polarization less than 1 percent, and a modulation transfer function close to theoretical limits, which was realized at less than 1 mm. The objective produced will have a resolution of around 15 m at the earth's surface from an orbit of 681 km and a total field of view of 167 km. M.S K.

A82-32912
QUANTITATIVE RELATIONSHIPS OF NEAR-SURFACE SPECTRA TO LANDSAT RADIOMETRIC DATA
S. E. MARSH and R. J. P LYON (Stanford University, Stanford, CA) Remote Sensing of Environment, vol. 10, Dec. 1980, p 241-261. Research supported by the U.S. Geological Survey. refs

It is shown that for typical homogeneous and moderately heterogeneous terrains, the number of samples required for estimating the mean reflectance of a pixel is small. No more than 9-20 samples are required to be within 2% reflectance at the 95% probability level. Coincident field measurements and satellite observations are used to test the equivalency and correlation of the reflectance data. It is noted that, before the Landsat data could be compared with the surface measurements, the satellite brightness values had to be converted to absolute radiometric units and corrected for atmospheric attenuation and scattering. A conversion method using a standard/target comparison, which indirectly compensates for atmospheric attenuation and scattering, produces a Landsat equivalent reflectance exhibiting a root-mean-square error of + or - 4% reflectance (compared with the surface measured value at 12 test sites). C.R.

A82-32915* National Aeronautics and Space Administration Goddard Space Flight Center, Greenbelt, Md.
SNOWPACK MONITORING IN NORTH AMERICA AND EURASIA USING PASSIVE MICROWAVE SATELLITE DATA
J L. FOSTER, A. RANGO, D. K. HALL, A. T. C. CHANG, L. J. ALLISON, and B. C DIESEN, III (NASA, Goddard Space Flight Center, Greenbelt, MD) Remote Sensing of Environment, vol 10, Dec. 1980, p. 285-298. refs

Areas of the Canadian high plains, the Montana and North Dakota high plains, and the steppes of central Russia have been studied in an effort to determine the utility of spaceborne microwave radiometers for monitoring snow depths in different geographic areas. Significant regression relationships between snow depth and microwave brightness temperatures were developed for each of these homogeneous areas. In each of the study areas investigated in this paper, Nimbus-6 (0.81 cm) ESMR data produced higher correlations than Nimbus-5 (1.55 cm) ESMR data in relating microwave brightness temperature to snow depth. It is difficult to extrapolate relationships between microwave brightness temperature and snow depth from one area to another because different geographic areas are likely to have different snowpack conditions. (Author)

A82-33296
INVESTIGATIONS OF POINT TRANSFER [UNTERSUCHUNGEN ZUR PUNKTUEBERTRAGUNG]
M. SIGLE (Stuttgart, Universitaet, Stuttgart, West Germany) Bildmessung und Luftbildwesen, vol 50, May 1, 1982, p. 91-100. In German refs

The effectiveness of various new instruments developed for point transfer in practical photogrammetry is discussed with emphasis on their accuracy and economy by controlled aerotriangulation. A comparison is made between signaled and artificially labeled connection points using controlled aerotriangulation selected according to the bundle method. Point transmission methods, picture coordinate measurements and block adjustments are discussed Investigations are conducted using the equipment of the firms Zeiss and Kern, and no significant difference is found for the transcribers Zeiss PM1 and Kern PMG2 (CPM1).
D L G

A82-33297
IMAGE QUALITY AND HEIGHT MEASUREMENT ACCURACY OF SERIAL SURVEY CAMERA IMAGERY FROM HIGH ALTITUDES [BEITRAEGE ZUR BILDQUALITAET UND HOEHENMESSGENAUIGKEIT VON REIHENMESSKAMMERAUFNAHMEN AUS GROESSEREN FLUGHOEHEN]
J SIEVERS and K. SCHUERER (Institut fuer angewandte Geodaesie, Frankfurt am Main, West Germany) Bildmessung und Luftbildwesen, vol. 50, May 1, 1982, p. 101-118. In German. refs

The image quality for imagery obtained in photomissions flying from heights of 6 to 14 km is determined using four cameras of different focal lengths and the aerial film material Agfa Aviphot Pan 200 Resolving power is determined using a tri-bar test target, and a method is developed to estimate height accuracy with the aid of statistics The influence of image quality on the model is taken into consideration, and a highlands area with differences in elevation up to 200 m is used as a terrestrial basis for comparison. D L.G.

A82-33442#
INFERENCE OF REFRACTIVITY PROFILES BY SATELLITE-TO-GROUND RF MEASUREMENTS
K. D ANDERSON (U.S Naval Ocean Systems Center, San Diego, CA) Radio Science, vol. 17, May-June 1982, p. 653-663 refs

A technique is described to infer an estimate of the tropospheric radio refractive index distribution from earth-based observations of a satellite-born beacon This technique, known as the direct inference technique (DIT) predicts the refractivity profile by comparing the observed interference pattern, created as the satellite moves through low elevation angles, to patterns generated

from a family of assumed refractivity profiles It is shown that DID correctly predicts the ducting environment for 12 of 22 satellite-to-ground RF measurements made during July and August 1978. Although the inferred profile geometry can differ significantly from the refractivity profile measured by an upper air sounding, the technique is moderately successful in predicting whether the true profile contains a ground-based or elevated duct. However, the overall reliability of predicting the dominant features of the duct (e.g., refractive gradient through the trapping layer, top height of the duct) is not adequate for operational usage. (Author)

A82-34222* National Aeronautics and Space Administration Goddard Space Flight Center, Greenbelt, Md
IRRADIANCE MEASUREMENT ERRORS DUE TO THE ASSUMPTION OF A LAMBERTIAN REFERENCE PANEL
D S. KIMES and J. A KIRCHNER (NASA, Goddard Space Flight Center, Earth Resources Branch, Greenbelt, MD) Remote Sensing of Environment, vol. 12, May 1982, p. 141-149. refs

A technique is presented for determining the error in diurnal irradiance measurements that results from the non-Lambertian behavior of a reference panel under various irradiance conditions. Spectral biconical reflectance factors of a spray-painted barium sulfate panel, along with simulated sky radiance data for clear and hazy skies at six solar zenith angles, were used to calculate the estimated panel irradiances and true irradiances for a nadir-looking sensor in two wavelength bands. The inherent errors in total spectral irradiance (0.68 microns) for a clear sky were 0.60, 6.0, 13.0, and 27.0% for solar zenith angles of 0, 45, 60, and 75 deg, respectively. The technique can be used to characterize the error of a specific panel used in field measurements, and thus eliminate any ambiguity of the effects of the type, preparation, and aging of the paint. (Author)

A82-34470
TECHNICAL AND ECONOMICAL CHARACTERISTICS OF THE AFA-TES-10M AERIAL CAMERA [TEKHNIKO-EKONOMICHESKIE POKAZATELI AEROFOTOAPPARATA AFA-TES-10M]
A G. VANIN Geodeziia i Kartografiia, Apr. 1982, p. 36-39. In Russian refs

The technical characteristics and economics of the AFA-TES-10M aerial camera are compared with those of the AFA-TES-100M camera which it replaces. Although a focal length of 100 mm makes both suitable for large-scale cartography, the newer camera, which makes use of a Russar-71 objective, exhibits reduced objective distortion and increased resolution in comparison with the AFA-TES-100M. A shorter operating cycle and an extended exposure range also allow a wider applicability and greater effectiveness in large-scale cartography. Analysis of the costs involved in producing topographic maps of a rolling terrain at various scales by the AFA-TES-10M indicates an overall savings as a result of reductions in labor costs, the amount of field validation and cameral photogrammetric processes required and specific capital investment, as well as an increase in the productivity of survey work. Development costs of the new system would be recovered typically in two years. A.L.W.

A82-34471
ANALYTICAL PROCESSING OF PHOTOGRAPHS TAKEN BY PAIRED CAMERAS [ANALITICHESKAIA OBRABOTKA FOTOSNIMKOV, POLUCHENNYKH SPARENNYMI FOTOKAMERAMI]
G. P. KUDRIAVTSEV Geodeziia i Kartografiia, Apr. 1982, p 39-41. In Russian

The use of direct analytical methods for the processing of photographs taken simultaneously by pairs of cameras with parallel optical axes mounted on a moving airborne or ground vehicle is examined. A method is presented whereby the angular and linear components of the external orientation of a stereo model may be computed from the positions of three reference points visible on each of the photographs, and then used to derive the geodesic coordinates. A computer algorithm based on the method has been used to derive a topographic layout of the geometrical elements and transverse and longitudinal profiles of a road based on strip photography taken by a camera pair mounted on a moving automobile A.L.W.

A82-34701
AMERICAN SOCIETY OF PHOTOGRAMMETRY, ANNUAL MEETING, 47TH, WASHINGTON, DC, FEBRUARY 22-27, 1981, ASP TECHNICAL PAPERS
Falls Church, VA, American Society of Photogrammetry, 1981. 662 p $12 50

Simple plotters for close-range photogrammetry are considered along with remote sensing of thermal subsurface terrain properties, the effect of mixtures of primary forest scence components on spectral variability, Landsat in the search for Appalachian hydrocarbons, and the exterior orientation of side looking sensors Attention is given to image processing with microcomputers in remote sensing, sensitometry in Canadian aerial survey, aerial camera vibration, raster scanning and its application in automated cartography, improved land use classifications from Landsat and Seasat satellite imagery registered to a common map base, and a quantitative method to test for similarity between photo interpreters. Other topics explored are related to remote sensing of geomorphological factors affecting the visibility of archaeological materials, the use of Skylab S190-B photography for small scale mapping, an optical data link for an airborne scanning system, and new instrumentation for direct photogrammetric mapping. G.R.

A82-34708
IMAGE PROCESSING WITH MICROCOMPUTERS IN REMOTE SENSING
F M. CADY (Montana State University, Bozeman, MT) and R M. HODGSON (Canterbury, University, Christchurch, New Zealand) In: American Society of Photogrammetry, Annual Meeting, 47th, Washington, DC, February 22-27, 1981, ASP Technical Papers. Falls Church, VA, American Society of Photogrammetry, 1981, p 140-149. refs

A description is given of a digital image processing system which has proved to be useful in a number of application areas In connection with the employment of a relatively low resolution sensor, it was possible to use relatively inexpensive computing components, memory, and bulk storage devices. The speed of operation for a wide range of application programs was high enough to allow the system to be useful for interactive image processing. The experience gained with the aid of the considered system indicates that similar results can be obtained with higher resolution arrays by utilizing higher performance, new generation microprocessors. The discussed system is based on the use of an eight-bit microprocessor with an addressing space of 65,536 locations G.R.

A82-34724
SENSITOMETRY IN CANADIAN AERIAL SURVEY
P D. CARMAN (National Research Council, Ottawa, Canada) In: American Society of Photogrammetry, Annual Meeting, 47th, Washington, DC, February 22-27, 1981, ASP Technical Papers Falls Church, VA, American Society of Photogrammetry, 1981, p. 285-295. refs

Since 1943, sensitometric control of the processing of aerial negatives has been used by the Royal Canadian Air Force (RCAF) in connection with the performance of its task to provide aerial photography for Canada. The sensitometers used by the RCAF suffered from a variety of problems which, however, could be overcome by making use of repair and recalibration facilities. The transfer of aerial photography assignments from the RCAF to a number of private companies in the 1950's made it appear desirable to employ sensitometers which could perform reliably without easy access to specialized repair facilities. Attention is given to a sensitometer which was designed to satisfy these requirements The design features of the new instrument are discussed, taking into account the light source, the spectral quality of illumination, the shutter, and the electrical supply. Aspects of sensitometer

calibration and verification are considered along with the uses of sensitometric control of aerial photography in Canada G.R

A82-34727
REMOTE SENSING OF THERMAL SUBSURFACE TERRAIN PROPERTIES
F. E. ALZOFON (Boeing Aerospace Co., Seattle, WA) In: American Society of Photogrammetry, Annual Meeting, 47th, Washington, DC, February 22-27, 1981, ASP Technical Papers. Falls Church, VA, American Society of Photogrammetry, 1981, p. 335-341. refs

It is noted that although the sensed radiation is generated and limited by heat flow through the material underlying the emitting surface, little attention appears to have been paid to the effect of variation in properties of the conducting materials on the information carried by the emitted radiation. As a consequence, variations in thermal radiation may be attributed solely to variation of the temperature and emissivity of the radiating surface However, it is shown that variation in radiant emittance can equally well be dominated by variation in the thermal conductivity of the underlying material. Criteria are derived under which either thermal conductivity variations or emissivity variations dominate radiant emittance data. A definition is given of threshold temperature; below the threshold, emissivity variations dominate, above it thermal conductivity variations dominate. Expressions are presented for the threshold temperature for various kinds of surface cooling C R.

A82-34737
AN OPTICAL DATA LINK FOR AIRBORNE SCANNING SYSTEM
M. J. GREEN (Wisconsin, University, Madison, WI) In: American Society of Photogrammetry, Annual Meeting, 47th, Washington, DC, February 22-27, 1981, ASP Technical Papers. Falls Church, VA, American Society of Photogrammetry, 1981, p. 476-482.

In connection with a study of oceanic thermal fronts, the Navy is interested in a thermal scanning system which could be used with their P-3 patrol aircraft. A suitable scanning system would be the RS-18A scanning thermal IR radiometer. However, an obstacle regarding the envisaged use of the instrument is related to the necessity to employ the aircraft without an introduction of any modifications. The obstacle has been overcome by making use of an optical data link which replaces the hardwire connections between the scanner and the power supply. The optical link is housed in a ten inch diameter tube which is clamped in position directly behind the scanner head G.R.

A82-34742
THE USE OF SKYLAB S-190B PHOTOGRAPHY FOR SMALL SCALE MAPPING
I. M. EL-HASSAN (Riyadh, University, Riyadh, Saudi Arabia) In: American Society of Photogrammetry, Annual Meeting, 47th, Washington, DC, February 22-27, 1981, ASP Technical Papers. Falls Church, VA, American Society of Photogrammetry, 1981, p. 536-543 refs

The use of the Skylab Earth Terrain Camera (S-190B) with 1:946,000 scale photography in small-scale mapping is investigated. The procedure used in making the measurements on the Skylab imagery is described An analytical absolute orientation is performed, and the results show that the photography could be used for mapping at scales of 1:100,000 and smaller. The photography used in the test comprises a strip of three photographs exposed on the SO-242 high-resolution color film. Second generation film transparencies made from the original film are used in the actual test. C.R.

A82-34746
COMPARISONS OF LAND COVER CLASSIFICATIONS FROM SELECTED REMOTE SENSING SYSTEMS
J B. CAMPBELL (Virginia Polytechnic Institute and State University, Blacksburg, VA) and F M. HENDERSON (New York, State University, Albany, NY) In: American Society of Photogrammetry, Annual Meeting, 47th, Washington, DC, February 22-27, 1981, ASP Technical Papers. Falls Church, VA, American Society of Photogrammetry, 1981, p. 618-626. refs

The present investigation is concerned with differences in accuracy of land cover maps generated by manual interpretation of several forms of remote sensing imagery. An area near Harrisburg, PA was imaged by K-band SLAR, the Landsat-1 MSS, the Landsat-3 RBV, and two Seasat SAR passes These images were manually interpreted to yield land cover parcels corresponding to the Level I categories considered by Anderson et al. (1976). The resulting interpretations were compared with the more detailed USGS land cover map of the same region to determine classification errors It is pointed out, however, that the results of this comparison cannot be interpreted as definitive assessments of the merits of each sensor system Continued research is necessary According to the current study, airborne radar imagery produced the best overall accuracy With respect to the four space-borne sensor systems the MSS and RBV images are preferable to the digitally processed Seasat SAR image with the optically processed Seasat SAR image being the least accurate system product. G.R.

A82-36018
THE USE OF MICROWAVE RADIOMETRY FOR THE DETERMINATION OF SNOW COVER HEIGHT [ISPOL'ZOVANIE SVCH RADIOMETRII DLIA OPREDELENIIA VYSOTY SNEZHNOGO POKROVA]
V. E. GERSHENZON, V. G. IRISOV, IU B. KHAPIN, and V S. ETKIN (Akademiia Nauk SSSR, Institut Kosmicheskikh Issledovanii, Moscow, USSR) Akademiia Nauk SSSR, Doklady, vol. 264, no. 3, 1982, p. 601-603. In Russian. refs

A method is proposed for determining the height of snow cover from remote measurements of the brightness temperatures in the wavelength range 1.5-0 34 cm. The method is validated by means of a model experiment and by comparing the results with direct measurements. The remote and direct measurements are found to correlate to within 5 cm. V.L.

A82-37809#
MICROWAVE SENSING FROM SPACE
H. SCHUESSLER (Dornier System GmbH, Friedrichshafen, West Germany) American Astronautical Society and Deutsche Gesellschaft fuer Luft- und Raumfahrt, Goddard Memorial Symposium on Spacelab, Space Platforms and the Future, 20th, Greenbelt, MD, Mar. 17-19, 1982, AAS 15 p. Research supported by the Bundesministerium fuer Forschung und Technologie (AAS PAPER 82-127)

The design, functions, and performance of satellite microwave sensor systems for earth imaging are described It is noted that microwave operations can be carried out in all weather and in day or night conditions, and that current satellite systems operate in the interval of 1-20 GHz. Applications for soil characterization, moisture, and wind vector measurements over the sea are described in terms of frequency selection, power, and antenna requirements. Sunsynchronous orbits offer the advantage of low power storage capabilities due to avoidance of eclipse conditions. Areas of development necessary to implement an SAR for GEO positioning are reviewed, and features of a microwave remote sensing experiment involving SAR operating at 9 6 GHz during the first Spacelab flight on the Shuttle are presented. Finally, details of the ERS-1 satellite, which will carry a radar altimeter, wind scatterometer, and SAR are outlined M.S.K.

A82-37812*# National Aeronautics and Space Administration. Goddard Space Flight Center, Greenbelt, Md.
SOLID STATE INSTRUMENTATION CONCEPTS FOR EARTH RESOURCE OBSERVATION
H. L. RICHARD (NASA, Goddard Space Flight Center, Advanced Land Observing Systems Studies Office, Greenbelt, MD) American Astronautical Society and Deutsche Gesellschaft fuer Luft- und Raumfahrt, Goddard Memorial Symposium on Spacelab, Space Platforms and the Future, 20th, Greenbelt, MD, Mar. 17-19, 1982, AAS 18 p refs
(AAS PAPER 82-132)

Late in 1980, specifications were prepared for detail design definition of a six band solid state multispectral instrument having three visible (VIS), one near infrared (NIR), and two short wave infrared (SWIR) bands. This instrument concept, known as the Multispectral Linear Array (MLA), also offered increased spatial resolution, on board gain and offset correction, and additional operational modes which would allow for cross track and stereoscopic viewing as well as a multialtitude operational capability. A description is presented of a summary of some of the salient features of four different MLA design concepts, as developed by four American companies. The designs ranged from the use of multiple refractive telescopes utilizing three groups of focal plane detectors electronic correlation processing for achieving spatial registration, and incorporating palladium silicide (PdSi) SWIR detectors, to a four-mirror all-reflective telecentric system utilizing a beam splitter for spatial registration. G.R

N82-22643*# National Aeronautics and Space Administration Goddard Space Flight Center, Greenbelt, Md.
USE OF NOAA/AVHRR VISIBLE AND NEAR-INFRARED DATA FOR LAND REMOTE SENSING
S. R. SCHNEIDER (NOAA)02(NOAA), D. F MCGINNIS, JR , and J. A. GATLIN Sep. 1981 55 p refs Sponsored in part by NOAA Prepared in cooperation with Earth Satellite Corp.
(NASA-TM-84186; NAS 1.15:84186; PB82-129388, NOAA-TR-NESS-84, NOAA-81100501) Avail NTIS HC A04/MF A01 CSCL 08L

The data were analyzed for their usefulness in monitoring lake ice, snowcover, water quality, crop condition and terrain classification on the H.P. 1000 computer interactive system. Terrain phenomena that were studied using LANDSAT MSS data could also be monitored with the NOAA-6 channels, but at a lesser resolution. T.M

N82-22865*# National Aeronautics and Space Administration Langley Research Center, Hampton, Va.
SEASAT: A SATELLITE SCATTEROMETER ILLUMINATION TIMES OF SELECTED IN SITU SITES
L. C. SCHROEDER, D. R. GOODRIDGE, J. C. BOBERLY, J. K. HUGHES, and J. L. SWEET Mar. 1982 120 p
(NASA-TM-83280; NAS 1.15:83280) Avail: NTIS HC A06/MF A01 CSCL 08J

A list of times that the SEASAT A Satellite Scatterometer (SASS) illuminated from directly above or directly abeam, selected surface sites where in situ winds were measured is provided. The list is ordered by the Greenwich Mean Time (GMT) of the midpoint of the illumination period (hit time) for a given surface site. The site identification, the orbit number and the direction from the subtrack in which the truth lies are provided. The accuracy of these times depends in part upon the ascending node times, which are estimated to be within + 1 sec, and on the illumination time relative to the ascending node, which is estimated to be within +6 seconds. The uncertainties in the times provided were judged to be sufficiently small to allow efficient and accurate extraction of SASS and in situ data at the selected surface sites. The list contains approximately six thousand hit times from 61 geographically dispersed sites. Author

N82-24264# Joint Publications Research Service, Arlington, Va.
PURPOSE, BACKGROUND OF 'INTERCOSMOS-21' MISSION
M. A. RIMSHA *In its* USSR Rept.· Space, No 15 (JPRS-80424) p 94-98 29 Mar. 1982 Transl. into ENGLISH from Zemlya Vselennaya (USSR), no. 5, Sep. - Oct. 1981 p 39-41
Avail: NTIS HC A07/MF A01

Research performed with satellites of the 'Intercosmos' series is discussed. Scientists have investigated short wave emissions of the Sun and the Earth's ionosphere and magnetosphere, cosmic rays and meteorite flows. Various technical systems were tested in these satellites. A transmitter of the 'beacon' type operated successfully in the first 'Intercosmos' satellites, while a special telemetric system later functioned in space and was recommended for further use. The unified telemetric system transmitted information directly to ground stations without the use of spacecraft instruments. S.L

N82-24489# Research Inst. of National Defence, Linkoeping (Sweden).
STUDY VISIT TO UNITED STATES LASER TECHNOLOGY CENTERS, 1981 [RAPPORT FRAAN USA-RESA INOM LASEROMRAADET, 1981]
O. STEINVALL Jan. 1982 29 p Partly in SWEDISH and ENGLISH
(FOA-C-30257-E1) Avail· NTIS HC A03/MF A01

Coherent infrared radar and coherent CO2 laser radar were studied. Information from visits to research laboratories and radar manufacturers is outlined, focusing on TEA lasers, heterodyne radiometers, laser absorption spectrometers, and transportable measurement radar. Airborne oceanographic lidar, laser cloud mappers, and oceanographic detection were examined. Infrared imaging systems, and hydrographic laser sounders were investigated Author (ESA)

N82-25602*# General Software Corp., Landover, Md
LANDSAT-D CONICAL SCANNER EVALUATION PLAN
S BILANOW and L. C CHEN, Principal Investigators Mar. 1982 102 p refs ERTS
(Contract NAS5-26205)
(E82-10340; NASA-CR-166790, NAS 1.26:166790, GSC-TR8203) Avail NTIS HC A06/MF A01 CSCL 14B

The planned activities involved in the inflight sensor calibration and performance evaluation are discussed and the supporting software requirements are specified The possible sensor error sources and their effects on sensor measurements are summarized. The methods by which the inflight sensor performance will be analyzed and the sensor modeling parameters will be calibrated are presented In addition, a brief discussion on the data requirement for the study is provided. T M.

N82-25610*# National Aeronautics and Space Administration. Langley Research Center, Hampton, Va.
RADIOMETER MISSION REQUIREMENTS FOR LARGE SPACE ANTENNA SYSTEMS
L. S. KEAFER, JR., P. SWANSON, and J. ECKERMAN May 1982 64 p refs
(NASA-TM-84478, NAS 1 15:84478) Avail: NTIS HC A04/MF A01 CSCL 20N

Requirements are defined for Earth observational microwave radiometry using large space antenna systems with apertures in the 50 to 200 meter range. General Earth observational needs, specific measurement requirements, orbital mission guidelines and constraints, and general radiometric requirements are defined. Specific measurements include soil moisture, water surface temperature, water roughness, ice boundaries, salinity, and water pollutants. Measurements with 10 to 1 km spatial resolution and 3 to 1 day temporal resolution are required. Author

N82-26642# Barringer Research Ltd , Rexdale (Ontario)
BREADBOARD GAS FILTER CORRELATION SPECTROMETER FOR ATMOSPHERIC MEASUREMENT OF HYDRAZINES AND NITROGEN DIOXIDE Final Report, Jan. 1977 - Apr. 1979
R. DICK Oct 1981 31 p refs
(Contract F33615-77-C-0604, AF PROJ. 7930)
(AD-A110688; TR-79-281, SAM-TR-81-11) Avail. NTIS HC A03/MF A01 CSCL 14B

This report describes the efforts to build a breadboard Gas Filter Correlation Spectrometer (GFSC) for the atmospheric measurement of hydrazines and nitrogen dioxide. The instrument was configured for use as an ambient monitor, with the possibility of conversion to a remote sensor by addition of a telescope. The final detection limits for the gases were: N2H4 = .3 ppm, UDHM = .23 ppm, MMH = .22 ppm, and N02 = 9 ppm GRA

N82-26741* National Aeronautics and Space Administration, Washington, D. C.
LANDSAT D TO TEST THEMATIC MAPPER, INAUGURATE OPERATIONAL SYSTEM
21 Jun. 1982 43 p
(NASA-NEWS-RELEASE-82-100, P82-10:03) Avail: NASA Scientific and Technical Information Facility, P. O. Box 8757, B.W.I Airport, Md. 21240 CSCL 22A

NASA will launch the Landsat D spacecraft on July 9, 1982 aboard a new, up-rated Delta 3920 expendable launch vehicle LANDSAT D will incorporate two highly sophisticated sensors; the flight proven multispectral scanner; and a new instrument expected to advance considerably the remote sensing capabilities of Earth resources satellites. The new sensor, the thematic mapper, provides data in seven spectral (light) bands with greatly improved spectral, spatial and radiometric resolution L.F.M.

N82-26743*# Pennsylvania State Univ., University Park Dept. of Meteorology
INTERACTIVE INITIALIZATION OF HEAT FLUX PARAMETERS FOR NUMERICAL MODELS USING SATELLITE TEMPERATURE MEASUREMENTS Quarterly Report, 1 Nov. 1981 - 1 Jun. 1982
T N. CARLSON, Principal Investigator 1 Jun. 1982 4 p HCMM
(Contract NAS5-26456)
(E82-10313; NASA-CR-168998; NAS 1.26:168998, QR-4) Avail NTIS HC A02/MF A01 CSCL 05B

Progress made in HCMM research, including testing the interactive minicomputer system and preparation of a paper on the analysis of regional scale soil moisture patterns, is summarized An exhibit on remote sensing including a videotape display of HCMM images, most of them of the State College area, was prepared. J.D.

N82-26744*# OAO Corp , Beltsville, Md.
LANDSAT-D THERMAL ANALYSIS AND DESIGN SUPPORT
1982 134 p ERTS
(Contract NAS5-25737)
(E82-10346; NASA-CR-166788; NAS 1.26:166788, OAO/TR-81/0033) Avail: NTIS HC A07/MF A01 CSCL 05B

Detailed thermal models of the LANDSAT-D Earth Sensor Assembly Module (ESAM), the Dummy Thematic Mapper (DTM), and a small thermal model of the LANDSAT-D spacecraft for a heater analysis were developed. These models were used to develop and verify the thermal design of the ESAM and DTM, to evaluate the aeroheating effects on ESAM during launch and to evaluate the thermal response of the LANDSAT-D assuming the hard-line heaters failed on with the spacecraft in the Space Transportation System (STS) orbiter bay. Results of model applications are summarized. T.M.

09

GENERAL

Includes economic analysis.

A82-22546
ANTIPROTONS FROM GALACTIC SOURCES OF COSMIC RAYS AND GAMMA RAYS
R COWSIK (Franklin Institute, Bartol Research Foundation, Newark, DE; Tata Institute of Fundamental Research, Bombay, India) and T. K GAISSER (Franklin Institute, Bartol Research Foundation, Newark, DE) In International Cosmic Ray Conference, 17th, Paris, France, July 13-25, 1981, Conference Papers. Volume 2 Gif-sur-Yvette, Essonne, France, Commissariat a l'Energie Atomique, 1981, p. 218-221. Research supported by the U S Department of Energy. refs

Recent observations of discrete galactic sources of gamma rays are examined in terms of a modified version of the nested leaky box model of Cowsik and Wilson (1973, 1975). It is shown that the modified model can account for the observed high fluxes of antiprotons The essential idea is that bright gamma-ray sources are surrounded by significantly more matter than most other sources of cosmic rays, they are thus strong sources of both secondary gamma rays and antiprotons, and at the same time efficient absorbers of heavy nuclei V.L.

A82-22547* George Mason Univ., Fairfax, Va.
CONFINEMENT AND ACCELERATION OF COSMIC RAYS IN GALACTIC SUPERBUBBLES
M KAFATOS (George Mason University, Fairfax, VA), F BRUHWEILER, and S SOFIA (NASA, Goddard Space Flight Center, Greenbelt, MD) In: International Cosmic Ray Conference, 17th, Paris, France, July 13-25, 1981, Conference Papers. Volume 2 Gif-sur-Yvette, Essonne, France, Commissariat a l'Energie Atomique, 1981, p 222-225. refs

The role of the newly discovered galactic superbubbles on the confinement and acceleration of cosmic rays is examined. It is shown that these structures naturally account for the lifetime and the local origin of the cosmic rays, as well as for the location of galactic gamma-ray sources not associated with pulsars.
(Author)

A82-22548
INTERACTIONS OF COSMIC RAYS WITH MOLECULAR CLOUDS
Y FUKUI and S. HAYAKAWA (Nagoya University, Nagoya, Japan) In: International Cosmic Ray Conference, 17th, Paris, France, July 13-25, 1981, Conference Papers. Volume 2 Gif-sur-Yvette, Essonne, France, Commissariat a l'Energie Atomique, 1981, p. 226-228.

The optical thickness of HI, tau, obtained from the dip of 21 cm line for cold clouds is found to depend on the linear size d as tau varies as d to the 0.44 power Cosmic rays responsible for the production of HI from H2 are appreciably absorbed in the inner part of the clouds. The tau-d relation indicates a nearly flat energy spectrum of cosmic rays at low energies (Author)

A82-22549
DERIVATION OF THE DISTRIBUTION OF SYNCHROTRON EMISSIVITY IN THE GALAXY FROM THE 408 MHZ ALL-SKY SURVEY
S. PHILLIPPS, S KEARSEY, J L. OSBORNE (Durham, University, Durham, England), C. G T. HASLAM, and H STOFFEL (Max-Planck-Institut fuer Radioastronomie, Bonn, West Germany) In: International Cosmic Ray Conference, 17th, Paris, France, July 13-25, 1981, Conference Papers Volume 2. Gif-sur-Yvette, Essonne, France, Commissariat a l'Energie Atomique, 1981, p. 229-232 refs

A82-22550
ANGULAR VARIATIONS OF NONTHERMAL RADIO EMISSION FROM THE GALAXY RELEVANT TO THE STRUCTURE OF INTERSTELLAR MAGNETIC FIELD
G. V. CHIBISOV (Akademiia Nauk SSSR, Fizicheskii Institut, Moscow, USSR) and V. S. PTUSKIN (Akademiia Nauk SSSR, Institut Zemnogo Magnetizma, Ionosfery i Rasprostraneniia Radiovoln, Troitsk, USSR) In: International Cosmic Ray Conference, 17th, Paris, France, July 13-25, 1981, Conference Papers Volume 2. Gif-sur-Yvette, Essonne, France, Commissariat a l'Energie Atomique, 1981, p. 233-235.

The relation between the correlation function of the intensity of galactic radio-emission at different directions and the correlation function of interstellar magnetic field at different points is found. This relation is shown to be used for the determination of random and regular components of magnetic field. Measurements at different frequencies clarify the character of cosmic ray propagation in the Galaxy, and in particular, distinguish between the diffusive and convective transfer of cosmic rays. (Author)

A82-22551
CONVECTIVE OUTFLOW OF COSMIC RAYS FROM THE GALAXY AND BACKGROUND RADIO EMISSION
V. A. DOGIEL, V. M. KOVALENKO, and V L PRISHCHEP (Akademiia Nauk SSSR, Fizicheskii Institut, Moscow, USSR) In: International Cosmic Ray Conference, 17th, Paris, France, July 13-25, 1981, Conference Papers Volume 2 Gif-sur-Yvette, Essonne, France, Commissariat a l'Energie Atomique, 1981, p. 236-239 refs

A82-22553
CONSEQUENCES OF AN INVERSE COMPTON EMISSION MODEL FOR EXTRAGALACTIC X-RAY SOURCES
P. BIERMANN and R SCHLICKEISER (Max-Planck-Institut fuer Radioastronomie, Bonn, West Germany) In: International Cosmic Ray Conference, 17th, Paris, France, July 13-25, 1981, Conference Papers. Volume 2 Gif-sur-Yvette, Essonne, France, Commissariat a l'Energie Atomique, 1981, p. 252-255. refs

An X-ray survey of flat spectrum radio sources is carried out. All sources are detected, among them two highly compact BL Lac type objects which show aligned triple X-ray sources. Interpreting these features as very large jets radiating X rays by inverse Compton scattering of microwave background photons leads to strong constraints on the process of acceleration and the energetics of the sources. C.R.

A82-22554
CALCULATED ISOTOPIC SOURCE COMPOSITION AND TESTS FOR ORIGIN AND PROPAGATION OF COSMIC RAYS WITH MASS NUMBERS LESS THAN OR EQUAL TO 62
J. H ADAMS, JR and M. M. SHAPIRO (U S. Navy, Naval Research Laboratory, Washington, DC) In: International Cosmic Ray Conference, 17th, Paris, France, July 13-25, 1981, Conference Papers. Volume 2. Gif-sur-Yvette, Essonne, France, Commissariat a l'Energie Atomique, 1981, p. 256-259. refs

Recent measurements of the nuclidic composition of cosmic-ray Ne and Mg are used to calculate their isotopic source compositions. In addition, the effects of these neutron-rich species on abundances of various secondary nuclides are presented. Implications of anomalies in the source composition for nucleosynthesis and/or evolution of the galactic composition are discussed. Finally, the arriving isotopic abundances Co-59, Co-57 and Ti-44, Ti-46 are calculated for time intervals much less than 50 years, much greater than 50 years, much less than 100,000 years, and much greater than 100,000 years between nucleosynthesis and acceleration to cosmic-ray energies. (Author)

A82-22556
COMPARATIVE ABUNDANCES IN SOLAR ENERGETIC PARTICLES AND IN GALACTIC COSMIC RAY SOURCES, AND THE NE-22 ANOMALY
J. P. MEYER (Commissariat a l'Energie Atomique, Centre d'Etudes Nucleaires de Saclay, Gif-sur-Yvette, Essonne, France) In. International Cosmic Ray Conference, 17th, Paris, France, July 13-25, 1981, Conference Papers. Volume 2. Gif-sur-Yvette, Essonne, France, Commissariat a l'Energie Atomique, 1981, p 265-268. refs

A82-22599
ON THE PHYSICAL SENSE OF THE CONSTANT OF SOLAR COSMIC RAY CORONAL PROPAGATION
G. A. BAZILEVSKAIA (Akademiia Nauk SSSR, Fizicheskii Institut, Moscow, USSR) and E. V VASHENIUK (Akademiia Nauk SSSR, Poliarnyi Geofizicheskii Institut, Apatity, USSR) In International Cosmic Ray Conference, 17th, Paris, France, July 13-25, 1981, Conference Papers. Volume 3. Gif-sur-Yvette, Essonne, France, Commissariat a l'Energie Atomique, 1981, p. 93-96. refs

An analysis is made of the time dependence of solar cosmic ray intensity and anisotropy Results show that the coronal time is the time of the escape of the bulk of the particles into the interplanetary space, and it is found that the generation of solar cosmic rays is almost simultaneous in the fast propagation region, which could be in the case of solar cosmic ray acceleration by the quasi-spheric shock wave This result is in agreement with values found by Bazilevskaya and Vashenyuk (1979) for the transit time of the first particles in the corona for high energy solar cosmic rays. D L G

A82-22603
THE INFLUENCE OF THE SECTOR STRUCTURE OF INTERPLANETARY MAGNETIC FIELD ON THE SOLAR COSMIC RAY CHARACTERISTICS
G. A. BAZILEVSKAIA (Akademiia Nauk SSSR, Fizicheskii Institut, Moscow, USSR) In: International Cosmic Ray Conference, 17th, Paris, France, July 13-25, 1981, Conference Papers. Volume 3 Gif-sur-Yvette, Essonne, France, Commissariat a l'Energie Atomique, 1981, p. 117-120. refs

A statistical study of solar cosmic-ray events from 1957 to 1968 is performed, taking into account only events with certain or probable association. The solar wind velocity is used to define the earth connection longitude on the sun and to map the longitude of sector boundaries. No sector boundary influence on registration probability of solar cosmic-rays is found, and the intensity time dependence seems to be controlled by coronal structures, which are situated lower in the solar atmosphere than where the sector boundaries are formed D.L.G.

A82-30850
SPACE TO THE EARTH [KOSMOS - ZEMLE]
A. A BOLSHOI, I V MESHCHERIAKOV, S. D. SILVESTROV, A V. TSEPELEV, and V. A. MASHCHENKO Moscow, Izdatel'stvo Nauka, 1981. 152 p. In Russian. refs

Several applications of space technology are discussed Attention is given to satellite communications systems, navigation satellites, space geodesy, meteorological satellites, and the remote sensing of earth resources. The principles underlying such applications and the design and operation of the appropriate systems are considered. B.J.

A82-31996
THE USE OF THE SPOT SATELLITE IN NATURAL RESOURCE EVALUATION [EL SATELITE SPOT EN LA EVALUACION DE LOS RECURSOS NATURALES]
P.-M. ADRIEN CIDA, vol. 5, no 5, 1980, p. 31-36 In Spanish.

The practical application of the remote sensing satellite SPOT to natural resources assessment in Latin America are discussed SPOT, which will be launched by the French government in 1984, will assume a nearly polar orbit at an altitude of 822 km and be able to scan a 60 km-wide area with 10-20 m sweeps of its multispectral scanner. Comparisons are made with the capabilities

of the ARGOS satellite, which has been in operation since 1974. The data to be collected by SPOT will be pertinent to research in agricultural land use, agricultural meteorology, hydrology, forest management, and mineralogical resources. Attention is given to the coordination of such research and the dissemination of its data by French government agencies. O C.

A82-33555
REMOTE SENSING OF THE EARTH'S RESOURCES - THE SOVIET EXPERIENCE
J. POPESCU British Interplanetary Society, Journal (Space Chronicle), vol. 35, June 1982, p. 273, 274.

The tools, techniques, and targets of Soviet remote sensing systems are explored. Satellite viewing results are rechecked by both aerial surveys and surface sampling for purposes of calibration and confirmation. A total of 1,260 Kosmos spacecraft were launched by 1979, and carried vidicons and microwave sensors for data acquisition. The Salyut space stations were also equipped with a multispectral scanner which featured 10 m resolution, could discern between wet and dry ground, and covered the range 0.46-0.89 microns. Additional instrumentation comprised a radio telescope, stereoscopic camera, and SAR. World grain crops are monitored to anticipate the world wheat market, regions of intense storm activity such as the Bermuda Triangle are studied, and weather conditions and evolution, particularly in Arctic shipping areas, are tracked Telemetry stations are located in five countries outside the Soviet Union. Instances of successful cosmonaut remote sensing for mineral prospecting, glacier mapping, and sea ice tracking to protect ocean-going vessels are cited. M.S.K.

A82-34116#
EARTH OBSERVATIONS FROM SPACE - TRENDS AND PROSPECTS
G BRACHET (Centre National d'Etudes Spatiales, Paris, France) In: International aerospace review, Proceedings of the First International Aerospace Symposium, Le Bourget, Seine-Saint-Denis, France, June 2, 3, 1981. New York, American Institute of Aeronautics and Astronautics, 1982, p. 215-223.

The instrumentation and missions of various earth observation satellites are outlined. Earth observation satellites are grouped into experimental types for testing instruments or observing techniques, operational meteorological satellites with on-line users, the Landsat series of satellites for performing whole-earth scanning using different EM wavelengths, and ocean and ice scanning satellites. The Tiros-N series of satellites included advanced very high resolution radiometers for sea-surface temperature measurements, a solar backscatter ultraviolet sensor for global ozone monitoring, and an advanced microwave sounding unit The GOES-D spacecraft carries an improved imaging radiometer for atmospheric vertical sounding, while the European Meteosat features a water vapor channel at 6-7 microns for upper atmosphere water vapor content assays. Landsat data has been useful in areas such as agriculture, forestry, urban planning, mapping, cartography, water resources studies, and geology. M S.K.

A82-34367#
ERS-1 EUROPEAN REMOTE SENSING SATELLITE
Dornier-Post (English Edition), no. 2, 1982, p. 24-29

The mission objectives and the components developed for the ERS-1 remote sensing satellite are discussed. The spacecraft is intended for use in weather forecasting, sea state forecasting, off-shore activities support, ship routing, ice monitoring, ocean pollution monitoring, scientific investigations of complex ocean interactions, and microwave sensing of land surfaces and coastal zones. A supply module provides power for the instruments and earth pointing. The data will be transmitted and possibly stored on board. Launched by the Ariane into a 675 km sunsynchronous orbit, ERS-1 will carry a sidelooking radar with SAR for high resolution land and ocean imaging and wave spectra plotting, and a wind scatterometer for measurements from 4-24 m/sec over the oceans A microwave radar serves for wave height, earth surface height, wind speed, and iced- or open-ocean determination. Launch is scheduled for 1987. M.S.K.

A82-36617*
SPACE SCIENCE FOR APPLICATIONS - THE HISTORY OF LANDSAT
P. E MACH In. Space science comes of age· Perspectives in the history of the space sciences; Proceedings of the Symposium, Washington, DC, March 23, 24, 1981 Washington, DC, Smithsonian Institution Press, 1981, p 135-148. NASA-supported research refs

The history of the Landsat project is discussed in terms of three historical phases, each characterized by a dominant problem. From 1964 to 1967, the challenge was to develop interagency cooperation and to achieve consensus on basic plans for the satellite Between 1968 and 1971, the cooperating agencies had to persuade the Bureau of the Budget to provide funding for the project Since 1972, the challenge to NASA has been to encourage applications of the Landsat data and plan the shift from an experimental program to an operational one. The tension between experimental and operational goals has run through all these phases, and the conflicts between agencies is detailed, as well as the interaction between technological and political systems. C.D.

N82-22620*# Lockheed Engineering and Management Services Co., Inc., Houston, Tex.
TEN-ECOSYSTEM STUDY Final Report
A. V MAZADE, Principal Investigator Aug. 1981 96 p refs Sponsored in part by USDA Original contains color imagery Original photography may be purchased from the EROS Data Center, Sioux Falls, S D. 57198. ERTS
(Contract NAS9-15800; PROJ. AGRISTARS)
(E82-10186; NASA-CR-167457, NAS 1.26:167457; LEMSCO-13491) Avail NTIS HC A05/MF A01 CSCL 13B

Remote sensing methodology developed for the Nationwide Forestry Applications Program utilize computer data processing procedures for performing inventories from satellite imagery The Ten-Ecosystem Study (TES) was developed to test the processing procedures in an intermediate-sized application study. The results of TES indicate that LANDSAT multispectral imagery and associated automatic data processing techniques can be used to distinguish softwood, hardwood, grassland, and water and make inventory of these classes with an accuracy of 70 percent or better. The technical problems encountered during the TES and the solutions and insights to these problems are discussed. The TES experience is useful in planning subsequent inventories utilizing remote sensing technology. T.M.

N82-22630# Committee on Science and Technology (U. S House)
CIVIL LAND REMOTE SENSING SYSTEM
Washington GPO 1982 77 p Presented by the Subcom on Space Sci. and Appl. of the Comm. on Sci. and Technol., 97th Congr., 1st Sess , Dec. 1981
(GPO-87-070) Avail Subcommittee on Space Science and Applications

Current remote sensing research and development activities, current planning for an operational system, and international remote sensing activities are summarized. Significant issues considered include: the role of government vis-a-vis the private sector, the way in which it can best serve both the public and the private sector, its role in future research and development, and regulations and terms it must mandate for a civil land remote sensing system. Legislation needed for government/industry joint ventures is also examined. A.R.H.

N82-23258*# National Aeronautics and Space Administration, Washington, D. C
OSTA-1 POST MISSION OPERATION REPORT
1982 17 p
(NASA-TM-84191, NAS 1.15:84191; S-420-81-01) Avail. NTIS HC A02/MF A01 CSCL 22A

The first science and applications payload for the space shuttle was carried on STS-2. The space shuttle's performance and systems were tested The Shuttle's capability of providing a platform

for scientific and applications research was demonstrated. The OSTA-1 payload was selected and developed to demonstrate this secondary objective. The experiments selected for the OSTA-1 payload were concerned with remote sensing of Earth resources, environmental quality, ocean conditions, meteorological phenomena and life sciences. These experiments demonstrated the Shuttle's capability for space research and the potential application of techniques for future remote sensing S.L.

N82-23568*# Environmental Research Inst of Michigan, Ann Arbor.
LANDSAT TECHNOLOGY TRANSFER TO THE PRIVATE AND PUBLIC SECTORS THROUGH COMMUNITY COLLEGES AND OTHER LOCALLY AVAILABLE INSTITUTIONS Final Report, 20 Dec. 1979 - 20 Dec. 1980
R. H. ROGERS, Principal Investigator Dec. 1980 59 p ERTS
(Contract NASW-3308)
(E82-10181; NASA-CR-168846; NAS 1.26.168846;
ERIM-147200-13-F) Avail: NTIS HC A04/MF A01 CSCL 05A

Major first year accomplishments are summarized and plans are provided for the next 12-month period for a program established by NASA with the Environmental Research Institute of Michigan to investigate methods of making LANDSAT technology readily available to a broader set of private sector firms through local community colleges. The program applies a network where the major participants are NASA, university or research institutes, community colleges, and obtain hands-on training in LANDSAT data analysis techniques, using a desk-top, interactive remote analysis station which communicates with a central computing facility via telephone line, and provides for generation of land cover maps and data products via remote command A.R H.

N82-24216# Centre National d'Etudes Spatiales, Toulouse (France)
HISTORY OF THE FRENCH SATELLITE SPACE PROGRAM [HISTORIQUE DU PROGRAMME SPATIALE SCIENTIFIQUE FRANCAIS]
J C. HUSSON *In its* The Technol of Spaceborne Sci Expt p 3-10 1981 In FRENCH
Avail: NTIS HC A99/MF A01

The amplitude of the French space program and the variety of research that supports it are discussed. Three objectives stand out: (1) develop space research and technology; (2) develop spacecraft and related technology; and (3) participate on a global scale in research into the terrestrial environment, space observation, and exploration of the solar system. Given this perspective, results concerning astronomy, planetology, geophysics, geodesy, meteorology, and biology are reviewed. Future projects in space manufacturing are also mentioned.
Author (ESA)

N82-24263# Joint Publications Research Service, Arlington, Va.
COST-EFFECTIVENESS OF GEOGRAPHIC SURVEYING FROM SPACE
M. Y. LEMESHEV, Y. V. SUKHOTIN, and A. F DEMIDOV *In its* USSR Rept.: Space, No. 15 (JPRS-80424) p 76-96 29 Mar 1982 refs Transl. into ENGLISH from Ekon. Mat Metody (USSR), v. 17, no. 5, Sep - Oct 1981 p 920-935
Avail: NTIS HC A07/MF A01

An economic evaluation of space based observation systems is presented The cost effectiveness of these satellite systems is discussed. S.L.

N82-24568*# National Conference of State Legislatures, Denver, Colo Remote Sensing Project.
A LEGISLATOR'S GUIDE TO LANDSAT
1982 33 p Sponsored by NASA. Original contains color imagery Original photography may be purchased from the EROS Data Center, Sioux Falls, S.D. 57198 ERTS
(E82-10290; NASA-CR-168859, NAS 1.26:168859) Avail: NTIS HC A03/MF A01 CSCL 05B

The LANDSAT satellite is an effective tool in meeting the natural resources data requirements of state and federal legislation. The availability of data from the satellite is beginning to have an impact on state legislature activities An overview of the history, operation, and data analysis techniques, is presented as well as a discussion of the advantages and limitations of this method of remote sensing. Applications are discussed in the areas of (1) land resource planning and management; (2) coastal zone management; (3) agriculture; (4) forestry; (5) routing and siting, (6) environmental monitoring; and (7) geological exploration. National and state sources from which information about LANDSAT technology is available are listed A R.H.

N82-26746*# Purdue Univ., Lafayette, Ind. Lab. of Applications of Remote Sensing.
KEY ISSUES IN THE ANALYSIS OF REMOTE SENSING DATA: A REPORT ON THE WORKSHOP
P. H. SWAIN, Principal Investigator Jun 1981 41 p Workshop held in West Lafayette, Ind., 22-23 Jun. 1981 ERTS
(Contract NAS9-15466)
(E82-10348; NASA-CR-167570; NAS 1.26:167570;
LARS-TR-062481) Avail NTIS HC A03/MF A01 CSCL 05B

The procedures of a workshop assessing the state of the art of machine analysis of remotely sensed data are summarized. Areas discussed were. data bases, image registration, image preprocessing operations, map oriented considerations, advanced digital systems, artificial intelligence methods, image classification, and improved classifier training Recommendations of areas for further research are presented. J D.

Typical Subject Index Listing

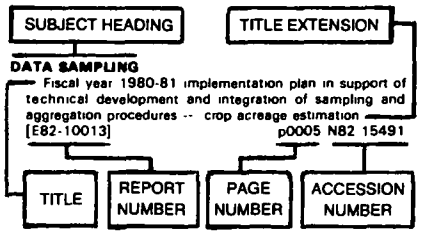

The subject heading is a key to the subject content of the document The title is used to provide a description of the subject matter When the title is insufficiently descriptive of the document content, the title extension is added, separated from the title by three hyphens The (NASA or AIAA) accession number and the page number are included in each entry to assist the user in locating the abstract in the abstract section (of this supplement) If applicable, a report number is also included as an aid in identifying the document Under any one subject heading, the accession numbers are arranged in sequence with the AIAA accession numbers appearing first

A

ABSORPTION SPECTRA
Remote sensing of leaf water content in the near infrared p 8 A82-32897
In situ ozone data for comparison with laser absorption remote sensor 1980 PEPE/NEROS program [NASA-TM-84471] p 30 N82-25661

ABSORPTION SPECTROSCOPY
Observation of the diurnal variation of atmospheric ozone p 26 A82-35895

ABSORPTIVITY
Sensitivity of Dobson total ozone estimations to wavelength band calibration uncertainties p 27 A82-36405
Dobson spectrophotometer calibrations, possible errors in ozone absorption coefficients, and errors due to interfering pollutant gases p 28 A82-36431

ABUNDANCE
The cosmic ray positron spectrum p 1 A82-22542
Calculated isotopic source composition and tests for origin and propagation of cosmic rays with mass numbers less than or equal to 62 p 83 A82-22554
Comparative abundances in solar energetic particles and in galactic cosmic ray sources, and the Ne-22 anomaly p 83 A82-22556
Mass per charge ratio in hot plasmas and cosmic ray source composition p 2 A82-22557
Cosmic ray composition from acceleration of thermal matter p 64 A82-22558
Interstellar grains as seeds for galactic cosmic rays p 2 A82-22561
On the stellar origin of the Ne-22 excess in cosmic rays p 21 A82-22562
Time and energy dependence of heavy ion abundances in solar flare energetic particle events p 22 A82-22605
High resolution measurements of solar flare isotopes p 22 A82-22606
Heavy-element abundances in He/3/-rich events p 5 A82-22611
A comparison of helium and heavy ion spectra in He/3/ rich solar flares with a model calculation p 5 A82-22612
On the anticorrelation between the He/3//He/4/ ratio and proton intensity in He/3/ rich flares p 40 A82-22613

ACCURACY
Investigations of point transfer p 78 A82-33296
Ten-Ecosystem Study --- Grand and Weld Counties, Colorado, Warren County, Pennsylvania, St Louis County, Minnesota, Sandoval County, New Mexico, Kershaw County, South Carolina, Fort Yukon, Alaska, Grays Harbor County, Washington, and Washington County, Missouri [E82-10186] p 84 N82-22620
Analysis of scanner data for crop inventories [E82-10192] p 10 N82-22626
AgRISTARS Preliminary technical results review of FY81 experiments, volume 2 Fiscal year 1981/1982 'corn and soybeans pilot' experiment [E82-10216] p 13 N82-23589
An analysis of LANDSAT MSS scene-to-scene registration accuracy [E82-10285] p 16 N82-24563

ACTINIDE SERIES
Laboratory studies of actinide metal-silicate fractionation p 49 A82-22306

AERIAL PHOTOGRAPHY
Detection of environmental disturbance using color aerial photography and thermal infrared imagery p 22 A82-29327
Description of gray level picture using a collection of density contour lines p 66 A82-29409
Color aerial photography in the plant sciences and related fields, Proceedings of the Eighth Biennial Workshop, Luray, VA, April 21-23, 1981 p 5 A82-29526
Development and application of panoramic aerial photography in forest pest management p 5 A82-29527
Riparian vegetation mapping in Northeastern California using high altitude color infrared aerial photography p 5 A82-29528
Inventory of wildlife habitat from color infrared aerial photography for Cobb Island, Virginia p 6 A82-29529
Considerations in using color infrared photographs for vegetative interpretation p 6 A82-29530
Color aerial photography detects nutrient status of loblolly pine plantations p 6 A82-29531
Application of 35mm color aerial photography to forest land change detection p 6 A82-29533
Estimating rangeland cover proportions with large-scale color-infrared aerial photographs p 6 A82-29534
Mapping riparian vegetation in Southeastern Oregon using digitized large scale color infra-red aerial photography p 6 A82-29535
Remote sensing of Douglas-fir trees newly infested by bark beetles p 6 A82-29536
Detection and damage assessment of citrus tree losses with aerial color infrared photography /ACIR/ p 7 A82-29538
An infrared exposure meter p 76 A82-29541
Thermography - A remote sensing method with many perspectives p 76 A82-29922
Problems of the interpretation of aerial and satellite images of industrial smoke p 23 A82-30307
Extraction of line shaped objects from aerial images using a special operator to analyze the profiles of functions p 67 A82-32033
Panoramic aerial photography in forest pest management p 7 A82-32701
Photogrammetric methods for mapping resource data from high altitude panoramic photography p 77 A82-32702
Estimating bark beetle-killed lodgepole pine with high altitude panoramic photography p 7 A82-32703
Estimating mountain pine beetle-killed ponderosa pine over the front range of Colorado with high altitude panoramic photography p 7 A82-32704
Optical bar panoramic photography for planning timber salvage in drought-stressed forests p 7 A82-32705
Evaluation of spruce-fir forests using small-format photographs p 8 A82-32707
Nearshore current pattern off south Texas - An interpretation from aerial photographs p 53 A82-32903
Image quality and height measurement accuracy of aerial survey camera imagery from high altitudes p 78 A82-33297
Skirt clouds associated with the Soufriere eruption of 17 April 1979 p 24 A82-33656
The use of Landsat-3 thermal data to help differentiate land covers p 25 A82-34218
Evaluation of the effectiveness of systematic image distortion compensation p 69 A82-34469
Technical and economical characteristics of the AFA-TES-10M aerial camera p 79 A82-34470
Analytical processing of photographs taken by paired cameras p 79 A82-34471
A quantitative method to test for similarity between photo interpreters p 69 A82-34722
Sensitometry in Canadian aerial survey p 79 A82-34724
Effects of altitude, focal length, and filter combinations on color infrared photography of citrus groves p 9 A82-34729
Remote sensing - A potential aid in the preparation of an urban tree inventory p 9 A82-34732
Use of aerial photography in determining land use and streamflow relationships on small developing watersheds p 60 A82-34736
Aerial photography vs Landsat for digital land-cover mapping in an urban watershed p 61 A82-34745
Present status of on-line analytical triangulation p 69 A82-34940
A quantitative multispectral analysis system for aerial photographs applied to coastal planning p 55 A82-37505

AERIAL RECONNAISSANCE
Aerogeophysical methods of finding uranium deposits --- Russian book p 41 A82-33402
Airborne gamma-ray spectrometer and magnetometer survey Roseau quadrangle, Minnesota, volume 1 [DE82-001031] p 43 N82-23621
Airborne gamma-ray spectrometer and magnetometer survey Barrow quadrangle, Alaska, volume 1 [DE82-000334] p 43 N82-23623
Airborne gamma-ray spectrometer and magnetometer survey Wainwright quadrangle, Alaska, volume 2 [DE82-000341] p 43 N82-23624
Airborne gamma-ray spectrometer and magnetometer survey Devil's Lake quadrangle, North Dakota, volume 1 [DE82-004161] p 44 N82-23635
Airborne gamma-ray spectrometer and magnetometer survey Devil's Lake quadrangle, North Dakota, volume 2 [DE82-004168] p 44 N82-23636
Airborne gamma-ray spectrometer and magnetometer survey Bemidji quadrangle, Minnesota, volume 1 [DE82-001032] p 44 N82-23637
Airborne gamma-ray spectrometer and magnetometer survey Bemidji quadrangle, Minnesota, volume 2 [DE82-001026] p 44 N82-23638
Airborne gamma-ray spectrometer and magnetometer survey Barrow quadranagle, Alaska, volume 2 [DE82-000342] p 46 N82-25623
Airborne gamma-ray spectrometer and magnetometer survey North/south tieline, volume 1 [DE82-005542] p 47 N82-27804
Airborne gamma-ray spectrometer and magnetometer survey North/south tieline, volume 2 [DE82-005570] p 47 N82-27805
Evaluation and combined geophysical interpretations of NURE and related geoscience data in the Van Horn, Pecos, Marfa, Fort Stockton, Presidido, and Emory Peak quadrangles, Texas, volume 1 [DE82-005554] p 47 N82-27808
Airborne gamma-ray spectrometer and magnetometer survey Huron Quadrangle, South Dakota [DE82-005540] p 48 N82-27814

Airborne gamma-ray spectrometer and magnetometer survey Chico Quadrangle, California
[DE82-005543] p 48 N82-27815

AEROSOLS

Effect of atmospheric conditions on remote sensing of vegetation parameters p 24 A82-32901
The effect of the spectral attenuation of UV radiation by aerosol on the total ozone measurements p 27 A82-36406

AFRICA

The mineralogy of global magnetic anomalies --- rock magnetic signatures and MAGSAT geological, and gravity correlations in West Africa
[E82-10305] p 45 N82-24579
An investigation of MAGSAT and complementary data emphasizing precambrian shields and adjacent areas of *West Africa and South America*
[E82-10316] p 38 N82-24589
An investigation of MAGSAT and complementary data emphasizing precambrian shields and adjacent areas of West Africa and South America
[E82-10317] p 38 N82-24590
An investigation of MAGSAT and complementary data emphasizing precambrian shields and adjacent areas of West Africa and South America
[E82-10318] p 38 N82-24591
Aeromagnetic and satellite magnetic anomaly mapping
[E82-10339] p 39 N82-25601

AGRICULTURE

Remote sensing of leaf water content in the near infrared p 8 A82-32897
Analysis of scanner data for crop inventories
[E82-10192] p 10 N82-22626
AgRISTARS Supporting research Spring small grains planting date distribution model
[E82-10208] p 12 N82-23581
AgRISTARS *Preliminary technical results review of* FY81 experiments, volume 2 Fiscal year 1981/1982 'corn and soybeans pilot' experiment
[E82-10216] p 13 N82-23589
Application of thermal model for pan evaporation to the hydrology of a defined medium, the sponge
[E82-10217] p 13 N82-23590
A meteorologically driven grain sorghum stress indicator model
[E82-10218] p 13 N82-23591
Selection of the Australian indicator region
[E82-10222] p 13 N82-23595
Agricultural Research Service research highlights in remote sensing for calendar year 1980
[E82-10228] p 14 N82-23601
AgRISTARS Agriculture and resources inventory surveys through aerospace remote sensing
[E82-10236] p 15 N82-23609
An analysis of LANDSAT MSS scene-to-scene registration accuracy
[E82-10285] p 16 N82-24563
An algorithm for automating the registration of USDA segment ground data to LANDSAT MSS data
[E82-10286] p 16 N82-24564
Plan of research for integrated soil moisture studies *Recommendations of the Soil Moisture Working Group*
[NASA-TM-84731] p 18 N82-25608
Association of spectral development patterns with development stages of corn
[E82-10353] p 19 N82-26751

AGRISTARS PROJECT

AgRISTARS Project management report Program review presentation to level 1, interagency coordination committee
[E82-10219] p 13 N82-23592
AgRISTARS Agriculture and resources inventory surveys through aerospace remote sensing
[E82-10236] p 15 N82-23609

AGROCLIMATOLOGY

A meteorologically driven maize stress indicator model
[E82-10112] p 11 N82-23564
Selection of the Australian indicator region
[E82-10222] p 13 N82-23595

AGROMETEOROLOGY

Spectral estimates of solar radiation intercepted by corn canopies
[E82-10003] p 18 N82-26742

AIR LAND INTERACTIONS

On the application of a model of boundary-layer flow over low hills to real terrain p 29 A82-36741

AIR MASSES

Comparison of ozone in polluted and clean air masses over Lake Michigan p 29 A82-36477

AIR POLLUTION

Problems of the interpretation of aerial and satellite images of industrial smoke p 23 A82-30307
Detection of volcanic smoke and ash-fall area at volcano Aso, from Landsat MSS data p 23 A82-31295
Detection of regional air pollution episodes utilizing satellite digital data in the visual range p 23 A82-31990
Aircraft measurements of NO/x/ in the lower troposphere above the coast of Japan p 26 A82-36247
Tropospheric CO measurement experiment from the second Space Shuttle flight p 27 A82-36292
Dobson spectrophotometer calibrations, possible errors in ozone absorption coefficients, and errors due to interfering pollutant gases p 28 A82-36431
Comparison of ozone in polluted and clean air masses over Lake Michigan p 29 A82-36477
Breadboard gas filter correlation spectrometer for atmospheric measurement of hydrazines and nitrogen dioxide
[AD-A110688] p 82 N82-26642
A study of atmospheric diffusion from the LANDSAT imagery --- pollution transport over the ocean
[E82-10360] p 58 N82-26758
Feasibility of laser-separation of 36 S and its use as an atmospheric tracer
[DE82-000965] p 30 N82-27737
Remote sensing of sulfur dioxide effects on vegetation *Volume 1 Summary*
[DE82-900580] p 31 N82-27802
Remote sensing of sulfur dioxide effects on vegetation Volume 2 Data
[DE82-900581] p 31 N82-27803

AIR QUALITY

In situ ozone data for comparison with laser absorption remote sensor 1980 PEPE/NEROS program
[NASA-TM-84471] p 30 N82-25661
Field measurements in support of dispersion modeling in complex terrain (1980)
[PB82-148644] p 39 N82-27882

AIR SAMPLING

The growth of snow in winter storms - An airborne observational study p 60 A82-33329

AIR WATER INTERACTIONS

Remote sensing of precipitable water over the oceans from Nimbus 7 microwave measurements p 49 A82-28907
Surface wind analyses for Seasat p 51 A82-29619
Estimation of the temperature of the upper boundary of cloud cover over the world ocean p 54 A82-36005
Interannual variations of outgoing IR associated with tropical circulation changes during 1974-1978 p 54 A82-36341
Analysis of ocean and atmosphere thermodynamical characteristics during the onset of southwest monsoon over the Arabian Sea p 57 N82-23945

AIRBORNE EQUIPMENT

Aircraft monitoring of surface carbon dioxide exchange p 23 A82-30293
A system design for a multispectral sensor using two-dimensional solid-state imaging arrays p 77 A82-31991
High spectral resolution airborne spectrometry p 77 A82-32443
The growth of snow in winter storms - An airborne observational study p 60 A82-33329
EPA's new bubble and banking policies --- for environmental monitoring p 25 A82-33865
An optical data link for airborne scanning system p 80 A82-34737
Study of the hydrological cycle by aerospace methods --- Russian book p 61 A82-35126
Evaluation of the accuracy of water-surface temperature measurement by means of airborne infrared radiometers p 62 A82-35136
Comparison of brightness indicatrixes of snow cover measured from an aircraft and calculated theoretically for different heights of the atmosphere p 62 A82-35140
Airborne gamma-ray spectrometer and magnetometer survey, Kingston quadrangle New York, volume 2C
[DE81-027161] p 46 N82-25621
Airborne gamma-ray spectrometer and magnetometer survey Barrow quadranagle, Alaska, volume 2
[DE82-000342] p 46 N82-25623

AIRBORNE/SPACEBORNE COMPUTERS

Bathymetric imaging p 69 A82-34720

ALASKA

Landsat digital analysis of the initial recovery of burned tundra at Kokolik River, Alaska p 8 A82-32913
Airborne gamma-ray spectrometer and magnetometer survey Barrow quadrangle, Alaska, volume 1
[DE82-000334] p 43 N82-23623
Airborne gamma-ray spectrometer and magnetometer *survey Wainwright quadrangle, Alaska, volume 2*
[DE82-000341] p 43 N82-23624
Airborne gamma-ray spectrometer and magnetometer survey Meade River quadrangle, Alaska, volume 2
[DE82-000340] p 43 N82-23626
Airborne gamma-ray spectrometer and magnetometer survey Teshekpuk quadrangle, Alaska, volume 2
[DE82-000310] p 43 N82-23627
Airborne gamma-ray spectrometer and magnetometer survey Harrison Bay quadrangle, Alaska, volume 2
[DE82-000315] p 43 N82-23628
Airborne gamma-ray spectrometer and magnetometer survey Beechey Pt , quadrangle, Alaska, volume 2
[DE82-000309] p 43 N82-23629
Airborne gamma-ray spectrometer and magnetometer survey Point Lay quadrangle, Alaska, volume 2
[DE82-000308] p 43 N82-23630
Airborne gamma-ray spectrometer and magnetometer survey Utukik River quadrangle, Alaska, volume 2
[DE82-000316] p 44 N82-23631
Airborne gamma-ray spectrometer and magnetometer *survey Sagavanirktok quadrangle, Alaska, volume 2*
[DE82-000311] p 44 N82-23632
Airborne gamma-ray spectrometer and magnetometer survey Lookout Ridge quadrangle, Alaska, volume 2
[DE82-000313] p 47 N82-25625
Ice distribution and winter surface circulation patterns, Kachemak Bay, Alaska
[AD-A110806] p 58 N82-26764

ALFALFA

Normal crop calendars Volume 3 The corn and soybean states of Illinois, Indiana, and Iowa
[E82-10221] p 13 N82-23594
A multi-frequency radiometric measurement of soil moisture content over bare and vegetated fields
[E82-10238] p 16 N82-23611

ALGAE

HCMM hydrological analysis in Utah
[E82-10328] p 63 N82-24601

ALGORITHMS

Multistage classification of multispectral Earth observational data The design approach
[E82-10213] p 72 N82-23586

ALTIMETERS

Intercomparison of wind speeds inferred by the SASS, altimeter, and SMMR p 52 A82-29621
Geoid height-age relation from Seasat altimeter profiles across the Mendocino Fracture Zone p 34 A82-32646

ALTITUDE

Effects of altitude, focal length, and filter combinations on color infrared photography of citrus groves p 9 A82-34729
Comparison of brightness indicatrixes of snow cover *measured from an aircraft and calculated theoretically for* different heights of the atmosphere p 62 A82-35140

AMMONIA

Ammonia and the NOx budget of the troposphere p 27 A82-36293

ANALYSIS OF VARIANCE

A comparison of stratified versus regression estimators p 11 N82-23133

ANGULAR CORRELATION

Angular variations of nonthermal radio emission from the Galaxy relevant to the structure of interstellar magnetic field p 83 A82-22550

ANGULAR DISTRIBUTION

Albedo and angular characteristics of the reflectance of *the underlying surface and clouds --- Russian book* p 33 A82-30849
Comparison of brightness indicatrixes of snow cover measured from an aircraft and calculated theoretically for *different heights of the atmosphere* p 62 A82-35140

ANGULAR MOMENTUM

Magnetic monopole pair and its observation in cosmic rays p 65 A82-22579

ANISOTROPY

On the physical sense of the constant of solar cosmic ray coronal propagation p 83 A82-22599

ANNUAL VARIATIONS

A study of the earth's radiation budget using a general circulation model p 52 A82-30666
The seasonal snow-line within the Fergana basin and the possibility of using it for hydrological forecasting p 61 A82-35131
Interannual variations of outgoing IR associated with tropical circulation changes during 1974-1978 p 54 A82-36341
Observations and analyses of the total amount of atmospheric ozone in the Beijing region and in the region of Jolmolungma Mountain in Tibet p 28 A82-36444
The seasonal variations of ozone and temperature in *the middle and the upper stratosphere* p 29 A82-36534

ANOMALIES

Airborne gamma-ray spectrometer and magnetometer survey, Toronto quadrangle New York, volume 2A
[DE81-027158] p 46 N82-25620
Airborne gamma-ray spectrometer and magnetometer survey, Rochester quadrangle New York, volume 2D
[DE81-027156] p 46 N82-25622

ANTARCTIC REGIONS
Magsat magnetic anomalies over Antarctica and the surrounding oceans p 32 A82-30787
Investigation of Antarctic crust and upper mantle using MAGSAT and other geophysical data
[E82-10308] p 37 N82-24582
Investigation of Antarctic crust and upper mantle using MAGSAT and other geophysical data
[E82-10309] p 37 N82-24583
ANTIPARTICLES
Magnetic monopole pair and its observation in cosmic rays p 65 A82-22579
ANTIPROTONS
Comparison of the measured antiproton flux with that predicted by the 'leaky box' model p 1 A82-22544
Dependence of earth spectrum of positrons and antiprotons on propagation models --- of cosmic radiation p 21 A82-22545
Antiprotons from galactic sources of cosmic rays and gamma rays p 82 A82-22546
ARABIAN SEA
On the space-time variability of ocean surface mixed layer characteristics of central and eastern Arabian sea during MONSOON-77 --- global atmospheric research program p 56 N82-23909
Analysis of ocean and atmosphere thermodynamical characteristics during the onset of southwest monsoon over the Arabian Sea p 57 N82-23945
ARCHITECTURE (COMPUTERS)
Design guidelines for satellite image data distribution systems p 70 A82-37048
ARCTIC OCEAN
Magsat magnetic anomalies over Antarctica and the surrounding oceans p 32 A82-30787
ARGENTINA
Analysis of scanner data for crop inventories
[E82-10192] p 10 N82-22626
AgRISTARS Project management report Program review presentation to level 1, interagency coordination committee --- Brazil, Argentina, U S corn belt, Great Plains Corridor
[E82-10231] p 15 N82-23604
Analysis of scanner data for crop inventories
[E82-10241] p 16 N82-24519
ARIZONA
The application of Heat Capacity Mapping Mission (HCMM) thermal data to snow hydrology --- Salt Verde Watershed and the southern Sierra Nevada
[E82-10191] p 62 N82-22625
Application of HCMM data to regional geologic analysis for mineral and energy resource evaluation
[E82-10153] p 45 N82-24518
NURE aerial gamma-ray and magnetic reconnaissance survey of portions of New Mexico, Arizona and Texas Volume 2 New Mexico-Carlsbad Quadrangle
[DE82-005527] p 48 N82-27810
ARTIFICIAL INTELLIGENCE
Key Issues in the Analysis of Remote Sensing Data A report on the workshop
[E82-10348] p 85 N82-26746
ASTROMETRY
On reference coordinate systems used in polar motion determinations p 33 A82-32090
ASTRONOMICAL COORDINATES
The definition of the terrestrial coordinate frame by long baseline interferometry p 33 A82-32084
ASTRONOMICAL MAPS
A color-ratio map of Mercury p 31 A82-22294
ASTRONOMICAL MODELS
The cosmic ray positron spectrum p 1 A82-22542
Comparison of the measured antiproton flux with that *predicted by the 'leaky box' model* p 1 A82-22544
Dependence of earth spectrum of positrons and antiprotons on propagation models --- of cosmic radiation p 21 A82-22545
Consequences of an inverse Compton emission model for extragalactic X-ray sources p 83 A82-22553
Model for solar hard X-ray bursts p 65 A82-22581
ASTRONOMICAL PHOTOMETRY
Subtleties in the flat-fielding of charge-coupled device /CCD/ images p 68 A82-32581
ATLANTIC OCEAN
Comparison data for Seasat altimetry in the western North Atlantic p 50 A82-29611
A study of atmospheric diffusion from the LANDSAT imagery --- pollution transport over the ocean
[E82-10360] p 58 N82-26758
ATMOSPHERIC ATTENUATION
Evaluation of atmospheric attenuation from SMMR brightness temperature for the Seasat satellite scatterometer p 51 A82-29618
Simplified techniques to study components of solar radiation under haze and clouds p 78 A82-32766
ATMOSPHERIC BOUNDARY LAYER
On the application of a model of boundary-layer flow over low hills to real terrain p 29 A82-36741
Marine boundary layer wind structure over the Bay of Bengal during Monex-79 --- Monsoon Experiment (MONEX) p 57 N82-23929
ATMOSPHERIC CHEMISTRY
Observation of the diurnal variation of atmospheric ozone p 26 A82-35895
The seasonal variations of ozone and temperature in the middle and the upper stratosphere p 29 A82-36534
ATMOSPHERIC CIRCULATION
Remote sensing of precipitable water over the oceans from Nimbus 7 microwave measurements p 49 A82-28907
A study of the earth's radiation budget using a general circulation model p 52 A82-30666
Interannual variations of outgoing IR associated with tropical circulation changes during 1974-1978 p 54 A82-36341
The impact of meteorological satellites on the First GARP Global Experiment (FGGE) --- First Global Atmospheric Research Program Global Experiment (FGGE) p 55 N82-23852
ATMOSPHERIC COMPOSITION
Total ozone variations 1970-74 using Backscattered Ultraviolet /BUV/ and ground-based observations p 26 A82-36053
Tropospheric CO measurement experiment from the second Space Shuttle flight p 27 A82-36292
Atmospheric ozone determination by solar occultation using the UV spectrometer on the Solar Maximum Mission p 27 A82-36362
Application of infrared techniques to the study of atmospheric ozone p 27 A82-36414
Total ozone retrieval from satellite Meteor 28 Fourier spectrometer measurements p 28 A82-36422
Observations and analyses of the total amount of atmospheric ozone in the Beijing region and in the region of Jolmolungma Mountain in Tibet p 28 A82-36444
In situ ozone data for comparison with laser absorption remote sensor 1980 PEPE/NEROS program
[NASA-TM-84471] p 30 N82-25661
ATMOSPHERIC DIFFUSION
A study of atmospheric diffusion from the LANDSAT imagery --- pollution transport over the ocean
[E82-10360] p 58 N82-26758
ATMOSPHERIC EFFECTS
Effect of atmospheric conditions on remote sensing of vegetation parameters p 24 A82-32901
Allowance for the effect of the atmosphere in the processing of satellite remote-sensing images p 70 A82-35141
ATMOSPHERIC IONIZATION
The determination of differential X-ray spectrum of the solar flare using ionospheric data p 65 A82-22582
ATMOSPHERIC MODELS
A study of the earth's radiation budget using a general circulation model p 52 A82-30666
The growth of snow in winter storms - An airborne observational study p 60 A82-33329
ATMOSPHERIC MOISTURE
Remote sensing of precipitable water over the oceans from Nimbus 7 microwave measurements p 49 A82-28907
Description of Seasat radiometer status and results p 52 A82-29622
Estimation of the precipitable water from the IR channel of the geostationary satellite p 55 A82-37196
ATMOSPHERIC OPTICS
Relating Landsat digital count values to ground reflectance for optically thin atmospheric conditions p 66 A82-29762
ATMOSPHERIC PRESSURE
Mean sea-level pressure in the Southern Hemisphere during the FGGE period --- First Global Atmospheric Research Program Global Experiment (FGGE), buoys p 55 N82-23856
Estimates of the statistical structure of the atmospheric pressure field in summer Monex-79 area p 57 N82-23939
ATMOSPHERIC RADIATION
Soft X-rays from the sunlit earth's atmosphere p 29 A82-37405
ATMOSPHERIC SOUNDING
Total ozone variations 1970-74 using Backscattered Ultraviolet /BUV/ and ground-based observations p 26 A82-36053
Microwave measurement of stratospheric and mesospheric ozone p 28 A82-36415
ATMOSPHERIC TEMPERATURE
Estimation of the temperature of the upper boundary of cloud cover over the world ocean p 54 A82-36005
The seasonal variations of ozone and temperature in the middle and the upper stratosphere p 29 A82-36534
Satellite radiation measurements for the retrieval of the vertical temperature profiles p 70 A82-36935
A meteorologically driven maize stress indicator model
[E82-10112] p 11 N82-23564
ATMOSPHERIC WINDOWS
Application of infrared techniques to the study of atmospheric ozone p 27 A82-36414
ATTITUDE CONTROL
LANDSAT-D conical scanner evaluation plan
[E82-10340] p 81 N82-25602
AURORAL ARCS
Extremely high latitude auroras p 76 A82-31020
AURORAL IRRADIATION
Large amplitude undulations on the equatorward boundary of the diffuse aurora p 76 A82-31019
AURORAL ZONES
Generation of the auroral kilometric radiation p 26 A82-35542
AUSTRALIA
Selection of the Australian indicator region
[E82-10222] p 13 N82-23595
The onset of the Australian Northwest monsoon during winter MONEX Broadscale flow revealed by an objective analysis scheme p 56 N82-23912
AUTOCORRELATION
The influence of autocorrelation in signature extraction An example from a geobotanical investigation of Cotter Basin, Montana
[E82-10341] p 46 N82-25603
AUTOMATIC WEATHER STATIONS
Remote automatic weather station for resource and fire management agencies
[PB82-107335] p 30 N82-23963
AUTOMATION
Extraction of line shaped objects from aerial images using a special operator to analyze the profiles of functions p 67 A82-32033
AVIONICS
Effective electromagnetic shielding in multilayer printed circuit boards
[AIAA 81-2333] p 59 A82-13528

B

BALTIC SEA
The METEOSAT Data Collection System and its application p 75 N82-26037
BARLEY
AgRISTARS Foreign commodity production forecasting The 1980 US/Canada wheat and barley exploratory experiment
[E82-10126] p 11 N82-23565
AgRISTARS Supporting research Spring small grains planting date distribution model
[E82-10208] p 12 N82-23581
Evaluation of the procedure for separating barley from other spring small grains --- North Dakota, South Dakota, Minnesota and Montana
[E82-10230] p 14 N82-23603
Description of the FORTRAN implementation of the spring small grains planting date distribution model
[E82-10235] p 15 N82-23608
Multilevel measurements of surface temperature over undulating terrain planted to barley
[E82-10245] p 16 N82-24523
Evaluation of HCMM data for assessing soil moisture and water table depth --- South Dakota
[E82-10329] p 18 N82-24602
BAROTROPIC FLOW
Impact of additional summer MONEX wind data on the *prediction of monsoon depressions during June - August* 1979 with two versions of primitive equation (PE) barotropic model --- Monsoon Experiment (MONEX) p 56 N82-23900
BAROTROPISM
Estimates of sea surface stress for summer MONEX from cloud motions --- global atmospheric research program p 56 N82-23910
BARREN LAND
A multi-frequency radiometric measurement of soil moisture content over bare and vegetated fields
[E82-10238] p 16 N82-23611
Multifrequency remote sensing of soil moisture --- Guymon, Oklahoma and Dalhart, Texas
[E82-10362] p 20 N82-26760
BATHYMETERS
Bathymetric imaging p 69 A82-34720
BAY ICE
Ice distribution and winter surface circulation patterns, Kachemak Bay, Alaska
[AD-A110806] p 58 N82-26764
BAYS (TOPOGRAPHIC FEATURES)
Marine boundary layer wind structure over the Bay of *Bengal during Monex-79 --- Monsoon Experiment* (MONEX) p 57 N82-23929

BEACHES
Fluid-sediment interactions on beaches and shelves
[AD-A110838] p 59 N82-26948
BEDROCK
Satellite image interpretation of the eastern Caledonian part of the Blue Road Geotraverse and its geological implications /Nordland, Vasterbotten, Scandinavia/
p 41 A82-30305
Characterization of the structure and tectonic of South America
[E82-10196] p 42 N82-23569
BEETLES
Remote sensing of Douglas-fir trees newly infested by bark beetles p 6 A82-29536
Estimating mountain pine beetle-killed ponderosa pine over the front range of Colorado with high altitude panoramic photography p 7 A82-32704
BERMUDA
Seasat altimeter height calibration --- related to sea surface heights near Bermuda p 49 A82-29603
BERYLLIUM 10
The cosmic ray positron spectrum p 1 A82-22542
BIBLIOGRAPHIES
The crustal structure and tectonics of South America
[E82-10319] p 38 N82-24592
BIOLUMINESCENCE
Laser-induced bioluminescence --- for remote sensing of marine organisms p 53 A82-32559
BIOMASS
Development of visible/infrared/microwave agriculture classification and biomass estimation algorithms --- Guyton, Oklahoma and Dalhart, Texas
[E82-10363] p 20 N82-26761
BLACK HOLES (ASTRONOMY)
Acceleration processes near massive black holes
p 3 A82-22572
BLIGHT
Detection and damage assessment of citrus tree losses with aerial color infrared photography /ACIR/
p 7 A82-29538
BOTSWANA
Overseas Geology And Mineral Resources number 56 A geological interpretation of LANDSAT imagery and air photography of Botswana
[OGMR-56] p 42 N82-22636
BOUNDARY LAYER FLOW
On the application of a model of boundary-layer flow over low hills to real terrain p 29 A82-36741
On the space-time variability of ocean surface mixed layer characteristics of central and eastern Arabian sea during MONSOON-77 --- global atmospheric research program p 56 N82-23909
BRAZIL
Structure, composition and thermal state of the crust in Brazil --- geomagnetic survey
[E82-10187] p 35 N82-22621
Dynamic study of the upper Sao Francisco river and Tres Marias reservoir using MSS/LANDSAT images --- BRazil
[E82-10291] p 63 N82-24569
A study of atmospheric diffusion from the LANDSAT imagery --- pollution transport over the ocean
[E82-10360] p 58 N82-26758
BREMSSTRAHLUNG
Computer simulation of the time dependence of the photon energy spectra produced in proton and electron bremstrahlung p 3 A82-22587
BRIGHTNESS DISTRIBUTION
Comparison of brightness indicatrixes of snow cover measured from an aircraft and calculated theoretically for different heights of the atmosphere p 62 A82-35140
BRIGHTNESS TEMPERATURE
Surface temperature determination from an amalgamation of GOES and TIROS-N radiance measurements p 66 A82-28905
Remote sensing of precipitable water over the oceans from Nimbus 7 microwave measurements
p 49 A82-28907
Evaluation of atmospheric attenuation from SMMR brightness temperature for the Seasat satellite scatterometer p 51 A82-29618
Snowpack monitoring in North America and Eurasia using passive microwave satellite data
p 78 A82-32915
Depression of brightness temperature of sea surfaces covered with monomolecular oil films relative to clean water surfaces at 1 43 GHz p 54 A82-33322
Analysis of scanner data for crop inventories
[E82-10192] p 10 N82-22626
A multi-frequency radiometric measurement of soil moisture content over bare and vegetated fields
[E82-10238] p 16 N82-23611
The effect of sea-surface Sun glitter on microwave radiometer measurements
[NASA-CR-169083] p 57 N82-26525
Relating thematic mapper bands TM3, TM4, and TM5 to agronomic variables for corn, cotton, sugarbeet, soybean, sorghum, sunflower and tobacco
[E82-10347] p 19 N82-26745
BUNDLES
A practical study of gross-error detection in bundle adjustment p 69 A82-34702
BUOYS
The impact of meteorological satellites on the First GARP Global Experiment (FGGE) --- First Global *Atmospheric Research Program Global Experiment* (FGGE) p 55 N82-23852

C

C BAND
C-band radar for determining surface soil moisture
p 10 A82-37194
CALIBRATING
Seasat altimeter height calibration --- related to sea surface heights near Bermuda p 49 A82-29603
Tidal and geodetic observations for the Seasat altimeter *calibration experiment* p 49 A82-29604
Sensitivity of Dobson total ozone estimations to *wavelength band calibration uncertainties*
p 27 A82-36405
Dobson spectrophotometer calibrations, possible errors in ozone absorption coefficients, and errors due to interfering pollutant gases p 28 A82-36431
C-band radar for determining surface soil moisture
p 10 A82-37194
CALIFORNIA
The application of Heat Capacity Mapping Mission (HCMM) thermal data to snow hydrology --- Salt Verde Watershed and the southern Sierra Nevada
[E82-10191] p 62 N82-22625
Multilevel measurements of surface temperature over undulating terrain planted to barley
[E82-10245] p 16 N82-24523
Airborne gamma-ray spectrometer and magnetometer survey Ukiah quadrangle, California, volume 1 --- uranium exploration
[DE82-005541] p 48 N82-27813
Airborne gamma-ray spectrometer and magnetometer survey Chico Quadrangle, California
[DE82-005543] p 48 N82-27815
CAMERAS
Image quality and height measurement accuracy of serial survey camera imagery from high altitudes
p 78 A82-33297
Analytical processing of photographs taken by paired cameras p 79 A82-34471
CANADA
Magnetic charts of Canada derived from Magsat data
p 32 A82-30778
AgRISTARS Foreign commodity production forecasting The 1980 US/Canada wheat and barley exploratory experiment
[E82-10126] p 11 N82-23565
CANOPIES (VEGETATION)
Effect of atmospheric conditions on remote sensing of vegetation parameters p 24 A82-32901
The response characteristics of vegetation in Landsat MSS digital data p 8 A82-32907
View angle effects in the radiometric measurement of plant canopy temperatures p 8 A82-32914
Appearance of irregular tree canopies in nighttime *high-resolution thermal infrared imagery*
p 68 A82-32916
Spectral properties of agricultural crops and soils measured from space, aerial, field, and laboratory sensors
[E82-10189] p 10 N82-22623
Diurnal changes in reflectance factor due to Sun-row direction interactions
[E82-10128] p 11 N82-23566
Structure of the St Francois Mountains and surrounding lead belt, S E Missouri Inferences from thermal IR and other data sets --- Ozard Plateau and St Francois Mountains
[E82-10205] p 11 N82-23578
Application of Computer Axial Tomography (CAT) to measuring crop canopy geometry --- corn and soybeans
[E82-10227] p 14 N82-23600
Linear polarization of light by two wheat canopies measured at many view angles
[E82-10229] p 14 N82-23602
A model of plant canopy polarization
[E82-10233] p 15 N82-23606
Canopy reflectance as influenced by solar illumination angle
[E82-10237] p 15 N82-23610
An analysis of LANDSAT MSS scene-to-scene registration accuracy
[E82-10285] p 16 N82-24563
An algorithm for automating the registration of USDA segment ground data to LANDSAT MSS data
[E82-10286] p 16 N82-24564
Evaluation of HCMM data for assessing soil moisture and water table depth --- South Dakota
[E82-10329] p 18 N82-24602
Spectral estimates of solar radiation intercepted by corn *canopies*
[E82-10003] p 18 N82-26742
Mapping of wildlife habitat in Farmington Bay, Utah
[E82-10354] p 19 N82-26752
Detection of variations in aspen forest habitat from LANDSAT digital data Bear River Range, Utah
[E82-10355] p 19 N82-26753
CANTILEVER BEAMS
Nonlinear theory for elastic beams and rods and its finite element representation
[WTHD-143] p 73 N82-24517
CARBON DIOXIDE
Influence of CO2 on melting of model granulite facies *assemblages - A model for the genesis of charnockites*
p 42 A82-36298
CARBON DIOXIDE CONCENTRATION
Aircraft monitoring of surface carbon dioxide exchange p 23 A82-30293
CARBON MONOXIDE
Tropospheric CO measurement experiment from the second Space Shuttle flight p 27 A82-36292
CARBON STARS
On the stellar origin of the Ne-22 excess in cosmic rays p 21 A82-22562
CELESTIAL GEODESY
Space to the earth --- Russian book on space technology applications p 83 A82-30850
CELESTIAL REFERENCE SYSTEMS
Establishment of terrestrial reference frames by new *observational techniques* p 33 A82-32078
On reference coordinate systems used in polar motion determinations p 33 A82-32090
Some considerations in the use of very-long-baseline-interferometry to establish reference coordinate systems for geodynamics p 34 A82-32096
CENTRAL AMERICA
Geotectonics of South America --- regional magnetic and gravity anomalies of South America
[E82-10320] p 38 N82-24593
CHARGE COUPLED DEVICES
Subtleties in the flat-fielding of charge-coupled device /CCD/ images p 68 A82-32581
CHARGED PARTICLES
Mass per charge ratio in hot plasmas and cosmic ray source composition p 2 A82-22557
Observations of interplanetary energetic charged particles from gamma-ray line solar flares
p 65 A82-22586
CHECKOUT
Interactive initialization of heat flux parameters for numerical models using satellite temperature measurements
[E82-10313] p 82 N82-26743
CHEMICAL COMPOSITION
Calculated isotopic source composition and tests for origin and propagation of cosmic rays with mass numbers less than or equal to 62 p 83 A82-22554
The charge and isotopic composition of Z equals 7-16 *cosmic ray nuclei at their source* p 64 A82-22555
Physical state of the birth place of cosmic rays and its implication to the acceleration processes
p 2 A82-22559
High resolution measurements of solar flare isotopes
p 22 A82-22606
CHEMICAL EFFECTS
Spectral scanning of experimental plots of SO2-affected winter wheat and soybeans for mission planning
p 6 A82-29537
CHEMICAL FRACTIONATION
Laboratory studies of actinide metal-silicate fractionation p 49 A82-22306
CHESAPEAKE BAY (US)
Analysis of ocean color scanner data from the Superflux III Experiment
[NASA-TM-83290] p 55 N82-23614
CHLOROPHYLLS
Analysis of ocean color scanner data from the Superflux III Experiment
[NASA-TM-83290] p 55 N82-23614
CHROMOSPHERE
Possible evidence for attenuation of an MHD shock by a magnetic neutral sheet in the solar corona
p 3 A82-22589
The model of the cosmic ray enrichment by helium-3
p 31 A82-22614
CIRCUIT BOARDS
Effective electromagnetic shielding in multilayer printed circuit boards
[AIAA 81-2333] p 59 A82-13528

CITIES
Remote sensing - A potential aid in the preparation of an urban tree inventory p 9 A82-34732
Longwave infrared observation of urban landscapes p 25 A82-34744

CITRUS TREES
Detection and damage assessment of citrus tree losses with aerial color infrared photography /ACIR/ p 7 A82-29538
Effects of altitude, focal length, and filter combinations on color infrared photography of citrus groves p 9 A82-34729

CLASSIFICATIONS
The use of prior probabilities in maximum likelihood classification of remotely sensed data p 68 A82-32904
Ten-Ecosystem Study --- Grand and Weld Counties, Colorado, Warren County, Pennsylvania, St Louis County, Minnesota, Sandoval County, New Mexico, Kershaw County, South Carolina, Fort Yukon, Alaska, Grays Harbor County, Washington, and Washington County, Missouri [E82-10186] p 84 N82-22620
AgRISTARS Foreign commodity production forecasting The 1980 US corn and soybeans exploratory experiment [E82-10206] p 11 N82-23579
Multistage classification of multispectral Earth observational data The design approach [E82-10213] p 72 N82-23586
Use and applicability of the vegetation component of the national site classification system --- Sumter National Forest, South Carolina [E82-10234] p 15 N82-23607
Analysis of scanner data for crop inventories [E82-10241] p 16 N82-24519
Analysis of thematic mapper simulator data acquired during winter season over Pearl River, Mississippi, test site [E82-10287] p 17 N82-24565
Key issues in the Analysis of Remote Sensing Data A report on the workshop [E82-10348] p 85 N82-26746
Development of visible/infrared/microwave agriculture classification and biomass estimation algorithms --- Guyton, Oklahoma and Dalhart, Texas [E82-10363] p 20 N82-26761

CLIMATE
The onset of the Australian Northwest monsoon during winter MONEX Broadscale flow revealed by an objective analysis scheme p 56 N82-23912

CLIMATOLOGY
A study of the earth's radiation budget using a general circulation model p 52 A82-30666
System albedo as sensed by satellites - Its definition and variability p 23 A82-32342
Plan of research for integrated soil moisture studies Recommendations of the Soil Moisture Working Group [NASA-TM-84731] p 18 N82-25608
Sea-Ice Mission Requirements for the US FIREX and Canada RADARSAT programs [NASA-CR-168984] p 57 N82-25609

CLOUD COVER
Simplified techniques to study components of solar radiation under haze and clouds p 78 A82-32766
Estimation of the temperature of the upper boundary of cloud cover over the world ocean p 54 A82-36005

CLOUD HEIGHT INDICATORS
The meteorological product - 'Cloud-top height' p 70 A82-36043

CLOUD PHOTOGRAPHY
Skirt clouds associated with the Soufriere eruption of 17 April 1979 p 24 A82-33656

CLOUD PHYSICS
Albedo and angular characteristics of the reflectance of the underlying surface and clouds --- Russian book p 33 A82-30849
Skirt clouds associated with the Soufriere eruption of 17 April 1979 p 24 A82-33656

CLOUDS (METEOROLOGY)
Representativeness of cloud motion winds deduced from GOES Indian Ocean satellite imagery for the description of the Indian summer monsoon --- superpressure balloons for the study of the Indian summer monsoon (BALSAMINE) p 55 N82-23879
Estimates of sea surface stress for summer MONEX from cloud motions --- global atmospheric research program p 56 N82-23910

COAL UTILIZATION
Remote sensing of sulfur dioxide effects on vegetation Volume 1 Summary [DE82-900580] p 31 N82-27802
Remote sensing of sulfur dioxide effects on vegetation Volume 2 Data [DE82-900581] p 31 N82-27803

COASTAL CURRENTS
Nearshore current pattern off south Texas - An interpretation from aerial photographs p 53 A82-32903
MONEX oceanographic observations along the East African coast --- global atmospheric research program p 56 N82-23908
Fluid-sediment interactions on beaches and shelves [AD-A110838] p 59 N82-26948

COASTAL WATER
Interpretation of surface-water circulation, Aransas Pass, Texas, using Landsat imagery p 60 A82-32896
A quantitative multispectral analysis system for aerial photographs applied to coastal planning p 55 A82-37505
Analysis of ocean color scanner data from the Superflux III Experiment [NASA-TM-83290] p 55 N82-23614
Thermal mapping, geothermal source location, natural effluents and plant stress in the Mediterranean coast of Spain [E82-10300] p 17 N82-24576
A study of atmospheric diffusion from the LANDSAT imagery --- pollution transport over the ocean [E82-10360] p 58 N82-26758
Meteorological and aircraft data for CUE 2 1973 [PB82-149246] p 59 N82-26949

COASTS
Coastal environment change analysis by Landsat MSS data p 54 A82-34219
Some empirical rules for forecasting fog and status over northern Florida, southern Georgia and adjacent coastal waters [PB82-154006] p 59 N82-27949

COHERENT RADAR
Study visit to United States laser technology centers, 1981 [FOA-C-30257-E1] p 81 N82-24489

COLD WEATHER
Use of thermal inertia determined by HCMM to predict nocturnal cold prone areas in Florida --- Everglades agricultural area and the west north central peninsula [E82-10299] p 17 N82-24575

COLOR CODING
Multidisciplinary investigations on HCMM data over middle Europe and Marocco --- southern Germany and Marrakesh, Morocco [E82-10315] p 74 N82-24588
Matrix data analysis Color/B and W coding is not always enough [AD-A111401] p 74 N82-25612

COLOR INFRARED PHOTOGRAPHY
Riparian vegetation mapping in Northeastern California using high altitude color infrared aerial photography p 5 A82-29528
Inventory of wildlife habitat from color infrared aerial photography for Cobb Island, Virginia p 6 A82-29529
Considerations in using color infrared photographs for vegetative interpretation p 6 A82-29530
Multi-resource inventory in interior Alaska p 6 A82-29532
Estimating rangeland cover proportions with large-scale color-infrared aerial photographs p 6 A82-29534
Mapping riparian vegetation in Southeastern Oregon using digitized large scale color infra-red aerial photography p 6 A82-29535
Remote sensing of Douglas-fir trees newly infested by bark beetles p 6 A82-29536
Detection and damage assessment of citrus tree losses with aerial color infrared photography /ACIR/ p 7 A82-29538
An infrared exposure meter p 76 A82-29541
Estimating bark beetle-killed lodgepole pine with high altitude panoramic photography p 7 A82-32703
Effects of altitude, focal length, and filter combinations on color infrared photography of citrus groves p 9 A82-34729
Use of Landsat multispectral scanner data in vegetation mapping of a forested area p 9 A82-34731
Aerial photography vs Landsat for digital land-cover mapping in an urban watershed p 61 A82-34745

COLOR PHOTOGRAPHY
A color-ratio map of Mercury p 31 A82-22294
Detection of environmental disturbance using color aerial photography and thermal infrared imagery p 22 A82-29327
Color aerial photography detects nutrient status of loblolly pine plantations p 6 A82-29531
Application of 35mm color aerial photography to forest land change detection p 6 A82-29533
Evaluation of spruce-fir forests using small-format photographs p 8 A82-32707
The use of Skylab S-190B photography for small scale mapping p 80 A82-34742
Multidisciplinary investigations on HCMM data over middle Europe and Marocco --- southern Germany and Marrakesh, Morocco [E82-10315] p 74 N82-24588
Mapping of wildlife habitat in Farmington Bay, Utah [E82-10354] p 19 N82-26752

COLOR TELEVISION
Terrain analysis from Landsat using a color TV enhancement system p 68 A82-32911

COLORADO
Application of thermal model for pan evaporation to the hydrology of a defined medium, the sponge [E82-10217] p 13 N82-23590
AgRISTARS Renewable resources inventory Land information support system implementation plan and schedule --- San Juan National Forest pilot test [E82-10224] p 14 N82-23597

COMMODITIES
A meteorologically driven grain sorghum stress indicator model [E82-10218] p 13 N82-23591

COMPARISON
An analysis of LANDSAT MSS scene-to-scene registration accuracy [E82-10285] p 16 N82-24563
An algorithm for automating the registration of USDA segment ground data to LANDSAT MSS data [E82-10286] p 16 N82-24564

COMPTON EFFECT
Consequences of an inverse Compton emission model for extragalactic X-ray sources p 83 A82-22553

COMPUTER COMPATIBLE TAPES
Computation with physical values from Landsat digital data p 68 A82-32709
Spherical harmonic representation of the main geomagnetic field for world charting and investigations of some fundamental problems of physics and geophysics [E82-10203] p 72 N82-23576
Investigation from Japanese MAGSAT team [E82-10239] p 73 N82-23612
An analysis of LANDSAT MSS scene-to-scene registration accuracy [E82-10285] p 16 N82-24563
An algorithm for automating the registration of USDA segment ground data to LANDSAT MSS data [E82-10286] p 16 N82-24564
Report of investigation from Japanese MAGSAT Team [E82-10322] p 74 N82-24595
Models and maps of the main field [E82-10327] p 74 N82-24600
Analysis of MAGSAT data of the Indian region [E82-10358] p 75 N82-26756
Comparison of storm-time changes of geomagnetic field at ground and MAGSAT altitudes [E82-10359] p 30 N82-26757

COMPUTER GRAPHICS
Development of three-dimensional spatial displays using a geographically based information system p 66 A82-29326
RAMS-1, a Resource Analysis and Mapping System p 69 A82-34726

COMPUTER PROGRAMS
The simultaneous employment of geodetic measurements for block adjustments using the method of independent models p 34 A82-33295
A practical study of gross-error detection in bundle adjustment p 69 A82-34702
Description of the FORTRAN implementation of the spring small grains planting date distribution model [E82-10235] p 15 N82-23608

COMPUTER SYSTEMS PROGRAMS
Development of three-dimensional spatial displays using a geographically based information system p 66 A82-29326

COMPUTER TECHNIQUES
A computerized spatial analysis system for assessing wildlife habitat from vegetation maps p 9 A82-34716
A quantitative method to test for similarity between photo interpreters p 69 A82-34722
Present status of on-line analytical triangulation p 69 A82-34940
Application of Computer Axial Tomography (CAT) to measuring crop canopy geometry --- corn and soybeans [E82-10227] p 14 N82-23600

COMPUTERIZED SIMULATION
Computer simulation of the time dependence of the photon energy spectra produced in proton and electron bremstrahlung p 3 A82-22587
A simulation study of soil moisture estimation by a space SAR p 60 A82-29333
Orbiting passive microwave sensor simulation applied to soil moisture estimation [E82-10343] p 18 N82-25605

CONFERENCES
International Cosmic Ray Conference, 17th, Paris, France, July 13-25, 1981, Conference Papers Volume 3 p 65 A82-22580
Color aerial photography in the plant sciences and related fields, Proceedings of the Eighth Biennial Workshop, Luray, VA, April 21-23, 1981 p 5 A82-29526
Imaging spectroscopy, Proceedings of the Seminar, Los Angeles, CA, February 10, 11, 1981 p 77 A82-32440
American Society of Photogrammetry, Annual Meeting, 47th, Washington, DC, February 22-27, 1981, ASP Technical Papers p 79 A82-34701

CONGRESSIONAL REPORTS
Civil land remote sensing system
[GPO-87-070] p 84 N82-22630
Streamlining and ensuring mineral development must begin at local land management levels
[EMD-82-10] p 29 N82-23043

CONICAL SCANNING
LANDSAT-D conical scanner evaluation plan
[E82-10340] p 81 N82-25602

CONIFERS
Remote sensing of Douglas-fir trees newly infested by bark beetles p 6 A82-29536
Estimating bark beetle-killed lodgepole pine with high altitude panoramic photography p 7 A82-32703
Estimating mountain pine beetle-killed ponderosa pine over the front range of Colorado with high altitude panoramic photography p 7 A82-32704

CONTINENTAL DRIFT
MAGSAT anomaly map and continental drift
[E82-10326] p 38 N82-24599

CONTINENTS
MAGSAT anomaly map and continental drift
[E82-10326] p 38 N82-24599

CONTOURS
Description of gray level picture using a collection of density contour lines p 66 A82-29409

CONVECTION
A statistical approach to rainfall estimation using satellite and conventional data
[NOAA-TR-NESS-89] p 63 N82-22854

CONVECTION CURRENTS
The influence of soil characteristics on regional convection differences above Northern Germany p 10 A82-37589

CONVECTIVE FLOW
Convective outflow of cosmic rays from the Galaxy and background radio emission p 83 A82-22551

COORDINATES
Reference coordinate systems for earth dynamics - A preview p 33 A82-32077

CORN
A meteorologically driven maize stress indicator model
[E82-10112] p 11 N82-23564
AgRISTARS Foreign commodity production forecasting The 1980 US corn and soybeans exploratory experiment
[E82-10206] p 11 N82-23579
Determination of the optimal level for combining area and yield estimates
[E82-10215] p 12 N82-23588
AgRISTARS Preliminary technical results review of FY81 experiments, volume 2 Fiscal year 1981/1982 'corn and soybeans pilot' experiment
[E82-10216] p 13 N82-23589
Application of Computer Axial Tomography (CAT) to measuring crop canopy geometry --- corn and soybeans
[E82-10227] p 14 N82-23600
Analysis of scanner data for crop inventories
[E82-10241] p 16 N82-24519
Spectral estimates of solar radiation intercepted by corn canopies
[E82-10003] p 18 N82-26742
Association of spectral development patterns with development stages of corn
[E82-10353] p 19 N82-26751

CORRELATION
On the anticorrelation between the He/3//He/4/ ratio and proton intensity in He/3/ rich flares p 40 A82-22613

COSMIC RAYS
Fragmentation of Fe nuclei on carbon, hydrogen and CH2 targets I - Individual charge changing and total cross sections II - Isotopic cross sections --- for interstellar cosmic ray propagation p 63 A82-22538
A report on the 'cosmic ray propagation problem' p 1 A82-22539
On the characteristics of the very low energy galactic cosmic rays in the interstellar space p 63 A82-22540
The question of short pathlengths in interstellar propagation p 1 A82-22541
Dependence of earth spectrum of positrons and antiprotons on propagation models --- of cosmic radiation p 21 A82-22545
Antiprotons from galactic sources of cosmic rays and gamma rays p 82 A82-22546
Confinement and acceleration of cosmic rays in galactic superbubbles p 82 A82-22547
Interactions of cosmic rays with molecular clouds p 82 A82-22548
Angular variations of nonthermal radio emission from the Galaxy relevant to the structure of interstellar magnetic field p 83 A82-22550
Convective outflow of cosmic rays from the Galaxy and background radio emission p 83 A82-22551
Steady-state cosmic ray electron spectrum under diffusion, convection, adiabatic deceleration and synchrotron losses p 1 A82-22552
Calculated isotopic source composition and tests for origin and propagation of cosmic rays with mass numbers less than or equal to 62 p 83 A82-22554
The charge and isotopic composition of Z equals 7-16 cosmic ray nuclei at their source p 64 A82-22555
Comparative abundances in solar energetic particles and in galactic cosmic ray sources, and the Ne-22 anomaly p 83 A82-22556
Mass per charge ratio in hot plasmas and cosmic ray source composition p 2 A82-22557
Cosmic ray composition from acceleration of thermal matter p 64 A82-22558
Physical state of the birth place of cosmic rays and its implication to the acceleration processes p 2 A82-22559
On volatility, first ionization potential, and s- and r-processes --- for Galactic cosmic ray sources p 2 A82-22560
Interstellar grains as seeds for galactic cosmic rays p 2 A82-22561
On the stellar origin of the Ne-22 excess in cosmic rays p 21 A82-22562
Origin of galactic cosmic rays from Ne isotopic composition p 2 A82-22563
Evidence for the stochastic acceleration of cosmic rays in supernova remnants p 2 A82-22564
Cosmic ray acceleration by stellar winds I - Total density, pressure and energy flux p 21 A82-22566
On the stellar origin of low energy cosmic rays p 21 A82-22567
Acceleration of cosmic rays in accretion shocks p 64 A82-22568
Remarks on cosmic ray origin p 21 A82-22569
Pulsar models and cosmic-ray acceleration p 21 A82-22570
The galactic origin of cosmic rays II
[CONF-810711-2] p 64 A82-22573
Extragalactic cosmic rays, their sources and spectrum p 40 A82-22574
Calculation of production rates of cosmogenic nuclides by Monte Carlo method p 64 A82-22576
Measurement of cosmogenic nuclides using a multi-crystal gamma-ray coincidence spectrometer --- for Mayo Belwa meteorite study p 64 A82-22577
Magnetic monopole pair and its observation in cosmic rays p 65 A82-22579
International Cosmic Ray Conference, 17th, Paris, France, July 13-25, 1981, Conference Papers Volume 3 p 65 A82-22580
The modulation characteristics of the 19th and 20th solar activity cycles p 59 A82-22615
11-year modulation and spectrum of cosmic rays in the interstellar space p 22 A82-22616
Features of cosmic ray variations due to variations in the total magnetic field of the sun p 49 A82-22619

COSMOCHEMISTRY
Laboratory studies of actinide metal-silicate fractionation p 49 A82-22306
The charge and isotopic composition of Z equals 7-16 cosmic ray nuclei at their source p 64 A82-22555
Nucleosynthesis of light and by-passed isotopes in the solar system matter p 64 A82-22578

COTTON
Airborne observed solar elevation and row direction effects on the near-IR/red ratio of cotton
[E82-10220] p 13 N82-23593

COULOMB COLLISIONS
Cosmic ray composition from acceleration of thermal matter p 64 A82-22558

COULOMB POTENTIAL
Coulombian energy losses and the nuclear composition of the solar cosmic rays p 4 A82-22610

CROP CALENDARS
Analysis of scanner data for crop inventories
[E82-10192] p 10 N82-22626
Evaluation of the Doraiswamy-Thompson winter wheat crop calendar model incorporating a modified spring restart sequence
[E82-10207] p 12 N82-23580
AgRISTARS Supporting research Spring small grains planting date distribution model
[E82-10208] p 12 N82-23581
Description of historical crop calendar data bases developed to support foreign commodity production forecasting project experiments
[E82-10209] p 12 N82-23582
AgRISTARS Preliminary technical results review of FY81 experiments, volume 2 Fiscal year 1981/1982 'corn and soybeans pilot' experiment
[E82-10216] p 13 N82-23589
A meteorologically driven grain sorghum stress indicator model
[E82-10218] p 13 N82-23591
AgRISTARS Project management report Program review presentation to level 1, interagency coordination committee
[E82-10219] p 13 N82-23592
Selection of the Australian indicator region
[E82-10222] p 13 N82-23595
AgRISTARS Project management report Program review presentation to level 1, interagency coordination committee --- Brazil, Argentina, U S corn belt, Great Plains Corridor
[E82-10231] p 15 N82-23604

CROP GROWTH
Color aerial photography detects nutrient status of loblolly pine plantations p 6 A82-29531
Spectral scanning of experimental plots of SO2-affected winter wheat and soybeans for mission planning p 6 A82-29537
Evaluation of the Doraiswamy-Thompson winter wheat crop calendar model incorporating a modified spring restart sequence
[E82-10207] p 12 N82-23580
AgRISTARS Supporting research Spring small grains planting date distribution model
[E82-10208] p 12 N82-23581
Description of historical crop calendar data bases developed to support foreign commodity production forecasting project experiments
[E82-10209] p 12 N82-23582
Application of thermal model for pan evaporation to the hydrology of a defined medium, the sponge
[E82-10217] p 13 N82-23590
A meteorologically driven grain sorghum stress indicator model
[E82-10218] p 13 N82-23591
AgRISTARS Project management report Program review presentation to level 1, interagency coordination committee
[E82-10219] p 13 N82-23592
Relating thematic mapper bands TM3, TM4, and TM5 to agronomic variables for corn, cotton, sugarbeet, soybean, sorghum, sunflower and tobacco
[E82-10347] p 19 N82-26745
Association of spectral development patterns with development stages of corn
[E82-10353] p 19 N82-26751

CROP IDENTIFICATION
Field size, length, and width distributions based on LACIE ground truth data --- large area crop inventory experiment p 8 A82-32909
Evaluation of NOAA-AVHRR data for crop assessment --- Advanced Very High Resolution Radiometer p 8 A82-34179
Analysis of scanner data for crop inventories
[E82-10192] p 10 N82-22626
AgRISTARS Foreign commodity production forecasting The 1980 US/Canada wheat and barley exploratory experiment
[E82-10126] p 11 N82-23565
Agricultural Research Service research highlights in remote sensing for calendar year 1980
[E82-10228] p 14 N82-23601
Evaluation of the procedure for separating barley from other spring small grains --- North Dakota, South Dakota, Minnesota and Montana
[E82-10230] p 14 N82-23603
AgRISTARS Agriculture and resources inventory surveys through aerospace remote sensing
[E82-10236] p 15 N82-23609
Canopy reflectance as influenced by solar illumination angle
[E82-10237] p 15 N82-23610
An algorithm for automating the registration of USDA segment ground data to LANDSAT MSS data
[E82-10286] p 16 N82-24564
Relating thematic mapper bands TM3, TM4, and TM5 to agronomic variables for corn, cotton, sugarbeet, soybean, sorghum, sunflower and tobacco
[E82-10347] p 19 N82-26745
Development of visible/infrared/microwave agriculture classification and biomass estimation algorithms --- Guyton, Oklahoma and Dalhart, Texas
[E82-10363] p 20 N82-26761

CROP INVENTORIES
Effects of altitude, focal length, and filter combinations on color infrared photography of citrus groves p 9 A82-34729
Analysis of scanner data for crop inventories [E82-10192] p 10 N82-22626
A comparison of stratified versus regression estimators p 11 N82-23133
Determination of the optimal level for combining area and yield estimates [E82-10215] p 12 N82-23588
AgRISTARS Preliminary technical results review of FY81 experiments, volume 2 Fiscal year 1981/1982 'corn and soybeans pilot' experiment [E82-10216] p 13 N82-23589
Normal crop calendars Volume 3 The corn and soybean states of Illinois, Indiana, and Iowa [E82-10221] p 13 N82-23594
Selection of the Australian indicator region [E82-10222] p 13 N82-23595
Analysis of scanner data for crop inventories [E82-10241] p 16 N82-24519
Inventory of wetlands and agricultural land cover in the upper Sevier River Basin, Utah [E82-10345] p 18 N82-25607
Spectral estimates of solar radiation intercepted by corn canopies [E82-10003] p 18 N82-26742

CROP VIGOR
Remote sensing of the weediness of crop fields p 5 A82-29435
Considerations in using color infrared photographs for vegetative interpretation p 6 A82-29530
Effects of vegetation canopy structure on remotely sensed canopy temperatures --- inferring plant water stress and yield p 8 A82-32905
Use of NOAA/AVHRR visible and near-infrared data for land remote sensing [NASA-TM-84186] p 81 N82-22643
AgRISTARS Preliminary technical results review of FY81 experiments, volume 2 Fiscal year 1981/1982 'corn and soybeans pilot' experiment [E82-10216] p 13 N82-23589
A meteorologically driven grain sorghum stress indicator model [E82-10218] p 13 N82-23591
AgRISTARS Early warning and crop condition assessment Plant cover, soil temperature, freeze, water stress, and evapotranspiration conditions [E82-10225] p 14 N82-23598
Application of Computer Axial Tomography (CAT) to measuring crop canopy geometry --- corn and soybeans [E82-10227] p 14 N82-23600
Multispectral determination of soil moisture-2 --- Guymon, Oklahoma and Dalhart, Texas [E82-10349] p 19 N82-26747

CRUSTAL FRACTURES
Geoid height-age relation from Seasat altimeter profiles across the Mendocino Fracture Zone p 34 A82-32646
Geodetic monitoring of tectonic information Toward a strategy p 35 N82-22832
Seismic and geodetic studies of the Imperial Valley, California [DE82-001686] p 39 N82-26915

CUMULONIMBUS CLOUDS
The onset of the Australian Northwest monsoon during winter MONEX Broadscale flow revealed by an objective analysis scheme p 56 N82-23912

CUMULUS CLOUDS
The use of contextual information to detect cumulus clouds and cloud shadows in Landsat data p 67 A82-32346
The influence of soil characteristics on regional convection differences above Northern Germany p 10 A82-37589

CURIE TEMPERATURE
Application of satellite magnetic anomaly data to Curie isotherm mapping p 70 A82-35824
MAGSAT and aeromagnetic data in the North American continent [E82-10193] p 71 N82-22627

CYCLOGENESIS
Analysis of ocean and atmosphere thermodynamical characteristics during the onset of southwest monsoon over the Arabian Sea p 57 N82-23945

D

DAMAGE ASSESSMENT
Detection and damage assessment of citrus tree losses with aerial color infrared photography /ACIR/ p 7 A82-29538

DATA ACQUISITION
Application of satellite magnetic anomaly data to Curie isotherm mapping p 70 A82-35824
Source assessment system [AD-A111223] p 75 N82-25613
SMS/GOES data collection platform system p 75 N82-26027

DATA BASE MANAGEMENT SYSTEMS
Source assessment system [AD-A111223] p 75 N82-25613

DATA BASES
A tentative ordering of all available solar energetic particles abundance observations I - The mass unbiased baseline II - Discussion and comparison with coronal abundances p 40 A82-22609
Description of historical crop calendar data bases developed to support foreign commodity production forecasting project experiments [E82-10209] p 12 N82-23582
Matrix data analysis Color/B and W coding is not always enough [AD-A111401] p 74 N82-25612
Key issues in the Analysis of Remote Sensing Data A report on the workshop [E82-10348] p 85 N82-26746
Exploration into technical procedures for vertical integration --- information systems [NASA-CR-166352] p 75 N82-26763

DATA COLLECTION PLATFORMS
The METEOSAT Data Collection System and its application p 75 N82-26037

DATA CONVERSION ROUTINES
MAGSAT for geomagnetic studies over Indian region [E82-10202] p 72 N82-23575
MAGSAT for geomagnetic studies over Indian region [E82-10296] p 73 N82-24572

DATA CORRELATION
Comparison data for Seasat altimetry in the western North Atlantic p 50 A82-29611
Preliminary evidence for the influence of physiography and scale upon the autocorrelation function of remotely sensed data p 67 A82-32343
Irrigation management with remote sensing --- Navajo Indian Irrigation Project [E82-10357] p 20 N82-26755

DATA LINKS
An optical data link for airborne scanning system p 80 A82-34737

DATA PROCESSING
The processing of satellite navigation data for marine geodesy p 34 A82-37175
Advanced technology for earth observation - Data processing [AAS PAPER 82-130] p 71 A82-37810
Ten-Ecosystem Study --- Grand and Weld Counties, Colorado, Warren County, Pennsylvania, St Louis County, Minnesota, Sandoval County, New Mexico, Kershaw County, South Carolina, Fort Yukon, Alaska, Grays Harbor County, Washington, and Washington County, Missouri [E82-10186] p 84 N82-22620
Use of NOAA/AVHRR visible and near-infrared data for land remote sensing [NASA-TM-84186] p 81 N82-22643
MAGSAT science investigations [E82-10199] p 71 N82-23572
Bathymetric and tectonics of Indian Ocean using MAGSAT data [E82-10204] p 36 N82-23577
AgRISTARS Foreign commodity production forecasting The 1980 US corn and soybeans exploratory experiment [E82-10206] p 11 N82-23579
Multistage classification of multispectral Earth observational data The design approach [E82-10213] p 72 N82-23586
AgRISTARS Project management report Program review presentation to level 1, interagency coordination committee [E82-10219] p 13 N82-23592
An algorithm for automating the registration of USDA segment ground data to LANDSAT MSS data [E82-10286] p 16 N82-24564
Investigation of the effects of external current systems on the MAGSAT data utilizing gnd cell modeling techniques [E82-10306] p 74 N82-24580
MAGSAT scalar and vector anomaly data analysis [E82-10307] p 74 N82-24581
An investigation of MAGSAT and complementary data emphasizing precambrian shields and adjacent areas of West Africa and South America [E82-10317] p 38 N82-24590
An investigation of MAGSAT and complementary data emphasizing precambrian shields and adjacent areas of West Africa and South America [E82-10318] p 38 N82-24591
Investigations of medium wavelength magnetic anomalies in the eastern Pacific using MAGSAT data [E82-10330] p 38 N82-24603
Aeromagnetic and satellite magnetic anomaly mapping [E82-10339] p 39 N82-25601
Interactive initialization of heat flux parameters for numerical models using satellite temperature measurements [E82-10313] p 82 N82-26743
Measurement of soil moisture trends with airborne scatterometers --- Guymon, Oklahoma and Dalhart, Texas [E82-10361] p 20 N82-26759

DATA REDUCTION
The use of prior probabilities in maximum likelihood classification of remotely sensed data p 68 A82-32904
Studies of high latitude current systems using MAGSAT vector data [E82-10188] p 71 N82-22622
MAGSAT and aeromagnetic data in the North American continent [E82-10193] p 71 N82-22627
Investigation of the effects of external current systems on the MAGSAT data utilizing grid cell modeling techniques [E82-10195] p 71 N82-22629
LANDSAT technology transfer to the private and public sectors through community colleges and other locally available institutions [E82-10181] p 85 N82-23568
Investigation of MAGSAT and TRIAD magnetometer data to provide corrective information on high-latitude external fields [E82-10201] p 72 N82-23574
Investigation of the effects of external current systems on the MAGSAT data utilizing grid cell modeling techniques [E82-10226] p 73 N82-23599
Report of MAGSAT project by Survey of India [E82-10293] p 73 N82-24570
Analysis of MAGSAT data of the Indian region [E82-10358] p 75 N82-26756

DATA SAMPLING
Sample design for estimating change in land use and land cover p 24 A82-32711
Measurement of soil moisture trends with airborne scatterometers --- Guymon, Oklahoma and Dalhart, Texas [E82-10361] p 20 N82-26759

DATA SMOOTHING
Improved definition of crustal magnetic anomalies for MAGSAT data [E82-10314] p 37 N82-24587

DATA SYSTEMS
Design guidelines for satellite image data distribution systems p 70 A82-37048
AgRISTARS Project management report Program review presentation to level 1, interagency coordination committee --- Brazil, Argentina, U S corn belt, Great Plains Corridor [E82-10231] p 15 N82-23604

DATA TRANSMISSION
Purpose, background of 'Intercosmos-21' mission p 81 N82-24264

DEATH VALLEY (CA)
Possible fault detection in Cottonball Basin, California An application of radar remote sensing p 41 A82-32898

DEER
Application of remote sensing to state and regional problems [E82-10288] p 30 N82-24566

DEFOLIATION
Defining the temporal window for monitoring forest canopy defoliation using Landsat p 9 A82-34730

DEFORESTATION
Monitoring deforestation in the eastern part of the state of Guerrero, Mexico p 9 A82-34733

DEHYDRATION
Remote sensing of leaf water content in the near infrared p 8 A82-32897

DELINEATION
Status and prospects of the automated processing of remote-sensing data /using forest surveys as an example/ p 10 A82-35139

DENSITY (NUMBER/VOLUME)
OSO-8 lower mesospheric ozone number density profiles p 28 A82-36472

DENSITY DISTRIBUTION
Description of gray level picture using a collection of density contour lines p 66 A82-29409
Information theory lateral density distribution for earth inferred from global gravity field p 35 A82-37962

DEPOSITS
Evaluation and combined geophysical interpretations of NURE and related geoscience data in the Van Horn, Pecos, Marfa, Fort Stockton, Presidio, and Emory Peak quadrangels, Texas
[DE82-005560] p 48 N82-27809
DESERTS
Desert locust habitat monitoring with satellite remote sensing A new technology for an old problem
p 7 A82-29747
Resource inventory techniques used in the California Desert Conservation Area p 23 A82-32441
DIFFRACTION LIMITED CAMERAS
Inversion of data from diffraction-limited multiwavelength remote sensors II - Nonlinear dependence of observables on the geophysical parameters p 77 A82-32658
DIFFUSE RADIATION
Large amplitude undulations on the equatorward boundary of the diffuse aurora p 76 A82-31019
DIGITAL DATA
Detection of regional air pollution episodes utilizing satellite digital data in the visual range
p 23 A82-31990
Computation with physical values from Landsat digital data p 68 A82-32709
Use of NOAA/AVHRR visible and near-infrared data for land remote sensing
[NASA-TM-84186] p 81 N82-22643
Computer-processed geophysical atlas of digital data for the East Coast margin of the United States from surface and spacecraft data
[AD-A111388] p 39 N82-25748
Detection of variations in aspen forest habitat from LANDSAT digital data Bear River Range, Utah
[E82-10355] p 19 N82-26753
DIGITAL FILTERS
Matrix data analysis Color/B and W coding is not always enough
[AD-A111401] p 74 N82-25612
DIGITAL RADAR SYSTEMS
The estimation of wave height from digitally processed SAR imagery p 67 A82-32347
DIGITAL SYSTEMS
Separation of diffuse from sharp-edged features in digital imagery p 68 A82-34225
DIGITAL TECHNIQUES
Mapping riparian vegetation in Southeastern Oregon using digitized large scale color infra-red aerial photography p 6 A82-29535
Digitally enhanced visual displays facilitate the analysis of Landsat imagery p 67 A82-32507
The response characteristics of vegetation in Landsat MSS digital data p 8 A82-32907
Image processing with microcomputers in remote sensing p 79 A82-34708
Terrain classification by Fourier analysis - Accuracy and economy p 69 A82-34723
Aerial photography vs Landsat for digital land-cover mapping in an urban watershed p 61 A82-34745
Matrix data analysis Color/B and W coding is not always enough
[AD-A111401] p 74 N82-25612
Key Issues in the Analysis of Remote Sensing Data A report on the workshop
[E82-10348] p 85 N82-26746
DISCONTINUITY
Satellite observations in FRONTS 80
[AD-A111080] p 58 N82-26766
DISPLAY DEVICES
Source assessment system
[AD-A111223] p 75 N82-25613
DIURNAL VARIATIONS
Observation of the diurnal variation of atmospheric ozone p 26 A82-35895
Diurnal changes in reflectance factor due to Sun-row direction interactions
[E82-10128] p 11 N82-23566
Registration of Heat Capacity Mapping Mission day and night images
[E82-10210] p 72 N82-23583
Application of HCMM data to regional geologic analysis for mineral and energy resource evaluation
[E82-10243] p 45 N82-24521
Delineation of soil temperature regimes from HCMM data
[E82-10298] p 17 N82-24574
Magnetic and gravity anomalies in the Americas
[E82-10312] p 37 N82-24586
Multidisciplinary investigations on HCMM data over middle Europe and Marocco --- southern Germany and Marrakesh, Morocco
[E82-10315] p 74 N82-24588
HCMM hydrological analysis in Utah
[E82-10328] p 63 N82-24601
Comparison of storm-time changes of geomagnetic field at ground and MAGSAT altitudes
[E82-10359] p 30 N82-26757
DRAINAGE
The application of Heat Capacity Mapping Mission (HCMM) thermal data to snow hydrology --- Salt Verde Watershed and the southern Sierra Nevada
[E82-10191] p 62 N82-22625
DRAINAGE PATTERNS
Dynamic study of the upper Sao Francisco river and Tres Marias reservoir using MSS/LANDSAT images --- BRazil
[E82-10291] p 63 N82-24569
DROUGHT
Remote sensing of leaf water content in the near infrared p 8 A82-32897
DYNAMIC CHARACTERISTICS
Sea-Ice Mission Requirements for the US FIREX and Canada RADARSAT programs
[NASA-CR-168984] p 57 N82-25609
DYNAMIC MODELS
Impact of additional summer MONEX wind data on the prediction of monsoon depressions during June - August 1979 with two versions of primitive equation (PE) barotropic model --- Monsoon Experiment (MONEX)
p 56 N82-23900

E

E REGION
Characteristics of field-aligned E-region irregularities over Iioka /36 N/, Japan I p 26 A82-36268
EARTH (PLANET)
Reference coordinate systems for earth dynamics - A preview p 33 A82-32077
Some considerations in the use of very-long-baseline-interferometry to establish reference coordinate systems for geodynamics p 34 A82-32096
MAGSAT anomaly map and continental drift
[E82-10326] p 38 N82-24599
Models and maps of the main field
[E82-10327] p 74 N82-24600
EARTH ALBEDO
Albedo and angular characteristics of the reflectance of the underlying surface and clouds --- Russian book
p 33 A82-30849
System albedo as sensed by satellites - Its definition and variability p 23 A82-32342
Comparison of satellite derived radiation budget measurements over MONEX during 1979 to 1980 --- Monsoon Experiment (MONEX) p 29 N82-23891
EARTH ATMOSPHERE
Soft X-rays from the sunlit earth's atmosphere
p 29 A82-37405
EARTH CORE
Information theory lateral density distribution for earth inferred from global gravity field p 35 A82-37962
Investigation of geomagnetic field forecasting and fluid dynamics of the core --- determination of the bundary between the core and mantle of the Earth
[E82-10198] p 35 N82-23571
Investigation of geomagnetic field forecasting and fluid dynamics of the core
[E82-10310] p 37 N82-24584
Investigation of geomagnetic field forecasting and fluid dynamics of the core
[E82-10342] p 39 N82-25604
EARTH CRUST
Initial vector magnetic anomaly map from Magsat
p 32 A82-30785
Spatial resolution and repeatability of Magsat crustal anomaly data over the Indian Ocean p 32 A82-30788
Verification of the crustal component in satellite magnetic data p 32 A82-30789
Preliminary interpretation of magnetic anomalies over Japan and its surrounding area p 33 A82-30796
Influence of CO2 on melting of model granulite facies assemblages - A model for the genesis of charnockites
p 42 A82-36298
Information theory lateral density distribution for earth inferred from global gravity field p 35 A82-37962
Structure, composition and thermal state of the crust in Brazil --- geomagnetic survey
[E82-10187] p 35 N82-22621
Crustal structures under the active volcanic areas of central and eastern Mediterranean (M-44)
[E82-10096] p 35 N82-23563
Equivalent source modeling of the main field using MAGSAT data
[E82-10151] p 71 N82-23567
Spherical-Earth gravity and magnetic anomaly modeling by Gauss-Legendre quadrature integration
[E82-10242] p 36 N82-24520
An equivalent layer magnetization model for the United States derived from MAGSAT data
[E82-10297] p 36 N82-24573
Analyzing the Broken Ridge area of the Indian Ocean using magnetic and gravity anomaly maps and geoid undulation and bathymetry data
[E82-10303] p 36 N82-24577
Investigating tectonic and bathymetric features of the Indian Ocean using MAGSAT magnetic anomaly data
[E82-10304] p 37 N82-24578
Investigation of Antarctic crust and upper mantle using MAGSAT and other geophysical data
[E82-10308] p 37 N82-24582
Investigation of Antarctic crust and upper mantle using MAGSAT and other geophysical data
[E82-10309] p 37 N82-24583
Magnetic and gravity anomalies in the Americas
[E82-10312] p 37 N82-24586
The crustal structure and tectonics of South America
[E82-10319] p 38 N82-24592
Use of MAGSAT anomaly data for crustal structure and mineral resources in the US Midcontinent
[E82-10321] p 46 N82-24594
Report of investigation from Japanese MAGSAT Team
[E82-10322] p 74 N82-24595
Use of MAGSAT anomaly data for crustal structure and mineral resources in the US Midcontinent
[E82-10323] p 46 N82-24596
MAGSAT anomaly map and continental drift
[E82-10326] p 38 N82-24599
Investigations of medium wavelength magnetic anomalies in the eastern Pacific using MAGSAT data
[E82-10330] p 38 N82-24603
Seismic and geodetic studies of the Imperial Valley, California
[DE82-001686] p 39 N82-26915
EARTH MANTLE
Information theory lateral density distribution for earth inferred from global gravity field p 35 A82-37962
Investigation of geomagnetic field forecasting and fluid dynamics of the core --- determination of the bundary between the core and mantle of the Earth
[E82-10198] p 35 N82-23571
Investigation of Antarctic crust and upper mantle using MAGSAT and other geophysical data
[E82-10308] p 37 N82-24582
Investigation of Antarctic crust and upper mantle using MAGSAT and other geophysical data
[E82-10309] p 37 N82-24583
EARTH MOVEMENTS
Geodetic monitoring of tectonic information Toward a strategy p 35 N82-22832
EARTH OBSERVATIONS (FROM SPACE)
Space to the earth --- Russian book on space technology applications p 83 A82-30850
The use of the SPOT satellite in natural resource evaluation p 83 A82-31996
Spectroscopic remote sensing for geological applications p 41 A82-32442
Thematic mapper - An overview of spectral band registration p 77 A82-32447
An optical objective lens for earth observations by satellites p 78 A82-32824
Infrared sensing of sea surface temperature from space p 53 A82-32902
Inference of refractivity profiles by satellite-to-ground RF measurements p 78 A82-33442
Remote sensing of the earth's resources - The Soviet experience p 84 A82-33555
Earth observations from space - Trends and prospects
p 84 A82-34116
ERS-1 European remote sensing satellite
p 84 A82-34367
Microwave sensing from space
[AAS PAPER 82-127] p 80 A82-37809
Advanced technology for earth observation - Data processing
[AAS PAPER 82-130] p 71 A82-37810
Civil land remote sensing system
[GPO-87-070] p 84 N82-22630
Radiometer mission requirements for large space antenna systems
[NASA-TM-84478] p 81 N82-25610
EARTH PLANETARY STRUCTURE
The definition of the terrestrial coordinate frame by long baseline interferometry p 33 A82-32084
MAGSAT anomaly map and continental drift
[E82-10326] p 38 N82-24599
EARTH RESOURCES
Multi-resource inventory in interior Alaska
p 6 A82-29532
The use of the SPOT satellite in natural resource evaluation p 83 A82-31996
Thematic mapper - An overview of spectral band registration p 77 A82-32447

Multispectral mapper - Imaging spectroscopy as applied to the mapping of earth resources p 77 A82-32448
Photogrammetric methods for mapping resource data from high altitude panoramic photography p 77 A82-32702
Aerogeophysical methods of finding uranium deposits --- Russian book p 41 A82-33402
Remote sensing of the earth's resources - The Soviet experience p 84 A82-33555
RAMS-1, a Resource Analysis and Mapping System p 69 A82-34726
Landsat D to yield more precise data p 70 A82-37200
Solid state instrumentation concepts for earth resource observation
[AAS PAPER 82-132] p 81 A82-37812
LANDSAT D to test thematic mapper, inaugurate operational system
[NASA-NEWS-RELEASE-82-100] p 82 N82-26741

EARTH RESOURCES INFORMATION SYSTEM
A new approach to multiresource inventories using remote sensing and geographic information systems technologies p 25 A82-34739

EARTH RESOURCES PROGRAM
An infrared exposure meter p 76 A82-29541
Resource inventory techniques used in the California Desert Conservation Area p 23 A82-32441
High spectral resolution airborne spectrometry p 77 A82-32443
Irrigation management with remote sensing --- Navajo Indian Irrigation Project
[E82-10357] p 20 N82-26755

EARTH RESOURCES SHUTTLE IMAGING RADAR
OSTA-1 Post Mission Operation Report
[NASA-TM-84191] p 84 N82-23258

EARTH ROTATION
On reference coordinate systems used in polar motion determinations p 33 A82-32090

EARTH SATELLITES
Cost-effectiveness of geographic surveying from space p 85 N82-24263

EARTH SURFACE
Surface temperature determination from an amalgamation of GOES and TIROS-N radiance measurements p 66 A82-28905
Relating Landsat digital count values to ground reflectance for optically thin atmospheric conditions p 66 A82-29762
Albedo and angular characteristics of the reflectance of the underlying surface and clouds --- Russian book p 33 A82-30849
Simplified techniques to study components of solar radiation under haze and clouds p 78 A82-32766
Experimental assessment of improved spatial resolution LANDSAT data
[AD-A110538] p 75 N82-26765

EARTH TIDES
Work related to the Blue Road Geotraverse at the Finnish Geodetic Institute p 32 A82-30306

EARTHQUAKES
Geodetic monitoring of tectonic deformation Toward a strategy
[NASA-CR-168784] p 35 N82-22846
Seismic and geodetic studies of the Imperial Valley, California
[DE82-001686] p 39 N82-26915

ECOLOGY
Landsat digital analysis of the initial recovery of burned tundra at Kokolik River, Alaska p 8 A82-32913
Use and applicability of the vegetation component of the national site classification system --- Sumter National Forest, South Carolina
[E82-10234] p 15 N82-23607

ECOSYSTEMS
Agricultural Research Service research highlights in remote sensing for calendar year 1980
[E82-10228] p 14 N82-23601

ELECTRIC CURRENT
Studies of high latitude current systems using MAGSAT vector data
[E82-10188] p 71 N82-22622
Investigation from Japanese MAGSAT team
[E82-10239] p 73 N82-23612
Investigation of Antarctic crust and upper mantle using MAGSAT and other geophysical data
[E82-10309] p 37 N82-24583
Report of investigation from Japanese MAGSAT Team
[E82-10322] p 74 N82-24595

ELECTRIC FIELDS
Generation of the auroral kilometric radiation p 26 A82-35542

ELECTROMAGNETIC FIELDS
Astrophysical scenarios for critically evaluating a zero-point field acceleration mechanism p 64 A82-22575

ELECTROMAGNETIC SHIELDING
Effective electromagnetic shielding in multilayer printed circuit boards
[AIAA 81-2333] p 59 A82-13528

ELECTRON DIFFUSION
Convective outflow of cosmic rays from the Galaxy and background radio emission p 83 A82-22551

ELECTRON ENERGY
The electron and positron spectra in primary cosmic rays p 1 A82-22543
Generation of the auroral kilometric radiation p 26 A82-35542

ELECTRON FLUX DENSITY
The model of the cosmic ray enrichment by helium-3 p 31 A82-22614

ELECTROPHOTOMETERS
Optical stop and focussing effects in the Dobson instrument p 28 A82-36428

ELEMENTARY PARTICLE INTERACTIONS
Measurement of cosmogenic nuclides using a multi-crystal gamma-ray coincidence spectrometer --- for Mayo Belwa meteorite study p 64 A82-22577

EMISSION SPECTRA
The cosmic ray positron spectrum p 1 A82-22542
Consequences of an inverse Compton emission model for extragalactic X-ray sources p 83 A82-22553
Stratospheric emission data analysis
[AD-A112337] p 76 N82-26907

EMISSIVITY
Derivation of the distribution of synchrotron emissivity in the Galaxy from the 408 MHz all-sky survey p 82 A82-22549
Emissivity and reflectance of the model sea surface for the use of AVHRR data of NOAA satellites p 52 A82-31294
Remote sensing of thermal subsurface terrain properties p 80 A82-34727

ENERGETIC PARTICLES
Comparative abundances in solar energetic particles and in galactic cosmic ray sources, and the Ne-22 anomaly p 83 A82-22556
Acceleration of cosmic rays in accretion shocks p 64 A82-22568
Observations of interplanetary energetic charged particles from gamma-ray line solar flares p 65 A82-22586
High-energy solar protons p 22 A82-22588
The relation of type II radio bursts to solar energetic particles observed at earth p 3 A82-22591
Energetic solar particle spectra according to Venera-11, 12 and Prognoz-5, 6 p 4 A82-22593
Evolution of the solar proton spectrum in interplanetary space p 4 A82-22594
Spacecraft determination of energetic particle propagation parameters - The 1 January 1978 solar event p 31 A82-22598
Time and energy dependence of heavy ion abundances in solar flare energetic particle events p 22 A82-22605
High resolution measurements of solar flare isotopes p 22 A82-22606
Observations of the ionization states of energetic particles accelerated in solar flares p 40 A82-22607
Is the neon composition of our sun, planetary or solar p 76 A82-22608
A tentative ordering of all available solar energetic particles abundance observations I - The mass unbiased baseline II - Discussion and comparison with coronal abundances p 40 A82-22609
On the anticorrelation between the He/3//He/4/ ratio and proton intensity in He/3/ rich flares p 40 A82-22613

ENERGY BUDGETS
Ammonia and the NOx budget of the troposphere p 27 A82-36293

ENERGY DISSIPATION
Steady-state cosmic ray electron spectrum under diffusion, convection, adiabatic deceleration and synchrotron losses p 1 A82-22552
Coulombian energy losses and the nuclear composition of the solar cosmic rays p 4 A82-22610

ENERGY SPECTRA
On the characteristics of the very low energy galactic cosmic rays in the interstellar space p 63 A82-22540
The electron and positron spectra in primary cosmic rays p 1 A82-22543
Dependence of earth spectrum of positrons and antiprotons on propagation models --- of cosmic radiation p 21 A82-22545
Extragalactic cosmic rays, their sources and spectrum p 40 A82-22574
Model for solar hard X-ray bursts p 65 A82-22581
Computer simulation of the time dependence of the photon energy spectra produced in proton and electron bremstrahlung p 3 A82-22587
A survey of solar protons and alpha differential spectra between 1 and greater than 400 MeV/nucleon p 4 A82-22592
Energetic solar particle spectra according to Venera-11, 12 and Prognoz-5, 6 p 4 A82-22593
Evolution of the solar proton spectrum in interplanetary space p 4 A82-22594
Preflare increases in solar cosmic rays relevant to the mode of energy accumulation in the active regions associated with large flares p 31 A82-22595
A comparison of helium and heavy ion spectra in He/3/ rich solar flares with a model calculation p 5 A82-22612
11-year modulation and spectrum of cosmic rays in the interstellar space p 22 A82-22616
The energy spectra of cosmic ray variations inferred from the stratospheric measurements in 1972-1979 p 5 A82-22617

ENTHALPY
Analysis of ocean and atmosphere thermodynamical characteristics during the onset of southwest monsoon over the Arabian Sea p 57 N82-23945

ENVIRONMENT EFFECTS
Landsat digital analysis of the initial recovery of burned tundra at Kokolik River, Alaska p 8 A82-32913

ENVIRONMENT POLLUTION
Environmental monitoring report of the Lawrence Berkeley Laboratory, 1980
[LBL-12604] p 29 N82-23793

ENVIRONMENTAL MONITORING
Detection of environmental disturbance using color aerial photography and thermal infrared imagery p 22 A82-29327
Desert locust habitat monitoring with satellite remote sensing A new technology for an old problem p 7 A82-29747
Aircraft monitoring of surface carbon dioxide exchange p 23 A82-30293
EPA's new bubble and banking policies --- for environmental monitoring p 25 A82-33865
Defining the temporal window for monitoring forest canopy defoliation using Landsat p 9 A82-34730
Monitoring deforestation in the eastern part of the state of Guerrero, Mexico p 9 A82-34733
Space science for applications - The history of Landsat p 84 A82-36617
Environmental monitoring report of the Lawrence Berkeley Laboratory, 1980
[LBL-12604] p 29 N82-23793
History of the French satellite space program p 85 N82-24216

ENVIRONMENTAL RESEARCH SATELLITES
ERS-1 European remote sensing satellite p 84 A82-34367

EQUATORIAL ELECTROJET
MAGSAT for geomagnetic studies over Indian region
[E82-10296] p 73 N82-24572

EQUATORIAL REGIONS
Comparison of storm-time changes of geomagnetic field at ground and at MAGSAT altitudes, part 2
[E82-10325] p 30 N82-24598

ERROR ANALYSIS
Seasat altimeter timing bias estimation p 50 A82-29609
Evaluation of the Seasat altimeter time tag bias p 50 A82-29610
A practical study of gross-error detection in bundle adjustment p 69 A82-34702
A quantitative method to test for similarity between photo interpreters p 69 A82-34722
Dobson spectrophotometer calibrations, possible errors in ozone absorption coefficients, and errors due to interfering pollutant gases p 28 A82-36431

ERS-1 (ESA SATELLITE)
ERS-1 European remote sensing satellite p 84 A82-34367

ESTIMATES
Determination of the optimal level for combining area and yield estimates
[E82-10215] p 12 N82-23588
AgRISTARS Preliminary technical results review of FY81 experiments, volume 2 Fiscal year 1981/1982 'corn and soybeans pilot' experiment
[E82-10216] p 13 N82-23589

ESTIMATING
Sample design for estimating change in land use and land cover p 24 A82-32711
A statistical approach to rainfall estimation using satellite and conventional data
[NOAA-TR-NESS-89] p 63 N82-22854
A comparison of stratified versus regression estimators p 11 N82-23133

ESTUARIES
Remote sensing in Scotland using data received from satellites - A study of the Tay Estuary region using Landsat multispectral scanning imagery p 62 A82-37501

EUROPE
Crustal structures under the active volcanic areas of central and eastern Mediterranean (M-44)
[E82-10096] p 35 N82-23563
Aeromagnetic and satellite magnetic anomaly mapping
[E82-10339] p 39 N82-25601

EUROPEAN SPACE AGENCY
ERS-1 European remote sensing satellite
p 84 A82-34367

EVALUATION
LANDSAT-D conical scanner evaluation plan
[E82-10340] p 81 N82-25602

EVAPORATION
A method for inferring available surface moisture using remote surface temperature measurements An assessment --- Kansas and St Louis, Missouri
[E82-10311] p 17 N82-24585

EVAPORATION RATE
Application of thermal model for pan evaporation to the hydrology of a defined medium, the sponge
[E82-10217] p 13 N82-23590

EVAPOTRANSPIRATION
Application of thermal model for pan evaporation to the hydrology of a defined medium, the sponge
[E82-10217] p 13 N82-23590
AgRISTARS Early warning and crop condition assessment Plant cover, soil temperature, freeze, water stress, and evapotranspiration conditions
[E82-10225] p 14 N82-23598

EXPERIMENTAL DESIGN
The impact of meteorological satellites on the First GARP Global Experiment (FGGE) --- First Global Atmospheric Research Program Global Experiment (FGGE) p 55 N82-23852

EXPLORATION
Airborne gamma-ray spectrometer and magnetometer survey Devil's Lake quadrangle, North Dakota, volume 1
[DE82-004161] p 44 N82-23635

EXTRAGALACTIC RADIO SOURCES
Consequences of an inverse Compton emission model for extragalactic X-ray sources p 83 A82-22553

F

FAR INFRARED RADIATION
Thermography - A remote sensing method with many perspectives p 76 A82-29922

FARM CROPS
Remote sensing of the weediness of crop fields
p 5 A82-29435
Spectral properties of agricultural crops and soils measured from space, aerial, field, and laboratory sensors
[E82-10189] p 10 N82-22623
Analysis of scanner data for crop inventories
[E82-10192] p 10 N82-22626
Spectral properties of agricultural crops and soils measured from space, aerial, field, and laboratory sensors
[E82-10212] p 12 N82-23585
Application of thermal model for pan evaporation to the hydrology of a defined medium, the sponge
[E82-10217] p 13 N82-23590
AgRISTARS Project management report Program review presentation to level 1, interagency coordination committee
[E82-10219] p 13 N82-23592

FARMLANDS
Thermal mapping, geothermal source location, natural effluents and plant stress in the Mediterranean coast of Spain
[E82-10300] p 17 N82-24576
Irrigated acreage in the Bear River Basin as of the 1975 growing season --- Idaho, Utah, and Wyoming
[E82-10356] p 20 N82-26754
Measurement of soil moisture trends with airborne scatterometers --- Guymon, Oklahoma and Dalhart, Texas
[E82-10361] p 20 N82-26759

FELSITE
Influence of CO2 on melting of model granulite facies assemblages - A model for the genesis of charnockites
p 42 A82-36298

FERTILIZERS
Color aerial photography detects nutrient status of loblolly pine plantations p 6 A82-29531

FIELD THEORY (PHYSICS)
Astrophysical scenarios for critically evaluating a zero-point field acceleration mechanism
p 64 A82-22575

FINITE ELEMENT METHOD
Nonlinear theory for elastic beams and rods and its finite element representation
[WTHD-143] p 73 N82-24517

FIRE DAMAGE
Landsat digital analysis of the initial recovery of burned tundra at Kokolik River, Alaska p 8 A82-32913

FIRE PREVENTION
Remote automatic weather station for resource and fire management agencies
[PB82-107335] p 30 N82-23963

FISHERIES
Technology and oceanography An assessment of Federal technologies for oceanographic research and monitoring Volume 2 Working papers on fishery research technology p 58 N82-26944

FLAT PATTERNS
Subtleties in the flat-fielding of charge-coupled device /CCD/ images p 68 A82-32581

FLIGHT PATHS
Airborne gamma-ray spectrometer and magnetometer survey Roseau quadrangle, Minnesota, volume 2
[DE82-001025] p 44 N82-23634

FLORIDA
Use of thermal inertia determined by HCMM to predict nocturnal cold prone areas in Florida --- Everglades agricultural area and the west north central peninsula
[E82-10299] p 17 N82-24575
Forest Resource Information System Phase 3 System transfer report
[E82-10344] p 18 N82-25606

FLOW MEASUREMENT
Fluid-sediment interactions on beaches and shelves
[AD-A110838] p 59 N82-26948

FLUID DYNAMICS
Investigation of geomagnetic field forecasting and fluid dynamics of the core
[E82-10342] p 39 N82-25604

FLUID FLOW
Fluid-sediment interactions on beaches and shelves
[AD-A110838] p 59 N82-26948

FOCUSING
Optical stop and focussing effects in the Dobson instrument p 28 A82-36428

FOG
Some empirical rules for forecasting fog and status over northern Florida, southern Georgia and adjacent coastal waters
[PB82-154006] p 59 N82-27949

FOLIAGE
Remote sensing of leaf water content in the near infrared p 8 A82-32897
Application of Computer Axial Tomography (CAT) to measuring crop canopy geometry --- corn and soybeans
[E82-10227] p 14 N82-23600

FORBUSH DECREASES
The approximate 1 GeV solar cosmic rays in the Forbush-effect of February 15, 1978 p 40 A82-22604

FORECASTING
AgRISTARS Foreign commodity production forecasting The 1980 US corn and soybeans exploratory experiment
[E82-10206] p 11 N82-23579
Determination of the optimal level for combining area and yield estimates
[E82-10215] p 12 N82-23588
AgRISTARS Preliminary technical results review of FY81 experiments, volume 2 Fiscal year 1981/1982 'corn and soybeans pilot' experiment
[E82-10216] p 13 N82-23589

FOREST MANAGEMENT
Development and application of panoramic aerial photography in forest pest management
p 5 A82-29527
Panoramic aerial photography in forest pest management p 7 A82-32701
Optical bar panoramic photography for planning timber salvage in drought-stressed forests p 7 A82-32705
Landsat detection of hardwood forest clearcuts
p 8 A82-32708
Defining the temporal window for monitoring forest canopy defoliation using Landsat p 9 A82-34730
AgRISTARS Renewable resources inventory Land information support system implementation plan and schedule --- San Juan National Forest pilot test
[E82-10224] p 14 N82-23597
Forest Resource Information System Phase 3 System transfer report
[E82-10344] p 18 N82-25606

FORESTS
Application of 35mm color aerial photography to forest land change detection p 6 A82-29533
Evaluation of spruce-fir forests using small-format photographs p 8 A82-32707
Use of Landsat multispectral scanner data in vegetation mapping of a forested area p 9 A82-34731
Water-balance differentiation of natural complexes on the basis of satellite photographs p 61 A82-35129
Status and prospects of the automated processing of remote-sensing data /using forest surveys as an example/ p 10 A82-35139
Ten-Ecosystem Study --- Grand and Weld Counties, Colorado, Warren County, Pennsylvania, St Louis County, Minnesota, Sandoval County, New Mexico, Kershaw County, South Carolina, Fort Yukon, Alaska, Grays Harbor County, Washington, and Washington County, Missouri
[E82-10186] p 84 N82-22620
AgRISTARS Renewable resources inventory Land information support system implementation plan and schedule --- San Juan National Forest pilot test
[E82-10224] p 14 N82-23597
Use and applicability of the vegetation component of the national site classification system --- Sumter National Forest, South Carolina
[E82-10234] p 15 N82-23607
An analysis of LANDSAT MSS scene-to-scene registration accuracy
[E82-10285] p 16 N82-24563
Analysis of thematic mapper simulator data acquired during winter season over Pearl River, Mississippi, test site
[E82-10287] p 17 N82-24565
Identifying environmental features for land management decisions --- Utah
[E82-10289] p 30 N82-24567
Detection of variations in aspen forest habitat from LANDSAT digital data Bear River Range, Utah
[E82-10355] p 19 N82-26753

FOURIER ANALYSIS
Terrain classification by Fourier analysis - Accuracy and economy p 69 A82-34723

FOURIER TRANSFORMATION
Terrain classification by Fourier analysis - Accuracy and economy p 69 A82-34723

FRAGMENTATION
Fragmentation of Fe nuclei on carbon, hydrogen and CH2 targets I - Individual charge changing and total cross sections II - Isotopic cross sections --- for interstellar cosmic ray propagation p 63 A82-22538

FRANCE
Spatial thermal radiometry contribution to the Massif Armoricain and the Massif Central France litho-structural study
[E82-10190] p 42 N82-22624

FREEZING
AgRISTARS Early warning and crop condition assessment Plant cover, soil temperature, freeze, water stress, and evapotranspiration conditions
[E82-10225] p 14 N82-23598

FRENCH SPACE PROGRAMS
History of the French satellite space program
p 85 N82-24216

FRESH WATER
Ice distribution and winter surface circulation patterns, Kachemak Bay, Alaska
[AD-A110806] p 58 N82-26764

G

GALACTIC NUCLEI
Origin of cosmic rays in galactic centre sources
p 3 A82-22571
Acceleration processes near massive black holes
p 3 A82-22572

GALACTIC RADIATION
On the characteristics of the very low energy galactic cosmic rays in the interstellar space p 63 A82-22540
Dependence of earth spectrum of positrons and antiprotons on propagation models --- of cosmic radiation p 21 A82-22545
Antiprotons from galactic sources of cosmic rays and gamma rays p 82 A82-22546
Confinement and acceleration of cosmic rays in galactic superbubbles p 82 A82-22547
Derivation of the distribution of synchrotron emissivity in the Galaxy from the 408 MHz all-sky survey
p 82 A82-22549
Angular variations of nonthermal radio emission from the Galaxy relevant to the structure of interstellar magnetic field p 83 A82-22550
Comparative abundances in solar energetic particles and in galactic cosmic ray sources, and the Ne-22 anomaly
p 83 A82-22556
Physical state of the birth place of cosmic rays and its implication to the acceleration processes
p 2 A82-22559
On volatility, first ionization potential, and s- and r-processes --- for Galactic cosmic ray sources
p 2 A82-22560
Interstellar grains as seeds for galactic cosmic rays
p 2 A82-22561

Origin of galactic cosmic rays from Ne isotopic composition p 2 A82-22563
The galactic origin of cosmic rays I [CONF-810711-1] p 2 A82-22565
Acceleration of cosmic rays in accretion shocks p 64 A82-22568
The galactic origin of cosmic rays II [CONF-810711-2] p 64 A82-22573
Extragalactic cosmic rays, their sources and spectrum p 40 A82-22574
International Cosmic Ray Conference, 17th, Paris, France, July 13-25, 1981, Conference Papers Volume 3 p 65 A82-22580
The approximate 1 GeV solar cosmic rays in the Forbush-effect of February 15, 1978 p 40 A82-22604
The modulation characteristics of the 19th and 20th solar activity cycles p 59 A82-22615

GALACTIC RADIO WAVES
Convective outflow of cosmic rays from the Galaxy and background radio emission p 83 A82-22551

GAMMA RAY ASTRONOMY
Confinement and acceleration of cosmic rays in galactic superbubbles p 82 A82-22547
Origin of cosmic rays in galactic centre sources p 3 A82-22571
Measurement of cosmogenic nuclides using a multi-crystal gamma-ray coincidence spectrometer --- for Mayo Belwa meteorite study p 64 A82-22577
Solar gamma-ray experiment on Astro-A satellite p 21 A82-22583
Unusual properties of particle events associated with solar flare gamma ray events p 65 A82-22585

GAMMA RAY SPECTRA
Interplanetary particle observations associated with solar flare gamma-ray line emission p 3 A82-22584
Observations of interplanetary energetic charged particles from gamma-ray line solar flares p 65 A82-22586
Airborne gamma-ray spectrometer and magnetometer survey International Falls quadrangle, Minnesota, volume 1 [DE82-004151] p 45 N82-23643
Airborne gamma-ray spectrometer and magnetometer survey International Falls quadrangle, Minnesota, volume 2 [DE82-004166] p 45 N82-23644
Airborne gamma-ray spectrometer and magnetometer survey Susanville quadrangle, California, volume 1 [DE82-005538] p 48 N82-27811
Airborne gamma-ray spectrometer and magnetometer survey Roseburg quadrangle, Oregon, volume 2 [DE82-005568] p 48 N82-27812

GAMMA RAY SPECTROMETERS
Measurement of cosmogenic nuclides using a multi-crystal gamma-ray coincidence spectrometer --- for Mayo Belwa meteorite study p 64 A82-22577
Airborne gamma-ray spectrometer and magnetometer survey Bemidji quadrangle, Minnesota, volume 1 [DE82-001032] p 44 N82-23637
Airborne gamma-ray spectrometer and magnetometer survey Bemidji quadrangle, Minnesota, volume 2 [DE82-001026] p 44 N82-23638
Airborne gamma-ray spectrometer and magnetometer survey Barrow quadranagle, Alaska, volume 2 [DE82-000342] p 46 N82-25623
Airborne gamma-ray spectrometer and magnetometer survey North/south tieline, volume 1 [DE82-005542] p 47 N82-27804
NURE aerial gamma-ray and magnetic reconnaissance survey of portions of New Mexico, Arizona and Texas Volume 2 New Mexico-Carlsbad Quadrangle [DE82-005527] p 48 N82-27810
Airborne gamma-ray spectrometer and magnetometer survey Huron Quadrangle, South Dakota [DE82-005540] p 48 N82-27814
Airborne gamma-ray spectrometer and magnetometer survey Chico Quadrangle, California [DE82-005543] p 48 N82-27815

GAMMA RAYS
Antiprotons from galactic sources of cosmic rays and gamma rays p 82 A82-22546
Airborne gamma-ray spectrometer and magnetometer survey North/south tieline, volume 2 [DE82-005570] p 47 N82-27805

GAS DETECTORS
Aircraft monitoring of surface carbon dioxide exchange p 23 A82-30293
Breadboard gas filter correlation spectrometer for atmospheric measurement of hydrazines and nitrogen dioxide [AD-A110688] p 82 N82-26642

GAS EXCHANGE
Aircraft monitoring of surface carbon dioxide exchange p 23 A82-30293

GAS TRANSPORT
Comparison of ozone in polluted and clean air masses over Lake Michigan p 29 A82-36477

GEOBOTANY
The influence of autocorrelation in signature extraction An example from a geobotanical investigation of Cotter Basin, Montana [E82-10341] p 46 N82-25603

GEOCENTRIC COORDINATES
Establishment of terrestrial reference frames by new observational techniques p 33 A82-32078
Origin and scale of coordinate systems in satellite geodesy p 34 A82-32099

GEODESY
Seasat altimeter height calibration --- related to sea surface heights near Bermuda p 49 A82-29603
Gravity model improvement for Seasat p 32 A82-29615
Work related to the Blue Road Geotraverse at the Finnish Geodetic Institute p 32 A82-30306
Reference coordinate systems for earth dynamics - A preview p 33 A82-32077
Geodetic monitoring of tectonic deformation Toward a strategy [NASA-CR-168784] p 35 N82-22846

GEODETIC COORDINATES
Origin and scale of coordinate systems in satellite geodesy p 34 A82-32099
Investigations of point transfer p 78 A82-33296
The processing of satellite navigation data for marine geodesy p 34 A82-37175

GEODETIC SURVEYS
Tidal and geodetic observations for the Seasat altimeter calibration experiment p 49 A82-29604
Seasat altimeter timing bias estimation p 50 A82-29609
Establishing geodetic-geodynamic parameters using lunar laser range measurements p 34 A82-33293
The simultaneous employment of geodetic measurements for block adjustments using the method of independent models p 34 A82-33295
Geodetic monitoring of tectonic information Toward a strategy p 35 N82-22832
Geodetic monitoring of tectonic deformation Toward a strategy [NASA-CR-168784] p 35 N82-22846
Seismic and geodetic studies of the Imperial Valley, California [DE82-001686] p 39 N82-26915

GEODYNAMICS
Establishment of terrestrial reference frames by new observational techniques p 33 A82-32078
Some considerations in the use of very-long-baseline-interferometry to establish reference coordinate systems for geodynamics p 34 A82-32096
Establishing geodetic-geodynamic parameters using lunar laser range measurements p 34 A82-33293
Investigation of geomagnetic field forecasting and fluid dynamics of the core --- determination of the bundary between the core and mantle of the Earth [E82-10198] p 35 N82-23571

GEOGRAPHY
Impacts of remote sensing on U S geography p 24 A82-32899
Exploration into technical procedures for vertical integration --- information systems [NASA-CR-166352] p 75 N82-26763

GEOIDS
Geoid height-age relation from Seasat altimeter profiles across the Mendocino Fracture Zone p 34 A82-32646

GEOLOGICAL FAULTS
Satellite image interpretation of the eastern Caledonian part of the Blue Road Geotraverse and its geological implications /Nordland, Vasterbotten, Scandinavia/ p 41 A82-30305
Possible fault detection in Cottonball Basin, California An application of radar remote sensing p 41 A82-32898
Comparing lineaments interpreted from Landsat imagery and topographic maps with reported faults in southwest Montana p 34 A82-34719
Structure of the Saint Francois Mountains and surrounding lead belt, S E Missouri Inference from thermal IR and other data sets [E82-10350] p 39 N82-26748

GEOLOGICAL SURVEYS
Magsat scalar anomaly distribution - The global perspective p 41 A82-30786
Aerogeophysical methods of finding uranium deposits --- Russian book p 41 A82-33402
Satellite and surface geophysical expression of anomalous crustal structure in Kentucky and Tennessee p 34 A82-34918
Airborne gamma-ray spectrometer and magnetometer survey, Kenora quadrangle, Minnesota, volume 1 [DE82-001029] p 43 N82-23625
Airborne gamma-ray spectrometer and magnetometer survey Roseau quadrangle, Minnesota, volume 2 [DE82-001025] p 44 N82-23634
Airborne gamma-ray spectrometer and magnetometer survey Devil's Lake quadrangle, North Dakota, volume 1 [DE82-004161] p 44 N82-23635
Airborne gamma-ray spectrometer and magnetometer survey Devil's Lake quadrangle, North Dakota, volume 2 [DE82-004168] p 44 N82-23636
Airborne gamma-ray spectrometer and magnetometer survey Hibbing quadrangle, Minnesota, volume 1 [DE82-004159] p 44 N82-23639
Airborne gamma-ray spectrometer and magnetometer survey Hibbing quadrangle, Minnesota, volume 2 [DE82-004165] p 45 N82-23640
Airborne gamma-ray spectrometer and magnetometer survey Aberdeen quadrangle, South Dakota, volume 1 [DE82-004152] p 45 N82-23641
Airborne gamma-ray spectrometer and magnetometer survey Aberdeen quadrangle, South Dakota, volume 2 [DE82-004164] p 45 N82-23642
Application of HCMM data to regional geologic analysis for mineral and energy resource evaluation [E82-10243] p 45 N82-24521
Use of MAGSAT anomaly data for crustal structure and mineral resources in the US Midcontinent [E82-10321] p 46 N82-24594
Use of MAGSAT anomaly data for crustal structure and mineral resources in the US Midcontinent [E82-10323] p 46 N82-24596
Airborne gamma-ray spectrometer and magnetometer survey Barrow quadranagle, Alaska, volume 2 [DE82-000342] p 46 N82-25623
An investigation into the utilization of HCMM thermal data for the discrimination of volcanic and Eolian geological units --- Newberry Volcano, Oregon [E82-10352] p 47 N82-26750
Airborne gamma-ray spectrometer and magnetometer survey North/south tieline, volume 1 [DE82-005542] p 47 N82-27804
Airborne gamma-ray spectrometer and magnetometer survey Susanville quadrangle, California, volume 1 [DE82-005538] p 48 N82-27811

GEOLOGY
Geodetic monitoring of tectonic deformation Toward a strategy [NASA-CR-168784] p 35 N82-22846

GEOMAGNETIC HOLLOW
Satellite and surface geophysical expression of anomalous crustal structure in Kentucky and Tennessee p 34 A82-34918

GEOMAGNETISM
Regional geological, tectonic and geophysical features of Nordland, Norway p 41 A82-30304
Magnetic charts of Canada derived from Magsat data p 32 A82-30778
Initial scalar magnetic anomaly map from Magsat p 32 A82-30784
Initial vector magnetic anomaly map from Magsat p 32 A82-30785
Magsat scalar anomaly distribution - The global perspective p 41 A82-30786
Magsat magnetic anomalies over Antarctica and the surrounding oceans p 32 A82-30787
Spatial resolution and repeatability of Magsat crustal anomaly data over the Indian Ocean p 32 A82-30788
Verification of the crustal component in satellite magnetic data p 32 A82-30789
A preliminary comparison of the Magsat data and aeromagnetic data in the continental U S p 32 A82-30790
A satellite magnetic model of northeastern South American aulacogens p 33 A82-30795
Preliminary interpretation of magnetic anomalies over Japan and its surrounding area p 33 A82-30796
Observed magnetic substorm signatures at synchronous altitude p 26 A82-35534
Structure, composition and thermal state of the crust in Brazil --- geomagnetic survey [E82-10187] p 35 N82-22621
Studies of high latitude current systems using MAGSAT vector data [E82-10188] p 71 N82-22622
MAGSAT and aeromagnetic data in the North American continent [E82-10193] p 71 N82-22627
Study of gravity and magnetic anomalies using MAGSAT data [E82-10194] p 35 N82-22628
Equivalent source modeling of the main field using MAGSAT data [E82-10151] p 71 N82-23567

Characterization of the structure and tectonic of South America
[E82-10196] p 42 N82-23569
Analyses of MAGSAT tracks crossing the study region in the Indian Ocean
[E82-10197] p 71 N82-23570
Investigation of geomagnetic field forecasting and fluid dynamics of the core --- determination of the bundary between the core and mantle of the Earth
[E82-10198] p 35 N82-23571
MAGSAT science investigations
[E82-10199] p 71 N82-23572
Investigation of MAGSAT and TRIAD magnetometer data to provide corrective information on high-latitude external fields
[E82-10201] p 72 N82-23574
MAGSAT for geomagnetic studies over Indian region
[E82-10202] p 72 N82-23575
Spherical harmonic representation of the main geomagnetic field for world charting and investigations of some fundamental problems of physics and geophysics
[E82-10203] p 72 N82-23576
Investigation of the effects of external current systems on the MAGSAT data utilizing grid cell modeling techniques
[E82-10226] p 73 N82-23599
Investigation of the effects of external current systems on the MAGSAT data utilizing grid cell modeling techniques
[E82-10232] p 73 N82-23605
Investigation from Japanese MAGSAT team
[E82-10239] p 73 N82-23612
Investigations of medium wavelength magnetic anomalies in the eastern Pacific using MAGSAT
[E82-10240] p 73 N82-23613
Airborne gamma-ray spectrometer and magnetometer survey Devil's Lake quadrangle, North Dakota, volume 1
[DE82-004161] p 44 N82-23635
Airborne gamma-ray spectrometer and magnetometer survey Devil's Lake quadrangle, North Dakota, volume 2
[DE82-004168] p 44 N82-23636
Airborne gamma-ray spectrometer and magnetometer survey Bemidji quadrangle, Minnesota, volume 1
[DE82-001032] p 44 N82-23637
Spherical-Earth gravity and magnetic anomaly modeling by Gauss-Legendre quadrature integration
[E82-10242] p 36 N82-24520
Investigation from Japanese MAGSAT Team Part A Crustal structure near Japan and in Antarctic station Part B Electric currents and hydromagnetic waves in the ionosphere and the magnetosphere
[E82-10244] p 36 N82-24522
Report of MAGSAT project by Survey of India
[E82-10293] p 73 N82-24570
MAGSAT for geomagnetic studies over Indian region
[E82-10296] p 73 N82-24572
An equivalent layer magnetization model for the United States derived from MAGSAT data
[E82-10297] p 36 N82-24573
Investigation of the effects of external current systems on the MAGSAT data utilizing grid cell modeling techniques
[E82-10306] p 74 N82-24580
MAGSAT scalar and vector anomaly data analysis
[E82-10307] p 74 N82-24581
Investigation of geomagnetic field forecasting and fluid dynamics of the core
[E82-10310] p 37 N82-24584
Magnetic and gravity anomalies in the Americas
[E82-10312] p 37 N82-24586
Improved definition of crustal magnetic anomalies for MAGSAT data
[E82-10314] p 37 N82-24587
An investigation of MAGSAT and complementary data emphasizing precambrian shields and adjacent areas of West Africa and South America
[E82-10316] p 38 N82-24589
An investigation of MAGSAT and complementary data emphasizing precambrian shields and adjacent areas of West Africa and South America
[E82-10317] p 38 N82-24590
An investigation of MAGSAT and complementary data emphasizing precambrian shields and adjacent areas of West Africa and South America
[E82-10318] p 38 N82-24591
Report of investigation from Japanese MAGSAT Team
[E82-10322] p 74 N82-24595
Comparison of storm-time changes of geomagnetic field at ground and at MAGSAT altitudes, part 2
[E82-10325] p 30 N82-24598
MAGSAT anomaly map and continental drift
[E82-10326] p 38 N82-24599
Models and maps of the main field
[E82-10327] p 74 N82-24600
Investigations of medium wavelength magnetic anomalies in the eastern Pacific using MAGSAT data
[E82-10330] p 38 N82-24603
Aeromagnetic and satellite magnetic anomaly mapping
[E82-10339] p 39 N82-25601
Investigation of geomagnetic field forecasting and fluid dynamics of the core
[E82-10342] p 39 N82-25604
A comparison of pole positions derived from GPS satellite and Navy navigation satellite observations
[AD-A110765] p 39 N82-26268
Comparison of storm-time changes of geomagnetic field at ground and MAGSAT altitudes
[E82-10359] p 30 N82-26757
The Earth's gravity field to degree and order 180 using SEASAT altimeter data, terrestrial gravity data and other data
[AD-A113098] p 40 N82-27900

GEOMETRIC RECTIFICATION (IMAGERY)
Evaluation of temporal registration of Landsat scenes p 67 A82-32345
Evaluation of VICAR software capability for land information support system needs --- Elk River quadrangle, Idaho
[E82-10223] p 73 N82-23596

GEOMORPHOLOGY
Preliminary evidence for the influence of physiography and scale upon the autocorrelation function of remotely sensed data p 67 A82-32343
Soufriere Volcano, St Vincent - Observations of its 1979 eruption from the ground, aircraft, and satellites p 24 A82-33652
Overseas Geology And Mineral Resources number 56 A geological interpretation of LANDSAT imagery and air photography of Botswana
[OGMR-56] p 42 N82-22636
Analyses of MAGSAT tracks crossing the study region in the Indian Ocean
[E82-10197] p 71 N82-23570
Structure of the Saint Francois Mountains and surrounding lead belt, S E Missouri Inference from thermal IR and other data sets
[E82-10350] p 39 N82-26748

GEOPHYSICAL FLUIDS
Investigation of geomagnetic field forecasting and fluid dynamics of the core
[E82-10342] p 39 N82-25604

GEOPHYSICAL SATELLITES
Satellite and surface geophysical expression of anomalous crustal structure in Kentucky and Tennessee p 34 A82-34918

GEOPHYSICS
Origin and scale of coordinate systems in satellite geodesy p 34 A82-32099
Inversion of data from diffraction-limited multiwavelength remote sensors II - Nonlinear dependence of observables on the geophysical parameters p 77 A82-32658
Spherical harmonic representation of the main geomagnetic field for world charting and investigations of some fundamental problems of physics and geophysics
[E82-10203] p 72 N82-23576
Computer-processed geophysical atlas of digital data for the East Coast margin of the United States from surface and spacecraft data
[AD-A111388] p 39 N82-25748
Airborne gamma-ray spectrometer and magnetometer survey North/south tieline, volume 1
[DE82-005542] p 47 N82-27804
Evaluation and combined geophysical interpretations of NURE and related geoscience data in the Van Horn, Pecos, Marfa, Fort Stockton, Presidido, and Emory Peak quadrangles, Texas, volume 1
[DE82-005554] p 47 N82-27808
Evaluation and combined geophysical interpretations of NURE and related geoscience data in the Van Horn, Pecos, Marfa, Fort Stockton, Presidio, and Emory Peak quadrangels, Texas
[DE82-005560] p 48 N82-27809
NURE aerial gamma-ray and magnetic reconnaissance survey of portions of New Mexico, Arizona and Texas Volume 2 New Mexico-Carlsbad Quadrangle
[DE82-005527] p 48 N82-27810
Airborne gamma-ray spectrometer and magnetometer survey Susanville quadrangle, California, volume 1
[DE82-005538] p 48 N82-27811
Airborne gamma-ray spectrometer and magnetometer survey Huron Quadrangle, South Dakota
[DE82-005540] p 48 N82-27814
Airborne gamma-ray spectrometer and magnetometer survey Chico Quadrangle, California
[DE82-005543] p 48 N82-27815

GEOS 3 SATELLITE
A search for seamounts in the southern Cook and Austral region p 52 A82-30810

GLACIERS
The use of space photographs in the mapping of glaciers and water bodies p 62 A82-37174

GLINT
The effect of sea-surface Sun glitter on microwave radiometer measurements
[NASA-CR-169083] p 57 N82-26525

GLOBAL ATMOSPHERIC RESEARCH PROGRAM
The impact of meteorological satellites on the First GARP Global Experiment (FGGE) --- First Global Atmospheric Research Program Global Experiment (FGGE) p 55 N82-23852
Mean sea-level pressure in the Southern Hemisphere during the FGGE period --- First Global Atmospheric Research Program Global Experiment (FGGE), buoys p 55 N82-23856
Comparison of satellite derived radiation budget measurements over MONEX during 1979 to 1980 --- Monsoon Experiment (MONEX) p 29 N82-23891
Short term influence radius of monsoonal overturnings --- First Global Atmospheric Research Program Global Experiment (FGGE) p 56 N82-23898
Impact of additional summer MONEX wind data on the prediction of monsoon depressions during June - August 1979 with two versions of primitive equation (PE) barotropic model --- Monsoon Experiment (MONEX) p 56 N82-23900

GLOBAL POSITIONING SYSTEM
A comparison of pole positions derived from GPS satellite and Navy navigation satellite observations
[AD-A110765] p 39 N82-26268

GOES SATELLITES
Digital and visual evaluation of GOES and TIROS/NOAA image data for cover type effects on snowfield observations p 60 A82-34735
SMS/GOES data collection platform system p 75 N82-26027

GOVERNMENT/INDUSTRY RELATIONS
Civil land remote sensing system
[GPO-87-070] p 84 N82-22630
LANDSAT technology transfer to the private and public sectors through community colleges and other locally available institutions
[E82-10181] p 85 N82-23568

GOVERNMENTS
A legislator's guide to LANDSAT
[E82-10290] p 85 N82-24568

GRAINS (FOOD)
Normal crop calendars Volume 3 The corn and soybean states of Illinois, Indiana, and Iowa
[E82-10221] p 13 N82-23594
Evaluation of the procedure for separating barley from other spring small grains --- North Dakota, South Dakota, Minnesota and Montana
[E82-10230] p 14 N82-23603
AgRISTARS Project management report Program review presentation to level 1, interagency coordination committee --- Brazil, Argentina, U S corn belt, Great Plains Corridor
[E82-10231] p 15 N82-23604
Description of the FORTRAN implementation of the spring small grains planting date distribution model
[E82-10235] p 15 N82-23608

GRASSLANDS
Ten-Ecosystem Study --- Grand and Weld Counties, Colorado, Warren County, Pennsylvania, St Louis County, Minnesota, Sandoval County, New Mexico, Kershaw County, South Carolina, Fort Yukon, Alaska, Grays Harbor County, Washington, and Washington County, Missouri
[E82-10186] p 84 N82-22620
A multi-frequency radiometric measurement of soil moisture content over bare and vegetated fields
[E82-10238] p 16 N82-23611

GRAVIMETRY
Work related to the Blue Road Geotraverse at the Finnish Geodetic Institute p 32 A82-30306

GRAVITATIONAL FIELDS
Gravity model improvement for Seasat p 32 A82-29615
The Earth's gravity field to degree and order 180 using SEASAT altimeter data, terrestrial gravity data and other data
[AD-A113098] p 40 N82-27900

GRAVITY ANOMALIES
Regional geological, tectonic and geophysical features of Nordland, Norway p 41 A82-30304
Work related to the Blue Road Geotraverse at the Finnish Geodetic Institute p 32 A82-30306
Study of gravity and magnetic anomalies using MAGSAT data
[E82-10194] p 35 N82-22628
Characterization of the structure and tectonic of South America
[E82-10196] p 42 N82-23569

Spherical-Earth gravity and magnetic anomaly modeling by Gauss-Legendre quadrature integration
[E82-10242] p 36 N82-24520
Analyzing the Broken Ridge area of the Indian Ocean using magnetic and gravity anomaly maps and geoid undulation and bathymetry data
[E82-10303] p 36 N82-24577
The mineralogy of global magnetic anomalies --- rock magnetic signatures and MAGSAT geological, and gravity correlations in West Africa
[E82-10305] p 45 N82-24579
Magnetic and gravity anomalies in the Americas
[E82-10312] p 37 N82-24586
Geotectonics of South America --- regional magnetic and gravity anomalies of South America
[E82-10320] p 38 N82-24593
Structure of the Saint Francois Mountains and surrounding lead belt, S E Missouri Inference from thermal IR and other data sets
[E82-10350] p 39 N82-26748
The Earth's gravity field to degree and order 180 using SEASAT altimeter data, terrestrial gravity data and other data
[AD-A113098] p 40 N82-27900

GRAVITY GRADIOMETERS
Evaluation and combined geophysical interpretations of NURE and related geoscience data in the Van Horn, Pecos, Marfa, Fort Stockton, Presidio, and Emory Peak quadrangels, Texas
[DE82-005560] p 48 N82-27809

GRAVITY WAVES
The observation of ocean surface phenomena using imagery from the Seasat synthetic aperture radar - An assessment p 52 A82-29623

GREAT LAKES (NORTH AMERICA)
Airborne gamma-ray spectrometer and magnetometer survey Bemidji quadrangle, Minnesota, volume 1
[DE82-001032] p 44 N82-23637
Airborne gamma-ray spectrometer and magnetometer survey Hibbing quadrangle, Minnesota, volume 1
[DE82-004159] p 44 N82-23639
Airborne gamma-ray spectrometer and magnetometer survey Hibbing quadrangle, Minnesota, volume 2
[DE82-004165] p 45 N82-23640

GREAT PLAINS CORRIDOR (NORTH AMERICA)
AgRISTARS Foreign commodity production forecasting The 1980 US/Canada wheat and barley exploratory experiment
[E82-10126] p 11 N82-23565
Evaluation of the procedure for separating barley from other spring small grains --- North Dakota, South Dakota, Minnesota and Montana
[E82-10230] p 14 N82-23603
AgRISTARS Project management report Program review presentation to level 1, interagency coordination committee --- Brazil, Argentina, U S corn belt, Great Plains Corridor
[E82-10231] p 15 N82-23604

GREAT SALT LAKE (UT)
Mapping of wildlife habitat in Farmington Bay, Utah
[E82-10354] p 19 N82-26752

GREEN WAVE EFFECT
Analysis of scanner data for crop inventories
[E82-10192] p 10 N82-22626

GREENLAND
The METEOSAT Data Collection System and its application p 75 N82-26037

GROUND SPEED
Magnetic anomalies as a reference for ground-speed and map-matching navigation p 32 A82-30314

GROUND TRUTH
Field size, length, and width distributions based on LACIE ground truth data --- large area crop inventory experiment p 8 A82-32909
Measuring sea surface temperature from satellites - A ground truth approach p 54 A82-32917
The use of Landsat-3 thermal data to help differentiate land covers p 25 A82-34218
Method for the analysis of the melting of a firn complex on the basis of aerospace photographs p 61 A82-35133
Analysis of scanner data for crop inventories
[E82-10192] p 10 N82-22626
SEASAT A satellite scatterometer illumination times of selected in situ sites
[NASA-TM-83280] p 81 N82-22865
AgRISTARS Preliminary technical results review of FY81 experiments, volume 2 Fiscal year 1981/1982 'corn and soybeans pilot' experiment
[E82-10216] p 13 N82-23589
An algorithm for automating the registration of USDA segment ground data to LANDSAT MSS data
[E82-10286] p 16 N82-24564
The mineralogy of global magnetic anomalies --- rock magnetic signatures and MAGSAT geological, and gravity correlations in West Africa
[E82-10305] p 45 N82-24579
Irrigation management with remote sensing --- Navajo Indian Irrigation Project
[E82-10357] p 20 N82-26755
Comparison of storm-time changes of geomagnetic field at ground and MAGSAT altitudes
[E82-10359] p 30 N82-26757
Measurement of soil moisture trends with airborne scatterometers --- Guymon, Oklahoma and Dalhart, Texas
[E82-10361] p 20 N82-26759

GROUND WATER
Evaluation of HCMM data for assessing soil moisture and water table depth --- South Dakota
[E82-10329] p 18 N82-24602

GROUND WIND
Surface wind analyses for Seasat p 51 A82-29619

GULF OF MEXICO
A ship and satellite view of hydrographic features in the western Gulf of Mexico p 53 A82-32651

GULF STREAM
Comparison data for Seasat altimetry in the western North Atlantic p 50 A82-29611

H

HABITATS
Inventory of wildlife habitat from color infrared aerial photography for Cobb Island, Virginia p 6 A82-29529
Desert locust habitat monitoring with satellite remote sensing A new technology for an old problem p 7 A82-29747
A computerized spatial analysis system for assessing wildlife habitat from vegetation maps p 9 A82-34716
Application of remote sensing to state and regional problems
[E82-10288] p 30 N82-24566
Identifying environmental features for land management decisions --- Utah
[E82-10289] p 30 N82-24567
Mapping of wildlife habitat in Farmington Bay, Utah
[E82-10354] p 19 N82-26752
Detection of variations in aspen forest habitat from LANDSAT digital data Bear River Range, Utah
[E82-10355] p 19 N82-26753

HARMONIC ANALYSIS
Gravity model improvement for Seasat p 32 A82-29615

HAZE
Simplified techniques to study components of solar radiation under haze and clouds p 78 A82-32766

HEAT FLUX
Interactive initialization of heat flux parameters for numerical models using satellite temperature measurements
[E82-10313] p 82 N82-26743

HEAT ISLANDS
A method for inferring available surface moisture using remote surface temperature measurements An assessment --- Kansas and St Louis, Missouri
[E82-10311] p 17 N82-24585

HEAT TRANSMISSION
Remote sensing of thermal subsurface terrain properties p 80 A82-34727

HEAVY IONS
Time and energy dependence of heavy ion abundances in solar flare energetic particle events p 22 A82-22605
A comparison of helium and heavy ion spectra in He/3/ rich solar flares with a model calculation p 5 A82-22612

HEAVY NUCLEI
Fragmentation of Fe nuclei on carbon, hydrogen and CH2 targets I - Individual charge changing and total cross sections II - Isotopic cross sections --- for interstellar cosmic ray propagation p 63 A82-22538
A report on the 'cosmic ray propagation problem' p 1 A82-22539
Heavy-element abundances in He/3/-rich events p 5 A82-22611

HELIOSPHERE
Azimuthal propagation of flare particles in the heliosphere p 66 A82-22590

HELIUM ISOTOPES
Heavy-element abundances in He/3/-rich events p 5 A82-22611
A comparison of helium and heavy ion spectra in He/3/ rich solar flares with a model calculation p 5 A82-22612
On the anticorrelation between the He/3//He/4/ ratio and proton intensity in He/3/ rich flares p 40 A82-22613
The model of the cosmic ray enrichment by helium-3 p 31 A82-22614

HIGH ALTITUDE
Estimating mountain pine beetle-killed ponderosa pine over the front range of Colorado with high altitude panoramic photography p 7 A82-32704

HIGH ALTITUDE TESTS
Image quality and height measurement accuracy of aerial survey camera imagery from high altitudes p 78 A82-33297

HIGH ENERGY ELECTRONS
Origin of cosmic rays in galactic centre sources p 3 A82-22571
A survey of solar protons and alpha differential spectra between 1 and greater than 400 MeV/nucleon p 4 A82-22592

HIGH RESOLUTION
High spectral resolution airborne spectrometry p 77 A82-32443
Evaluation of NOAA-AVHRR data for crop assessment --- Advanced Very High Resolution Radiometer p 8 A82-34179

HIGH TEMPERATURE PLASMAS
Mass per charge ratio in hot plasmas and cosmic ray source composition p 2 A82-22557

HISTOGRAMS
Airborne gamma-ray spectrometer and magnetometer survey Roseau quadrangle, Minnesota, volume 1
[DE82-001031] p 43 N82-23621
Airborne gamma-ray spectrometer and magnetometer survey Roseau quadrangle, Minnesota, volume 2
[DE82-001025] p 44 N82-23634
Airborne gamma-ray spectrometer and magnetometer survey Bemidji quadrangle, Minnesota, volume 2
[DE82-001026] p 44 N82-23638

HISTORIES
Space science for applications - The history of Landsat p 84 A82-36617

HURRICANES
Seasat wind and wave observations of northeast Pacific hurricane Iva, August 13, 1978 p 52 A82-29624

HYDRAZINES
Breadboard gas filter correlation spectrometer for atmospheric measurement of hydrazines and nitrogen dioxide
[AD-A110688] p 82 N82-26642

HYDROCARBONS
Landsat in the search for Appalachian hydrocarbons p 42 A82-34721

HYDRODYNAMICS
The use of satellite photographs to study snow-cover dynamics and to determine the average water discharge of the Amudarya during a vegetation period p 61 A82-35132

HYDROGEN ATOMS
Interactions of cosmic rays with molecular clouds p 82 A82-22548

HYDROGEOLOGY
Spatial thermal radiometry contribution to the Massif Armoricain and the Massif Central France litho-structural study
[E82-10190] p 42 N82-22624

HYDROGRAPHY
A ship and satellite view of hydrographic features in the western Gulf of Mexico p 53 A82-32651
Bias correction procedures for airborne laser hydrography
[PB82-130089] p 63 N82-22644

HYDROLOGY
Automated classification of runoff coefficients from Landsat multispectral data p 60 A82-34734
Study of the hydrological cycle by aerospace methods --- Russian book p 61 A82-35126
Principles and methods of the study of the hydrological cycle on the basis of aerospace data p 61 A82-35127
Water-balance differentiation of natural complexes on the basis of satellite photographs p 61 A82-35129
The possibility of using remote-sensing methods to study the hydrology of elementary watersheds p 61 A82-35130
The use of space photographs in the mapping of glaciers and water bodies p 62 A82-37174
The application of Heat Capacity Mapping Mission (HCMM) thermal data to snow hydrology --- Salt Verde Watershed and the southern Sierra Nevada
[E82-10191] p 62 N82-22625
Application of thermal model for pan evaporation to the hydrology of a defined medium, the sponge
[E82-10217] p 13 N82-23590
AgRISTARS Agriculture and resources inventory surveys through aerospace remote sensing
[E82-10236] p 15 N82-23609
HCMM hydrological analysis in Utah
[E82-10328] p 63 N82-24601

Plan of research for integrated soil moisture studies Recommendations of the Soil Moisture Working Group
[NASA-TM-84731] p 18 N82-25608
The METEOSAT Data Collection System and its application p 75 N82-26037
Ice distribution and winter surface circulation patterns, Kachemak Bay, Alaska
[AD-A110806] p 58 N82-26764

HYGROSCOPICITY
Application of thermal model for pan evaporation to the hydrology of a defined medium, the sponge
[E82-10217] p 13 N82-23590

I

ICE FORMATION
Sea-Ice Mission Requirements for the US FIREX and Canada RADARSAT programs
[NASA-CR-168984] p 57 N82-25609
Ice distribution and winter surface circulation patterns, Kachemak Bay, Alaska
[AD-A110806] p 58 N82-26764

ICE MAPPING
The use of space photographs in the mapping of glaciers and water bodies p 62 A82-37174
Movement of ice markers measured by satellite ranging
[R-240] p 59 N82-27816

ICE REPORTING
Sea-Ice Mission Requirements for the US FIREX and Canada RADARSAT programs
[NASA-CR-168984] p 57 N82-25609

IDAHO
Evaluation of VICAR software capability for land information support system needs --- Elk River quadrangle, Idaho
[E82-10223] p 73 N82-23596
Irrigated acreage in the Bear River Basin as of the 1975 growing season --- Idaho, Utah, and Wyoming
[E82-10356] p 20 N82-26754

ILLINOIS
Normal crop calendars Volume 3 The corn and soybean states of Illinois, Indiana, and Iowa
[E82-10221] p 13 N82-23594

IMAGE CORRELATORS
Analytical processing of photographs taken by paired cameras p 79 A82-34471

IMAGE ENHANCEMENT
Digitally enhanced visual displays facilitate the analysis of Landsat imagery p 67 A82-32507
Terrain analysis from Landsat using a color TV enhancement system p 68 A82-32911
Separation of diffuse from sharp-edged features in digital imagery p 68 A82-34225
Evaluation of the effectiveness of systematic image distortion compensation p 69 A82-34469
Allowance for the effect of the atmosphere in the processing of satellite remote-sensing images p 70 A82-35141
Structure of the St Francois Mountains and surrounding lead belt, S E Missouri Inferences from thermal IR and other data sets --- Ozard Plateau and St Francois Mountains
[E82-10205] p 11 N82-23578

IMAGE MOTION COMPENSATION
Evaluation of the effectiveness of systematic image distortion compensation p 69 A82-34469

IMAGE PROCESSING
Development of three-dimensional spatial displays using a geographically based information system p 66 A82-29326
The use of residual images in Landsat image analysis p 66 A82-29328
Description of gray level picture using a collection of density contour lines p 66 A82-29409
Evaluation of temporal registration of Landsat scenes p 67 A82-32345
The estimation of wave height from digitally processed SAR imagery p 67 A82-32347
Inversion of data from diffraction-limited multiwavelength remote sensors II - Nonlinear dependence of observables on the geophysical parameters p 77 A82-32658
Evaluation of NOAA-AVHRR data for crop assessment --- Advanced Very High Resolution Radiometer p 8 A82-34179
Coastal environment change analysis by Landsat MSS data p 54 A82-34219
Separation of diffuse from sharp-edged features in digital imagery p 68 A82-34225
A practical study of gross-error detection in bundle adjustment p 69 A82-34702
Image processing with microcomputers in remote sensing p 79 A82-34708
An information-theoric spatial transform p 69 A82-34717
Improved land use classification from Landsat and Seasat satellite imagery registered to a common map base p 25 A82-34743
Status and prospects of the automated processing of remote-sensing data /using forest surveys as an example/ p 10 A82-35139
Allowance for the effect of the atmosphere in the processing of satellite remote-sensing images p 70 A82-35141
Design guidelines for satellite image data distribution systems p 70 A82-37048
Ten-Ecosystem Study --- Grand and Weld Counties, Colorado, Warren County, Pennsylvania, St Louis County, Minnesota, Sandoval County, New Mexico, Kershaw County, South Carolina, Fort Yukon, Alaska, Grays Harbor County, Washington, and Washington County, Missouri
[E82-10186] p 84 N82-22620
Registration of Heat Capacity Mapping Mission day and night images
[E82-10210] p 72 N82-23583
Evaluation of VICAR software capability for land information support system needs --- Elk River quadrangle, Idaho
[E82-10223] p 73 N82-23596
Application of HCMM data to regional geologic analysis for mineral and energy resource evaluation
[E82-10243] p 45 N82-24521
Delineation of soil temperature regimes from HCMM data
[E82-10298] p 17 N82-24574
Thermal mapping, geothermal source location, natural effluents and plant stress in the Mediterranean coast of Spain
[E82-10300] p 17 N82-24576
Multidisciplinary investigations on HCMM data over middle Europe and Marocco --- southern Germany and Marrakesh, Morocco
[E82-10315] p 74 N82-24588
Forest Resource Information System Phase 3 System transfer report
[E82-10344] p 18 N82-25606
Image understanding research
[AD-A110746] p 74 N82-25611
Matrix data analysis Color/B and W coding is not always enough
[AD-A111401] p 74 N82-25612
Coordination of stereo image registration and pixel classification
[AD-A111307] p 75 N82-25614
Key Issues in the Analysis of Remote Sensing Data A report on the workshop
[E82-10348] p 85 N82-26746

IMAGE RESOLUTION
Appearance of irregular tree canopies in nighttime high-resolution thermal infrared imagery p 68 A82-32916
Image quality and height measurement accuracy of serial survey camera imagery from high altitudes p 78 A82-33297
Spatial resolution requirements for urban studies p 29 A82-37502
Evaluation of the soil moisture prediction accuracy of a space radar using simulation techniques --- Kansas
[E82-10351] p 19 N82-26749

IMAGING TECHNIQUES
Imaging spectroscopy, Proceedings of the Seminar, Los Angeles, CA, February 10, 11, 1981 p 77 A82-32440
Subtleties in the flat-fielding of charge-coupled device /CCD/ images p 68 A82-32581
Evaluation of the effectiveness of systematic image distortion compensation p 69 A82-34469
Bathymetric imaging p 69 A82-34720
Comparisons of land cover classifications from selected remote sensing systems p 80 A82-34746
Coordination of stereo image registration and pixel classification
[AD-A111307] p 75 N82-25614

INDIA
MAGSAT for geomagnetic studies over Indian region
[E82-10202] p 72 N82-23575
On the space-time variability of ocean surface mixed layer characteristics of central and eastern Arabian sea during MONSOON-77 --- global atmospheric research program p 56 N82-23909
Report of MAGSAT project by Survey of India
[E82-10293] p 73 N82-24570
MAGSAT for geomagnetic studies over Indian region
[E82-10296] p 73 N82-24572
Analysis of MAGSAT data of the Indian region
[E82-10358] p 75 N82-26756

INDIAN OCEAN
Spatial resolution and repeatability of Magsat crustal anomaly data over the Indian Ocean p 32 A82-30788
Analyses of MAGSAT tracks crossing the study region in the Indian Ocean
[E82-10197] p 71 N82-23570
Bathymetric and tectonics of Indian Ocean using MAGSAT data
[E82-10204] p 36 N82-23577
Analyzing the Broken Ridge area of the Indian Ocean using magnetic and gravity anomaly maps and geoid undulation and bathymetry data
[E82-10303] p 36 N82-24577
Investigating tectonic and bathymetric features of the Indian Ocean using MAGSAT magnetic anomaly data
[E82-10304] p 37 N82-24578

INDIANA
Normal crop calendars Volume 3 The corn and soybean states of Illinois, Indiana, and Iowa
[E82-10221] p 13 N82-23594

INDUSTRIAL AREAS
Site selection and engineering issues for a major industrial complex - Application of image and map interpretation p 25 A82-34711

INDUSTRIAL WASTES
Problems of the interpretation of aerial and satellite images of industrial smoke p 23 A82-30307

INERTIAL COORDINATES
Reference coordinate systems for earth dynamics - A preview p 33 A82-32077

INFESTATION
Development and application of panoramic aerial photography in forest pest management p 5 A82-29527
Remote sensing of Douglas-fir trees newly infested by bark beetles p 6 A82-29536
Estimating bark beetle-killed lodgepole pine with high altitude panoramic photography p 7 A82-32703
Estimating mountain pine beetle-killed ponderosa pine over the front range of Colorado with high altitude panoramic photography p 7 A82-32704
Defining the temporal window for monitoring forest canopy defoliation using Landsat p 9 A82-34730

INFORMATION DISSEMINATION
Design guidelines for satellite image data distribution systems p 70 A82-37048
LANDSAT technology transfer to the private and public sectors through community colleges and other locally available institutions
[E82-10181] p 85 N82-23568

INFORMATION SYSTEMS
Cost-effectiveness of geographic surveying from space p 85 N82-24263
Forest Resource Information System Phase 3 System transfer report
[E82-10344] p 18 N82-25606
Exploration into technical procedures for vertical integration --- information systems
[NASA-CR-166352] p 75 N82-26763

INFORMATION THEORY
An information-theoric spatial transform p 69 A82-34717
Information theory lateral density distribution for earth inferred from global gravity field p 35 A82-37962

INFRARED DETECTORS
An infrared exposure meter p 76 A82-29541

INFRARED IMAGERY
Detection of environmental disturbance using color aerial photography and thermal infrared imagery p 22 A82-29327
Remote sensing of leaf water content in the near infrared p 8 A82-32897
View angle effects in the radiometric measurement of plant canopy temperatures p 8 A82-32914
Appearance of irregular tree canopies in nighttime high-resolution thermal infrared imagery p 68 A82-32916
Satellite radiation measurements for the retrieval of the vertical temperature profiles p 70 A82-36935
Determination of winter temperature patterns, fronts, and surface currents in the Yellow Sea and East China Sea from satellite imagery p 55 A82-37195
Estimation of the precipitable water from the IR channel of the geostationary satellite p 55 A82-37196
A statistical approach to rainfall estimation using satellite and conventional data
[NOAA-TR-NESS-89] p 63 N82-22854
Registration of Heat Capacity Mapping Mission day and night images
[E82-10210] p 72 N82-23583
Use of thermal inertia determined by HCMM to predict nocturnal cold prone areas in Florida --- Everglades agricultural area and the west north central peninsula
[E82-10299] p 17 N82-24575

INFRARED INSTRUMENTS
Infrared sensing of sea surface temperature from space p 53 A82-32902

INFRARED PHOTOGRAPHY
Color aerial photography in the plant sciences and related fields, Proceedings of the Eighth Biennial Workshop, Luray, VA, April 21-23, 1981 p 5 A82-29526

Thermography - A remote sensing method with many perspectives p 76 A82-29922
Geostationary satellite observations of the April 1979 Soufriere eruptions p 24 A82-33654
Mapping of wildlife habitat in Farmington Bay, Utah [E82-10354] p 19 N82-26752
INFRARED RADAR
Study visit to United States laser technology centers, 1981 [FOA-C-30257-E1] p 81 N82-24489
INFRARED RADIATION
Interannual variations of outgoing IR associated with tropical circulation changes during 1974-1978 p 54 A82-36341
Structure of the Saint Francois Mountains and surrounding lead belt, S E Missouri Inference from thermal IR and other data sets [E82-10350] p 39 N82-26748
INFRARED RADIOMETERS
High spectral resolution airborne spectrometry p 77 A82-32443
Evaluation of the accuracy of water-surface temperature measurement by means of airborne infrared radiometers p 62 A82-35136
OSTA-1 Post Mission Operation Report [NASA-TM-84191] p 84 N82-23258
INFRARED SCANNERS
Remote sensing of tornadic storms from geosynchronous satellite infrared digital data p 23 A82-32348
Longwave infrared observation of urban landscapes p 25 A82-34744
LANDSAT-D conical scanner evaluation plan [E82-10340] p 81 N82-25602
INFRARED SPECTRA
Airborne observed solar elevation and row direction effects on the near-IR/red ratio of cotton [E82-10220] p 13 N82-23593
Development of visible/infrared/microwave agriculture classification and biomass estimation algorithms --- Guyton, Oklahoma and Dalhart, Texas [E82-10363] p 20 N82-26761
INFRARED SPECTROMETERS
Total ozone retrieval from satellite Meteor 28 Fourier spectrometer measurements p 28 A82-36422
INFRARED SPECTROSCOPY
Application of infrared techniques to the study of atmospheric ozone p 27 A82-36414
INSOLATION
Ground support data from July 10 to July 29, 1978, for HCMM thermal satellite data of the Powder River Basin, Wyoming [E82-10211] p 72 N82-23584
INSTRUMENT ERRORS
Sea-state-related altitude errors in the Seasat radar altimeter p 50 A82-29608
Evaluation of the Seasat altimeter time tag bias p 50 A82-29610
Magnetic anomalies as a reference for ground-speed and map-matching navigation p 32 A82-30314
Irradiance measurement errors due to the assumption of a Lambertian reference panel p 79 A82-34222
The effect of the spectral attenuation of UV radiation by aerosol on the total ozone measurements p 27 A82-36406
Optical stop and focussing effects in the Dobson instrument p 28 A82-36428
INSTRUMENT PACKAGES
LANDSAT-D thermal analysis and design support [E82-10346] p 82 N82-26744
INSTRUMENTS
Investigations of point transfer p 78 A82-33296
INTEGRATED CIRCUITS
Image understanding research [AD-A110746] p 74 N82-25611
INTERCOSMOS SATELLITES
Purpose, background of 'Intercosmos-21' mission p 81 N82-24264
INTERGALACTIC MEDIA
Extragalactic cosmic rays, their sources and spectrum p 40 A82-22574
Astrophysical scenarios for critically evaluating a zero-point field acceleration mechanism p 64 A82-22575
INTERPLANETARY MAGNETIC FIELDS
A description of relativistic solar particle propagation p 4 A82-22600
Low-energy particles in interplanetary magnetic field near the sectorial boundary on September 26, 1977 p 4 A82-22602
The influence of the sector structure of interplanetary magnetic field on the solar cosmic ray characteristics p 83 A82-22603
INTERPLANETARY MEDIUM
Time and energy dependence of heavy ion abundances in solar flare energetic particle events p 22 A82-22605
INTERPLANETARY SPACE
Interplanetary particle observations associated with solar flare gamma-ray line emission p 3 A82-22584
Observations of interplanetary energetic charged particles from gamma-ray line solar flares p 65 A82-22586
Evolution of the solar proton spectrum in interplanetary space p 4 A82-22594
Spacecraft determination of energetic particle propagation parameters - The 1 January 1978 solar event p 31 A82-22598
On the physical sense of the constant of solar cosmic ray coronal propagation p 83 A82-22599
Non-flare injection of protons into interplanetary space p 4 A82-22601
INTERSTELLAR MAGNETIC FIELDS
Angular variations of nonthermal radio emission from the Galaxy relevant to the structure of interstellar magnetic field p 83 A82-22550
INTERSTELLAR MATTER
Confinement and acceleration of cosmic rays in galactic superbubbles p 82 A82-22547
Steady-state cosmic ray electron spectrum under diffusion, convection, adiabatic deceleration and synchrotron losses p 1 A82-22552
Interstellar grains as seeds for galactic cosmic rays p 2 A82-22561
On the stellar origin of low energy cosmic rays p 21 A82-22567
INTERSTELLAR RADIATION
The question of short pathlengths in interstellar propagation p 1 A82-22541
The electron and positron spectra in primary cosmic rays p 1 A82-22543
INTERSTELLAR SPACE
On the characteristics of the very low energy galactic cosmic rays in the interstellar space p 63 A82-22540
Remarks on cosmic ray origin p 21 A82-22569
11-year modulation and spectrum of cosmic rays in the interstellar space p 22 A82-22616
INVENTORIES
Multi-resource inventory in interior Alaska p 6 A82-29532
A new approach to multiresource inventories using remote sensing and geographic information systems technologies p 25 A82-34739
INVERSE SCATTERING
Consequences of an inverse Compton emission model for extragalactic X-ray sources p 83 A82-22553
ION EMISSION
Coulombian energy losses and the nuclear composition of the solar cosmic rays p 4 A82-22610
ION IMPLANTATION
Is the neon composition of our sun, planetary or solar p 76 A82-22608
ION MOTION
On the stellar origin of low energy cosmic rays p 21 A82-22567
ION PRODUCTION RATES
Evidence for the stochastic acceleration of cosmic rays in supernova remnants p 2 A82-22564
IONIZATION CROSS SECTIONS
Observations of the ionization states of energetic particles accelerated in solar flares p 40 A82-22607
IONIZATION POTENTIALS
On volatility, first ionization potential, and s- and r-processes --- for Galactic cosmic ray sources p 2 A82-22560
A tentative ordering of all available solar energetic particles abundance observations I - The mass unbiased baseline II - Discussion and comparison with coronal abundances p 40 A82-22609
IONOSPHERE
Investigation from Japanese MAGSAT team [E82-10239] p 73 N82-23612
Report of investigation from Japanese MAGSAT Team [E82-10322] p 74 N82-24595
IONOSPHERIC CURRENTS
Investigation of the effects of external current systems on the MAGSAT data utilizing grid cell modeling techniques [E82-10195] p 71 N82-22629
Investigation of the effects of external current systems on the MAGSAT data utilizing grid cell modeling techniques [E82-10226] p 73 N82-23599
Investigation of the effects of external current systems on the MAGSAT data utilizing grid cell modeling techniques [E82-10232] p 73 N82-23605
Investigation from Japanese MAGSAT team [E82-10239] p 73 N82-23612
Investigation from Japanese MAGSAT Team Part A Crustal structure near Japan and in Antarctic station Part B Electric currents and hydromagnetic waves in the ionosphere and the magnetosphere [E82-10244] p 36 N82-24522
Investigation of the effects of external current systems on the MAGSAT data utilizing grid cell modeling techniques [E82-10306] p 74 N82-24580
Report of investigation from Japanese MAGSAT Team [E82-10322] p 74 N82-24595
IONOSPHERIC DRIFT
Characteristics of field-aligned E-region irregularities over Ioka /36 N/, Japan I p 26 A82-36268
IONOSPHERIC ELECTRON DENSITY
Generation of the auroral kilometric radiation p 26 A82-35542
IONOSPHERIC SOUNDING
The determination of differential X-ray spectrum of the solar flare using ionospheric data p 65 A82-22582
IOWA
Determination of the optimal level for combining area and yield estimates [E82-10215] p 12 N82-23588
Normal crop calendars Volume 3 The corn and soybean states of Illinois, Indiana, and Iowa [E82-10221] p 13 N82-23594
IRON
Fragmentation of Fe nuclei on carbon, hydrogen and CH2 targets I - Individual charge changing and total cross sections II - Isotopic cross sections --- for interstellar cosmic ray propagation p 63 A82-22538
IRRADIANCE
Irradiance measurement errors due to the assumption of a Lambertian reference panel p 79 A82-34222
IRRIGATION
Problems associated with remotely detecting and monitoring saline sites within irrigated Alberta p 9 A82-34710
Irrigated acreage in the Bear River Basin as of the 1975 growing season --- Idaho, Utah, and Wyoming [E82-10356] p 20 N82-26754
ISOTHERMS
Application of satellite magnetic anomaly data to Curie isotherm mapping p 70 A82-35824
ISOTOPE EFFECT
Airborne gamma-ray spectrometer and magnetometer survey Huron Quadrangle, South Dakota [DE82-005540] p 48 N82-27814
ISOTOPES
Nucleosynthesis of light and by-passed isotopes in the solar system matter p 64 A82-22578
High resolution measurements of solar flare isotopes p 22 A82-22606
ISOTOPIC ENRICHMENT
The charge and isotopic composition of Z equals 7-16 cosmic ray nuclei at their source p 64 A82-22555
The model of the cosmic ray enrichment by helium-3 p 31 A82-22614
ISOTOPIC LABELING
Feasibility of laser-separation of 36 S and its use as an atmospheric tracer [DE82-000965] p 30 N82-27737
ITALY
Crustal structures under the active volcanic areas of central and eastern Mediterranean (M-44) [E82-10096] p 35 N82-23563

J

JAPAN
Investigation from Japanese MAGSAT team [E82-10239] p 73 N82-23612
Investigation from Japanese MAGSAT Team Part A Crustal structure near Japan and in Antarctic station Part B Electric currents and hydromagnetic waves in the ionosphere and the magnetosphere [E82-10244] p 36 N82-24522
Report of investigation from Japanese MAGSAT Team [E82-10322] p 74 N82-24595

K

KALIHARI BASIN (AFRICA)
Overseas Geology And Mineral Resources number 56 A geological interpretation of LANDSAT imagery and air photography of Botswana [OGMR-56] p 42 N82-22636
KANSAS
Application of thermal model for pan evaporation to the hydrology of a defined medium, the sponge [E82-10217] p 13 N82-23590

Evaluation of the soil moisture prediction accuracy of a space radar using simulation techniques --- Kansas
[E82-10351] p 19 N82-26749
KENTUCKY
Satellite and surface geophysical expression of anomalous crustal structure in Kentucky and Tennessee
p 34 A82-34918
KILOMETRIC WAVES
Generation of the auroral kilometric radiation
p 26 A82-35542
KINETIC EQUATIONS
Estimates of sea surface stress for summer MONEX from cloud motions --- global atmospheric research program p 56 N82-23910

L

LAKE ICE
Use of NOAA/AVHRR visible and near-infrared data for land remote sensing
[NASA-TM-84186] p 81 N82-22643
LAKE MICHIGAN
Comparison of ozone in polluted and clean air masses over Lake Michigan p 29 A82-36477
LAMBERT SURFACE
Irradiance measurement errors due to the assumption of a Lambertian reference panel p 79 A82-34222
LAND MANAGEMENT
Resource inventory techniques used in the California Desert Conservation Area p 23 A82-32441
Problems associated with remotely detecting and monitoring saline sites within irrigated Alberta
p 9 A82-34710
AgRISTARS Renewable resources inventory Land information support system implementation plan and schedule --- San Juan National Forest pilot test
[E82-10224] p 14 N82-23597
Identifying environmental features for land management decisions --- Utah
[E82-10289] p 30 N82-24567
LAND USE
Detecting residential land-use development at the urban fringe p 22 A82-29332
Preliminary evidence for the influence of physiography and scale upon the autocorrelation function of remotely sensed data p 67 A82-32343
Sample design for estimating change in land use and land cover p 24 A82-32711
Site selection and engineering issues for a major industrial complex - Application of image and map interpretation p 25 A82-34711
Use of aerial photography in determining land use and streamflow relationships on small developing watersheds
p 60 A82-34736
Improved land use classification from Landsat and Seasat satellite imagery registered to a common map base p 25 A82-34743
Aerial photography vs Landsat for digital land-cover mapping in an urban watershed p 61 A82-34745
Comparisons of land cover classifications from selected remote sensing systems p 80 A82-34746
Spatial resolution requirements for urban studies
p 29 A82-37502
Streamlining and ensuring mineral development must begin at local land management levels
[EMD-82-10] p 29 N82-23043
AgRISTARS Preliminary technical results review of FY81 experiments, volume 2 Fiscal year 1981/1982 'corn and soybeans pilot' experiment
[E82-10216] p 13 N82-23589
AgRISTARS Renewable resources inventory Land information support system implementation plan and schedule --- San Juan National Forest pilot test
[E82-10224] p 14 N82-23597
An analysis of LANDSAT MSS scene-to-scene registration accuracy
[E82-10285] p 16 N82-24563
Application of remote sensing to state and regional problems
[E82-10288] p 30 N82-24566
A method for inferring available surface moisture using remote surface temperature measurements An assessment --- Kansas and St Louis, Missouri
[E82-10311] p 17 N82-24585
Forest Resource Information System Phase 3 System transfer report
[E82-10344] p 18 N82-25606
Inventory of wetlands and agricultural land cover in the upper Sevier River Basin, Utah
[E82-10345] p 18 N82-25607
Exploration into technical procedures for vertical integration --- information systems
[NASA-CR-166352] p 75 N82-26763
LANDSAT D
Landsat D to yield more precise data
p 70 A82-37200
LANDSAT-D conical scanner evaluation plan
[E82-10340] p 81 N82-25602
LANDSAT D to test thematic mapper, inaugurate operational system
[NASA-NEWS-RELEASE-82-100] p 82 N82-26741
LANDSAT-D thermal analysis and design support
[E82-10346] p 82 N82-26744
LANDSAT SATELLITES
Development of three-dimensional spatial displays using a geographically based information system
p 66 A82-29326
The use of residual images in Landsat image analysis
p 66 A82-29328
Desert locust habitat monitoring with satellite remote sensing A new technology for an old problem
p 7 A82-29747
Relating Landsat digital count values to ground reflectance for optically thin atmospheric conditions
p 66 A82-29762
Regional geological, tectonic and geophysical features of Nordland, Norway p 41 A82-30304
Satellite image interpretation of the eastern Caledonian part of the Blue Road Geotraverse and its geological implications /Nordland, Vasterbotten, Scandinavia/
p 41 A82-30305
Detection of volcanic smoke and ash-fall area at volcano Aso, from Landsat MSS data p 23 A82-31295
Evaluation of temporal registration of Landsat scenes
p 67 A82-32345
Resource inventory techniques used in the California Desert Conservation Area p 23 A82-32441
Digitally enhanced visual displays facilitate the analysis of Landsat imagery p 67 A82-32507
Computation with physical values from Landsat digital data p 68 A82-32709
Monitoring land-cover change by principal component analysis of multitemporal Landsat data
p 68 A82-32906
The response characteristics of vegetation in Landsat MSS digital data p 8 A82-32907
Quantitative relationships of near-surface spectra to Landsat radiometric data p 78 A82-32912
Coastal environment change analysis by Landsat MSS data p 54 A82-34219
An information-theoric spatial transform
p 69 A82-34717
Defining the temporal window for monitoring forest canopy defoliation using Landsat p 9 A82-34730
Use of Landsat multispectral scanner data in vegetation mapping of a forested area p 9 A82-34731
Automated classification of runoff coefficients from Landsat multispectral data p 60 A82-34734
A new approach to multiresource inventories using remote sensing and geographic information systems technologies p 25 A82-34739
Improved land use classification from Landsat and Seasat satellite imagery registered to a common map base p 25 A82-34743
Aerial photography vs Landsat for digital land-cover mapping in an urban watershed p 61 A82-34745
Space science for applications - The history of Landsat p 84 A82-36617
Remote sensing in Scotland using data received from satellites - A study of the Tay Estuary region using Landsat multispectral scanning imagery p 62 A82-37501
Remote sensing of salt marsh vegetation in the first four proposed Thematic Mapper bands
p 10 A82-37503
Use of LANDSAT data to define soil boundaries in Carroll County, Missouri p 10 N82-23116
A legislator's guide to LANDSAT
[E82-10290] p 85 N82-24568
Exploration into technical procedures for vertical integration --- information systems
[NASA-CR-166352] p 75 N82-26763
Experimental assessment of improved spatial resolution LANDSAT data
[AD-A110538] p 75 N82-26765
LANDSAT 3
The use of Landsat-3 thermal data to help differentiate land covers p 25 A82-34218
LARGE AREA CROP INVENTORY EXPERIMENT
Field size, length, and width distributions based on LACIE ground truth data --- large area crop inventory experiment p 8 A82-32909
LARGE SPACE TELESCOPE
Radiometer mission requirements for large space antenna systems
[NASA-TM-84478] p 81 N82-25610
LASER APPLICATIONS
Laser-induced bioluminescence --- for remote sensing of marine organisms p 53 A82-32559
Bias correction procedures for airborne laser hydrography
[PB82-130089] p 63 N82-22644
Study visit to United States laser technology centers, 1981
[FOA-C-30257-E1] p 81 N82-24489
Feasibility of laser-separation of 36 S and its use as an atmospheric tracer
[DE82-000965] p 30 N82-27737
LASER RANGE FINDERS
Establishing geodetic-geodynamic parameters using lunar laser range measurements p 34 A82-33293
LASER SPECTROMETERS
In situ ozone data for comparison with laser absorption remote sensor 1980 PEPE/NEROS program
[NASA-TM-84471] p 30 N82-25661
LEASING
Streamlining and ensuring mineral development must begin at local land management levels
[EMD-82-10] p 29 N82-23043
LEAVES
Remote sensing of leaf water content in the near infrared p 8 A82-32897
Spectral properties of agricultural crops and soils measured from space, aerial, field, and laboratory sensors
[E82-10189] p 10 N82-22623
LENSES
An optical objective lens for earth observations by satellites p 78 A82-32824
LESSER ANTILLES
Soufriere Volcano, St Vincent - Observations of its 1979 eruption from the ground, aircraft, and satellites
p 24 A82-33652
LIGNITE
Application of remote sensing to state and regional problems
[E82-10288] p 30 N82-24566
LINEAR POLARIZATION
Linear polarization of light by two wheat canopies measured at many view angles
[E82-10229] p 14 N82-23602
LITHOLOGY
Spatial thermal radiometry contribution to the Massif Armoricain and the Massif Central France litho-structural study
[E82-10190] p 42 N82-22624
Crustal structures under the active volcanic areas of central and eastern Mediterranean (M-44)
[E82-10096] p 35 N82-23563
LITHOSPHERE
A satellite magnetic model of northeastern South American aulacogens p 33 A82-30795
LOCUSTS
Desert locust habitat monitoring with satellite remote sensing A new technology for an old problem
p 7 A82-29747
LONG RANGE WEATHER FORECASTING
On the space-time variability of ocean surface mixed layer characteristics of central and eastern Arabian sea during MONSOON-77 --- global atmospheric research program p 56 N82-23909
LUNAR RANGEFINDING
Establishing geodetic-geodynamic parameters using lunar laser range measurements p 34 A82-33293
LUNAR SOIL
Is the neon composition of our sun, planetary or solar
p 76 A82-22608

M

MAGNESIUM ISOTOPES
Calculated isotopic source composition and tests for origin and propagation of cosmic rays with mass numbers less than or equal to 62 p 83 A82-22554
MAGNETIC ANOMALIES
Magnetic anomalies as a reference for ground-speed and map-matching navigation p 32 A82-30314
Initial scalar magnetic anomaly map from Magsat
p 32 A82-30784
Initial vector magnetic anomaly map from Magsat
p 32 A82-30785
Magsat scalar anomaly distribution - The global perspective p 41 A82-30786
Magsat magnetic anomalies over Antarctica and the surrounding oceans p 32 A82-30787
Spatial resolution and repeatability of Magsat crustal anomaly data over the Indian Ocean p 32 A82-30788
Verification of the crustal component in satellite magnetic data p 32 A82-30789
A preliminary comparison of the Magsat data and aeromagnetic data in the continental U S
p 32 A82-30790
A satellite magnetic model of northeastern South American aulacogens p 33 A82-30795

Preliminary interpretation of magnetic anomalies over Japan and its surrounding area p 33 A82-30796
Satellite and surface geophysical expression of anomalous crustal structure in Kentucky and Tennessee p 34 A82-34918
Application of satellite magnetic anomaly data to Curie isotherm mapping p 70 A82-35824
Structure, composition and thermal state of the crust in Brazil --- geomagnetic survey
[E82-10187] p 35 N82-22621
Study of gravity and magnetic anomalies using MAGSAT data
[E82-10194] p 35 N82-22628
Crustal structures under the active volcanic areas of central and eastern Mediterranean (M-44)
[E82-10096] p 35 N82-23563
Characterization of the structure and tectonic of South America
[E82-10196] p 42 N82-23569
Analyses of MAGSAT tracks crossing the study region in the Indian Ocean
[E82-10197] p 71 N82-23570
MAGSAT science investigations
[E82-10199] p 71 N82-23572
MAGSAT for geomagnetic studies over Indian region
[E82-10202] p 72 N82-23575
Bathymetric and tectonics of Indian Ocean using MAGSAT data
[E82-10204] p 36 N82-23577
Investigation from Japanese MAGSAT team
[E82-10239] p 73 N82-23612
Investigations of medium wavelength magnetic anomalies in the eastern Pacific using MAGSAT
[E82-10240] p 73 N82-23613
Airborne gamma-ray spectrometer and magnetometer survey Roseau quadrangle, Minnesota, volume 1
[DE82-001031] p 43 N82-23621
Airborne gamma-ray spectrometer and magnetometer survey Hibbing quadrangle, Minnesota, volume 1
[DE82-004159] p 44 N82-23639
Airborne gamma-ray spectrometer and magnetometer survey Hibbing quadrangle, Minnesota, volume 2
[DE82-004165] p 45 N82-23640
Airborne gamma-ray spectrometer and magnetometer survey Aberdeen quadrangle, South Dakota, volume 1
[DE82-004152] p 45 N82-23641
Airborne gamma-ray spectrometer and magnetometer survey Aberdeen quadrangle, South Dakota, volume 2
[DE82-004164] p 45 N82-23642
Spherical-Earth gravity and magnetic anomaly modeling by Gauss-Legendre quadrature integration
[E82-10242] p 36 N82-24520
Investigation from Japanese MAGSAT Team Part A Crustal structure near Japan and in Antarctic station Part B Electric currents and hydromagnetic waves in the ionosphere and the magnetosphere
[E82-10244] p 36 N82-24522
Report of MAGSAT project by Survey of India
[E82-10293] p 73 N82-24570
MAGSAT for geomagnetic studies over Indian region
[E82-10296] p 73 N82-24572
An equivalent layer magnetization model for the United States derived from MAGSAT data
[E82-10297] p 36 N82-24573
Analyzing the Broken Ridge area of the Indian Ocean using magnetic and gravity anomaly maps and geoid undulation and bathymetry data
[E82-10303] p 36 N82-24577
Investigating tectonic and bathymetric features of the Indian Ocean using MAGSAT magnetic anomaly data
[E82-10304] p 37 N82-24578
The mineralogy of global magnetic anomalies --- rock magnetic signatures and MAGSAT geological, and gravity correlations in West Africa
[E82-10305] p 45 N82-24579
MAGSAT scalar and vector anomaly data analysis
[E82-10307] p 74 N82-24581
Investigation of Antarctic crust and upper mantle using MAGSAT and other geophysical data
[E82-10308] p 37 N82-24582
Investigation of Antarctic crust and upper mantle using MAGSAT and other geophysical data
[E82-10309] p 37 N82-24583
Magnetic and gravity anomalies in the Americas
[E82-10312] p 37 N82-24586
Improved definition of crustal magnetic anomalies for MAGSAT data
[E82-10314] p 37 N82-24587
An investigation of MAGSAT and complementary data emphasizing precambrian shields and adjacent areas of West Africa and South America
[E82-10316] p 38 N82-24589
An investigation of MAGSAT and complementary data emphasizing precambrian shields and adjacent areas of West Africa and South America
[E82-10317] p 38 N82-24590
An investigation of MAGSAT and complementary data emphasizing precambrian shields and adjacent areas of West Africa and South America
[E82-10318] p 38 N82-24591
Geotectonics of South America --- regional magnetic and gravity anomalies of South America
[E82-10320] p 38 N82-24593
Use of MAGSAT anomaly data for crustal structure and mineral resources in the US Midcontinent
[E82-10321] p 46 N82-24594
Report of investigation from Japanese MAGSAT Team
[E82-10322] p 74 N82-24595
Use of MAGSAT anomaly data for crustal structure and mineral resources in the US Midcontinent
[E82-10323] p 46 N82-24596
Comparison of storm-time changes of geomagnetic field at ground and at MAGSAT altitudes, part 2
[E82-10325] p 30 N82-24598
MAGSAT anomaly map and continental drift
[E82-10326] p 38 N82-24599
Models and maps of the main field
[E82-10327] p 74 N82-24600
Investigations of medium wavelength magnetic anomalies in the eastern Pacific using MAGSAT data
[E82-10330] p 38 N82-24603
Aeromagnetic and satellite magnetic anomally mapping
[E82-10339] p 39 N82-25601
Airborne gamma-ray spectrometer and magnetometer survey, Kingston quadrangle New York, volume 2C
[DE81-027161] p 46 N82-25621
Analysis of MAGSAT data of the Indian region
[E82-10358] p 75 N82-26756

MAGNETIC DISTURBANCES

Studies of high latitude current systems using MAGSAT vector data
[E82-10188] p 71 N82-22622

MAGNETIC EFFECTS

Features of cosmic ray variations due to variations in the total magnetic field of the sun p 49 A82-22619

MAGNETIC FIELDS

Investigation of the effects of external current systems on the MAGSAT data utilizing grid cell modeling techniques
[E82-10306] p 74 N82-24580

MAGNETIC FLUX

Investigation of geomagnetic field forecasting and fluid dynamics of the core --- determination of the bundary between the core and mantle of the Earth
[E82-10198] p 35 N82-23571
Investigation of geomagnetic field forecasting and fluid dynamics of the core
[E82-10310] p 37 N82-24584

MAGNETIC MEASUREMENT

Airborne gamma-ray spectrometer and magnetometer survey Susanville quadrangle, California, volume 1
[DE82-005538] p 48 N82-27811
Airborne gamma-ray spectrometer and magnetometer survey Roseburg quadrangle, Oregon, volume 2
[DE82-005568] p 48 N82-27812

MAGNETIC MONOPOLES

Magnetic monopole pair and its observation in cosmic rays p 65 A82-22579

MAGNETIC POLES

A comparison of pole positions derived from GPS satellite and Navy navigation satellite observations
[AD-A110765] p 39 N82-26268

MAGNETIC SIGNATURES

Observed magnetic substorm signatures at synchronous altitude p 26 A82-35534
Investigation of MAGSAT and TRIAD magnetometer data to provide corrective information on high-latitude external fields
[E82-10201] p 72 N82-23574

MAGNETIC STORMS

Comparison of storm-time changes of geomagnetic field at ground and MAGSAT altitudes
[E82-10359] p 30 N82-26757

MAGNETIC SURVEYS

Magnetic charts of Canada derived from Magsat data p 32 A82-30778
Verification of the crustal component in satellite magnetic data p 32 A82-30789
Structure, composition and thermal state of the crust in Brazil --- geomagnetic survey
[E82-10187] p 35 N82-22621
MAGSAT and aeromagnetic data in the North American continent
[E82-10193] p 71 N82-22627
Investigation of the effects of external current systems on the MAGSAT data utilizing grid cell modeling techniques
[E82-10195] p 71 N82-22629
Equivalent source modeling of the main field using MAGSAT data
[E82-10151] p 71 N82-23567
MAGSAT for geomagnetic studies over Indian region
[E82-10202] p 72 N82-23575
Spherical harmonic representation of the main geomagnetic field for world charting and investigations of some fundamental problems of physics and geophysics
[E82-10203] p 72 N82-23576
Investigation of the effects of external current systems on the MAGSAT data utilizing grid cell modeling techniques
[E82-10226] p 73 N82-23599
Investigation of the effects of external current systems on the MAGSAT data utilizing grid cell modeling techniques
[E82-10232] p 73 N82-23605
Investigation from Japanese MAGSAT team
[E82-10239] p 73 N82-23612
Airborne gamma-ray spectrometer and magnetometer survey Roseau quadrangle, Minnesota, volume 1
[DE82-001031] p 43 N82-23621
Airborne gamma-ray spectrometer and magnetometer survey Barrow quadrangle, Alaska, volume 1
[DE82-000334] p 43 N82-23623
Airborne gamma-ray spectrometer and magnetometer survey Wainwright quadrangle, Alaska, volume 2
[DE82-000341] p 43 N82-23624
Airborne gamma-ray spectrometer and magnetometer survey Meade River quadrangle, Alaska, volume 2
[DE82-000340] p 43 N82-23626
Airborne gamma-ray spectrometer and magnetometer survey Teshekpuk quadrangle, Alaska, volume 2
[DE82-000310] p 43 N82-23627
Airborne gamma-ray spectrometer and magnetometer survey Harrison Bay quadrangle, Alaska, volume 2
[DE82-000315] p 43 N82-23628
Airborne gamma-ray spectrometer and magnetometer survey Beechey Pt , quadrangle, Alaska, volume 2
[DE82-000309] p 43 N82-23629
Airborne gamma-ray spectrometer and magnetometer survey Point Lay quadrangle, Alaska, volume 2
[DE82-000308] p 43 N82-23630
Airborne gamma-ray spectrometer and magnetometer survey Utukik River quadrangle, Alaska, volume 2
[DE82-000316] p 44 N82-23631
Airborne gamma-ray spectrometer and magnetometer survey Sagavanirktok quadrangle, Alaska, volume 2
[DE82-000311] p 44 N82-23632
Airborne gamma-ray spectrometer and magnetometer survey Duluth quadrangle, Minnesota, volume 2
[DE82-001027] p 44 N82-23633
Airborne gamma-ray spectrometer and magnetometer survey Devil's Lake quadrangle, North Dakota, volume 1
[DE82-004161] p 44 N82-23635
Airborne gamma-ray spectrometer and magnetometer survey Devil's Lake quadrangle, North Dakota, volume 2
[DE82-004168] p 44 N82-23636
Airborne gamma-ray spectrometer and magnetometer survey Bemidji quadrangle, Minnesota, volume 1
[DE82-001032] p 44 N82-23637
Airborne gamma-ray spectrometer and magnetometer survey International Falls quadrangle, Minnesota, volume 1
[DE82-004151] p 45 N82-23643
Airborne gamma-ray spectrometer and magnetometer survey International Falls quadrangle, Minnesota, volume 2
[DE82-004166] p 45 N82-23644
Investigation from Japanese MAGSAT Team Part A Crustal structure near Japan and in Antarctic station Part B Electric currents and hydromagnetic waves in the ionosphere and the magnetosphere
[E82-10244] p 36 N82-24522
MAGSAT for geomagnetic studies over Indian region
[E82-10296] p 73 N82-24572
Investigation of geomagnetic field forecasting and fluid dynamics of the core
[E82-10310] p 37 N82-24584
Use of MAGSAT anomaly data for crustal structure and mineral resources in the US Midcontinent
[E82-10323] p 46 N82-24596
Investigation of geomagnetic field forecasting and fluid dynamics of the core
[E82-10342] p 39 N82-25604
Airborne gamma-ray spectrometer and magnetometer survey, Toronto quadrangle New York, volume 2A
[DE81-027158] p 46 N82-25620
Airborne gamma-ray spectrometer and magnetometer survey, Kingston quadrangle New York, volume 2C
[DE81-027161] p 46 N82-25621
Airborne gamma-ray spectrometer and magnetometer survey, Rochester quadrangle New York, volume 2D
[DE81-027156] p 46 N82-25622
Airborne gamma-ray spectrometer and magnetometer survey Lookout Ridge quadrangle, Alaska, volume 2
[DE82-000313] p 47 N82-25625

Airborne gamma-ray spectrometer and magnetometer survey North/south tieline, volume 1
[DE82-005542] p 47 N82-27804
Airborne gamma-ray spectrometer and magnetometer survey North/south tieline, volume 2
[DE82-005570] p 47 N82-27805
Evaluation and combined geophysical interpretations of NURE and related geoscience data in the Van Horn, Pecos, Marfa, Fort Stockton, Presidido, and Emory Peak quadrangles, Texas, volume 1
[DE82-005554] p 47 N82-27808
Evaluation and combined geophysical interpretations of NURE and related geoscience data in the Van Horn, Pecos, Marfa, Fort Stockton, Presidio, and Emory Peak quadrangels, Texas
[DE82-005560] p 48 N82-27809
NURE aerial gamma-ray and magnetic reconnaissance survey of portions of New Mexico, Arizona and Texas Volume 2 New Mexico-Carlsbad Quadrangle
[DE82-005527] p 48 N82-27810
Airborne gamma-ray spectrometer and magnetometer survey Ukiah quadrangle, California, volume 1 --- uranium exploration
[DE82-005541] p 48 N82-27813
Airborne gamma-ray spectrometer and magnetometer survey Huron Quadrangle, South Dakota
[DE82-005540] p 48 N82-27814
Airborne gamma-ray spectrometer and magnetometer survey Chico Quadrangle, California
[DE82-005543] p 48 N82-27815

MAGNETIC VARIATIONS
Comparison of storm-time changes of geomagnetic field at ground and at MAGSAT altitudes, part 2
[E82-10325] p 30 N82-24598
Comparison of storm-time changes of geomagnetic field at ground and MAGSAT altitudes
[E82-10359] p 30 N82-26757

MAGNETIZATION
Satellite and surface geophysical expression of anomalous crustal structure in Kentucky and Tennessee
p 34 A82-34918

MAGNETOHYDRODYNAMIC WAVES
The galactic origin of cosmic rays I
[CONF-810711-1] p 2 A82-22565
Possible evidence for attenuation of an MHD shock by a magnetic neutral sheet in the solar corona
p 3 A82-22589

MAGNETOMETERS
Airborne gamma-ray spectrometer and magnetometer survey Barrow quadranagle, Alaska, volume 2
[DE82-000342] p 46 N82-25623

MAGNETOSPHERE
Investigation of the effects of external current systems on the MAGSAT data utilizing grid cell modeling techniques
[E82-10232] p 73 N82-23605
Investigation from Japanese MAGSAT team
[E82-10239] p 73 N82-23612
Investigation from Japanese MAGSAT Team Part A Crustal structure near Japan and in Antarctic station Part B Electric currents and hydromagnetic waves in the ionosphere and the magnetosphere
[E82-10244] p 36 N82-24522
Investigation of the effects of external current systems on the MAGSAT data utilizing grid cell modeling techniques
[E82-10306] p 74 N82-24580
Report of investigation from Japanese MAGSAT Team
[E82-10322] p 74 N82-24595

MAGSAT SATELLITES
Initial scalar magnetic anomaly map from Magsat
p 32 A82-30784
Initial vector magnetic anomaly map from Magsat
p 32 A82-30785
Magsat scalar anomaly distribution - The global perspective p 41 A82-30786
Magsat magnetic anomalies over Antarctica and the surrounding oceans p 32 A82-30787
Spatial resolution and repeatability of Magsat crustal anomaly data over the Indian Ocean p 32 A82-30788
Verification of the crustal component in satellite magnetic data p 32 A82-30789
A preliminary comparison of the Magsat data and aeromagnetic data in the continental U S
p 32 A82-30790
A satellite magnetic model of northeastern South American aulacogens p 33 A82-30795
Preliminary interpretation of magnetic anomalies over Japan and its surrounding area p 33 A82-30796

MANAGEMENT INFORMATION SYSTEMS
AgRISTARS Renewable resources inventory Land information support system implementation plan and schedule --- San Juan National Forest pilot test
[E82-10224] p 14 N82-23597

MANNED SPACECRAFT
Remote sensing of the earth's resources - The Soviet experience p 84 A82-33555

MAP MATCHING GUIDANCE
Magnetic anomalies as a reference for ground-speed and map-matching navigation p 32 A82-30314

MAPPING
Work related to the Blue Road Geotraverse at the Finnish Geodetic Institute p 32 A82-30306
American Society of Photogrammetry, Annual Meeting, 47th, Washington, DC, February 22-27, 1981, ASP Technical Papers p 79 A82-34701
Comparisons of land cover classifications from selected remote sensing systems p 80 A82-34746
Study of gravity and magnetic anomalies using MAGSAT data
[E82-10194] p 35 N82-22628
Airborne gamma-ray spectrometer and magnetometer survey Roseau quadrangle, Minnesota, volume 1
[DE82-001031] p 43 N82-23621
Airborne gamma-ray spectrometer and magnetometer survey Roseau quadrangle, Minnesota, volume 2
[DE82-001025] p 44 N82-23634
Airborne gamma-ray spectrometer and magnetometer survey Bemidji quadrangle, Minnesota, volume 2
[DE82-001026] p 44 N82-23638
Airborne gamma-ray spectrometer and magnetometer survey Hibbing quadrangle, Minnesota, volume 1
[DE82-004159] p 44 N82-23639
Airborne gamma-ray spectrometer and magnetometer survey Hibbing quadrangle, Minnesota, volume 2
[DE82-004165] p 45 N82-23640
Airborne gamma-ray spectrometer and magnetometer survey Aberdeen quadrangle, South Dakota, volume 1
[DE82-004152] p 45 N82-23641
Airborne gamma-ray spectrometer and magnetometer survey Aberdeen quadrangle, South Dakota, volume 2
[DE82-004164] p 45 N82-23642
Report of MAGSAT project by Survey of India
[E82-10293] p 73 N82-24570
Magnetic and gravity anomalies in the Americas
[E82-10312] p 37 N82-24586
Image understanding research
[AD-A110746] p 74 N82-25611
Matrix data analysis Color/B and W coding is not always enough
[AD-A111401] p 74 N82-25612
Source assessment system
[AD-A111223] p 75 N82-25613
Airborne gamma-ray spectrometer and magnetometer survey Chico Quadrangle, California
[DE82-005543] p 48 N82-27815

MAPS
The crustal structure and tectonics of South America
[E82-10319] p 38 N82-24592
Report of investigation from Japanese MAGSAT Team
[E82-10322] p 74 N82-24595
MAGSAT anomaly map and continental drift
[E82-10326] p 38 N82-24599
Models and maps of the main field
[E82-10327] p 74 N82-24600
Computer-processed geophysical atlas of digital data for the East Coast margin of the United States from surface and spacecraft data
[AD-A111388] p 39 N82-25748
Evaluation and combined geophysical interpretations of NURE and related geoscience data in the Van Horn, Pecos, Marfa, Fort Stockton, Presidio, and Emory Peak quadrangels, Texas
[DE82-005560] p 48 N82-27809

MARINE BIOLOGY
Laser-induced bioluminescence --- for remote sensing of marine organisms p 53 A82-32559
Technology and oceanography An assessment of Federal technologies for oceanographic research and monitoring Volume 2 Working papers on fishery research technology p 58 N82-26944

MARINE ENVIRONMENTS
A study of atmospheric diffusion from the LANDSAT imagery --- pollution transport over the ocean
[E82-10360] p 58 N82-26758

MARINE METEOROLOGY
Retrieval of ocean surface and atmospheric parameters from multichannel microwave radiometric measurements
p 53 A82-31995
Estimation of the temperature of the upper boundary of cloud cover over the world ocean p 54 A82-36005
Estimation of the precipitable water from the IR channel of the geostationary satellite p 55 A82-37196
Marine boundary layer wind structure over the Bay of Bengal during Monex-79 --- Monsoon Experiment (MONEX) p 57 N82-23929

MARINE RESOURCES
Technology and oceanography An assessment of Federal technologies for oceanographic research and monitoring Volume 2 Working papers on fishery research technology p 58 N82-26944

MARINE TECHNOLOGY
The processing of satellite navigation data for marine geodesy p 34 A82-37175
Technology and oceanography An assessment of Federal technologies for oceanographic research and monitoring Volume 2 Working papers on fishery research technology p 58 N82-26944

MARINER 10 SPACE PROBE
A color-ratio map of Mercury p 31 A82-22294

MARSHLANDS
Remote sensing of salt marsh vegetation in the first four proposed Thematic Mapper bands
p 10 A82-37503

MASS RATIOS
Mass per charge ratio in hot plasmas and cosmic ray source composition p 2 A82-22557

MASSIFS
Spatial thermal radiometry contribution to the Massif Armoricain and the Massif Central France litho-structural study
[E82-10190] p 42 N82-22624

MATCHING
An algorithm for automating the registration of USDA segment ground data to LANDSAT MSS data
[E82-10286] p 16 N82-24564

MATHEMATICAL MODELS
A comparison of helium and heavy ion spectra in He/3/ rich solar flares with a model calculation
p 5 A82-22612
Gravity model improvement for Seasat
p 32 A82-29615
A comparative study of microwave radiometer observations over snowfields with radiative transfer model calculations --- for water runoff estimation
p 60 A82-32910
Application of satellite magnetic anomaly data to Curie isotherm mapping p 70 A82-35824
A meteorologically driven maize stress indicator model
[E82-10112] p 11 N82-23564
Topographic slope correction for analysis of thermal infrared images
[E82-10214] p 36 N82-23587
Report of MAGSAT project by Survey of India
[E82-10293] p 73 N82-24570
An equivalent layer magnetization model for the United States derived from MAGSAT data
[E82-10297] p 36 N82-24573

MATRICES (MATHEMATICS)
Matrix data analysis Color/B and W coding is not always enough
[AD-A111401] p 74 N82-25612

MAXIMUM ENTROPY METHOD
Information theory lateral density distribution for earth inferred from global gravity field p 35 A82-37962

MAXIMUM LIKELIHOOD ESTIMATES
The use of prior probabilities in maximum likelihood classification of remotely sensed data
p 68 A82-32904

MEAN FREE PATH
Spacecraft determination of energetic particle propagation parameters - The 1 January 1978 solar event p 31 A82-22598

MEASUREMENT
Movement of ice markers measured by satellite ranging
[R-240] p 59 N82-27816

MEDITERRANEAN SEA
Crustal structures under the active volcanic areas of central and eastern Mediterranean (M-44)
[E82-10096] p 35 N82-23563
Thermal mapping, geothermal source location, natural effluents and plant stress in the Mediterranean coast of Spain
[E82-10300] p 17 N82-24576

MELTING
The use of satellite photographs to study snow-cover dynamics and to determine the average water discharge of the Amudarya during a vegetation period
p 61 A82-35132
Method for the analysis of the melting of a firn complex on the basis of aerospace photographs
p 61 A82-35133
Experience with the compilation of maps of snow-cover melting in the central part of the European USSR on the basis of satellite data p 62 A82-35134

MELTS (CRYSTAL GROWTH)
Influence of CO2 on melting of model granulite facies assemblages - A model for the genesis of charnockites
p 42 A82-36298

MERCURY (PLANET)
A color-ratio map of Mercury p 31 A82-22294

MESON-MESON INTERACTIONS
Magnetic monopole pair and its observation in cosmic rays p 65 A82-22579
MESOSCALE PHENOMENA
High resolution satellite observations of mesoscale oceanography in the Tasman Sea, 1978 - 1979 [E82-10324] p 57 N82-24597
MESOSPHERE
Observation of the diurnal variation of atmospheric ozone p 26 A82-35895
Microwave measurement of stratospheric and mesospheric ozone p 28 A82-36415
OSO-8 lower mesospheric ozone number density profiles p 28 A82-36472
METEORITIC COMPOSITION
Measurement of cosmogenic nuclides using a multi-crystal gamma-ray coincidence spectrometer --- for Mayo Belwa meteorite study p 64 A82-22577
METEOROLOGICAL CHARTS
Meteorological and aircraft data for CUE 2 1973 [PB82-149246] p 59 N82-26949
METEOROLOGICAL PARAMETERS
Retrieval of ocean surface and atmospheric parameters from multichannel microwave radiometric measurements p 53 A82-31995
Meteorological analysis of the eruption of Soufriere in April 1979 p 24 A82-33655
The meteorological product - 'Cloud-top height' p 70 A82-36043
Ground support data from July 10 to July 29, 1978, for HCMM thermal satellite data of the Powder River Basin, Wyoming [E82-10211] p 72 N82-23584
A meteorologically driven grain sorghum stress indicator model [E82-10218] p 13 N82-23591
METEOROLOGICAL SATELLITES
System albedo as sensed by satellites - Its definition and variability p 23 A82-32342
The seasonal snow-line within the Fergana basin and the possibility of using it for hydrological forecasting p 61 A82-35131
Estimation of the temperature of the upper boundary of cloud cover over the world ocean p 54 A82-36005
METEOROLOGY
The METEOSAT Data Collection System and its application p 75 N82-26037
METEOSAT SATELLITE
The meteorological product - 'Cloud-top height' p 70 A82-36043
MEXICO
Monitoring deforestation in the eastern part of the state of Guerrero, Mexico p 9 A82-34733
MICROCOMPUTERS
Image processing with microcomputers in remote sensing p 79 A82-34708
MICRODENSITOMETERS
Application of scanning microdensitometer data in selected plant science case studies p 7 A82-29539
MICROWAVE EMISSION
A multi-frequency radiometric measurement of soil moisture content over bare and vegetated fields [E82-10238] p 16 N82-23611
MICROWAVE EQUIPMENT
Intercomparison of wind speeds inferred by the SASS, altimeter, and SMMR p 52 A82-29621
MICROWAVE IMAGERY
Remote sensing of precipitable water over the oceans from Nimbus 7 microwave measurements p 49 A82-28907
MICROWAVE RADIOMETERS
Evaluation of atmospheric attenuation from SMMR brightness temperature for the Seasat satellite scatterometer p 51 A82-29618
Intercomparison of wind speeds inferred by the SASS, altimeter, and SMMR p 52 A82-29621
Description of Seasat radiometer status and results p 52 A82-29622
Retrieval of ocean surface and atmospheric parameters from multichannel microwave radiometric measurements p 53 A82-31995
Inversion of data from diffraction-limited multiwavelength remote sensors II - Nonlinear dependence of observables on the geophysical parameters p 77 A82-32658
A comparative study of microwave radiometer observations over snowfields with radiative transfer model calculations --- for water runoff estimation p 60 A82-32910
Snowpack monitoring in North America and Eurasia using passive microwave satellite data p 78 A82-32915
The use of microwave radiometry for the determination of snow cover height p 80 A82-36018
Microwave measurement of stratospheric and mesospheric ozone p 28 A82-36415
Orbiting passive microwave sensor simulation applied to soil moisture estimation [E82-10343] p 18 N82-25605
Radiometer mission requirements for large space antenna systems [NASA-TM-84478] p 81 N82-25610
MICROWAVE SCATTERING
Intercomparison of wind speeds inferred by the SASS, altimeter, and SMMR p 52 A82-29621
On the synthetic aperture radar imaging of ocean surface waves p 53 A82-32881
Characteristics of 13 9 GHz radar scattering from oil films on the sea surface p 54 A82-33438
MICROWAVE SENSORS
Seasat measurement system evaluation - Achievements and limitations p 49 A82-29601
Microwave sensing from space [AAS PAPER 82-127] p 80 A82-37809
Orbiting passive microwave sensor simulation applied to soil moisture estimation [E82-10343] p 18 N82-25605
Multifrequency remote sensing of soil moisture --- Guymon, Oklahoma and Dalhart, Texas [E82-10362] p 20 N82-26760
The use of soil texture and field capacity to normalize microwave soil moisture measurements Some problems p 20 N82-26762
MICROWAVE SPECTRA
Development of visible/infrared/microwave agriculture classification and biomass estimation algorithms --- Guyton, Oklahoma and Dalhart, Texas [E82-10363] p 20 N82-26761
MICROWAVES
The possibility of using remote-sensing methods to study the hydrology of elementary watersheds p 61 A82-35130
The effect of sea-surface Sun glitter on microwave radiometer measurements [NASA-CR-169083] p 57 N82-26525
MIDLATITUDE ATMOSPHERE
Characteristics of field-aligned E-region irregularities over Iioka /36 N/, Japan I p 26 A82-36268
MILKY WAY GALAXY
Derivation of the distribution of synchrotron emissivity in the Galaxy from the 408 MHz all-sky survey p 82 A82-22549
Angular variations of nonthermal radio emission from the Galaxy relevant to the structure of interstellar magnetic field p 83 A82-22550
Convective outflow of cosmic rays from the Galaxy and background radio emission p 83 A82-22551
MINERAL DEPOSITS
Overseas Geology And Mineral Resources number 56 A geological interpretation of LANDSAT imagery and air photography of Botswana [OGMR-56] p 42 N82-22636
Streamlining and ensuring mineral development must begin at local land management levels [EMD-82-10] p 29 N82-23043
Airborne gamma-ray spectrometer and magnetometer survey Roseau quadrangle, Minnesota, volume 1 [DE82-001031] p 43 N82-23621
Airborne gamma-ray spectrometer and magnetometer survey Barrow quadrangle, Alaska, volume 1 [DE82-000334] p 43 N82-23623
Airborne gamma-ray spectrometer and magnetometer survey Wainwright quadrangle, Alaska, volume 2 [DE82-000341] p 43 N82-23624
Airborne gamma-ray spectrometer and magnetometer survey, Kenora quadrangle, Minnesota, volume 1 [DE82-001029] p 43 N82-23625
Airborne gamma-ray spectrometer and magnetometer survey Roseau quadrangle, Minnesota, volume 2 [DE82-001025] p 44 N82-23634
Airborne gamma-ray spectrometer and magnetometer survey Hibbing quadrangle, Minnesota, volume 1 [DE82-004159] p 44 N82-23639
Airborne gamma-ray spectrometer and magnetometer survey Hibbing quadrangle, Minnesota, volume 2 [DE82-004165] p 45 N82-23640
Airborne gamma-ray spectrometer and magnetometer survey Aberdeen quadrangle, South Dakota, volume 1 [DE82-004152] p 45 N82-23641
Airborne gamma-ray spectrometer and magnetometer survey Aberdeen quadrangle, South Dakota, volume 2 [DE82-004164] p 45 N82-23642
Use of MAGSAT anomaly data for crustal structure and mineral resources in the US Midcontinent [E82-10321] p 46 N82-24594
Airborne gamma-ray spectrometer and magnetometer survey, Toronto quadrangle New York, volume 2A [DE81-027158] p 46 N82-25620
Airborne gamma-ray spectrometer and magnetometer survey, Rochester quadrangle New York, volume 2D [DE81-027156] p 46 N82-25622
Evaluation and combined geophysical interpretations of NURE and related geoscience data in the Van Horn, Pecos, Marfa, Fort Stockton, Presidido, and Emory Peak quadrangles, Texas, volume 1 [DE82-005554] p 47 N82-27808
NURE aerial gamma-ray and magnetic reconnaissance survey of portions of New Mexico, Arizona and Texas Volume 2 New Mexico-Carlsbad Quadrangle [DE82-005527] p 48 N82-27810
MINERAL EXPLORATION
Aerogeophysical methods of finding uranium deposits --- Russian book p 41 A82-33402
Landsat in the search for Appalachian hydrocarbons p 42 A82-34721
Airborne gamma-ray spectrometer and magnetometer survey Barrow quadrangle, Alaska, volume 1 [DE82-000334] p 43 N82-23623
Airborne gamma-ray spectrometer and magnetometer survey Wainwright quadrangle, Alaska, volume 2 [DE82-000341] p 43 N82-23624
Airborne gamma-ray spectrometer and magnetometer survey Meade River quadrangle, Alaska, volume 2 [DE82-000340] p 43 N82-23626
Airborne gamma-ray spectrometer and magnetometer survey Teshekpuk quadrangle, Alaska, volume 2 [DE82-000310] p 43 N82-23627
Airborne gamma-ray spectrometer and magnetometer survey Harrison Bay quadrangle, Alaska, volume 2 [DE82-000315] p 43 N82-23628
Airborne gamma-ray spectrometer and magnetometer survey Beechey Pt, quadrangle, Alaska, volume 2 [DE82-000309] p 43 N82-23629
Airborne gamma-ray spectrometer and magnetometer survey Point Lay quadrangle, Alaska, volume 2 [DE82-000308] p 43 N82-23630
Airborne gamma-ray spectrometer and magnetometer survey Utukik River quadrangle, Alaska, volume 2 [DE82-000316] p 44 N82-23631
Airborne gamma-ray spectrometer and magnetometer survey Sagavanirktok quadrangle, Alaska, volume 2 [DE82-000311] p 44 N82-23632
Airborne gamma-ray spectrometer and magnetometer survey Duluth quadrangle, Minnesota, volume 2 [DE82-001027] p 44 N82-23633
Airborne gamma-ray spectrometer and magnetometer survey International Falls quadrangle, Minnesota, volume 1 [DE82-004151] p 45 N82-23643
Airborne gamma-ray spectrometer and magnetometer survey International Falls quadrangle, Minnesota, volume 2 [DE82-004166] p 45 N82-23644
Application of HCMM data to regional geologic analysis for mineral and energy resource evaluation [E82-10153] p 45 N82-24518
Application of HCMM data to regional geologic analysis for mineral and energy resource evaluation [E82-10243] p 45 N82-24521
Use of MAGSAT anomaly data for crustal structure and mineral resources in the US Midcontinent [E82-10323] p 46 N82-24596
Airborne gamma-ray spectrometer and magnetometer survey, Kingston quadrangle New York, volume 2C [DE81-027161] p 46 N82-25621
Airborne gamma-ray spectrometer and magnetometer survey Barrow quadranagle, Alaska, volume 2 [DE82-000342] p 46 N82-25623
Airborne gamma-ray spectrometer and magnetometer survey Lookout Ridge quadrangle, Alaska, volume 2 [DE82-000313] p 47 N82-25625
Airborne gamma-ray spectrometer and magnetometer survey North/south tieline, volume 2 [DE82-005570] p 47 N82-27805
Airborne gamma-ray spectrometer and magnetometer survey Sioux Falls quadrangle, South Dakota, volume 1 [DE82-005533] p 47 N82-27806
Airborne gamma-ray spectrometer and magnetometer survey Sioux Falls quadrangle, South Dakota, volume 2 [DE82-005574] p 47 N82-27807
Airborne gamma-ray spectrometer and magnetometer survey Ukiah quadrangle, California, volume 1 --- uranium exploration [DE82-005541] p 48 N82-27813
MINERALOGY
Influence of CO2 on melting of model granulite facies assemblages - A model for the genesis of charnockites p 42 A82-36298
The mineralogy of global magnetic anomalies --- rock magnetic signatures and MAGSAT geological, and gravity correlations in West Africa [E82-10305] p 45 N82-24579
MINICOMPUTERS
Interactive initialization of heat flux parameters for numerical models using satellite temperature measurements [E82-10313] p 82 N82-26743

MINNESOTA
AgRISTARS Supporting research Spring small grains planting date distribution model
[E82-10208] p 12 N82-23581
Airborne gamma-ray spectrometer and magnetometer survey Duluth quadrangle, Minnesota, volume 2
[DE82-001027] p 44 N82-23633
Airborne gamma-ray spectrometer and magnetometer survey Bemidji quadrangle, Minnesota, volume 1
[DE82-001032] p 44 N82-23637
Airborne gamma-ray spectrometer and magnetometer survey Bemidji quadrangle, Minnesota, volume 2
[DE82-001026] p 44 N82-23638
Airborne gamma-ray spectrometer and magnetometer survey Hibbing quadrangle, Minnesota, volume 1
[DE82-004159] p 44 N82-23639
Airborne gamma-ray spectrometer and magnetometer survey Hibbing quadrangle, Minnesota, volume 2
[DE82-004165] p 45 N82-23640
Airborne gamma-ray spectrometer and magnetometer survey International Falls quadrangle, Minnesota, volume 1
[DE82-004151] p 45 N82-23643
Airborne gamma-ray spectrometer and magnetometer survey International Falls quadrangle, Minnesota, volume 2
[DE82-004166] p 45 N82-23644

MISSISSIPPI
Analysis of thematic mapper simulator data acquired during winter season over Pearl River, Mississippi, test site
[E82-10287] p 17 N82-24565
Application of remote sensing to state and regional problems
[E82-10288] p 30 N82-24566

MISSOURI
Structure of the St Francois Mountains and surrounding lead belt, S E Missouri Inferences from thermal IR and other data sets
[E82-10200] p 36 N82-23573
Structure of the St Francois Mountains and surrounding lead belt, S E Missouri Inferences from thermal IR and other data sets --- Ozard Plateau and St Francois Mountains
[E82-10205] p 11 N82-23578
Structure of the Saint Francois Mountains and surrounding lead belt, S E Missouri Inference from thermal IR and other data sets
[E82-10350] p 39 N82-26748

MODELS
Investigation of the effects of external current systems on the MAGSAT data utilizing grid cell modeling techniques
[E82-10226] p 73 N82-23599

MODULATION TRANSFER FUNCTION
11-year modulation and spectrum of cosmic rays in the interstellar space p 22 A82-22616

MOISTURE CONTENT
Remote sensing of leaf water content in the near infrared p 8 A82-32897
Effect of atmospheric conditions on remote sensing of vegetation parameters p 24 A82-32901
Application of thermal model for pan evaporation to the hydrology of a defined medium, the sponge
[E82-10217] p 13 N82-23590
Relating thematic mapper bands TM3, TM4, and TM5 to agronomic variables for corn, cotton, sugarbeet, soybean, sorghum, sunflower and tobacco
[E82-10347] p 19 N82-26745

MOLECULAR CLOUDS
Interactions of cosmic rays with molecular clouds p 82 A82-22548

MONOMOLECULAR FILMS
Depression of brightness temperature of sea surfaces covered with monomolecular oil films relative to clean water surfaces at 1 43 GHz p 54 A82-33322

MONSOONS
The impact of meteorological satellites on the First GARP Global Experiment (FGGE) --- First Global Atmospheric Research Program Global Experiment (FGGE) p 55 N82-23852
Representativeness of cloud motion winds deduced from GOES Indian Ocean satellite imagery for the description of the Indian summer monsoon --- superpressure balloons for the study of the Indian summer monsoon (BALSAMINE) p 55 N82-23879
Comparison of satellite derived radiation budget measurements over MONEX during 1979 to 1980 --- Monsoon Experiment (MONEX) p 29 N82-23891
Short term influence radius of monsoonal overturnings --- First Global Atmospheric Research Program Global Experiment (FGGE) p 56 N82-23898
Impact of additional summer MONEX wind data on the prediction of monsoon depressions during June - August 1979 with two versions of primitive equation (PE) barotropic model --- Monsoon Experiment (MONEX) p 56 N82-23900
MONEX oceanographic observations along the East African coast --- global atmospheric research program p 56 N82-23908
Estimates of sea surface stress for summer MONEX from cloud motions --- global atmospheric research program p 56 N82-23910
The onset of the Australian Northwest monsoon during winter MONEX Broadscale flow revealed by an objective analysis scheme p 56 N82-23912
Marine boundary layer wind structure over the Bay of Bengal during Monex-79 --- Monsoon Experiment (MONEX) p 57 N82-23929
Estimates of the statistical structure of the atmospheric pressure field in summer Monex-79 area p 57 N82-23939
Analysis of ocean and atmosphere thermodynamical characteristics during the onset of southwest monsoon over the Arabian Sea p 57 N82-23945

MONTANA
AgRISTARS Supporting research Spring small grains planting date distribution model
[E82-10208] p 12 N82-23581
The influence of autocorrelation in signature extraction An example from a geobotanical investigation of Cotter Basin, Montana
[E82-10341] p 46 N82-25603

MONTE CARLO METHOD
Calculation of production rates of cosmogenic nuclides by Monte Carlo method p 64 A82-22576
A description of relativistic solar particle propagation p 4 A82-22600

MOROCCO
Multidisciplinary investigations on HCMM data over middle Europe and Marocco --- southern Germany and Marrakesh, Morocco
[E82-10315] p 74 N82-24588

MOUNTAINS
Method for the analysis of the melting of a firn complex on the basis of aerospace photographs p 61 A82-35133
Structure of the St Francois Mountains and surrounding lead belt, S E Missouri Inferences from thermal IR and other data sets
[E82-10200] p 36 N82-23573
Structure of the Saint Francois Mountains and surrounding lead belt, S E Missouri Inference from thermal IR and other data sets
[E82-10350] p 39 N82-26748

MULTISPECTRAL BAND SCANNERS
Detecting residential land-use development at the urban fringe p 22 A82-29332
Detection of volcanic smoke and ash-fall area at volcano Aso, from Landsat MSS data p 23 A82-31295
A system design for a multispectral sensor using two-dimensional solid-state imaging arrays p 77 A82-31991
Spectroscopic remote sensing for geological applications p 41 A82-32442
Thematic mapper - An overview of spectral band registration p 77 A82-32447
Multispectral mapper - Imaging spectroscopy as applied to the mapping of earth resources p 77 A82-32448
The use of prior probabilities in maximum likelihood classification of remotely sensed data p 68 A82-32904
Quantitative relationships of near-surface spectra to Landsat radiometric data p 78 A82-32912
EPA's new bubble and banking policies --- for environmental monitoring p 25 A82-33865
The use of Landsat-3 thermal data to help differentiate land covers p 25 A82-34218
Coastal environment change analysis by Landsat MSS data p 54 A82-34219
Use of Landsat multispectral scanner data in vegetation mapping of a forested area p 9 A82-34731
Comparisons of land cover classifications from selected remote sensing systems p 80 A82-34746
Remote sensing in Scotland using data received from satellites - A study of the Tay Estuary region using Landsat multispectral scanning imagery p 62 A82-37501
Remote sensing of salt marsh vegetation in the first four proposed Thematic Mapper bands p 10 A82-37503
Solid state instrumentation concepts for earth resource observation
[AAS PAPER 82-132] p 81 A82-37812
OSTA-1 Post Mission Operation Report
[NASA-TM-84191] p 84 N82-23258
LANDSAT D to test thematic mapper, inaugurate operational system
[NASA-NEWS-RELEASE-82-100] p 82 N82-26741

MULTISPECTRAL LINEAR ARRAYS
Advanced technology for earth observation - Data processing
[AAS PAPER 82-130] p 71 A82-37810

MULTISPECTRAL PHOTOGRAPHY
Imaging spectroscopy, Proceedings of the Seminar, Los Angeles, CA, February 10, 11, 1981 p 77 A82-32440
Resource inventory techniques used in the California Desert Conservation Area p 23 A82-32441
Landsat detection of hardwood forest clearcuts p 8 A82-32708
An information-theoric spatial transform p 69 A82-34717
Allowance for the effect of the atmosphere in the processing of satellite remote-sensing images p 70 A82-35141
Landsat D to yield more precise data p 70 A82-37200
A quantitative multispectral analysis system for aerial photographs applied to coastal planning p 55 A82-37505
Ten-Ecosystem Study --- Grand and Weld Counties, Colorado, Warren County, Pennsylvania, St Louis County, Minnesota, Sandoval County, New Mexico, Kershaw County, South Carolina, Fort Yukon, Alaska, Grays Harbor County, Washington, and Washington County, Missouri
[E82-10186] p 84 N82-22620
An analysis of LANDSAT MSS scene-to-scene registration accuracy
[E82-10285] p 16 N82-24563

N

NAUTICAL CHARTS
A search for seamounts in the southern Cook and Austral region p 52 A82-30810

NAVIGATION
Spherical harmonic representation of the main geomagnetic field for world charting and investigations of some fundamental problems of physics and geophysics
[E82-10203] p 72 N82-23576

NAVIGATION INSTRUMENTS
Magnetic anomalies as a reference for ground-speed and map-matching navigation p 32 A82-30314

NAVIGATION SATELLITES
The processing of satellite navigation data for marine geodesy p 34 A82-37175

NEARSHORE WATER
Nearshore current pattern off south Texas - An interpretation from aerial photographs p 53 A82-32903

NEON ISOTOPES
Calculated isotopic source composition and tests for origin and propagation of cosmic rays with mass numbers less than or equal to 62 p 83 A82-22554
Comparative abundances in solar energetic particles and in galactic cosmic ray sources, and the Ne-22 anomaly p 83 A82-22556
On the stellar origin of the Ne-22 excess in cosmic rays p 21 A82-22562
Origin of galactic cosmic rays from Ne isotopic composition p 2 A82-22563
Is the neon composition of our sun, planetary or solar p 76 A82-22608

NEUTRAL SHEETS
Possible evidence for attenuation of an MHD shock by a magnetic neutral sheet in the solar corona p 3 A82-22589

NEUTRON FLUX DENSITY
The approximate 1 GeV solar cosmic rays in the Forbush-effect of February 15, 1978 p 40 A82-22604
Primary spectral variations of cosmic rays above 1 GV p 5 A82-22618

NEUTRON SPECTRA
Primary spectral variations of cosmic rays above 1 GV p 5 A82-22618

NEUTRON SPECTROMETERS
Primary spectral variations of cosmic rays above 1 GV p 5 A82-22618

NEUTRON STARS
Acceleration of cosmic rays in accretion shocks p 64 A82-22568
Pulsar models and cosmic-ray acceleration p 21 A82-22570

NEW MEXICO
NURE aerial gamma-ray and magnetic reconnaissance survey of portions of New Mexico, Arizona and Texas Volume 2 New Mexico-Carlsbad Quadrangle
[DE82-005527] p 48 N82-27810

NIMBUS SATELLITES
Snowpack monitoring in North America and Eurasia using passive microwave satellite data p 78 A82-32915

NIMBUS 4 SATELLITE
Total ozone variations 1970-74 using Backscattered Ultraviolet /BUV/ and ground-based observations p 26 A82-36053
NITROGEN
Soft X-rays from the sunlit earth's atmosphere p 29 A82-37405
NITROGEN DIOXIDE
Breadboard gas filter correlation spectrometer for atmospheric measurement of hydrazines and nitrogen dioxide
[AD-A110688] p 82 N82-26642
NITROGEN OXIDES
Aircraft measurements of NO/x/ in the lower troposphere above the coast of Japan p 26 A82-36247
Ammonia and the NOx budget of the troposphere p 27 A82-36293
NOAA SATELLITES
Geographic location of individual pixels --- for thermal infrared digital data processing p 68 A82-32900
Measuring sea surface temperature from satellites - A ground truth approach p 54 A82-32917
Short term influence radius of monsoonal overturnings --- First Global Atmospheric Research Program Global Experiment (FGGE) p 56 N82-23898
NOAA 6 SATELLITE
Evaluation of NOAA-AVHRR data for crop assessment --- Advanced Very High Resolution Radiometer p 8 A82-34179
NONLINEAR SYSTEMS
Nonlinear theory for elastic beams and rods and its finite element representation
[WTHD-143] p 73 N82-24517
NORTH AMERICA
Study of gravity and magnetic anomalies using MAGSAT data
[E82-10194] p 35 N82-22628
Use of MAGSAT anomaly data for crustal structure and mineral resources in the US Midcontinent
[E82-10321] p 46 N82-24594
NORTH DAKOTA
AgRISTARS Supporting research Spring small grains planting date distribution model
[E82-10208] p 12 N82-23581
Application of thermal model for pan evaporation to the hydrology of a defined medium, the sponge
[E82-10217] p 13 N82-23590
Airborne gamma-ray spectrometer and magnetometer survey Devil's Lake quadrangle, North Dakota, volume 1
[DE82-004161] p 44 N82-23635
Airborne gamma-ray spectrometer and magnetometer survey Devil's Lake quadrangle, North Dakota, volume 2
[DE82-004168] p 44 N82-23636
NORTH SEA
The METEOSAT Data Collection System and its application p 75 N82-26037
NUCLEAR FUSION
Nucleosynthesis of light and by-passed isotopes in the solar system matter p 64 A82-22578
NUCLIDES
Calculated isotopic source composition and tests for origin and propagation of cosmic rays with mass numbers less than or equal to 62 p 83 A82-22554
Calculation of production rates of cosmogenic nuclides by Monte Carlo method p 64 A82-22576
Measurement of cosmogenic nuclides using a multi-crystal gamma-ray coincidence spectrometer --- for Mayo Belwa meteorite study p 64 A82-22577
NUMERICAL ANALYSIS
Generation of the auroral kilometric radiation p 26 A82-35542
NUTRIENTS
Color aerial photography detects nutrient status of loblolly pine plantations p 6 A82-29531

O

O STARS
On the stellar origin of low energy cosmic rays p 21 A82-22567
OCCULTATION
OSO-8 lower mesospheric ozone number density profiles p 28 A82-36472
OCEAN BOTTOM
Geoid height-age relation from Seasat altimeter profiles across the Mendocino Fracture Zone p 34 A82-32646
OCEAN COLOR SCANNER
Analysis of ocean color scanner data from the Superflux III Experiment
[NASA-TM-83290] p 55 N82-23614
OCEAN CURRENTS
Seasat altimeter determination of ocean current variability p 50 A82-29613
A ship and satellite view of hydrographic features in the western Gulf of Mexico p 53 A82-32651
Determination of winter temperature patterns, fronts, and surface currents in the Yellow Sea and East China Sea from satellite imagery p 55 A82-37195
Ice distribution and winter surface circulation patterns, Kachemak Bay, Alaska
[AD-A110806] p 58 N82-26764
OCEAN DATA ACQUISITIONS SYSTEMS
Technology and oceanography An assessment of Federal technologies for oceanographic research and monitoring Volume 2 Working papers on fishery research technology p 58 N82-26944
OCEAN DYNAMICS
Estimates of sea surface stress for summer MONEX from cloud motions --- global atmospheric research program p 56 N82-23910
Satellite observations in FRONTS 80
[AD-A111080] p 58 N82-26766
OCEAN MODELS
An empirical determination of the effects of sea state bias on Seasat altimetry p 50 A82-29607
The Seasat altimeter mean sea surface model p 51 A82-29614
OCEAN SURFACE
Remote sensing of precipitable water over the oceans from Nimbus 7 microwave measurements p 49 A82-28907
The Seasat altimeter data and its accuracy assessment p 49 A82-29602
Seasat altimeter height calibration --- related to sea surface heights near Bermuda p 49 A82-29603
Tidal and geodetic observations for the Seasat altimeter calibration experiment p 49 A82-29604
An empirical determination of the effects of sea state bias on Seasat altimetry p 50 A82-29607
Sea-state-related altitude errors in the Seasat radar altimeter p 50 A82-29608
Seasat altimeter timing bias estimation p 50 A82-29609
The Seasat altimeter mean sea surface model p 51 A82-29614
The Seasat-A satellite scatterometer - The geophysical evaluation of remotely sensed wind vectors over the ocean p 51 A82-29616
The relationship between wind vector and normalized radar cross section used to derive Seasat-A Satellite Scatterometer winds p 51 A82-29617
Surface wind analyses for Seasat p 51 A82-29619
The observation of ocean surface phenomena using imagery from the Seasat synthetic aperture radar - An assessment p 52 A82-29623
Seasat wind and wave observations of northeast Pacific hurricane Iva, August 13, 1978 p 52 A82-29624
Emissivity and reflectance of the model sea surface for the use of AVHRR data of NOAA satellites p 52 A82-31294
On the synthetic aperture radar imaging of ocean surface waves p 53 A82-32881
Ocean wave height measurement with SEASAT SAR using speckle diversity p 53 A82-32882
Infrared sensing of sea surface temperature from space p 53 A82-32902
Measuring sea surface temperature from satellites - A ground truth approach p 54 A82-32917
Depression of brightness temperature of sea surfaces covered with monomolecular oil films relative to clean water surfaces at 1 43 GHz p 54 A82-33322
Characteristics of 13 9 GHz radar scattering from oil films on the sea surface p 54 A82-33438
Satellite observations of sea surface temperature around the British Isles p 54 A82-33717
Pulse-to-pulse correlation in satellite radar altimeters --- for ocean wave height measurement p 55 A82-37390
Mean sea-level pressure in the Southern Hemisphere during the FGGE period --- First Global Atmospheric Research Program Global Experiment (FGGE), buoys p 55 N82-23856
On the space-time variability of ocean surface mixed layer characteristics of central and eastern Arabian sea during MONSOON-77 --- global atmospheric research program p 56 N82-23909
Estimates of sea surface stress for summer MONEX from cloud motions --- global atmospheric research program p 56 N82-23910
Analysis of ocean and atmosphere thermodynamical characteristics during the onset of southwest monsoon over the Arabian Sea p 57 N82-23945
The effect of sea-surface Sun glitter on microwave radiometer measurements
[NASA-CR-169083] p 57 N82-26525
Ice distribution and winter surface circulation patterns, Kachemak Bay, Alaska
[AD-A110806] p 58 N82-26764
Satellite observations in FRONTS 80
[AD-A111080] p 58 N82-26766
OCEAN TEMPERATURE
Seasat altimeter determination of ocean current variability p 50 A82-29613
Description of Seasat radiometer status and results p 52 A82-29622
Infrared sensing of sea surface temperature from space p 53 A82-32902
Measuring sea surface temperature from satellites - A ground truth approach p 54 A82-32917
Satellite observations of sea surface temperature around the British Isles p 54 A82-33717
Interannual variations of outgoing IR associated with tropical circulation changes during 1974-1978 p 54 A82-36341
On the space-time variability of ocean surface mixed layer characteristics of central and eastern Arabian sea during MONSOON-77 --- global atmospheric research program p 56 N82-23909
Rapid oceanographic data gathering Some problems in using remote sensing to determine the horizontal and vertical thermal distributions in the Northeast Pacific Ocean
[AD-A111005] p 58 N82-26945
OCEANOGRAPHIC PARAMETERS
Waveheight and wind speed measurements from the Seasat radar altimeter p 50 A82-29612
Retrieval of ocean surface and atmospheric parameters from multichannel microwave radiometric measurements p 53 A82-31995
MONEX oceanographic observations along the East African coast --- global atmospheric research program p 56 N82-23908
OCEANOGRAPHY
Seasat measurement system evaluation - Achievements and limitations p 49 A82-29601
Magsat magnetic anomalies over Antarctica and the surrounding oceans p 32 A82-30787
A search for seamounts in the southern Cook and Austral region p 52 A82-30810
The processing of satellite navigation data for marine geodesy p 34 A82-37175
High resolution satellite observations of mesoscale oceanography in the Tasman Sea, 1978 - 1979
[E82-10324] p 57 N82-24597
Ice distribution and winter surface circulation patterns, Kachemak Bay, Alaska
[AD-A110806] p 58 N82-26764
Meteorological and aircraft data for CUE 2 1973
[PB82-149246] p 59 N82-26949
OIL SLICKS
Emissivity and reflectance of the model sea surface for the use of AVHRR data of NOAA satellites p 52 A82-31294
Depression of brightness temperature of sea surfaces covered with monomolecular oil films relative to clean water surfaces at 1 43 GHz p 54 A82-33322
Characteristics of 13 9 GHz radar scattering from oil films on the sea surface p 54 A82-33438
OKLAHOMA
Application of thermal model for pan evaporation to the hydrology of a defined medium, the sponge
[E82-10217] p 13 N82-23590
ON-LINE SYSTEMS
Present status of on-line analytical triangulation p 69 A82-34940
OPTICAL FILTERS
Effects of altitude, focal length, and filter combinations on color infrared photography of citrus groves p 9 A82-34729
OPTICAL PROPERTIES
Bias correction procedures for airborne laser hydrography
[PB82-130089] p 63 N82-22644
OPTICAL RADAR
Airborne lidar measurements of the Soufriere eruption of 17 April 1979 p 24 A82-33657
OPTICAL SCANNERS
An optical data link for airborne scanning system p 80 A82-34737
OPTICAL THICKNESS
Interactions of cosmic rays with molecular clouds p 82 A82-22548
Relating Landsat digital count values to ground reflectance for optically thin atmospheric conditions p 66 A82-29762
OPTIMIZATION
Determination of the optimal level for combining area and yield estimates
[E82-10215] p 12 N82-23588

OREGON
An investigation into the utilization of HCMM thermal data for the discrimination of volcanic and Eolian geological units --- Newberry Volcano, Oregon
[E82-10352] p 47 N82-26750
Meteorological and aircraft data for CUE 2 1973
[PB82-149246] p 59 N82-26949
Airborne gamma-ray spectrometer and magnetometer survey Chico Quadrangle, California
[DE82-005543] p 48 N82-27815

OROGRAPHY
On the application of a model of boundary-layer flow over low hills to real terrain p 29 A82-36741
The influence of soil characteristics on regional convection differences above Northern Germany p 10 A82-37589

OSCILLATIONS
Fluid-sediment interactions on beaches and shelves
[AD-A110838] p 59 N82-26948

OSO-8
OSO-8 lower mesospheric ozone number density profiles p 28 A82-36472

OSTA-1 PAYLOAD
OSTA-1 Post Mission Operation Report
[NASA-TM-84191] p 84 N82-23258

OXYGEN SPECTRA
Soft X-rays from the sunlit earth's atmosphere p 29 A82-37405

OZONE
Total ozone variations 1970-74 using Backscattered Ultraviolet /BUV/ and ground-based observations p 26 A82-36053
Atmospheric ozone determination by solar occultation using the UV spectrometer on the Solar Maximum Mission p 27 A82-36362
Application of infrared techniques to the study of atmospheric ozone p 27 A82-36414
Observations and analyses of the total amount of atmospheric ozone in the Beijing region and in the region of Jolmolungma Mountain in Tibet p 28 A82-36444
Comparison of ozone in polluted and clean air masses over Lake Michigan p 29 A82-36477
The seasonal variations of ozone and temperature in the middle and the upper stratosphere p 29 A82-36534
In situ ozone data for comparison with laser absorption remote sensor 1980 PEPE/NEROS program
[NASA-TM-84471] p 30 N82-25661

OZONOMETRY
Observation of the diurnal variation of atmospheric ozone p 26 A82-35895
Sensitivity of Dobson total ozone estimations to wavelength band calibration uncertainties p 27 A82-36405
The effect of the spectral attenuation of UV radiation by aerosol on the total ozone measurements p 27 A82-36406
Microwave measurement of stratospheric and mesospheric ozone p 28 A82-36415
Total ozone retrieval from satellite Meteor 28 Fourier spectrometer measurements p 28 A82-36422
Dobson spectrophotometer calibrations, possible errors in ozone absorption coefficients, and errors due to interfering pollutant gases p 28 A82-36431
OSO-8 lower mesospheric ozone number density profiles p 28 A82-36472

P

PACIFIC OCEAN
A search for seamounts in the southern Cook and Austral region p 52 A82-30810
Investigations of medium wavelength magnetic anomalies in the eastern Pacific using MAGSAT
[E82-10240] p 73 N82-23613
Short term influence radius of monsoonal overturnings --- First Global Atmospheric Research Program Global Experiment (FGGE) p 56 N82-23898
High resolution satellite observations of mesoscale oceanography in the Tasman Sea, 1978 - 1979
[E82-10324] p 57 N82-24597
Investigations of medium wavelength magnetic anomalies in the eastern Pacific using MAGSAT data
[E82-10330] p 38 N82-24603
Satellite observations in FRONTS 80
[AD-A111080] p 58 N82-26766
Rapid oceanographic data gathering Some problems in using remote sensing to determine the horizontal and vertical thermal distributions in the Northeast Pacific Ocean
[AD-A111005] p 58 N82-26945

PAIN
Thermal mapping, geothermal source location, natural effluents and plant stress in the Mediterranean coast of Spain
[E82-10300] p 17 N82-24576

PALEOMAGNETISM
MAGSAT anomaly map and continental drift
[E82-10326] p 38 N82-24599

PANORAMIC CAMERAS
Development and application of panoramic aerial photography in forest pest management p 5 A82-29527
Photogrammetric methods for mapping resource data from high altitude panoramic photography p 77 A82-32702
Estimating mountain pine beetle-killed ponderosa pine over the front range of Colorado with high altitude panoramic photography p 7 A82-32704
Optical bar panoramic photography for planning timber salvage in drought-stressed forests p 7 A82-32705
Technical and economical characteristics of the AFA-TES-10M aerial camera p 79 A82-34470

PANORAMIC SCANNING
Panoramic aerial photography in forest pest management p 7 A82-32701

PARTICLE ACCELERATION
Confinement and acceleration of cosmic rays in galactic superbubbles p 82 A82-22547
Cosmic ray composition from acceleration of thermal matter p 64 A82-22558
Physical state of the birth place of cosmic rays and its implication to the acceleration processes p 2 A82-22559
Evidence for the stochastic acceleration of cosmic rays in supernova remnants p 2 A82-22564
The galactic origin of cosmic rays I
[CONF-810711-1] p 2 A82-22565
Cosmic ray acceleration by stellar winds I - Total density, pressure and energy flux p 21 A82-22566
Acceleration of cosmic rays in accretion shocks p 64 A82-22568
Remarks on cosmic ray origin p 21 A82-22569
Pulsar models and cosmic-ray acceleration p 21 A82-22570
Acceleration processes near massive black holes p 3 A82-22572
The galactic origin of cosmic rays II
[CONF-810711-2] p 64 A82-22573
Astrophysical scenarios for critically evaluating a zero-point field acceleration mechanism p 64 A82-22575
Interplanetary particle observations associated with solar flare gamma-ray line emission p 3 A82-22584
Computer simulation of the time dependence of the photon energy spectra produced in proton and electron bremsstrahlung p 3 A82-22587
High-energy solar protons p 22 A82-22588
A survey of solar protons and alpha differential spectra between 1 and greater than 400 MeV/nucleon p 4 A82-22592
Preflare increases in solar cosmic rays relevant to the mode of energy accumulation in the active regions associated with large flares p 31 A82-22595
On the physical sense of the constant of solar cosmic ray coronal propagation p 83 A82-22599
Time and energy dependence of heavy ion abundances in solar flare energetic particle events p 22 A82-22605
Observations of the ionization states of energetic particles accelerated in solar flares p 40 A82-22607
Coulombian energy losses and the nuclear composition of the solar cosmic rays p 4 A82-22610

PARTICLE DIFFUSION
The cosmic ray positron spectrum p 1 A82-22542

PARTICLE EMISSION
Interplanetary particle observations associated with solar flare gamma-ray line emission p 3 A82-22584
Unusual properties of particle events associated with solar flare gamma ray events p 65 A82-22585

PARTICLE ENERGY
On the characteristics of the very low energy galactic cosmic rays in the interstellar space p 63 A82-22540
Cosmic ray acceleration by stellar winds I - Total density, pressure and energy flux p 21 A82-22566
On the stellar origin of low energy cosmic rays p 21 A82-22567
11-year modulation and spectrum of cosmic rays in the interstellar space p 22 A82-22616

PARTICLE FLUX DENSITY
Comparison of the measured antiproton flux with that predicted by the 'leaky box' model p 1 A82-22544
Cosmic ray acceleration by stellar winds I - Total density, pressure and energy flux p 21 A82-22566
Energetic solar particle spectra according to Venera-11, 12 and Prognoz-5, 6 p 4 A82-22593
The modulation characteristics of the 19th and 20th solar activity cycles p 59 A82-22615
Features of cosmic ray variations due to variations in the total magnetic field of the sun p 49 A82-22619

PARTICLE INTERACTIONS
Interactions of cosmic rays with molecular clouds p 82 A82-22548
Cosmic ray composition from acceleration of thermal matter p 64 A82-22558
Calculation of production rates of cosmogenic nuclides by Monte Carlo method p 64 A82-22576

PARTICLE MOTION
A report on the 'cosmic ray propagation problem' p 1 A82-22539
Azimuthal propagation of flare particles in the heliosphere p 66 A82-22590
Spacecraft determination of energetic particle propagation parameters - The 1 January 1978 solar event p 31 A82-22598

PARTICLE PRODUCTION
Extragalactic cosmic rays, their sources and spectrum p 40 A82-22574
Calculation of production rates of cosmogenic nuclides by Monte Carlo method p 64 A82-22576

PARTICLE SIZE DISTRIBUTION
Fine particles in the Soufriere eruption plume p 24 A82-33659
The effect of the spectral attenuation of UV radiation by aerosol on the total ozone measurements p 27 A82-36406

PARTICLE SPIN
Magnetic monopole pair and its observation in cosmic rays p 65 A82-22579

PARTICLE TRAJECTORIES
The question of short pathlengths in interstellar propagation p 1 A82-22541

PARTICULATE SAMPLING
Fine particles in the Soufriere eruption plume p 24 A82-33659

PATTERN RECOGNITION
Description of gray level picture using a collection of density contour lines p 66 A82-29409
Separation of diffuse from sharp-edged features in digital imagery p 68 A82-34225
Multistage classification of multispectral Earth observational data The design approach
[E82-10213] p 72 N82-23586
AgRISTARS Project management report Program review presentation to level 1, interagency coordination committee
[E82-10219] p 13 N82-23592
Analysis of scanner data for crop inventories
[E82-10241] p 16 N82-24519
Analysis of thematic mapper simulator data acquired during winter season over Pearl River, Mississippi, test site
[E82-10287] p 17 N82-24565
Thermal mapping, geothermal source location, natural effluents and plant stress in the Mediterranean coast of Spain
[E82-10300] p 17 N82-24576
Image understanding research
[AD-A110746] p 74 N82-25611
Association of spectral development patterns with development stages of corn
[E82-10353] p 19 N82-26751

PATTERN REGISTRATION
Registration of Heat Capacity Mapping Mission day and night images
[E82-10210] p 72 N82-23583
An analysis of LANDSAT MSS scene-to-scene registration accuracy
[E82-10285] p 16 N82-24563
An algorithm for automating the registration of USDA segment ground data to LANDSAT MSS data
[E82-10286] p 16 N82-24564
Forest Resource Information System Phase 3 System transfer report
[E82-10344] p 18 N82-25606
Key Issues in the Analysis of Remote Sensing Data A report on the workshop
[E82-10348] p 85 N82-26746

PENNSYLVANIA
Interactive initialization of heat flux parameters for numerical models using satellite temperature measurements
[E82-10313] p 82 N82-26743

PERFORMANCE PREDICTION
Investigations of point transfer p 78 A82-33296

PERFORMANCE TESTS
The simultaneous employment of geodetic measurements for block adjustments using the method of independent models p 34 A82-33295

PERIODIC VARIATIONS
Features of cosmic ray variations due to variations in the total magnetic field of the sun p 49 A82-22619

Principles and methods of the study of the hydrological cycle on the basis of aerospace data p 61 A82-35127
PERTURBATION
Investigation of the effects of external current systems on the MAGSAT data utilizing grid cell modeling techniques
[E82-10226] p 73 N82-23599
PETROLOGY
Influence of CO2 on melting of model granulite facies assemblages - A model for the genesis of charnockites p 42 A82-36298
PHENOLOGY
A meteorologically driven maize stress indicator model
[E82-10112] p 11 N82-23564
AgRISTARS Foreign commodity production forecasting The 1980 US/Canada wheat and barley exploratory experiment
[E82-10126] p 11 N82-23565
Evaluation of the Doraiswamy-Thompson winter wheat crop calendar model incorporating a modified spring restart sequence
[E82-10207] p 12 N82-23580
AgRISTARS Supporting research Spring small grains planting date distribution model
[E82-10208] p 12 N82-23581
A meteorologically driven grain sorghum stress indicator model
[E82-10218] p 13 N82-23591
PHOTOGEOLOGY
Spectroscopic remote sensing for geological applications p 41 A82-32442
Possible fault detection in Cottonball Basin, California An application of radar remote sensing p 41 A82-32898
Aerogeophysical methods of finding uranium deposits --- Russian book p 41 A82-33402
Comparing lineaments interpreted from Landsat imagery and topographic maps with reported faults in southwest Montana p 34 A82-34719
Landsat in the search for Appalachian hydrocarbons p 42 A82-34721
Significance of tectonics in linear feature detection and interpretation on satellite images p 42 A82-37198
Overseas Geology And Mineral Resources number 56 A geological interpretation of LANDSAT imagery and air photography of Botswana
[OGMR-56] p 42 N82-22636
Multidisciplinary investigations on HCMM data over middle Europe and Marocco --- southern Germany and Marrakesh, Morocco
[E82-10315] p 74 N82-24588
An investigation into the utilization of HCMM thermal data for the discrimination of volcanic and Eolian geological units --- Newberry Volcano, Oregon
[E82-10352] p 47 N82-26750
PHOTOGONIOMETERS
Irradiance measurement errors due to the assumption of a Lambertian reference panel p 79 A82-34222
PHOTOGRAMMETRY
Photogrammetric methods for mapping resource data from high altitude panoramic photography p 77 A82-32702
Geographic location of individual pixels --- for thermal infrared digital data processing p 68 A82-32900
The simultaneous employment of geodetic measurements for block adjustments using the method of independent models p 34 A82-33295
Investigations of point transfer p 78 A82-33296
American Society of Photogrammetry, Annual Meeting, 47th, Washington, DC, February 22-27, 1981, ASP Technical Papers p 79 A82-34701
A practical study of gross-error detection in bundle adjustment p 69 A82-34702
Present status of on-line analytical triangulation p 69 A82-34940
Coordination of stereo image registration and pixel classification
[AD-A111307] p 75 N82-25614
PHOTOGRAPHIC FILM
Considerations in using color infrared photographs for vegetative interpretation p 6 A82-29530
An infrared exposure meter p 76 A82-29541
Image quality and height measurement accuracy of aerial survey camera imagery from high altitudes p 78 A82-33297
Sensitometry in Canadian aerial survey p 79 A82-34724
PHOTOGRAPHIC PROCESSING
Analytical processing of photographs taken by paired cameras p 79 A82-34471
PHOTOGRAPHY
Detection and damage assessment of citrus tree losses with aerial color infrared photography /ACIR/ p 7 A82-29538
PHOTOINTERPRETATION
Detecting residential land-use development at the urban fringe p 22 A82-29332
Development and application of panoramic aerial photography in forest pest management p 5 A82-29527
Considerations in using color infrared photographs for vegetative interpretation p 6 A82-29530
Multi-resource inventory in interior Alaska p 6 A82-29532
Estimating rangeland cover proportions with large-scale color-infrared aerial photographs p 6 A82-29534
Detection and damage assessment of citrus tree losses with aerial color infrared photography /ACIR/ p 7 A82-29538
Application of scanning microdensitometer data in selected plant science case studies p 7 A82-29539
Satellite image interpretation of the eastern Caledonian part of the Blue Road Geotraverse and its geological implications /Nordland, Vasterbotten, Scandinavia/ p 41 A82-30305
Problems of the interpretation of aerial and satellite images of industrial smoke p 23 A82-30307
Extraction of line shaped objects from aerial images using a special operator to analyze the profiles of functions p 67 A82-32033
Dependent feature trees for density approximation I - Optimal construction and classification results p 67 A82-32344
The use of contextual information to detect cumulus clouds and cloud shadows in Landsat data p 67 A82-32346
Evaluation of spruce-fir forests using small-format photographs p 8 A82-32707
Sample design for estimating change in land use and land cover p 24 A82-32711
Interpretation of surface-water circulation, Aransas Pass, Texas, using Landsat imagery p 60 A82-32896
Monitoring land-cover change by principal component analysis of multitemporal Landsat data p 68 A82-32906
Terrain analysis from Landsat using a color TV enhancement system p 68 A82-32911
Coastal environment change analysis by Landsat MSS data p 54 A82-34219
Site selection and engineering issues for a major industrial complex - Application of image and map interpretation p 25 A82-34711
A computerized spatial analysis system for assessing wildlife habitat from vegetation maps p 9 A82-34716
Comparing lineaments interpreted from Landsat imagery and topographic maps with reported faults in southwest Montana p 34 A82-34719
A quantitative method to test for similarity between photo interpreters p 69 A82-34722
Digital and visual evaluation of GOES and TIROS/NOAA image data for cover type effects on snowfield observations p 60 A82-34735
Status and prospects of the automated processing of remote-sensing data /using forest surveys as an example/ p 10 A82-35139
Significance of tectonics in linear feature detection and interpretation on satellite images p 42 A82-37198
LANDSAT technology transfer to the private and public sectors through community colleges and other locally available institutions
[E82-10181] p 85 N82-23568
Multidisciplinary investigations on HCMM data over middle Europe and Marocco --- southern Germany and Marrakesh, Morocco
[E82-10315] p 74 N82-24588
Mapping of wildlife habitat in Farmington Bay, Utah
[E82-10354] p 19 N82-26752
Irrigated acreage in the Bear River Basin as of the 1975 growing season --- Idaho, Utah, and Wyoming
[E82-10356] p 20 N82-26754
Exploration into technical procedures for vertical integration --- information systems
[NASA-CR-166352] p 75 N82-26763
PHOTOMAPPING
Riparian vegetation mapping in Northeastern California using high altitude color infrared aerial photography p 5 A82-29528
Multi-resource inventory in interior Alaska p 6 A82-29532
Mapping riparian vegetation in Southeastern Oregon using digitized large scale color infra-red aerial photography p 6 A82-29535
Application of scanning microdensitometer data in selected plant science case studies p 7 A82-29539
Regional geological, tectonic and geophysical features of Nordland, Norway p 41 A82-30304
Dependent feature trees for density approximation I - Optimal construction and classification results p 67 A82-32344
Spectroscopic remote sensing for geological applications p 41 A82-32442
Multispectral mapper - Imaging spectroscopy as applied to the mapping of earth resources p 77 A82-32448
Digitally enhanced visual displays facilitate the analysis of Landsat imagery p 67 A82-32507
Landsat detection of hardwood forest clearcuts p 8 A82-32708
Computation with physical values from Landsat digital data p 68 A82-32709
Impacts of remote sensing on U S geography p 24 A82-32899
Geographic location of individual pixels --- for thermal infrared digital data processing p 68 A82-32900
Technical and economical characteristics of the AFA-TES-10M aerial camera p 79 A82-34470
A computerized spatial analysis system for assessing wildlife habitat from vegetation maps p 9 A82-34716
Use of Landsat multispectral scanner data in vegetation mapping of a forested area p 9 A82-34731
The use of Skylab S-190B photography for small scale mapping p 80 A82-34742
Aerial photography vs Landsat for digital land-cover mapping in an urban watershed p 61 A82-34745
The use of space photographs in the mapping of glaciers and water bodies p 62 A82-37174
Relating thematic mapper bands TM3, TM4, and TM5 to agronomic variables for corn, cotton, sugarbeet, soybean, sorghum, sunflower and tobacco
[E82-10347] p 19 N82-26745
Mapping of wildlife habitat in Farmington Bay, Utah
[E82-10354] p 19 N82-26752
PHOTOMAPS
Experience with the compilation of maps of snow-cover melting in the central part of the European USSR on the basis of satellite data p 62 A82-35134
PHOTON BEAMS
Computer simulation of the time dependence of the photon energy spectra produced in proton and electron bremstrahlung p 3 A82-22587
PHOTOOXIDATION
Ammonia and the NOx budget of the troposphere p 27 A82-36293
PHOTOSYNTHESIS
Spectral estimates of solar radiation intercepted by corn canopies
[E82-10003] p 18 N82-26742
PLANET EPHEMERIDES
The Seasat altimeter data and its accuracy assessment p 49 A82-29602
The Seasat altimeter mean sea surface model p 51 A82-29614
PLANETARY MAGNETIC FIELDS
MAGSAT anomaly map and continental drift
[E82-10326] p 38 N82-24599
Models and maps of the main field
[E82-10327] p 74 N82-24600
PLANETARY MAPPING
A color-ratio map of Mercury p 31 A82-22294
Initial vector magnetic anomaly map from Magsat p 32 A82-30785
PLANKTON
HCMM hydrological analysis in Utah
[E82-10328] p 63 N82-24601
PLANT STRESS
A meteorologically driven maize stress indicator model
[E82-10112] p 11 N82-23564
Evaluation of the Doraiswamy-Thompson winter wheat crop calendar model incorporating a modified spring restart sequence
[E82-10207] p 12 N82-23580
A meteorologically driven grain sorghum stress indicator model
[E82-10218] p 13 N82-23591
AgRISTARS Early warning and crop condition assessment Plant cover, soil temperature, freeze, water stress, and evapotranspiration conditions
[E82-10225] p 14 N82-23598
Multilevel measurements of surface temperature over undulating terrain planted to barley
[E82-10245] p 16 N82-24523
Thermal mapping, geothermal source location, natural effluents and plant stress in the Mediterranean coast of Spain
[E82-10300] p 17 N82-24576
Multispectral determination of soil moisture-2 --- Guymon, Oklahoma and Dalhart, Texas
[E82-10349] p 19 N82-26747
PLANTING
Diurnal changes in reflectance factor due to Sun-row direction interactions
[E82-10128] p 11 N82-23566
AgRISTARS Supporting research Spring small grains planting date distribution model
[E82-10208] p 12 N82-23581

A meteorologically driven grain sorghum stress indicator model
[E82-10218] p 13 N82-23591
Airborne observed solar elevation and row direction effects on the near-IR/red ratio of cotton
[E82-10220] p 13 N82-23593
Description of the FORTRAN implementation of the spring small grains planting date distribution model
[E82-10235] p 15 N82-23608
PLANTS (BOTANY)
Color aerial photography in the plant sciences and related fields, Proceedings of the Eighth Biennial Workshop, Luray, VA, April 21-23, 1981
p 5 A82-29526
Remote sensing of leaf water content in the near infrared p 8 A82-32897
Landsat digital analysis of the initial recovery of burned tundra at Kokolik River, Alaska p 8 A82-32913
The influence of autocorrelation in signature extraction An example from a geobotanical investigation of Cotter Basin, Montana
[E82-10341] p 46 N82-25603
PLASMA COMPOSITION
A tentative ordering of all available solar energetic particles abundance observations I - The mass unbiased baseline II - Discussion and comparison with coronal abundances p 40 *A82-22609*
PLATES (TECTONICS)
Regional geological, tectonic and geophysical features of Nordland, Norway p 41 A82-30304
A satellite magnetic model of northeastern South American aulacogens p 33 A82-30795
An investigation of MAGSAT and complementary data emphasizing precambrian shields and adjacent areas of West Africa and South America
[E82-10316] p 38 N82-24589
An investigation of MAGSAT and complementary data emphasizing precambrian shields and adjacent areas of West Africa and South America
[E82-10317] p 38 N82-24590
An investigation of MAGSAT and complementary data emphasizing precambrian shields and adjacent areas of West Africa and South America
[E82-10318] p 38 N82-24591
Geotectonics of South America --- regional magnetic and gravity anomalies of South America
[E82-10320] p 38 N82-24593
PLUMES
Meteorological analysis of the eruption of Soufriere in April 1979 p 24 A82-33655
Airborne lidar measurements of the Soufriere eruption of 17 April 1979 p 24 A82-33657
Fine particles in the Soufriere eruption plume
p 24 A82-33659
In situ ozone data for comparison with laser absorption remote sensor 1980 PEPE/NEROS program
[NASA-TM-84471] p 30 N82-25661
POGO
Verification of the crustal component in satellite magnetic data p 32 A82-30789
POLAR CAPS
Extremely high latitude auroras p 76 A82-31020
POLAR ORBITS
Comparison of satellite derived radiation budget measurements over MONEX during 1979 to 1980 --- Monsoon Experiment (MONEX) p 29 N82-23891
POLAR REGIONS
Studies of high latitude current systems using MAGSAT vector data
[E82-10188] p 71 N82-22622
Investigation from Japanese MAGSAT Team Part A Crustal structure near Japan and in Antarctic station Part B Electric currents and hydromagnetic waves in the ionosphere and the magnetosphere
[E82-10244] p 36 N82-24522
POLAR SUBSTORMS
Observed magnetic substorm signatures at synchronous altitude p 26 A82-35534
POLAR WANDERING (GEOLOGY)
On reference coordinate systems used in polar motion determinations p 33 A82-32090
A comparison of pole positions derived from GPS satellite and Navy navigation satellite observations
[AD-A110765] p 39 N82-26268
POLARIZED LIGHT
A model of plant canopy polarization
[E82-10233] p 15 N82-23606
POLLUTION MONITORING
Problems of the interpretation of aerial and satellite images of industrial smoke p 23 A82-30307
Detection of regional air pollution episodes utilizing satellite digital data in the visual range
p 23 A82-31990
Depression of brightness temperature of sea surfaces covered with monomolecular oil films relative to clean water surfaces at 1 43 GHz p 54 A82-33322
EPA's new bubble and banking policies --- for environmental monitoring p 25 A82-33865
The use of remote-sensing data to identify the space-time variability of the quality of natural waters
p 62 A82-35138
Aircraft measurements of NO/x/ in the lower troposphere above the coast of Japan
p 26 A82-36247
Tropospheric CO measurement experiment from the second Space Shuttle flight p 27 A82-36292
A quantitative multispectral analysis system for aerial photographs applied to coastal planning
p 55 A82-37505
Feasibility of laser-separation of 36 S and its use as an atmospheric tracer
[DE82-000965] p 30 N82-27737
POLLUTION TRANSPORT
Aircraft measurements of NO/x/ in the lower troposphere above the coast of Japan
p 26 A82-36247
A study of atmospheric diffusion from the LANDSAT imagery --- pollution transport over the ocean
[E82-10360] p 58 N82-26758
Feasibility of laser-separation of 36 S and its use as an atmospheric tracer
[DE82-000965] p 30 N82-27737
Field measurements in support of dispersion modeling in complex terrain (1980)
[PB82-148644] p 39 N82-27882
POSITION (LOCATION)
A comparison of pole positions derived from GPS satellite and Navy navigation satellite observations
[AD-A110765] p 39 N82-26268
POSITRONS
The cosmic ray positron spectrum p 1 A82-22542
The electron and positron spectra in primary cosmic rays p 1 A82-22543
Dependence of earth spectrum of positrons and antiprotons on propagation models --- of cosmic radiation p 21 A82-22545
POSTMISSION ANALYSIS (SPACECRAFT)
OSTA-1 Post Mission Operation Report
[NASA-TM-84191] p 84 N82-23258
POTASSIUM
Airborne gamma-ray spectrometer and magnetometer survey Roseau quadrangle, Minnesota, volume 2
[DE82-001025] p 44 N82-23634
Airborne gamma-ray spectrometer and magnetometer survey Bemidji quadrangle, Minnesota, volume 2
[DE82-001026] p 44 N82-23638
Airborne gamma-ray spectrometer and magnetometer survey, Kingston quadrangle New York, volume 2C
[DE81-027161] p 46 N82-25621
Airborne gamma-ray spectrometer and magnetometer survey, Rochester quadrangle New York, volume 2D
[DE81-027156] p 46 N82-25622
Airborne gamma-ray spectrometer and magnetometer survey Lookout Ridge quadrangle, Alaska, volume 2
[DE82-000313] p 47 N82-25625
Airborne gamma-ray spectrometer and magnetometer survey Sioux Falls quadrangle, South Dakota, volume 1
[DE82-005533] p 47 N82-27806
POTENTIAL FIELDS
Spherical-Earth gravity and magnetic anomaly modeling by Gauss-Legendre quadrature integration
[E82-10242] p 36 N82-24520
POWER SPECTRA
Terrain classification by Fourier analysis - Accuracy and economy p 69 A82-34723
Investigation of Antarctic crust and upper mantle using MAGSAT and other geophysical data
[E82-10308] p 37 N82-24582
PRECIPITATION (METEOROLOGY)
Remote sensing of precipitable water over the oceans from Nimbus 7 microwave measurements
p 49 A82-28907
PRIMARY COSMIC RAYS
The electron and positron spectra in primary cosmic rays p 1 A82-22543
Comparison of the measured antiproton flux with that predicted by the 'leaky box' model p 1 A82-22544
The galactic origin of cosmic rays I
[CONF-810711-1] p 2 A82-22565
Origin of cosmic rays in galactic centre sources
p 3 A82-22571
The energy spectra of cosmic ray variations inferred from the stratospheric measurements in 1972-1979
p 5 A82-22617
Primary spectral variations of cosmic rays above 1 GV
p 5 A82-22618
PRIMITIVE EQUATIONS
Impact of additional summer MONEX wind data on the prediction of monsoon depressions during June - August 1979 with two versions of primitive equation (PE) barotropic model --- Monsoon Experiment (MONEX)
p 56 N82-23900
PRINTED CIRCUITS
Effective electromagnetic shielding in multilayer printed circuit boards
[AIAA 81-2333] p 59 A82-13528
PROBABILITY DENSITY FUNCTIONS
Dependent feature trees for density approximation I - Optimal construction and classification results
p 67 A82-32344
PROBABILITY THEORY
The use of prior probabilities in maximum likelihood classification of remotely sensed data
p 68 A82-32904
PROJECT PLANNING
Plan of research for integrated soil moisture studies Recommendations of the Soil Moisture Working Group
[NASA-TM-84731] p 18 N82-25608
PROPAGATION MODES
A report on the 'cosmic ray propagation problem'
p 1 A82-22539
PROTON ENERGY
Origin of cosmic rays in galactic centre sources
p 3 A82-22571
High-energy solar protons p 22 A82-22588
PROTON FLUX DENSITY
Evolution of the solar proton spectrum in interplanetary space p 4 A82-22594
Comparison of solar proton activity in 1967 and 1969 with that in 1978 and 1979 as measured onboard Venera 4, 6, 11, 12 space probes p 31 A82-22596
The solar proton fluxes in April, 1979
p 66 A82-22597
A description of relativistic solar particle propagation
p 4 A82-22600
Non-flare injection of protons into interplanetary space
p 4 A82-22601
On the anticorrelation between the He/3//He/4/ ratio and proton intensity in He/3/ rich flares
p 40 A82-22613
The energy spectra of cosmic ray variations inferred from the stratospheric measurements in 1972-1979
p 5 A82-22617
PULSARS
Pulsar models and cosmic-ray acceleration
p 21 A82-22570
PULSE RADAR
Pulse-to-pulse correlation in satellite radar altimeters --- for ocean wave height measurement p 55 A82-37390

Q

QUANTITATIVE ANALYSIS
Quantitative relationships of near-surface spectra to Landsat radiometric data p 78 A82-32912
QUANTUM THEORY
Astrophysical scenarios for critically evaluating a zero-point field acceleration mechanism
p 64 A82-22575
QUARTZ
Influence of CO2 on melting of model granulite facies assemblages - A model for the genesis of charnockites
p 42 A82-36298

R

RADAR
Movement of ice markers measured by satellite ranging
[R-240] p 59 N82-27816
RADAR CROSS SECTIONS
The relationship between wind vector and normalized radar cross section used to derive Seasat-A Satellite Scatterometer winds p 51 A82-29617
RADAR DETECTION
Possible fault detection in Cottonball Basin, California An application of radar remote sensing
p 41 A82-32898
RADAR ECHOES
Characteristics of field-aligned E-region irregularities over Ioka /36 N/, Japan I p 26 A82-36268
RADAR EQUIPMENT
Pulse-to-pulse correlation in satellite radar altimeters --- for ocean wave height measurement p 55 A82-37390
RADAR GEOLOGY
An investigation into the utilization of HCMM thermal data for the discrimination of volcanic and Eolian geological units --- Newberry Volcano, Oregon
[E82-10352] p 47 N82-26750
RADAR IMAGERY
A simulation study of soil moisture estimation by a space SAR p 60 A82-29333
The observation of ocean surface phenomena using imagery from the Seasat synthetic aperture radar - An assessment p 52 A82-29623

The estimation of wave height from digitally processed SAR imagery p 67 A82-32347
On the synthetic aperture radar imaging of ocean surface waves p 53 A82-32881
Ocean wave height measurement with SEASAT SAR using speckle diversity p 53 A82-32882
Possible fault detection in Cottonball Basin, California An application of radar remote sensing p 41 A82-32898
Interpretation of vegetative cover in wetlands using four-channel SAR imagery p 9 A82-34706
C-band radar for determining surface soil moisture p 10 A82-37194
Evaluation of the soil moisture prediction accuracy of a space radar using simulation techniques --- Kansas [E82-10351] p 19 N82-26749

RADAR MEASUREMENT
Airborne lidar measurements of the Soufriere eruption of 17 April 1979 p 24 A82-33657
The use of soil texture and field capacity to normalize microwave soil moisture measurements Some problems p 20 N82-26762

RADAR SCATTERING
Characteristics of 13 9 GHz radar scattering from oil films on the sea surface p 54 A82-33438
The use of soil texture and field capacity to normalize microwave soil moisture measurements Some problems p 20 N82-26762

RADAR TARGETS
The recognition of extended targets - SAR images for level and hilly terrain p 33 A82-31994

RADIANCE
Surface temperature determination from an amalgamation of GOES and TIROS-N radiance measurements p 66 A82-28905
Effect of atmospheric conditions on remote sensing of vegetation parameters p 24 A82-32901
Influence of sky radiance distribution on the ratio technique for estimating bidirectional reflectance p 70 A82-35650
Ground support data from July 10 to July 29, 1978, for HCMM thermal satellite data of the Powder River Basin, Wyoming [E82-10211] p 72 N82-23584

RADIANT FLUX DENSITY
The charge and isotopic composition of Z equals 7-16 cosmic ray nuclei at their source p 64 A82-22555
Comparison of brightness indicatrixes of snow cover measured from an aircraft and calculated theoretically for different heights of the atmosphere p 62 A82-35140

RADIATION COUNTERS
Relating Landsat digital count values to ground reflectance for optically thin atmospheric conditions p 66 A82-29762

RADIATION DISTRIBUTION
Derivation of the distribution of synchrotron emissivity in the Galaxy from the 408 MHz all-sky survey p 82 A82-22549
Influence of sky radiance distribution on the ratio technique for estimating bidirectional reflectance p 70 A82-35650

RADIATION HAZARDS
Environmental monitoring report of the Lawrence Berkeley Laboratory, 1980 [LBL-12604] p 29 N82-23793

RADIATION MEASUREMENT
Comparison of satellite derived radiation budget measurements over MONEX during 1979 to 1980 --- Monsoon Experiment (MONEX) p 29 N82-23891

RADIATION PRESSURE
Cosmic ray acceleration by stellar winds I - Total density, pressure and energy flux p 21 A82-22566

RADIATION SOURCES
The charge and isotopic composition of Z equals 7-16 cosmic ray nuclei at their source p 64 A82-22555
Mass per charge ratio in hot plasmas and cosmic ray source composition p 2 A82-22557
The galactic origin of cosmic rays II [CONF-810711-2] p 64 A82-22573

RADIATION SPECTRA
Airborne gamma-ray spectrometer and magnetometer survey Roseau quadrangle, Minnesota, volume 1 [DE82-001031] p 43 N82-23621
Airborne gamma-ray spectrometer and magnetometer survey Hibbing quadrangle, Minnesota, volume 1 [DE82-004159] p 44 N82-23639
Airborne gamma-ray spectrometer and magnetometer survey Hibbing quadrangle, Minnesota, volume 2 [DE82-004165] p 45 N82-23640
Airborne gamma-ray spectrometer and magnetometer survey Aberdeen quadrangle, South Dakota, volume 1 [DE82-004152] p 45 N82-23641
Airborne gamma-ray spectrometer and magnetometer survey Aberdeen quadrangle, South Dakota, volume 2 [DE82-004164] p 45 N82-23642

RADIATIVE TRANSFER
A comparative study of microwave radiometer observations over snowfields with radiative transfer model calculations --- for water runoff estimation p 60 A82-32910
Spatial thermal radiometry contribution to the Massif Armoricain and the Massif Central France litho-structural study [E82-10190] p 42 N82-22624
Application of HCMM data to regional geologic analysis for mineral and energy resource evaluation [E82-10243] p 45 N82-24521
Multispectral determination of soil moisture-2 --- Guymon, Oklahoma and Dalhart, Texas [E82-10349] p 19 N82-26747

RADIO ALTIMETERS
The Seasat altimeter data and its accuracy assessment p 49 A82-29602
Seasat altimeter height calibration --- related to sea surface heights near Bermuda p 49 A82-29603
Tidal and geodetic observations for the Seasat altimeter calibration experiment p 49 A82-29604
An empirical determination of the effects of sea state bias on Seasat altimetry p 50 A82-29607
Sea-state-related altitude errors in the Seasat radar altimeter p 50 A82-29608
Seasat altimeter timing bias estimation p 50 A82-29609
Evaluation of the Seasat altimeter time tag bias p 50 A82-29610
Comparison data for Seasat altimetry in the western North Atlantic p 50 A82-29611
Waveheight and wind speed measurements from the Seasat radar altimeter p 50 A82-29612
Seasat altimeter determination of ocean current variability p 50 A82-29613
The Seasat altimeter mean sea surface model p 51 A82-29614
Pulse-to-pulse correlation in satellite radar altimeters --- for ocean wave height measurement p 55 A82-37390

RADIO AURORAS
Large amplitude undulations on the equatorward boundary of the diffuse aurora p 76 A82-31019

RADIO EMISSION
Angular variations of nonthermal radio emission from the Galaxy relevant to the structure of interstellar magnetic field p 83 A82-22550

RADIO FREQUENCY INTERFERENCE
Inference of refractivity profiles by satellite-to-ground RF measurements p 78 A82-33442

RADIO PROBING
Influence of sky radiance distribution on the ratio technique for estimating bidirectional reflectance p 70 A82-35650

RADIO SOURCES (ASTRONOMY)
The definition of the terrestrial coordinate frame by long baseline interferometry p 33 A82-32084
Some considerations in the use of very-long-baseline-interferometry to establish reference coordinate systems for geodynamics p 34 A82-32096

RADIO WAVE REFRACTION
Inference of refractivity profiles by satellite-to-ground RF measurements p 78 A82-33442

RADIOMETERS
Evaluation of NOAA-AVHRR data for crop assessment --- Advanced Very High Resolution Radiometer p 8 A82-34179
Airborne gamma-ray spectrometer and magnetometer survey Devil's Lake quadrangle, North Dakota, volume 2 [DE82-004168] p 44 N82-23636
Airborne gamma-ray spectrometer and magnetometer survey, Toronto quadrangle New York, volume 2A [DE81-027158] p 46 N82-25620
Airborne gamma-ray spectrometer and magnetometer survey, Rochester quadrangle New York, volume 2D [DE81-027156] p 46 N82-25622
Irrigation management with remote sensing --- Navajo Indian Irrigation Project [E82-10357] p 20 N82-26755
Satellite observations in FRONTS 80 [AD-A111080] p 58 N82-26766
Airborne gamma-ray spectrometer and magnetometer survey North/south tieline, volume 1 [DE82-005542] p 47 N82-27804

RADIOMETRIC CORRECTION
Quantitative relationships of near-surface spectra to Landsat radiometric data p 78 A82-32912
View angle effects in the radiometric measurement of plant canopy temperatures p 8 A82-32914
Measuring sea surface temperature from satellites - A ground truth approach p 54 A82-32917

RADIOMETRIC RESOLUTION
Evaluation of VICAR software capability for land information support system needs --- Elk River quadrangle, Idaho [E82-10223] p 73 N82-23596

RAIN
A statistical approach to rainfall estimation using satellite and conventional data [NOAA-TR-NESS-89] p 63 N82-22854

RANGELANDS
Estimating rangeland cover proportions with large-scale color-infrared aerial photographs p 6 A82-29534
An analysis of LANDSAT MSS scene-to-scene registration accuracy [E82-10285] p 16 N82-24563

REFLECTANCE
Application of Computer Axial Tomography (CAT) to measuring crop canopy geometry --- corn and soybeans [E82-10227] p 14 N82-23600
Canopy reflectance as influenced by solar illumination angle [E82-10237] p 15 N82-23610
Irrigated acreage in the Bear River Basin as of the 1975 growing season --- Idaho, Utah, and Wyoming [E82-10356] p 20 N82-26754

REFLECTED WAVES
System albedo as sensed by satellites - Its definition and variability p 23 A82-32342

REFRACTIVITY
Inference of refractivity profiles by satellite-to-ground RF measurements p 78 A82-33442

REGIONAL PLANNING
A legislator's guide to LANDSAT [E82-10290] p 85 N82-24568

REGRESSION ANALYSIS
A comparison of stratified versus regression estimators p 11 N82-23133

RELATIVISTIC ELECTRON BEAMS
Steady-state cosmic ray electron spectrum under diffusion, convection, adiabatic deceleration and synchrotron losses p 1 A82-22552

RELATIVISTIC PARTICLES
A description of relativistic solar particle propagation p 4 A82-22600

RELIABILITY ENGINEERING
A practical study of gross-error detection in bundle adjustment p 69 A82-34702

RELIEF MAPS
Bathymetric imaging p 69 A82-34720

REMOTE SENSING
Detection of environmental disturbance using color aerial photography and thermal infrared imagery p 22 A82-29327
A simulation study of soil moisture estimation by a space SAR p 60 A82-29333
Remote sensing of the weediness of crop fields p 5 A82-29435
Color aerial photography in the plant sciences and related fields, Proceedings of the Eighth Biennial Workshop, Luray, VA, April 21-23, 1981 p 5 A82-29526
Development and application of panoramic aerial photography in forest pest management p 5 A82-29527
Riparian vegetation mapping in Northeastern California using high altitude color infrared aerial photography p 5 A82-29528
Inventory of wildlife habitat from color infrared aerial photography for Cobb Island, Virginia p 6 A82-29529
Color aerial photography detects nutrient status of loblolly pine plantations p 6 A82-29531
Application of 35mm color aerial photography to forest land change detection p 6 A82-29533
Remote sensing of Douglas-fir trees newly infested by bark beetles p 6 A82-29536
Spectral scanning of experimental plots of SO2-affected winter wheat and soybeans for mission planning p 6 A82-29537
Application of scanning microdensitometer data in selected plant science case studies p 7 A82-29539
The Seasat-A satellite scatterometer - The geophysical evaluation of remotely sensed wind vectors over the ocean p 51 A82-29616
Desert locust habitat monitoring with satellite remote sensing A new technology for an old problem p 7 A82-29747
Thermography - A remote sensing method with many perspectives p 76 A82-29922
Space to the earth --- Russian book on space technology applications p 83 A82-30850
The use of the SPOT satellite in natural resource evaluation p 83 A82-31996
Extraction of line shaped objects from aerial images using a special operator to analyze the profiles of functions p 67 A82-32033

Remote sensing of tornadic storms from geosynchronous satellite infrared digital data p 23 A82-32348
Imaging spectroscopy, Proceedings of the Seminar, Los Angeles, CA, February 10, 11, 1981 p 77 A82-32440
Spectroscopic remote sensing for geological applications p 41 A82-32442
High spectral resolution airborne spectrometry p 77 A82-32443
Laser-induced bioluminescence --- for remote sensing of marine organisms p 53 A82-32559
Impacts of remote sensing on U S geography p 24 A82-32899
Effect of atmospheric conditions on remote sensing of vegetation parameters p 24 A82-32901
Infrared sensing of sea surface temperature from space p 53 A82-32902
Nearshore current pattern off south Texas - An interpretation from aerial photographs p 53 A82-32903
The use of prior probabilities in maximum likelihood classification of remotely sensed data p 68 *A82-32904*
Quantitative relationships of near-surface spectra to Landsat radiometric data p 78 A82-32912
Snowpack monitoring in North America and Eurasia using passive microwave satellite data p 78 A82-32915
Appearance of irregular tree canopies in nighttime high-resolution thermal infrared imagery p 68 A82-32916
Remote sensing of the earth's resources - The Soviet experience p 84 A82-33555
Irradiance measurement errors due to the assumption of a Lambertian reference panel p 79 A82-34222
ERS-1 European remote sensing satellite p 84 A82-34367
American Society of Photogrammetry, Annual Meeting, 47th, Washington, DC, February 22-27, 1981, ASP Technical Papers p 79 A82-34701
Image processing with microcomputers in remote sensing p 79 A82-34708
Site selection and engineering issues for a major industrial complex - Application of image and map interpretation p 25 A82-34711
RAMS-1, a Resource Analysis and Mapping System p 69 *A82-34726*
Remote sensing of thermal subsurface terrain properties p 80 A82-34727
Remote sensing - A potential aid in the preparation of an urban tree inventory p 9 A82-34732
Monitoring deforestation in the eastern part of the state of Guerrero, Mexico p 9 A82-34733
Digital and visual evaluation of GOES and TIROS/NOAA image data for cover type effects on snowfield observations p 60 A82-34735
A new approach to multiresource inventories using remote sensing and geographic information systems technologies p 25 A82-34739
Comparisons of land cover classifications from selected remote sensing systems p 80 A82-34746
Study of the hydrological cycle by aerospace methods --- Russian book p 61 A82-35126
Principles and methods of the study of the hydrological cycle on the basis of aerospace data p 61 A82-35127
The possibility of using remote-sensing methods to study the hydrology of elementary watersheds p 61 A82-35130
The seasonal snow-line within the Fergana basin and the possibility of using it for hydrological forecasting p 61 A82-35131
The use of remote-sensing data to identify the space-time variability of the quality of natural waters p 62 A82-35138
Status and prospects of the automated processing of remote-sensing data /using forest surveys as an example/ p 10 A82-35139
Allowance for the effect of the atmosphere in the processing of satellite remote-sensing images p 70 A82-35141
The use of microwave radiometry for the determination of snow cover height p 80 A82-36018
Microwave measurement of stratospheric and mesospheric ozone p 28 A82-36415
Space science for applications - The history of Landsat p 84 A82-36617
Satellite radiation measurements for the retrieval of the vertical temperature profiles p 70 A82-36935
Landsat D to yield more precise data p 70 A82-37200
Spatial resolution requirements for urban studies p 29 A82-37502
Remote sensing of salt marsh vegetation in the first four proposed Thematic Mapper bands p 10 A82-37503
Advanced technology for earth observation - Data processing
[AAS PAPER 82-130] p 71 A82-37810
Solid state instrumentation concepts for earth resource observation
[AAS PAPER 82-132] p 81 A82-37812
Civil land remote sensing system
[GPO-87-070] p 84 N82-22630
Use of NOAA/AVHRR visible and near-infrared data for land remote sensing
[NASA-TM-84186] p 81 N82-22643
AgRISTARS Renewable resources inventory Land information support system implementation plan and schedule --- San Juan National Forest pilot test
[E82-10224] p 14 N82-23597
Agricultural Research Service research highlights in remote sensing for calendar year 1980
[E82-10228] p 14 N82-23601
Cost-effectiveness of geographic surveying from space p 85 N82-24263
Plan of research for integrated soil moisture studies Recommendations of the Soil Moisture Working Group
[NASA-TM-84731] p 18 *N82-25608*
Experimental assessment of improved spatial resolution LANDSAT data
[AD-A110538] p 75 N82-26765
Rapid oceanographic data gathering Some problems in using remote sensing to determine the horizontal and vertical thermal distributions in the Northeast Pacific Ocean
[AD-A111005] p 58 N82-26945
Remote sensing of sulfur dioxide effects on vegetation *Volume 1 Summary*
[DE82-900580] p 31 N82-27802
Remote sensing of sulfur dioxide effects on vegetation Volume 2 Data
[DE82-900581] p 31 N82-27803

REMOTE SENSORS
Magnetic anomalies as a reference for ground-speed *and map-matching navigation* p 32 *A82-30314*
A system design for a multispectral sensor using two-dimensional solid-state imaging arrays p 77 A82-31991
Inversion of data from diffraction-limited multiwavelength remote sensors II - Nonlinear dependence of observables on the geophysical parameters p 77 A82-32658
An optical objective lens for earth observations by satellites p 78 A82-32824
View angle effects in the radiometric measurement of plant canopy temperatures p 8 A82-32914
Characteristics of 13 9 GHz radar scattering from oil films on the sea surface p 54 A82-33438
EPA's new bubble and banking policies --- for environmental monitoring p 25 A82-33865
An information-theoric spatial transform p 69 A82-34717
Bathymetric imaging p 69 A82-34720
Longwave infrared observation of urban landscapes p 25 A82-34744
Evaluation of the accuracy of water-surface temperature measurement by means of airborne infrared radiometers p 62 A82-35136
Microwave sensing from space
[AAS PAPER 82-127] *p 80 A82-37809*
Orbiting passive microwave sensor simulation applied to soil moisture estimation
[E82-10343] p 18 N82-25605
In situ ozone data for comparison with laser absorption remote sensor 1980 PEPE/NEROS program
[NASA-TM-84471] p 30 N82-25661

RESEARCH
Agricultural Research Service research highlights in remote sensing for calendar year 1980
[E82-10228] p 14 N82-23601

RESEARCH FACILITIES
Environmental monitoring report of the Lawrence Berkeley Laboratory, 1980
[LBL-12604] p 29 *N82-23793*

RESEARCH MANAGEMENT
Plan of research for integrated soil moisture studies Recommendations of the Soil Moisture Working Group
[NASA-TM-84731] p 18 N82-25608

RESERVOIRS
Dynamic study of the upper Sao Francisco river and Tres Marias reservoir using MSS/LANDSAT images --- BRazil
[E82-10291] p 63 N82-24569

RESIDENTIAL AREAS
Detecting residential land-use development at the urban fringe p 22 A82-29332

RESOURCES MANAGEMENT
Multi-resource inventory in interior Alaska p 6 A82-29532
Streamlining and ensuring mineral development must *begin at local land management levels*
[EMD-82-10] p 29 N82-23043
Agricultural Research Service research highlights in remote sensing for calendar year 1980
[E82-10228] p 14 N82-23601
AgRISTARS Agriculture and resources inventory surveys through aerospace remote sensing
[E82-10236] p 15 *N82-23609*
Remote automatic weather station for resource and fire management agencies
[PB82-107335] p 30 N82-23963
A legislator's guide to LANDSAT
[E82-10290] p 85 N82-24568

RESPONSE BIAS
Bias correction procedures for airborne laser hydrography
[PB82-130089] p 63 N82-22644

RETURN BEAM VIDICONS
Comparisons of land cover classifications from selected remote sensing systems p 80 A82-34746

RHEOLOGY
Fluid-sediment interactions on beaches and shelves
[AD-A110838] p 59 N82-26948

RING CURRENTS
Improved definition of crustal magnetic anomalies for MAGSAT data
[E82-10314] p 37 N82-24587

RIVER BASINS
The seasonal snow-line within the Fergana basin and the possibility of using it for hydrological forecasting p 61 A82-35131
The use of satellite photographs to study snow-cover dynamics and to determine the average water discharge of the Amudarya during a vegetation period p 61 A82-35132
Analysis of thematic mapper simulator data acquired during winter season over Pearl River, Mississippi, test site
[E82-10287] p 17 N82-24565
Irrigated acreage in the Bear River Basin as of the 1975 growing season --- Idaho, Utah, and Wyoming
[E82-10356] *p 20 N82-26754*

RIVERS
The use of satellite photographs to study snow-cover dynamics and to determine the average water discharge of the Amudarya during a vegetation period p 61 A82-35132
Airborne gamma-ray spectrometer and magnetometer survey Utukik River quadrangle, Alaska, volume 2
[DE82-000316] p 44 N82-23631
Dynamic study of the upper Sao Francisco river and Tres Marias reservoir using MSS/LANDSAT images --- BRazil
[E82-10291] p 63 N82-24569

ROCKS
The mineralogy of global magnetic anomalies --- rock magnetic signatures and MAGSAT geological, and gravity correlations in West Africa
[E82-10305] p 45 N82-24579

RODS
Nonlinear theory for elastic beams and rods and its finite element representation
[WTHD-143] p 73 N82-24517

RURAL LAND USE
Monitoring deforestation in the eastern part of the state of Guerrero, Mexico p 9 A82-34733
Analysis of scanner data for crop inventories
[E82-10192] p 10 N82-22626
Determination of the optimal level for combining area and yield estimates
[E82-10215] p 12 N82-23588

S

SALINITY
Problems associated with remotely detecting and monitoring saline sites within irrigated Alberta p 9 A82-34710

SANDS
Remote sensing in Scotland using data received from satellites - A study of the Tay Estuary region using Landsat multispectral scanning imagery p 62 A82-37501
Fluid-sediment interactions on beaches and shelves
[AD-A110838] p 59 N82-26948

SATELLITE ANTENNAS
Movement of ice markers measured by satellite ranging
[R-240] p 59 N82-27816

SATELLITE DESIGN
LANDSAT-D thermal analysis and design support
[E82-10346] p 82 N82-26744

SATELLITE GROUND SUPPORT
Advanced technology for earth observation - Data *processing*
[AAS PAPER 82-130] p 71 A82-37810

SATELLITE GROUND TRACKS
Evaluation of the Seasat altimeter time tag bias p 50 A82-29610
SATELLITE OBSERVATION
Solar gamma-ray experiment on Astro-A satellite p 21 A82-22583
The relation of type II radio bursts to solar energetic particles observed at earth p 3 A82-22591
A survey of solar protons and alpha differential spectra between 1 and greater than 400 MeV/nucleon p 4 A82-22592
Energetic solar particle spectra according to Venera-11, 12 and Prognoz-5, 6 p 4 A82-22593
Spacecraft determination of energetic particle propagation parameters - The 1 January 1978 solar event p 31 A82-22598
Low-energy particles in interplanetary magnetic field near the sectorial boundary on September 26, 1977 p 4 A82-22602
Surface temperature determination from an amalgamation of GOES and TIROS-N radiance measurements p 66 A82-28905
The observation of ocean surface phenomena using imagery from the Seasat synthetic aperture radar - An assessment p 52 A82-29623
A study of the earth's radiation budget using a general circulation model p 52 A82-30666
Magsat scalar anomaly distribution - The global perspective p 41 A82-30786
A satellite magnetic model of northeastern South American aulacogens p 33 A82-30795
Extremely high latitude auroras p 76 A82-31020
Emissivity and reflectance of the model sea surface for the use of AVHRR data of NOAA satellites p 52 A82-31294
Origin and scale of coordinate systems in satellite geodesy p 34 A82-32099
System albedo as sensed by satellites - Its definition and variability p 23 A82-32342
Geoid height-age relation from Seasat altimeter profiles across the Mendocino Fracture Zone p 34 A82-32646
An optical objective lens for earth observations by satellites p 78 A82-32824
Geostationary satellite observations of the April 1979 Soufriere eruptions p 24 A82-33654
Earth observations from space - Trends and prospects p 84 A82-34116
Observed magnetic substorm signatures at synchronous altitude p 26 A82-35534
Estimation of the precipitable water from the IR channel of the geostationary satellite p 55 A82-37196
Soft X-rays from the sunlit earth's atmosphere p 29 A82-37405
Microwave sensing from space [AAS PAPER 82-127] p 80 A82-37809
A statistical approach to rainfall estimation using satellite and conventional data [NOAA-TR-NESS-89] p 63 N82-22854
Comparison of satellite derived radiation budget measurements over MONEX during 1979 to 1980 --- Monsoon Experiment (MONEX) p 29 N82-23891
History of the French satellite space program p 85 N82-24216
A comparison of pole positions derived from GPS satellite and Navy navigation satellite observations [AD-A110765] p 39 N82-26268
SATELLITE SOUNDING
Magnetic charts of Canada derived from Magsat data p 32 A82-30778
Initial scalar magnetic anomaly map from Magsat p 32 A82-30784
Remote sensing of tornadic storms from geosynchronous satellite infrared digital data p 23 A82-32348
Satellite observations of sea surface temperature around the British Isles p 54 A82-33717
Total ozone retrieval from satellite Meteor 28 Fourier spectrometer measurements p 28 A82-36422
Satellite radiation measurements for the retrieval of the vertical temperature profiles p 70 A82-36935
SATELLITE TELEVISION
The seasonal snow-line within the Fergana basin and the possibility of using it for hydrological forecasting p 61 A82-35131
SATELLITE TEMPERATURE
LANDSAT-D thermal analysis and design support [E82-10346] p 82 N82-26744
SATELLITE TRACKING
Spatial resolution and repeatability of Magsat crustal anomaly data over the Indian Ocean p 32 A82-30788
Representativeness of cloud motion winds deduced from GOES Indian Ocean satellite imagery for the description of the Indian summer monsoon --- superpressure balloons for the study of the Indian summer monsoon (BALSAMINE) p 55 N82-23879
SATELLITE TRANSMISSION
Purpose, background of 'Intercosmos-21' mission p 81 N82-24264
SATELLITE-BORNE INSTRUMENTS
Seasat measurement system evaluation - Achievements and limitations p 49 A82-29601
The Seasat altimeter data and its accuracy assessment p 49 A82-29602
Tidal and geodetic observations for the Seasat altimeter calibration experiment p 49 A82-29604
Waveheight and wind speed measurements from the Seasat radar altimeter p 50 A82-29612
Seasat altimeter determination of ocean current variability p 50 A82-29613
The Seasat altimeter mean sea surface model p 51 A82-29614
The Seasat-A satellite scatterometer - The geophysical evaluation of remotely sensed wind vectors over the ocean p 51 A82-29616
The relationship between wind vector and normalized radar cross section used to derive Seasat-A Satellite Scatterometer winds p 51 A82-29617
Evaluation of atmospheric attenuation from SMMR brightness temperature for the Seasat satellite scatterometer p 51 A82-29618
Intercomparison of wind speeds inferred by the SASS, altimeter, and SMMR p 52 A82-29621
Description of Seasat radiometer status and results p 52 A82-29622
Seasat wind and wave observations of northeast Pacific hurricane Iva, August 13, 1978 p 52 A82-29624
Space to the earth --- Russian book on space technology applications p 83 A82-30850
Inference of refractivity profiles by satellite-to-ground RF measurements p 78 A82-33442
Evaluation of NOAA-AVHRR data for crop assessment --- Advanced Very High Resolution Radiometer p 8 A82-34179
Allowance for the effect of the atmosphere in the processing of satellite remote-sensing images p 70 A82-35141
Application of satellite magnetic anomaly data to Curie isotherm mapping p 70 A82-35824
Pulse-to-pulse correlation in satellite radar altimeters --- for ocean wave height measurement p 55 A82-37390
Advanced technology for earth observation - Data processing [AAS PAPER 82-130] p 71 A82-37810
LANDSAT-D conical scanner evaluation plan [E82-10340] p 81 N82-25602
Orbiting passive microwave sensor simulation applied to soil moisture estimation [E82-10343] p 18 N82-25605
SATELLITE-BORNE PHOTOGRAPHY
The use of residual images in Landsat image analysis p 66 A82-29328
Satellite image interpretation of the eastern Caledonian part of the Blue Road Geotraverse and its geological implications /Nordland, Vasterbotten, Scandinavia/ p 41 A82-30305
Problems of the interpretation of aerial and satellite images of industrial smoke p 23 A82-30307
Large amplitude undulations on the equatorward boundary of the diffuse aurora p 76 A82-31019
Detection of volcanic smoke and ash-fall area at volcano Aso, from Landsat MSS data p 23 A82-31295
Detection of regional air pollution episodes utilizing satellite digital data in the visual range p 23 A82-31990
Dependent feature trees for density approximation I - Optimal construction and classification results p 67 A82-32344
Evaluation of temporal registration of Landsat scenes p 67 A82-32345
The use of contextual information to detect cumulus clouds and cloud shadows in Landsat data p 67 A82-32346
Resource inventory techniques used in the California Desert Conservation Area p 23 A82-32441
Digitally enhanced visual displays facilitate the analysis of Landsat imagery p 67 A82-32507
A ship and satellite view of hydrographic features in the western Gulf of Mexico p 53 A82-32651
Landsat detection of hardwood forest clearcuts p 8 A82-32708
Computation with physical values from Landsat digital data p 68 A82-32709
Geographic location of individual pixels --- for thermal infrared digital data processing p 68 A82-32900
Monitoring land-cover change by principal component analysis of multitemporal Landsat data p 68 A82-32906
The response characteristics of vegetation in Landsat MSS digital data p 8 A82-32907
Field size, length, and width distributions based on LACIE ground truth data --- large area crop inventory experiment p 8 A82-32909
Terrain analysis from Landsat using a color TV enhancement system p 68 A82-32911
Problems associated with remotely detecting and monitoring saline sites within irrigated Alberta p 9 A82-34710
Comparing lineaments interpreted from Landsat imagery and topographic maps with reported faults in southwest Montana p 34 A82-34719
Landsat in the search for Appalachian hydrocarbons p 42 A82-34721
Digital and visual evaluation of GOES and TIROS/NOAA image data for cover type effects on snowfield observations p 60 A82-34735
A new approach to multiresource inventories using remote sensing and geographic information systems technologies p 25 A82-34739
The use of Skylab S-190B photography for small scale mapping p 80 A82-34742
Study of the hydrological cycle by aerospace methods --- Russian book p 61 A82-35126
Principles and methods of the study of the hydrological cycle on the basis of aerospace data p 61 A82-35127
Water-balance differentiation of natural complexes on the basis of satellite photographs p 61 A82-35129
The use of satellite photographs to study snow-cover dynamics and to determine the average water discharge of the Amudarya during a vegetation period p 61 A82-35132
Method for the analysis of the melting of a firn complex on the basis of aerospace photographs p 61 A82-35133
Experience with the compilation of maps of snow-cover melting in the central part of the European USSR on the basis of satellite data p 62 A82-35134
Status and prospects of the automated processing of remote-sensing data /using forest surveys as an example/ p 10 A82-35139
The meteorological product - 'Cloud-top height' p 70 A82-36043
Space science for applications - The history of Landsat p 84 A82-36617
Design guidelines for satellite image data distribution systems p 70 A82-37048
The use of space photographs in the mapping of glaciers and water bodies p 62 A82-37174
Determination of winter temperature patterns, fronts, and surface currents in the Yellow Sea and East China Sea from satellite imagery p 55 A82-37195
Significance of tectonics in linear feature detection and interpretation on satellite images p 42 A82-37198
Landsat D to yield more precise data p 70 A82-37200
SCALE (RATIO)
Origin and scale of coordinate systems in satellite geodesy p 34 A82-32099
SCANNING
Application of scanning microdensitometer data in selected plant science case studies p 7 A82-29539
SCATTEROMETERS
The Seasat-A satellite scatterometer - The geophysical evaluation of remotely sensed wind vectors over the ocean p 51 A82-29616
The relationship between wind vector and normalized radar cross section used to derive Seasat-A Satellite Scatterometer winds p 51 A82-29617
Evaluation of atmospheric attenuation from SMMR brightness temperature for the Seasat satellite scatterometer p 51 A82-29618
Surface wind analyses for Seasat p 51 A82-29619
Intercomparison of wind speeds inferred by the SASS, altimeter, and SMMR p 52 A82-29621
SEASAT A satellite scatterometer illumination times of selected in situ sites [NASA-TM-83280] p 81 N82-22865
Measurement of soil moisture trends with airborne scatterometers --- Guymon, Oklahoma and Dalhart, Texas [E82-10361] p 20 N82-26759
SCENE ANALYSIS
Landsat digital analysis of the initial recovery of burned tundra at Kokolik River, Alaska p 8 A82-32913
Coastal environment change analysis by Landsat MSS data p 54 A82-34219
Separation of diffuse from sharp-edged features in digital imagery p 68 A82-34225
An analysis of LANDSAT MSS scene-to-scene registration accuracy [E82-10285] p 16 N82-24563
Image understanding research [AD-A110746] p 74 N82-25611

SCHEDULES
AgRISTARS Renewable resources inventory Land information support system implementation plan and schedule --- San Juan National Forest pilot test
[E82-10224] p 14 N82-23597
SEA ICE
Sea-Ice Mission Requirements for the US FIREX and Canada RADARSAT programs
[NASA-CR-168984] p 57 N82-25609
SEA STATES
Seasat altimeter height calibration --- related to sea surface heights near Bermuda p 49 A82-29603
An empirical determination of the effects of sea state bias on Seasat altimetry p 50 A82-29607
Sea-state-related altitude errors in the Seasat radar altimeter p 50 A82-29608
The METEOSAT Data Collection System and its application p 75 N82-26037
SEA TRUTH
A ship and satellite view of hydrographic features in the western Gulf of Mexico p 53 A82-32651
SEA WATER
Technology and oceanography An assessment of Federal technologies for oceanographic research and monitoring Volume 2 Working papers on fishery research technology p 58 N82-26944
SEAMOUNTS
A search for seamounts in the southern Cook and Austral region p 52 A82-30810
SEAS
High resolution satellite observations of mesoscale oceanography in the Tasman Sea, 1978 - 1979
[E82-10324] p 57 N82-24597
SEASAT SATELLITES
Seasat measurement system evaluation - Achievements and limitations p 49 A82-29601
The Seasat altimeter data and its accuracy assessment p 49 A82-29602
Tidal and geodetic observations for the Seasat altimeter calibration experiment p 49 A82-29604
An empirical determination of the effects of sea state bias on Seasat altimetry p 50 A82-29607
Sea-state-related altitude errors in the Seasat radar altimeter p 50 A82-29608
Seasat altimeter timing bias estimation p 50 A82-29609
Evaluation of the Seasat altimeter time tag bias p 50 A82-29610
Waveheight and wind speed measurements from the Seasat radar altimeter p 50 A82-29612
Seasat altimeter determination of ocean current variability p 50 A82-29613
The Seasat altimeter mean sea surface model p 51 A82-29614
Gravity model improvement for Seasat p 32 A82-29615
Evaluation of atmospheric attenuation from SMMR brightness temperature for the Seasat satellite scatterometer p 51 A82-29618
Intercomparison of wind speeds inferred by the SASS, altimeter, and SMMR p 52 A82-29621
Description of Seasat radiometer status and results p 52 A82-29622
The observation of ocean surface phenomena using *imagery from the Seasat synthetic aperture radar - An* assessment p 52 A82-29623
Seasat wind and wave observations of northeast Pacific hurricane Iva, August 13, 1978 p 52 A82-29624
A search for seamounts in the southern Cook and Austral region p 52 A82-30810
The estimation of wave height from digitally processed SAR imagery p 67 A82-32347
Ocean wave height measurement with SEASAT SAR using speckle diversity p 53 A82-32882
Improved land use classification from Landsat and Seasat satellite imagery registered to a common map base p 25 A82-34743
SEASAT-A SATELLITE
Seasat altimeter height calibration --- related to sea *surface heights near Bermuda* p 49 A82-29603
The Seasat-A satellite scatterometer - The geophysical evaluation of remotely sensed wind vectors over the ocean p 51 A82-29616
The relationship between wind vector and normalized radar cross section used to derive Seasat-A Satellite Scatterometer winds p 51 A82-29617
Surface wind analyses for Seasat p 51 A82-29619
SEASAT A satellite scatterometer illumination times of selected in situ sites
[NASA-TM-83280] p 81 N82-22865
SECONDARY COSMIC RAYS
The cosmic ray positron spectrum p 1 A82-22542
SECULAR VARIATIONS
Investigation of geomagnetic field forecasting and fluid dynamics of the core
[E82-10310] p 37 N82-24584
SEDIMENT TRANSPORT
Dynamic study of the upper Sao Francisco river and Tres Marias reservoir using MSS/LANDSAT images --- BRazil
[E82-10291] p 63 N82-24569
SEDIMENTS
Fluid-sediment interactions on beaches and shelves
[AD-A110838] p 59 N82-26948
SEISMOLOGY
Geodetic monitoring of tectonic information Toward a strategy p 35 N82-22832
Seismic and geodetic studies of the Imperial Valley, California
[DE82-001686] p 39 N82-26915
SENSITIVITY
Orbiting passive microwave sensor simulation applied to soil moisture estimation
[E82-10343] p 18 N82-25605
SENSITOMETRY
Sensitometry in Canadian aerial survey p 79 A82-34724
SHADOWS
The use of contextual information to detect cumulus clouds and cloud shadows in Landsat data p 67 A82-32346
SHOCK FRONTS
The model of the cosmic ray enrichment by helium-3 p 31 A82-22614
SHOCK WAVE PROPAGATION
Possible evidence for attenuation of an MHD shock by a magnetic neutral sheet in the solar corona p 3 A82-22589
On the physical sense of the constant of solar cosmic ray coronal propagation p 83 A82-22599
SHOCK WAVES
Mass per charge ratio in hot plasmas and cosmic ray source composition p 2 A82-22557
Observations of the ionization states of energetic particles accelerated in solar flares p 40 A82-22607
SHORELINES
Airborne gamma-ray spectrometer and magnetometer survey Meade River quadrangle, Alaska, volume 2
[DE82-000340] p 43 N82-23626
Airborne gamma-ray spectrometer and magnetometer survey Harrison Bay quadrangle, Alaska, volume 2
[DE82-000315] p 43 N82-23628
Airborne gamma-ray spectrometer and magnetometer survey Beechey Pt, quadrangle, Alaska, volume 2
[DE82-000309] p 43 N82-23629
Airborne gamma-ray spectrometer and magnetometer survey Point Lay quadrangle, Alaska, volume 2
[DE82-000308] p 43 N82-23630
Airborne gamma-ray spectrometer and magnetometer survey Utukik River quadrangle, Alaska, volume 2
[DE82-000316] p 44 N82-23631
Identifying environmental features for land management decisions --- Utah
[E82-10289] p 30 N82-24567
Fluid-sediment interactions on beaches and shelves
[AD-A110838] p 59 N82-26948
SIERRA NEVADA MOUNTAINS (CA)
The application of Heat Capacity Mapping Mission (HCMM) thermal data to snow hydrology --- Salt Verde *Watershed and the southern Sierra Nevada*
[E82-10191] p 62 N82-22625
SIGNAL PROCESSING
Ocean wave height measurement with SEASAT SAR using speckle diversity p 53 A82-32882
SIGNAL TRANSMISSION
Establishing geodetic-geodynamic parameters using lunar laser range measurements p 34 A82-33293
SIGNATURE ANALYSIS
Irrigation management with remote sensing --- Navajo Indian Irrigation Project
[E82-10357] p 20 N82-26755
SILICATES
Laboratory studies of actinide metal-silicate fractionation p 49 A82-22306
SILICON RADIATION DETECTORS
Simplified techniques to study components of solar radiation under haze and clouds p 78 A82-32766
SITE SELECTION
Site selection and engineering issues for a major industrial complex - Application of image and map interpretation p 25 A82-34711
SEASAT A satellite scatterometer illumination times of selected in situ sites
[NASA-TM-83280] p 81 N82-22865
SKY RADIATION
Influence of sky radiance distribution on the ratio technique for estimating bidirectional reflectance p 70 A82-35650
SKYLAB PROGRAM
The use of Skylab S-190B photography for small scale mapping p 80 A82-34742
SLOPES
Structure of the St Francois Mountains and surrounding lead belt, S E Missouri Inferences from thermal IR and other data sets --- Ozard Plateau and St Francois Mountains
[E82-10205] p 11 N82-23578
Topographic slope correction for analysis of thermal infrared images
[E82-10214] p 36 N82-23587
Application of HCMM data to regional geologic analysis for mineral and energy resource evaluation
[E82-10243] p 45 N82-24521
SMOKE
Problems of the interpretation of aerial and satellite images of industrial smoke p 23 A82-30307
Detection of volcanic smoke and ash-fall area at volcano *Aso, from Landsat MSS data* p 23 A82-31295
SMS 1
Geostationary satellite observations of the April 1979 Soufriere eruptions p 24 A82-33654
SNOW
The growth of snow in winter storms - An airborne observational study p 60 A82-33329
SNOW COVER
A comparative study of microwave radiometer observations over snowfields with radiative transfer model calculations --- for water runoff estimation p 60 A82-32910
Snowpack monitoring in North America and Eurasia using passive microwave satellite data p 78 A82-32915
Digital and visual evaluation of GOES and TIROS/NOAA image data for cover type effects on snowfield observations p 60 A82-34735
The seasonal snow-line within the Fergana basin and the possibility of using it for hydrological forecasting p 61 A82-35131
The use of satellite photographs to study snow-cover dynamics and to determine the average water discharge of the Amudarya during a vegetation period p 61 A82-35132
Method for the analysis of the melting of a firn complex *on the basis of aerospace photographs* p 61 A82-35133
Experience with the compilation of maps of snow-cover melting in the central part of the European USSR on the basis of satellite data p 62 A82-35134
Comparison of brightness indicatrixes of snow cover measured from an aircraft and calculated theoretically for different heights of the atmosphere p 62 A82-35140
The use of microwave radiometry for the determination of snow cover height p 80 A82-36018
The application of Heat Capacity Mapping Mission *(HCMM) thermal data to snow hydrology --- Salt Verde* Watershed and the southern Sierra Nevada
[E82-10191] p 62 N82-22625
Use of NOAA/AVHRR visible and near-infrared data for land remote sensing
[NASA-TM-84186] p 81 N82-22643
SOIL MAPPING
Problems associated with remotely detecting and monitoring saline sites within irrigated Alberta p 9 A82-34710
The influence of soil characteristics on regional *convection differences above Northern Germany* p 10 A82-37589
Overseas Geology And Mineral Resources number 56 A geological interpretation of LANDSAT imagery and air photography of Botswana
[OGMR-56] p 42 N82-22636
Use of LANDSAT data to define soil boundaries in Carroll County, Missouri p 10 N82-23116
AgRISTARS Agriculture and resources inventory surveys through aerospace remote sensing
[E82-10236] p 15 N82-23609
SOIL MOISTURE
A simulation study of soil moisture estimation by a space SAR p 60 A82-29333
Remote sensing of leaf water content in the near *infrared* p 8 A82-32897
Landsat digital analysis of the initial recovery of burned tundra at Kokolik River, Alaska p 8 A82-32913
The possibility of using remote-sensing methods to study the hydrology of elementary watersheds p 61 A82-35130
C-band radar for determining surface soil moisture p 10 A82-37194
The influence of soil characteristics on regional convection differences above Northern Germany p 10 A82-37589
A meteorologically driven maize stress indicator model
[E82-10112] p 11 N82-23564
Spectral properties of agricultural crops and soils measured from space, aerial, field, and laboratory sensors
[E82-10212] p 12 N82-23585

Application of thermal model for pan evaporation to the hydrology of a defined medium, the sponge
[E82-10217] p 13 N82-23590
A meteorologically driven grain sorghum stress indicator model
[E82-10218] p 13 N82-23591
AgRISTARS Early warning and crop condition assessment Plant cover, soil temperature, freeze, water stress, and evapotranspiration conditions
[E82-10225] p 14 N82-23598
A multi-frequency radiometric measurement of soil moisture content over bare and vegetated fields
[E82-10238] p 16 N82-23611
Multilevel measurements of surface temperature over undulating terrain planted to barley
[E82-10245] p 16 N82-24523
Thermal mapping, geothermal source location, natural effluents and plant stress in the Mediterranean coast of Spain
[E82-10300] p 17 N82-24576
A method for inferring available surface moisture using remote surface temperature measurements An assessment --- Kansas and St Louis, Missouri
[E82-10311] p 17 N82-24585
Evaluation of HCMM data for assessing soil moisture and water table depth --- South Dakota
[E82-10329] p 18 N82-24602
Orbiting passive microwave sensor simulation applied to soil moisture estimation
[E82-10343] p 18 N82-25605
Plan of research for integrated soil moisture studies Recommendations of the Soil Moisture Working Group
[NASA-TM-84731] p 18 N82-25608
Interactive initialization of heat flux parameters for numerical models using satellite temperature measurements
[E82-10313] p 82 N82-26743
Multispectral determination of soil moisture-2 --- Guymon, Oklahoma and Dalhart, Texas
[E82-10349] p 19 N82-26747
Evaluation of the soil moisture prediction accuracy of a space radar using simulation techniques --- Kansas
[E82-10351] p 19 N82-26749
Detection of variations in aspen forest habitat from LANDSAT digital data Bear River Range, Utah
[E82-10355] p 19 N82-26753
Measurement of soil moisture trends with airborne scatterometers --- Guymon, Oklahoma and Dalhart, Texas
[E82-10361] p 20 N82-26759
Multifrequency remote sensing of soil moisture --- Guymon, Oklahoma and Dalhart, Texas
[E82-10362] p 20 N82-26760
The use of soil texture and field capacity to normalize microwave soil moisture measurements Some problems p 20 N82-26762

SOIL SCIENCE
Use of LANDSAT data to define soil boundaries in Carroll County, Missouri p 10 N82-23116

SOILS
Spectral properties of agricultural crops and soils measured from space, aerial, field, and laboratory sensors
[E82-10189] p 10 N82-22623
Spectral properties of agricultural crops and soils measured from space, aerial, field, and laboratory sensors
[E82-10212] p 12 N82-23585
Delineation of soil temperature regimes from HCMM data
[E82-10298] p 17 N82-24574
Use of thermal inertia determined by HCMM to predict nocturnal cold prone areas in Florida --- Everglades agricultural area and the west north central peninsula
[E82-10299] p 17 N82-24575
The use of soil texture and field capacity to normalize microwave soil moisture measurements Some problems p 20 N82-26762

SOLAR ACTIVITY
Comparison of solar proton activity in 1967 and 1969 with that in 1978 and 1979 as measured onboard Venera 4, 6, 11, 12 space probes p 31 A82-22596
The solar proton fluxes in April, 1979 p 66 A82-22597
Non-flare injection of protons into interplanetary space p 4 A82-22601

SOLAR ACTIVITY EFFECTS
International Cosmic Ray Conference, 17th, Paris, France, July 13-25, 1981, Conference Papers Volume 3 p 65 A82-22580
Model for solar hard X-ray bursts p 65 A82-22581
Solar gamma-ray experiment on Astro-A satellite p 21 A82-22583
High-energy solar protons p 22 A82-22588
Preflare increases in solar cosmic rays relevant to the mode of energy accumulation in the active regions associated with large flares p 31 A82-22595
The modulation characteristics of the 19th and 20th solar activity cycles p 59 A82-22615

SOLAR ATMOSPHERE
Azimuthal propagation of flare particles in the heliosphere p 66 A82-22590
The influence of the sector structure of interplanetary magnetic field on the solar cosmic ray characteristics p 83 A82-22603

SOLAR CORONA
Possible evidence for attenuation of an MHD shock by a magnetic neutral sheet in the solar corona p 3 A82-22589
Azimuthal propagation of flare particles in the heliosphere p 66 A82-22590
On the physical sense of the constant of solar cosmic ray coronal propagation p 83 A82-22599
Observations of the ionization states of energetic particles accelerated in solar flares p 40 A82-22607
A tentative ordering of all available solar energetic particles abundance observations I - The mass unbiased baseline II - Discussion and comparison with coronal abundances p 40 A82-22609

SOLAR CORPUSCULAR RADIATION
Azimuthal propagation of flare particles in the heliosphere p 66 A82-22590
The relation of type II radio bursts to solar energetic particles observed at earth p 3 A82-22591
Energetic solar particle spectra according to Venera-11, 12 and Prognoz-5, 6 p 4 A82-22593
A tentative ordering of all available solar energetic particles abundance observations I - The mass unbiased baseline II - Discussion and comparison with coronal abundances p 40 A82-22609
Heavy-element abundances in He/3/-rich events p 5 A82-22611

SOLAR COSMIC RAYS
Comparative abundances in solar energetic particles and in galactic cosmic ray sources, and the Ne-22 anomaly p 83 A82-22556
International Cosmic Ray Conference, 17th, Paris, France, July 13-25, 1981, Conference Papers Volume 3 p 65 A82-22580
Preflare increases in solar cosmic rays relevant to the mode of energy accumulation in the active regions associated with large flares p 31 A82-22595
On the physical sense of the constant of solar cosmic ray coronal propagation p 83 A82-22599
A description of relativistic solar particle propagation p 4 A82-22600
Low-energy particles in interplanetary magnetic field near the sectorial boundary on September 26, 1977 p 4 A82-22602
The influence of the sector structure of interplanetary magnetic field on the solar cosmic ray characteristics p 83 A82-22603
The approximate 1 GeV solar cosmic rays in the Forbush-effect of February 15, 1978 p 40 A82-22604
Coulombian energy losses and the nuclear composition of the solar cosmic rays p 4 A82-22610
The model of the cosmic ray enrichment by helium-3 p 31 A82-22614
Primary spectral variations of cosmic rays above 1 GV p 5 A82-22618

SOLAR CYCLES
The modulation characteristics of the 19th and 20th solar activity cycles p 59 A82-22615

SOLAR ELECTRONS
Unusual properties of particle events associated with solar flare gamma ray events p 65 A82-22585
Low-energy particles in interplanetary magnetic field near the sectorial boundary on September 26, 1977 p 4 A82-22602

SOLAR FLARES
International Cosmic Ray Conference, 17th, Paris, France, July 13-25, 1981, Conference Papers Volume 3 p 65 A82-22580
Model for solar hard X-ray bursts p 65 A82-22581
The determination of differential X-ray spectrum of the solar flare using ionospheric data p 65 A82-22582
Solar gamma-ray experiment on Astro-A satellite p 21 A82-22583
Interplanetary particle observations associated with solar flare gamma-ray line emission p 3 A82-22584
Unusual properties of particle events associated with solar flare gamma ray events p 65 A82-22585
Observations of interplanetary energetic charged particles from gamma-ray line solar flares p 65 A82-22586
High-energy solar protons p 22 A82-22588
Azimuthal propagation of flare particles in the heliosphere p 66 A82-22590
The relation of type II radio bursts to solar energetic particles observed at earth p 3 A82-22591
A survey of solar protons and alpha differential spectra between 1 and greater than 400 MeV/nucleon p 4 A82-22592
Energetic solar particle spectra according to Venera-11, 12 and Prognoz-5, 6 p 4 A82-22593
Evolution of the solar proton spectrum in interplanetary space p 4 A82-22594
Preflare increases in solar cosmic rays relevant to the mode of energy accumulation in the active regions associated with large flares p 31 A82-22595
Spacecraft determination of energetic particle propagation parameters - The 1 January 1978 solar event p 31 A82-22598
The influence of the sector structure of interplanetary magnetic field on the solar cosmic ray characteristics p 83 A82-22603
Time and energy dependence of heavy ion abundances in solar flare energetic particle events p 22 A82-22605
High resolution measurements of solar flare isotopes p 22 A82-22606
Observations of the ionization states of energetic particles accelerated in solar flares p 40 A82-22607
Is the neon composition of our sun, planetary or solar p 76 A82-22608
A comparison of helium and heavy ion spectra in He/3/ rich solar flares with a model calculation p 5 A82-22612
On the anticorrelation between the He/3//He/4/ ratio and proton intensity in He/3/ rich flares p 40 A82-22613
Primary spectral variations of cosmic rays above 1 GV p 5 A82-22618

SOLAR FLUX DENSITY
The solar proton fluxes in April, 1979 p 66 A82-22597

SOLAR MAGNETIC FIELD
Features of cosmic ray variations due to variations in the total magnetic field of the sun p 49 A82-22619

SOLAR MAXIMUM MISSION
Interplanetary particle observations associated with solar flare gamma-ray line emission p 3 A82-22584
Unusual properties of particle events associated with solar flare gamma ray events p 65 A82-22585
Atmospheric ozone determination by solar occultation using the UV spectrometer on the Solar Maximum Mission p 27 A82-36362

SOLAR ORBITS
Some considerations in the use of very-long-baseline-interferometry to establish reference coordinate systems for geodynamics p 34 A82-32096

SOLAR POSITION
Diurnal changes in reflectance factor due to Sun-row direction interactions
[E82-10128] p 11 N82-23566
Airborne observed solar elevation and row direction effects on the near-IR/red ratio of cotton
[E82-10220] p 13 N82-23593
Canopy reflectance as influenced by solar illumination angle
[E82-10237] p 15 N82-23610
The effect of sea-surface Sun glitter on microwave radiometer measurements
[NASA-CR-169083] p 57 N82-26525

SOLAR PROMINENCES
Non-flare injection of protons into interplanetary space p 4 A82-22601

SOLAR PROTONS
Unusual properties of particle events associated with solar flare gamma ray events p 65 A82-22585
High-energy solar protons p 22 A82-22588
A survey of solar protons and alpha differential spectra between 1 and greater than 400 MeV/nucleon p 4 A82-22592
Evolution of the solar proton spectrum in interplanetary space p 4 A82-22594
Comparison of solar proton activity in 1967 and 1969 with that in 1978 and 1979 as measured onboard Venera 4, 6, 11, 12 space probes p 31 A82-22596
The solar proton fluxes in April, 1979 p 66 A82-22597
Non-flare injection of protons into interplanetary space p 4 A82-22601
Low-energy particles in interplanetary magnetic field near the sectorial boundary on September 26, 1977 p 4 A82-22602

SOLAR RADIATION
Simplified techniques to study components of solar radiation under haze and clouds p 78 A82-32766
Spectral estimates of solar radiation intercepted by corn canopies
[E82-10003] p 18 N82-26742

SOLAR SYSTEM
Nucleosynthesis of light and by-passed isotopes in the solar system matter p 64 A82-22578

SOLAR WIND
High resolution measurements of solar flare isotopes p 22 A82-22606
Is the neon composition of our sun, planetary or solar p 76 A82-22608
11-year modulation and spectrum of cosmic rays in the interstellar space p 22 A82-22616

SOLAR WIND VELOCITY
Non-flare injection of protons into interplanetary space p 4 A82-22601
The influence of the sector structure of interplanetary magnetic field on the solar cosmic ray characteristics p 83 A82-22603

SOLAR X-RAYS
Model for solar hard X-ray bursts p 65 A82-22581
The determination of differential X-ray spectrum of the solar flare using ionospheric data p 65 A82-22582
Solar gamma-ray experiment on Astro-A satellite p 21 A82-22583
Interplanetary particle observations associated with solar flare gamma-ray line emission p 3 A82-22584
Observations of interplanetary energetic charged particles from gamma-ray line solar flares p 65 A82-22586
Soft X-rays from the sunlit earth's atmosphere p 29 A82-37405

SOLID STATE DEVICES
A system design for a multispectral sensor using two-dimensional solid-state imaging arrays p 77 A82-31991
Solid state instrumentation concepts for earth resource observation
[AAS PAPER 82-132] p 81 A82-37812

SOMALIA
MONEX oceanographic observations along the East African coast --- global atmospheric research program p 56 N82-23908

SORGHUM
A meteorologically driven grain sorghum stress indicator model
[E82-10218] p 13 N82-23591
Normal crop calendars Volume 3 The corn and soybean states of Illinois, Indiana, and Iowa
[E82-10221] p 13 N82-23594

SOUTH AMERICA
Study of gravity and magnetic anomalies using MAGSAT data
[E82-10194] p 35 N82-22628
Characterization of the structure and tectonic of South America
[E82-10196] p 42 N82-23569
Magnetic and gravity anomalies in the Americas
[E82-10312] p 37 N82-24586
An investigation of MAGSAT and complementary data emphasizing precambrian shields and adjacent areas of West Africa and South America
[E82-10316] p 38 N82-24589
An investigation of MAGSAT and complementary data emphasizing precambrian shields and adjacent areas of West Africa and South America
[E82-10317] p 38 N82-24590
The crustal structure and tectonics of South America
[E82-10319] p 38 N82-24592
Geotectonics of South America --- regional magnetic and gravity anomalies of South America
[E82-10320] p 38 N82-24593

SOUTH CAROLINA
Use and applicability of the vegetation component of the national site classification system --- Sumter National Forest, South Carolina
[E82-10234] p 15 N82-23607

SOUTH DAKOTA
AgRISTARS Supporting research Spring small grains planting date distribution model
[E82-10208] p 12 N82-23581
Airborne gamma-ray spectrometer and magnetometer survey Aberdeen quadrangle, South Dakota, volume 1
[DE82-004152] p 45 N82-23641
Airborne gamma-ray spectrometer and magnetometer survey Aberdeen quadrangle, South Dakota, volume 2
[DE82-004164] p 45 N82-23642
Evaluation of HCMM data for assessing soil moisture and water table depth --- South Dakota
[E82-10329] p 18 N82-24602
Airborne gamma-ray spectrometer and magnetometer survey Sioux Falls quadrangle, South Dakota, volume 1
[DE82-005533] p 47 N82-27806
Airborne gamma-ray spectrometer and magnetometer survey Sioux Falls quadrangle, South Dakota, volume 2
[DE82-005574] p 47 N82-27807
Airborne gamma-ray spectrometer and magnetometer survey Huron Quadrangle, South Dakota
[DE82-005540] p 48 N82-27814

SOUTHERN HEMISPHERE
Mean sea-level pressure in the Southern Hemisphere during the FGGE period --- First Global Atmospheric Research Program Global Experiment (FGGE), buoys p 55 N82-23856

SOYBEANS
Spectral scanning of experimental plots of SO2-affected winter wheat and soybeans for mission planning p 6 A82-29537
Effects of vegetation canopy structure on remotely sensed canopy temperatures --- inferring plant water stress and yield p 8 A82-32905
Diurnal changes in reflectance factor due to Sun-row direction interactions
[E82-10128] p 11 N82-23566
AgRISTARS Foreign commodity production forecasting The 1980 US corn and soybeans exploratory experiment
[E82-10206] p 11 N82-23579
Determination of the optimal level for combining area and yield estimates
[E82-10215] p 12 N82-23588
AgRISTARS Preliminary technical results review of FY81 experiments, volume 2 Fiscal year 1981/1982 'corn and soybeans pilot' experiment
[E82-10216] p 13 N82-23589
Normal crop calendars Volume 3 The corn and soybean states of Illinois, Indiana, and Iowa
[E82-10221] p 13 N82-23594
Application of Computer Axial Tomography (CAT) to measuring crop canopy geometry --- corn and soybeans
[E82-10227] p 14 N82-23600
AgRISTARS Project management report Program review presentation to level 1, interagency coordination committee --- Brazil, Argentina, U S corn belt, Great Plains Corridor
[E82-10231] p 15 N82-23604
Canopy reflectance as influenced by solar illumination angle
[E82-10237] p 15 N82-23610
Analysis of scanner data for crop inventories
[E82-10241] p 16 N82-24519

SPACE EXPLORATION
History of the French satellite space program p 85 N82-24216

SPACE MISSIONS
ERS-1 European remote sensing satellite p 84 A82-34367

SPACE NAVIGATION
Space to the earth --- Russian book on space technology applications p 83 A82-30850

SPACE PLATFORMS
SMS/GOES data collection platform system p 75 N82-26027

SPACE TRANSPORTATION SYSTEM 2 FLIGHT
Tropospheric CO measurement experiment from the second Space Shuttle flight p 27 A82-36292
OSTA-1 Post Mission Operation Report
[NASA-TM-84191] p 84 N82-23258

SPACE-TIME FUNCTIONS
On the space-time variability of ocean surface mixed layer characteristics of central and eastern Arabian sea during MONSOON-77 --- global atmospheric research program p 56 N82-23909

SPACEBORNE PHOTOGRAPHY
Imaging spectroscopy, Proceedings of the Seminar, Los Angeles, CA, February 10, 11, 1981 p 77 A82-32440

SPACEBORNE TELESCOPES
An optical objective lens for earth observations by satellites p 78 A82-32824

SPACECRAFT COMMUNICATION
Space to the earth --- Russian book on space technology applications p 83 A82-30850

SPACECRAFT INSTRUMENTS
Purpose, background of 'Intercosmos-21' mission p 81 N82-24264

SPACECRAFT LAUNCHING
LANDSAT D to test thematic mapper, inaugurate operational system
[NASA-NEWS-RELEASE-82-100] p 82 N82-26741

SPACECRAFT MODULES
LANDSAT-D thermal analysis and design support
[E82-10346] p 82 N82-26744

SPACETENNAS
Radiometer mission requirements for large space antenna systems
[NASA-TM-84478] p 81 N82-25610

SPATIAL DISTRIBUTION
The use of remote-sensing data to identify the space-time variability of the quality of natural waters p 62 A82-35138

SPATIAL FILTERING
Inversion of data from diffraction-limited multiwavelength remote sensors II - Nonlinear dependence of observables on the geophysical parameters p 77 A82-32658

SPATIAL RESOLUTION
Spatial resolution requirements for urban studies p 29 A82-37502

SPECKLE PATTERNS
Ocean wave height measurement with SEASAT SAR using speckle diversity p 53 A82-32882

SPECTRAL BANDS
Measurement of soil moisture trends with airborne scatterometers --- Guymon, Oklahoma and Dalhart, Texas
[E82-10361] p 20 N82-26759
Development of visible/infrared/microwave agriculture classification and biomass estimation algorithms --- Guyton, Oklahoma and Dalhart, Texas
[E82-10363] p 20 N82-26761

SPECTRAL RECONNAISSANCE
Agricultural Research Service research highlights in remote sensing for calendar year 1980
[E82-10228] p 14 N82-23601
Airborne gamma-ray spectrometer and magnetometer survey Barrow quadrangle, Alaska, volume 1
[DE82-000334] p 43 N82-23623
Airborne gamma-ray spectrometer and magnetometer survey Meade River quadrangle, Alaska, volume 2
[DE82-000340] p 43 N82-23626
Airborne gamma-ray spectrometer and magnetometer survey Teshekpuk quadrangle, Alaska, volume 2
[DE82-000310] p 43 N82-23627
Airborne gamma-ray spectrometer and magnetometer survey Harrison Bay quadrangle, Alaska, volume 2
[DE82-000315] p 43 N82-23628
Airborne gamma-ray spectrometer and magnetometer survey Beechey Pt, quadrangle, Alaska, volume 2
[DE82-000309] p 43 N82-23629
Airborne gamma-ray spectrometer and magnetometer survey Point Lay quadrangle, Alaska, volume 2
[DE82-000308] p 43 N82-23630
Airborne gamma-ray spectrometer and magnetometer survey Utukik River quadrangle, Alaska, volume 2
[DE82-000316] p 44 N82-23631
Airborne gamma-ray spectrometer and magnetometer survey Sagavanirktok quadrangle, Alaska, volume 2
[DE82-000311] p 44 N82-23632
Airborne gamma-ray spectrometer and magnetometer survey Duluth quadrangle, Minnesota, volume 2
[DE82-001027] p 44 N82-23633
Airborne gamma-ray spectrometer and magnetometer survey Ukiah quadrangle, California, volume 1 --- uranium exploration
[DE82-005541] p 48 N82-27813

SPECTRAL REFLECTANCE
Remote sensing of the weediness of crop fields p 5 A82-29435
Spectral scanning of experimental plots of SO2-affected winter wheat and soybeans for mission planning p 6 A82-29537
Relating Landsat digital count values to ground reflectance for optically thin atmospheric conditions p 66 A82-29762
Albedo and angular characteristics of the reflectance of the underlying surface and clouds --- Russian book p 33 A82-30849
Emissivity and reflectance of the model sea surface for the use of AVHRR data of NOAA satellites p 52 A82-31294
System albedo as sensed by satellites - Its definition and variability p 23 A82-32342
Remote sensing of leaf water content in the near infrared p 8 A82-32897
Quantitative relationships of near-surface spectra to Landsat radiometric data p 78 A82-32912
Influence of sky radiance distribution on the ratio technique for estimating bidirectional reflectance p 70 A82-35650
Spectral properties of agricultural crops and soils measured from space, aerial, field, and laboratory sensors
[E82-10189] p 10 N82-22623
Analysis of scanner data for crop inventories
[E82-10192] p 10 N82-22626
Diurnal changes in reflectance factor due to Sun-row direction interactions
[E82-10128] p 11 N82-23566
Spectral properties of agricultural crops and soils measured from space, aerial, field, and laboratory sensors
[E82-10212] p 12 N82-23585
Airborne observed solar elevation and row direction effects on the near-IR/red ratio of cotton
[E82-10220] p 13 N82-23593
Relating thematic mapper bands TM3, TM4, and TM5 to agronomic variables for corn, cotton, sugarbeet, soybean, sorghum, sunflower and tobacco
[E82-10347] p 19 N82-26745

Association of spectral development patterns with development stages of corn
[E82-10353] p 19 N82-26751
Detection of variations in aspen forest habitat from LANDSAT digital data Bear River Range, Utah
[E82-10355] p 19 N82-26753

SPECTRAL SENSITIVITY
Sensitivity of Dobson total ozone estimations to wavelength band calibration uncertainties
p 27 A82-36405
Optical slop and focussing effects in the Dobson instrument p 28 A82-36428
Analysis of thematic mapper simulator data acquired during winter season over Pearl River, Mississippi, test site
[E82-10287] p 17 N82-24565
Multifrequency remote sensing of soil moisture --- Guymon, Oklahoma and Dalhart, Texas
[E82-10362] p 20 N82-26760
Development of visible/infrared/microwave agriculture classification and biomass estimation algorithms --- Guyton, Oklahoma and Dalhart, Texas
[E82-10363] p 20 N82-26761

SPECTRAL SIGNATURES
Landsat digital analysis of the initial recovery of burned tundra at Kokolik River, Alaska p 8 A82-32913
Improved land use classification from Landsat and Seasat satellite imagery registered to a common map base p 25 A82-34743
Spectral properties of agricultural crops and soils measured from space, aerial, field, and laboratory sensors
[E82-10189] p 10 N82-22623
Spectral properties of agricultural crops and soils measured from space, aerial, field, and laboratory sensors
[E82-10212] p 12 N82-23585
Airborne observed solar elevation and row direction effects on the near-IR/red ratio of cotton
[E82-10220] p 13 N82-23593
Linear polarization of light by two wheat canopies measured at many view angles
[E82-10229] p 14 N82-23602
Canopy reflectance as influenced by solar illumination angle
[E82-10237] p 15 N82-23610
Analysis of scanner data for crop inventories
[E82-10241] p 16 N82-24519
Analysis of thematic mapper simulator data acquired during winter season over Pearl River, Mississippi, test site
[E82-10287] p 17 N82-24565
The influence of autocorrelation in signature extraction An example from a geobotanical investigation of Cotter Basin, Montana
[E82-10341] p 46 N82-25603
Spectral estimates of solar radiation intercepted by corn canopies
[E82-10003] p 18 N82-26742
Multispectral determination of soil moisture-2 --- Guymon, Oklahoma and Dalhart, Texas
[E82-10349] p 19 N82-26747
Detection of variations in aspen forest habitat from LANDSAT digital data Bear River Range, Utah
[E82-10355] p 19 N82-26753

SPECTROMETERS
Breadboard gas filter correlation spectrometer for atmospheric measurement of hydrazines and nitrogen dioxide
[AD-A110688] p 82 N82-26642
Airborne gamma-ray spectrometer and magnetometer survey North/south tieline, volume 2
[DE82-005570] p 47 N82-27805

SPECTROPHOTOMETERS
Optical slop and focussing effects in the Dobson instrument p 28 A82-36428
Observations and analyses of the total amount of atmospheric ozone in the Beijing region and in the region of Jolmolungma Mountain in Tibet p 28 A82-36444

SPECTRORADIOMETERS
Emissivity and reflectance of the model sea surface for the use of AVHRR data of NOAA satellites
p 52 A82-31294
High spectral resolution airborne spectrometry
p 77 A82-32443
Thematic mapper - An overview of spectral band registration p 77 A82-32447

SPECTROSCOPIC ANALYSIS
Imaging spectroscopy, Proceedings of the Seminar, Los Angeles, CA, February 10, 11, 1981 p 77 A82-32440
Multispectral mapper - Imaging spectroscopy as applied to the mapping of earth resources p 77 A82-32448

SPECTRUM ANALYSIS
Spectroscopic remote sensing for geological applications p 41 A82-32442
Total ozone retrieval from satellite Meteor 28 Fourier spectrometer measurements p 28 A82-36422
Observations and analyses of the total amount of atmospheric ozone in the Beijing region and in the region of Jolmolungma Mountain in Tibet p 28 A82-36444
MAGSAT science investigations
[E82-10199] p 71 N82-23572
Investigation of Antarctic crust and upper mantle using MAGSAT and other geophysical data
[E82-10308] p 37 N82-24582
Irrigation management with remote sensing --- Navajo Indian Irrigation Project
[E82-10357] p 20 N82-26755

SPECULAR REFLECTION
A model of plant canopy polarization
[E82-10233] p 15 N82-23606

SPHERICAL HARMONICS
Spherical harmonic representation of the main geomagnetic field for world charting and investigations of some fundamental problems of physics and geophysics
[E82-10203] p 72 N82-23576
Improved definition of crustal magnetic anomalies for MAGSAT data
[E82-10314] p 37 N82-24587

SPIRAL GALAXIES
Derivation of the distribution of synchrotron emissivity in the Galaxy from the 408 MHz all-sky survey
p 82 A82-22549

SPONGES (MATERIALS)
Application of thermal model for pan evaporation to the hydrology of a defined medium, the sponge
[E82-10217] p 13 N82-23590

SPOT (FRENCH SATELLITE)
The use of the SPOT satellite in natural resource evaluation p 83 A82-31996

STATISTICAL ANALYSIS
Monitoring land-cover change by principal component analysis of multitemporal Landsat data
p 68 A82-32906
Image quality and height measurement accuracy of serial survey camera imagery from high altitudes
p 78 A82-33297
The effect of the spectral attenuation of UV radiation by aerosol on the total ozone measurements
p 27 A82-36406
A statistical approach to rainfall estimation using satellite and conventional data
[NOAA-TR-NESS-89] p 63 N82-22854
Estimates of the statistical structure of the atmospheric pressure field in summer Monex-79 area
p 57 N82-23939

STEADY STATE
Steady-state cosmic ray electron spectrum under diffusion, convection, adiabatic deceleration and synchrotron losses p 1 A82-22552

STELLAR EVOLUTION
Nucleosynthesis of light and by-passed isotopes in the solar system matter p 64 A82-22578

STELLAR MAGNETIC FIELDS
Acceleration processes near massive black holes
p 3 A82-22572

STELLAR MASS ACCRETION
Acceleration of cosmic rays in accretion shocks
p 64 A82-22568

STELLAR MODELS
Pulsar models and cosmic-ray acceleration
p 21 A82-22570

STELLAR OCCULTATION
Atmospheric ozone determination by solar occultation using the UV spectrometer on the Solar Maximum Mission p 27 A82-36362

STELLAR RADIATION
On the stellar origin of the Ne-22 excess in cosmic rays p 21 A82-22562
On the stellar origin of low energy cosmic rays
p 21 A82-22567

STELLAR WINDS
Cosmic ray acceleration by stellar winds I - Total density, pressure and energy flux p 21 A82-22566

STEREOPHOTOGRAPHY
Application of 35mm color aerial photography to forest land change detection p 6 A82-29533
Analytical processing of photographs taken by paired cameras p 79 A82-34471

STEREOSCOPY
Coordination of stereo image registration and pixel classification
[AD-A111307] p 75 N82-25614

STOCHASTIC PROCESSES
Evidence for the stochastic acceleration of cosmic rays in supernova remnants p 2 A82-22564
Preliminary evidence for the influence of physiography and scale upon the autocorrelation function of remotely sensed data p 67 A82-32343

STORMS (METEOROLOGY)
The growth of snow in winter storms - An airborne observational study p 60 A82-33329
Comparison of storm-time changes of geomagnetic field at ground and at MAGSAT altitudes, part 2
[E82-10325] p 30 N82-24598

STRATIFICATION
A comparison of stratified versus regression estimators p 11 N82-23133

STRATIFIED FLOW
On the application of a model of boundary-layer flow over low hills to real terrain p 29 A82-36741

STRATOSPHERE
Airborne lidar measurements of the Soufriere eruption of 17 April 1979 p 24 A82-33657
Observation of the diurnal variation of atmospheric ozone p 26 A82-35895
Microwave measurement of stratospheric and mesospheric ozone p 28 A82-36415
The seasonal variations of ozone and temperature in the middle and the upper stratosphere
p 29 A82-36534

STRATOSPHERE RADIATION
The energy spectra of cosmic ray variations inferred from the stratospheric measurements in 1972-1979
p 5 A82-22617
Stratospheric emission data analysis
[AD-A112337] p 76 N82-26907

STREAMS
Use of aerial photography in determining land use and streamflow relationships on small developing watersheds
p 60 A82-34736

STRESS (BIOLOGY)
Remote sensing of leaf water content in the near infrared p 8 A82-32897
Effects of vegetation canopy structure on remotely sensed canopy temperatures --- inferring plant water stress and yield p 8 A82-32905

STRESS MEASUREMENT
Estimates of sea surface stress for summer MONEX from cloud motions --- global atmospheric research program p 56 N82-23910

STRIP MINING
Application of remote sensing to state and regional problems
[E82-10288] p 30 N82-24566

STRUCTURAL BASINS
The influence of autocorrelation in signature extraction An example from a geobotanical investigation of Cotter Basin, Montana
[E82-10341] p 46 N82-25603

STRUCTURAL PROPERTIES (GEOLOGY)
Regional geological, tectonic and geophysical features of Nordland, Norway p 41 A82-30304
Satellite image interpretation of the eastern Caledonian part of the Blue Road Geotraverse and its geological implications /Nordland, Vasterbotten, Scandinavia/
p 41 A82-30305
Comparing lineaments interpreted from Landsat imagery and topographic maps with reported faults in southwest Montana p 34 A82-34719
Terrain classification by Fourier analysis - Accuracy and economy p 69 A82-34723
Significance of tectonics in linear feature detection and interpretation on satellite images p 42 A82-37198
Spatial thermal radiometry contribution to the Massif Armoricain and the Massif Central France litho-structural study
[E82-10190] p 42 N82-22624
Geodetic monitoring of tectonic information Toward a strategy p 35 N82-22832
Structure of the St Francois Mountains and surrounding lead belt, S E Missouri Inferences from thermal IR and other data sets
[E82-10200] p 36 N82-23573
Application of HCMM data to regional geologic analysis for mineral and energy resource evaluation
[E82-10153] p 45 N82-24518
Thermal mapping, geothermal source location, natural effluents and plant stress in the Mediterranean coast of Spain
[E82-10300] p 17 N82-24576
Analyzing the Broken Ridge area of the Indian Ocean using magnetic and gravity anomaly maps and geoid undulation and bathymetry data
[E82-10303] p 36 N82-24577
Investigating tectonic and bathymetric features of the Indian Ocean using MAGSAT magnetic anomaly data
[E82-10304] p 37 N82-24578
Magnetic and gravity anomalies in the Americas
[E82-10312] p 37 N82-24586

STRUCTURAL STABILITY
Nonlinear theory for elastic beams and rods and its finite element representation
[WTHD-143] p 73 N82-24517

SUGAR BEETS
Normal crop calendars Volume 3 The corn and soybean states of Illinois, Indiana, and Iowa
[E82-10221] p 13 N82-23594
SUGAR CANE
Use of thermal inertia determined by HCMM to predict nocturnal cold prone areas in Florida --- Everglades agricultural area and the west north central peninsula
[E82-10299] p 17 N82-24575
SULFUR DIOXIDES
Spectral scanning of experimental plots of SO2-affected winter wheat and soybeans for mission planning
p 6 A82-29537
Remote sensing of sulfur dioxide effects on vegetation Volume 1 Summary
[DE82-900580] p 31 N82-27802
Remote sensing of sulfur dioxide effects on vegetation Volume 2 Data
[DE82-900581] p 31 N82-27803
SUMMER
Impact of additional summer MONEX wind data on the prediction of monsoon depressions during June - August 1979 with two versions of primitive equation (PE) barotropic model --- Monsoon Experiment (MONEX)
p 56 N82-23900
Estimates of sea surface stress for summer MONEX from cloud motions --- global atmospheric research program p 56 N82-23910
SUPERNOVA REMNANTS
Evidence for the stochastic acceleration of cosmic rays in supernova remnants p 2 A82-22564
SUPERNOVAE
The galactic origin of cosmic rays I
[CONF-810711-1] p 2 A82-22565
Nucleosynthesis of light and by-passed isotopes in the solar system matter p 64 A82-22578
SURFACE PROPERTIES
Experimental assessment of improved spatial resolution LANDSAT data
[AD-A110538] p 75 N82-26765
SURFACE ROUGHNESS
Multispectral determination of soil moisture-2 --- Guymon, Oklahoma and Dalhart, Texas
[E82-10349] p 19 N82-26747
Evaluation of the soil moisture prediction accuracy of a space radar using simulation techniques --- Kansas
[E82-10351] p 19 N82-26749
Multifrequency remote sensing of soil moisture --- Guymon, Oklahoma and Dalhart, Texas
[E82-10362] p 20 N82-26760
SURFACE TEMPERATURE
Surface temperature determination from an amalgamation of GOES and TIROS-N radiance measurements p 66 A82-28905
Infrared sensing of sea surface temperature from space p 53 A82-32902
Effects of vegetation canopy structure on remotely sensed canopy temperatures --- inferring plant water stress and yield p 8 A82-32905
Measuring sea surface temperature from satellites - A ground truth approach p 54 A82-32917
Satellite observations of sea surface temperature around the British Isles p 54 A82-33717
Evaluation of the accuracy of water-surface temperature measurement by means of airborne infrared radiometers
p 62 A82-35136
Determination of winter temperature patterns, fronts, and surface currents in the Yellow Sea and East China Sea from satellite imagery p 55 A82-37195
The application of Heat Capacity Mapping Mission (HCMM) thermal data to snow hydrology --- Salt Verde Watershed and the southern Sierra Nevada
[E82-10191] p 62 N82-22625
Evaluation of the Doraiswamy-Thompson winter wheat crop calendar model incorporating a modified spring restart sequence
[E82-10207] p 12 N82-23580
AgRISTARS Early warning and crop condition assessment Plant cover, soil temperature, freeze, water stress, and evapotranspiration conditions
[E82-10225] p 14 N82-23598
Delineation of soil temperature regimes from HCMM data
[E82-10298] p 17 N82-24574
Use of thermal inertia determined by HCMM to predict nocturnal cold prone areas in Florida --- Everglades agricultural area and the west north central peninsula
[E82-10299] p 17 N82-24575
Thermal mapping, geothermal source location, natural effluents and plant stress in the Mediterranean coast of Spain
[E82-10300] p 17 N82-24576
A method for inferring available surface moisture using remote surface temperature measurements An assessment --- Kansas and St Louis, Missouri
[E82-10311] p 17 N82-24585
High resolution satellite observations of mesoscale oceanography in the Tasman Sea, 1978 - 1979
[E82-10324] p 57 N82-24597
SURFACE WATER
Interpretation of surface-water circulation, Aransas Pass, Texas, using Landsat imagery p 60 A82-32896
SYNCHRONOUS METEOROLOGICAL SATELLITE
SMS/GOES data collection platform system
p 75 N82-26027
SYNCHRONOUS SATELLITES
Observed magnetic substorm signatures at synchronous altitude p 26 A82-35534
SYNCHROTRON RADIATION
Derivation of the distribution of synchrotron emissivity in the Galaxy from the 408 MHz all-sky survey
p 82 A82-22549
Steady-state cosmic ray electron spectrum under diffusion, convection, adiabatic deceleration and synchrotron losses p 1 A82-22552
SYNTHETIC APERTURE RADAR
A simulation study of soil moisture estimation by a space SAR p 60 A82-29333
The observation of ocean surface phenomena using imagery from the Seasat synthetic aperture radar - An assessment p 52 A82-29623
The recognition of extended targets - SAR images for level and hilly terrain p 33 A82-31994
The estimation of wave height from digitally processed SAR imagery p 67 A82-32347
On the synthetic aperture radar imaging of ocean surface waves p 53 A82-32881
Ocean wave height measurement with SEASAT SAR using speckle diversity p 53 A82-32882
Interpretation of vegetative cover in wetlands using four-channel SAR imagery p 9 A82-34706
Comparisons of land cover classifications from selected remote sensing systems p 80 A82-34746
Microwave sensing from space
[AAS PAPER 82-127] p 80 A82-37809
Evaluation of the soil moisture prediction accuracy of a space radar using simulation techniques --- Kansas
[E82-10351] p 19 N82-26749
SYSTEMS
Meteorological and aircraft data for CUE 2 1973
[PB82-149246] p 59 N82-26949
SYSTEMS ENGINEERING
A system design for a multispectral sensor using two-dimensional solid-state imaging arrays
p 77 A82-31991
Design guidelines for satellite image data distribution systems p 70 A82-37048

T

TARGET RECOGNITION
The recognition of extended targets - SAR images for level and hilly terrain p 33 A82-31994
TECHNOLOGY ASSESSMENT
Seasat measurement system evaluation - Achievements and limitations p 49 A82-29601
Impacts of remote sensing on U S geography
p 24 A82-32899
TECHNOLOGY TRANSFER
Civil land remote sensing system
[GPO-87-070] p 84 N82-22630
LANDSAT technology transfer to the private and public sectors through community colleges and other locally available institutions
[E82-10181] p 85 N82-23568
Forest Resource Information System Phase 3 System transfer report
[E82-10344] p 18 N82-25606
TECTONICS
Significance of tectonics in linear feature detection and interpretation on satellite images p 42 A82-37198
Geodetic monitoring of tectonic information Toward a strategy p 35 N82-22832
Geodetic monitoring of tectonic deformation Toward a strategy
[NASA-CR-168784] p 35 N82-22846
Characterization of the structure and tectonic of South America
[E82-10196] p 42 N82-23569
Bathymetric and tectonics of Indian Ocean using MAGSAT data
[E82-10204] p 36 N82-23577
An equivalent layer magnetization model for the United States derived from MAGSAT data
[E82-10297] p 36 N82-24573
Analyzing the Broken Ridge area of the Indian Ocean using magnetic and gravity anomaly maps and geoid undulation and bathymetry data
[E82-10303] p 36 N82-24577
Investigating tectonic and bathymetric features of the Indian Ocean using MAGSAT magnetic anomaly data
[E82-10304] p 37 N82-24578
The crustal structure and tectonics of South America
[E82-10319] p 38 N82-24592
Geotectonics of South America --- regional magnetic and gravity anomalies of South America
[E82-10320] p 38 N82-24593
Seismic and geodetic studies of the Imperial Valley, California
[DE82-001686] p 39 N82-26915
TELEMETRY
Purpose, background of 'Intercosmos-21' mission
p 81 N82-24264
TEMPERATURE DISTRIBUTION
Surface temperature determination from an amalgamation of GOES and TIROS-N radiance measurements p 66 A82-28905
Effects of vegetation canopy structure on remotely sensed canopy temperatures --- inferring plant water stress and yield p 8 A82-32905
Rapid oceanographic data gathering Some problems in using remote sensing to determine the horizontal and vertical thermal distributions in the Northeast Pacific Ocean
[AD-A111005] p 58 N82-26945
TEMPERATURE EFFECTS
A meteorologically driven grain sorghum stress indicator model
[E82-10218] p 13 N82-23591
LANDSAT-D thermal analysis and design support
[E82-10346] p 82 N82-26744
TEMPERATURE MEASUREMENT
View angle effects in the radiometric measurement of plant canopy temperatures p 8 A82-32914
Appearance of irregular tree canopies in nighttime high-resolution thermal infrared imagery
p 68 A82-32916
Measuring sea surface temperature from satellites - A ground truth approach p 54 A82-32917
Evaluation of the accuracy of water-surface temperature measurement by means of airborne infrared radiometers
p 62 A82-35136
Interactive initialization of heat flux parameters for numerical models using satellite temperature measurements
[E82-10313] p 82 N82-26743
TEMPERATURE PROFILES
Satellite radiation measurements for the retrieval of the vertical temperature profiles p 70 A82-36935
TEMPORAL DISTRIBUTION
The use of remote-sensing data to identify the space-time variability of the quality of natural waters
p 62 A82-35138
TERRADYNAMICS
Origin and scale of coordinate systems in satellite geodesy p 34 A82-32099
TERRAIN ANALYSIS
The recognition of extended targets - SAR images for level and hilly terrain p 33 A82-31994
Terrain analysis from Landsat using a color TV enhancement system p 68 A82-32911
Bathymetric imaging p 69 A82-34720
Terrain classification by Fourier analysis - Accuracy and economy p 69 A82-34723
Remote sensing of thermal subsurface terrain properties p 80 A82-34727
Use of NOAA/AVHRR visible and near-infrared data for land remote sensing
[NASA-TM-84186] p 81 N82-22643
Topographic slope correction for analysis of thermal infrared images
[E82-10214] p 36 N82-23587
Field measurements in support of dispersion modeling in complex terrain (1980)
[PB82-148644] p 39 N82-27882
TERRESTRIAL RADIATION
A study of the earth's radiation budget using a general circulation model p 52 A82-30666
TEXAS
AgRISTARS Early warning and crop condition assessment Plant cover, soil temperature, freeze, water stress, and evapotranspiration conditions
[E82-10225] p 14 N82-23598
Evaluation and combined geophysical interpretations of NURE and related geoscience data in the Van Horn, Pecos, Marfa, Fort Stockton, Presidido, and Emory Peak quadrangles, Texas, volume 1
[DE82-005554] p 47 N82-27808
Evaluation and combined geophysical interpretations of NURE and related geoscience data in the Van Horn, Pecos, Marfa, Fort Stockton, Presidio, and Emory Peak quadrangels, Texas
[DE82-005560] p 48 N82-27809

TEXTURES
The use of soil texture and field capacity to normalize microwave soil moisture measurements Some problems p 20 N82-26762
THEMATIC MAPPING
Preliminary evidence for the influence of physiography and scale upon the autocorrelation function of remotely sensed data p 67 A82-32343
Thematic mapper - An overview of spectral band registration p 77 A82-32447
Multispectral mapper - Imaging spectroscopy as applied to the mapping of earth resources p 77 A82-32448
RAMS-1, a Resource Analysis and Mapping System p 69 A82-34726
Improved land use classification from Landsat and Seasat satellite imagery registered to a common map base p 25 A82-34743
Water-balance differentiation of natural complexes on the basis of satellite photographs p 61 A82-35129
Remote sensing of salt marsh vegetation in the first four proposed Thematic Mapper bands p 10 A82-37503
Overseas Geology And Mineral Resources number 56 A geological interpretation of LANDSAT imagery and air photography of Botswana
[OGMR-56] p 42 N82-22636
Analysis of thematic mapper simulator data acquired during winter season over Pearl River, Mississippi, test site
[E82-10287] p 17 N82-24565
Identifying environmental features for land management decisions --- Utah
[E82-10289] p 30 N82-24567
A legislator's guide to LANDSAT
[E82-10290] p 85 N82-24568
The influence of autocorrelation in signature extraction An example from a geobotanical investigation of Cotter Basin, Montana
[E82-10341] p 46 N82-25603
LANDSAT D to test thematic mapper, inaugurate operational system
[NASA-NEWS-RELEASE-82-100] p 82 N82-26741
Relating thematic mapper bands TM3, TM4, and TM5 to agronomic variables for corn, cotton, sugarbeet, soybean, sorghum, sunflower and tobacco
[E82-10347] p 19 N82-26745
Detection of variations in aspen forest habitat from LANDSAT digital data Bear River Range, Utah
[E82-10355] p 19 N82-26753
Evaluation and combined geophysical interpretations of NURE and related geoscience data in the Van Horn, Pecos, Marfa, Fort Stockton, Presidio, and Emory Peak quadrangels, Texas
[DE82-005560] p 48 N82-27809
THERMAL CONDUCTIVITY
Remote sensing of thermal subsurface terrain properties p 80 A82-34727
THERMAL MAPPING
Thermography - A remote sensing method with many perspectives p 76 A82-29922
Geographic location of individual pixels --- for thermal infrared digital data processing p 68 A82-32900
View angle effects in the radiometric measurement of plant canopy temperatures p 8 A82-32914
Appearance of irregular tree canopies in nighttime high-resolution thermal infrared imagery p 68 A82-32916
The use of Landsat-3 thermal data to help differentiate land covers p 25 A82-34218
An optical data link for airborne scanning system p 80 A82-34737
Longwave infrared observation of urban landscapes p 25 A82-34744
Application of satellite magnetic anomaly data to Curie isotherm mapping p 70 A82-35824
Landsat D to yield more precise data p 70 A82-37200
Spatial thermal radiometry contribution to the Massif Armoricain and the Massif Central France litho-structural study
[E82-10190] p 42 N82-22624
The application of Heat Capacity Mapping Mission (HCMM) thermal data to snow hydrology --- Salt Verde Watershed and the southern Sierra Nevada
[E82-10191] p 62 N82-22625
Structure of the St Francois Mountains and surrounding lead belt, S E Missouri Inferences from thermal IR and other data sets
[E82-10200] p 36 N82-23573
Structure of the St Francois Mountains and surrounding lead belt, S E Missouri Inferences from thermal IR and other data sets --- Ozard Plateau and St Francois Mountains
[E82-10205] p 11 N82-23578
Registration of Heat Capacity Mapping Mission day and night images
[E82-10210] p 72 N82-23583
Topographic slope correction for analysis of thermal infrared images
[E82-10214] p 36 N82-23587
Application of HCMM data to regional geologic analysis for mineral and energy resource evaluation
[E82-10153] p 45 N82-24518
Application of HCMM data to regional geologic analysis for mineral and energy resource evaluation
[E82-10243] p 45 N82-24521
Multilevel measurements of surface temperature over undulating terrain planted to barley
[E82-10245] p 16 N82-24523
Delineation of soil temperature regimes from HCMM data
[E82-10298] p 17 N82-24574
Use of thermal inertia determined by HCMM to predict nocturnal cold prone areas in Florida --- Everglades agricultural area and the west north central peninsula
[E82-10299] p 17 N82-24575
Thermal mapping, geothermal source location, natural effluents and plant stress in the Mediterranean coast of Spain
[E82-10300] p 17 N82-24576
A method for inferring available surface moisture using remote surface temperature measurements An assessment --- Kansas and St Louis, Missouri
[E82-10311] p 17 N82-24585
Multidisciplinary investigations on HCMM data over middle Europe and Marocco --- southern Germany and Marrakesh, Morocco
[E82-10315] p 74 N82-24588
High resolution satellite observations of mesoscale oceanography in the Tasman Sea, 1978 - 1979
[E82-10324] p 57 N82-24597
HCMM hydrological analysis in Utah
[E82-10328] p 63 N82-24601
Evaluation of HCMM data for assessing soil moisture and water table depth --- South Dakota
[E82-10329] p 18 N82-24602
Structure of the Saint Francois Mountains and surrounding lead belt, S E Missouri Inference from thermal IR and other data sets
[E82-10350] p 39 N82-26748
An investigation into the utilization of HCMM thermal data for the discrimination of volcanic and Eolian geological units --- Newberry Volcano, Oregon
[E82-10352] p 47 N82-26750
Evaluation and combined geophysical interpretations of NURE and related geoscience data in the Van Horn, Pecos, Marfa, Fort Stockton, Presidio, and Emory Peak quadrangles, Texas, volume 1
[DE82-005554] p 47 N82-27808
THERMAL RADIATION
Cosmic ray composition from acceleration of thermal matter p 64 A82-22558
Effects of vegetation canopy structure on remotely sensed canopy temperatures --- inferring plant water stress and yield p 8 A82-32905
Remote sensing of thermal subsurface terrain properties p 80 A82-34727
THORIUM
Airborne gamma-ray spectrometer and magnetometer survey Roseau quadrangle, Minnesota, volume 2
[DE82-001025] p 44 N82-23634
Airborne gamma-ray spectrometer and magnetometer survey Bemidji quadrangle, Minnesota, volume 2
[DE82-001026] p 44 N82-23638
Airborne gamma-ray spectrometer and magnetometer survey Lookout Ridge quadrangle, Alaska, volume 2
[DE82-000313] p 47 N82-25625
Airborne gamma-ray spectrometer and magnetometer survey Sioux Falls quadrangle, South Dakota, volume 1
[DE82-005533] p 47 N82-27806
TIDAL FLATS
Remote sensing in Scotland using data received from satellites - A study of the Tay Estuary region using Landsat multispectral scanning imagery p 62 A82-37501
TIDES
Tidal and geodetic observations for the Seasat altimeter calibration experiment p 49 A82-29604
TIMBER INVENTORY
Optical bar panoramic photography for planning timber salvage in drought-stressed forests p 7 A82-32705
Landsat detection of hardwood forest clearcuts p 8 A82-32708
Remote sensing - A potential aid in the preparation of an urban tree inventory p 9 A82-34732
Ten-Ecosystem Study --- Grand and Weld Counties, Colorado, Warren County, Pennsylvania, St Louis County, Minnesota, Sandoval County, New Mexico, Kershaw County, South Carolina, Fort Yukon, Alaska, Grays Harbor County, Washington, and Washington County, Missouri
[E82-10186] p 84 N82-22620
AgRISTARS Renewable resources inventory Land information support system implementation plan and schedule --- San Juan National Forest pilot test
[E82-10224] p 14 N82-23597
Analysis of thematic mapper simulator data acquired during winter season over Pearl River, Mississippi, test site
[E82-10287] p 17 N82-24565
TIMBER VIGOR
Remote sensing of Douglas-fir trees newly infested by bark beetles p 6 A82-29536
Panoramic aerial photography in forest pest management p 7 A82-32701
Estimating bark beetle-killed lodgepole pine with high altitude panoramic photography p 7 A82-32703
Evaluation of spruce-fir forests using small-format photographs p 8 A82-32707
TIME DEPENDENCE
Computer simulation of the time dependence of the photon energy spectra produced in proton and electron bremsstrahlung p 3 A82-22587
TIME LAG
Seasat altimeter timing bias estimation p 50 A82-29609
Evaluation of the Seasat altimeter time tag bias p 50 A82-29610
Geodetic monitoring of tectonic information Toward a strategy p 35 N82-22832
TIROS N SERIES SATELLITES
Digital and visual evaluation of GOES and TIROS/NOAA image data for cover type effects on snowfield observations p 60 A82-34735
TOBACCO
Normal crop calendars Volume 3 The corn and soybean states of Illinois, Indiana, and Iowa
[E82-10221] p 13 N82-23594
TOMOGRAPHY
Application of Computer Axial Tomography (CAT) to measuring crop canopy geometry --- corn and soybeans
[E82-10227] p 14 N82-23600
TOPOGRAPHY
Comparison data for Seasat altimetry in the western North Atlantic p 50 A82-29611
The simultaneous employment of geodetic measurements for block adjustments using the method of independent models p 34 A82-33295
Structure of the St Francois Mountains and surrounding lead belt, S E Missouri Inferences from thermal IR and other data sets --- Ozard Plateau and St Francois Mountains
[E82-10205] p 11 N82-23578
Topographic slope correction for analysis of thermal infrared images
[E82-10214] p 36 N82-23587
TORNADOES
Remote sensing of tornadic storms from geosynchronous satellite infrared digital data p 23 A82-32348
TRACE CONTAMINANTS
Dobson spectrophotometer calibrations, possible errors in ozone absorption coefficients, and errors due to interfering pollutant gases p 28 A82-36431
TRANSFORMATIONS (MATHEMATICS)
An information-theoric spatial transform p 69 A82-34717
TRANSMITTANCE
Spectral properties of agricultural crops and soils measured from space, aerial, field, and laboratory sensors
[E82-10189] p 10 N82-22623
TRAVELING IONOSPHERIC DISTURBANCES
Characteristics of field-aligned E-region irregularities over Iioka /36 N/, Japan I p 26 A82-36268
TREES (MATHEMATICS)
Dependent feature trees for density approximation I - Optimal construction and classification results p 67 A82-32344
TREES (PLANTS)
Remote sensing - A potential aid in the preparation of an urban tree inventory p 9 A82-34732
Ten-Ecosystem Study --- Grand and Weld Counties, Colorado, Warren County, Pennsylvania, St Louis County, Minnesota, Sandoval County, New Mexico, Kershaw County, South Carolina, Fort Yukon, Alaska, Grays Harbor County, Washington, and Washington County, Missouri
[E82-10186] p 84 N82-22620
TRIANGULATION
Present status of on-line analytical triangulation p 69 A82-34940
TROPICAL METEOROLOGY
Interannual variations of outgoing IR associated with tropical circulation changes during 1974-1978 p 54 A82-36341

TROPICAL REGIONS
The impact of meteorological satellites on the First GARP Global Experiment (FGGE) --- First Global Atmospheric Research Program Global Experiment (FGGE) p 55 N82-23852
TROPOSPHERE
Fine particles in the Soufriere eruption plume p 24 A82-33659
Aircraft measurements of NO/x/ in the lower troposphere above the coast of Japan p 26 A82-36247
Tropospheric CO measurement experiment from the second Space Shuttle flight p 27 A82-36292
Ammonia and the NOx budget of the troposphere p 27 A82-36293
TROPOSPHERIC SCATTERING
Inference of refractivity profiles by satellite-to-ground RF measurements p 78 A82-33442
TUNDRA
Landsat digital analysis of the initial recovery of burned tundra at Kokolik River, Alaska p 8 A82-32913
TURBIDITY
Interpretation of surface-water circulation, Aransas Pass, Texas, using Landsat imagery p 60 A82-32896
Nearshore current pattern off south Texas - An interpretation from aerial photographs p 53 A82-32903
TYPE 2 BURSTS
The relation of type II radio bursts to solar energetic particles observed at earth p 3 A82-22591

U

U.S.S.R. SPACE PROGRAM
Remote sensing of the earth's resources - The Soviet experience p 84 A82-33555
ULTRAVIOLET ABSORPTION
The effect of the spectral attenuation of UV radiation by aerosol on the total ozone measurements p 27 A82-36406
ULTRAVIOLET SPECTROMETERS
Atmospheric ozone determination by solar occultation using the UV spectrometer on the Solar Maximum Mission p 27 A82-36362
ULTRAVIOLET SPECTROPHOTOMETERS
Sensitivity of Dobson total ozone estimations to wavelength band calibration uncertainties p 27 A82-36405
Dobson spectrophotometer calibrations, possible errors in ozone absorption coefficients, and errors due to interfering pollutant gases p 28 A82-36431
OSO-8 lower mesospheric ozone number density profiles p 28 A82-36472
UNDERWATER OPTICS
Bias correction procedures for airborne laser hydrography
[PB82-130089] p 63 N82-22644
UNITED KINGDOM
Satellite observations of sea surface temperature around the British Isles p 54 A82-33717
The METEOSAT Data Collection System and its application p 75 N82-26037
UNITED STATES OF AMERICA
MAGSAT and aeromagnetic data in the North American continent
[E82-10193] p 71 N82-22627
AgRISTARS Foreign commodity production forecasting The 1980 US/Canada wheat and barley exploratory experiment
[E82-10126] p 11 N82-23565
An equivalent layer magnetization model for the United States derived from MAGSAT data
[E82-10297] p 36 N82-24573
Magnetic and gravity anomalies in the Americas
[E82-10312] p 37 N82-24586
Use of MAGSAT anomaly data for crustal structure and mineral resources in the US Midcontinent
[E82-10321] p 46 N82-24594
Use of MAGSAT anomaly data for crustal structure and mineral resources in the US Midcontinent
[E82-10323] p 46 N82-24596
UNIVERSITY PROGRAM
LANDSAT technology transfer to the private and public sectors through community colleges and other locally available institutions
[E82-10181] p 85 N82-23568
UPWELLING WATER
Meteorological and aircraft data for CUE 2 1973
[PB82-149246] p 59 N82-26949
URANIUM
Airborne gamma-ray spectrometer and magnetometer survey Barrow quadrangle, Alaska, volume 1
[DE82-000334] p 43 N82-23623
Airborne gamma-ray spectrometer and magnetometer survey Wainwright quadrangle, Alaska, volume 2
[DE82-000341] p 43 N82-23624
Airborne gamma-ray spectrometer and magnetometer survey, Kenora quadrangle, Minnesota, volume 1
[DE82-001029] p 43 N82-23625
Airborne gamma-ray spectrometer and magnetometer survey Meade River quadrangle, Alaska, volume 2
[DE82-000340] p 43 N82-23626
Airborne gamma-ray spectrometer and magnetometer survey Teshekpuk quadrangle, Alaska, volume 2
[DE82-000310] p 43 N82-23627
Airborne gamma-ray spectrometer and magnetometer survey Harrison Bay quadrangle, Alaska, volume 2
[DE82-000315] p 43 N82-23628
Airborne gamma-ray spectrometer and magnetometer survey Beechey Pt , quadrangle, Alaska, volume 2
[DE82-000309] p 43 N82-23629
Airborne gamma-ray spectrometer and magnetometer survey Point Lay quadrangle, Alaska, volume 2
[DE82-000308] p 43 N82-23630
Airborne gamma-ray spectrometer and magnetometer survey Utukik River quadrangle, Alaska, volume 2
[DE82-000316] p 44 N82-23631
Airborne gamma-ray spectrometer and magnetometer survey Sagavanirktok quadrangle, Alaska, volume 2
[DE82-000311] p 44 N82-23632
Airborne gamma-ray spectrometer and magnetometer survey Duluth quadrangle, Minnesota, volume 2
[DE82-001027] p 44 N82-23633
Airborne gamma-ray spectrometer and magnetometer survey Roseau quadrangle, Minnesota, volume 2
[DE82-001025] p 44 N82-23634
Airborne gamma-ray spectrometer and magnetometer survey Devil's Lake quadrangle, North Dakota, volume 1
[DE82-004161] p 44 N82-23635
Airborne gamma-ray spectrometer and magnetometer survey Devil's Lake quadrangle, North Dakota, volume 2
[DE82-004168] p 44 N82-23636
Airborne gamma-ray spectrometer and magnetometer survey Bemidji quadrangle, Minnesota, volume 1
[DE82-001032] p 44 N82-23637
Airborne gamma-ray spectrometer and magnetometer survey Bemidji quadrangle, Minnesota, volume 2
[DE82-001026] p 44 N82-23638
Airborne gamma-ray spectrometer and magnetometer survey Hibbing quadrangle, Minnesota, volume 1
[DE82-004159] p 44 N82-23639
Airborne gamma-ray spectrometer and magnetometer survey Hibbing quadrangle, Minnesota, volume 2
[DE82-004165] p 45 N82-23640
Airborne gamma-ray spectrometer and magnetometer survey Aberdeen quadrangle, South Dakota, volume 1
[DE82-004152] p 45 N82-23641
Airborne gamma-ray spectrometer and magnetometer survey Aberdeen quadrangle, South Dakota, volume 2
[DE82-004164] p 45 N82-23642
Airborne gamma-ray spectrometer and magnetometer survey International Falls quadrangle, Minnesota, volume 1
[DE82-004151] p 45 N82-23643
Airborne gamma-ray spectrometer and magnetometer survey International Falls quadrangle, Minnesota, volume 2
[DE82-004166] p 45 N82-23644
Airborne gamma-ray spectrometer and magnetometer survey, Toronto quadrangle New York, volume 2A
[DE81-027158] p 46 N82-25620
Airborne gamma-ray spectrometer and magnetometer survey, Kingston quadrangle New York, volume 2C
[DE81-027161] p 46 N82-25621
Airborne gamma-ray spectrometer and magnetometer survey, Rochester quadrangle New York, volume 2D
[DE81-027156] p 46 N82-25622
Airborne gamma-ray spectrometer and magnetometer survey Barrow quadranagle, Alaska, volume 2
[DE82-000342] p 46 N82-25623
Airborne gamma-ray spectrometer and magnetometer survey Lookout Ridge quadrangle, Alaska, volume 2
[DE82-000313] p 47 N82-25625
Airborne gamma-ray spectrometer and magnetometer survey North/south tieline, volume 2
[DE82-005570] p 47 N82-27805
Airborne gamma-ray spectrometer and magnetometer survey Sioux Falls quadrangle, South Dakota, volume 1
[DE82-005533] p 47 N82-27806
Airborne gamma-ray spectrometer and magnetometer survey Sioux Falls quadrangle, South Dakota, volume 2
[DE82-005574] p 47 N82-27807
Airborne gamma-ray spectrometer and magnetometer survey Susanville quadrangle, California, volume 1
[DE82-005538] p 48 N82-27811
Airborne gamma-ray spectrometer and magnetometer survey Roseburg quadrangle, Oregon, volume 2
[DE82-005568] p 48 N82-27812
Airborne gamma-ray spectrometer and magnetometer survey Ukiah quadrangle, California, volume 1 --- uranium exploration
[DE82-005541] p 48 N82-27813
URBAN RESEARCH
Spatial resolution requirements for urban studies p 29 A82-37502
A legislator's guide to LANDSAT
[E82-10290] p 85 N82-24568
USER MANUALS (COMPUTER PROGRAMS)
Description of the FORTRAN implementation of the spring small grains planting date distribution model
[E82-10235] p 15 N82-23608
UTAH
Identifying environmental features for land management decisions --- Utah
[E82-10289] p 30 N82-24567
HCMM hydrological analysis in Utah
[E82-10328] p 63 N82-24601
Inventory of wetlands and agricultural land cover in the upper Sevier River Basin, Utah
[E82-10345] p 18 N82-25607
Mapping of wildlife habitat in Farmington Bay, Utah
[E82-10354] p 19 N82-26752
Detection of variations in aspen forest habitat from LANDSAT digital data Bear River Range, Utah
[E82-10355] p 19 N82-26753
Irrigated acreage in the Bear River Basin as of the 1975 growing season --- Idaho, Utah, and Wyoming
[E82-10356] p 20 N82-26754

V

VARIABILITY
Determination of the optimal level for combining area and yield estimates
[E82-10215] p 12 N82-23588
On the space-time variability of ocean surface mixed layer charactenstics of central and eastern Arabian sea during MONSOON-77 --- global atmospheric research program p 56 N82-23909
VEGETATION
Color aerial photography in the plant sciences and related fields, Proceedings of the Eighth Biennial Workshop, Luray, VA, April 21-23, 1981 p 5 A82-29526
Estimating rangeland cover proportions with large-scale color-infrared aerial photographs p 6 A82-29534
Mapping riparian vegetation in Southeastern Oregon using digitized large scale color infra-red aerial photography p 6 A82-29535
Application of scanning microdensitometer data in selected plant science case studies p 7 A82-29539
Effects of vegetation canopy structure on remotely sensed canopy temperatures --- inferring plant water stress and yield p 8 A82-32905
Interpretation of vegetative cover in wetlands using four-channel SAR imagery p 9 A82-34706
Use of Landsat multispectral scanner data in vegetation mapping of a forested area p 9 A82-34731
Remote sensing of salt marsh vegetation in the first four proposed Thematic Mapper bands p 10 A82-37503
Use and applicability of the vegetation component of the national site classification system --- Sumter National Forest, South Carolina
[E82-10234] p 15 N82-23607
AgRISTARS Agriculture and resources inventory surveys through aerospace remote sensing
[E82-10236] p 15 N82-23609
A method for inferring available surface moisture using remote surface temperature measurements An assessment --- Kansas and St Louis, Missouri
[E82-10311] p 17 N82-24585
Measurement of soil moisture trends with airborne scatterometers --- Guymon, Oklahoma and Dalhart, Texas
[E82-10361] p 20 N82-26759
Multifrequency remote sensing of soil moisture --- Guymon, Oklahoma and Dalhart, Texas
[E82-10362] p 20 N82-26760
Remote sensing of sulfur dioxide effects on vegetation Volume 1 Summary
[DE82-900580] p 31 N82-27802
Remote sensing of sulfur dioxide effects on vegetation Volume 2 Data
[DE82-900581] p 31 N82-27803
VEGETATION GROWTH
Riparian vegetation mapping in Northeastern California using high altitude color infrared aerial photography p 5 A82-29528

Landsat digital analysis of the initial recovery of burned tundra at Kokolik River, Alaska p 8 A82-32913
Multispectral determination of soil moisture-2 --- Guymon, Oklahoma and Dalhart, Texas
[E82-10349] p 19 N82-26747
Development of visible/infrared/microwave agriculture classification and biomass estimation algorithms --- Guyton, Oklahoma and Dalhart, Texas
[E82-10363] p 20 N82-26761

VENERA SATELLITES
Comparison of solar proton activity in 1967 and 1969 with that in 1978 and 1979 as measured onboard Venera 4, 6, 11, 12 space probes p 31 A82-22596

VENERA 11 SATELLITE
The solar proton fluxes in April, 1979 p 66 A82-22597

VERTICAL DISTRIBUTION
Aircraft measurements of NO/x/ in the lower troposphere above the coast of Japan p 26 A82-36247
Ammonia and the NOx budget of the troposphere p 27 A82-36293

VERY LONG BASE INTERFEROMETRY
Work related to the Blue Road Geotraverse at the Finnish Geodetic Institute p 32 A82-30306
The definition of the terrestrial coordinate frame by long baseline interferometry p 33 A82-32084
Some considerations in the use of very-long-baseline-interferometry to establish reference coordinate systems for geodynamics p 34 A82-32096

VIEW EFFECTS
Effect of atmospheric conditions on remote sensing of vegetation parameters p 24 A82-32901
View angle effects in the radiometric measurement of plant canopy temperatures p 8 A82-32914

VISUAL AIDS
Interactive initialization of heat flux parameters for numerical models using satellite temperature measurements
[E82-10313] p 82 N82-26743

VISUAL OBSERVATION
Detection of regional air pollution episodes utilizing satellite digital data in the visual range p 23 A82-31990

VOLATILITY
On volatility, first ionization potential, and s- and r-processes --- for Galactic cosmic ray sources p 2 A82-22560

VOLCANOES
Soufriere Volcano, St Vincent - Observations of its 1979 eruption from the ground, aircraft, and satellites p 24 A82-33652
Crustal structures under the active volcanic areas of central and eastern Mediterranean (M-44)
[E82-10096] p 35 N82-23563
An investigation into the utilization of HCMM thermal data for the discrimination of volcanic and Eolian geological units --- Newberry Volcano, Oregon
[E82-10352] p 47 N82-26750

VOLCANOLOGY
Detection of volcanic smoke and ash-fall area at volcano Aso, from Landsat MSS data p 23 A82-31295
Geostationary satellite observations of the April 1979 Soufriere eruptions p 24 A82-33654
Meteorological analysis of the eruption of Soufriere in April 1979 p 24 A82-33655
Skirt clouds associated with the Soufriere eruption of 17 April 1979 p 24 A82-33656
Airborne lidar measurements of the Soufriere eruption of 17 April 1979 p 24 A82-33657
Fine particles in the Soufriere eruption plume p 24 A82-33659
Overseas Geology And Mineral Resources number 56 A geological interpretation of LANDSAT imagery and air photography of Botswana
[OGMR-56] p 42 N82-22636
Seismic and geodetic studies of the Imperial Valley, California
[DE82-001686] p 39 N82-26915

W

WATER BALANCE
Water-balance differentiation of natural complexes on the basis of satellite photographs p 61 A82-35129
The possibility of using remote-sensing methods to study the hydrology of elementary watersheds p 61 A82-35130

WATER CIRCULATION
Interpretation of surface-water circulation, Aransas Pass, Texas, using Landsat imagery p 60 A82-32896
Sea-Ice Mission Requirements for the US FIREX and Canada RADARSAT programs
[NASA-CR-168984] p 57 N82-25609

WATER COLOR
Analysis of ocean color scanner data from the Superflux III Experiment
[NASA-TM-83290] p 55 N82-23614

WATER DEPTH
Bias correction procedures for airborne laser hydrography
[PB82-130089] p 63 N82-22644
Bathymetric and tectonics of Indian Ocean using MAGSAT data
[E82-10204] p 36 N82-23577
Analyzing the Broken Ridge area of the Indian Ocean using magnetic and gravity anomaly maps and geoid undulation and bathymetry data
[E82-10303] p 36 N82-24577
Investigating tectonic and bathymetric features of the Indian Ocean using MAGSAT magnetic anomaly data
[E82-10304] p 37 N82-24578

WATER FLOW
The use of satellite photographs to study snow-cover dynamics and to determine the average water discharge of the Amudarya during a vegetation period p 61 A82-35132

WATER POLLUTION
Characteristics of 13 9 GHz radar scattering from oil films on the sea surface p 54 A82-33438
A quantitative multispectral analysis system for aerial photographs applied to coastal planning p 55 A82-37505

WATER QUALITY
The use of remote-sensing data to identify the space-time variability of the quality of natural waters p 62 A82-35138
Use of NOAA/AVHRR visible and near-infrared data for land remote sensing
[NASA-TM-84186] p 81 N82-22643
HCMM hydrological analysis in Utah
[E82-10328] p 63 N82-24601

WATER RESOURCES
A comparative study of microwave radiometer observations over snowfields with radiative transfer model calculations --- for water runoff estimation p 60 A82-32910
Use of aerial photography in determining land use and streamflow relationships on small developing watersheds p 60 A82-34736
The possibility of using remote-sensing methods to study the hydrology of elementary watersheds p 61 A82-35130
The seasonal snow-line within the Fergana basin and the possibility of using it for hydrological forecasting p 61 A82-35131
The use of remote-sensing data to identify the space-time variability of the quality of natural waters p 62 A82-35138
Ten-Ecosystem Study --- Grand and Weld Counties, Colorado, Warren County, Pennsylvania, St Louis County, Minnesota; Sandoval County, New Mexico, Kershaw County, South Carolina, Fort Yukon, Alaska, Grays Harbor County, Washington, and Washington County, Missouri
[E82-10186] p 84 N82-22620

WATER RUNOFF
A comparative study of microwave radiometer observations over snowfields with radiative transfer model calculations --- for water runoff estimation p 60 A82-32910
Automated classification of runoff coefficients from Landsat multispectral data p 60 A82-34734
The application of Heat Capacity Mapping Mission (HCMM) thermal data to snow hydrology --- Salt Verde Watershed and the southern Sierra Nevada
[E82-10191] p 62 N82-22625

WATER TABLES
Evaluation of HCMM data for assessing soil moisture and water table depth --- South Dakota
[E82-10329] p 18 N82-24602

WATER TEMPERATURE
Evaluation of the accuracy of water-surface temperature measurement by means of airborne infrared radiometers p 62 A82-35136

WATER VAPOR
Estimation of the precipitable water from the IR channel of the geostationary satellite p 55 A82-37196

WATER WAVES
The Seasat altimeter data and its accuracy assessment p 49 A82-29602
An empirical determination of the effects of sea state bias on Seasat altimetry p 50 A82-29607
Sea-state-related altitude errors in the Seasat radar altimeter p 50 A82-29608
Waveheight and wind speed measurements from the Seasat radar altimeter p 50 A82-29612
Seasat wind and wave observations of northeast Pacific hurricane Iva, August 13, 1978 p 52 A82-29624
The estimation of wave height from digitally processed SAR imagery p 67 A82-32347
On the synthetic aperture radar imaging of ocean surface waves p 53 A82-32881
Ocean wave height measurement with SEASAT SAR using speckle diversity p 53 A82-32882
Pulse-to-pulse correlation in satellite radar altimeters --- for ocean wave height measurement p 55 A82-37390

WATERSHEDS
Automated classification of runoff coefficients from Landsat multispectral data p 60 A82-34734
Use of aerial photography in determining land use and streamflow relationships on small developing watersheds p 60 A82-34736
Dynamic study of the upper Sao Francisco river and Tres Marias reservoir using MSS/LANDSAT images --- BRazil
[E82-10291] p 63 N82-24569

WAVE ATTENUATION
Possible evidence for attenuation of an MHD shock by a magnetic neutral sheet in the solar corona p 3 A82-22589

WAVE FRONTS
Satellite observations in FRONTS 80
[AD-A111080] p 58 N82-26766

WAVEFORMS
Sea-state-related altitude errors in the Seasat radar altimeter p 50 A82-29608

WEATHER FORECASTING
Impact of additional summer MONEX wind data on the prediction of monsoon depressions during June - August 1979 with two versions of primitive equation (PE) barotropic model --- Monsoon Experiment (MONEX) p 56 N82-23900
Some empirical rules for forecasting fog and status over northern Florida, southern Georgia and adjacent coastal waters
[PB82-154006] p 59 N82-27949

WEST GERMANY
Multidisciplinary investigations on HCMM data over middle Europe and Marocco --- southern Germany and Marrakesh, Morocco
[E82-10315] p 74 N82-24588

WEST INDIES
An investigation of MAGSAT and complementary data emphasizing precambrian shields and adjacent areas of West Africa and South America
[E82-10316] p 38 N82-24589

WETLANDS
Interpretation of vegetative cover in wetlands using four-channel SAR imagery p 9 A82-34706
Application of remote sensing to state and regional problems
[E82-10288] p 30 N82-24566
Identifying environmental features for land management decisions --- Utah
[E82-10289] p 30 N82-24567
Inventory of wetlands and agricultural land cover in the upper Sevier River Basin, Utah
[E82-10345] p 18 N82-25607
Irrigated acreage in the Bear River Basin as of the 1975 growing season --- Idaho, Utah, and Wyoming
[E82-10356] p 20 N82-26754

WHEAT
Spectral scanning of experimental plots of SO2-affected winter wheat and soybeans for mission planning p 6 A82-29537
AgRISTARS Foreign commodity production forecasting The 1980 US/Canada wheat and barley exploratory experiment
[E82-10126] p 11 N82-23565
Evaluation of the Doraiswamy-Thompson winter wheat crop calendar model incorporating a modified spring restart sequence
[E82-10207] p 12 N82-23580
AgRISTARS Supporting research Spring small grains planting date distribution model
[E82-10208] p 12 N82-23581
Selection of the Australian indicator region
[E82-10222] p 13 N82-23595
Linear polarization of light by two wheat canopies measured at many view angles
[E82-10229] p 14 N82-23602
A model of plant canopy polarization
[E82-10233] p 15 N82-23606
Description of the FORTRAN implementation of the spring small grains planting date distribution model
[E82-10235] p 15 N82-23608

WILDLIFE
Inventory of wildlife habitat from color infrared aerial photography for Cobb Island, Virginia p 6 A82-29529
A computerized spatial analysis system for assessing wildlife habitat from vegetation maps p 9 A82-34716
Mapping of wildlife habitat in Farmington Bay, Utah
[E82-10354] p 19 N82-26752

WIND DIRECTION
Some empirical rules for forecasting fog and status over northern Florida, southern Georgia and adjacent coastal waters
[PB82-154006] p 59 N82-27949
WIND MEASUREMENT
The Seasat-A satellite scatterometer - The geophysical evaluation of remotely sensed wind vectors over the ocean p 51 A82-29616
The relationship between wind vector and normalized radar cross section used to derive Seasat-A Satellite Scatterometer winds p 51 A82-29617
Surface wind analyses for Seasat p 51 A82-29619
Seasat wind and wave observations of northeast Pacific hurricane Iva, August 13, 1978 p 52 A82-29624
SEASAT A satellite scatterometer illumination times of selected in situ sites
[NASA-TM-83280] p 81 N82-22865
WIND VARIATIONS
Representativeness of cloud motion winds deduced from GOES Indian Ocean satellite imagery for the description of the Indian summer monsoon --- superpressure balloons for the study of the Indian summer monsoon (BALSAMINE) p 55 N82-23879
Estimates of sea surface stress for summer MONEX from cloud motions --- global atmospheric research program p 56 N82-23910
WIND VELOCITY
On the application of a model of boundary-layer flow over low hills to real terrain p 29 A82-36741
The effect of sea-surface Sun glitter on microwave radiometer measurements
[NASA-CR-169083] p 57 N82-26525
WIND VELOCITY MEASUREMENT
The Seasat altimeter data and its accuracy assessment p 49 A82-29602
Waveheight and wind speed measurements from the Seasat radar altimeter p 50 A82-29612
Intercomparison of wind speeds inferred by the SASS, altimeter, and SMMR p 52 A82-29621
Description of Seasat radiometer status and results p 52 A82-29622
WINDOWS (INTERVALS)
Defining the temporal window for monitoring forest canopy defoliation using Landsat p 9 A82-34730
WINTER
The growth of snow in winter storms - An airborne observational study p 60 A82-33329
Determination of winter temperature patterns, fronts, and surface currents in the Yellow Sea and East China Sea from satellite imagery p 55 A82-37195
The onset of the Australian Northwest monsoon during winter MONEX Broadscale flow revealed by an objective analysis scheme p 56 N82-23912
Analysis of thematic mapper simulator data acquired during winter season over Pearl River, Mississippi, test site
[E82-10287] p 17 N82-24565
Ice distribution and winter surface circulation patterns, Kachemak Bay, Alaska
[AD-A110806] p 58 N82-26764
WOLF-RAYET STARS
On the stellar origin of the Ne-22 excess in cosmic rays p 21 A82-22562
WYOMING
Ground support data from July 10 to July 29, 1978, for HCMM thermal satellite data of the Powder River Basin, Wyoming
[E82-10211] p 72 N82-23584
Irrigated acreage in the Bear River Basin as of the 1975 growing season --- Idaho, Utah, and Wyoming
[E82-10356] p 20 N82-26754

X

X RAY SOURCES
Consequences of an inverse Compton emission model for extragalactic X-ray sources p 83 A82-22553
X RAY SPECTRA
The determination of differential X-ray spectrum of the solar flare using ionospheric data p 65 A82-22582

Y

YIELD
AgRISTARS Supporting research Spring small grains planting date distribution model
[E82-10208] p 12 N82-23581
Determination of the optimal level for combining area and yield estimates
[E82-10215] p 12 N82-23588
AgRISTARS Preliminary technical results review of FY81 experiments, volume 2 Fiscal year 1981/1982 'corn and soybeans pilot' experiment
[E82-10216] p 13 N82-23589
Association of spectral development patterns with development stages of corn
[E82-10353] p 19 N82-26751

Z

ZERO POINT ENERGY
Astrophysical scenarios for critically evaluating a zero-point field acceleration mechanism p 64 A82-22575

Typical Personal Author Index Listing

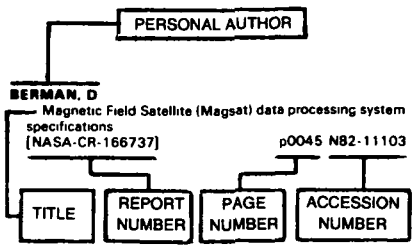

Listings in this index are arranged alphabetically by personal author The title of the document provides the user with a brief description of the subject matter The report number helps to indicate the type of document listed (e.g , NASA report, translation, NASA contractor report) The page and accession numbers are located beneath and to the right of the title, e g., p0045 N82-11103 Under any one author's name the accession numbers are arranged in sequence with the AIAA accession numbers appearing first

A

ADAMS, J. H., JR.
Calculated isotopic source composition and tests for origin and propagation of cosmic rays with mass numbers less than or equal to 62 p 83 A82-22554

ADRIEN, P -M.
The use of the SPOT satellite in natural resource evaluation p 83 A82-31996

AGARWAL, B. N. P
Analysis of MAGSAT data of the Indian region [E82-10358] p 75 N82-26756

AGARWAL, P. K.
Analysis of MAGSAT data of the Indian region [E82-10358] p 75 N82-26756

AGUI, T.
Description of gray level picture using a collection of density contour lines p 66 A82-29409

AIKEN, C. L. V.
Evaluation and combined geophysical interpretations of NURE and related geoscience data in the Van Horn, Pecos, Marfa, Fort Stockton, Presidido, and Emory Peak quadrangles, Texas, volume 1 [DE82-005554] p 47 N82-27808
Evaluation and combined geophysical interpretations of NURE and related geoscience data in the Van Horn, Pecos, Marfa, Fort Stockton, Presidio, and Emory Peak quadrangels, Texas [DE82-005560] p 48 N82-27809

AIKIN, A. C.
Atmospheric ozone determination by solar occultation using the UV spectrometer on the Solar Maximum Mission p 27 A82-36362

ALIMUKHAMEDOV, M. A.
The use of space photographs in the mapping of glaciers and water bodies p 62 A82-37174

ALKEZWEENY, A. J.
Comparison of ozone in polluted and clean air masses over Lake Michigan p 29 A82-36477

ALLEN, L. H., JR.
Use of thermal inertia determined by HCMM to predict nocturnal cold prone areas in Florida [E82-10299] p 17 N82-24575

ALLISON, L J.
Snowpack monitoring in North America and Eurasia using passive microwave satellite data p 78 A82-32915

ALLISON, R. A.
Panoramic aerial photography in forest pest management p 7 A82-32701

ALVO, P.
Aircraft monitoring of surface carbon dioxide exchange p 23 A82-30293

ALZOFON, F. E.
Remote sensing of thermal subsurface terrain properties p 80 A82-34727

ANDERSON, J. E
Analysis of thematic mapper simulator data acquired during winter season over Pearl River, Mississippi, test site [E82-10287] p 17 N82-24565

ANDERSON, K. D.
Inference of refractivity profiles by satellite-to-ground RF measurements p 78 A82-33442

ANDREWS, J C.
High resolution satellite observations of mesoscale oceanography in the Tasman Sea, 1978 - 1979 [E82-10324] p 57 N82-24597

AOKI, T.
Estimation of the precipitable water from the IR channel of the geostationary satellite p 55 A82-37196

ARONOFF, S.
Detection of environmental disturbance using color aerial photography and thermal infrared imagery p 22 A82-29327

ARORA, B R
MAGSAT for geomagnetic studies over Indian region [E82-10202] p 72 N82-23575
MAGSAT for geomagnetic studies over Indian region [E82-10296] p 73 N82-24572

ARTLEY, J. A.
AgRISTARS Supporting research Spring small grains planting date distribution model [E82-10208] p 12 N82-23581
Application of thermal model for pan evaporation to the hydrology of a defined medium, the sponge [E82-10217] p 13 N82-23590
Description of the FORTRAN implementation of the spring small grains planting date distribution model [E82-10235] p 15 N82-23608

ARUR, M. G.
Analysis of MAGSAT data of the Indian region [E82-10358] p 75 N82-26756

ARVIDSON, R. E.
Structure of the St Francois Mountains and surrounding lead belt, S E Missouri Inferences from thermal IR and other data sets [E82-10200] p 36 N82-23573
Structure of the St Francois Mountains and surrounding lead belt, S E Missouri Inferences from thermal IR and other data sets [E82-10205] p 11 N82-23578
Structure of the Saint Francois Mountains and surrounding lead belt, S E Missouri Inference from thermal IR and other data sets [E82-10350] p 39 N82-26748

ASKARI, F
Automated classification of runoff coefficients from Landsat multispectral data p 60 A82-34734

AUDOUZE, J.
Origin of galactic cosmic rays from Ne isotopic composition p 2 A82-22563

AUGUSTSSON, T. R.
Ammonia and the NOx budget of the troposphere p 27 A82-36293

AVASTE, O.
Estimation of the temperature of the upper boundary of cloud cover over the world ocean p 54 A82-36005

AXFORD, W. I.
Cosmic ray acceleration by stellar winds I - Total density, pressure and energy flux p 21 A82-22566

B

BABKINA, L. P.
Experience with the compilation of maps of snow-cover melting in the central part of the European USSR on the basis of satellite data p 62 A82-35134

BADHWAR, G.
Field size, length, and width distributions based on LACIE ground truth data p 8 A82-32909

BAINS, S P. S.
Analysis of MAGSAT data of the Indian region [E82-10358] p 75 N82-26756

BALICK, L. K.
Appearance of irregular tree canopies in nighttime high-resolution thermal infrared imagery p 68 A82-32916

BALLANI, L.
Establishing geodetic-geodynamic parameters using lunar laser range measurements p 34 A82-33293

BARABANOVA, N G.
Evaluation of the effectiveness of systematic image distortion compensation p 69 A82-34469

BARBE, A.
Application of infrared techniques to the study of atmospheric ozone p 27 A82-36414

BARNES, J. C.
The application of Heat Capacity Mapping Mission (HCMM) thermal data to snow hydrology [E82-10191] p 62 N82-22625

BARR, S.
Meteorological analysis of the eruption of Soufriere in April 1979 p 24 A82-33655
Skirt clouds associated with the Soufriere eruption of 17 April 1979 p 24 A82-33656

BARRACLOUGH, D. R
Spherical harmonic representation of the main geomagnetic field for world charting and investigations of some fundamental problems of physics and geophysics [E82-10203] p 72 N82-23576

BARTON, J C
Measurement of cosmogenic nuclides using a multi-crystal gamma-ray coincidence spectrometer p 64 A82-22577

BASHER, R. E.
Sensitivity of Dobson total ozone estimations to wavelength band calibration uncertainties p 27 A82-36405
Optical stop and focussing effects in the Dobson instrument p 28 A82-36428

BAUER, M. E.
Spectral properties of agricultural crops and soils measured from space, aerial, field, and laboratory sensors [E82-10189] p 10 N82-22623
Diurnal changes in reflectance factor due to Sun-row direction interactions [E82-10128] p 11 N82-23566
Spectral properties of agricultural crops and soils measured from space, aerial, field, and laboratory sensors [E82-10212] p 12 N82-23585
Multistage classification of multispectral Earth observational data The design approach [E82-10213] p 72 N82-23586
Determination of the optimal level for combining area and yield estimates [E82-10215] p 12 N82-23588
Application of Computer Axial Tomography (CAT) to measuring crop canopy geometry [E82-10227] p 14 N82-23600
Linear polarization of light by two wheat canopies measured at many view angles [E82-10229] p 14 N82-23602
Canopy reflectance as influenced by solar illumination angle [E82-10237] p 15 N82-23610
Spectral estimates of solar radiation intercepted by corn canopies [E82-10003] p 18 N82-26742

BAUM, W. A.
Subtleties in the flat-fielding of charge-coupled device /CCD/ images p 68 A82-32581

BAUMGARDNER, R. W., JR.
Interpretation of surface-water circulation, Aransas Pass, Texas, using Landsat imagery p 60 A82-32896
BAZILEVSKAIA, G. A.
On the physical sense of the constant of solar cosmic ray coronal propagation p 83 A82-22599
The influence of the sector structure of interplanetary magnetic field on the solar cosmic ray characteristics p 83 A82-22603
BELIAVSKII, A. I.
Remote sensing of the weediness of crop fields p 5 A82-29435
BENDER, P. L.
Establishment of terrestrial reference frames by new observational techniques p 33 A82-32078
BENDURA, R. J.
In situ ozone data for comparison with laser absorption remote sensor 1980 PEPE/NEROS program [NASA-TM-84471] p 30 N82-25661
BENTLEY, C. R
Magsat magnetic anomalies over Antarctica and the surrounding oceans p 32 A82-30787
Investigation of Antarctic crust and upper mantle using MAGSAT and other geophysical data [E82-10308] p 37 N82-24582
Investigation of Antarctic crust and upper mantle using MAGSAT and other geophysical data [E82-10309] p 37 N82-24583
BENTON, E. R.
Investigation of geomagnetic field forecasting and fluid dynamics of the core [E82-10198] p 35 N82-23571
Investigation of geomagnetic field forecasting and fluid dynamics of the core [E82-10310] p 37 N82-24584
Investigation of geomagnetic field forecasting and fluid dynamics of the core [E82-10342] p 39 N82-25604
BERLIN, G. L.
Possible fault detection in Cottonball Basin, California An application of radar remote sensing p 41 A82-32898
BERNARD, R.
C-band radar for determining surface soil moisture p 10 A82-37194
BERNSTEIN, R. L.
Seasat altimeter determination of ocean current variability p 50 A82-29613
BESSELING, J. F.
Nonlinear theory for elastic beams and rods and its finite element representation [WTHD-143] p 73 N82-24517
BEUTLER, G A.
Evaluation of HCMM data for assessing soil moisture and water table depth [E82-10329] p 18 N82-24602
BHARGAVA, B. N.
MAGSAT for geomagnetic studies over Indian region [E82-10202] p 72 N82-23575
BIBRING, J.-P.
Interstellar grains as seeds for galactic cosmic rays p 2 A82-22561
BIEHL, L. L.
Diurnal changes in reflectance factor due to Sun-row direction interactions [E82-10128] p 11 N82-23566
Linear polarization of light by two wheat canopies measured at many view angles [E82-10229] p 14 N82-23602
BIERMANN, P.
Consequences of an inverse Compton emission model for extragalactic X-ray sources p 83 A82-22553
BILANOW, S.
LANDSAT-D conical scanner evaluation plan [E82-10340] p 81 N82-25602
BINENKO, V. I.
Albedo and angular characteristics of the reflectance of the underlying surface and clouds p 33 A82-30849
BIRRER, I. J.
Evaluation of atmospheric attenuation from SMMR brightness temperature for the Seasat satellite scatterometer p 51 A82-29618
BISIGNANI, W. T.
Design guidelines for satellite image data distribution systems p 70 A82-37048
BISWAS, S
On the stellar origin of low energy cosmic rays p 21 A82-22567
Coulombian energy losses and the nuclear composition of the solar cosmic rays p 4 A82-22610
BLAZQUEZ, C. H.
Detection and damage assessment of citrus tree losses with aerial color infrared photography /ACIR/ p 7 A82-29538
Effects of altitude, focal length, and filter combinations on color infrared photography of citrus groves p 9 A82-34729
BLODGET, H. W.
Landsat in the search for Appalachian hydrocarbons p 42 A82-34721
BLOKH, G. M.
Preflare increases in solar cosmic rays relevant to the mode of energy accumulation in the active regions associated with large flares p 31 A82-22595
BLUME, H -J. C.
Depression of brightness temperature of sea surfaces covered with monomolecular oil films relative to clean water surfaces at 1 43 GHz p 54 A82-33322
BOBERLY, J. C.
SEASAT A satellite scatterometer illumination times of selected in situ sites [NASA-TM-83280] p 81 N82-22865
BOGGS, D H.
The Seasat-A satellite scatterometer - The geophysical evaluation of remotely sensed wind vectors over the ocean p 51 A82-29616
The relationship between wind vector and normalized radar cross section used to derive Seasat-A Satellite Scatterometer winds p 51 A82-29617
BOLSHOI, A. A
Space to the earth p 83 A82-30850
BONNER, K. G
Riparian vegetation mapping in Northeastern California using high altitude color infrared aerial photography p 5 A82-29528
Estimating rangeland cover proportions with large-scale color-infrared aerial photographs p 6 A82-29534
BORN, G. H.
Seasat measurement system evaluation - Achievements and limitations p 49 A82-29601
The Seasat altimeter data and its accuracy assessment p 49 A82-29602
An empirical determination of the effects of sea state bias on Seasat altimetry p 50 A82-29607
Seasat altimeter determination of ocean current variability p 50 A82-29613
BOWEN, R. A.
The meteorological product - 'Cloud-top height' p 70 A82-36043
BOWIN, C.
Computer-processed geophysical atlas of digital data for the East Coast margin of the United States from surface and spacecraft data [AD-A111388] p 39 N82-25748
BOWLEY, C J
The application of Heat Capacity Mapping Mission (HCMM) thermal data to snow hydrology [E82-10191] p 62 N82-22625
BRACALENTE, E. M.
The Seasat-A satellite scatterometer - The geophysical evaluation of remotely sensed wind vectors over the ocean p 51 A82-29616
Evaluation of atmospheric attenuation from SMMR brightness temperature for the Seasat satellite scatterometer p 51 A82-29618
BRACH, E. J.
Aircraft monitoring of surface carbon dioxide exchange p 23 A82-30293
BRACHET, G.
Earth observations from space - Trends and prospects p 84 A82-34116
BRAILE, L. W.
Verification of the crustal component in satellite magnetic data p 32 A82-30789
Study of gravity and magnetic anomalies using MAGSAT data [E82-10194] p 35 N82-22628
Spherical-Earth gravity and magnetic anomaly modeling by Gauss-Legendre quadrature integration [E82-10242] p 36 N82-24520
Magnetic and gravity anomalies in the Americas [E82-10312] p 37 N82-24586
Aeromagnetic and satellite magnetic anomaly mapping [E82-10339] p 39 N82-25601
BRAMMER, R. F.
Spatial resolution and repeatability of Magsat crustal anomaly data over the Indian Ocean p 32 A82-30788
BRAUN, B.
Satellite radiation measurements for the retrieval of the vertical temperature profiles p 70 A82-36935
BRAUTIGAM, D. A.
Fragmentation of Fe nuclei on carbon, hydrogen and CH2 targets I - Individual charge changing and total cross sections II - Isotopic cross sections p 63 A82-22538
BROOKS, D. A.
A ship and satellite view of hydrographic features in the western Gulf of Mexico p 53 A82-32651
BROWN, G. S.
Waveheight and wind speed measurements from the Seasat radar altimeter p 50 A82-29612
BROWN, J.
Landsat digital analysis of the initial recovery of burned tundra at Kokolik River, Alaska p 8 A82-32913
BROWN, O. B.
MONEX oceanographic observations along the East African coast p 56 N82-23908
BROWN, R. A.
The Seasat-A satellite scatterometer - The geophysical evaluation of remotely sensed wind vectors over the ocean p 51 A82-29616
Surface wind analyses for Seasat p 51 A82-29619
BROWN, R. D.
Improved definition of crustal magnetic anomalies for MAGSAT data [E82-10314] p 37 N82-24587
BROWN, W. E., JR.
Seasat wind and wave observations of northeast Pacific hurricane Iva, August 13, 1978 p 52 A82-29624
BRUHWEILER, F.
Confinement and acceleration of cosmic rays in galactic superbubbles p 82 A82-22547
BUCKNER, E
Color aerial photography detects nutrient status of loblolly pine plantations p 6 A82-29531
BUDD, J T. C.
Remote sensing of salt marsh vegetation in the first four proposed Thematic Mapper bands p 10 A82-37503
BUNSCH-MAKAREWICZ, Z.
Satellite radiation measurements for the retrieval of the vertical temperature profiles p 70 A82-36935
BURKE, H.-H. K.
Detection of regional air pollution episodes utilizing satellite digital data in the visual range p 23 A82-31990
BURNETT, D. S.
Laboratory studies of actinide metal-silicate fractionation p 49 A82-22306
BURNS, R.
Source assessment system [AD-A111223] p 75 N82-25613
BURROWS, J R
Studies of high latitude current systems using MAGSAT vector data [E82-10188] p 71 N82-22622
BYRNE, G. F.
Monitoring land-cover change by principal component analysis of multitemporal Landsat data p 68 A82-32906
Separation of diffuse from sharp-edged features in digital imagery p 68 A82-34225

C

CADY, F. M.
A system design for a multispectral sensor using two-dimensional solid-state imaging arrays p 77 A82-31991
Image processing with microcomputers in remote sensing p 79 A82-34708
CAMPBELL, J B
Comparisons of land cover classifications from selected remote sensing systems p 80 A82-34746
CANNON, W. H.
The definition of the terrestrial coordinate frame by long baseline interferometry p 33 A82-32084
CARDONE, V. J.
Surface wind analyses for Seasat p 51 A82-29619
Intercomparison of wind speeds inferred by the SASS, altimeter, and SMMR p 52 A82-29621
CARLE, C.
Movement of ice markers measured by satellite ranging [R-240] p 59 N82-27816
CARLSON, T. N.
A method for inferring available surface moisture using remote surface temperature measurements An assessment [E82-10311] p 17 N82-24585
Interactive initialization of heat flux parameters for numerical models using satellite temperature measurements [E82-10313] p 82 N82-26743
CARMAN, P. D.
Sensitometry in Canadian aerial survey p 79 A82-34724
CARMICHAEL, R. S
Use of MAGSAT anomaly data for crustal structure and mineral resources in the US Midcontinent [E82-10321] p 46 N82-24594

Use of MAGSAT anomaly data for crustal structure and mineral resources in the US Midcontinent
[E82-10323] p 46 N82-24596

CARNES, J G.
AgRISTARS Foreign commodity production forecasting The 1980 US corn and soybeans exploratory experiment
[E82-10206] p 11 N82-23579

CARSEY, F. D.
Sea-Ice Mission Requirements for the US FIREX and Canada RADARSAT programs
[NASA-CR-168984] p 57 N82-25609

CASSE, M.
Mass per charge ratio in hot plasmas and cosmic ray source composition p 2 A82-22557
On the stellar origin of the Ne-22 excess in cosmic rays p 21 A82-22562
Origin of galactic cosmic rays from Ne isotopic composition p 2 A82-22563

CAYLOR, J.
Optical bar panoramic photography for planning timber salvage in drought-stressed forests p 7 A82-32705

CESARSKY, C. J
Mass per charge ratio in hot plasmas and cosmic ray source composition p 2 A82-22557
Interstellar grains as seeds for galactic cosmic rays p 2 A82-22561

CHANDRA, S
The seasonal variations of ozone and temperature in the middle and the upper stratosphere p 29 A82-36534

CHANG, A. T. C
Remote sensing of precipitable water over the oceans from Nimbus 7 microwave measurements p 49 A82-28907
Retrieval of ocean surface and atmospheric parameters from multichannel microwave radiometric measurements p 53 A82-31995
A comparative study of microwave radiometer observations over snowfields with radiative transfer model calculations p 60 A82-32910
Snowpack monitoring in North America and Eurasia using passive microwave satellite data p 78 A82-32915

CHANG, H D.
Remote sensing of precipitable water over the oceans from Nimbus 7 microwave measurements p 49 A82-28907

CHANG, S.
High spectral resolution airborne spectrometry p 77 A82-32443

CHAPELL, J. H.
Fragmentation of Fe nuclei on carbon, hydrogen and CH2 targets I - Individual charge changing and total cross sections II - Isotopic cross sections p 63 A82-22538

CHARAKHCHIAN, A. N.
Features of cosmic ray variations due to variations in the total magnetic field of the sun p 49 A82-22619

CHARAKHCHIAN, T N.
The energy spectra of cosmic ray variations inferred from the stratospheric measurements in 1972-1979 p 5 A82-22617
Features of cosmic ray variations due to variations in the total magnetic field of the sun p 49 A82-22619

CHARLES, P. A.
Soft X-rays from the sunlit earth's atmosphere p 29 A82-37405

CHARLTON, J. A.
Remote sensing in Scotland using data received from satellites - A study of the Tay Estuary region using Landsat multispectral scanning imagery p 62 A82-37501

CHEN, E.
Use of thermal inertia determined by HCMM to predict nocturnal cold prone areas in Florida
[E82-10299] p 17 N82-24575

CHEN, L. C
LANDSAT-D conical scanner evaluation plan
[E82-10340] p 81 N82-25602

CHENEY, R. E.
Comparison data for Seasat altimetry in the western North Atlantic p 50 A82-29611

CHERNOV, V. IU.
The seasonal snow-line within the Fergana basin and the possibility of using it for hydrological forecasting p 61 A82-35131

CHIBISOV, G. V.
Angular variations of nonthermal radio emission from the Galaxy relevant to the structure of interstellar magnetic field p 83 A82-22550

CHIEZE, J. P.
Origin of galactic cosmic rays from Ne isotopic composition p 2 A82-22563

CHITTINENI, C. B.
Dependent feature trees for density approximation I - Optimal construction and classification results p 67 A82-32344

CHRISTMAN, C.
A color-ratio map of Mercury p 31 A82-22294

CHUAN, R. L.
Fine particles in the Soufriere eruption plume p 24 A82-33659

CHUCHKOV, E. A.
The approximate 1 GeV solar cosmic rays in the Forbush-effect of February 15, 1978 p 40 A82-22604

CICONE, R. C.
Analysis of scanner data for crop inventories
[E82-10192] p 10 N82-22626
Analysis of scanner data for crop inventories
[E82-10241] p 16 N82-24519

CIESLA, W. M
Development and application of panoramic aerial photography in forest pest management p 5 A82-29527
Panoramic aerial photography in forest pest management p 7 A82-32701

CLARK, B. V.
Orbiting passive microwave sensor simulation applied to soil moisture estimation
[E82-10343] p 18 N82-25605

CLARK, C A
Use and applicability of the vegetation component of the national site classification system
[E82-10234] p 15 N82-23607

CLARK, J.
Improved land use classification from Landsat and Seasat satellite imagery registered to a common map base p 25 A82-34743

CLARK, J. R.
Application of remote sensing to state and regional problems
[E82-10288] p 30 N82-24566

CLARK, L. D., JR.
Inventory of wetlands and agricultural land cover in the upper Sevier River Basin, Utah
[E82-10345] p 18 N82-25607
Irrigated acreage in the Bear River Basin as of the 1975 growing season
[E82-10356] p 20 N82-26754

COLEMAN, R.
A search for seamounts in the southern Cook and Austral region p 52 A82-30810

COLES, R. L.
Magnetic charts of Canada derived from Magsat data p 32 A82-30778

COLGATE, S A.
The galactic origin of cosmic rays I
[CONF-810711-1] p 2 A82-22565
The galactic origin of cosmic rays II
[CONF-810711-2] p 64 A82-22573

COLLINS, W.
High spectral resolution airborne spectrometry p 77 A82-32443

COLWELL, R. N.
Digitally enhanced visual displays facilitate the analysis of Landsat imagery p 67 A82-32507

CONCANNON, D. M
Mapping riparian vegetation in Southeastern Oregon using digitized large scale color infra-red aerial photography p 6 A82-29535

CONGALTON, R. G.
A quantitative method to test for similarity between photo interpreters p 69 A82-34722

CONNELL, E.
Advanced technology for earth observation - Data processing
[AAS PAPER 82-130] p 71 A82-37810

COOK, P. W
An analysis of LANDSAT MSS scene-to-scene registration accuracy
[E82-10285] p 16 N82-24563

COVAULT, C
Landsat D to yield more precise data p 70 A82-37200

COWSIK, R.
Antiprotons from galactic sources of cosmic rays and gamma rays p 82 A82-22546
Acceleration of cosmic rays in accretion shocks p 64 A82-22568

CRACKNELL, A. P
Remote sensing in Scotland using data received from satellites - A study of the Tay Estuary region using Landsat multispectral scanning imagery p 62 A82-37501

CRAPPER, P. F.
Monitoring land-cover change by principal component analysis of multitemporal Landsat data p 68 A82-32906
Separation of diffuse from sharp-edged features in digital imagery p 68 A82-34225

CRIST, E. P.
Association of spectral development patterns with development stages of corn
[E82-10353] p 19 N82-26751

CROMBIE, M. A.
Coordination of stereo image registration and pixel classification
[AD-A111307] p 75 N82-25614

CROSWELL, W. F
Characteristics of 13 9 GHz radar scattering from oil films on the sea surface p 54 A82-33438

CSILLAG, F.
Significance of tectonics in linear feature detection and interpretation on satellite images p 42 A82-37198

D

DAIBOG, E I.
Energetic solar particle spectra according to Venera-11, 12 and Prognoz-5, 6 p 4 A82-22593

DALKE, G
Multidisciplinary investigations on HCMM data over middle Europe and Marocco
[E82-10315] p 74 N82-24588

DANA, R W.
An infrared exposure meter p 76 A82-29541

DAUGHTRY, C. S. T.
Spectral properties of agricultural crops and soils measured from space, aerial, field, and laboratory sensors
[E82-10189] p 10 N82-22623
Spectral properties of agricultural crops and soils measured from space, aerial, field, and laboratory sensors
[E82-10212] p 12 N82-23585
Canopy reflectance as influenced by solar illumination angle
[E82-10237] p 15 N82-23610
Spectral estimates of solar radiation intercepted by corn canopies
[E82-10003] p 18 N82-26742

DAVE, J. V.
Effect of atmospheric conditions on remote sensing of vegetation parameters p 24 A82-32901

DAVIDSON, N. E.
The onset of the Australian Northwest monsoon during winter MONEX Broadscale flow revealed by an objective analysis scheme p 56 N82-23912

DAVIDSON, S. E.
Use of LANDSAT data to define soil boundaries in Carroll County, Missouri p 10 N82-23116

DAVIS, W. E.
Comparison of ozone in polluted and clean air masses over Lake Michigan p 29 A82-36477

DAVIS, W. M
Improved definition of crustal magnetic anomalies for MAGSAT data
[E82-10314] p 37 N82-24587

DAWSON, E.
Magnetic charts of Canada derived from Magsat data p 32 A82-30778

DAY, R. L.
Delineation of soil temperature regimes from HCMM data
[E82-10298] p 17 N82-24574

DEARAGON, A. M.
Thermal mapping, geothermal source location, natural effluents and plant stress in the Mediterranean coast of Spain
[E82-10300] p 17 N82-24576

DEBRUNNER, H.
A description of relativistic solar particle propagation p 4 A82-22600

DEJESUSPARADA, N
Dynamic study of the upper Sao Francisco river and Tres Marias reservoir using MSS/LANDSAT images
[E82-10291] p 63 N82-24569
Comparison of storm-time changes of geomagnetic field at ground and at MAGSAT altitudes, part 2
[E82-10325] p 30 N82-24598
Comparison of storm-time changes of geomagnetic field at ground and MAGSAT altitudes
[E82-10359] p 30 N82-26757
A study of atmospheric diffusion from the LANDSAT imagery
[E82-10360] p 58 N82-26758

DELAND, M. R
EPA's new bubble and banking policies p 25 A82-33865

DELASCUEVAS, R. N.
Thermal mapping, geothermal source location, natural effluents and plant stress in the Mediterranean coast of Spain
[E82-10300] p 17 N82-24576

DELEUR, M. S.
Experience with the compilation of maps of snow-cover melting in the central part of the European USSR on the basis of satellite data p 62 A82-35134

DEMIDOV, A. F.
Cost-effectiveness of geographic surveying from space p 85 N82-24263
DESBOIS, M.
Representativeness of cloud motion winds deduced from GOES Indian Ocean satellite imagery for the description of the Indian summer monsoon p 55 N82-23879
DESJARDINS, R. L.
Aircraft monitoring of surface carbon dioxide exchange p 23 A82-30293
DESSLER, A. J
Pulsar models and cosmic-ray acceleration p 21 A82-22570
DEUELL, R. L.
Digital and visual evaluation of GOES and TIROS/NOAA image data for cover type effects on snowfield observations p 60 A82-34735
DIACHENKO, L. N.
Albedo and angular characteristics of the reflectance of the underlying surface and clouds p 33 A82-30849
DIAMANTE, J. M.
Tidal and geodetic observations for the Seasat altimeter calibration experiment p 49 A82-29604
DICK, R.
Breadboard gas filter correlation spectrometer for atmospheric measurement of hydrazines and nitrogen dioxide
[AD-A110688] p 82 N82-26642
DIDWALL, E
Improved definition of crustal magnetic anomalies for MAGSAT data
[E82-10314] p 37 N82-24587
DIESEN, B. C., III
Snowpack monitoring in North America and Eurasia using passive microwave satellite data p 78 A82-32915
DILLMAN, R. D
Estimating mountain pine beetle-killed ponderosa pine over the front range of Colorado with high altitude panoramic photography p 7 A82-32704
DIORDIENKO, L. V
Aerogeophysical methods of finding uranium deposits p 41 A82-33402
DOBSON, C.
A simulation study of soil moisture estimation by a space SAR p 60 A82-29333
DOBSON, M. C.
Evaluation of the soil moisture prediction accuracy of a space radar using simulation techniques
[E82-10351] p 19 N82-26749
DOGIEL, V. A.
Convective outflow of cosmic rays from the Galaxy and background radio emission p 83 A82-22551
DOME, G.
The relationship between wind vector and normalized radar cross section used to derive Seasat-A Satellite Scatterometer winds p 51 A82-29617
DOME, G. J.
The Seasat-A satellite scatterometer - The geophysical evaluation of remotely sensed wind vectors over the ocean p 51 A82-29616
Evaluation of atmospheric attenuation from SMMR brightness temperature for the Seasat satellite scatterometer p 51 A82-29618
DOMINGO, V.
Non-flare injection of protons into interplanetary space p 4 A82-22601
DOUGLAS, B. C.
Tidal and geodetic observations for the Seasat altimeter calibration experiment p 49 A82-29604
DOUMA, M.
High spectral resolution airborne spectrometry p 77 A82-32443
DOWNS, A L.
Digital and visual evaluation of GOES and TIROS/NOAA image data for cover type effects on snowfield observations p 60 A82-34735
DUCRUIX, J.
MAGSAT anomaly map and continental drift
[E82-10326] p 38 N82-24599
Models and maps of the main field
[E82-10327] p 74 N82-24600
DUEPPE, R -D
The simultaneous employment of geodetic measurements for block adjustments using the method of independent models p 34 A82-33295
DUFFY, B.
Application of remote sensing to state and regional problems
[E82-10288] p 30 N82-24566
DUGGIN, M. J.
Evaluation of NOAA-AVHRR data for crop assessment p 8 A82-34179
DUNKLE, K.
Computer-processed geophysical atlas of digital data for the East Coast margin of the United States from surface and spacecraft data
[AD-A111388] p 39 N82-25748
DURGAPRASAD, N.
On the stellar origin of low energy cosmic rays p 21 A82-22567
DURPAIRE, J -P.
An optical objective lens for earth observations by satellites p 78 A82-32824
DUYBKIN, I. A.
Estimates of the statistical structure of the atmospheric pressure field in summer Monex-79 area p 57 N82-23939
DWORAK, T. Z.
Problems of the interpretation of aerial and satellite images of industrial smoke p 23 A82-30307
DYKSTRA, J
Experimental assessment of improved spatial resolution LANDSAT data
[AD-A110538] p 75 N82-26765
DZHORZHIO, M V
The use of satellite photographs to study snow-cover dynamics and to determine the average water discharge of the Amudarya during a vegetation period p 61 A82-35132
DZIEWULSKA-LOSIOWA, A.
The effect of the spectral attenuation of UV radiation by aerosol on the total ozone measurements p 27 A82-36406

E

EASTER, R. C.
Comparison of ozone in polluted and clean air masses over Lake Michigan p 29 A82-36477
EBERHARD, W
Field measurements in support of dispersion modeling in complex terrain (1980)
[PB82-148644] p 39 N82-27882
ECKERMAN, J.
Radiometer mission requirements for large space antenna systems
[NASA-TM-84478] p 81 N82-25610
EDWARDS, G J.
Detection and damage assessment of citrus tree losses with aerial color infrared photography /ACIR/ p 7 A82-29538
EL-HAKIM, S. F.
A practical study of gross-error detection in bundle adjustment p 69 A82-34702
EL-HASSAN, I. M.
The use of Skylab S-190B photography for small scale mapping p 80 A82-34742
ELMAN, R I.
Status and prospects of the automated processing of remote-sensing data /using forest surveys as an example/ p 10 A82-35139
EMERY, B. A.
OSO-8 lower mesospheric ozone number density profiles p 28 A82-36472
ENGLAND, C. F.
Satellite observations of sea surface temperature around the British Isles p 54 A82-33717
ERMAKOV, S. I.
Comparison of solar proton activity in 1967 and 1969 with that in 1978 and 1979 as measured onboard Venera 4, 6, 11, 12 space probes p 31 A82-22596
The solar proton fluxes in April, 1979 p 66 A82-22597
ESTES, J. E.
Impacts of remote sensing on U S geography p 24 A82-32899
Multispectral determination of soil moisture-2
[E82-10349] p 19 N82-26747
ETKIN, V. S.
The use of microwave radiometry for the determination of snow cover height p 80 A82-36018
EVANS, R. D.
Dobson spectrophotometer calibrations, possible errors in ozone absorption coefficients, and errors due to interfering pollutant gases p 28 A82-36431
EVENSON, P.
Unusual properties of particle events associated with solar flare gamma ray events p 65 A82-22585
The relation of type II radio bursts to solar energetic particles observed at earth p 3 A82-22591

F

FAINTICH, M B.
Matrix data analysis Color/B and W coding is not always enough
[AD-A111401] p 74 N82-25612
FAN, C. J.
Relating thematic mapper bands TM3, TM4, and TM5 to agronomic variables for corn, cotton, sugarbeet, soybean, sorghum, sunflower and tobacco
[E82-10347] p 19 N82-26745
FAN, C. Y.
Observations of the ionization states of energetic particles accelerated in solar flares p 40 A82-22607
FAUST, N. L
Automated classification of runoff coefficients from Landsat multispectral data p 60 A82-34734
FEDCHENKO, P. P
Remote sensing of the weediness of crop fields p 5 A82-29435
FEDI, M.
Crustal structures under the active volcanic areas of central and eastern Mediterranean (M-44)
[E82-10096] p 35 N82-23563
FEDOR, L. S.
Waveheight and wind speed measurements from the Seasat radar altimeter p 50 A82-29612
Intercomparison of wind speeds inferred by the SASS, altimeter, and SMMR p 52 A82-29621
FEISTER, U.
Total ozone retrieval from satellite Meteor 28 Fourier spectrometer measurements p 28 A82-36422
FINLEY, R. J.
Interpretation of surface-water circulation, Aransas Pass, Texas, using Landsat imagery p 60 A82-32896
FIRSOV, IU. G
The processing of satellite navigation data for marine geodesy p 34 A82-37175
FISK, L. A
Observations of the ionization states of energetic particles accelerated in solar flares p 40 A82-22607
FISKE, R. S
Soufriere Volcano, St Vincent - Observations of its 1979 eruption from the ground, aircraft, and satellites p 24 A82-33652
FLEIG, A. J
Total ozone variations 1970-74 using Backscattered Ultraviolet /BUV/ and ground-based observations p 26 A82-36053
FLICK, R. E
Fluid-sediment interactions on beaches and shelves
[AD-A110838] p 59 N82-26948
FORMAN, M A.
Cosmic ray acceleration by stellar winds I - Total density, pressure and energy flux p 21 A82-22566
FOSTER, J. L.
Snowpack monitoring in North America and Eurasia using passive microwave satellite data p 78 A82-32915
FRAWLEY, J. F.
Improved definition of crustal magnetic anomalies for MAGSAT data
[E82-10314] p 37 N82-24587
FREDERIKSEN, P.
Terrain classification by Fourier analysis - Accuracy and economy p 69 A82-34723
FREIER, P. S.
A report on the 'cosmic ray propagation problem' p 1 A82-22539
FREUDENSTEIN, W. H.
Thematic mapper - An overview of spectral band registration p 77 A82-32447
FREY, H.
Magsat scalar anomaly distribution - The global perspective p 41 A82-30786
FROST, V. S.
The recognition of extended targets - SAR images for level and hilly terrain p 33 A82-31994
FUCHS, J. E.
A multi-frequency radiometric measurement of soil moisture content over bare and vegetated fields
[E82-10238] p 16 N82-23611
FUKUI, Y.
Interactions of cosmic rays with molecular clouds p 82 A82-22548
FUKUSHIMA, N.
Preliminary interpretation of magnetic anomalies over Japan and its surrounding area p 33 A82-30796
Investigation from Japanese MAGSAT team
[E82-10239] p 73 N82-23612
Investigation from Japanese MAGSAT Team Part A Crustal structure near Japan and in Antarctic station Part B Electric currents and hydromagnetic waves in the ionosphere and the magnetosphere
[E82-10244] p 36 N82-24522

Report of investigation from Japanese MAGSAT Team
[E82-10322] p 74 N82-24595
FULLER, W. H , JR.
Airborne lidar measurements of the Soufriere eruption of 17 April 1979 p 24 A82-33657

G

GABRIELSEN, R H
Regional geological, tectonic and geophysical features of Nordland, Norway p 41 A82-30304
GAISSER, T. K.
Antiprotons from galactic sources of cosmic rays and gamma rays p 82 A82-22546
GALDEANO, A.
MAGSAT anomaly map and continental drift
[E82-10326] p 38 N82-24599
GALLIHER, S. C.
An equivalent layer magnetization model for the United States derived from MAGSAT data
[E82-10297] p 36 N82-24573
GALLO, K. P
Spectral estimates of solar radiation intercepted by corn canopies
[E82-10003] p 18 N82-26742
GARCIA-MUNOZ, M
The question of short pathlengths in interstellar propagation p 1 A82-22541
GAROFALO, D.
Experimental assessment of improved spatial resolution LANDSAT data
[AD-A110538] p 75 N82-26765
GASPARINI, P.
Crustal structures under the active volcanic areas of central and eastern Mediterranean (M-44)
[E82-10096] p 35 N82-23563
GATLIN, J. A.
Use of NOAA/AVHRR visible and near-infrared data for land remote sensing
[NASA-TM-84186] p 81 N82-22643
GATTO, L. W
Ice distribution and winter surface circulation patterns, Kachemak Bay, Alaska
[AD-A110806] p 58 N82-26764
GAUSMAN, H. W.
AgRISTARS Early warning and crop condition assessment Plant cover, soil temperature, freeze, water stress, and evapotranspiration conditions
[E82-10225] p 14 N82-23598
GERSHENZON, V. E.
The use of microwave radiometry for the determination of snow cover height p 80 A82-36018
GERTSENOVA, K. N.
Evaluation of the effectiveness of systematic image distortion compensation p 69 A82-34469
GESCHKE, A.
Thermography - A remote sensing method with many perspectives p 76 A82-29922
GILER, M.
Origin of cosmic rays in galactic centre sources p 3 A82-22571
GINZBURG, V. L.
Remarks on cosmic ray origin p 21 A82-22569
GIRE, C.
Models and maps of the main field
[E82-10327] p 74 N82-24600
GLAZAR, W. S.
A multi-frequency radiometric measurement of soil moisture content over bare and vegetated fields
[E82-10238] p 16 N82-23611
GLOECKLER, G.
Observations of interplanetary energetic charged particles from gamma-ray line solar flares p 65 A82-22586
Time and energy dependence of heavy ion abundances in solar flare energetic particle events p 22 A82-22605
Observations of the ionization states of energetic particles accelerated in solar flares p 40 A82-22607
A comparison of helium and heavy ion spectra in He/3/ rich solar flares with a model calculation p 5 A82-22612
GOETTELMAN, R. C.
Airborne observed solar elevation and row direction effects on the near-IR/red ratio of cotton
[E82-10220] p 13 N82-23593
GOETZ, A. F H.
Spectroscopic remote sensing for geological applications p 41 A82-32442
GOLDBERG, P. A.
Remote sensing - A potential aid in the preparation of an urban tree inventory p 9 A82-34732
GOMBOSI, T. I
Spacecraft determination of energetic particle propagation parameters - The 1 January 1978 solar event p 31 A82-22598
GONZALEZ, F. I.
Seasat wind and wave observations of northeast Pacific hurricane Iva, August 13, 1978 p 52 A82-29624
GOODELL, P. C.
Evaluation and combined geophysical interpretations of NURE and related geoscience data in the Van Horn, Pecos, Marfa, Fort Stockton, Presidido, and Emory Peak quadrangles, Texas, volume 1
[DE82-005554] p 47 N82-27808
GOODELL, R. C.
Evaluation and combined geophysical interpretations of NURE and related geoscience data in the Van Horn, Pecos, Marfa, Fort Stockton, Presidio, and Emory Peak quadrangels, Texas
[DE82-005560] p 48 N82-27809
GOODMAN, J. M.
Terrain analysis from Landsat using a color TV enhancement system p 68 A82-32911
GOODRIDGE, D. R.
SEASAT A satellite scatterometer illumination times of selected in situ sites
[NASA-TM-83280] p 81 N82-22865
GOODSPEED, M. J.
Separation of diffuse from sharp-edged features in digital imagery p 68 A82-34225
GORNEY, D. J.
Generation of the auroral kilometric radiation p 26 A82-35542
GOSS-ZUREK, R.
Satellite radiation measurements for the retrieval of the vertical temperature profiles p 70 A82-36935
GOULD, W. I
A multi-frequency radiometric measurement of soil moisture content over bare and vegetated fields
[E82-10238] p 16 N82-23611
GOWARD, S. N.
Longwave infrared observation of urban landscapes p 25 A82-34744
GRAHAM, M. H.
An algorithm for automating the registration of USDA segment ground data to LANDSAT MSS data
[E82-10286] p 16 N82-24564
GRASS, R. D
Dobson spectrophotometer calibrations, possible errors in ozone absorption coefficients, and errors due to interfering pollutant gases p 28 A82-36431
GREBOWSKY, G.
Evaluation of temporal registration of Landsat scenes p 67 A82-32345
GREEN, G.
Spacecraft determination of energetic particle propagation parameters - The 1 January 1978 solar event p 31 A82-22598
GREEN, M. J.
An optical data link for airborne scanning system p 80 A82-34737
GREILING, R.
Satellite image interpretation of the eastern Caledonian part of the Blue Road Geotraverse and its geological implications /Nordland, Vasterbotten, Scandinavia/ p 41 A82-30305
GRIGORIAN, O P.
Preflare increases in solar cosmic rays relevant to the mode of energy accumulation in the active regions associated with large flares p 31 A82-22595
GRIN, A. M.
Principles and methods of the study of the hydrological cycle on the basis of aerospace data p 61 A82-35127
GROCH, W -D.
Extraction of line shaped objects from aerial images using a special operator to analyze the profiles of functions p 67 A82-32033
GUDMANDSEN, P.
Movement of ice markers measured by satellite ranging
[R-240] p 59 N82-27816
GUENTHER, G. C.
Bias correction procedures for airborne laser hydrography
[PB82-130089] p 63 N82-22644
GUPTA, S. R M.
Analysis of MAGSAT data of the Indian region
[E82-10358] p 75 N82-26756
GURNEY, C M.
The use of contextual information to detect cumulus clouds and cloud shadows in Landsat data p 67 A82-32346
GUSSENHOVEN, M. S.
Extremely high latitude auroras p 76 A82-31020
GUYMER, T.
Surface wind analyses for Seasat p 51 A82-29619
GUZA, R. T.
Fluid-sediment interactions on beaches and shelves
[AD-A110838] p 59 N82-26948
GUZIK, T G.
The question of short pathlengths in interstellar propagation p 1 A82-22541

H

HABGOOD, F.
Overseas Geology And Mineral Resources number 56 A geological interpretation of LANDSAT imagery and air photography of Botswana
[OGMR-56] p 42 N82-22636
HAFKER, W. R.
Landsat detection of hardwood forest clearcuts p 8 A82-32708
HAGGERTY, S E.
The mineralogy of global magnetic anomalies
[E82-10305] p 45 N82-24579
HAJIC, E. J.
Multispectral determination of soil moisture-2
[E82-10349] p 19 N82-26747
HALBERSTAM, I. M.
The relationship between wind vector and normalized radar cross section used to derive Seasat-A Satellite Scatterometer winds p 51 A82-29617
HALL, D. K
Landsat digital analysis of the initial recovery of burned tundra at Kokolik River, Alaska p 8 A82-32913
Snowpack monitoring in North America and Eurasia using passive microwave satellite data p 78 A82-32915
HALL, D. L.
Design guidelines for satellite image data distribution systems p 70 A82-37048
HALL, L.
Experimental assessment of improved spatial resolution LANDSAT data
[AD-A110538] p 75 N82-26765
HALL, P. M.
Remote sensing of Douglas-fir trees newly infested by bark beetles p 6 A82-29536
HANCOCK, D. W., III
Sea-state-related altitude errors in the Seasat radar altimeter p 50 A82-29608
HAPKE, B.
A color-ratio map of Mercury p 31 A82-22294
HARKER, D. B.
Problems associated with remotely detecting and monitoring saline sites within irrigated Alberta p 9 A82-34710
HARLAN, C.
Irrigation management with remote sensing
[E82-10357] p 20 N82-26755
HARQUIST, T. W.
Evidence for the stochastic acceleration of cosmic rays in supernova remnants p 2 A82-22564
HARRISON, C. G. A.
Investigations of medium wavelength magnetic anomalies in the eastern Pacific using MAGSAT
[E82-10240] p 73 N82-23613
Investigations of medium wavelength magnetic anomalies in the eastern Pacific using MAGSAT data
[E82-10330] p 38 N82-24603
HARTMANN, D. L.
Interannual variations of outgoing IR associated with tropical circulation changes during 1974-1978 p 54 A82-36341
HASLAM, C. G. T.
Derivation of the distribution of synchrotron emissivity in the Galaxy from the 408 MHz all-sky survey p 82 A82-22549
HASTINGS, D A.
An investigation of MAGSAT and complementary data emphasizing precambrian shields and adjacent areas of West Africa and South America
[E82-10316] p 38 N82-24589
An investigation of MAGSAT and complementary data emphasizing precambrian shields and adjacent areas of West Africa and South America
[E82-10317] p 38 N82-24590
An investigation of MAGSAT and complementary data emphasizing precambrian shields and adjacent areas of West Africa and South America
[E82-10318] p 38 N82-24591
HATFIELD, J. L.
Multilevel measurements of surface temperature over undulating terrain planted to barley
[E82-10245] p 16 N82-24523
HAWKINS, J.
Surface wind analyses for Seasat p 51 A82-29619
HAWKINS, J D.
Meteorological and aircraft data for CUE 2 1973
[PB82-149246] p 59 N82-26949

HAYAKAWA, S.
Interactions of cosmic rays with molecular clouds p 82 A82-22548
HAYDEN, C. M.
Surface temperature determination from an amalgamation of GOES and TIROS-N radiance measurements p 66 A82-28905
HAYDN, R.
Multidisciplinary investigations on HCMM data over middle Europe and Marocco
[E82-10315] p 74 N82-24588
HAYNE, G S.
Sea-state-related altitude errors in the Seasat radar altimeter p 50 A82-29608
HEAD, J. W., III
An investigation into the utilization of HCMM thermal data for the discrimination of volcanic and Eolian geological units
[E82-10352] p 47 N82-26750
HEATH, D. F.
Total ozone variations 1970-74 using Backscattered Ultraviolet /BUV/ and ground-based observations p 26 A82-36053
HEFFNER, P.
Advanced technology for earth observation - Data processing
[AAS PAPER 82-130] p 71 A82-37810
HEFFTER, J. L.
Meteorological analysis of the eruption of Soufriere in April 1979 p 24 A82-33655
HEGG, K. M.
Multi-resource inventory in interior Alaska p 6 A82-29532
HEILMAN, J.
Irrigation management with remote sensing
[E82-10357] p 20 N82-26755
HEILMAN, J. L.
Evaluation of HCMM data for assessing soil moisture and water table depth
[E82-10329] p 18 N82-24602
HEILMAN, W. E.
Evaluation of HCMM data for assessing soil moisture and water table depth
[E82-10329] p 18 N82-24602
HEINEN, J. T.
Inventory of wildlife habitat from color infrared aerial photography for Cobb Island, Virginia p 6 A82-29529
A computerized spatial analysis system for assessing wildlife habitat from vegetation maps p 9 A82-34716
HENDERSON-SELLERS, A
System albedo as sensed by satellites - Its definition and variability p 23 A82-32342
HENDERSON, F. M.
Comparisons of land cover classifications from selected remote sensing systems p 80 A82-34746
HENKEL, J.
Multidisciplinary investigations on HCMM data over middle Europe and Marocco
[E82-10315] p 74 N82-24588
HERMAN, I. P.
Feasibility of laser-separation of 36 S and its use as an atmospheric tracer
[DE82-000965] p 30 N82-27737
HICKMAN, G. D.
Laser-induced bioluminescence p 53 A82-32559
HIDE, R.
Spherical harmonic representation of the main geomagnetic field for world charting and investigations of some fundamental problems of physics and geophysics
[E82-10203] p 72 N82-23576
HIELKEMA, J. U.
Desert locust habitat monitoring with satellite remote sensing A new technology for an old problem p 7 A82-29747
HILL, G. W.
Nearshore current pattern off south Texas - An interpretation from aerial photographs p 53 A82-32903
HILTON, B. M.
Multispectral determination of soil moisture-2
[E82-10349] p 19 N82-26747
HINTON, B. B.
Estimates of sea surface stress for summer MONEX from cloud motions p 56 N82-23910
HINZE, W J.
Verification of the crustal component in satellite magnetic data p 32 A82-30789
A satellite magnetic model of northeastern South American aulacogens p 33 A82-30795
Study of gravity and magnetic anomalies using MAGSAT data
[E82-10194] p 35 N82-22628
Spherical-Earth gravity and magnetic anomaly modeling by Gauss-Legendre quadrature integration
[E82-10242] p 36 N82-24520
Magnetic and gravity anomalies in the Americas
[E82-10312] p 37 N82-24586
Aeromagnetic and satellite magnetic anomaly mapping
[E82-10339] p 39 N82-25601
Evaluation and combined geophysical interpretations of *NURE and related geoscience data in the Van Horn, Pecos,* Marfa, Fort Stockton, Presidido, and Emory Peak quadrangles, Texas, volume 1
[DE82-005554] p 47 N82-27808
Evaluation and combined geophysical interpretations of NURE and related geoscience data in the Van Horn, Pecos, Marfa, Fort Stockton, Presidio, and Emory Peak quadrangels, Texas
[DE82-005560] p 48 N82-27809
HIRASIMA, Y
Solar gamma-ray experiment on Astro-A satellite p 21 A82-22583
HIXSON, M. M.
Determination of the optimal level for combining area and yield estimates
[E82-10215] p 12 N82-23588
HODGES, T.
AgRISTARS Supporting research Spring small grains planting date distribution model
[E82-10208] p 12 N82-23581
HODGSON, R. M.
A system design for a multispectral sensor using two-dimensional solid-state imaging arrays p 77 A82-31991
Image processing with microcomputers in remote sensing p 79 A82-34708
HOELL, J. M.
Ammonia and the NOx budget of the troposphere p 27 A82-36293
HOLTZMAN, J
A simulation study of soil moisture estimation by a space SAR p 60 A82-29333
HOLTZMAN, J. C.
The recognition of extended targets - SAR images for level and hilly terrain p 33 A82-31994
Evaluation of the soil moisture prediction accuracy of a space radar using simulation techniques
[E82-10351] p 19 N82-26749
HONG, J.-K.
Coastal environment change analysis by Landsat MSS data p 54 A82-34219
HORN, F W., JR.
Detection and damage assessment of citrus tree losses with aerial color infrared photography /ACIR/ p 7 A82-29538
Effects of altitude, focal length, and filter combinations on color infrared photography of citrus groves p 9 A82-34729
HORNER, R J
Initial scalar magnetic anomaly map from Magsat p 32 A82-30784
Initial vector magnetic anomaly map from Magsat p 32 A82-30785
HORNIBROOK, M.
High resolution satellite observations of mesoscale oceanography in the Tasman Sea, 1978 - 1979
[E82-10324] p 57 N82-24597
HORSTMAN, K. C.
Possible fault detection in Cottonball Basin, California An application of radar remote sensing p 41 A82-32898
HORVATH, R.
Analysis of scanner data for crop inventories
[E82-10192] p 10 N82-22626
Analysis of scanner data for crop inventories
[E82-10241] p 16 N82-24519
HOVESTADT, D
Observations of interplanetary energetic charged particles from gamma-ray line solar flares p 65 A82-22586
Time and energy dependence of heavy ion abundances in solar flare energetic particle events p 22 A82-22605
Observations of the ionization states of energetic particles accelerated in solar flares p 40 A82-22607
A comparison of helium and heavy ion spectra in He/3/ rich solar flares with a model calculation p 5 A82-22612
HOVET, H.
The METEOSAT Data Collection System and its application p 75 N82-26037
HOWE, R C.
Comparing lineaments interpreted from Landsat imagery and topographic maps with reported faults in southwest Montana p 34 A82-34719
HUGHES, J. K.
SEASAT A satellite scatterometer illumination times of selected in situ sites
[NASA-TM-83280] p 81 N82-22865
HUGHES, N. A
System albedo as sensed by satellites - Its definition and variability p 23 A82-32342
HUGHES, T. J.
Studies of high latitude current systems using MAGSAT vector data
[E82-10188] p 71 N82-22622
HUMMER-MILLER, S.
Registration of Heat Capacity Mapping Mission day and night images
[E82-10210] p 72 N82-23583
Ground support data from July 10 to July 29, 1978, for HCMM thermal satellite data of the Powder River Basin, Wyoming
[E82-10211] p 72 N82-23584
HUNG, R. J.
Remote sensing of tornadic storms from geosynchronous satellite infrared digital data p 23 A82-32348
HUNT, G E.
Satellite observations of sea surface temperature around the British Isles p 54 A82-33717
HUNT, W. H.
Airborne lidar measurements of the Soufriere eruption of 17 April 1979 p 24 A82-33657
HUNTER, R. E.
Nearshore current pattern off south Texas - An interpretation from aerial photographs p 53 A82-32903
HUSSON, J C.
History of the French satellite space program p 85 N82-24216

I

IAROVOI, B D.
The processing of satellite navigation data for marine geodesy p 34 A82-37175
IDSO, S B.
View angle effects in the radiometric measurement of plant canopy temperatures p 8 A82-32914
IISAKA, J.
Coastal environment change analysis by Landsat MSS data p 54 A82-34219
INMAN, D L.
Fluid-sediment interactions on beaches and shelves
[AD-A110838] p 59 N82-26948
INOUE, T.
Estimation of the precipitable water from the IR channel of the geostationary satellite p 55 A82-37196
IPAVICH, F. M.
Observations of the ionization states of energetic particles accelerated in solar flares p 40 A82-22607
IRISOV, V. G.
The use of microwave radiometry for the determination of snow cover height p 80 A82-36018
ISMAIL, S.
Large amplitude undulations on the equatorward boundary of the diffuse aurora p 76 A82-31019
IVANOV, A. V.
On the synthetic aperture radar imaging of ocean surface waves p 53 A82-32881
IWATA, A.
Aircraft measurements of NO/x/ in the lower troposphere above the coast of Japan p 26 A82-36247

J

JACKSON, D. D.
Seismic and geodetic studies of the Imperial Valley, California
[DE82-001686] p 39 N82-26915
JACKSON, R. D.
View angle effects in the radiometric measurement of plant canopy temperatures p 8 A82-32914
Airborne observed solar elevation and row direction effects on the near-IR/red ratio of cotton
[E82-10220] p 13 N82-23593
Multilevel measurements of surface temperature over undulating terrain planted to barley
[E82-10245] p 16 N82-24523
JACOBI, O.
Terrain classification by Fourier analysis - Accuracy and economy p 69 A82-34723
JAIN, A.
Ocean wave height measurement with SEASAT SAR using speckle diversity p 53 A82-32882
JAYNES, R. A.
Inventory of wetlands and agricultural land cover in the upper Sevier River Basin, Utah
[E82-10345] p 18 N82-25607
Mapping of wildlife habitat in Farmington Bay, Utah
[E82-10354] p 19 N82-26752

Detection of variations in aspen forest habitat from LANDSAT digital data Bear River Range, Utah
[E82-10355] p 19 N82-26753
Irrigated acreage in the Bear River Basin as of the 1975 growing season
[E82-10356] p 20 N82-26754
JENSEN, J. R.
Detecting residential land-use development at the urban fringe p 22 A82-29332
Impacts of remote sensing on U S geography p 24 A82-32899
JOBUSCH, C D.
Determination of the optimal level for combining area and yield estimates
[E82-10215] p 12 N82-23588
JOHNSON, H. B.
Resource inventory techniques used in the California Desert Conservation Area p 23 A82-32441
JOHNSON, J. W.
Characteristics of 13 9 GHz radar scattering from oil films on the sea surface p 54 A82-33438
JOHNSON, L.
Landsat digital analysis of the initial recovery of burned tundra at Kokolik River, Alaska p 8 A82-32913
JONES, C. L.
Measurement of soil moisture trends with airborne scatterometers
[E82-10361] p 20 N82-26759
Multifrequency remote sensing of soil moisture
[E82-10362] p 20 N82-26760
Development of visible/infrared/microwave agriculture classification and biomass estimation algorithms
[E82-10363] p 20 N82-26761
JONES, J H.
Laboratory studies of actinide metal-silicate fractionation p 49 A82-22306
JONES, P H.
Use of thermal inertia determined by HCMM to predict nocturnal cold prone areas in Florida
[E82-10299] p 17 N82-24575
JONES, W. L.
The Seasat-A satellite scatterometer - The geophysical evaluation of remotely sensed wind vectors over the ocean p 51 A82-29616
The relationship between wind vector and normalized radar cross section used to derive Seasat-A Satellite Scatterometer winds p 51 A82-29617
JOSEPH, M. G.
On the space-time variability of ocean surface mixed layer characteristics of central and eastern Arabian sea during MONSOON-77 p 56 N82-23909
JOUVE, P.
Application of infrared techniques to the study of atmospheric ozone p 27 A82-36414
JUNKIN, B. G
Development of three-dimensional spatial displays using a geographically based information system p 66 A82-29326
JUPP, D. L. B.
The use of residual images in Landsat image analysis p 66 A82-29328

K

KAFATOS, M.
Confinement and acceleration of cosmic rays in galactic superbubbles p 82 A82-22547
Acceleration processes near massive black holes p 3 A82-22572
KALCIC, M. T
Analysis of thematic mapper simulator data acquired during winter season over Pearl River, Mississippi, test site
[E82-10287] p 17 N82-24565
KANE, R. P.
Comparison of storm-time changes of geomagnetic field at ground and at MAGSAT altitudes, part 2
[E82-10325] p 30 N82-24598
Comparison of storm-time changes of geomagnetic field at ground and MAGSAT altitudes
[E82-10359] p 30 N82-26757
KASPRZHAK, K.
The possibility of using remote-sensing methods to study the hydrology of elementary watersheds p 61 A82-35130
KATIBAH, E F.
Use of Landsat multispectral scanner data in vegetation mapping of a forested area p 9 A82-34731
KAUFMANN, H.
Multidisciplinary investigations on HCMM data over middle Europe and Marocco
[E82-10315] p 74 N82-24588
KAUTH, R J.
Analysis of scanner data for crop inventories
[E82-10192] p 10 N82-22626
Analysis of scanner data for crop inventories
[E82-10241] p 16 N82-24519
KAWAMURA, M.
Report of investigation from Japanese MAGSAT Team
[E82-10322] p 74 N82-24595
KEAFER, L. S., JR.
Radiometer mission requirements for large space antenna systems
[NASA-TM-84478] p 81 N82-25610
KEARSEY, S
Derivation of the distribution of synchrotron emissivity in the Galaxy from the 408 MHz all-sky survey p 82 A82-22549
KECSKEMETY, K.
Spacecraft determination of energetic particle propagation parameters - The 1 January 1978 solar event p 31 A82-22598
KEEVALLIK, S.
Estimation of the temperature of the upper boundary of cloud cover over the world ocean p 54 A82-36005
KELLER, G. R.
Characterization of the structure and tectonic of South America
[E82-10196] p 42 N82-23569
The crustal structure and tectonics of South America
[E82-10319] p 38 N82-24592
Geotectonics of South America
[E82-10320] p 38 N82-24593
Evaluation and combined geophysical interpretations of NURE and related geoscience data in the Van Horn, Pecos, Marfa, Fort Stockton, Presidido, and Emory Peak quadrangles, Texas, volume 1
[DE82-005554] p 47 N82-27808
Evaluation and combined geophysical interpretations of NURE and related geoscience data in the Van Horn, Pecos, Marfa, Fort Stockton, Presidio, and Emory Peak quadrangels, Texas
[DE82-005560] p 48 N82-27809
KELNER, S. R.
Computer simulation of the time dependence of the photon energy spectra produced in proton and electron bremstrahlung p 3 A82-22587
KENNARD, R E.
Preliminary evidence for the influence of physiography and scale upon the autocorrelation function of remotely sensed data p 67 A82-32343
KESSLER, R
Interpretation of vegetative cover in wetlands using four-channel SAR imagery p 9 A82-34706
KHACHATURIAN, G O.
The solar proton fluxes in April, 1979 p 66 A82-22597
KHAPIN, IU. B.
The use of microwave radiometry for the determination of snow cover height p 80 A82-36018
KHORRAM, S
Use of Landsat multispectral scanner data in vegetation mapping of a forested area p 9 A82-34731
KHOSLA, K. L.
Analysis of MAGSAT data of the Indian region
[E82-10358] p 75 N82-26756
KHOTILOVSKAIA, T. G.
Comparison of solar proton activity in 1967 and 1969 with that in 1978 and 1979 as measured onboard Venera 4, 6, 11, 12 space probes p 31 A82-22596
KIARNER, O
Estimation of the temperature of the upper boundary of cloud cover over the world ocean p 54 A82-36005
KILGORE, R. W.
Application of Computer Axial Tomography (CAT) to measuring crop canopy geometry
[E82-10227] p 14 N82-23600
KIMES, D. S.
Effects of vegetation canopy structure on remotely sensed canopy temperatures p 8 A82-32905
View angle effects in the radiometric measurement of plant canopy temperatures p 8 A82-32914
Irradiance measurement errors due to the assumption of a Lambertian reference panel p 79 A82-34222
KIPFINGER, R
Ground support data from July 10 to July 29, 1978, for HCMM thermal satellite data of the Powder River Basin, Wyoming
[E82-10211] p 72 N82-23584
KIRCHNER, J. A.
Irradiance measurement errors due to the assumption of a Lambertian reference panel p 79 A82-34222
Influence of sky radiance distribution on the ratio technique for estimating bidirectional reflectance p 70 A82-35650
KISH, J. C.
Fragmentation of Fe nuclei on carbon, hydrogen and CH2 targets I - Individual charge changing and total cross sections II - Isotopic cross sections p 63 A82-22538
KLECKER, B.
Observations of interplanetary energetic charged particles from gamma-ray line solar flares p 65 A82-22586
Observations of the ionization states of energetic particles accelerated in solar flares p 40 A82-22607
A comparison of helium and heavy ion spectra in He/3/ rich solar flares with a model calculation p 5 A82-22612
KLEIN, W. H.
Estimating bark beetle-killed lodgepole pine with high altitude panoramic photography p 7 A82-32703
KLEMAS, V
Determination of winter temperature patterns, fronts, and surface currents in the Yellow Sea and East China Sea from satellite imagery p 55 A82-37195
KLOSKO, S. M.
Gravity model improvement for Seasat p 32 A82-29615
KLUMPAR, D. M.
Investigation of the effects of external current systems on the MAGSAT data utilizing grid cell modeling techniques
[E82-10195] p 71 N82-22629
Investigation of the effects of external current systems on the MAGSAT data utilizing grid cell modeling techniques
[E82-10226] p 73 N82-23599
Investigation of the effects of external current systems on the MAGSAT data utilizing grid cell modeling techniques
[E82-10232] p 73 N82-23605
Investigation of the effects of external current systems on the MAGSAT data utilizing grid cell modeling techniques
[E82-10306] p 74 N82-24580
KOBAYASHI, K.
Report of investigation from Japanese MAGSAT Team
[E82-10322] p 74 N82-24595
KOCHAROV, L. G.
The model of the cosmic ray enrichment by helium-3 p 31 A82-22614
KOLACZEK, B.
On reference coordinate systems used in polar motion determinations p 33 A82-32090
KOLENKIEWICZ, R.
Seasat altimeter height calibration p 49 A82-29603
KOLLENKARK, J. C.
Diurnal changes in reflectance factor due to Sun-row direction interactions
[E82-10128] p 11 N82-23566
Canopy reflectance as influenced by solar illumination angle
[E82-10237] p 15 N82-23610
KOLOSOV, P. A.
Principles and methods of the study of the hydrological cycle on the basis of aerospace data p 61 A82-35127
KOMHYR, W D.
Dobson spectrophotometer calibrations, possible errors in ozone absorption coefficients, and errors due to interfering pollutant gases p 28 A82-36431
KONDO, I.
Solar gamma-ray experiment on Astro-A satellite p 21 A82-22583
KONDO, Y.
Aircraft measurements of NO/x/ in the lower troposphere above the coast of Japan p 26 A82-36247
KONDRATEV, K. IA.
Remote sensing of the weediness of crop fields p 5 A82-29435
Albedo and angular characteristics of the reflectance of the underlying surface and clouds p 33 A82-30849
Study of the hydrological cycle by aerospace methods p 61 A82-35126
KONO, M.
Preliminary interpretation of magnetic anomalies over Japan and its surrounding area p 33 A82-30796
KONTOR, N. N.
Evolution of the solar proton spectrum in interplanetary space p 4 A82-22594
Comparison of solar proton activity in 1967 and 1969 with that in 1978 and 1979 as measured onboard Venera 4, 6, 11, 12 space probes p 31 A82-22596
The solar proton fluxes in April, 1979 p 66 A82-22597
The modulation characteristics of the 19th and 20th solar activity cycles p 59 A82-22615
KORZOV, V. I.
Albedo and angular characteristics of the reflectance of the underlying surface and clouds p 33 A82-30849
KOTOV, IU. D.
Computer simulation of the time dependence of the photon energy spectra produced in proton and electron bremstrahlung p 3 A82-22587

KOTTMEIER, C.
The influence of soil characteristics on regional convection differences above Northern Germany p 10 A82-37589
KOVALENKO, V. M
Convective outflow of cosmic rays from the Galaxy and background radio emission p 83 A82-22551
KOZIN, I. D.
The determination of differential X-ray spectrum of the solar flare using ionospheric data p 65 A82-22582
KOZODEROV, V. V.
Comparison of brightness indicatrixes of snow cover measured from an aircraft and calculated theoretically for different heights of the atmosphere p 62 A82-35140
Allowance for the effect of the atmosphere in the processing of satellite remote-sensing images p 70 A82-35141
KRAINEV, M. B.
On the characteristics of the very low energy galactic cosmic rays in the interstellar space p 63 A82-22540
KRASNOV, A. I.
Aerogeophysical methods of finding uranium deposits p 41 A82-33402
KRATKY, V.
Present status of on-line analytical triangulation p 69 A82-34940
KREIDL, T. J.
Subtleties in the flat-fielding of charge-coupled device /CCD/ images p 68 A82-32581
KRIULKOV, V. A.
The use of remote-sensing data to identify the space-time variability of the quality of natural waters p 62 A82-35138
KRUEGER, A. F.
Geostationary satellite observations of the April 1979 Soufriere eruptions p 24 A82-33654
KUDRIAVTSEV, G P.
Analytical processing of photographs taken by paired cameras p 79 A82-34471
KULKANNI, P L.
Impact of additional summer MONEX wind data on the prediction of monsoon depressions during June - August 1979 with two versions of primitive equation (PE) barotropic model p 56 N82-23900
KULKARNI, A. A.
Impact of additional summer MONEX wind data on the prediction of monsoon depressions during June - August 1979 with two versions of primitive equation (PE) barotropic model p 56 N82-23900
KUNOW, H
Spacecraft determination of energetic particle propagation parameters - The 1 January 1978 solar event p 31 A82-22598
KUO, J. T.
High spectral resolution airborne spectrometry p 77 A82-32443
KURILOVA, IU. V.
Study of the hydrological cycle by aerospace methods p 61 A82-35126
Principles and methods of the study of the hydrological cycle on the basis of aerospace data p 61 A82-35127
KURT, V. G.
Energetic solar particle spectra according to Venera-11, 12 and Prognoz-5, 6 p 4 A82-22593
Spacecraft determination of energetic particle propagation parameters - The 1 January 1978 solar event p 31 A82-22598
KUZEVSKII, B. M.
Preflare increases in solar cosmic rays relevant to the *mode of energy accumulation in the active regions* associated with large flares p 31 A82-22595
KUZHEVSKII, B M.
Low-energy particles in interplanetary magnetic field near the sectorial boundary on September 26, 1977 p 4 A82-22602
KUZNETSOVA, R. I.
Nucleosynthesis of light and by-passed isotopes in the solar system matter p 64 A82-22578

L

LABOVITZ, M. L.
Preliminary evidence for the influence of physiography and scale upon the autocorrelation function of remotely sensed data p 67 A82-32343
The influence of autocorrelation in signature extraction An example from a geobotanical investigation of Cotter Basin, Montana
[E82-10341] p 46 N82-25603
LAL, S. J.
Analysis of MAGSAT data of the Indian region
[E82-10358] p 75 N82-26756
LAMBECK, K.
A search for seamounts in the southern Cook and Austral region p 52 A82-30810
LAME, D. B.
Seasat measurement system evaluation - Achievements and limitations p 49 A82-29601
LANDGRAF, K. F.
Inventory of wetlands and agricultural land cover in the upper Sevier River Basin, Utah
[E82-10345] p 18 N82-25607
Irrigated acreage in the Bear River Basin as of the 1975 growing season
[E82-10356] p 20 N82-26754
LANDGREBE, D. A
Multistage classification of multispectral Earth observational data The design approach
[E82-10213] p 72 N82-23586
LANGEL, R A.
Initial scalar magnetic anomaly map from Magsat p 32 A82-30784
Initial vector magnetic anomaly map from Magsat p 32 A82-30785
LANGLEY, P G.
A new approach to multiresource inventories using remote sensing and geographic information systems technologies p 25 A82-34739
LAPCHENKOV, S. T
The use of remote-sensing data to identify the space-time variability of the quality of natural waters p 62 A82-35138
LARSON, F R.
Multi-resource inventory in interior Alaska p 6 A82-29532
LATHAM, A. R.
High resolution satellite observations of mesoscale oceanography in the Tasman Sea, 1978 - 1979
[E82-10324] p 57 N82-24597
LAVRUKHINA, A. K.
Nucleosynthesis of light and by-passed isotopes in the solar system matter p 64 A82-22578
LAZAREWICZ, A. R
Spatial resolution and repeatability of Magsat crustal anomaly data over the Indian Ocean p 32 A82-30788
Analyses of MAGSAT tracks crossing the study region in the Indian Ocean
[E82-10197] p 71 N82-23570
Bathymetric and tectonics of Indian Ocean using MAGSAT data
[E82-10204] p 36 N82-23577
Analyzing the Broken Ridge area of the Indian Ocean using magnetic and gravity anomaly maps and geoid undulation and bathymetry data
[E82-10303] p 36 N82-24577
Investigating tectonic and bathymetric features of the Indian Ocean using MAGSAT magnetic anomaly data
[E82-10304] p 37 N82-24578
LEAMER, R. W
AgRISTARS Early warning and crop condition assessment Plant cover, soil temperature, freeze, water stress, and evapotranspiration conditions
[E82-10225] p 14 N82-23598
LEAN, J. L.
Observation of the diurnal variation of atmospheric ozone p 26 A82-35895
LEATON, B R
Spherical harmonic representation of the main geomagnetic field for world charting and investigations of some fundamental problems of physics and geophysics
[E82-10203] p 72 N82-23576
LEBEDEV, A. V.
Water-balance differentiation of natural complexes on the basis of satellite photographs p 61 A82-35129
LEE, L. C.
Generation of the auroral kilometric radiation p 26 A82-35542
LEE, M. A.
Acceleration of cosmic rays in accretion shocks p 64 A82-22568
LEE, R B., III
In situ ozone data for comparison with laser absorption remote sensor 1980 PEPE/NEROS program
[NASA-TM-84471] p 30 N82-25661
LEES, R. D.
Multispectral determination of soil moisture-2
[E82-10349] p 19 N82-26747
The use of soil texture and field capacity to normalize microwave soil moisture measurements Some problems p 20 N82-26762
LEGECKIS, R. V.
A ship and satellite view of hydrographic features in the western Gulf of Mexico p 53 A82-32651
LEMESHEV, M. Y.
Cost-effectiveness of geographic surveying from space p 85 N82-24263
LEMOUEL, J. L.
MAGSAT anomaly map and continental drift
[E82-10326] p 38 N82-24599
Models and maps of the main field
[E82-10327] p 74 N82-24600
LEONARD, R. K
Dobson spectrophotometer calibrations, possible errors in ozone absorption coefficients, and errors due to interfering pollutant gases p 28 A82-36431
LERCH, F. J.
Gravity model improvement for Seasat p 32 A82-29615
LERCHE, I.
Steady-state cosmic ray electron spectrum under diffusion, convection, adiabatic deceleration and synchrotron losses p 1 A82-22552
LEROY, M. J
Airborne observed solar elevation and row direction effects on the near-IR/red ratio of cotton
[E82-10220] p 13 N82-23593
LESNIK, IU N
The use of space photographs in the mapping of glaciers and water bodies p 62 A82-37174
LEVINE, J S.
Ammonia and the NOx budget of the troposphere p 27 A82-36293
LIDIAK, E. G.
Characterization of the structure and tectonic of South America
[E82-10196] p 42 N82-23569
The crustal structure and tectonics of South America
[E82-10319] p 38 N82-24592
Geotectonics of South America
[E82-10320] p 38 N82-24593
LIEBMANN, B
Interannual variations of outgoing IR associated with tropical circulation changes during 1974-1978 p 54 A82-36341
LILLESAND, T. M.
Application of scanning microdensitometer data in selected plant science case studies p 7 A82-29539
Digital and visual evaluation of GOES and TIROS/NOAA image data for cover type effects on snowfield observations p 60 A82-34735
LINDEN, D S.
Mapping riparian vegetation in Southeastern Oregon using digitized large scale color infra-red aerial photography p 6 A82-29535
LIPES, R. G.
Description of Seasat radiometer status and results p 52 A82-29622
LISTON, R. L.
Photogrammetric methods for mapping resource data from high altitude panoramic photography p 77 A82-32702
LIUBIMOV, G. P
Comparison of solar proton activity in 1967 and 1969 with that in 1978 and 1979 as measured onboard Venera 4, 6, 11, 12 space probes p 31 A82-22596
The approximate 1 GeV solar cosmic rays in the Forbush-effect of February 15, 1978 p 40 A82-22604
The modulation characteristics of the 19th and 20th solar activity cycles p 59 A82-22615
LIUBOVNYI, N. D.
Allowance for the effect of the atmosphere in the processing of satellite remote-sensing images p 70 A82-35141
LLEBARIA, A.
A quantitative multispectral analysis system for aerial photographs applied to coastal planning p 55 A82-37505
LO, K. K.
The growth of snow in winter storms - An airborne observational study p 60 A82-33329
LOCKWOOD, J A.
A description of relativistic solar particle propagation p 4 A82-22600
LOGACHEV, IU. I.
Energetic solar particle spectra according to Venera-11, 12 and Prognoz-5, 6 p 4 A82-22593
Spacecraft determination of energetic particle propagation parameters - The 1 January 1978 solar event p 31 A82-22598
LONGACRE, M. B.
A satellite magnetic model of northeastern South American aulacogens p 33 A82-30795
LOWES, F. J.
Spherical harmonic representation of the main geomagnetic field for world charting and investigations of some fundamental problems of physics and geophysics
[E82-10203] p 72 N82-23576
LU, T
Magnetic monopole pair and its observation in cosmic rays p 65 A82-22579
LUCA, A. J.
Spherical-Earth gravity and magnetic anomaly modeling by Gauss-Legendre quadrature integration
[E82-10242] p 36 N82-24520
LUI, A. T. Y.
Large amplitude undulations on the equatorward boundary of the diffuse aurora p 76 A82-31019

LUNDELL, G. W.
Rapid oceanographic data gathering Some problems in using remote sensing to determine the horizontal and vertical thermal distributions in the Northeast Pacific Ocean
[AD-A111005] p 58 N82-26945
LUO, L.
Magnetic monopole pair and its observation in cosmic rays p 65 A82-22579
LYNCH, R. V., III
Laser-induced bioluminescence p 53 A82-32559
LYON, R. J. P.
Quantitative relationships of near-surface spectra to Landsat radiometric data p 78 A82-32912
LYONS, A.
Color aerial photography detects nutrient status of loblolly pine plantations p 6 A82-29531

M

MAALOEE, J.
Movement of ice markers measured by satellite ranging
[R-240] p 59 N82-27816
MACDONALD, F. B
A survey of solar protons and alpha differential spectra between 1 and greater than 400 MeV/nucleon p 4 A82-22592
MACFARLANE, N.
Remote sensing in Scotland using data received from satellites - A study of the Tay Estuary region using Landsat multispectral scanning imagery p 62 A82-37501
MACH, P. E.
Space science for applications - The history of Landsat p 84 A82-36617
MADILL, R. J.
RAMS-1, a Resource Analysis and Mapping System p 69 A82-34726
MAEDA, H.
Report of investigation from Japanese MAGSAT Team
[E82-10322] p 74 N82-24595
MAGNESS, E. R.
Evaluation of the procedure for separating barley from other spring small grains
[E82-10230] p 14 N82-23603
MAKINEN, J.
Work related to the Blue Road Geotraverse at the Finnish Geodetic Institute p 32 A82-30306
MALILA, W. A.
Analysis of scanner data for crop inventories
[E82-10192] p 10 N82-22626
Analysis of scanner data for crop inventories
[E82-10241] p 16 N82-24519
MALIN, J. T.
AgRISTARS Foreign Commodity production forecasting The 1980 US corn and soybeans exploratory experiment
[E82-10206] p 11 N82-23579
MALIN, M. C.
Bathymetric imaging p 69 A82-34720
MALIN, S. R. C.
Spherical harmonic representation of the main geomagnetic field for world charting and investigations of some fundamental problems of physics and geophysics
[E82-10203] p 72 N82-23576
MALINIE, G.
Origin of galactic cosmic rays from Ne isotopic composition p 2 A82-22563
MALLICK, D. I. J.
Overseas Geology And Mineral Resources number 56 A geological interpretation of LANDSAT imagery and air photography of Botswana
[OGMR-56] p 42 N82-22636
MANTOVANI, M. S. M.
Crustal structures under the active volcanic areas of central and eastern Mediterranean (M-44)
[E82-10096] p 35 N82-23563
MARCHE, P.
Application of infrared techniques to the study of atmospheric ozone p 27 A82-36414
MARSH, J. G.
Seasat altimeter timing bias estimation p 50 A82-29609
The Seasat altimeter mean sea surface model p 51 A82-29614
Gravity model improvement for Seasat p 32 A82-29615
MARSH, S. E.
Quantitative relationships of near-surface spectra to Landsat radiometric data p 78 A82-32912
MARSHALL, S.
High spectral resolution airborne spectrometry p 77 A82-32443
MARTIN, C. F.
Seasat altimeter height calibration p 49 A82-29603
MARTIN, P.
C-band radar for determining surface soil moisture p 10 A82-37194
MARTIN, T. V.
The Seasat altimeter mean sea surface model p 51 A82-29614
MARTINELL, J.
Azimuthal propagation of flare particles in the heliosphere p 66 A82-22590
MARTSOLF, J. D.
Use of thermal inertia determined by HCMM to predict nocturnal cold prone areas in Florida
[E82-10299] p 17 N82-24575
MASHCHENKO, V. A.
Space to the earth p 83 A82-30850
MASON, G. M.
Time and energy dependence of heavy ion abundances in solar flare energetic particle events p 22 A82-22605
MASTERSON, R. P., JR.
Tidal and geodetic observations for the Seasat altimeter calibration experiment p 49 A82-29604
MASUOKA, E. J.
The influence of autocorrelation in signature extraction An example from a geobotanical investigation of Cotter Basin, Montana
[E82-10341] p 46 N82-25603
MATHIEU, E.
An optical objective lens for earth observations by satellites p 78 A82-32824
MATSUBARA, K.
Description of gray level picture using a collection of density contour lines p 66 A82-29409
MAW, K. D
Exploration into technical procedures for vertical integration
[NASA-CR-166352] p 75 N82-26763
MAYHEW, M. A.
Satellite and surface geophysical expression of anomalous crustal structure in Kentucky and Tennessee p 34 A82-34918
Application of satellite magnetic anomaly data to Curie isotherm mapping p 70 A82-35824
An equivalent layer magnetization model for the United States derived from MAGSAT data
[E82-10297] p 36 N82-24573
MAYO, K. K.
The use of residual images in Landsat image analysis p 66 A82-29328
Monitoring land-cover change by principal component analysis of multitemporal Landsat data p 68 A82-32906
MAZADE, A. V
Ten-Ecosystem Study
[E82-10186] p 84 N82-22620
MCAVANEY, B. J.
The onset of the Australian Northwest monsoon during winter MONEX Broadscale flow revealed by an objective analysis scheme p 56 N82-23912
MCBRIDE, J. L.
The onset of the Australian Northwest monsoon during winter MONEX Broadscale flow revealed by an objective analysis scheme p 56 N82-23912
MCCARTHY, J.
Evaluation of spruce-fir forests using small-format photographs p 8 A82-32707
MCCLOY, K. R.
The response characteristics of vegetation in Landsat MSS digital data p 8 A82-32907
MCCONAGHY, D. C
Geographic location of individual pixels p 68 A82-32900
Measuring sea surface temperature from satellites - A ground truth approach p 54 A82-32917
MCDOUGAL, D S.
In situ ozone data for comparison with laser absorption remote sensor 1980 PEPE/NEROS program
[NASA-TM-84471] p 30 N82-25661
MCFARLAND, M. J.
Measurement of soil moisture trends with airborne scatterometers
[E82-10361] p 20 N82-26759
Multifrequency remote sensing of soil moisture
[E82-10362] p 20 N82-26760
Development of visible/infrared/microwave agriculture classification and biomass estimation algorithms
[E82-10363] p 20 N82-26761
MCGINNIS, D. F., JR.
Use of NOAA/AVHRR visible and near-infrared data for land remote sensing
[NASA-TM-84186] p 81 N82-22643
MCGUIRE, R. E.
A survey of solar protons and alpha differential spectra between 1 and greater than 400 MeV/nucleon p 4 A82-22592
MCKENZIE, D. L.
Soft X-rays from the sunlit earth's atmosphere p 29 A82-37405
MCLEAN, J A.
Remote sensing of Douglas-fir trees newly infested by bark beetles p 6 A82-29536
MCLEOD, R. G.
Resource inventory techniques used in the California Desert Conservation Area p 23 A82-32441
MCMANUS, J.
Remote sensing in Scotland using data received from satellites - A study of the Tay Estuary region using Landsat multispectral scanning imagery p 62 A82-37501
MCMILLAN, K
Remote sensing in Scotland using data received from satellites - A study of the Tay Estuary region using Landsat multispectral scanning imagery p 62 A82-37501
MCMURTREY, J. E., III
A multi-frequency radiometric measurement of soil moisture content over bare and vegetated fields
[E82-10238] p 16 N82-23611
MEAD, D. R.
Multi-resource inventory in interior Alaska p 6 A82-29532
MEAD, R. A.
Inventory of wildlife habitat from color infrared aerial photography for Cobb Island, Virginia p 6 A82-29529
A computerized spatial analysis system for assessing wildlife habitat from vegetation maps p 9 A82-34716
A quantitative method to test for similarity between photo interpreters p 69 A82-34722
MEDLIN, G.
Ocean wave height measurement with SEASAT SAR using speckle diversity p 53 A82-32882
MEISNER, D. E.
Application of scanning microdensitometer data in selected plant science case studies p 7 A82-29539
Digital and visual evaluation of GOES and TIROS/NOAA image data for cover type effects on snowfield observations p 60 A82-34735
MENG, C.-I.
Large amplitude undulations on the equatorward boundary of the diffuse aurora p 76 A82-31019
MENZEL, W P.
Surface temperature determination from an amalgamation of GOES and TIROS-N radiance measurements p 66 A82-28905
MEROLA, J. A.
Detection of variations in aspen forest habitat from LANDSAT digital data Bear River Range, Utah
[E82-10355] p 19 N82-26753
MESHCHERIAKOV, I. V.
Space to the earth p 83 A82-30850
MEWALDT, R. A.
High resolution measurements of solar flare isotopes p 22 A82-22606
MEYER, J. P.
Comparative abundances in solar energetic particles and in galactic cosmic ray sources, and the Ne-22 anomaly p 83 A82-22556
On volatility, first ionization potential, and s- and r-processes p 2 A82-22560
A tentative ordering of all available solar energetic particles abundance observations I - The mass unbiased baseline II - Discussion and comparison with coronal abundances p 40 A82-22609
MEYER, M. P.
Application of 35mm color aerial photography to forest land change detection p 6 A82-29533
MEYER, P.
Unusual properties of particle events associated with solar flare gamma ray events p 65 A82-22585
The relation of type II radio bursts to solar energetic particles observed at earth p 3 A82-22591
MICHEL, F. C.
Pulsar models and cosmic-ray acceleration p 21 A82-22570
MICHEL, R. J.
Exploration into technical procedures for vertical integration
[NASA-CR-166352] *p 75 N82-26763*
MILLARD, J P.
Airborne observed solar elevation and row direction effects on the near-IR/red ratio of cotton
[E82-10220] p 13 N82-23593
Multilevel measurements of surface temperature over undulating terrain planted to barley
[E82-10245] p 16 N82-24523
MILLER, A. J.
Total ozone variations 1970-74 using Backscattered Ultraviolet /BUV/ and ground-based observations p 26 A82-36053
MILLER, K. H.
Design guidelines for satellite image data distribution systems p 70 A82-37048

MILLER, N L.
Application of 35mm color aerial photography to forest land change detection p 6 A82-29533
MILLER, S. H.
Application of HCMM data to regional geologic analysis for mineral and energy resource evaluation
[E82-10153] p 45 N82-24518
Application of HCMM data to regional geologic analysis for mineral and energy resource evaluation
[E82-10243] p 45 N82-24521
MILLER, W. F.
Application of remote sensing to state and regional problems
[E82-10288] p 30 N82-24566
MILLIER, F.
OSO-8 lower mesospheric ozone number density profiles p 28 A82-36472
MILLIGAN, J.
Computer-processed geophysical atlas of digital data for the East Coast margin of the United States from surface and spacecraft data
[AD-A111388] p 39 N82-25748
MILMAN, A. S.
Retrieval of ocean surface and atmospheric parameters from multichannel microwave radiometric measurements p 53 A82-31995
MILTON, E. J.
Remote sensing of salt marsh vegetation in the first four proposed Thematic Mapper bands p 10 A82-37503
MINCHEW, K.
Application of remote sensing to state and regional problems
[E82-10288] p 30 N82-24566
MIYAZAKI, Y.
Report of investigation from Japanese MAGSAT Team
[E82-10322] p 74 N82-24595
MOBIUS, E.
A comparison of helium and heavy ion spectra in He/3/ rich solar flares with a model calculation p 5 A82-22612
MOE, J. L.
Effective electromagnetic shielding in multilayer printed circuit boards
[AIAA 81-2333] p 59 A82-13528
MONACO, F.
Crustal structures under the active volcanic areas of central and eastern Mediterranean (M-44)
[E82-10096] p 35 N82-23563
MOORE, D.
Irrigation management with remote sensing
[E82-10357] p 20 N82-26755
MOORE, D. G
Evaluation of HCMM data for assessing soil moisture and water table depth
[E82-10329] p 18 N82-24602
MOORE, R. K.
A simulation study of soil moisture estimation by a space SAR p 60 A82-29333
Evaluation of atmospheric attenuation from SMMR brightness temperature for the Seasat satellite scatterometer p 51 A82-29618
Evaluation of the soil moisture prediction accuracy of a space radar using simulation techniques
[E82-10351] p 19 N82-26749
MORFILL, G. E.
Evidence for the stochastic acceleration of cosmic rays in supernova remnants p 2 A82-22564
MORITA, Y.
Aircraft measurements of NO/x/ in the lower troposphere above the coast of Japan p 26 A82-36247
MORK, M. B. E.
Regional geological, tectonic and geophysical features of Nordland, Norway p 41 A82-30304
MOROZOVA, T. I.
The solar proton fluxes in April, 1979 p 66 A82-22597
MOSHER, J.
A color-ratio map of Mercury p 31 A82-22294
MROCZYNSKI, R. P.
Forest Resource Information System Phase 3 System transfer report
[E82-10344] p 18 N82-25606
MUASHER, M. J.
Multistage classification of multispectral Earth observational data The design approach
[E82-10213] p 72 N82-23586
MUELLER, D.
The influence of soil characteristics on regional convection differences above Northern Germany p 10 A82-37589
MUELLER, I. I.
Reference coordinate systems for earth dynamics - A preview p 33 A82-32077
MUKAREVA, G. B.
Aerogeophysical methods of finding uranium deposits p 41 A82-33402
MUKHENBERG, V. V.
Albedo and angular characteristics of the reflectance of the underlying surface and clouds p 33 A82-30849
MULLAN, D. J.
Possible evidence for attenuation of an MHD shock by a magnetic neutral sheet in the solar corona p 3 A82-22589
MURPHY, P.
High spectral resolution airborne spectrometry p 77 A82-32443
MURTHA, P. A.
Remote sensing of Douglas-fir trees newly infested by bark beetles p 6 A82-29536
MURTY, P. G. K.
On the space-time variability of ocean surface mixed layer characteristics of central and eastern Arabian sea during MONSOON-77 p 56 N82-23909
MYERS, V.
Irrigation management with remote sensing
[E82-10357] p 20 N82-26755

N

NAGAI, T.
Observed magnetic substorm signatures at synchronous altitude p 26 A82-35534
NAGATANI, R. M.
Total ozone variations 1970-74 using Backscattered Ultraviolet /BUV/ and ground-based observations p 26 A82-36053
NAKAJIMA, M.
Description of gray level picture using a collection of density contour lines p 66 A82-29409
NAMKEN, L. N.
AgRISTARS Early warning and crop condition assessment Plant cover, soil temperature, freeze, water stress, and evapotranspiration conditions
[E82-10225] p 14 N82-23598
NANDI, A.
Magnetic charts of Canada derived from Magsat data p 32 A82-30778
NAUTIYAL, C. M.
Is the neon composition of our sun, planetary or solar p 76 A82-22608
NEGI, J G
Analysis of MAGSAT data of the Indian region
[E82-10358] p 75 N82-26756
NEKHIN, S. S.
Evaluation of the effectiveness of systematic image distortion compensation p 69 A82-34469
NELSON, R.
Evaluation of temporal registration of Landsat scenes p 67 A82-32345
NELSON, R. F.
Defining the temporal window for monitoring forest canopy defoliation using Landsat p 9 A82-34730
NESS, S. D.
Evaluation of HCMM data for assessing soil moisture and water table depth
[E82-10329] p 18 N82-24602
NEUENSCHWANDER, H.
A description of relativistic solar particle propagation p 4 A82-22600
NEVATIA, R.
Image understanding research
[AD-A110746] p 74 N82-25611
NEWITT, L. R.
Magnetic charts of Canada derived from Magsat data p 32 A82-30778
NEWTON, R. W.
Orbiting passive microwave sensor simulation applied to soil moisture estimation
[E82-10343] p 18 N82-25605
NG, L. K.
The electron and positron spectra in primary cosmic rays p 1 A82-22543
Comparison of the measured antiproton flux with that predicted by the 'leaky box' model p 1 A82-22544
NIKITIN, A. M.
Evaluation of the accuracy of water-surface temperature measurement by means of airborne infrared radiometers p 62 A82-35136
NILSSON, C. S.
High resolution satellite observations of mesoscale oceanography in the Tasman Sea, 1978 - 1979
[E82-10324] p 57 N82-24597
NIXON, P. R.
AgRISTARS Early warning and crop condition assessment Plant cover, soil temperature, freeze, water stress, and evapotranspiration conditions
[E82-10225] p 14 N82-23598
NORRIS, D. D
Imaging spectroscopy, Proceedings of the Seminar, Los Angeles, CA, February 10, 11, 1981 p 77 A82-32440
NOSACHEV, V. I
The use of remote-sensing data to identify the space-time variability of the quality of natural waters p 62 A82-35138
NOVIKOV, IU. B.
Aerogeophysical methods of finding uranium deposits p 41 A82-33402
NUZHDIN, P. V.
Analysis of ocean and atmosphere thermodynamical characteristics during the onset of southwest monsoon over the Arabian Sea p 57 N82-23945

O

OGALLAGHER, J J
Observations of the ionization states of energetic particles accelerated in solar flares p 40 A82-22607
OGAWA, K.
Report of investigation from Japanese MAGSAT Team
[E82-10322] p 74 N82-24595
OHLHORST, C W.
Analysis of ocean color scanner data from the Superflux III Experiment
[NASA-TM-83290] p 55 N82-23614
OKUDAIRA, K.
Solar gamma-ray experiment on Astro-A satellite p 21 A82-22583
OLSON, C. E., JR.
Evaluation of spruce-fir forests using small-format photographs p 8 A82-32707
ORMSBY, J P.
Landsat digital analysis of the initial recovery of burned tundra at Kokolik River, Alaska p 8 A82-32913
The use of Landsat-3 thermal data to help differentiate land covers p 25 A82-34218
OSBORNE, J. L.
Derivation of the distribution of synchrotron emissivity in the Galaxy from the 408 MHz all-sky survey p 82 A82-22549
OSHIMA, S.
Report of investigation from Japanese MAGSAT Team
[E82-10322] p 74 N82-24595
OSOKIN, N. I.
Method for the analysis of the melting of a firn complex on the basis of aerospace photographs p 61 A82-35133
OVERLAND, J E.
Surface wind analyses for Seasat p 51 A82-29619
OWE, M
Use of aerial photography in determining land use and streamflow relationships on small developing watersheds p 60 A82-34736

P

PACCA, I. I. G.
Structure, composition and thermal state of the crust in Brazil
[E82-10187] p 35 N82-22621
PAEGLE, J.
Short term influence radius of monsoonal overturnings p 56 N82-23898
PAIRMAN, D.
A system design for a multispectral sensor using two-dimensional solid-state imaging arrays p 77 A82-31991
PALUZZI, P. R
Bathymetric imaging p 69 A82-34720
PANKRATOVA, E I.
Experience with the compilation of maps of snow-cover melting in the central part of the European USSR on the basis of satellite data p 62 A82-35134
PARIS, J. F.
Orbiting passive microwave sensor simulation applied to soil moisture estimation
[E82-10343] p 18 N82-25605
PARKE, M. E.
The Seasat altimeter data and its accuracy assessment p 49 A82-29602
PASSARELLI, R. E., JR.
The growth of snow in winter storms - An airborne observational study p 60 A82-33329
PAUL, J A.
On the stellar origin of the Ne-22 excess in cosmic rays p 21 A82-22562
Origin of galactic cosmic rays from Ne isotopic composition p 2 A82-22563

PAYNE, R. W.
AgRISTARS Foreign commodity production forecasting The 1980 US/Canada wheat and barley exploratory experiment
[E82-10126] p 11 N82-23565
PERESLEGINA, N. V.
Comparison of solar proton activity in 1967 and 1969 with that in 1978 and 1979 as measured onboard Venera 4, 6, 11, 12 space probes p 31 A82-22596
The modulation characteristics of the 19th and 20th solar activity cycles p 59 A82-22615
PEREZ-PERAZA, J.
Cosmic ray composition from acceleration of thermal matter p 64 A82-22558
Azimuthal propagation of flare particles in the heliosphere p 66 A82-22590
PESSES, M. E.
Observations of interplanetary energetic charged particles from gamma-ray line solar flares p 65 A82-22586
On the anticorrelation between the He/3//He/4/ ratio and proton intensity in He/3/ rich flares p 40 A82-22613
PETEHERYCH, S
Surface wind analyses for Seasat p 51 A82-29619
PETERSEN, G. W.
Delineation of soil temperature regimes from HCMM data
[E82-10298] p 17 N82-24574
PHILIPSON, W. R.
Landsat detection of hardwood forest clearcuts p 8 A82-32708
PHILLIPPS, S.
Derivation of the distribution of synchrotron emissivity in the Galaxy from the 408 MHz all-sky survey p 82 A82-22549
PHILLIPS, J. D.
Initial scalar magnetic anomaly map from Magsat p 32 A82-30784
Initial vector magnetic anomaly map from Magsat p 32 A82-30785
PHYSICK, W. L.
Mean sea-level pressure in the Southern Hemisphere during the FGGE period p 55 N82-23856
PIERATTINI, D.
Crustal structures under the active volcanic areas of central and eastern Mediterranean (M-44)
[E82-10096] p 35 N82-23563
PIERCE, J.
Optical bar panoramic photography for planning timber salvage in drought-stressed forests p 7 A82-32705
PIERSON, W. J.
The Seasat-A satellite scatterometer - The geophysical evaluation of remotely sensed wind vectors over the ocean p 51 A82-29616
The relationship between wind vector and normalized radar cross section used to derive Seasat-A Satellite Scatterometer winds p 51 A82-29617
Surface wind analyses for Seasat p 51 A82-29619
PINGITORE, N. E
Evaluation and combined geophysical interpretations of NURE and related geoscience data in the Van Horn, Pecos, Marfa, Fort Stockton, Presidido, and Emory Peak quadrangles, Texas, volume 1
[DE82-005554] p 47 N82-27808
Evaluation and combined geophysical interpretations of NURE and related geoscience data in the Van Horn, Pecos, Marfa, Fort Stockton, Presidio, and Emory Peak quadrangels, Texas
[DE82-005560] p 48 N82-27809
PINTER, P J., JR.
View angle effects in the radiometric measurement of plant canopy temperatures p 8 A82-32914
PITCHFORD, W. M.
Orbiting passive microwave sensor simulation applied to soil moisture estimation
[E82-10343] p 18 N82-25605
PITTS, D. E.
Field size, length, and width distributions based on LACIE ground truth data p 8 A82-32909
PIWINSKI, D.
Evaluation of NOAA-AVHRR data for crop assessment p 8 A82-34179
PLACE, M.
Experimental assessment of improved spatial resolution LANDSAT data
[AD-A110538] p 75 N82-26765
PLACE, M. C.
A new approach to multiresource inventories using remote sensing and geographic information systems technologies p 25 A82-34739
POKROVSKII, O. M.
Remote sensing of the weediness of crop fields p 5 A82-29435
PONT, W.
Analysis of scanner data for crop inventories
[E82-10192] p 10 N82-22626
POPESCU, J.
Remote sensing of the earth's resources - The Soviet experience p 84 A82-33555
PORTER, D. L.
Tidal and geodetic observations for the Seasat altimeter calibration experiment p 49 A82-29604
POTEMRA, T. A.
Investigation of MAGSAT and TRIAD magnetometer data to provide corrective information on high-latitude external fields
[E82-10201] p 72 N82-23574
POVINEC, P.
Calculation of production rates of cosmogenic nuclides by Monte Carlo method p 64 A82-22576
POWERS, J. S.
An information-theoric spatial transform p 69 A82-34717
PRABHAKARA, C.
Remote sensing of precipitable water over the oceans from Nimbus 7 microwave measurements p 49 A82-28907
PRISHCHEP, V. L.
Convective outflow of cosmic rays from the Galaxy and background radio emission p 83 A82-22551
PRISLEY, S. P.
A computerized spatial analysis system for assessing wildlife habitat from vegetation maps p 9 A82-34716
PROTHEROE, R. J.
The cosmic ray positron spectrum p 1 A82-22542
PTUSKIN, V. S.
Angular variations of nonthermal radio emission from the Galaxy relevant to the structure of interstellar magnetic field p 83 A82-22550
Remarks on cosmic ray origin p 21 A82-22569

Q

QUIRK, B. K
Aerial photography vs Landsat for digital land-cover mapping in an urban watershed p 61 A82-34745

R

RAJARAM, R.
MAGSAT for geomagnetic studies over Indian region
[E82-10202] p 72 N82-23575
MAGSAT for geomagnetic studies over Indian region
[E82-10296] p 73 N82-24572
RAMAN, K. V. S.
On the space-time variability of ocean surface mixed layer characteristics of central and eastern Arabian sea during MONSOON-77 p 56 N82-23909
RAMATY, R.
Interplanetary particle observations associated with solar flare gamma-ray line emission p 3 A82-22584
RAMBERG, I. B.
Regional geological, tectonic and geophysical features of Nordland, Norway p 41 A82-30304
RAMSEIER, R. O
Sea-Ice Mission Requirements for the US FIREX and Canada RADARSAT programs
[NASA-CR-168984] p 57 N82-25609
RANGARAJAN, G. K.
MAGSAT for geomagnetic studies over Indian region
[E82-10202] p 72 N82-23575
MAGSAT for geomagnetic studies over Indian region
[E82-10296] p 73 N82-24572
RANGO, A.
Snowpack monitoring in North America and Eurasia using passive microwave satellite data p 78 A82-32915
RANSON, K. J.
Diurnal changes in reflectance factor due to Sun-row direction interactions
[E82-10128] p 11 N82-23566
RAO, D R. K.
MAGSAT for geomagnetic studies over Indian region
[E82-10202] p 72 N82-23575
MAGSAT for geomagnetic studies over Indian region
[E82-10296] p 73 N82-24572
RAO, M. N.
Is the neon composition of our sun, planetary or solar p 76 A82-22608
RAO, P. K.
Comparison of satellite derived radiation budget measurements over MONEX during 1979 to 1980 p 29 N82-23891
RAO, R. R.
On the space-time variability of ocean surface mixed layer characteristics of central and eastern Arabian sea during MONSOON-77 p 56 N82-23909
RAPP, R. H.
The Earth's gravity field to degree and order 180 using SEASAT altimeter data, terrestrial gravity data and other data
[AD-A113098] p 40 N82-27900
RASTOGI, R. G.
MAGSAT for geomagnetic studies over Indian region
[E82-10202] p 72 N82-23575
MAGSAT for geomagnetic studies over Indian region
[E82-10296] p 73 N82-24572
RAVA, B.
A color-ratio map of Mercury p 31 A82-22294
RAVET, F. W.
A meteorologically driven maize stress indicator model
[E82-10112] p 11 N82-23564
Evaluation of the Doraiswamy-Thompson winter wheat crop calendar model incorporating a modified spring restart sequence
[E82-10207] p 12 N82-23580
A meteorologically driven grain sorghum stress indicator model
[E82-10218] p 13 N82-23591
RAY, R. D.
Improved definition of crustal magnetic anomalies for MAGSAT data
[E82-10314] p 37 N82-24587
REAMES, D. V.
Heavy-element abundances in He/3/-rich events p 5 A82-22611
REAMES, V.
Interplanetary particle observations associated with solar flare gamma-ray line emission p 3 A82-22584
REED, C. R.
Selection of the Australian indicator region
[E82-10222] p 13 N82-23595
REGAN, R. D
Improved definition of crustal magnetic anomalies for MAGSAT data
[E82-10314] p 37 N82-24587
REGINATO, R. J
View angle effects in the radiometric measurement of plant canopy temperatures p 8 A82-32914
Multilevel measurements of surface temperature over undulating terrain planted to barley
[E82-10245] p 16 N82-24523
REICHLE, H. G., JR.
Tropospheric CO measurement experiment from the second Space Shuttle flight p 27 A82-36292
RHODES, E.
Effects of altitude, focal length, and filter combinations on color infrared photography of citrus groves p 9 A82-34729
RICHARD, H. L.
Solid state instrumentation concepts for earth resource observation
[AAS PAPER 82-132] p 81 A82-37812
RICHARDS, M. A.
An empirical determination of the effects of sea state bias on Seasat altimetry p 50 A82-29607
RICHARDSON, A. J.
Relating Landsat digital count values to ground reflectance for optically thin atmospheric conditions p 66 A82-29762
AgRISTARS Early warning and crop condition assessment Plant cover, soil temperature, freeze, water stress, and evapotranspiration conditions
[E82-10225] p 14 N82-23598
RICKS, E. L.
Some empirical rules for forecasting fog and status over northern Florida, southern Georgia and adjacent coastal waters
[PB82-154006] p 59 N82-27949
RIDD, M. K.
Irrigated acreage in the Bear River Basin as of the 1975 growing season
[E82-10356] p 20 N82-26754
RIMSHA, M. A.
Purpose, background of 'Intercosmos-21' mission p 81 N82-24264
RITCHIE, J. C.
Agricultural Research Service research highlights in remote sensing for calendar year 1980
[E82-10228] p 14 N82-23601
RITZWOLLER, M. H.
Magsat magnetic anomalies over Antarctica and the surrounding oceans p 32 A82-30787
ROBERTSON, D. S.
Some considerations in the use of very-long-baseline-interferometry to establish reference coordinate systems for geodynamics p 34 A82-32096
ROBINOVE, C. J.
Computation with physical values from Landsat digital data p 68 A82-32709

ROBINSON, B F.
Spectral properties of agricultural crops and soils measured from space, aerial, field, and laboratory sensors
[E82-10189] p 10 N82-22623
Diurnal changes in reflectance factor due to Sun-row direction interactions
[E82-10128] p 11 N82-23566
Spectral properties of agricultural crops and soils measured from space, aerial, field, and laboratory sensors
[E82-10212] p 12 N82-23585
Linear polarization of light by two wheat canopies measured at many view angles
[E82-10229] p 14 N82-23602
ROBLE, R. G.
OSO-8 lower mesospheric ozone number density profiles p 28 A82-36472
ROBSON, A.
The METEOSAT Data Collection System and its application p 75 N82-26037
ROCHESTER, M. G.
The definition of the terrestrial coordinate frame by long baseline interferometry p 33 A82-32084
RODRIGUES, V
SMS/GOES data collection platform system p 75 N82-26027
RODRIGUEZ-BEJARANO, D.
Monitoring deforestation in the eastern part of the state of Guerrero, Mexico p 9 A82-34733
ROGERS, R. H
LANDSAT technology transfer to the private and public sectors through community colleges and other locally available institutions
[E82-10181] p 85 N82-23568
ROGERS, T. G.
Total ozone variations 1970-74 using Backscattered Ultraviolet /BUV/ and ground-based observations p 26 A82-36053
ROSBOROUGH, G. W
An empirical determination of the effects of sea state bias on Seasat altimetry p 50 A82-29607
ROSENFIELD, G. H.
Sample design for estimating change in land use and land cover p 24 A82-32711
ROSENKRANZ, P. W.
Inversion of data from diffraction-limited multiwavelength remote sensors II - Nonlinear dependence of observables on the geophysical parameters p 77 A82-32658
ROSENTHAL, W. D.
Multifrequency remote sensing of soil moisture
[E82-10362] p 20 N82-26760
Development of visible/infrared/microwave agriculture classification and biomass estimation algorithms
[E82-10363] p 20 N82-26761
ROSETHAL, W. D.
Measurement of soil moisture trends with airborne scatterometers
[E82-10361] p 20 N82-26759
ROSHAL, A S.
Computer simulation of the time dependence of the photon energy spectra produced in proton and electron bremstrahlung p 3 A82-22587
ROSS, G. A.
Detection of environmental disturbance using color aerial photography and thermal infrared imagery p 22 A82-29327
ROTHENFLUG, R.
Mass per charge ratio in hot plasmas and cosmic ray source composition p 2 A82-22557
ROY, M.
MAGSAT for geomagnetic studies over Indian region
[E82-10202] p 72 N82-23575
MAGSAT for geomagnetic studies over Indian region
[E82-10296] p 73 N82-24572
ROY, R. F.
Evaluation and combined geophysical interpretations of NURE and related geoscience data in the Van Horn, Pecos, Marfa, Fort Stockton, Presidido, and Emory Peak quadrangles, Texas, volume 1
[DE82-005554] p 47 N82-27808
Evaluation and combined geophysical interpretations of NURE and related geoscience data in the Van Horn, Pecos, Marfa, Fort Stockton, Presidio, and Emory Peak quadrangels, Texas
[DE82-005560] p 48 N82-27809
RUBINCAM, D. P.
Information theory lateral density distribution for earth inferred from global gravity field p 35 A82-37962
RUEDA, A.
Astrophysical scenarios for critically evaluating a zero-point field acceleration mechanism p 64 A82-22575
RUGGE, H. R
Soft X-rays from the sunlit earth's atmosphere p 29 A82-37405
RUSSKIKH, V. N
Computer simulation of the time dependence of the photon energy spectra produced in proton and electron bremstrahlung p 3 A82-22587
RYLAND, G.
Evaluation of NOAA-AVHRR data for crop assessment p 8 A82-34179

S

SAHAI, B
Analysis of MAGSAT data of the Indian region
[E82-10358] p 75 N82-26756
SAID, S S.
Origin of cosmic rays in galactic centre sources p 3 A82-22571
SAILOR, R. V.
Spatial resolution and repeatability of Magsat crustal anomaly data over the Indian Ocean p 32 A82-30788
Analyses of MAGSAT tracks crossing the study region in the Indian Ocean
[E82-10197] p 71 N82-23570
Bathymetric and tectonics of Indian Ocean using MAGSAT data
[E82-10204] p 36 N82-23577
Analyzing the Broken Ridge area of the Indian Ocean using magnetic and gravity anomaly maps and geoid undulation and bathymetry data
[E82-10303] p 36 N82-24577
Investigating tectonic and bathymetric features of the Indian Ocean using MAGSAT magnetic anomaly data
[E82-10304] p 37 N82-24578
SAKAI, H
Stratospheric emission data analysis
[AD-A112337] p 76 N82-26907
SAKURAI, K.
Physical state of the birth place of cosmic rays and its implication to the acceleration processes p 2 A82-22559
SALAZAR, W.
Optical bar panoramic photography for planning timber salvage in drought-stressed forests p 7 A82-32705
SALMON, J. R.
On the application of a model of boundary-layer flow over low hills to real terrain p 29 A82-36741
SANAHUJA, B.
Non-flare injection of protons into interplanetary space p 4 A82-22601
SANDWELL, D. T.
Geoid height-age relation from Seasat altimeter profiles across the Mendocino Fracture Zone p 34 A82-32646
SAPP, C. D.
Spectral scanning of experimental plots of SO2-affected winter wheat and soybeans for mission planning p 6 A82-29537
Remote sensing of sulfur dioxide effects on vegetation Volume 1 Summary
[DE82-900580] p 31 N82-27802
Remote sensing of sulfur dioxide effects on vegetation Volume 2 Data
[DE82-900581] p 31 N82-27803
SAUNDERS, R W.
Satellite observations of sea surface temperature around the British Isles p 54 A82-33717
SAUSEN, T M.
Dynamic study of the upper Sao Francisco river and Tres Marias reservoir using MSS/LANDSAT images
[E82-10291] p 63 N82-24569
SAVENKO, I. A.
High-energy solar protons p 22 A82-22588
SAWATZKY, D. L.
Registration of Heat Capacity Mapping Mission day and night images
[E82-10210] p 72 N82-23583
SAWCHUK, A. A.
Image understanding research
[AD-A110746] p 74 N82-25611
SAWHNEY, J. L.
Report of MAGSAT project by Survey of India
[E82-10293] p 73 N82-24570
SCANVIC, J. Y
Spatial thermal radiometry contribution to the Massif Armoricain and the Massif Central France litho-structural study
[E82-10190] p 42 N82-22624
SCARPACE, F. L.
Aerial photography vs Landsat for digital land-cover mapping in an urban watershed p 61 A82-34745
SCHABER, G. G.
Possible fault detection in Cottonball Basin, California An application of radar remote sensing p 41 A82-32898
SCHLEIMER, G E.
Environmental monitoring report of the Lawrence Berkeley Laboratory, 1980
[LBL-12604] p 29 N82-23793
SCHLICKEISER, R
Consequences of an inverse Compton emission model for extragalactic X-ray sources p 83 A82-22553
SCHLICKE6SER, R.
Steady-state cosmic ray electron spectrum under diffusion, convection, adiabatic deceleration and synchrotron losses p 1 A82-22552
SCHMUGGE, T. J
A multi-frequency radiometric measurement of soil moisture content over bare and vegetated fields
[E82-10238] p 16 N82-23611
SCHNEIDER, S. R.
Use of NOAA/AVHRR visible and near-infrared data for land remote sensing
[NASA-TM-84186] p 81 N82-22643
SCHNETZLER, C. C.
Initial vector magnetic anomaly map from Magsat p 32 A82-30785
SCHOLER, M.
Observations of the ionization states of energetic particles accelerated in solar flares p 40 A82-22607
A comparison of helium and heavy ion spectra in He/3/ rich solar flares with a model calculation p 5 A82-22612
SCHOTT, F.
MONEX oceanographic observations along the East African coast p 56 N82-23908
SCHROEDER, L. C.
The Seasat-A satellite scatterometer - The geophysical evaluation of remotely sensed wind vectors over the ocean p 51 A82-29616
The relationship between wind vector and normalized radar cross section used to derive Seasat-A Satellite Scatterometer winds p 51 A82-29617
SEASAT A satellite scatterometer illumination times of selected in situ sites
[NASA-TM-83280] p 81 N82-22865
SCHUBERT, G
Geoid height-age relation from Seasat altimeter profiles across the Mendocino Fracture Zone p 34 A82-32646
SCHUEPP, P H
Aircraft monitoring of surface carbon dioxide exchange p 23 A82-30293
SCHUERER, K.
Image quality and height measurement accuracy of serial survey camera imagery from high altitudes p 78 A82-33297
SCHUESSLER, H.
Microwave sensing from space
[AAS PAPER 82-127] p 80 A82-37809
SCHUTZ, B E
Evaluation of the Seasat altimeter time tag bias p 50 A82-29610
SCULLY-POWER, P.
High resolution satellite observations of mesoscale oceanography in the Tasman Sea, 1978 - 1979
[E82-10324] p 57 N82-24597
SECROUN, C.
Application of infrared techniques to the study of atmospheric ozone p 27 A82-36414
SEEVERS, P. M.
Considerations in using color infrared photographs for vegetative interpretation p 6 A82-29530
SEIN, E.
An optical objective lens for earth observations by satellites p 78 A82-32824
SELLMAN, A
Analysis of scanner data for crop inventories
[E82-10192] p 10 N82-22626
SENN, R. H.
Source assessment system
[AD-A111223] p 75 N82-25613
SETH, A.
MAGSAT for geomagnetic studies over Indian region
[E82-10202] p 72 N82-23575
SETHURAMAN, S.
Marine boundary layer wind structure over the Bay of Bengal during Monex-79 p 57 N82-23929
SEXTON, J. L.
Verification of the crustal component in satellite magnetic data p 32 A82-30789
SEYFARTH, B. R.
An analysis of LANDSAT MSS scene-to-scene registration accuracy
[E82-10285] p 16 N82-24563
SHABELA, F.
The possibility of using remote-sensing methods to study the hydrology of elementary watersheds p 61 A82-35130
SHANMUGAM, K. S.
The recognition of extended targets - SAR images for level and hilly terrain p 33 A82-31994

SHAPIRO, M. M.
Calculated isotopic source composition and tests for origin and propagation of cosmic rays with mass numbers less than or equal to 62 p 83 A82-22554
Acceleration processes near massive black holes p 3 A82-22572
Extragalactic cosmic rays, their sources and spectrum p 40 A82-22574
SHARIK, T L.
A computerized spatial analysis system for assessing wildlife habitat from vegetation maps p 9 A82-34716
SHCHEGLOVA, O. P.
The seasonal snow-line within the Fergana basin and the possibility of using it for hydrological forecasting p 61 A82-35131
SHEFFIELD, C.
A new approach to multiresource inventories using remote sensing and geographic information systems technologies p 25 A82-34739
Experimental assessment of improved spatial resolution LANDSAT data
[AD-A110538] p 75 N82-26765
SHIUE, J. C.
A comparative study of microwave radiometer observations over snowfields with radiative transfer model calculations p 60 A82-32910
SHKABURA, N. A.
Estimates of the statistical structure of the atmospheric pressure field in summer Monex-79 area p 57 N82-23939
SHLIAKHOVA, L. A.
The use of remote-sensing data to identify the space-time variability of the quality of natural waters p 62 A82-35138
SHUKOWSKY, W.
Structure, composition and thermal state of the crust in Brazil
[E82-10187] p 35 N82-22621
SHUM, C
Evaluation of the Seasat altimeter time tag bias p 50 A82-29610
SIDRAN, M.
Infrared sensing of sea surface temperature from space p 53 A82-32902
SIEVERS, J.
Image quality and height measurement accuracy of serial survey camera imagery from high altitudes p 78 A82-33297
SIGLE, M
Investigations of point transfer p 78 A82-33296
SIGLER, G. B.
Matrix data analysis Color/B and W coding is not always enough
[AD-A111401] p 74 N82-25612
SIGURDSSON, H
Soufriere Volcano, St Vincent - Observations of its 1979 eruption from the ground, aircraft, and satellites p 24 A82-33652
SIKKA, D. R.
Impact of additional summer MONEX wind data on the prediction of monsoon depressions during June - August 1979 with two versions of primitive equation (PE) barotropic model p 56 N82-23900
SILBERBERG, R
Acceleration processes near massive black holes p 3 A82-22572
Extragalactic cosmic rays, their sources and spectrum p 40 A82-22574
SILVESTROV, S. D.
Space to the earth p 83 A82-30850
SIMONETT, D S.
Impacts of remote sensing on U S geography p 24 A82-32899
Multispectral determination of soil moisture-2
[E82-10349] p 19 N82-26747
SIMPSON, G. A.
Fragmentation of Fe nuclei on carbon, hydrogen and CH2 targets I - Individual charge changing and total cross sections II - Isotopic cross sections p 63 A82-22538
SIMPSON, J. A
The question of short pathlengths in interstellar propagation p 1 A82-22541
SIMPSON, J. D.
Matrix data analysis Color/B and W coding is not always enough
[AD-A111401] p 74 N82-25612
SINGH, B. P.
MAGSAT for geomagnetic studies over Indian region
[E82-10202] p 72 N82-23575
MAGSAT for geomagnetic studies over Indian region
[E82-10296] p 73 N82-24572
SINGH, S. S.
Impact of additional summer MONEX wind data on the prediction of monsoon depressions during June - August 1979 with two versions of primitive equation (PE) barotropic model p 56 N82-23900
SINHA, S.
Impact of additional summer MONEX wind data on the prediction of monsoon depressions during June - August 1979 with two versions of primitive equation (PE) barotropic model p 56 N82-23900
SITNIKOVA, M. V
The use of satellite photographs to study snow-cover dynamics and to determine the average water discharge of the Amudarya during a vegetation period p 61 A82-35132
SKINNER, A. C.
Overseas Geology And Mineral Resources number 56 A geological interpretation of LANDSAT imagery and air photography of Botswana
[OGMR-56] p 42 N82-22636
SLINGO, J. M.
A study of the earth's radiation budget using a general circulation model p 52 A82-30666
SMALLWOOD, M. D.
The application of Heat Capacity Mapping Mission (HCMM) thermal data to snow hydrology
[E82-10191] p 62 N82-22625
SMIKA, D.
Evaluation of the Doraiswamy-Thompson winter wheat crop calendar model incorporating a modified spring restart sequence
[E82-10207] p 12 N82-23580
SMIRNOV, V. A.
Aerogeophysical methods of finding uranium deposits p 41 A82-33402
SMITH, H. J. P
Atmospheric ozone determination by solar occultation using the UV spectrometer on the Solar Maximum Mission p 27 A82-36362
SMITH, J A
Influence of sky radiance distribution on the ratio technique for estimating bidirectional reflectance p 70 A82-35650
SMITH, M.
Source assessment system
[AD-A111223] p 75 N82-25613
SMITH, R. E
Remote sensing of tornadic storms from geosynchronous satellite infrared digital data p 23 A82-32348
SMITH, W. L.
Surface temperature determination from an amalgamation of GOES and TIROS-N radiance measurements p 66 A82-28905
SOFIA, S.
Confinement and acceleration of cosmic rays in galactic superbubbles p 82 A82-22547
SOKOL, S.
Airborne lidar measurements of the Soufriere eruption of 17 April 1979 p 24 A82-33657
SOLOMON, J. L.
Application of remote sensing to state and regional problems
[E82-10288] p 30 N82-24566
SOMOGYI, A. J.
Spacecraft determination of energetic particle propagation parameters - The 1 January 1978 solar event p 31 A82-22598
SON, K. H
A preliminary comparison of the Magsat data and aeromagnetic data in the continental U S p 32 A82-30790
SOSNINA, E A.
Estimates of the statistical structure of the atmospheric pressure field in summer Monex-79 area p 57 N82-23939
SPAENKUCH, D.
Total ozone retrieval from satellite Meteor 28 Fourier spectrometer measurements p 28 A82-36422
SPALDING, J. D.
High resolution measurements of solar flare isotopes p 22 A82-22606
SPEECHLEY, G. C.
High resolution satellite observations of mesoscale oceanography in the Tasman Sea, 1978 - 1979
[E82-10324] p 57 N82-24597
STEFFENS, V
Spacecraft determination of energetic particle propagation parameters - The 1 January 1978 solar event p 31 A82-22598
STEINVALL, O.
Study visit to United States laser technology centers, 1981
[FOA-C-30257-E1] p 81 N82-24489
STEPHENS, S. A.
Dependence of earth spectrum of positrons and antiprotons on propagation models p 21 A82-22545
STEPINA, T. I.
The solar proton fluxes in April, 1979 p 66 A82-22597
The modulation characteristics of the 19th and 20th solar activity cycles p 59 A82-22615
STEWART, R H.
The observation of ocean surface phenomena using imagery from the Seasat synthetic aperture radar - An assessment p 52 A82-29623
STILES, J.
A simulation study of soil moisture estimation by a space SAR p 60 A82-29333
STILES, J. A.
The recognition of extended targets - SAR images for level and hilly terrain p 33 A82-31994
Evaluation of the soil moisture prediction accuracy of a space radar using simulation techniques
[E82-10351] p 19 N82-26749
STOFFEL, H
Derivation of the distribution of synchrotron emissivity in the Galaxy from the 408 MHz all-sky survey p 82 A82-22549
STOKER, P H.
Primary spectral variations of cosmic rays above 1 GV p 5 A82-22618
STOLPOVSKII, V G.
Energetic solar particle spectra according to Venera-11, 12 and Prognoz-5, 6 p 4 A82-22593
STONE, E C.
High resolution measurements of solar flare isotopes p 22 A82-22606
STOZHKOV, IU I.
The energy spectra of cosmic ray variations inferred from the stratospheric measurements in 1972-1979 p 5 A82-22617
STRAHLER, A H
The use of prior probabilities in maximum likelihood classification of remotely sensed data p 68 A82-32904
STUART, D. W.
Meteorological and aircraft data for CUE 2 1973
[PB82-149246] p 59 N82-26949
SUKHIKH, V I
Status and prospects of the automated processing of remote-sensing data /using forest surveys as an example/ p 10 A82-35139
SUKHOTIN, Y. V.
Cost-effectiveness of geographic surveying from space p 85 N82-24263
SUOMI, V. E.
The impact of meteorological satellites on the First GARP Global Experiment (FGGE) p 55 N82-23852
SVIRZHEVSKAIA, A K
The energy spectra of cosmic ray variations inferred from the stratospheric measurements in 1972-1979 p 5 A82-22617
SWAIN, P H
Key Issues in the Analysis of Remote Sensing Data A report on the workshop
[E82-10348] p 85 N82-26746
SWANSON, P.
Radiometer mission requirements for large space antenna systems
[NASA-TM-84478] p 81 N82-25610
SWEET, J. L.
SEASAT A satellite scatterometer illumination times of selected in situ sites
[NASA-TM-83280] p 81 N82-22865
SZENTGALI, A
Spacecraft determination of energetic particle propagation parameters - The 1 January 1978 solar event p 31 A82-22598

T

TAKACS, H. C
A comparison of stratified versus regression estimators p 11 N82-23133
TAKAGI, M
Aircraft measurements of NO/x/ in the lower troposphere above the coast of Japan p 26 A82-36247
TAKASHIMA, T.
Emissivity and reflectance of the model sea surface for the use of AVHRR data of NOAA satellites p 52 A82-31294
TAKAYAMA, Y.
Emissivity and reflectance of the model sea surface for the use of AVHRR data of NOAA satellites p 52 A82-31294
TAN, L. C.
The electron and positron spectra in primary cosmic rays p 1 A82-22543
Comparison of the measured antiproton flux with that predicted by the 'leaky box' model p 1 A82-22544
TANAKA, M.
Report of investigation from Japanese MAGSAT Team
[E82-10322] p 74 N82-24595

TANAKA, T.
Characteristics of field-aligned E-region irregularities over Ioka /36 N/, Japan I p 26 A82-36268
TANAKA, Y.
Detection of volcanic smoke and ash-fall area at volcano Aso, from Landsat MSS data p 23 A82-31295
TAPLEY, B. D.
The Seasat altimeter data and its accuracy assessment p 49 A82-29602
Evaluation of the Seasat altimeter time tag bias p 50 A82-29610
TAYLOR, M L.
Source assessment system [AD-A111223] p 75 N82-25613
TAYLOR, P A
On the application of a model of boundary-layer flow over low hills to real terrain p 29 A82-36741
TAYLOR, T. W.
A meteorologically driven maize stress indicator model [E82-10112] p 11 N82-23564
Evaluation of the Doraiswamy-Thompson winter wheat crop calendar model incorporating a modified spring restart sequence [E82-10207] p 12 N82-23580
A meteorologically driven grain sorghum stress indicator model [E82-10218] p 13 N82-23591
TELEKI, G
On reference coordinate systems used in polar motion determinations p 33 A82-32090
TEMNIKOV, S. N.
Evaluation of the accuracy of water-surface temperature measurement by means of airborne infrared radiometers p 62 A82-35136
THEIS, S. W.
Measurement of soil moisture trends with airborne scatterometers [E82-10361] p 20 N82-26759
Multifrequency remote sensing of soil moisture [E82-10362] p 20 N82-26760
Development of visible/infrared/microwave agriculture classification and biomass estimation algorithms [E82-10363] p 20 N82-26761
THELEN, B
Analysis of scanner data for crop inventories [E82-10192] p 10 N82-22626
THOMAS, H H.
Satellite and surface geophysical expression of anomalous crustal structure in Kentucky and Tennessee p 34 A82-34918
THOMAS, M. H. B.
The estimation of wave height from digitally processed SAR imagery p 67 A82-32347
THOMAS, R W L.
Bias correction procedures for airborne laser hydrography [PB82-130089] p 63 N82-22644
THOMPSON, D. M.
Comparing lineaments interpreted from Landsat imagery and topographic maps with reported faults in southwest Montana p 34 A82-34719
THOMPSON, T. W.
Seasat wind and wave observations of northeast Pacific hurricane Iva, August 13, 1978 p 52 A82-29624
THOMSEN, B.
Subtleties in the flat-fielding of charge-coupled device /CCD/ images p 68 A82-32581
THONY, J. L.
C-band radar for determining surface soil moisture p 10 A82-37194
TIMOSHENKO, A. M.
The use of space photographs in the mapping of glaciers and water bodies p 62 A82-37174
TOKAR, S.
Calculation of production rates of cosmogenic nuclides by Monte Carlo method p 64 A82-22576
TOLL, D. L.
Detecting residential land-use development at the urban fringe p 22 A82-29332
Preliminary evidence for the influence of physiography and scale upon the autocorrelation function of remotely sensed data p 67 A82-32343
TORSANI, J. A.
A study of atmospheric diffusion from the LANDSAT imagery [E82-10360] p 58 N82-26758
TRENCHARD, M. H.
Application of thermal model for pan evaporation to the hydrology of a defined medium, the sponge [E82-10217] p 13 N82-23590
TRIVEDI, N B.
Comparison of storm-time changes of geomagnetic field at ground and at MAGSAT altitudes, part 2 [E82-10325] p 30 N82-24598
Comparison of storm-time changes of geomagnetic field at ground and MAGSAT altitudes [E82-10359] p 30 N82-26757
TRIVEDI, S. S.
On the stellar origin of low energy cosmic rays p 21 A82-22567
Coulombian energy losses and the nuclear composition of the solar cosmic rays p 4 A82-22610
TSAREV, B. K.
The use of satellite photographs to study snow-cover dynamics and to determine the average water discharge of the Amudarya during a vegetation period p 61 A82-35132
TSEPELEV, A. V.
Space to the earth p 83 A82-30850
TSUCHIYA, K.
Detection of volcanic smoke and ash-fall area at volcano Aso, from Landsat MSS data p 23 A82-31295
TUCKER, C. J.
Remote sensing of leaf water content in the near infrared p 8 A82-32897
TUCKER, G. B
Mean sea-level pressure in the Southern Hemisphere during the FGGE period p 55 N82-23856
TULUPOV, V. I.
The approximate 1 GeV solar cosmic rays in the Forbush-effect of February 15, 1978 p 40 A82-22604
TUNHEIM, J. A.
Evaluation of HCMM data for assessing soil moisture and water table depth [E82-10329] p 18 N82-24602
TVEITEN, B.
Regional geological, tectonic and geophysical features of Nordland, Norway p 41 A82-30304
TYREN, C.
Magnetic anomalies as a reference for ground-speed and map-matching navigation p 32 A82-30314

U

ULABY, F. T.
A simulation study of soil moisture estimation by a space SAR p 60 A82-29333
Evaluation of the soil moisture prediction accuracy of a space radar using simulation techniques [E82-10351] p 19 N82-26749
ULBRICHT, K A.
Remote sensing in Scotland using data received from satellites - A study of the Tay Estuary region using Landsat multispectral scanning imagery p 62 A82-37501
UYEDA, S.
Report of investigation from Japanese MAGSAT Team [E82-10322] p 74 N82-24595

V

VALERIO, C.
A quantitative multispectral analysis system for aerial photographs applied to coastal planning p 55 A82-37505
VAN ROESSEL, J.
A new approach to multiresource inventories using remote sensing and geographic information systems technologies p 25 A82-34739
VAN ZEE, C J.
Estimating rangeland cover proportions with large-scale color-infrared aerial photographs p 6 A82-29534
VANCE, D. L.
Remote automatic weather station for resource and fire management agencies [PB82-107335] p 30 N82-23963
VANDERBILT, A. S.
Linear polarization of light by two wheat canopies measured at many view angles [E82-10229] p 14 N82-23602
VANDERBILT, V. C.
Spectral properties of agricultural crops and soils measured from space, aerial, field, and laboratory sensors [E82-10189] p 10 N82-22623
Diurnal changes in reflectance factor due to Sun-row direction interactions [E82-10128] p 11 N82-23566
Spectral properties of agricultural crops and soils measured from space, aerial, field, and laboratory sensors [E82-10212] p 12 N82-23585
Application of Computer Axial Tomography (CAT) to measuring crop canopy geometry [E82-10227] p 14 N82-23600
Linear polarization of light by two wheat canopies measured at many view angles [E82-10229] p 14 N82-23602
A model of plant canopy polarization [E82-10233] p 15 N82-23606
Canopy reflectance as influenced by solar illumination angle [E82-10237] p 15 N82-23610
VANIN, A. G.
Technical and economical characteristics of the AFA-TES-10M aerial camera p 79 A82-34470
VANWOERT, M L
Satellite observations in FRONTS 80 [AD-A111080] p 58 N82-26766
VASHENIUK, E V
On the physical sense of the constant of solar cosmic ray coronal propagation p 83 A82-22599
VAUCLIN, M
C-band radar for determining surface soil moisture p 10 A82-37194
VENKATESAN, T. R.
Is the neon composition of our sun, planetary or solar p 76 A82-22608
VENKATESWARAN, S. V.
Characteristics of field-aligned E-region irregularities over Ioka /36 N/, Japan I p 26 A82-36268
VERA, J. W.
Design guidelines for satellite image data distribution systems p 70 A82-37048
VESECKY, J. F.
The observation of ocean surface phenomena using imagery from the Seasat synthetic aperture radar - An assessment p 52 A82-29623
VIDAL-MADJAR, D.
C-band radar for determining surface soil moisture p 10 A82-37194
VISWANADHAM, Y.
A study of atmospheric diffusion from the LANDSAT imagery [E82-10360] p 58 N82-26758
VOGT, R. E.
High resolution measurements of solar flare isotopes p 22 A82-22606
VOLODICHEV, N. N
High-energy solar protons p 22 A82-22588
VON FRESE, R. R. B
Verification of the crustal component in satellite magnetic data p 32 A82-30789
A satellite magnetic model of northeastern South American aulacogens p 33 A82-30795
VON ROSENVINGE, T. T.
Interplanetary particle observations associated with solar flare gamma-ray line emission p 3 A82-22584
A survey of solar protons and alpha differential spectra between 1 and greater than 400 MeV/nucleon p 4 A82-22592
Heavy-element abundances in He/3/-rich events p 5 A82-22611
VONFRESE, R. R. B.
Study of gravity and magnetic anomalies using MAGSAT data [E82-10194] p 35 N82-22628
Spherical-Earth gravity and magnetic anomaly modeling by Gauss-Legendre quadrature integration [E82-10242] p 36 N82-24520
Magnetic and gravity anomalies in the Americas [E82-10312] p 37 N82-24586
Aeromagnetic and satellite magnetic anomaly mapping [E82-10339] p 39 N82-25601
VYSOKOOSTROVSKAIA, E. B.
Aerogeophysical methods of finding uranium deposits p 41 A82-33402

W

WAGNER, A. F
A description of relativistic solar particle propagation p 4 A82-22600
WALLIS, D. D.
Studies of high latitude current systems using MAGSAT vector data [E82-10188] p 71 N82-22622
WALMSLEY, J. L.
On the application of a model of boundary-layer flow over low hills to real terrain p 29 A82-36741
WALSH, E. J.
Pulse-to-pulse correlation in satellite radar altimeters p 55 A82-37390
WANG, J R
A multi-frequency radiometric measurement of soil moisture content over bare and vegetated fields [E82-10238] p 16 N82-23611
WARD, N. R.
Satellite observations of sea surface temperature around the British Isles p 54 A82-33717

WARREN, J. R.
Remote automatic weather station for resource and fire management agencies
[PB82-107335] p 30 N82-23963
WASILEWSKI, P J.
Satellite and surface geophysical expression of anomalous crustal structure in Kentucky and Tennessee p 34 A82-34918
WATERS, J. W.
Microwave measurement of stratospheric and mesospheric ozone p 28 A82-36415
WATSON, K.
Registration of Heat Capacity Mapping Mission day and night images
[E82-10210] p 72 N82-23583
Ground support data from July 10 to July 29, 1978, for HCMM thermal satellite data of the Powder River Basin, Wyoming
[E82-10211] p 72 N82-23584
Topographic slope correction for analysis of thermal infrared images
[E82-10214] p 36 N82-23587
Application of HCMM data to regional geologic analysis for mineral and energy resource evaluation
[E82-10153] p 45 N82-24518
Application of HCMM data to regional geologic analysis for mineral and energy resource evaluation
[E82-10243] p 45 N82-24521
WAY, D. S.
Site selection and engineering issues for a major industrial complex - Application of image and map interpretation p 25 A82-34711
WDOWCZYK, J
Origin of cosmic rays in galactic centre sources p 3 A82-22571
WEBB, G. M.
Cosmic ray acceleration by stellar winds I - Total density, pressure and energy flux p 21 A82-22566
WEBBER, W. R.
Fragmentation of Fe nuclei on carbon, hydrogen and CH2 targets I - Individual charge changing and total cross sections II - Isotopic cross sections p 63 A82-22538
The charge and isotopic composition of Z equals 7-16 cosmic ray nuclei at their source p 64 A82-22555
WEBER, F P.
Panoramic aerial photography in forest pest management p 7 A82-32701
WEDLER, E
Interpretation of vegetative cover in wetlands using four-channel SAR imagery p 9 A82-34706
WEEKS, W. F.
Sea-Ice Mission Requirements for the US FIREX and Canada RADARSAT programs
[NASA-CR-168984] p 57 N82-25609
WEFEL, J. P
The question of short pathlengths in interstellar propagation p 1 A82-22541
WEI, D
Observations and analyses of the total amount of atmospheric ozone in the Beijing region and in the region of Jolmolungma Mountain in Tibet p 28 A82-36444
WEISS, H.
Time and energy dependence of heavy ion abundances in solar flare energetic particle events p 22 A82-22605
Observations of the ionization states of energetic particles accelerated in solar flares p 40 A82-22607
WEISSMAN, D. E.
Seasat wind and wave observations of northeast Pacific hurricane Iva, August 13, 1978 p 52 A82-29624
WELCH, R.
Spatial resolution requirements for urban studies p 29 A82-37502
WELLMAN, J. B.
Multispectral mapper - Imaging spectroscopy as applied to the mapping of earth resources p 77 A82-32448
WEN, C.
Observations and analyses of the total amount of atmospheric ozone in the Beijing region and in the region of Jolmolungma Mountain in Tibet p 28 A82-36444
WENDLANDT, R F.
Influence of CO2 on melting of model granulite facies assemblages - A model for the genesis of charnockites p 42 A82-36298
WENTZ, F. J
The Seasat-A satellite scatterometer - The geophysical evaluation of remotely sensed wind vectors over the ocean p 51 A82-29616
The relationship between wind vector and normalized radar cross section used to derive Seasat-A Satellite Scatterometer winds p 51 A82-29617
Evaluation of atmospheric attenuation from SMMR brightness temperature for the Seasat satellite scatterometer p 51 A82-29618
Intercomparison of wind speeds inferred by the SASS, altimeter, and SMMR p 52 A82-29621
The effect of sea-surface Sun glitter on microwave radiometer measurements
[NASA-CR-169083] p 57 N82-26525
WENZEL, K.-P.
Non-flare injection of protons into interplanetary space p 4 A82-22601
WESELY, M. L.
Simplified techniques to study components of solar radiation under haze and clouds p 78 A82-32766
WEST, W L., III
Description of historical crop calendar data bases developed to support foreign commodity production forecasting project experiments
[E82-10209] p 12 N82-23582
Normal crop calendars Volume 3 The corn and soybean states of Illinois, Indiana, and Iowa
[E82-10221] p 13 N82-23594
WESTIN, F C
Evaluation of HCMM data for assessing soil moisture and water table depth
[E82-10329] p 18 N82-24602
WHITE, W. B.
Estimating mountain pine beetle-killed ponderosa pine over the front range of Colorado with high altitude panoramic photography p 7 A82-32704
WHITEHEAD, V.
Evaluation of NOAA-AVHRR data for crop assessment p 8 A82-34179
WHITNEY, L. F., JR.
A statistical approach to rainfall estimation using satellite and conventional data
[NOAA-TR-NESS-89] p 63 N82-22854
WHRITNER, R. H
Seasat altimeter determination of ocean current variability p 50 A82-29613
WIBBERENZ, G.
Spacecraft determination of energetic particle propagation parameters - The 1 January 1978 solar event p 31 A82-22598
WIEGAND, C. L.
AgRISTARS Early warning and crop condition assessment Plant cover, soil temperature, freeze, water stress, and evapotranspiration conditions
[E82-10225] p 14 N82-23598
WILES, K. G.
Effective electromagnetic shielding in multilayer printed circuit boards
[AIAA 81-2333] p 59 A82-13528
WILKERSON, J. C.
Surface wind analyses for Seasat p 51 A82-29619
WILLAND, J. H.
The application of Heat Capacity Mapping Mission (HCMM) thermal data to snow hydrology
[E82-10191] p 62 N82-22625
WILLIAMS, B. G.
Separation of diffuse from sharp-edged features in digital imagery p 68 A82-34225
WILLIAMS, T. H L.
Terrain analysis from Landsat using a color TV enhancement system p 68 A82-32911
WILLIAMSON, R. G.
Seasat altimeter timing bias estimation p 50 A82-29609
Gravity model improvement for Seasat p 32 A82-29615
WILLIE, R. D.
Mapping of wildlife habitat in Farmington Bay, Utah
[E82-10354] p 19 N82-26752
WILSON, M. D.
Studies of high latitude current systems using MAGSAT vector data
[E82-10188] p 71 N82-22622
WILSON, R. L.
Spherical harmonic representation of the main geomagnetic field for world charting and investigations of some fundamental problems of physics and geophysics
[E82-10203] p 72 N82-23576
WILSON, S. K.
Appearance of irregular tree canopies in nighttime high-resolution thermal infrared imagery p 68 A82-32916
WINANT, C. D.
Fluid-sediment interactions on beaches and shelves
[AD-A110838] p 59 N82-26948
WINTERBERGER, K. C.
Multi-resource inventory in interior Alaska p 6 A82-29532
WITTER, J. A.
Evaluation of spruce-fir forests using small-format photographs p 8 A82-32707
WOICESHYN, P M.
Surface wind analyses for Seasat p 51 A82-29619
WOLFENDALE, A. W
Origin of cosmic rays in galactic centre sources p 3 A82-22571
WON, I. J.
A preliminary comparison of the Magsat data and aeromagnetic data in the continental U S p 32 A82-30790
WONG, H. K.
Generation of the auroral kilometric radiation p 26 A82-35542
WOODEN, W. H., II
A comparison of pole positions derived from GPS satellite and Navy navigation satellite observations
[AD-A110765] p 39 N82-26268
WOODGATE, B.
Atmospheric ozone determination by solar occultation using the UV spectrometer on the Solar Maximum Mission p 27 A82-36362
WOODS, D. C
Fine particles in the Soufriere eruption plume p 24 A82-33659
WRIGHT, L. H.
Application of remote sensing to state and regional problems
[E82-10288] p 30 N82-24566
WU, C.
Ocean wave height measurement with SEASAT SAR using speckle diversity p 53 A82-32882
WU, C. S.
Generation of the auroral kilometric radiation p 26 A82-35542
WURTELE, M
Surface wind analyses for Seasat p 51 A82-29619
WYLIE, D. P.
Estimates of sea surface stress for summer MONEX from cloud motions p 56 N82-23910

Y

YAMAURA, Y
Detection of volcanic smoke and ash-fall area at volcano Aso, from Landsat MSS data p 23 A82-31295
YANAGISAWA, M.
Preliminary interpretation of magnetic anomalies over Japan and its surrounding area p 33 A82-30796
YANAGITA, S.
Unusual properties of particle events associated with solar flare gamma ray events p 65 A82-22585
The relation of type II radio bursts to solar energetic particles observed at earth p 3 A82-22591
YAO, S. S.
Evaluation of VICAR software capability for land information support system needs
[E82-10223] p 73 N82-23596
AgRISTARS Renewable resources inventory Land information support system implementation plan and schedule
[E82-10224] p 14 N82-23597
YOSHIMORI, M.
Model for solar hard X-ray bursts p 65 A82-22581
Solar gamma-ray experiment on Astro-A satellite p 21 A82-22583
YOUKHANA, S.
Influence of sky radiance distribution on the ratio technique for estimating bidirectional reflectance p 70 A82-35650
YUKUTAKE, T
Preliminary interpretation of magnetic anomalies over Japan and its surrounding area p 33 A82-30796
Report of investigation from Japanese MAGSAT Team
[E82-10322] p 74 N82-24595

Z

ZAITSEV, V. G.
Aerogeophysical methods of finding uranium deposits p 41 A82-33402
ZANDLO, J. A.
Surface temperature determination from an amalgamation of GOES and TIROS-N radiance measurements p 66 A82-28905
ZAVOLOKIN, IU. V.
The use of remote-sensing data to identify the space-time variability of the quality of natural waters p 62 A82-35138
ZELDOVICH, M A.
Low-energy particles in interplanetary magnetic field near the sectorial boundary on September 26, 1977 p 4 A82-22602
ZHENG, Q. A.
Determination of winter temperature patterns, fronts, and surface currents in the Yellow Sea and East China Sea from satellite imagery p 55 A82-37195
ZIELINSKI, J. B.
Origin and scale of coordinate systems in satellite geodesy p 34 A82-32099

ZUBOV, E. I.
Aerogeophysical methods of finding uranium deposits
p 41 A82-33402
ZUSMANOVICH, A. G.
11-year modulation and spectrum of cosmic rays in the interstellar space p 22 A82-22616

Typical Corporate Source Index Listing

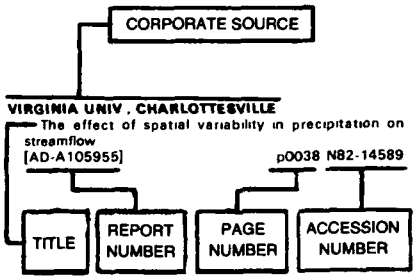

The title of the document is used to provide a brief description of the subject matter. The page number and the accession number are included in each entry to assist the user in locating the abstract in the abstract section. If applicable, a report number is also included as an aid in identifying the document.

A

Aerospace Corp , El Segundo, Calif.
Generation of the auroral kilometric radiation p 26 A82-35542
Soft X-rays from the sunlit earth's atmosphere p 29 A82-37405

Agricultural Research Services, Beltsville, Md.
Agricultural Research Service research highlights in remote sensing for calendar year 1980
[E82-10228] p 14 N82-23601

Alabama Univ., Huntsville.
Remote sensing of tornadic storms from geosynchronous satellite infrared digital data p 23 A82-32348

Alaska Univ., Fairbanks.
Generation of the auroral kilometric radiation p 26 A82-35542

All-Union Scientific Research Inst. of Hydrometeorological Information, Moscow (USSR)
Analysis of ocean and atmosphere thermodynamical characteristics during the onset of southwest monsoon over the Arabian Sea p 57 N82-23945

Analytic Sciences Corp., Reading, Mass.
Spatial resolution and repeatability of Magsat crustal anomaly data over the Indian Ocean p 32 A82-30788
Analyses of MAGSAT tracks crossing the study region in the Indian Ocean
[E82-10197] p 71 N82-23570
Bathymetric and tectonics of Indian Ocean using MAGSAT data
[E82-10204] p 36 N82-23577
Analyzing the Broken Ridge area of the Indian Ocean using magnetic and gravity anomaly maps and geoid undulation and bathymetry data
[E82-10303] p 36 N82-24577
Investigating tectonic and bathymetric features of the Indian Ocean using MAGSAT magnetic anomaly data
[E82-10304] p 37 N82-24578

Applied Physics Lab , Johns Hopkins Univ., Laurel, Md.
Investigation of MAGSAT and TRIAD magnetometer data to provide corrective information on high-latitude external fields
[E82-10201] p 72 N82-23574

Arizona State Univ., Tempe.
Bathymetric imaging p 69 A82-34720

Arizona Univ., Tucson
Observations of the ionization states of energetic particles accelerated in solar flares p 40 A82-22607

Army Cold Regions Research and Engineering Lab , Hanover, N. H.
Landsat digital analysis of the initial recovery of burned tundra at Kokolik River, Alaska p 8 A82-32913
Ice distribution and winter surface circulation patterns, Kachemak Bay, Alaska
[AD-A110806] p 58 N82-26764

Army Engineer Topographic Labs , Fort Belvoir, Va.
Coordination of stereo image registration and pixel classification
[AD-A111307] p 75 N82-25614

Atmospheric Environment Service, Downsview (Ontario).
Surface wind analyses for Seasat p 51 A82-29619

Australian 'cal Meteorology Research Center, Melbourne.
The onset of the Australian Northwest monsoon during winter MONEX Broadscale flow revealed by an objective analysis scheme p 56 N82-23912

B

Barringer Research Ltd., Rexdale (Ontario)
Breadboard gas filter correlation spectrometer for atmospheric measurement of hydrazines and nitrogen dioxide
[AD-A110688] p 82 N82-26642

Bell Telephone Labs., Inc., Holmdel, N. J
Evaluation of atmospheric attenuation from SMMR brightness temperature for the Seasat satellite scatterometer p 51 A82-29618

Bendix Field Engineering Corp , Grand Junction, Colo
Airborne gamma-ray spectrometer and magnetometer survey Roseau quadrangle, Minnesota, volume 1
[DE82-001031] p 43 N82-23621
NURE aerial gamma-ray and magnetic reconnaissance survey of portions of New Mexico, Arizona and Texas Volume 2 New Mexico-Carlsbad Quadrangle
[DE82-005527] p 48 N82-27810
Airborne gamma-ray spectrometer and magnetometer survey Susanville quadrangle, California, volume 1
[DE82-005538] p 48 N82-27811
Airborne gamma-ray spectrometer and magnetometer survey Roseburg quadrangle, Oregon, volume 2
[DE82-005568] p 48 N82-27812
Airborne gamma-ray spectrometer and magnetometer survey Huron Quadrangle, South Dakota
[DE82-005540] p 48 N82-27814
Airborne gamma-ray spectrometer and magnetometer survey Chico Quadrangle, California
[DE82-005543] p 48 N82-27815

Brigham Young Univ., Provo, Utah
HCMM hydrological analysis in Utah
[E82-10328] p 63 N82-24601

Brookhaven National Lab , Upton, N. Y.
Marine boundary layer wind structure over the Bay of Bengal during Monex-79 p 57 N82-23929

Brown Univ., Providence, R. I.
An investigation into the utilization of HCMM thermal data for the discrimination of volcanic and Eolian geological units
[E82-10352] p 47 N82-26750

Brunswick Corp., Costa Mesa, Calif.
Fine particles in the Soufriere eruption plume p 24 A82-33659

Bureau de Recherches Geologiques et Minieres, Minieres, Paris (France).
Spatial thermal radiometry contribution to the Massif Armoricain and the Massif Central France litho-structural study
[E82-10190] p 42 N82-22624

Business and Technological Systems, Inc., Seabrook, Md.
Application of satellite magnetic anomaly data to Curie isotherm mapping p 70 A82-35824
Equivalent source modeling of the main field using MAGSAT data
[E82-10151] p 71 N82-23567
MAGSAT science investigations
[E82-10199] p 71 N82-23572
An equivalent layer magnetization model for the United States derived from MAGSAT data
[E82-10297] p 36 N82-24573

C

California Inst. of Tech., Pasadena.
Laboratory studies of actinide metal-silicate fractionation p 49 A82-22306
High resolution measurements of solar flare isotopes p 22 A82-22606

California Univ., Berkeley. Lawrence Berkeley Lab.
Environmental monitoring report of the Lawrence Berkeley Laboratory, 1980
[LBL-12604] p 29 N82-23793

California Univ , La Jolla.
Seasat altimeter determination of ocean current variability p 50 A82-29613
The observation of ocean surface phenomena using imagery from the Seasat synthetic aperture radar - An assessment p 52 A82-29623

California Univ., Livermore Lawrence Livermore Lab
Seismic and geodetic studies of the Imperial Valley, California
[DE82-001686] p 39 N82-26915
Feasibility of laser-separation of 36 S and its use as an atmospheric tracer
[DE82-000965] p 30 N82-27737

California Univ., Los Angeles.
Surface wind analyses for Seasat p 51 A82-29619
Geoid height-age relation from Seasat altimeter profiles across the Mendocino Fracture Zone p 34 A82-32646

California Univ , Santa Barbara.
The use of prior probabilities in maximum likelihood classification of remotely sensed data p 68 A82-32904
Multispectral determination of soil moisture-2
[E82-10349] p 19 N82-26747
The use of soil texture and field capacity to normalize microwave soil moisture measurements Some problems p 20 N82-26762

Carson Helicopters, Inc., Perkasie, Pa.
NURE aerial gamma-ray and magnetic reconnaissance survey of portions of New Mexico, Arizona and Texas Volume 2 New Mexico-Carlsbad Quadrangle
[DE82-005527] p 48 N82-27810

Centre National d'Etudes Spatiales, Toulouse (France).
History of the French satellite space program p 85 N82-24216

Centre National de la Recherche Scientifique, Paris (France).
Representativeness of cloud motion winds deduced from GOES Indian Ocean satellite imagery for the description of the Indian summer monsoon p 55 N82-23879

Chicago Univ., Ill.
The question of short pathlengths in interstellar propagation p 1 A82-22541
Unusual properties of particle events associated with solar flare gamma ray events p 65 A82-22585
The relation of type II radio bursts to solar energetic particles observed at earth p 3 A82-22591
Observations of the ionization states of energetic particles accelerated in solar flares p 40 A82-22607

City Coll. of the City Univ. of New York.
Surface wind analyses for Seasat p 51 A82-29619

City Univ of New York, N. Y.
The Seasat-A satellite scatterometer - The geophysical evaluation of remotely sensed wind vectors over the ocean p 51 A82-29616
The relationship between wind vector and normalized radar cross section used to derive Seasat-A Satellite Scatterometer winds p 51 A82-29617

Colorado State Univ , Fort Collins.
Influence of sky radiance distribution on the ratio technique for estimating bidirectional reflectance p 70 A82-35650

SOURCE

Colorado Univ., Boulder.
Investigation of geomagnetic field forecasting and fluid dynamics of the core
[E82-10198] p 35 N82-23571
Investigation of geomagnetic field forecasting and fluid dynamics of the core
[E82-10310] p 37 N82-24584
Investigation of geomagnetic field forecasting and fluid dynamics of the core
[E82-10342] p 39 N82-25604
Columbia Univ., New York.
High spectral resolution airborne spectrometry p 77 A82-32443
Longwave infrared observation of urban landscapes p 25 A82-34744
Committee on Science and Technology (U S House)
Civil land remote sensing system
[GPO-87-070] p 84 N82-22630
Commonwealth Scientific and Industrial Research Organization, Mordialoc (Australia)
Mean sea-level pressure in the Southern Hemisphere during the FGGE period p 55 N82-23856
Comptroller General of the United States, Washington, D.C.
Streamlining and ensuring mineral development must begin at local land management levels
[EMD-82-10] p 29 N82-23043
Computer Sciences Corp , Silver Spring, Md
Remote sensing of precipitable water over the oceans from Nimbus 7 microwave measurements p 49 A82-28907
Initial scalar magnetic anomaly map from Magsat p 32 A82-30784
Initial vector magnetic anomaly map from Magsat p 32 A82-30785
Preliminary evidence for the influence of physiography and scale upon the autocorrelation function of remotely sensed data p 67 A82-32343
Consiglio Nazionale delle Ricerche, Naples (Italy).
Crustal structures under the active volcanic areas of central and eastern Mediterranean (M-44)
[E82-10096] p 35 N82-23563
Cornell Univ , Ithaca, N. Y.
Landsat detection of hardwood forest clearcuts p 8 A82-32708

D

Defence Science and Technology Organisation, Edgecliff (Australia).
High resolution satellite observations of mesoscale oceanography in the Tasman Sea, 1978 - 1979
[E82-10324] p 57 N82-24597
Defense Mapping Agency Aerospace Center, St. Louis, Mo.
Matrix data analysis Color/B and W coding is not always enough
[AD-A111401] p 74 N82-25612
***Defense Mapping Agency Hydrographic and* Topographic Center, Washington, D.C.**
A comparison of pole positions derived from GPS satellite and Navy navigation satellite observations
[AD-A110765] p 39 N82-26268
Department of Agriculture, Houston, Tex
Evaluation of the Doraiswamy-Thompson winter wheat crop calendar model incorporating a modified spring restart sequence
[E82-10207] p 12 N82-23580

E

Earth Satellite Corp., Washington, D. C
Use of NOAA/AVHRR visible and near-infrared data for land remote sensing
[NASA-TM-84186] p 81 N82-22643
Experimental assessment of improved spatial resolution LANDSAT data
[AD-A110538] p 75 N82-26765
Environmental Research and Technology, Inc., Concord, Mass.
The application of Heat Capacity Mapping Mission (HCMM) thermal data to snow hydrology
[E82-10191] p 62 N82-22625
Environmental Research Inst. of Michigan, Ann Arbor.
Analysis of scanner data for crop inventories
[E82-10192] p 10 N82-22626
LANDSAT technology transfer to the private and public sectors through community colleges and other locally available institutions
[E82-10181] p 85 N82-23568
Analysis of scanner data for crop inventories
[E82-10241] p 16 N82-24519
Association of spectral development patterns with development stages of corn
[E82-10353] p 19 N82-26751
Environmental Systems Research Inst., Redlands, Calif
Exploration into technical procedures for vertical integration
[NASA-CR-166352] p 75 N82-26763
European Space Agency, Toulouse (France).
The METEOSAT Data Collection System and its application p 75 N82-26037
Evangel Coll., Springfield, Mo.
Use of LANDSAT data to define soil boundaries in Carroll County, Missouri p 10 N82-23116
EG & G Washington Analytical Services Center, Inc., Riverdale, Md
Seasat altimeter height calibration p 49 A82-29603
Seasat altimeter timing bias estimation p 50 A82-29609
The Seasat altimeter mean sea surface model p 51 A82-29614
Gravity model improvement for Seasat p 32 A82-29615
EG and G Washington Analytical Services Center, Inc., Rockville, Md.
Bias correction procedures for airborne laser hydrography
[PB82-130089] p 63 N82-22644

F

Florida Dept of Transportation, Tallahassee.
Effects of altitude, focal length, and filter combinations on color infrared photography of citrus groves p 9 A82-34729
Florida State Univ., Tallahassee
Meteorological and aircraft data for CUE 2 1973
[PB82-149246] p 59 N82-26949
Florida Univ., Gainesville.
Use of thermal inertia determined by HCMM to predict nocturnal cold prone areas in Florida
[E82-10299] p 17 N82-24575
Florida Univ., Lake Alfred.
Detection and damage assessment of citrus tree losses with aerial color infrared photography /ACIR/ p 7 A82-29538
Effects of altitude, focal length, and filter combinations on color infrared photography of citrus groves p 9 A82-34729

G

General Electric Co., Philadelphia, Pa.
The Seasat-A satellite scatterometer - The geophysical evaluation of remotely sensed wind vectors over the ocean p 51 A82-29616
General Software Corp., Landover, Md.
LANDSAT-D conical scanner evaluation plan
[E82-10340] p 81 N82-25602
Geological Survey, Denver, Colo.
Registration of Heat Capacity Mapping Mission day and night images
[E82-10210] p 72 N82-23583
Ground support data from July 10 to July 29, 1978, for HCMM thermal satellite data of the Powder River Basin, Wyoming
[E82-10211] p 72 N82-23584
Topographic slope correction for analysis of thermal infrared images
[E82-10214] p 36 N82-23587
Application of HCMM data to regional geologic analysis for mineral and energy resource evaluation
[E82-10153] p 45 N82-24518
Application of HCMM data to regional geologic analysis for mineral and energy resource evaluation
[E82-10243] p 45 N82-24521
Geological Survey, Reston, Va.
Initial scalar magnetic anomaly map from Magsat p 32 A82-30784
Initial vector magnetic anomaly map from Magsat p 32 A82-30785
George Mason Univ., Fairfax, Va.
Confinement and acceleration of cosmic rays in galactic superbubbles p 82 A82-22547

H

Herzberg Inst. of Astrophysics, Ottawa (Ontario)
Studies of high latitude current systems using MAGSAT vector data
[E82-10188] p 71 N82-22622
High Life Helicopters, Inc , Puyallup, Wash
Airborne gamma-ray spectrometer and magnetometer survey, Toronto quadrangle New York, volume 2A
[DE81-027158] p 46 N82-25620
Airborne gamma-ray spectrometer and magnetometer survey, Kingston quadrangle New York, volume 2C
[DE81-027161] p 46 N82-25621
Airborne gamma-ray spectrometer and magnetometer survey, Rochester quadrangle New York, volume 2D
[DE81-027156] p 46 N82-25622
Hofstra Univ., Hempstead, N. Y.
Seasat wind and wave observations of northeast Pacific hurricane Iva, August 13, 1978 p 52 A82-29624

I

Indian Inst. of Geomagnetism, Bombay
MAGSAT for geomagnetic studies over Indian region
[E82-10202] p 72 N82-23575
MAGSAT for geomagnetic studies over Indian region
[E82-10296] p 73 N82-24572
Indian Inst of Tropical Meteorology, Poona
Impact of additional summer MONEX wind data on the prediction of monsoon depressions during June - August 1979 with two versions of primitive equation (PE) barotropic model p 56 N82-23900
Institute of Geological Sciences, Edinburgh (Scotland).
Spherical harmonic representation of the main geomagnetic field for world charting and investigations of some fundamental problems of physics and geophysics
[E82-10203] p 72 N82-23576
Institute of Oceanographic Sciences, Wormley (England).
Surface wind analyses for Seasat p 51 A82-29619
Instituto de Pesquisas Espaciais, Sao Jose dos Campos (Brazil).
Dynamic study of the upper Sao Francisco river and Tres Marias reservoir using MSS/LANDSAT images
[E82-10291] p 63 N82-24569
Comparison of storm-time changes of geomagnetic field at ground and at MAGSAT altitudes, part 2
[E82-10325] p 30 N82-24598
SMS/GOES data collection platform system p 75 N82-26027
Comparison of storm-time changes of geomagnetic field at ground and MAGSAT altitudes
[E82-10359] p 30 N82-26757
A study of atmospheric diffusion from the LANDSAT imagery
[E82-10360] p 58 N82-26758
Instituto Geografico Nacional, Madrid (Spain).
Thermal mapping, geothermal source location, natural effluents and plant stress in the Mediterranean coast of Spain
[E82-10300] p 17 N82-24576
***Intermountain Forest and Range Experiment Station,* Ogden, Utah.**
Remote automatic weather station for resource and fire management agencies
[PB82-107335] p 30 N82-23963
Iowa Univ., Iowa City
Use of MAGSAT anomaly data for crustal structure and mineral resources in the US Midcontinent
[E82-10321] p 46 N82-24594
Use of MAGSAT anomaly data for crustal structure and mineral resources in the US Midcontinent
[E82-10323] p 46 N82-24596

J

***Jet Propulsion Lab., California Inst of Tech.,* Pasadena.**
A color-ratio map of Mercury p 31 A82-22294
Seasat measurement system evaluation - Achievements and limitations p 49 A82-29601
The Seasat altimeter data and its accuracy assessment p 49 A82-29602
An empirical determination of the effects of sea state bias on Seasat altimetry p 50 A82-29607
Seasat altimeter determination of ocean current variability p 50 A82-29613
The Seasat-A satellite scatterometer - The geophysical evaluation of remotely sensed wind vectors over the ocean p 51 A82-29616
The relationship between wind vector and normalized radar cross section used to derive Seasat-A Satellite Scatterometer winds p 51 A82-29617
Surface wind analyses for Seasat p 51 A82-29619
Description of Seasat radiometer status and results p 52 A82-29622
The observation of ocean surface phenomena using imagery from the Seasat synthetic aperture radar - An assessment p 52 A82-29623

Seasat wind and wave observations of northeast Pacific hurricane Iva, August 13, 1978 p 52 A82-29624
Resource inventory techniques used in the California Desert Conservation Area p 23 A82-32441
Spectroscopic remote sensing for geological applications p 41 A82-32442
Multispectral mapper - Imaging spectroscopy as applied to the mapping of earth resources p 77 A82-32448
Ocean wave height measurement with SEASAT SAR using speckle diversity p 53 A82-32882
Bathymetric imaging p 69 A82-34720
Improved land use classification from Landsat and Seasat satellite imagery registered to a common map base p 25 A82-34743
Microwave measurement of stratospheric and mesospheric ozone p 28 A82-36415
Sea-Ice Mission Requirements for the US FIREX and Canada RADARSAT programs
[NASA-CR-168984] p 57 N82-25609

Joint Inst for Lab. Astrophysics, Boulder, Colo.
Establishment of terrestrial reference frames by new observational techniques p 33 A82-32078

Joint Publications Research Service, Arlington, Va.
Cost-effectiveness of geographic surveying from space p 85 N82-24263
Purpose, background of 'Intercosmos-21' mission p 81 N82-24264

K

Kansas Univ. Center for Research, Inc , Lawrence.
The Seasat-A satellite scatterometer - The geophysical evaluation of remotely sensed wind vectors over the ocean p 51 A82-29616
The relationship between wind vector and normalized radar cross section used to derive Seasat-A Satellite Scatterometer winds p 51 A82-29617
Evaluation of atmospheric attenuation from SMMR brightness temperature for the Seasat satellite scatterometer p 51 A82-29618
The recognition of extended targets - SAR images for level and hilly terrain p 33 A82-31994
Evaluation of the soil moisture prediction accuracy of a space radar using simulation techniques
[E82-10351] p 19 N82-26749

L

Lincoln Lab., Mass. Inst. of Tech , Lexington.
Detection of regional air pollution episodes utilizing satellite digital data in the visual range p 23 A82-31990

Liverpool Univ. (England).
System albedo as sensed by satellites - Its definition and variability p 23 A82-32342

Lockheed Engineering and Management Services Co., Inc., Houston, Tex.
Evaluation of NOAA-AVHRR data for crop assessment p 8 A82-34179
Ten-Ecosystem Study
[E82-10186] p 84 N82-22620
AgRISTARS Foreign commodity production forecasting The 1980 US/Canada wheat and barley exploratory experiment
[E82-10126] p 11 N82-23565
AgRISTARS Foreign commodity production forecasting The 1980 US corn and soybeans exploratory experiment
[E82-10206] p 11 N82-23579
AgRISTARS Supporting research Spring small grains planting date distribution model
[E82-10208] p 12 N82-23581
Description of historical crop calendar data bases developed to support foreign commodity production forecasting project experiments
[E82-10209] p 12 N82-23582
Application of thermal model for pan evaporation to the hydrology of a defined medium, the sponge
[E82-10217] p 13 N82-23590
Normal crop calendars Volume 3 The corn and soybean states of Illinois, Indiana, and Iowa
[E82-10221] p 13 N82-23594
Selection of the Australian indicator region
[E82-10222] p 13 N82-23595
Evaluation of VICAR software capability for land information support system needs
[E82-10223] p 73 N82-23596
AgRISTARS Renewable resources inventory Land information support system implementation plan and schedule
[E82-10224] p 14 N82-23597
Evaluation of the procedure for separating barley from other spring small grains
[E82-10230] p 14 N82-23603
Use and applicability of the vegetation component of the national site classification system
[E82-10234] p 15 N82-23607
Description of the FORTRAN implementation of the spring small grains planting date distribution model
[E82-10235] p 15 N82-23608

Lowell Observatory, Flagstaff, Ariz.
Subtleties in the flat-fielding of charge-coupled device /CCD/ images p 68 A82-32581

Lunar and Planetary Inst., Houston, Tex.
Influence of CO2 on melting of model granulite facies assemblages - A model for the genesis of charnockites p 42 A82-36298

M

Main Geophysical Observatory, Leningrad (USSR).
Estimates of the statistical structure of the atmospheric pressure field in summer Monex-79 area p 57 N82-23939

Maryland Univ., College Park.
Observations of interplanetary energetic charged particles from gamma-ray line solar flares p 65 A82-22586
A survey of solar protons and alpha differential spectra between 1 and greater than 400 MeV/nucleon p 4 A82-22592
Time and energy dependence of heavy ion abundances in solar flare energetic particle events p 22 A82-22605
Observations of the ionization states of energetic particles accelerated in solar flares p 40 A82-22607
A comparison of helium and heavy ion spectra in He/3/ rich solar flares with a model calculation p 5 A82-22612
On the anticorrelation between the He/3//He/4/ ratio and proton intensity in He/3/ rich flares p 40 A82-22613
Generation of the auroral kilometric radiation p 26 A82-35542

Massachusetts Inst of Tech., Cambridge.
Inversion of data from diffraction-limited multiwavelength remote sensors II - Nonlinear dependence of observables on the geophysical parameters p 77 A82-32658

Massachusetts Univ., Amherst.
The mineralogy of global magnetic anomalies
[E82-10305] p 45 N82-24579
Stratospheric emission data analysis
[AD-A112337] p 76 N82-26907

Max-Planck-Institut fuer Extraterrestrische Physik, Garching (West Germany)
Observations of interplanetary energetic charged particles from gamma-ray line solar flares p 65 A82-22586
Observations of the ionization states of energetic particles accelerated in solar flares p 40 A82-22607

Max-Planck-Institut fuer Physik und Astrophysik, Garching (West Germany)
Time and energy dependence of heavy ion abundances in solar flare energetic particle events p 22 A82-22605
A comparison of helium and heavy ion spectra in He/3/ rich solar flares with a model calculation p 5 A82-22612

Measurement Concept Corp , Rome, N. Y.
Source assessment system
[AD-A111223] p 75 N82-25613

Miami Univ., Fla.
Investigations of medium wavelength magnetic anomalies in the eastern Pacific using MAGSAT
[E82-10240] p 73 N82-23613
MONEX oceanographic observations along the East African coast p 56 N82-23908
Investigations of medium wavelength magnetic anomalies in the eastern Pacific using MAGSAT data
[E82-10330] p 38 N82-24603

Minnesota Univ., St. Paul.
Application of scanning microdensitometer data in selected plant science case studies p 7 A82-29539

Mississippi State Univ., Mississippi State.
Application of remote sensing to state and regional problems
[E82-10288] p 30 N82-24566

Mississippi State Univ., State College.
A comparison of stratified versus regression estimators p 11 N82-23133

Morgan State Coll., Baltimore, Md.
Relating thematic mapper bands TM3, TM4, and TM5 to agronomic variables for corn, cotton, sugarbeet, soybean, sorghum, sunflower and tobacco
[E82-10347] p 19 N82-26745

N

National Academy of Sciences - National Research Council, Washington, D C.
Geodetic monitoring of tectonic information Toward a strategy p 35 N82-22832
Geodetic monitoring of tectonic deformation Toward a strategy
[NASA-CR-168784] p 35 N82-22846

National Aeronautics and Space Administration. Ames Research Center, Moffett Field, Calif.
Airborne observed solar elevation and row direction effects on the near-IR/red ratio of cotton
[E82-10220] p 13 N82-23593
Multilevel measurements of surface temperature over undulating terrain planted to barley
[E82-10245] p 16 N82-24523

National Aeronautics and Space Administration. Earth Resources Labs , Bay St. Louis, Miss.
Development of three-dimensional spatial displays using a geographically based information system p 66 A82-29326

National Aeronautics and Space Administration. Goddard Inst. for Space Studies, New York.
System albedo as sensed by satellites - Its definition and variability p 23 A82-32342
Longwave infrared observation of urban landscapes p 25 A82-34744

National Aeronautics and Space Administration. Goddard Space Flight Center, Greenbelt, Md.
The cosmic ray positron spectrum p 1 A82-22542
Confinement and acceleration of cosmic rays in galactic superbubbles p 82 A82-22547
Interplanetary particle observations associated with solar flare gamma-ray line emission p 3 A82-22584
A survey of solar protons and alpha differential spectra between 1 and greater than 400 MeV/nucleon p 4 A82-22592
Heavy-element abundances in He/3/-rich events p 5 A82-22611
Remote sensing of precipitable water over the oceans from Nimbus 7 microwave measurements p 49 A82-28907
Detecting residential land-use development at the urban fringe p 22 A82-29332
Seasat altimeter height calibration p 49 A82-29603
Seasat altimeter timing bias estimation p 50 A82-29609
Comparison data for Seasat altimetry in the western North Atlantic p 50 A82-29611
The Seasat altimeter mean sea surface model p 51 A82-29614
Gravity model improvement for Seasat p 32 A82-29615
Initial scalar magnetic anomaly map from Magsat p 32 A82-30784
Initial vector magnetic anomaly map from Magsat p 32 A82-30785
Magsat scalar anomaly distribution - The global perspective p 41 A82-30786
Retrieval of ocean surface and atmospheric parameters from multichannel microwave radiometric measurements p 53 A82-31995
Preliminary evidence for the influence of physiography and scale upon the autocorrelation function of remotely sensed data p 67 A82-32343
Evaluation of temporal registration of Landsat scenes p 67 A82-32345
Remote sensing of leaf water content in the near infrared p 8 A82-32897
Effects of vegetation canopy structure on remotely sensed canopy temperatures p 8 A82-32905
A comparative study of microwave radiometer observations over snowfields with radiative transfer model calculations p 60 A82-32910
Landsat digital analysis of the initial recovery of burned tundra at Kokolik River, Alaska p 8 A82-32913
View angle effects in the radiometric measurement of plant canopy temperatures p 8 A82-32914
Snowpack monitoring in North America and Eurasia using passive microwave satellite data p 78 A82-32915
The use of Landsat-3 thermal data to help differentiate land covers p 25 A82-34218
Irradiance measurement errors due to the assumption of a Lambertian reference panel p 79 A82-34222
Landsat in the search for Appalachian hydrocarbons p 42 A82-34721
Defining the temporal window for monitoring forest canopy defoliation using Landsat p 9 A82-34730
Use of aerial photography in determining land use and streamflow relationships on small developing watersheds p 60 A82-34736
Satellite and surface geophysical expression of anomalous crustal structure in Kentucky and Tennessee p 34 A82-34918

Influence of sky radiance distribution on the ratio technique for estimating bidirectional reflectance p 70 A82-35650

Total ozone variations 1970-74 using Backscattered Ultraviolet /BUV/ and ground-based observations p 26 A82-36053

Atmospheric ozone determination by solar occultation using the UV spectrometer on the Solar Maximum Mission p 27 A82-36362

The seasonal variations of ozone and temperature in the middle and the upper stratosphere p 29 A82-36534

Advanced technology for earth observation - Data processing
[AAS PAPER 82-130] p 71 A82-37810

Solid state instrumentation concepts for earth resource observation
[AAS PAPER 82-132] p 81 A82-37812

Information theory lateral density distribution for earth inferred from global gravity field p 35 A82-37962

Use of NOAA/AVHRR visible and near-infrared data for land remote sensing
[NASA-TM-84186] p 81 N82-22643

A multi-frequency radiometric measurement of soil moisture content over bare and vegetated fields
[E82-10238] p 16 N82-23611

The influence of autocorrelation in signature extraction An example from a geobotanical investigation of Cotter Basin, Montana
[E82-10341] p 46 N82-25603

National Aeronautics and Space Administration. John F. Kennedy Space Center, Cocoa Beach, Fla

Detection and damage assessment of citrus tree losses with aerial color infrared photography /ACIR/ p 7 A82-29538

Effects of altitude, focal length, and filter combinations on color infrared photography of citrus groves p 9 A82-34729

National Aeronautics and Space Administration Langley Research Center, Hampton, Va.

The Seasat-A satellite scatterometer - The geophysical evaluation of remotely sensed wind vectors over the ocean p 51 A82-29616

The relationship between wind vector and normalized radar cross section used to derive Seasat-A Satellite Scatterometer winds p 51 A82-29617

Evaluation of atmospheric attenuation from SMMR brightness temperature for the Seasat satellite scatterometer p 51 A82-29618

Depression of brightness temperature of sea surfaces covered with monomolecular oil films relative to clean water surfaces at 1 43 GHz p 54 A82-33322

Characteristics of 13 9 GHz radar scattering from oil films on the sea surface p 54 A82-33438

Airborne lidar measurements of the Soufriere eruption of 17 April 1979 p 24 A82-33657

Fine particles in the Soufriere eruption plume p 24 A82-33659

Tropospheric CO measurement experiment from the second Space Shuttle flight p 27 A82-36292

Ammonia and the NOx budget of the troposphere p 27 A82-36293

SEASAT A satellite scatterometer illumination times of selected in situ sites
[NASA-TM-83280] p 81 N82-22865

Analysis of ocean color scanner data from the Superflux III Experiment
[NASA-TM-83290] p 55 N82-23614

Radiometer mission requirements for large space antenna systems
[NASA-TM-84478] p 81 N82-25610

In situ ozone data for comparison with laser absorption remote sensor 1980 PEPE/NEROS program
[NASA-TM-84471] p 30 N82-25661

National Aeronautics and Space Administration. Lyndon B. Johnson Space Center, Houston, Tex.

Field size, length, and width distributions based on LACIE ground truth data p 8 A82-32909

A meteorologically driven maize stress indicator model
[E82-10112] p 11 N82-23564

AgRISTARS Preliminary technical results review of FY81 experiments, volume 2 Fiscal year 1981/1982 'corn and soybeans pilot' experiment
[E82-10216] p 13 N82-23589

A meteorologically driven grain sorghum stress indicator model
[E82-10218] p 13 N82-23591

AgRISTARS Project management report Program review presentation to level 1, interagency coordination committee
[E82-10219] p 13 N82-23592

AgRISTARS Project management report Program review presentation to level 1, interagency coordination committee
[E82-10231] p 15 N82-23604

AgRISTARS Agriculture and resources inventory surveys through aerospace remote sensing
[E82-10236] p 15 N82-23609

National Aeronautics and Space Administration Marshall Space Flight Center, Huntsville, Ala.

Remote sensing of tornadic storms from geosynchronous satellite infrared digital data p 23 A82-32348

National Aeronautics and Space Administration. National Space Technology Labs , Bay Saint Louis, Miss.

An analysis of LANDSAT MSS scene-to-scene registration accuracy
[E82-10285] p 16 N82-24563

An algorithm for automating the registration of USDA segment ground data to LANDSAT MSS data
[E82-10286] p 16 N82-24564

Analysis of thematic mapper simulator data acquired during winter season over Pearl River, Mississippi, test site
[E82-10287] p 17 N82-24565

National Aeronautics and Space Administration Wallops Flight Center, Wallops Island, Va.

Sea-state-related altitude errors in the Seasat radar altimeter p 50 A82-29608

Pulse-to-pulse correlation in satellite radar altimeters p 55 A82-37390

National Aeronautics and Space Administration, Washington, D. C.

OSTA-1 Post Mission Operation Report
[NASA-TM-84191] p 84 N82-23258

Plan of research for integrated soil moisture studies Recommendations of the Soil Moisture Working Group
[NASA-TM-84731] p 18 N82-25608

LANDSAT D to test thematic mapper, inaugurate operational system
[NASA-NEWS-RELEASE-82-100] p 82 N82-26741

National Bureau of Standards, Boulder, Colo.

Establishment of terrestrial reference frames by new observational techniques p 33 A82-32078

National Conference of State Legislatures, Denver, Colo.

A legislator's guide to LANDSAT
[E82-10290] p 85 N82-24568

National Meteorological Center, Washington, D. C.

Total ozone variations 1970-74 using Backscattered Ultraviolet /BUV/ and ground-based observations p 26 A82-36053

Short term influence radius of monsoonal overturnings p 56 N82-23898

National Oceanic and Atmospheric Administration, Bay St Louis, Miss

Surface wind analyses for Seasat p 51 A82-29619

National Oceanic and Atmospheric Administration, Boulder, Colo

Intercomparison of wind speeds inferred by the SASS, altimeter, and SMMR p 52 A82-29621

Field measurements in support of dispersion modeling in complex terrain (1980)
[PB82-148644] p 39 N82-27882

National Oceanic and Atmospheric Administration, Rockville, Md.

Bias correction procedures for airborne laser hydrography
[PB82-130089] p 63 N82-22644

A statistical approach to rainfall estimation using satellite and conventional data
[NOAA-TR-NESS-89] p 63 N82-22854

National Oceanic and Atmospheric Administration, Seattle, Wash

Surface wind analyses for Seasat p 51 A82-29619

Seasat wind and wave observations of northeast Pacific hurricane Iva, August 13, 1978 p 52 A82-29624

National Oceanic and Atmospheric Administration, Washington, D. C

Comparison of satellite derived radiation budget measurements over MONEX during 1979 to 1980 p 29 N82-23891

National Weather Service, Fort Worth, Tex

Some empirical rules for forecasting fog and status over northern Florida, southern Georgia and adjacent coastal waters
[PB82-154006] p 59 N82-27949

Natural Environment Research Council, London (England).

Overseas Geology And Mineral Resources number 56 A geological interpretation of LANDSAT imagery and air photography of Botswana
[OGMR-56] p 42 N82-22636

Naval Physical and Oceanographic Lab , Cochin (India).

On the space-time variability of ocean surface mixed layer characteristics of central and eastern Arabian sea during MONSOON-77 p 56 N82-23909

Naval Postgraduate School, Monterey, Calif.

Rapid oceanographic data gathering Some problems in using remote sensing to determine the horizontal and vertical thermal distributions in the Northeast Pacific Ocean
[AD-A111005] p 58 N82-26945

New Hampshire Univ , Durham.

Fragmentation of Fe nuclei on carbon, hydrogen and CH2 targets I - Individual charge changing and total cross sections II - Isotopic cross sections p 63 A82-22538

The charge and isotopic composition of Z equals 7-16 cosmic ray nuclei at their source p 64 A82-22555

Observations of the ionization states of energetic particles accelerated in solar flares p 40 A82-22607

New York State Univ , Syracuse.

Evaluation of NOAA-AVHRR data for crop assessment p 8 A82-34179

North Carolina State Coll., Raleigh.

A preliminary comparison of the Magsat data and aeromagnetic data in the continental U S p 32 A82-30790

North Carolina State Univ., Raleigh

MAGSAT and aeromagnetic data in the North American continent
[E82-10193] p 71 N82-22627

MAGSAT scalar and vector anomaly data analysis
[E82-10307] p 74 N82-24581

O

Ocean Weather, Inc., White Plains, N.Y.

Surface wind analyses for Seasat p 51 A82-29619

Intercomparison of wind speeds inferred by the SASS, altimeter, and SMMR p 52 A82-29621

Office of Technology Assessment, Washington, D. C

Technology and oceanography An assessment of Federal technologies for oceanographic research and monitoring Volume 2 Working papers on fishery research technology p 58 N82-26944

Ohio State Univ., Columbus

Reference coordinate systems for earth dynamics - A preview p 33 A82-32077

The Earth's gravity field to degree and order 180 using SEASAT altimeter data, terrestrial gravity data and other data
[AD-A113098] p 40 N82-27900

OAO Corp , Beltsville, Md.

LANDSAT-D thermal analysis and design support
[E82-10346] p 82 N82-26744

P

Paris VI Univ. (France).

MAGSAT anomaly map and continental drift
[E82-10326] p 38 N82-24599

Models and maps of the main field
[E82-10327] p 74 N82-24600

Pennsylvania State Univ , University Park.

Delineation of soil temperature regimes from HCMM data
[E82-10298] p 17 N82-24574

A method for inferring available surface moisture using remote surface temperature measurements An assessment
[E82-10311] p 17 N82-24585

Interactive initialization of heat flux parameters for numerical models using satellite temperature measurements
[E82-10313] p 82 N82-26743

Phoenix Corp., McLean, Va

Improved definition of crustal magnetic anomalies for MAGSAT data
[E82-10314] p 37 N82-24587

Pittsburg Univ., Pa

A color-ratio map of Mercury p 31 A82-22294

Planetary Science Inst., Pasadena, Calif.

Seasat wind and wave observations of northeast Pacific hurricane Iva, August 13, 1978 p 52 A82-29624

Purdue Univ., Lafayette, Ind.

Verification of the crustal component in satellite magnetic data p 32 A82-30789

A satellite magnetic model of northeastern South American aulacogens p 33 A82-30795

Spectral properties of agricultural crops and soils measured from space, aerial, field, and laboratory sensors
[E82-10189] p 10 N82-22623

Study of gravity and magnetic anomalies using MAGSAT data
[E82-10194] p 35 N82-22628

Diurnal changes in reflectance factor due to Sun-row direction interactions
[E82-10128] p 11 N82-23566

Spectral properties of agricultural crops and soils measured from space, aerial, field, and laboratory sensors
[E82-10212] p 12 N82-23585
Multistage classification of multispectral Earth observational data The design approach
[E82-10213] p 72 N82-23586
Determination of the optimal level for combining area and yield estimates
[E82-10215] p 12 N82-23588
Application of Computer Axial Tomography (CAT) to measuring crop canopy geometry
[E82-10227] p 14 N82-23600
Linear polarization of light by two wheat canopies measured at many view angles
[E82-10229] p 14 N82-23602
A model of plant canopy polarization
[E82-10233] p 15 N82-23606
Canopy reflectance as influenced by solar illumination angle
[E82-10237] p 15 N82-23610
Spherical-Earth gravity and magnetic anomaly modeling by Gauss-Legendre quadrature integration
[E82-10242] p 36 N82-24520
Magnetic and gravity anomalies in the Americas
[E82-10312] p 37 N82-24586
Aeromagnetic and satellite magnetic anomaly mapping
[E82-10339] p 39 N82-25601
Forest Resource Information System Phase 3 System transfer report
[E82-10344] p 18 N82-25606
Spectral estimates of solar radiation intercepted by corn canopies
[E82-10003] p 18 N82-26742
Key Issues in the Analysis of Remote Sensing Data A report on the workshop
[E82-10348] p 85 N82-26746

Q

QEB, Inc., Lakewood, Colo.
Airborne gamma-ray spectrometer and magnetometer survey, Toronto quadrangle New York, volume 2A
[DE81-027158] p 46 N82-25620
Airborne gamma-ray spectrometer and magnetometer survey, Kingston quadrangle New York, volume 2C
[DE81-027161] p 46 N82-25621
Airborne gamma-ray spectrometer and magnetometer survey, Rochester quadrangle New York, volume 2D
[DE81-027156] p 46 N82-25622

R

Remote Sensing Systems, Sausalito, Calif.
The Seasat-A satellite scatterometer - The geophysical evaluation of remotely sensed wind vectors over the ocean p 51 A82-29616
The relationship between wind vector and normalized radar cross section used to derive Seasat-A Satellite Scatterometer winds p 51 A82-29617
Evaluation of atmospheric attenuation from SMMR brightness temperature for the Seasat satellite scatterometer p 51 A82-29618
Intercomparison of wind speeds inferred by the SASS, altimeter, and SMMR p 52 A82-29621
The effect of sea-surface Sun glitter on microwave radiometer measurements
[NASA-CR-169083] p 57 N82-26525
Research Inst. of National Defence, Linkoeping (Sweden).
Study visit to United States laser technology centers, 1981
[FOA-C-30257-E1] p 81 N82-24489

S

Sanders Associates, Inc., Nashua, N. H.
High spectral resolution airborne spectrometry p 77 A82-32443
Santa Barbara Research Center, Goleta, Calif
Thematic mapper - An overview of spectral band registration p 77 A82-32447
Sao Paulo Univ. (Brazil).
Structure, composition and thermal state of the crust in Brazil
[E82-10187] p 35 N82-22621
Science and Education Administration, Weslaco, Tex.
AgRISTARS Early warning and crop condition assessment Plant cover, soil temperature, freeze, water stress, and evapotranspiration conditions
[E82-10225] p 14 N82-23598
Scripps Institution of Oceanography, La Jolla, Calif
Satellite observations in FRONTS 80
[AD-A111080] p 58 N82-26766
Fluid-sediment interactions on beaches and shelves
[AD-A110838] p 59 N82-26948
South Carolina Univ., Columbia.
Detecting residential land-use development at the urban fringe p 22 A82-29332
South Dakota State Univ, Brookings.
Evaluation of HCMM data for assessing soil moisture and water table depth
[E82-10329] p 18 N82-24602
Irrigation management with remote sensing
[E82-10357] p 20 N82-26755
Stanford Univ., Calif
The observation of ocean surface phenomena using imagery from the Seasat synthetic aperture radar - An assessment p 52 A82-29623
Survey of India, Dehra Dun.
Report of MAGSAT project by Survey of India
[E82-10293] p 73 N82-24570
Analysis of MAGSAT data of the Indian region
[E82-10358] p 75 N82-26756
Systems and Applied Sciences Corp., Riverdale, Md.
Retrieval of ocean surface and atmospheric parameters from multichannel microwave radiometric measurements p 53 A82-31995

T

Technical Univ. of Denmark, Lyngby
Movement of ice markers measured by satellite ranging
[R-240] p 59 N82-27816
Technicolor Graphic Services, Inc., Sioux Falls, S Dak
An investigation of MAGSAT and complementary data emphasizing precambrian shields and adjacent areas of West Africa and South America
[E82-10316] p 38 N82-24589
An investigation of MAGSAT and complementary data emphasizing precambrian shields and adjacent areas of West Africa and South America
[E82-10317] p 38 N82-24590
An investigation of MAGSAT and complementary data emphasizing precambrian shields and adjacent areas of West Africa and South America
[E82-10318] p 38 N82-24591
Technische Hogeschool, Delft (Netherlands).
Nonlinear theory for elastic beams and rods and its finite element representation
[WTHD-143] p 73 N82-24517
Tennessee Valley Authority, Chattanooga.
Remote sensing of sulfur dioxide effects on vegetation Volume 1 Summary
[DE82-900580] p 31 N82-27802
Remote sensing of sulfur dioxide effects on vegetation Volume 2 Data
[DE82-900581] p 31 N82-27803
Texas A&M Univ., College Station.
Orbiting passive microwave sensor simulation applied to soil moisture estimation
[E82-10343] p 18 N82-25605
Multispectral determination of soil moisture-2
[E82-10349] p 19 N82-26747
Measurement of soil moisture trends with airborne scatterometers
[E82-10361] p 20 N82-26759
Multifrequency remote sensing of soil moisture
[E82-10362] p 20 N82-26760
Development of visible/infrared/microwave agriculture classification and biomass estimation algorithms
[E82-10363] p 20 N82-26761
Texas Univ. at Austin.
Interpretation of surface-water circulation, Aransas Pass, Texas, using Landsat imagery p 60 A82-32896
Texas Univ. at Dallas.
Investigation of the effects of external current systems on the MAGSAT data utilizing grid cell modeling techniques
[E82-10226] p 73 N82-23599
Investigation of the effects of external current systems on the MAGSAT data utilizing grid cell modeling techniques
[E82-10232] p 73 N82-23605
Texas Univ. at Dallas, Richardson.
Investigation of the effects of external current systems on the MAGSAT data utilizing grid cell modeling techniques
[E82-10195] p 71 N82-22629
Investigation of the effects of external current systems on the MAGSAT data utilizing grid cell modeling techniques
[E82-10306] p 74 N82-24580
Texas Univ. at El Paso.
Characterization of the structure and tectonic of South America
[E82-10196] p 42 N82-23569
The crustal structure and tectonics of South America
[E82-10319] p 38 N82-24592
Geotectonics of South America
[E82-10320] p 38 N82-24593
Texas Univ., Austin.
The Seasat altimeter data and its accuracy assessment p 49 A82-29602
An empirical determination of the effects of sea state bias on Seasat altimetry p 50 A82-29607
Evaluation of the Seasat altimeter time tag bias p 50 A82-29610
Texas Univ., El Paso.
Evaluation and combined geophysical interpretations of NURE and related geoscience data in the Van Horn, Pecos, Marfa, Fort Stockton, Presidido, and Emory Peak quadrangles, Texas, volume 1
[DE82-005554] p 47 N82-27808
Evaluation and combined geophysical interpretations of NURE and related geoscience data in the Van Horn, Pecos, Marfa, Fort Stockton, Presidio, and Emory Peak quadrangels, Texas
[DE82-005560] p 48 N82-27809
Tokyo Univ. (Japan).
Investigation from Japanese MAGSAT team
[E82-10239] p 73 N82-23612
Investigation from Japanese MAGSAT Team Part A Crustal structure near Japan and in Antarctic station Part B Electric currents and hydromagnetic waves in the ionosphere and the magnetosphere
[E82-10244] p 36 N82-24522
Report of investigation from Japanese MAGSAT Team
[E82-10322] p 74 N82-24595

U

University of Southern California, Los Angeles
Image understanding research
[AD-A110746] p 74 N82-25611
Utah Univ., Salt Lake City.
Identifying environmental features for land management decisions
[E82-10289] p 30 N82-24567
Inventory of wetlands and agricultural land cover in the upper Sevier River Basin, Utah
[E82-10345] p 18 N82-25607
Mapping of wildlife habitat in Farmington Bay, Utah
[E82-10354] p 19 N82-26752
Detection of variations in aspen forest habitat from LANDSAT digital data Bear River Range, Utah
[E82-10355] p 19 N82-26753
Irrigated acreage in the Bear River Basin as of the 1975 growing season
[E82-10356] p 20 N82-26754

V

Visidyne, Inc., Woburn, Mass.
Atmospheric ozone determination by solar occultation using the UV spectrometer on the Solar Maximum Mission p 27 A82-36362

W

Washington Univ., Seattle.
The Seasat-A satellite scatterometer - The geophysical evaluation of remotely sensed wind vectors over the ocean p 51 A82-29616
Surface wind analyses for Seasat p 51 A82-29619
Washington Univ., St. Louis, Mo.
Structure of the St Francois Mountains and surrounding lead belt, S E Missouri Inferences from thermal IR and other data sets
[E82-10200] p 36 N82-23573
Structure of the St Francois Mountains and surrounding lead belt, S E Missouri Inferences from thermal IR and other data sets
[E82-10205] p 11 N82-23578
Structure of the Saint Francois Mountains and surrounding lead belt, S E Missouri Inference from thermal IR and other data sets
[E82-10350] p 39 N82-26748
Western Geophysical Co. of America, Houston, Tex.
Airborne gamma-ray spectrometer and magnetometer survey Roseau quadrangle, Minnesota, volume 1
[DE82-001031] p 43 N82-23621
Airborne gamma-ray spectrometer and magnetometer survey Barrow quadrangle, Alaska, volume 1
[DE82-000334] p 43 N82-23623

Airborne gamma-ray spectrometer and magnetometer survey Wainwright quadrangle, Alaska, volume 2
[DE82-000341] p 43 N82-23624
Airborne gamma-ray spectrometer and magnetometer survey, Kenora quadrangle, Minnesota, volume 1
[DE82-001029] p 43 N82-23625
Airborne gamma-ray spectrometer and magnetometer survey Meade River quadrangle, Alaska, volume 2
[DE82-000340] p 43 N82-23626
Airborne gamma-ray spectrometer and magnetometer survey Teshekpuk quadrangle, Alaska, volume 2
[DE82-000310] p 43 *N82-23627*
Airborne gamma-ray spectrometer and magnetometer survey Harrison Bay quadrangle, Alaska, volume 2
[DE82-000315] p 43 N82-23628
Airborne gamma-ray spectrometer and magnetometer survey Beechey Pt , quadrangle, Alaska, volume 2
[DE82-000309] p 43 N82-23629
Airborne gamma-ray spectrometer and magnetometer survey Point Lay quadrangle, Alaska, volume 2
[DE82-000308] p 43 N82-23630
Airborne gamma-ray spectrometer and magnetometer survey Utukik River quadrangle, Alaska, volume 2
[DE82-000316] p 44 N82-23631
Airborne gamma-ray spectrometer and magnetometer survey Sagavanirktok quadrangle, Alaska, volume 2
[DE82-000311] p 44 N82-23632
Airborne gamma-ray spectrometer and magnetometer *survey Duluth quadrangle, Minnesota, volume 2*
[DE82-001027] p 44 N82-23633
Airborne gamma-ray spectrometer and magnetometer survey Roseau quadrangle, Minnesota, volume 2
[DE82-001025] p 44 N82-23634
Airborne gamma-ray spectrometer and magnetometer survey Devil's Lake quadrangle, North Dakota, volume 1
[DE82-004161] p 44 N82-23635
Airborne gamma-ray spectrometer and magnetometer survey Devil's Lake quadrangle, North Dakota, volume 2
[DE82-004168] p 44 N82-23636
Airborne gamma-ray spectrometer and magnetometer survey Bemidji quadrangle, Minnesota, volume 1
[DE82-001032] p 44 N82-23637
Airborne gamma-ray spectrometer and magnetometer *survey Bemidji quadrangle, Minnesota, volume 2*
[DE82-001026] p 44 N82-23638
Airborne gamma-ray spectrometer and magnetometer survey Hibbing quadrangle, Minnesota, volume 1
[DE82-004159] p 44 N82-23639
Airborne gamma-ray spectrometer and magnetometer survey Hibbing quadrangle, Minnesota, volume 2
[DE82-004165] p 45 N82-23640
Airborne gamma-ray spectrometer and magnetometer survey Aberdeen quadrangle, South Dakota, volume 1
[DE82-004152] p 45 N82-23641
Airborne gamma-ray spectrometer and magnetometer survey Aberdeen quadrangle, South Dakota, volume 2
[DE82-004164] p 45 N82-23642
Airborne gamma-ray spectrometer and magnetometer survey International Falls quadrangle, Minnesota, volume 1
[DE82-004151] p 45 N82-23643
Airborne gamma-ray spectrometer and magnetometer survey International Falls quadrangle, Minnesota, volume 2
[DE82-004166] p 45 N82-23644
Airborne gamma-ray spectrometer and magnetometer *survey Barrow quadranagle, Alaska, volume 2*
[DE82-000342] p 46 N82-25623
Airborne gamma-ray spectrometer and magnetometer survey Lookout Ridge quadrangle, Alaska, volume 2
[DE82-000313] p 47 N82-25625
Airborne gamma-ray spectrometer and magnetometer survey North/south tieline, volume 1
[DE82-005542] p 47 N82-27804
Airborne gamma-ray spectrometer and magnetometer survey North/south tieline, volume 2
[DE82-005570] p 47 N82-27805
Airborne gamma-ray spectrometer and magnetometer survey Sioux Falls quadrangle, South Dakota, volume 1
[DE82-005533] p 47 N82-27806
Airborne gamma-ray spectrometer and magnetometer survey Sioux Falls quadrangle, South Dakota, volume 2
[DE82-005574] p 47 N82-27807
Airborne gamma-ray spectrometer and magnetometer survey Ukiah quadrangle, California, volume 1
[DE82-005541] p 48 N82-27813
Airborne gamma-ray spectrometer and magnetometer survey Huron Quadrangle, South Dakota
[DE82-005540] p 48 N82-27814
Airborne gamma-ray spectrometer and magnetometer survey Chico Quadrangle, California
[DE82-005543] p 48 N82-27815

Wisconsin Univ., Madison.
Magsat magnetic anomalies over Antarctica and the surrounding oceans p 32 A82-30787
The impact of meteorological satellites on the First *GARP Global Experiment (FGGE)* p 55 *N82-23852*
Estimates of sea surface stress for summer MONEX from cloud motions p 56 N82-23910
Investigation of Antarctic crust and upper mantle using MAGSAT and other geophysical data
[E82-10308] p 37 *N82-24582*
Investigation of Antarctic crust and upper mantle using MAGSAT and other geophysical data
[E82-10309] p 37 N82-24583

Woods Hole Oceanographic Institution, Mass.
Computer-processed geophysical atlas of digital data for the East Coast margin of the United States from surface and spacecraft data
[AD-A111388] p 39 N82-25748

Wyle Labs., Inc., Hampton, Va.
Airborne lidar measurements of the Soufriere eruption of 17 April 1979 p 24 A82-33657

Z

Zentralstelle fuer Geo-Photogrammetrie und Fernerkundung, Munich (West Germany).
Multidisciplinary investigations on HCMM data over middle Europe and Marocco
[E82-10315] p 74 N82-24588

Typical Contract Number Index Listing

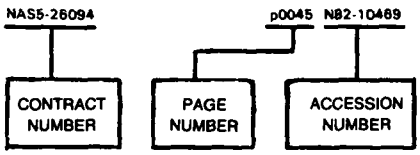

Listings in this index are arranged alphanumerically by contract number. Under each contract number, the accession numbers denoting documents that have been produced as a result of research done under that contract are arranged in ascending order with the AIAA accession numbers appearing first. The accession number denotes the number by which the citation is identified in the abstract section. Preceding the accession number is the page number on which the citation may be found.

AF PROJ 2309 p 40 N82-27900
AF PROJ 2310 p 76 N82-26907
AF PROJ 4303 p 75 N82-25613
AF PROJ 7930 p 82 N82-26642
AF-AFOSR-79-0010 p 76 A82-31019
AF-AFOSR-79-0012 p 76 A82-31020
BMFT-RV14-B8/74 p 65 A82-22586
p 40 A82-22607
p 5 A82-22612
BMFT-01-OI-017-ZA/WF/WRK-1754 p 40 A82-22607
BMFT-01-0I-017-ZA/WF/WRK-1754 p 65 A82-22586
CIT-44-727600 p 29 A82-37405
CNES-214 p 10 A82-37194
CNES-272 p 10 A82-37194
DAAK70-80-C-0016 p 75 N82-26765
DACW39-77-C-0073 p 70 A82-35650
DARG29-79-C-0199 p 70 A82-35650
DARPA ORDER 3119 p 74 N82-25611
DE-AC13-76GJ-01664 p 43 N82-23621
p 43 N82-23623
p 43 N82-23624
p 43 N82-23625
p 43 N82-23626
p 43 N82-23627
p 43 N82-23629
p 43 N82-23630
p 44 N82-23631
p 44 N82-23632
p 44 N82-23633
p 44 N82-23634
p 44 N82-23635
p 44 N82-23636
p 44 N82-23637
p 44 N82-23638
p 44 N82-23639
p 45 N82-23640
p 45 N82-23641
p 45 N82-23642
p 45 N82-23643
p 45 N82-23644
p 46 N82-25623
p 47 N82-25625
p 47 N82-27804
p 47 N82-27805
p 47 N82-27806
p 47 N82-27807
p 47 N82-27808
p 48 N82-27809
p 48 N82-27810
p 48 N82-27811
p 48 N82-27812
p 48 N82-27814
p 48 N82-27815
DE-AC13-76GJ-016664 p 43 N82-23628
DE-AC13-79CJ-01692 p 46 N82-25621
DE-AC13-79GJ-01664 p 48 N82-27813
DE-AC13-79GJ-01692 p 46 N82-25620
p 46 N82-25622
DE-14-08-0001-16439 p 38 N82-24590
DFG-SCHL-201/1 p 1 A82-22552
DFG-4810/79 p 33 A82-32077
DI-14-08-0001-16439 p 38 N82-24589
DI-14-08-0001-21249 p 38 N82-24591
DOT-FA78WAI-850 p 28 A82-36431
EPA-IAG-D8-E721 p 31 N82-27802
p 31 N82-27803
EPA-5-536-4 p 27 A82-36406
ESA-4422/80 p 78 A82-32824
ESA-4634/81 p 59 N82-27816
F04701-79-C-0080 p 29 A82-37405
F04701-80-C-0081 p 26 A82-35542
F19628-79-C-0027 p 40 N82-27900
F19628-79-C-0062 p 76 N82-26907
F19628-80-C-0021 p 60 A82-33329
F19628-81-K-0032 p 76 A82-31020
F30602-80-C-0040 p 75 N82-25613
F33615-77-C-0604 p 82 N82-26642
F33615-80-C-1080 p 74 N82-25611
JPL-954703 p 50 A82-29610
JPL-954958 p 57 N82-26525
JPL-955832 p 77 A82-32443
NAGW-95 p 30 N82-24567
p 18 N82-25607
p 19 N82-26752
p 19 N82-26753
p 20 N82-26754
NAG5-10 p 77 A82-32658
NAG5-12 p 19 N82-26745
NAG5-152 p 34 A82-32646
NAG5-37 p 20 N82-26755
NASA ORDER A-65111-B p 75 N82-26763
NASA ORDER S-40198B p 14 N82-23598
NASA ORDER S-40255-B p 16 N82-24523
NASA ORDER S-40256-B p 36 N82-23587
NASA ORDER S-65000-B p 33 A82-32078
NASW-3308 p 85 N82-23568
NASW-3338 p 29 A82-37405
NASW-3389 p 42 A82-36298
NAS1-15301 p 23 A82-31990
NAS1-16032 p 52 A82-29621
NAS5-11063 p 22 A82-22605
NAS5-20062 p 65 A82-22586
p 40 A82-22607
p 5 A82-22612
p 40 A82-22613
NAS5-20674 p 65 A82-22585
p 3 A82-22591
NAS5-20721 p 22 A82-22606
NAS5-20986 p 60 A82-32896
NAS5-22929 p 77 A82-32658
NAS5-23315 p 29 A82-37405
NAS5-24200 p 77 A82-32447
NAS5-24206 p 18 N82-24602
NAS5-24316 p 62 N82-22625
NAS5-25030 p 32 A82-30789
p 33 A82-30795
p 36 N82-24520
NAS5-25451 p 68 A82-32581
NAS5-25488 p 68 A82-32581
NAS5-25720 p 70 A82-35824
NAS5-25731 p 1 A82-22541
NAS5-25735 p 22 A82-22605
NAS5-25737 p 82 N82-26744
NAS5-25807 p 19 N82-26749
NAS5-25882 p 37 N82-24587
NAS5-25957 p 35 N82-23571
p 37 N82-24584
p 39 N82-25604
NAS5-25977 p 32 A82-30787
p 37 N82-24582
p 37 N82-24583
NAS5-26047 p 71 N82-23567
NAS5-26157 p 32 A82-30790
p 71 N82-22627
NAS5-26205 p 74 N82-24581
NAS5-26309 p 81 N82-25602
p 71 N82-22629
p 73 N82-23599
p 73 N82-23605
p 74 N82-24580
NAS5-26326 p 42 N82-23569
p 38 N82-24592
p 38 N82-24593
NAS5-26328 p 71 N82-23572
p 36 N82-24573
NAS5-26414 p 45 N82-24579
NAS5-26424 p 32 A82-30788
p 71 N82-23570
p 36 N82-23577
p 36 N82-24577
p 37 N82-24578
NAS5-26425 p 46 N82-24594
p 46 N82-24596
NAS5-26453 p 17 N82-24575
NAS5-26456 p 82 N82-26743
NAS5-26533 p 36 N82-23573
p 11 N82-23578
p 39 N82-26748
NAS5-26728 p 47 N82-26750
NAS7-100 p 49 A82-29601
p 50 A82-29613
p 52 A82-29621
p 52 A82-29622
p 52 A82-29624
p 33 A82-31994
p 23 A82-32441
p 41 A82-32442
p 77 A82-32448
p 53 A82-32882
p 68 A82-32904
p 69 A82-34720
p 25 A82-34743
p 57 N82-25609
NAS8-33235 p 29 A82-37405
NAS8-33726 p 23 A82-32348
NAS9-15325 p 18 N82-25606
NAS9-15466 p 10 N82-22623
p 11 N82-23566
p 12 N82-23585
p 72 N82-23586
p 12 N82-23588
p 14 N82-23600
p 14 N82-23602
p 15 N82-23606
p 15 N82-23610
p 18 N82-26742
p 85 N82-26746
NAS9-15476 p 10 N82-22626
p 16 N82-24519
NAS9-15509 p 68 A82-32904
NAS9-15800 p 84 N82-22620
p 11 N82-23565
p 11 N82-23579
p 12 N82-23581
p 12 N82-23582
p 13 N82-23590
p 13 N82-23594
p 13 N82-23595
p 73 N82-23596
p 14 N82-23597
p 14 N82-23603
p 15 N82-23607
p 15 N82-23608
NAS9-16514 p 8 A82-34179
NAS9-16538 p 19 N82-26751
NCC5-5 p 19 N82-26747
NERC-GR3/3941 p 23 A82-32342
NGL-14-001-006 p 1 A82-22541
NGL-21-002-005 p 26 A82-35542
NGL-24-005-263 p 7 A82-29539
NGL-25-001-054 p 30 N82-24566
NGL-33-010-171 p 8 A82-32708
NGR-05-002-160 p 22 A82-22606
NGR-21-002-224 p 40 A82-22607
NGR-21-002-316 p 22 A82-22605
p 40 A82-22607
NGR-30-002-052 p 63 A82-22538

	p 64	A82-22555
NOAA-MO-A01-78-00-4318	p 52	A82-29623
NOAA-MO-A01-78-00-4325	p 50	A82-29610
NOAA-NA-79SAC00723	p 50	A82-29612
NOAA-NA-80AAD0019	p 60	A82-34735
NSF ATM-77-24843	p 26	A82-36268
NSF ATM-78-20936-01	p 3	A82-22589
NSF ATM-79-13097	p 56	N82-23910
NSF ATM-79-23240	p 76	A82-31019
NSF ATM-79-25987	p 76	A82-31019
NSF ATM-81-16045	p 26	A82-35542
NSF ENG-78-24432	p 77	A82-32443
NSF OCE-77-27735	p 59	N82-26949
NSF OCE-78-22481	p 53	A82-32651
NSF OCE-79-24606	p 53	A82-32651
NSF SPI-80-03978	p 19	N82-26753
NSF 78-07369	p 54	A82-36341
NSF 81-06099	p 54	A82-36341
NSG-2377	p 68	A82-32904
NSG-5134	p 20	N82-26759
	p 20	N82-26760
	p 20	N82-26761
NSG-5265	p 33	A82-32077
NSG-5266	p 18	N82-25605
NSG-7202	p 49	A82-22306
NTNF PROJECT 18108075	p 41	A82-30304
N00014-75-C-0300	p 59	N82-26948
N00014-75-C-0356	p 52	A82-29623
N00014-80-C-0440	p 58	N82-26766
N00014-80-C-0673	p 53	A82-32559
N00014-82-C-0019	p 39	N82-25748
PROJ AGRISTARS	p 84	N82-22620
	p 10	N82-22623
	p 11	N82-23564
	p 11	N82-23565
	p 11	N82-23566
	p 11	N82-23579
	p 12	N82-23580
	p 12	N82-23581
	p 12	N82-23582
	p 12	N82-23585
	p 72	N82-23586
	p 12	N82-23588
	p 13	N82-23589
	p 13	N82-23590
	p 13	N82-23591
	p 13	N82-23592
	p 13	N82-23593
	p 13	N82-23594
	p 13	N82-23595
	p 73	N82-23596
	p 14	N82-23597
	p 14	N82-23598
	p 14	N82-23600
	p 14	N82-23601
	p 14	N82-23602
	p 14	N82-23603
	p 15	N82-23604
	p 15	N82-23606
	p 15	N82-23607
	p 15	N82-23608
	p 15	N82-23609
	p 15	N82-23610
	p 16	N82-23611
	p 16	N82-24519
	p 16	N82-24563
	p 16	N82-24564
	p 17	N82-24565
	p 18	N82-26742
	p 19	N82-26751
USDA-23-178	p 8	A82-32707
USDA-53-3187-8-25	p 7	A82-32704
W-7405-ENG-48	p 29	N82-23793
	p 39	N82-26915
	p 30	N82-27737
146-20-10-29	p 30	N82-25661
146-40-01-04	p 57	N82-25609
146-40-05-05	p 81	N82-22865
146-40-15-07	p 55	N82-23614
506-62-43-01	p 81	N82-25610

Typical Report/Accession Number Index Listing

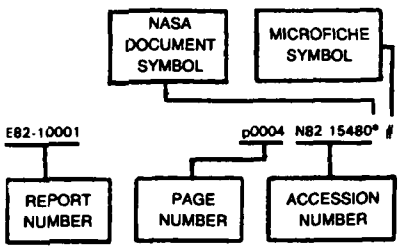

Listings in this index are arranged alphanumerically by report number The page number indicates the page on which the citation is located. The accession number denotes the number by which the citation is identified. An asterisk (*) indicates that the item is a NASA report. A pound sign (#) indicates that the item is available on microfiche

AAS PAPER 82-127 p 80 A82-37809 #
AAS PAPER 82-130 p 71 A82-37810* #
AAS PAPER 82-132 p 81 A82-37812* #

AD-A110538 p 75 N82-26765 #
AD-A110688 p 82 N82-26642 #
AD-A110746 p 74 N82-25611 #
AD-A110765 p 39 N82-26268 #
AD-A110806 p 58 N82-26764 #
AD-A110838 p 59 N82-26948 #
AD-A111005 p 58 N82-26945 #
AD-A111080 p 58 N82-26766 #
AD-A111223 p 75 N82-25613 #
AD-A111307 p 75 N82-25614 #
AD-A111388 p 39 N82-25748 #
AD-A111401 p 74 N82-25612 #
AD-A112337 p 76 N82-26907 #
AD-A113098 p 40 N82-27900 #

AFGL-TR-82-0019 p 40 N82-27900 #
AFGL-TR-82-0055 p 76 N82-26907 #

AIAA 81-2333 p 59 A82-13528 #

AP-J0-04111 p 15 N82-23609* #

AR-002-695 p 57 N82-24597* #

B-205344 p 29 N82-23043 #

CONF-810711-1 p 2 A82-22565 #
CONF-810711-2 p 64 A82-22573 #

CRREL-81-22 p 58 N82-26764 #

CRSC-82-1 p 19 N82-26752* #
CRSC-82-2 p 19 N82-26753* #
CRSC-82-3 p 20 N82-26754* #

CUEA-74 p 59 N82-26949 #

DC-YI-04211 p 16 N82-24564* #

DC-Y1-04156 p 16 N82-24563* #

DE81-027156 p 46 N82-25622 #
DE81-027158 p 46 N82-25620 #
DE81-027161 p 46 N82-25621 #
DE82-000308 p 43 N82-23630 #
DE82-000309 p 43 N82-23629 #
DE82-000310 p 43 N82-23627 #
DE82-000311 p 44 N82-23632 #
DE82-000313 p 47 N82-25625 #
DE82-000315 p 43 N82-23628 #
DE82-000316 p 44 N82-23631 #
DE82-000334 p 43 N82-23623 #
DE82-000340 p 43 N82-23626 #
DE82-000341 p 43 N82-23624 #
DE82-000342 p 46 N82-25623 #
DE82-000965 p 30 N82-27737 #
DE82-001025 p 44 N82-23634 #
DE82-001026 p 44 N82-23638 #
DE82-001027 p 44 N82-23633 #
DE82-001029 p 43 N82-23625 #
DE82-001031 p 43 N82-23621 #
DE82-001032 p 44 N82-23637 #
DE82-001686 p 39 N82-26915 #
DE82-004151 p 45 N82-23643 #
DE82-004152 p 45 N82-23641 #
DE82-004159 p 44 N82-23639 #
DE82-004161 p 44 N82-23635 #
DE82-004164 p 45 N82-23642 #
DE82-004165 p 45 N82-23640 #
DE82-004166 p 45 N82-23644 #
DE82-004168 p 44 N82-23636 #
DE82-005527 p 48 N82-27810 #
DE82-005533 p 47 N82-27806 #
DE82-005538 p 48 N82-27811 #
DE82-005540 p 48 N82-27814 #
DE82-005541 p 48 N82-27813 #
DE82-005542 p 47 N82-27804 #
DE82-005543 p 48 N82-27815 #
DE82-005554 p 47 N82-27808 #
DE82-005560 p 48 N82-27809 #
DE82-005568 p 48 N82-27812 #
DE82-005570 p 47 N82-27805 #
DE82-005574 p 47 N82-27807 #
DE82-900580 p 31 N82-27802 #
DE82-900581 p 31 N82-27803 #

DGS-322 p 40 N82-27900 #

E/S-1234 p 75 N82-26765 #

EMD-82-10 p 29 N82-23043 #

EPA-600/7-81-114 p 31 N82-27803 #
EPA-660/7-81-113 p 31 N82-27802 #

ERIM-147200-13-F p 85 N82-23568* #
ERIM-152400-4-P p 10 N82-22626* #
ERIM-152400-6-P p 16 N82-24519* #
ERIM-160300-7-T p 19 N82-26751* #

ERT-P-2061-F p 62 N82-22625* #

ESA-CR(P)-1547 p 59 N82-27816 #

ETL-R034 p 75 N82-25614 #

ETL-0268 p 75 N82-26765 #

EW-R1-04147 p 14 N82-23601* #

EW-UI-04119 p 11 N82-23564* #

EW-U1-04103 p 14 N82-23598* #
EW-U1-04144 p 13 N82-23593* #
EW-U1-04208 p 13 N82-23591* #
EW-U1-04212 p 12 N82-23580* #

E82-10003 p 18 N82-26742* #
E82-10096 p 35 N82-23563* #
E82-10112 p 11 N82-23564* #
E82-10126 p 11 N82-23565* #
E82-10128 p 11 N82-23566* #
E82-10151 p 71 N82-23567* #
E82-10153 p 45 N82-24518* #
E82-10181 p 85 N82-23568* #
E82-10186 p 84 N82-22620* #
E82-10187 p 35 N82-22621* #
E82-10188 p 71 N82-22622* #
E82-10189 p 10 N82-22623* #
E82-10190 p 42 N82-22624* #
E82-10191 p 62 N82-22625* #
E82-10192 p 10 N82-22626* #
E82-10193 p 71 N82-22627* #
E82-10194 p 35 N82-22628* #
E82-10195 p 71 N82-22629* #
E82-10196 p 42 N82-23569* #
E82-10197 p 71 N82-23570* #
E82-10198 p 35 N82-23571* #
E82-10199 p 71 N82-23572* #
E82-10200 p 36 N82-23573* #
E82-10201 p 72 N82-23574* #
E82-10202 p 72 N82-23575* #
E82-10203 p 72 N82-23576* #
E82-10204 p 36 N82-23577* #
E82-10205 p 11 N82-23578* #
E82-10206 p 11 N82-23579* #
E82-10207 p 12 N82-23580* #
E82-10208 p 12 N82-23581* #
E82-10209 p 12 N82-23582* #
E82-10210 p 72 N82-23583* #
E82-10211 p 72 N82-23584* #
E82-10212 p 12 N82-23585* #
E82-10213 p 72 N82-23586* #
E82-10214 p 36 N82-23587* #
E82-10215 p 12 N82-23588* #
E82-10216 p 13 N82-23589* #
E82-10217 p 13 N82-23590* #
E82-10218 p 13 N82-23591* #
E82-10219 p 13 N82-23592* #
E82-10220 p 13 N82-23593* #
E82-10221 p 13 N82-23594* #
E82-10222 p 13 N82-23595* #
E82-10223 p 73 N82-23596* #
E82-10224 p 14 N82-23597* #
E82-10225 p 14 N82-23598* #
E82-10226 p 73 N82-23599* #
E82-10227 p 14 N82-23600* #
E82-10228 p 14 N82-23601* #
E82-10229 p 14 N82-23602* #
E82-10230 p 14 N82-23603* #
E82-10231 p 15 N82-23604* #
E82-10232 p 73 N82-23605* #
E82-10233 p 15 N82-23606* #
E82-10234 p 15 N82-23607* #
E82-10235 p 15 N82-23608* #
E82-10236 p 15 N82-23609* #
E82-10237 p 15 N82-23610* #
E82-10238 p 16 N82-23611* #
E82-10239 p 73 N82-23612* #
E82-10240 p 73 N82-23613* #
E82-10241 p 16 N82-24519* #
E82-10242 p 36 N82-24520* #
E82-10243 p 45 N82-24521* #
E82-10244 p 36 N82-24522* #
E82-10245 p 16 N82-24523* #
E82-10285 p 16 N82-24563* #
E82-10286 p 16 N82-24564* #
E82-10287 p 17 N82-24565* #
E82-10288 p 30 N82-24566* #
E82-10289 p 30 N82-24567* #
E82-10290 p 85 N82-24568* #
E82-10291 p 63 N82-24569* #
E82-10293 p 73 N82-24570* #
E82-10296 p 73 N82-24572* #
E82-10297 p 36 N82-24573* #
E82-10298 p 17 N82-24574* #
E82-10299 p 17 N82-24575* #
E82-10300 p 17 N82-24576* #
E82-10303 p 36 N82-24577* #
E82-10304 p 37 N82-24578* #
E82-10305 p 45 N82-24579* #
E82-10306 p 74 N82-24580* #
E82-10307 p 74 N82-24581* #
E82-10308 p 37 N82-24582* #
E82-10309 p 37 N82-24583* #
E82-10310 p 37 N82-24584* #
E82-10311 p 17 N82-24585* #
E82-10312 p 37 N82-24586* #
E82-10313 p 82 N82-26743* #
E82-10314 p 37 N82-24587* #
E82-10315 p 74 N82-24588* #
E82-10316 p 38 N82-24589* #
E82-10317 p 38 N82-24590* #
E82-10318 p 38 N82-24591* #
E82-10319 p 38 N82-24592* #
E82-10320 p 38 N82-24593* #
E82-10321 p 46 N82-24594* #

E82-10322 p 74 N82-24595* #
E82-10323 p 46 N82-24596* #
E82-10324 p 57 N82-24597* #
E82-10325 p 30 N82-24598* #
E82-10326 p 38 N82-24599* #
E82-10327 p 74 N82-24600* #
E82-10328 p 63 N82-24601* #
E82-10329 p 18 N82-24602* #
E82-10330 p 38 N82-24603* #
E82-10339 p 39 N82-25601* #
E82-10340 p 81 N82-25602* #
E82-10341 p 46 N82-25603* #
E82-10342 p 39 N82-25604* #
E82-10343 p 18 N82-25605* #
E82-10344 p 18 N82-25606* #
E82-10345 p 18 N82-25607* #
E82-10346 p 82 N82-26744* #
E82-10347 p 19 N82-26745* #
E82-10348 p 85 N82-26746* #
E82-10349 p 19 N82-26747* #
E82-10350 p 39 N82-26748* #
E82-10351 p 19 N82-26749* #
E82-10352 p 47 N82-26750* #
E82-10353 p 19 N82-26751* #
E82-10354 p 19 N82-26752* #
E82-10355 p 19 N82-26753* #
E82-10356 p 20 N82-26754* #
E82-10357 p 20 N82-26755* #
E82-10358 p 75 N82-26756* #
E82-10359 p 30 N82-26757* #
E82-10360 p 58 N82-26758* #
E82-10361 p 20 N82-26759* #
E82-10362 p 20 N82-26760* #
E82-10363 p 20 N82-26761* #

FC-J1-04175-VOL-2 p 13 N82-23589* #
FC-J1-04181 p 15 N82-23604* #

FC-LO-00472 p 14 N82-23603* #

FC-L1-04096 p 11 N82-23579* #
FC-L1-04127 p 11 N82-23565* #
FC-L1-04142 p 12 N82-23582* #
FC-L1-04145 p 13 N82-23595* #
FC-L1-04172 p 13 N82-23594* #
FC-L1-04192 p 13 N82-23590* #

FC-P1-04197 p 12 N82-23588* #

FOA-C-30257-E1 p 81 N82-24489 #

FSGTR/INT-116 p 30 N82-23963 #

FSU-MET-STU-81/5 p 59 N82-26949 #

GJBX-211-81-VOL-2A p 46 N82-25620 #
GJBX-211-81-VOL-2C p 46 N82-25621 #
GJBX-211-81-VOL-2D p 46 N82-25622 #
GJBX-295-81-VOL-1 p 43 N82-23623 #
GJBX-295-81-VOL-2 p 46 N82-25623 #
GJBX-296-81-VOL-2 p 43 N82-23624 #
GJBX-297-81-VOL-2 p 43 N82-23626 #
GJBX-298-81-VOL-2 p 43 N82-23627 #
GJBX-299-81-VOL-2 p 43 N82-23628 #
GJBX-300-81-VOL-2 p 43 N82-23629 #
GJBX-301-81-VOL-2 p 43 N82-23630 #
GJBX-302-81-VOL-2 p 44 N82-23631 #
GJBX-303-81-VOL-2 p 47 N82-25625 #
GJBX-306-81-VOL-2 p 44 N82-23632 #
GJBX-328-81-VOL-1 p 43 N82-23625 #
GJBX-329-81-VOL-1 p 43 N82-23621 #
GJBX-329-81-VOL-2 p 44 N82-23634 #
GJBX-330-81-VOL-2 p 44 N82-23633 #
GJBX-331-81-VOL-1 p 44 N82-23637 #
GJBX-331-81-VOL-2 p 44 N82-23638 #
GJBX-354-81-VOL-1 p 44 N82-23635 #
GJBX-354-81-VOL-2 p 44 N82-23636 #
GJBX-355-81-VOL-1 p 44 N82-23639 #
GJBX-355-81-VOL-2 p 45 N82-23640 #
GJBX-356-81-VOL-1 p 45 N82-23643 #
GJBX-356-81-VOL-2 p 45 N82-23644 #
GJBX-357-81-VOL-1 p 45 N82-23641 #
GJBX-357-81-VOL-2 p 45 N82-23642 #
GJBX-365-81 p 47 N82-27808 #
GJBX-365-81-VOL-2 p 48 N82-27809 #
GJBX-386-81-VOL-1 p 47 N82-27804 #
GJBX-386-81-VOL-2 p 47 N82-27805 #
GJBX-388-81-VOL-2 p 48 N82-27812 #
GJBX-389-81-VOL-1 p 47 N82-27806 #
GJBX-389-81-VOL-2 p 47 N82-27807 #
GJBX-390-81-VOL-1 p 48 N82-27813 #
GJBX-405-81-VOL-1 p 48 N82-27814 #
GJBX-407-81-VOL-1 p 48 N82-27815 #
GJBX-410-81-VOL-1 p 48 N82-27811 #
GJBX-412-81-VOL-2C p 48 N82-27810 #

GPO-87-070 p 84 N82-22630 #

GSC-TR8203 p 81 N82-25602* #

INPE-2249-TDL/066 p 63 N82-24569* #
INPE-2284-PRE/060 p 58 N82-26758* #
INPE-2297-RPE/401 p 30 N82-26757* #
INPE-2367-RA/161-PT-2 p 30 N82-24598* #

ISBN-0-11-884138-6 p 42 N82-22636 #

IT-E2-04235 p 19 N82-26751* #

JPL-9950-652 p 57 N82-26525* #

JSC-16752 p 14 N82-23603* #
JSC-16858 p 12 N82-23581* #
JSC-17122 p 15 N82-23607* #
JSC-17138 p 11 N82-23579* #
JSC-17143 p 14 N82-23598* #
JSC-17398 p 15 N82-23609* #
JSC-173991 p 11 N82-23564* #
JSC-17406 p 11 N82-23565* #
JSC-17414 p 15 N82-23608* #
JSC-17417 p 12 N82-23582* #
JSC-17420 p 13 N82-23593* #
JSC-17421 p 13 N82-23595* #
JSC-17431 p 73 N82-23596* #
JSC-17432 p 13 N82-23594* #
JSC-17433-VOL-2 p 13 N82-23589* #
JSC-17434 p 14 N82-23597* #
JSC-17438 p 15 N82-23604* #
JSC-17440 p 13 N82-23590* #
JSC-17792 p 13 N82-23592* #
JSC-17797 p 13 N82-23591* #
JSC-17801 p 12 N82-23580* #

LA-UR-81-965 p 2 A82-22565 #
LA-UR-81-966 p 64 A82-22573 #

LARS-TR-060881 p 14 N82-23600* #
LARS-TR-062481 p 85 N82-26746* #
LARS-TR-090981 p 14 N82-23602* #

LARS-030182 p 18 N82-26742* #
LARS-060580 p 15 N82-23606* #
LARS-07138 p 10 N82-22623* #
LARS-071380 p 12 N82-23585* #
LARS-073081 p 18 N82-25606* #
LARS-090881 p 11 N82-23566* #
LARS-101281 p 12 N82-23588* #
LARS-101481 p 72 N82-23586* #

LBL-12604 p 29 N82-23793 #

LEMSCO-13491 p 84 N82-22620* #
LEMSCO-14598 p 14 N82-23603* #
LEMSCO-15173 p 15 N82-23607* #
LEMSCO-15682 p 13 N82-23595* #
LEMSCO-16018 p 12 N82-23581* #
LEMSCO-16573 p 11 N82-23579* #
LEMSCO-16854 p 15 N82-23608* #
LEMSCO-16921 p 11 N82-23565* #
LEMSCO-16929 p 12 N82-23582* #
LEMSCO-16935 p 13 N82-23590* #
LEMSCO-16944 p 13 N82-23594* #
LEMSCO-17269 p 73 N82-23596* #
LEMSCO-17276 p 14 N82-23597* #

LRS-021681 p 15 N82-23610* #

M-38 p 73 N82-24572* #

NAS 1 15 83280 p 81 N82-22865* #
NAS 1 15 83290 p 55 N82-23614* #
NAS 1 15 83842 p 16 N82-23611* #
NAS 1 15 83871 p 46 N82-25603* #
NAS 1 15 84186 p 81 N82-22643* #
NAS 1 15 84191 p 84 N82-23258* #
NAS 1 15 84201 p 11 N82-23564* #
NAS 1 15 84202 p 15 N82-23609* #
NAS 1 15 84203 p 13 N82-23592* #
NAS 1 15 84204 p 13 N82-23593* #
NAS 1 15 84205 p 15 N82-23604* #
NAS 1 15 84206 p 13 N82-23589* #
NAS 1 15 84471 p 30 N82-25661* #
NAS 1 15 84478 p 81 N82-25610* #
NAS 1 15 84694 p 16 N82-24563* #
NAS 1 15 84695 p 16 N82-24564* #
NAS 1 15 84696 p 17 N82-24565* #
NAS 1 15 84731 p 18 N82-25608* #
NAS 1 15 84740 p 13 N82-23591* #
NAS 1 26 16740 p 11 N82-23565* #
NAS 1 26 160888 p 14 N82-23603* #
NAS 1 26 161047 p 10 N82-22626* #
NAS 1 26 166352 p 75 N82-26763* #
NAS 1 26 166788 p 82 N82-26744* #
NAS 1 26 166790 p 81 N82-25602* #
NAS 1 26 166801 p 19 N82-26749* #
NAS 1 26 167391 p 16 N82-24519* #
NAS 1 26 167397 p 14 N82-23600* #
NAS 1 26 167402 p 15 N82-23610* #
NAS 1 26 167403 p 11 N82-23566* #
NAS 1 26 167406 p 13 N82-23595* #
NAS 1 26 167408 p 14 N82-23601* #
NAS 1 26 167411 p 15 N82-23608* #
NAS 1 26 167415 p 15 N82-23606* #
NAS 1 26 167416 p 15 N82-23607* #
NAS 1 26 167419 p 14 N82-23602* #
NAS 1 26 167440 p 14 N82-23598* #
NAS 1 26 167441 p 14 N82-23597* #
NAS 1 26 167442 p 73 N82-23596* #
NAS 1 26 167446 p 13 N82-23594* #
NAS 1 26 167457 p 84 N82-22620* #
NAS 1 26 167479 p 13 N82-23590* #
NAS 1 26 167485 p 11 N82-23579* #
NAS 1 26 167486 p 12 N82-23580* #
NAS 1 26 167487 p 12 N82-23581* #
NAS 1 26 167488 p 12 N82-23582* #
NAS 1 26 167507 p 12 N82-23585* #
NAS 1 26 167508 p 72 N82-23586* #
NAS 1 26 167511 p 12 N82-23588* #
NAS 1 26 167544 p 18 N82-25606* #
NAS 1 26 167570 p 85 N82-26746* #
NAS 1 26 167604 p 19 N82-26751* #
NAS 1 26 168536 p 71 N82-23567* #
NAS 1 26 168538 p 45 N82-24518* #
NAS 1 26 168615 p 35 N82-22621* #
NAS 1 26 168616 p 71 N82-22622* #
NAS 1 26 168617 p 10 N82-22623* #
NAS 1 26 168618 p 42 N82-22624* #
NAS 1 26 168619 p 62 N82-22625* #
NAS 1 26 168620 p 71 N82-22627* #
NAS 1 26 168621 p 35 N82-22628* #
NAS 1 26 168622 p 71 N82-22629* #
NAS 1 26 168623 p 42 N82-23569* #
NAS 1 26 168624 p 71 N82-23570* #
NAS 1 26 168625 p 35 N82-23571* #
NAS 1 26 168627 p 36 N82-23573* #
NAS 1 26 168628 p 72 N82-23574* #
NAS 1 26 168629 p 72 N82-23575* #
NAS 1 26 168630 p 72 N82-23576* #
NAS 1 26 168631 p 36 N82-23577* #
NAS 1 26 168632 p 11 N82-23578* #
NAS 1 26 168755 p 73 N82-23612* #
NAS 1 26 168756 p 73 N82-23613* #
NAS 1 26 168772 p 72 N82-23584* #
NAS 1 26 168774 p 36 N82-23587* #
NAS 1 26 168784 p 35 N82-22846* #
NAS 1 26 168800 p 73 N82-23599* #
NAS 1 26 168801 p 73 N82-23605* #
NAS 1 26 168823 p 36 N82-24520* #
NAS 1 26 168824 p 45 N82-24521* #
NAS 1 26 168825 p 36 N82-24522* #
NAS 1 26 168826 p 16 N82-24523* #
NAS 1 26 168845 p 35 N82-23563* #
NAS 1 26 168846 p 85 N82-23568* #
NAS 1 26 168856 p 19 N82-26745* #
NAS 1 26 168857 p 30 N82-24566* #
NAS 1 26 168859 p 85 N82-24568* #
NAS 1 26 168860 p 63 N82-24569* #
NAS 1 26 168865 p 73 N82-24572* #
NAS 1 26 168866 p 36 N82-24573* #
NAS 1 26 168867 p 17 N82-24574* #
NAS 1 26 168868 p 17 N82-24575* #
NAS 1 26 168869 p 17 N82-24576* #
NAS 1 26 168878 p 36 N82-24577* #
NAS 1 26 168879 p 37 N82-24578* #
NAS 1 26 168880 p 45 N82-24579* #
NAS 1 26 168881 p 74 N82-24580* #
NAS 1 26 168882 p 74 N82-24581* #
NAS 1 26 168883 p 37 N82-24582* #
NAS 1 26 168884 p 37 N82-24583* #
NAS 1 26 168885 p 37 N82-24584* #
NAS 1 26 168886 p 17 N82-24585* #
NAS 1 26 168888 p 37 N82-24586* #
NAS 1 26 168889 p 37 N82-24587* #
NAS 1 26 168895 p 38 N82-24590* #
NAS 1 26 168896 p 38 N82-24591* #
NAS 1 26 168897 p 38 N82-24589* #
NAS 1 26 168898 p 38 N82-24592* #
NAS 1 26 168899 p 38 N82-24593* #
NAS 1 26 168900 p 46 N82-24594* #
NAS 1 26 168901 p 74 N82-24595* #
NAS 1 26 168902 p 46 N82-24596* #
NAS 1 26 168903 p 57 N82-24597* #
NAS 1 26 168904 p 30 N82-24598* #
NAS 1 26 168905 p 38 N82-24599* #
NAS 1 26 168906 p 74 N82-24600* #
NAS 1 26 168907 p 63 N82-24601* #
NAS 1 26 168909 p 38 N82-24603* #
NAS 1 26 168910 p 74 N82-24588* #

NAS 1 26 168916 p 73 N82-24570* #
NAS 1 26 168944 p 18 N82-24602* #
NAS 1 26 168958 p 39 N82-25601* #
NAS 1 26 168959 p 39 N82-25604* #
NAS 1 26 168960 p 18 N82-25605* #
NAS 1 26 168967 p 19 N82-26747* #
NAS 1 26 168969 p 39 N82-26748* #
NAS 1 26 168975 p 19 N82-26752* #
NAS 1 26 168976 p 19 N82-26753* #
NAS 1 26 168977 p 20 N82-26754* #
NAS 1 26 168978 p 20 N82-26755* #
NAS 1 26 168979 p 75 N82-26756* #
NAS 1 26 168980 p 30 N82-26757* #
NAS 1 26 168981 p 58 N82-26758* #
NAS 1 26 168984 p 57 N82-25609* #
NAS 1 26 168996 p 47 N82-26750* #
NAS 1 26 168998 p 82 N82-26743* #
NAS 1 26 169010 p 20 N82-26759* #
NAS 1 26 169011 p 20 N82-26760* #
NAS 1 26 169032 p 18 N82-26742* #
NAS 1 26 169083 p 57 N82-26525* #

NASA-CR-160888 p 14 N82-23603* #
NASA-CR-161047 p 10 N82-22626* #
NASA-CR-166352 p 75 N82-26763* #
NASA-CR-166788 p 82 N82-26744* #
NASA-CR-166790 p 81 N82-25602* #
NASA-CR-166801 p 19 N82-26749* #
NASA-CR-167391 p 16 N82-24519* #
NASA-CR-167397 p 14 N82-23600* #
NASA-CR-167402 p 15 N82-23610* #
NASA-CR-167403 p 11 N82-23566* #
NASA-CR-167404 p 11 N82-23565* #
NASA-CR-167406 p 13 N82-23595* #
NASA-CR-167408 p 14 N82-23601* #
NASA-CR-167411 p 15 N82-23608* #
NASA-CR-167415 p 15 N82-23606* #
NASA-CR-167416 p 15 N82-23607* #
NASA-CR-167419 p 14 N82-23602* #
NASA-CR-167440 p 14 N82-23598* #
NASA-CR-167441 p 14 N82-23597* #
NASA-CR-167442 p 73 N82-23596* #
NASA-CR-167446 p 13 N82-23594* #
NASA-CR-167457 p 84 N82-22620* #
NASA-CR-167479 p 13 N82-23590* #
NASA-CR-167485 p 11 N82-23579* #
NASA-CR-167486 p 12 N82-23580* #
NASA-CR-167487 p 12 N82-23581* #
NASA-CR-167488 p 12 N82-23582* #
NASA-CR-167507 p 12 N82-23585* #
NASA-CR-167508 p 72 N82-23586* #
NASA-CR-167511 p 12 N82-23588* #
NASA-CR-167544 p 18 N82-25606* #
NASA-CR-167570 p 85 N82-26746* #
NASA-CR-167604 p 19 N82-26751* #
NASA-CR-167643 p 18 N82-26742* #
NASA-CR-168536 p 71 N82-23567* #
NASA-CR-168538 p 45 N82-24518* #
NASA-CR-168615 p 35 N82-22621* #
NASA-CR-168616 p 71 N82-22622* #
NASA-CR-168617 p 10 N82-22623* #
NASA-CR-168618 p 42 N82-22624* #
NASA-CR-168619 p 62 N82-22625* #
NASA-CR-168620 p 71 N82-22627* #
NASA-CR-168621 p 35 N82-22628* #
NASA-CR-168622 p 71 N82-22629* #
NASA-CR-168623 p 42 N82-23569* #
NASA-CR-168624 p 71 N82-23570* #
NASA-CR-168625 p 35 N82-23571* #
NASA-CR-168626 p 71 N82-23572* #
NASA-CR-168627 p 36 N82-23573* #
NASA-CR-168628 p 72 N82-23574* #
NASA-CR-168629 p 72 N82-23575* #
NASA-CR-168630 p 72 N82-23576* #
NASA-CR-168631 p 36 N82-23577* #
NASA-CR-168632 p 11 N82-23578* #
NASA-CR-168755 p 73 N82-23612* #
NASA-CR-168756 p 73 N82-23613* #
NASA-CR-168772 p 72 N82-23584* #
NASA-CR-168773 p 72 N82-23583* #
NASA-CR-168774 p 36 N82-23587* #
NASA-CR-168784 p 35 N82-22846* #
NASA-CR-168800 p 73 N82-23599* #
NASA-CR-168801 p 73 N82-23605* #
NASA-CR-168823 p 36 N82-24520* #
NASA-CR-168824 p 45 N82-24521* #
NASA-CR-168825 p 36 N82-24522* #
NASA-CR-168826 p 16 N82-24523* #
NASA-CR-168845 p 35 N82-23563* #
NASA-CR-168846 p 85 N82-23568* #
NASA-CR-168856 p 19 N82-26745* #
NASA-CR-168857 p 30 N82-24566* #
NASA-CR-168858 p 30 N82-24567* #
NASA-CR-168859 p 85 N82-24568* #
NASA-CR-168860 p 63 N82-24569* #
NASA-CR-168865 p 73 N82-24572* #
NASA-CR-168866 p 36 N82-24573* #
NASA-CR-168867 p 17 N82-24574* #
NASA-CR-168868 p 17 N82-24575* #
NASA-CR-168869 p 17 N82-24576* #
NASA-CR-168878 p 36 N82-24577* #
NASA-CR-168879 p 37 N82-24578* #
NASA-CR-168880 p 45 N82-24579* #
NASA-CR-168881 p 74 N82-24580* #
NASA-CR-168882 p 74 N82-24581* #
NASA-CR-168883 p 37 N82-24582* #
NASA-CR-168884 p 37 N82-24583* #
NASA-CR-168885 p 37 N82-24584* #
NASA-CR-168886 p 17 N82-24585* #
NASA-CR-168888 p 37 N82-24586* #
NASA-CR-168889 p 37 N82-24587* #
NASA-CR-168895 p 38 N82-24590* #
NASA-CR-168896 p 38 N82-24591* #
NASA-CR-168897 p 38 N82-24589* #
NASA-CR-168898 p 38 N82-24592* #
NASA-CR-168899 p 38 N82-24593* #
NASA-CR-168900 p 46 N82-24594* #
NASA-CR-168901 p 74 N82-24595* #
NASA-CR-168902 p 46 N82-24596* #
NASA-CR-168903 p 57 N82-24597* #
NASA-CR-168904 p 30 N82-24598* #
NASA-CR-168905 p 38 N82-24599* #
NASA-CR-168906 p 74 N82-24600* #
NASA-CR-168907 p 63 N82-24601* #
NASA-CR-168909 p 38 N82-24603* #
NASA-CR-168910 p 74 N82-24588* #
NASA-CR-168916 p 73 N82-24570* #
NASA-CR-168944 p 18 N82-24602* #
NASA-CR-168958 p 39 N82-25601* #
NASA-CR-168959 p 39 N82-25604* #
NASA-CR-168960 p 18 N82-25605* #
NASA-CR-168961 p 18 N82-25607* #
NASA-CR-168967 p 19 N82-26747* #
NASA-CR-168969 p 39 N82-26748* #
NASA-CR-168975 p 19 N82-26752* #
NASA-CR-168976 p 19 N82-26753* #
NASA-CR-168977 p 20 N82-26754* #
NASA-CR-168978 p 20 N82-26755* #
NASA-CR-168979 p 75 N82-26756* #
NASA-CR-168980 p 30 N82-26757* #
NASA-CR-168981 p 58 N82-26758* #
NASA-CR-168984 p 57 N82-25609* #
NASA-CR-168996 p 47 N82-26750* #
NASA-CR-168998 p 82 N82-26743* #
NASA-CR-169010 p 20 N82-26759* #
NASA-CR-169011 p 20 N82-26760* #
NASA-CR-169012 p 20 N82-26761* #
NASA-CR-169083 p 57 N82-26525* #

NASA-NEWS-RELEASE-82-100 p 82 N82-26741* #

NASA-TM-83280 p 81 N82-22865* #
NASA-TM-83290 p 55 N82-23614* #
NASA-TM-83842 p 16 N82-23611* #
NASA-TM-83871 p 46 N82-25603* #
NASA-TM-84186 p 81 N82-22643* #
NASA-TM-84191 p 84 N82-23258* #
NASA-TM-84201 p 11 N82-23564* #
NASA-TM-84202 p 15 N82-23609* #
NASA-TM-84203 p 13 N82-23592* #
NASA-TM-84204 p 13 N82-23593* #
NASA-TM-84205 p 15 N82-23604* #
NASA-TM-84206 p 13 N82-23589* #
NASA-TM-84471 p 30 N82-25661* #
NASA-TM-84478 p 81 N82-25610* #
NASA-TM-84694 p 16 N82-24563* #
NASA-TM-84695 p 16 N82-24564* #
NASA-TM-84696 p 17 N82-24565* #
NASA-TM-84731 p 18 N82-25608* #
NASA-TM-84740 p 13 N82-23591* #

NOAA-TM-NWS-SR-104 p 59 N82-27949 #

NOAA-TR-NESS-84 p 81 N82-22643* #
NOAA-TR-NESS-89 p 63 N82-22854 #

NOAA-TR-OTES-03 p 63 N82-22644 #

NOAA-81100501 p 81 N82-22643* #
NOAA-81102005 p 39 N82-27882 #
NOAA-8110502 p 63 N82-22644 #
NOAA-81111608 p 59 N82-27949 #

NPS68-81-006 p 58 N82-26945 #

NSF/IDOE-81-88 p 59 N82-26949 #

NSTL/ERL-198 p 16 N82-24563* #
NSTL/ERL-201 p 16 N82-24564* #
NSTL/ERL-202 p 17 N82-24565* #

OAO/TR-81/0033 p 82 N82-26744* #
OGMR-56 p 42 N82-22636 #

PB82-107335 p 30 N82-23963 #
PB82-129388 p 81 N82-22643* #
PB82-130089 p 63 N82-22644 #
PB82-137118 p 35 N82-22846* #
PB82-148644 p 39 N82-27882 #
PB82-149246 p 59 N82-26949 #
PB82-154006 p 59 N82-27949 #

PR-1 p 72 N82-23575* #
PR-1325-1 p 71 N82-23570* #
PR-1325-4 p 37 N82-24578* #
PR-2 p 73 N82-24572* #
PR-3 p 71 N82-22622* #
PR-3 p 73 N82-23612* #
PR-4 p 36 N82-24522* #
PR-5 p 74 N82-24595* #

P82-10 03 p 82 N82-26741* #

QPR-3 p 63 N82-24601* #
QPR-9 p 37 N82-24584* #

QR-4 p 46 N82-24596* #
QR-4 p 82 N82-26743* #
QR-5 p 71 N82-23567* #
QR-5 p 46 N82-24594* #

QSTPR-4 p 73 N82-23605* #
QSTPR-5 p 73 N82-23599* #
QSTPR-6 p 35 N82-23571* #
QSTPR-8 p 37 N82-24582* #
QSTPR-8 p 39 N82-25604* #
QSTPR-9 p 37 N82-24583* #

QSTRP-5 p 71 N82-22629* #

R-240 p 59 N82-27816 #

RADC-TR-81-303 p 75 N82-25613 #

RANRL-1/82 p 57 N82-24597* #

REPT-2 p 75 N82-26756* #
REPT-3 p 75 N82-26756* #
REPT-80-SGN-848-GEO-REPT-3 p 42 N82-22624* #

RR-LO-00466 p 15 N82-23607* #

RR-L1-00641 p 14 N82-23597* #
RR-L1-17269 p 73 N82-23596* #

RR-Y1-04217 p 17 N82-24565* #

RSC-3458-129 p 20 N82-26760* #
RSC-3458-131 p 20 N82-26759* #
RSC-3753 p 18 N82-25605* #

RSL-TR-429-1 p 19 N82-26749* #

RSS-TR-110481 p 57 N82-26525* #

S-420-81-01 p 84 N82-23258* #

SAM-TR-81-11 p 82 N82-26642 #

SAPR-16 p 30 N82-24566* #

SCIENTIFIC-12 p 40 N82-27900 #

SDSU-RSI-82-02 p 20 N82-26755* #

SDSU-RS1-81-04 p 18 N82-24602* #

SIO-REF-81-27 p 59 N82-26948 #
SIO-REF-81-38 p 58 N82-26766 #

SM-GI-04178 p 16 N82-23611* #

SR-J1-04195 p 13 N82-23592* #

SR-L1-00309 p 15 N82-23608* #
SR-L1-04032 p 12 N82-23581* #

SR-P1-04039 p 15 N82-23610* #
SR-P1-04139 p 14 N82-23602* #
SR-P1-04140 p 11 N82-23566* #
SR-P1-04141 p 14 N82-23600* #
SR-P1-04170 p 15 N82-23606* #
SR-P1-04194 p 72 N82-23586* #
SR-P1-04200 p 10 N82-22623* #
SR-P1-04200 p 12 N82-23585* #
SR-P2-04236 p 18 N82-26742* #

STPR-6 p 74 N82-24580* #

TR-79-281	p 82	N82-26642	#
TVA/ONR/ARP-81/5-VOL-1	p 31	N82-27802	#
TVA/ONR/ARP-81/6-VOL-2	p 31	N82-27803	#
UCID-19167	p 30	N82-27737	#
UCRL-15382	p 39	N82-26915	#
UMASS-ARF-82-321	p 76	N82-26907	#
USCIPI-1050	p 74	N82-25611	#
USGS-OFR-80-469	p 72	N82-23584*	#
UTD-E0533-01	p 71	N82-22629*	#
WHOI-81-104	p 39	N82-25748	#
WTHD-143	p 73	N82-24517	#

Typical Accession Number Index Listing

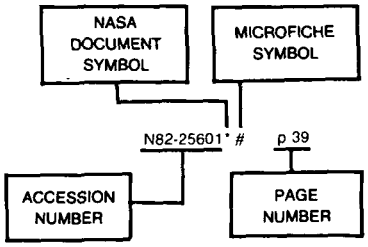

Listings in this index are arranged alphanumerically by accession number. The page number listed to the right indicates the page on which the citation is located. An asterisk (*) indicates that the item is a NASA report. A pound sign (#) indicates that the item is available on microfiche.

A82-13528 # p 59
A82-22294* # p 31
A82-22306* # p 49
A82-22538* # p 63
A82-22539 # p 1
A82-22540 # p 63
A82-22541* # p 1
A82-22542* # p 1
A82-22543 # p 1
A82-22544 # p 1
A82-22545 # p 21
A82-22546 # p 82
A82-22547* # p 82
A82-22548 # p 82
A82-22549 # p 82
A82-22550 # p 83
A82-22551 # p 83
A82-22552 # p 1
A82-22553 # p 83
A82-22554 # p 83
A82-22555* # p 64
A82-22556 # p 83
A82-22557 # p 2
A82-22558 # p 64
A82-22559 # p 2
A82-22560 # p 2
A82-22561 # p 2
A82-22562 # p 21
A82-22563 # p 2
A82-22564 # p 2
A82-22565 # p 2
A82-22566 # p 21
A82-22567 # p 21
A82-22568 # p 64
A82-22569 # p 21
A82-22570 # p 21
A82-22571 # p 3
A82-22572 # p 3
A82-22573 # p 64
A82-22574 # p 40
A82-22575 # p 64
A82-22576 # p 64
A82-22577 # p 64
A82-22578 # p 64
A82-22579 # p 65
A82-22580 p 65
A82-22581 # p 65
A82-22582 # p 65
A82-22583 # p 21
A82-22584* # p 3
A82-22585* # p 65
A82-22586* # p 65
A82-22587 # p 3
A82-22588 # p 22
A82-22589 # p 3
A82-22590 # p 66
A82-22591* # p 3
A82-22592* # p 4
A82-22593 # p 4
A82-22594 # p 4
A82-22595 # p 31
A82-22596 # p 31
A82-22597 # p 66
A82-22598 # p 31
A82-22599 # p 83
A82-22600 # p 4
A82-22601 # p 4
A82-22602 # p 4
A82-22603 # p 83
A82-22604 # p 40
A82-22605* # p 22
A82-22606* # p 22
A82-22607* # p 40
A82-22608 # p 76
A82-22609 # p 40
A82-22610 # p 4
A82-22611* # p 5
A82-22612* # p 5
A82-22613* # p 40
A82-22614 # p 31
A82-22615 # p 59
A82-22616 # p 22
A82-22617 # p 5
A82-22618 # p 5
A82-22619 # p 49
A82-28905 # p 66
A82-28907* # p 49
A82-29326* # p 66
A82-29327 # p 22
A82-29328 # p 66
A82-29332* # p 22
A82-29333 # p 60
A82-29409 # p 66
A82-29435 # p 5
A82-29526 p 5
A82-29527 # p 5
A82-29528 # p 5
A82-29529 # p 6
A82-29530 # p 6
A82-29531 # p 6
A82-29532 # p 6
A82-29533 # p 6
A82-29534 # p 6
A82-29535 # p 6
A82-29536 # p 6
A82-29537 # p 6
A82-29538* # p 7
A82-29539* # p 7
A82-29541 # p 76
A82-29601* # p 49
A82-29602* # p 49
A82-29603* # p 49
A82-29604 # p 49
A82-29607* # p 50
A82-29608* # p 50
A82-29609* # p 50
A82-29610* # p 50
A82-29611* # p 50
A82-29612 # p 50
A82-29613* # p 50
A82-29614* # p 51
A82-29615* # p 32
A82-29616* # p 51
A82-29617* # p 51
A82-29618* # p 51
A82-29619* # p 51
A82-29621* # p 52
A82-29622* # p 52
A82-29623* # p 52
A82-29624* # p 52
A82-29747 # p 7
A82-29762 # p 66
A82-29922 # p 76
A82-30293 # p 23
A82-30304 # p 41
A82-30305 # p 41
A82-30306 # p 32
A82-30307 # p 23
A82-30314 # p 32
A82-30666 # p 52
A82-30778 # p 32
A82-30784* # p 32
A82-30785* # p 32
A82-30786* # p 41
A82-30787* # p 32
A82-30788* # p 32
A82-30789* # p 32
A82-30790* # p 32
A82-30795* # p 33
A82-30796 # p 33
A82-30810 # p 52
A82-30849 # p 33
A82-30850 # p 83
A82-31019 # p 76
A82-31020 # p 76
A82-31294 # p 52
A82-31295 # p 23
A82-31990* # p 23
A82-31991 # p 77
A82-31994* # p 33
A82-31995* # p 53
A82-31996 # p 83
A82-32033 # p 67
A82-32077* # p 33
A82-32078* # p 33
A82-32084 # p 33
A82-32090 # p 33
A82-32096 # p 34
A82-32099 # p 34
A82-32342* # p 23
A82-32343* # p 67
A82-32344 # p 67
A82-32345* # p 67
A82-32346 # p 67
A82-32347 # p 67
A82-32348* # p 23
A82-32440 p 77
A82-32441* # p 23
A82-32442* # p 41
A82-32443* # p 77
A82-32447* # p 77
A82-32448* # p 77
A82-32507 # p 67
A82-32559 # p 53
A82-32581* # p 68
A82-32646* # p 34
A82-32651 # p 53
A82-32658* # p 77
A82-32701 # p 7
A82-32702 # p 77
A82-32703 # p 7
A82-32704 # p 7
A82-32705 # p 7
A82-32707 # p 8
A82-32708* # p 8
A82-32709 # p 68
A82-32711 # p 24
A82-32766 # p 78
A82-32824 # p 78
A82-32881 # p 53
A82-32882* # p 53
A82-32896* # p 60
A82-32897* # p 8
A82-32898 # p 41
A82-32899 # p 24
A82-32900 # p 68
A82-32901 # p 24
A82-32902 # p 53
A82-32903 # p 53
A82-32904* # p 68
A82-32905* # p 8
A82-32906 # p 68
A82-32907 # p 8
A82-32909* # p 8
A82-32910* # p 60
A82-32911 # p 68
A82-32912 # p 78
A82-32913* # p 8
A82-32914* # p 8
A82-32915* # p 78
A82-32916 # p 68
A82-32917 # p 54
A82-33293 # p 34
A82-33295 # p 34
A82-33296 # p 78
A82-33297 # p 78
A82-33322* # p 54
A82-33329 # p 60
A82-33402 # p 41
A82-33438* # p 54
A82-33442 # p 78
A82-33555 # p 84
A82-33652 # p 24
A82-33654 # p 24
A82-33655 # p 24
A82-33656 # p 24
A82-33657* # p 24
A82-33659* # p 24
A82-33717 # p 54
A82-33865 # p 25
A82-34116 # p 84
A82-34179* # p 8
A82-34218* # p 25
A82-34219 # p 54
A82-34222* # p 79
A82-34225 # p 68
A82-34367 # p 84
A82-34469 # p 69
A82-34470 # p 79
A82-34471 # p 79
A82-34701 p 79
A82-34702 # p 69
A82-34706 # p 9
A82-34708 # p 79
A82-34710 # p 9
A82-34711 # p 25
A82-34716 # p 9
A82-34717 # p 69
A82-34719 # p 34
A82-34720* # p 69
A82-34721* # p 42
A82-34722 # p 69
A82-34723 # p 69
A82-34724 # p 79
A82-34726 # p 69
A82-34727 # p 80
A82-34729* # p 9
A82-34730* # p 9
A82-34731 # p 9
A82-34732 # p 9
A82-34733 # p 9
A82-34734 # p 60
A82-34735 # p 60
A82-34736* # p 60
A82-34737 # p 80
A82-34739 # p 25
A82-34742 # p 80
A82-34743* # p 25
A82-34744* # p 25
A82-34745 # p 61
A82-34746 # p 80
A82-34918* # p 34
A82-34940 # p 69
A82-35126 p 61
A82-35127 # p 61
A82-35129 # p 61
A82-35130 # p 61
A82-35131 # p 61
A82-35132 # p 61
A82-35133 # p 61
A82-35134 # p 62
A82-35136 # p 62
A82-35138 # p 62
A82-35139 # p 10
A82-35140 # p 62
A82-35141 # p 70
A82-35534 # p 26
A82-35542* # p 26
A82-35650* # p 70
A82-35824* # p 70
A82-35895 # p 26
A82-36005 # p 54
A82-36018 # p 80
A82-36043 # p 70
A82-36053* # p 26
A82-36247 # p 26
A82-36268 # p 26
A82-36292* # p 27
A82-36293* # p 27
A82-36298* # p 42
A82-36341 # p 54
A82-36362* # p 27
A82-36405 # p 27
A82-36406 # p 27
A82-36414 # p 27
A82-36415* # p 28
A82-36422 # p 28
A82-36428 # p 28
A82-36431 # p 28
A82-36444 # p 28
A82-36472 # p 28
A82-36477 # p 29
A82-36534* # p 29
A82-36617* # p 84
A82-36741 # p 29
A82-36935 # p 70
A82-37048 # p 70
A82-37174 # p 62
A82-37175 # p 34
A82-37194 # p 10
A82-37195 # p 55
A82-37196 # p 55
A82-37198 # p 42
A82-37200 # p 70
A82-37390* # p 55
A82-37405* # p 29
A82-37501 # p 62
A82-37502 # p 29
A82-37503 # p 10
A82-37505 # p 55
A82-37589 # p 10
A82-37809 # p 80
A82-37810* # p 71
A82-37812* # p 81
A82-37962* # p 35

N82-22620* # p 84
N82-22621* # p 35
N82-22622* # p 71
N82-22623* # p 10
N82-22624* # p 42
N82-22625* # p 62
N82-22626* # p 10
N82-22627* # p 71
N82-22628* # p 35
N82-22629* # p 71
N82-22630 # p 84
N82-22636 # p 42
N82-22643* # p 81

N82-22644 # p 63
N82-22832 # p 35
N82-22846* # p 35
N82-22854 # p 63
N82-22865* # p 81
N82-23043 # p 29
N82-23116* # p 10
N82-23133* # p 11
N82-23258* # p 84
N82-23563* # p 35
N82-23564* # p 11
N82-23565* # p 11
N82-23566* # p 11
N82-23567* # p 71
N82-23568* # p 85
N82-23569* # p 42
N82-23570* # p 71
N82-23571* # p 35
N82-23572* # p 71
N82-23573* # p 36
N82-23574* # p 72
N82-23575* # p 72
N82-23576* # p 72
N82-23577* # p 36
N82-23578* # p 11
N82-23579* # p 11
N82-23580* # p 12
N82-23581* # p 12
N82-23582* # p 12
N82-23583* # p 72
N82-23584* # p 72
N82-23585* # p 12
N82-23586* # p 72
N82-23587* # p 36
N82-23588* # p 12
N82-23589* # p 13
N82-23590* # p 13
N82-23591* # p 13
N82-23592* # p 13
N82-23593* # p 13
N82-23594* # p 13
N82-23595* # p 13
N82-23596* # p 73
N82-23597* # p 14
N82-23598* # p 14
N82-23599* # p 73
N82-23600* # p 14
N82-23601* # p 14
N82-23602* # p 14
N82-23603* # p 14
N82-23604* # p 15
N82-23605* # p 73
N82-23606* # p 15
N82-23607* # p 15
N82-23608* # p 15
N82-23609* # p 15
N82-23610* # p 15
N82-23611* # p 16
N82-23612* # p 73
N82-23613* # p 73
N82-23614* # p 55
N82-23621 # p 43
N82-23623 # p 43
N82-23624 # p 43
N82-23625 # p 43
N82-23626 # p 43
N82-23627 # p 43
N82-23628 # p 43
N82-23629 # p 43
N82-23630 # p 43
N82-23631 # p 44
N82-23632 # p 44
N82-23633 # p 44
N82-23634 # p 44
N82-23635 # p 44
N82-23636 # p 44
N82-23637 # p 44
N82-23638 # p 44
N82-23639 # p 44
N82-23640 # p 45
N82-23641 # p 45
N82-23642 # p 45
N82-23643 # p 45
N82-23644 # p 45
N82-23793 # p 29
N82-23852 p 55
N82-23856 p 55
N82-23879 p 55
N82-23891 p 29
N82-23898 p 56
N82-23900 p 56
N82-23908 p 56
N82-23909 p 56
N82-23910 p 56
N82-23912 p 56
N82-23929 p 57
N82-23939 p 57
N82-23945 # p 57
N82-23963 # p 30
N82-24216 # p 85
N82-24263 # p 85
N82-24264 # p 81
N82-24489 # p 81
N82-24517 # p 73
N82-24518* # p 45
N82-24519* # p 16
N82-24520* # p 36
N82-24521* # p 45
N82-24522* # p 36
N82-24523* # p 16
N82-24563* # p 16
N82-24564* # p 16
N82-24565* # p 17
N82-24566* # p 30
N82-24567* # p 30
N82-24568* # p 85
N82-24569* # p 63
N82-24570* # p 73
N82-24572* # p 73
N82-24573* # p 36
N82-24574* # p 17
N82-24575* # p 17
N82-24576* # p 17
N82-24577* # p 36
N82-24578* # p 37
N82-24579* # p 45
N82-24580* # p 74
N82-24581* # p 74
N82-24582* # p 37
N82-24583* # p 37
N82-24584* # p 37
N82-24585* # p 17
N82-24586* # p 37
N82-24587* # p 37
N82-24588* # p 74
N82-24589* # p 38
N82-24590* # p 38
N82-24591* # p 38
N82-24592* # p 38
N82-24593* # p 38
N82-24594* # p 46
N82-24595* # p 74
N82-24596* # p 46
N82-24597* # p 57
N82-24598* # p 30
N82-24599* # p 38
N82-24600* # p 74
N82-24601* # p 63
N82-24602* # p 18
N82-24603* # p 38
N82-25601* # p 39
N82-25602* # p 81
N82-25603* # p 46
N82-25604* # p 39
N82-25605* # p 18
N82-25606* # p 18
N82-25607* # p 18
N82-25608* # p 18
N82-25609* # p 57
N82-25610* # p 81
N82-25611 # p 74
N82-25612 # p 74
N82-25613 # p 75
N82-25614 # p 75
N82-25620 # p 46
N82-25621 # p 46
N82-25622 # p 46
N82-25623 # p 46
N82-25625 # p 47
N82-25661* # p 30
N82-25748 # p 39
N82-26027 # p 75
N82-26037 # p 75
N82-26268 # p 39
N82-26525* # p 57
N82-26642 # p 82
N82-26741* # p 82
N82-26742* # p 18
N82-26743* # p 82
N82-26744* # p 82
N82-26745* # p 19
N82-26746* # p 85
N82-26747* # p 19
N82-26748* # p 39
N82-26749* # p 19
N82-26750* # p 47
N82-26751* # p 19
N82-26752* # p 19
N82-26753* # p 19
N82-26754* # p 20
N82-26755* # p 20
N82-26756* # p 75
N82-26757* # p 30
N82-26758* # p 58
N82-26759* # p 20
N82-26760* # p 20
N82-26761* # p 20
N82-26762 # p 20
N82-26763* # p 75
N82-26764 # p 58
N82-26765 # p 75
N82-26766 # p 58
N82-26907 # p 76
N82-26915 # p 39
N82-26944 # p 58
N82-26945 # p 58
N82-26948 # p 59
N82-26949 # p 59
N82-27737 # p 30
N82-27802 # p 31
N82-27803 # p 31
N82-27804 # p 47
N82-27805 # p 47
N82-27806 # p 47
N82-27807 # p 47
N82-27808 # p 47
N82-27809 # p 48
N82-27810 # p 48
N82-27811 # p 48
N82-27812 # p 48
N82-27813 # p 48
N82-27814 # p 48
N82-27815 # p 48
N82-27816 # p 59
N82-27882 # p 39
N82-27900 # p 40
N82-27949 # p 59

1. Report No. NASA SP-7041(35)	2 Government Accession No	3. Recipient's Catalog No
4 Title and Subtitle EARTH RESOURCES A Continuing Bibliography (Issue 35)		5 Report Date October 1982 6. Performing Organization Code
7 Author(s)		8. Performing Organization Report No
9 Performing Organization Name and Address National Aeronautics and Space Administration Washington, D.C. 20546		10. Work Unit No. 11 Contract or Grant No.
12. Sponsoring Agency Name and Address		13 Type of Report and Period Covered 14 Sponsoring Agency Code
15. Supplementary Notes		

16. Abstract

This bibliography list 587 reports, articles, and other documents introduced into the NASA Scientific and Technical Information System between July 1, and September 30, 1982. Emphasis is placed on the use of remote sensing and geophysical instrumentation in spacecraft and aircraft to survey and inventory natural resources and urban areas. Subject matter is grouped according to agriculture and forestry, environmental changes and cultural resources, geodesy and cartography, geology and mineral resources, hydrology and water management, data processing and distribution systems, instrumentation and sensors, and economic analysis.

17. Key Words (Suggested by Author(s))	18. Distribution Statement
Bibliographies Earth Resources Remote Sensors	Unclassified - Unlimited

19. Security Classif. (of this report)	20. Security Classif. (of this page)	21. No. of Pages	22. Price*
Unclassified	Unclassified	164	$10.50 HC

*For sale by the National Technical Information Service, Springfield, Virginia 22161

NASA-Langley, 1982

PUBLIC COLLECTIONS OF NASA DOCUMENTS

DOMESTIC

NASA distributes its technical documents and bibliographic tools to eleven special libraries located in the organizations listed below. Each library is prepared to furnish the public such services as reference assistance, interlibrary loans, photocopy service, and assistance in obtaining copies of NASA documents for retention.

CALIFORNIA
University of California, Berkeley
COLORADO
University of Colorado, Boulder
DISTRICT OF COLUMBIA
Library of Congress
GEORGIA
Georgia Institute of Technology, Atlanta
ILLINOIS
The John Crerar Library, Chicago
MASSACHUSETTS
Massachusetts Institute of Technology, Cambridge
MISSOURI
Linda Hall Library, Kansas City
NEW YORK
Columbia University, New York
OKLAHOMA
University of Oklahoma, Bizzell Library
PENNSYLVANIA
Carnegie Library of Pittsburgh
WASHINGTON
University of Washington, Seattle

NASA publications (those indicated by an '*' following the accession number) are also received by the following public and free libraries.

CALIFORNIA
Los Angeles Public Library
San Diego Public Library
COLORADO
Denver Public Library
CONNECTICUT
Hartford Public Library
MARYLAND
Enoch Pratt Free Library, Baltimore
MASSACHUSETTS
Boston Public Library
MICHIGAN
Detroit Public Library
MINNESOTA
Minneapolis Public Library and Information Center
NEW JERSEY
Trenton Public Library
NEW YORK
Brooklyn Public Library
Buffalo and Erie County Public Library
Rochester Public Library
New York Public Library
OHIO
Akron Public Library
Cincinnati and Hamilton County Public Library
Cleveland Public Library
Dayton Public Library
Toledo and Lucas County Public Library
TEXAS
Dallas Public Library
Fort Worth Public Library
WASHINGTON
Seattle Public Library
WISCONSIN
Milwaukee Public Library

An extensive collection of NASA and NASA-sponsored documents and aerospace publications available to the public for reference purposes is maintained by the American Institute of Aeronautics and Astronautics, Technical Information Service, 555 West 57th Street 12th Floor New York, New York 10019.

EUROPEAN

An extensive collection of NASA and NASA-sponsored publications is maintained by the British Library Lending Division Boston Spa Wetherby Yorkshire England. By virtue of arrangements other than with NASA, the British Library Lending Division also has available many of the non-NASA publications cited in *STAR*. European requesters may purchase facsimile copy of microfiche of NASA and NASA-sponsored documents those identified by both the symbols # and * from ESA - Information Retrieval Service European Space Agency 8-10 rue Mario-Nikis, 75738 Paris CEDEX 15 France.

3 1 SP-7041, 821215 S03487BSR
NASA
SCIEN & TECH INFO FACILITY
ATTN: REFERENCE & RETRIEVAL DEPT
P O BOX 8757 BWI ARPRT
BALTIMORE MD 21240